# Geotechnics of High Water Content Materials

TUNCER B. EDIL
AND PATRICK J. FOX
EDITORS

ASTM

STP 1374

STP 1374

# *Geotechnics of High Water Content Materials*

*Tuncer B. Edil and Patrick J. Fox, editors*

### Photocopy Rights

### Peer Review Policy

Each paper published in this volume was evaluated by two peer reviewers and at least one editor. The authors addressed all of the reviewers' comments to the satisfaction of both the technical editor(s) and the ASTM Committee on Publications.

To make technical information available as quickly as possible, the peer-reviewed papers in this publication were prepared "camera-ready" as submitted by the authors.

The quality of the papers in this publication reflects not only the obvious efforts of the authors and the technical editor(s), but also the work of the peer reviewers. In keeping with long-standing publication practices, ASTM maintains the anonymity of the peer reviewers. The ASTM Committee on Publications acknowledges with appreciation their dedication and contribution of time and effort on behalf of ASTM.

# Foreword

This publication, *Geotechnics of High Water Content Materials*, contains papers presented at the symposium of the same name held in Memphis, Tennessee, on 28–29 January 1999. The symposium was sponsored by ASTM Committee D18 on Soil and Rock and the D18.18 Subcommittee on Peats and Organic Soils. The symposium was chaired by Tuncer B. Edil, University of Wisconsin-Madison and Patrick J. Fox, University of California-Los Angeles.

# Contents

GEOTECHNICS OF HIGH WATER CONTENT MATERIALS

# Overview

A symposium sponsored by ASTM Subcommittee D18.18 on Peats and Organic Soils was held on 28–29 January 1999 at the Peabody Hotel in Memphis, Tennessee. The objective of the symposium was to bring together representatives of academia, government, and industry from around the world to discuss advances in research and practice involving geotechnics of high water content materials. The international flavor of the symposium and technical papers attest to the world-wide interest in such problems.

The papers contained in this volume cover a broad range of topics. Various types of high water content materials are discussed, including peats and organic soils, soft silts and clays, bentonite slurries, paper sludges, wastewater sludges, dredgings, lime wastes, and mine tailings. Several papers address contaminated materials. Geotechnical problems include handling and disposal, dewatering, stabilization, hydraulic performance, settlement, stability, in situ testing, and construction. The papers highlight recent developments in these areas with emphasis given to construction on marginal lands and dewatering and disposal of high water content waste materials.

## Background

Construction on marginal lands is becoming increasingly necessary for economic reasons. Foundation soils for these projects, such as soft clays and peats, typically have high water content, high compressibility, and low shear strength. There is also considerable interest in the economic and environmentally safe disposal of high water content waste materials. Applications in which waste materials can be reused beneficially take on even more importance. The successful design, construction, operation, and in some cases reclamation of such projects involve predictions of geotechnical behavior in terms of hydraulic conduction, settlement, and shear strength, often as a function of time. This, in turn, requires reliable material characterization and modeling that accounts for differences in behavior as compared to conventional soils. Likewise, there is a need for laboratory and field tests to measure material properties and, in some cases, a need for specialized techniques of construction.

## Contents

### Keynote Paper

The keynote paper provides an excellent overview of the geotechnics of high water content materials. A generation of slurried wastes is described, and material properties for a wide variety of waste materials are compared with those of natural soils. The paper identifies limitations in current knowledge and discusses a broad range of engineering concepts that are relevant to practical problems. The paper notes that current capabilities of engineering analysis far exceed the quality and/or quantity of input data in most cases and that improved methods for material and site characterization are needed.

### Fundamentals, Theory, and Modeling

Large strain consolidation theory is recognized as the appropriate framework for modeling volume change due to material self-weight and applied surface loads. User-friendly computer codes

and chart solutions bring this capability to engineering practice. The characterization of void ratio–effective stress and void ratio–hydraulic conductivity relationships at low effective stress and the establishment of initial void ratio for numerical analysis are still challenging problems for large strain consolidation modeling. Interesting test methods for evaluation of these relationships are proposed in this volume, and their validity is demonstrated. Use of the centrifuge for accelerated testing of sedimentation and self-weight consolidation holds special promise in this context. Instrumented columns provide insight into the process of transition from a suspension to a structured material and the development of geotechnical properties such as density, modulus, and shear strength. Currently, no ASTM standards exist for slurry sedimentation and consolidation testing.

Secondary compression and creep effects can be important for high water content materials, especially those that contain organic matter. Settlement behavior referred to as "tertiary compression" is also observed in peats, dredgings, and paper sludges. This phenomenon has been attributed to biodegradation and gas generation. However, recent studies have demonstrated that treatment of specimens for bacterial activity does not entirely remove the effect. A paper in this volume discusses the incorporation of various creep models into finite element codes. Such codes represent a needed development in the numerical simulation of field behavior.

Measurement of undrained shear strength for very soft materials and characterization of its development with consolidation remains a challenging problem. Conventional field equipment generally cannot adequately differentiate low values of shear strength. Vane shear still remains the method of choice although cone penetration is also used in sufficiently strong materials. Materials that contain fibers, such as peats and certain sludges, may exhibit internal fiber reinforcement effects, including strength anisotropy and a low coefficient of lateral earth pressure. Conventional soil strength models and testing procedures may not be applicable to such materials.

Papers are presented that deal with fundamental microstructural behavior of wastewater sludges and clay slurries. Issues of material flocculation, gas generation, and flow localization through channels are significant and require us to reevaluate basic assumptions of consolidation theory (e.g., continuum flow) for the modeling of rapidly dewatering or decomposing materials.

**Laboratory Investigations**

Hydraulic properties of high water content materials are important for the prediction of consolidation rate and the evaluation of potential use as a hydraulic barrier. Hydraulic conductivity testing of paper sludge may be complicated by gas generation. Refrigeration can be used to control gas during testing. As paper sludge is soft and plastic, fluid flow is not governed by macrostructure features (e.g., cracks, fissures, and clods). Consequently, hydraulic conductivity tests performed on small specimens taken from paper sludge liners can be used for quality control purposes. This material also has an effective sorptive capacity for heavy metals. Paper sludge liners may undergo significant consolidation after construction, which both improves strength and decreases hydraulic conductivity.

Dewatering is a primary concern for the disposal of high water content materials. Papers in this volume describe how to efficiently dewater slurries and estimate the quantity of exuded liquid. The quantity of water released from sludgy or pasty wastes is important in determining leaching potential and for water balance analyses associated with disposal activities. Centrifugal systems and other innovative separation techniques can produce efficient dewatering.

Chemical stabilization of high water content materials is used to increase strength and minimize leaching of contaminants. Addition of binders, typically Portland cement, to harbor dredgings and waste sludges results in solidification from both drying and hydration reactions. Significant leaching, especially of heavy metals, can occur after cement stabilization if the initial water content is high. Leaching is substantially reduced for chemical stabilization of dewatered (i.e., low water content) sludges due to their lower hydraulic conductivity.

Thermal properties of high water content materials are needed for problems involving heat transfer. Use of thermal probes is shown to be effective in characterizing the heat capacity and thermal conductivity of peats, industrial sludge, bentonite slurry, and municipal solid waste. Peat has a heat capacity similar to water and municipal solid waste has a value similar to air, illustrating that heat capacity is greatly influenced by water content. Values of thermal conductivity for high water content materials are generally less than those for sands and silts due to their high void ratio.

## Field Performance

Geophysical methods have seen great advancement in recent years and their application to high water content materials holds particular promise. An in situ density and shear modulus profiling system for soft deposits, called a soil stiffness probe, is described in this volume. The probe was used to define the transition from suspension to continuous soil and the presence of gas lenses in a pond of contaminated dredge spoils. A correlation between shear modulus and undrained shear strength was also found. Geophysical methods can be used to characterize soft deposits for which conventional sampling and laboratory testing of undisturbed specimens would be difficult or impossible.

Field performance of highway embankments founded on lime waste and soft clays are described in this volume. The analyses show that conventional consolidation theory, with adjustments for large settlement and ramp loading, may give reasonable estimates of settlement but underestimates rate of pore pressure dissipation. The reason for the discrepancy in pore pressure response is not clear.

## Case Histories

Construction over soft soils may encounter difficult problems of supporting equipment and structural loads. Use of low ground pressure equipment, geosynthetic reinforcement, lightweight fill, and winter construction procedures may circumvent such problems. In one case history, a sludge lagoon was capped during winter by flooding the upper crust of frozen sludge with water, thus producing a strong ice layer. A woven geotextile was then placed over the ice, followed by a lightweight cap consisting of a wood chip/soil mixture placed using low ground pressure equipment. The geotextile provided safety during construction against possible breaking of the frozen surface. After construction, the geotextile served as a separation/filter/reinforcement layer under the constructed cap.

Dredging and disposal of marine sediments in an abandoned rock quarry is described in another case history. Large strain self-weight consolidation modeling with careful characterization of material consistency from suspension to structured soil is shown to give good estimates of disposal pond capacity. Modeling of the sediment accretion process in the disposal pond was not found to have a large effect on long-term settlement estimates.

The effect of construction dewatering on soft silty clay and peat deposits and supported structures is presented in this volume. The finite element method is effectively used to optimize design of a dewatering system for a deep excavation to prevent excessive total and differential settlement. Simplified analytical approaches often result in poor predictions due to the complexity of the problem. Rapid transient drawdown of the groundwater table can result in significant compression of peat due to its high hydraulic conductivity.

Another paper describes procedures for the construction of reinforced soil walls on soft ground. Design details such as interpanel spacing joints that accommodate large total and differential settlements are presented for several walls.

## Concluding Remarks

Technical papers in this volume provide state-of-the-art information for geotechnical engineering involving high water content materials. The field has evolved in terms of new material types and ap-

plications, use of geosynthetics and in situ testing, and environmental issues that must be addressed. Large-strain consolidation theory and related material characterization techniques are now used routinely. As such, ASTM standards for slurry consolidation and corresponding parameter determination are needed. ASTM standards are also needed for sample preparation of chemically stabilized materials. In situ testing will likely see increased future use for material characterization due to the difficulties of conventional undisturbed sampling and testing. Geosynthetics are also expected to play an increasing role in future projects. Progress in this field occurs as traditional soil mechanics concepts are adapted to a range of material properties and behavior that is outside that of typical natural soils. The presence of fibers, organic matter, and chemical constituents can also introduce significant complexities. Thus, the need continues for future investigations to increase our understanding of these difficult materials.

The editors wish to express their appreciation to all those who participated in the symposium. Particular thanks are extended to those who contributed papers, to the reviewers of the papers, to ASTM Committee D18 on Soil and Rock for sponsoring the symposium through Subcommittee D18.18 on Peats and Organic Soils, and to the editorial staff of ASTM.

*Tuncer B. Edil*
University of Wisconsin, Madison, WI;
    Symposium Chairman and Editor

*Patrick J. Fox*
University of California, Los Angeles, CA;
    Symposium Chairman and Editor

**Fundamentals, Theory, and Modeling**

Raymond J. Krizek[1]

**Geotechnics of High Water Content Materials**

---

**Abstract:** Reasonable estimates indicate that approximately a billion cubic meters of
high water content soil-like wastes are produced annually worldwide, and a large portion
of these are deposited hydraulically in diked impoundment areas, some of which are
among the largest earth structures in the world. The major problems emanating from this
disposal method are the difficulty in dewatering the wastes, their low strength and
hydraulic conductivity, their high compressibility, their potential to contaminate the
groundwater, the stability of the confining dikes, and the ultimate reclamation of the
disturbed land. Following a brief explanation of how many of these wastes are generated,
quantitative values for key engineering properties are summarized and compared for a
wide variety of waste materials and some reference soils. Then, many concepts that have
been applied with success will be presented together with the advantages each offers, the
difficulties involved in using it, and the limitations in our knowledge. Discussed briefly
will be state-of-practice developments in mathematical modeling, laboratory testing and
associated interpretations, and material property formulations.

**Keywords:** high water content, soil-like wastes, process tailings, ore, disposal, diked
impoundment area, dewatering, high compressibility, low strength, low hydraulic
conductivity, disturbed land, reclamation

## Introduction

The disposal of high water content soil-like wastes and reclamation of the
disturbed land pose one of the major challenges facing geotechnical engineers.
Notwithstanding the progress made in recent decades to better understand this problem
and find solutions to specific cases, the growing desire for a risk-free environment,
greater concern for public safety, evolving regulatory criteria, increased legal liability,
advancing technology, and the need to integrate reclamation into the planning and design
process (Taylor and D'Appolonia, 1977; Vick, 1990) dictate that much more remains to
be done. In addition to the high water content and associated dewatering difficulty, two
of the major problems with these wastes lie in their large volume and great variability.

---

[1] Stanley F. Pepper Professor, Dept. of Civil Engineering, Northwestern University,
    2145 Sheridan Road, Evanston, IL 60208.

3

While it is hard to obtain reliable current disposal volumes for most of these wastes, a conservative estimate of the annual total worldwide is on the order of a billion cubic meters or more, and from an engineering point of view, the impoundments for these wastes are among the largest earth structures in the world. It is not uncommon for an impoundment area to have side lengths of a kilometer or more and dikes 50 or more meters high. Among the highly variable slurried wastes are taconite tailings, dredged spoil, red mud, phosphate slimes, paper mill sludge, precious metal tailings, uranium tailings, flue gas desulfurization sludge, tar sand wastes, gypsum tailings, coal refuse, flyash, and a large variety of other process waste materials. Each of these wastes has its own particular characteristics, and while certain general principles apply, each must be handled with appropriate recognition for its unique peculiarities.

For all practical purposes at the present time, the most common economically feasible way in which to dispose of these slurried soil-like wastes is to deposit them hydraulically in confined impoundment areas. The major problems emanating from this disposal method are (a) the difficulty and resultant long times that are required to dewater the wastes, (b) the low strength, low hydraulic conductivity, and high compressibility of the wastes, (c) the contaminants in the wastes that may leach into the groundwater, (d) the stability of the dikes forming the impoundment area, (e) the storage capacity or design life of the impoundment area, and (f) the availability of land for the impoundment areas and the final use that can be made of this land after disposal of the wastes. It is clear, however, that the planning, design, operation, and reclamation of impoundment areas containing high water content wastes is becoming increasingly interdisciplinary in nature and requires complementary expertise in many diverse fields beyond traditional geotechnical engineering.

## Objective

The objective of this paper is to provide an overview of the problems associated with the disposal of high water content (often slurried) wastes and the variety of solutions that are available to address these problems. As such, the intent is to provide an overall perspective and general framework within which to categorize certain problems, rather than detailed methodologies of how to design and implement specific solutions. This will be accomplished by first reviewing how many of these wastes are generated and the underlying reasons why they are difficult to handle. Then, quantitative values for the plasticity, compressibility, hydraulic conductivity, and "zero effective stress" void ratio of a wide variety of waste materials, together with some reference soils, will be compared at water contents well beyond those normally encountered in conventional geotechnical engineering practice. And finally, numerous concepts which merit consideration when determining a solution to a specific problem will be discussed, together with the advantages each offers, the difficulties involved in using it, and the limitations in our knowledge.

## Generation of Wastes

Most slurried wastes are produced by processing an ore and extracting from it the constituents of interest (such as gold, copper, iron, aluminum, phosphate, etc.). To better

understand the nature of the wastes produced, it is helpful to have a basic knowledge of how the ores are processed to remove the minerals of value. Although the extraction process may vary considerably with each individual ore – and even from plant to plant for essentially the same ore – certain steps in the process are fundamental for many ores (Vick, 1990).

*Crushing and Grinding*

At the heart of most milling processes are crushing and grinding the ore, after which various different techniques are used to remove the minerals of interest. Crushing is usually performed in stages to reduce the rock to a size that can be fed into grinding equipment; secondary crushing reduces half-meter size fragments from primary crushing to particles on the order of 1 or 2 mm. Then, grinding primarily by rod mills or ball mills further reduces the size of the particles produced by crushing; since ball mills generally produce smaller particles, they are often used sequentially after rod mills to obtain a particle size gradation on the order of 0.5 mm or less. Grinding is the final operation in the physical reduction of ore, and the final gradation depends on the degree of particle breakdown in the hard rock and the clay content in the ore. For example, copper tailings often consist largely of silicate particles produced by grinding the parent rock, whereas phosphate slimes consist primarily of clay particles from the ore rather than particle breakdown from grinding. Particles produced from hard rock are usually hard and highly angular, while those from shales and similar materials with a high clay content have a hardness and shape compatible with the clay particles in the ore.

*Concentration*

Since the particles produced by grinding will vary in mineral content, the goal of concentration is to separate those particles with high mineral value from those with little or no value. This is usually accomplished by gravity separation, magnetic separation, or froth flotation. Gravity separation is normally performed with water and requires that the mineral and its parent rock have very different specific gravities; the desired particles (either lighter or heavier) are separated and collected, and remaining particles are discharged as tailings. Magnetic separation is used frequently for the extraction of iron particles; the magnetic particles are collected via a belt or drum separator, and the nonmagnetic particles become tailings. Froth flotation is the most widely used concentration method; it is a highly complex physiochemical process in which mineral-bearing particles in a water suspension are made water repellant and receptive to attachment to air bubbles. Particles with higher mineral content then rise to the surface of a froth which is skimmed off, and the remaining particles become tailings. The chemicals used as flotation agents sometimes cause environmental problems with the tailings, such as cyanide used to froth the lead in galena.

*Leaching*

Leaching involves the removal of minerals from the ground particles of an ore by direct contact with a solvent – usually a strong acid or alkaline solution – and often leads

to environmental problems. For example, acid leaching of uranium or copper oxide ores produces a tailings effluent with a pH in the range of 1 to 3, and sodium cyanide with lime as a pH modifier is a common reagent for extraction of gold and silver. Leaching may also change the physical characteristics of the tailings. As one example, the acid leaching of a uranium ore converted the montmorillonite clay minerals in the original ore to predominantly kaolinite in the tailings as the result of a calcium-sodium replacement.

*Heating*

Heating either the slurry suspension or the ground itself is sometimes used to extract minerals. Examples include the extraction of oil from oil sands and the production of phosphoric acid fertilizer from phosphate rock concentrate. The resulting tailings are handled in slurry form.

*Thickening*

The final step in the milling process is to remove some of the water from the tailings-water slurry before it is discharged into the disposal area. This is commonly done with thickeners, which consist of a tank with rotating arms that convey the settled solids to the center of the tank where they are collected and pumped to the disposal area. This thickening process is sometimes accomplished with hydrocyclones or with drum or belt filters, which use vacuum suction to dewater the slurry through a cloth or screen. After the thickened tailings are transported in slurry form and deposited in an impoundment area, the coarser particles settle from suspension and the supernatant water with reagents and colloidal particles is collected, whenever possible, and returned to the mill for reuse as process water. However, the presence of contaminants sometimes precludes recirculation because it would reduce the extraction efficiency. What is left in the disposal area is a high water content soil-like waste material which must be dewatered in some fashion.

**Material Properties of Slurried Wastes**

This section summarizes much of the available data on the engineering properties that govern the post-depositional behavior of slurried wastes. Indices and properties will be compared for a variety of materials over ranges that extend well beyond those normally encountered in conventional geotechnical engineering practice. Virtually all finite-strain theories describing the consolidation and desiccation of these wastes are strongly dependent on the determination of an "initial" or "zero effective stress" void ratio and relationships among the effective stress, void ratio, and hydraulic conductivity. In their excellent paper on the design capacity of slurried waste ponds, Carrier, Bromwell, and Somogyi (1983) presented a comprehensive set of figures and equations that describe these relationships well. In some cases, classical small-strain consolidation theory can be used advantageously, and guidelines for estimating the compression index and coefficient of consolidation are discussed.

*Plasticity*

Figure 1 shows a plasticity chart with approximate ranges for the liquid limit and plasticity index for a wide variety of clays and slurried wastes, as well as several naturally occurring clays and specifically prepared samples of calcium and sodium montmorillonite.  As can be seen, the values for most of these materials plot slightly above the A-line in the zone typically characteristic of highly compressible materials.  In addition to the wastes already discussed, including a variety of dredged materials, this figure contains data from oil sand sludges and China clay tailings.  The oil sand sludge consists primarily of kaolinite clay with some smectite, together with some fine silt and residue bitumen, and the China clay tailings (from the manufacture of fine china) consist of micaceous silt and are generally nonplastic.  The Maumee River dredgings and the FGD sludge tend to be rather silty, and the applicability of the Atterberg tests is questionable, thus suggesting a reason for their position below the A-line.  The red muds, which also plot below the A-line, contain little to no mineral components.  Dredged materials from a given location tend to exhibit little variability, but taken collectively, their range becomes quite large; note in particular, the differences between fresh water and sea water dredged materials.
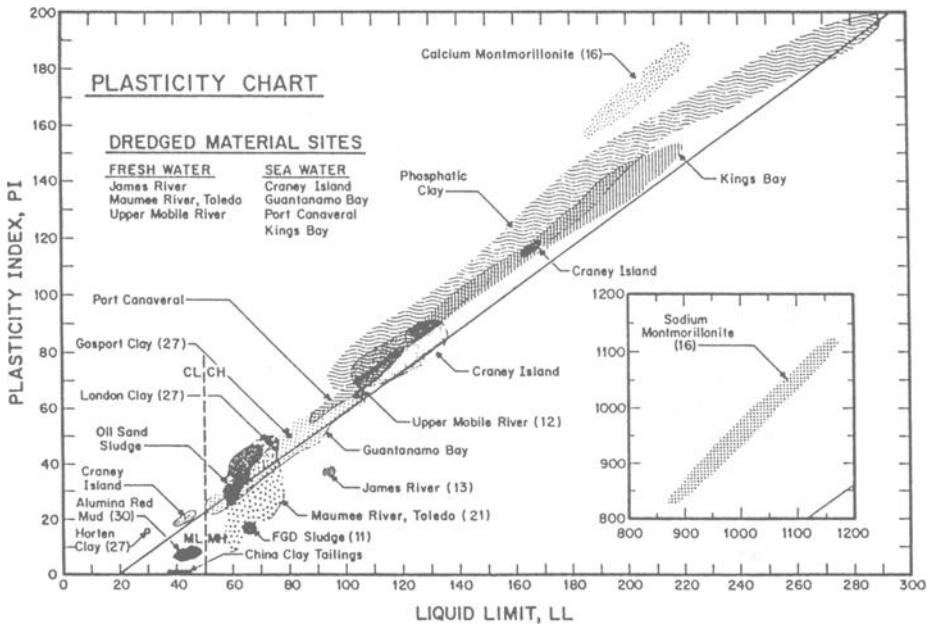


Figure 1- *Atterberg Limits of Fine-Grained Mineral Waste Materials and Clays (after Carrier, Bromwell, and Somogyi, 1983)*

*Initial Void Ratio*

When considering a dilute slurry of suspended particles (the void ratio may be on the order of 50 or 100), the term "void ratio" makes little sense, and a preferred term is "solids content." The term "void ratio" becomes meaningful only when the slurry suspension becomes a "soil" or "soil-like material." This occurs at the end of sedimentation and the onset of self-weight consolidation, or when the particles come into contact with each other and initiate the transfer of effective stress; this value is termed the "initial" or "zero effective stress" void ratio, and it provides the origin for measuring strains in the material of any point during its consolidation history. Although simple to define conceptually, it is difficult in practice to determine when this situation actually occurs, and the selection of an initial void ratio is somewhat arbitrary. The initial void ratio can be determined experimentally by measuring the void ratio of a sample (a) recovered from the surface after sedimentation is considered to be complete or (b) sedimented in a container from a slurry having an initial solids content similar to that in the field. Alternatively, Carrier, Bromwell, and Somogyi (1983) suggest that the water content corresponding to the value of the initial void ratio is about seven times the liquid limit, and pursuant to a study of large-strain consolidation of kaolin slurries, Monte and Krizek (1976) suggest five times the liquid limit. Some typical values for the initial void ratio of a few wastes are about 10-12 for red mud and FGD sludge, 10-20 for freshwater dredgings, and 15-30 for sea water dredgings and phosphate slimes. Although the choice of a value for the initial void ratio may affect the predicted time to complete a given amount of consolidation by weeks or months relative to the total consolidation time of many years, it has little effect on the calculated storage capacity of an impoundment area because the hydraulic conductivity and associated rate of consolidation are very high for high void ratios and decrease quickly as the void ratio decreases.

*Compressibility*

The compressibility of various fine-grain wastes and a few clays for comparison is summarized in Figure 2. These materials span an enormous range in compressibility with void ratios from about 20 to less than 1, and many involve material behavior at much lower effective stresses and much higher void ratios than normally encountered in geotechnical engineering. Some of the available mathematical models can accommodate experimental compressibility data (i.e. observed void ratios at known effective stresses) directly and employ various interpolation schemes to calculate the appropriate compressibility. However, most models require that some form of mathematical relationship be specified. Monte and Krizek (1976) used a power relationship of the form $\overline{\sigma} = M\varepsilon^{N}$, where $\overline{\sigma}$ is the vertical effective stress, $\varepsilon$ is the vertical strain, and $M$ and $N$ are empirical coefficients. According to Carrier, Bromwell, and Somogyi (1983), the compressibility of many wastes can be approximated by $e = A\overline{\sigma}^{B}$ where $e$ is the void ratio, and $A$ and $B$ (which is negative) are empirical coefficients that depend on the particular material and vary over a wide range. For high values of stress, this equation predicts unreasonably low values for the void ratio and is therefore invalid; in this case, the more conventional compression index, $C_c$, tends to govern the compressibility.

From this equation, it follows that the coefficient of compressibility, $a_v$, is given by:

$$a_v = -\frac{de}{d\overline{\sigma}} = -AB\overline{\sigma}^{B-1}$$

where $a_v$ is always positive (since $B$ is always negative) and varies greatly (perhaps three orders of magnitude or more) with effective stress and type of material. The most useful laboratory device for measuring the compressibility of high void ratio sediments is the slurry consolidometer (Sheeran and Krizek, 1971). Although the compressibility of a material is sufficient to predict the final volume, the time rate of volume change requires information on the relationship between the hydraulic conductivity and the void ratio.
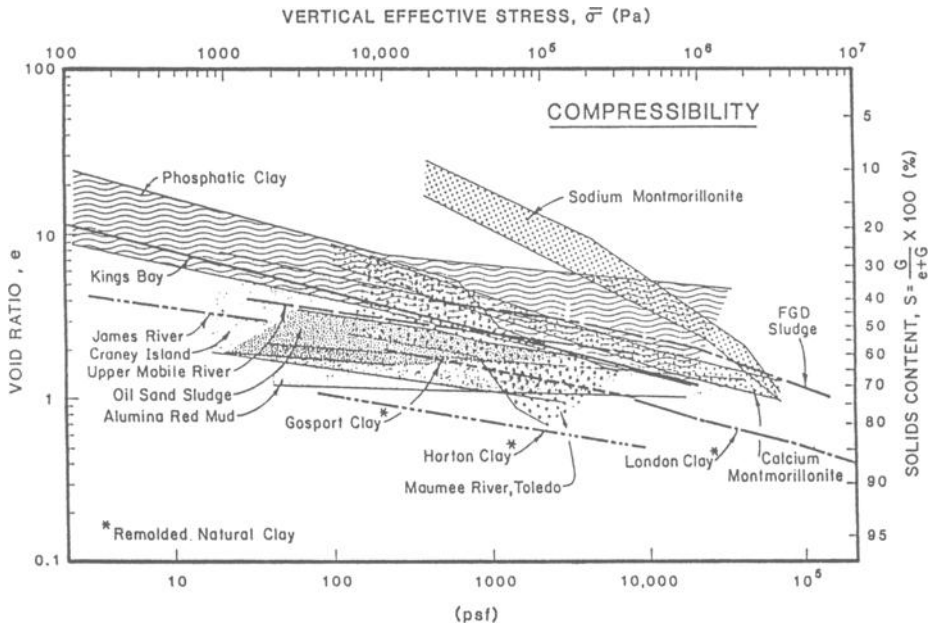


Figure 2 - *Compressibility of Fine-Grained Mineral Waste Materials and Remolded Clays (after Carrier, Bromwell, and Somogyi, 1983)*

*Hydraulic Conductivity*

Except for a few models that either incorporate experimental data or use the coefficient of consolidation, all others require a relationship between the hydraulic conductivity and the void ratio. Of all the components that comprise the problem under consideration, the hydraulic conductivity relationship is arguably the most important and the most difficult to quantify. Hydraulic conductivity values for a wide range of waste materials and two montmorillonite clays are summarized in Figure 3. Note that this graph spans eight orders of magnitude for the hydraulic conductivity from essentially impermeable to approximately the hydraulic conductivity of silt, with the waste materials spanning somewhat more than four orders of magnitude. Among the many empirical relationships used for the hydraulic conductivity are: $k = (1 + e)(S + Te)$ (Monte and

Krizek, 1976); $k = Ce^D$ (Somogyi, 1979); and $k = Ee^F/(1+e)$ (Carrier, Bromwell, and Somogyi, 1983), where e is the void ratio and S, T, C, D, E, and F are empirical constants. If laboratory hydraulic conductivity tests are conducted, sufficiently small gradients must be used to avoid seepage-induced consolidation during the test process.
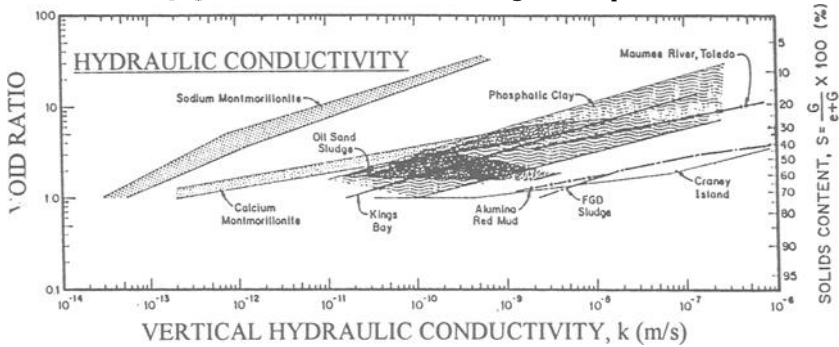


Figure 3 - *Hydraulic Conductivity of Fine-Grained Mineral Waste Materials and Remolded Clays (after Carrier, Bromwell, and Somogyi, 1983)*

Alternatively, Znidarcic (1982) presented a method for estimating the hydraulic conductivity from constant rate of deformation slurry consolidation test results, and Huerta, Kriegsmann, and Krizek (1988) present a means for back-calculating the hydraulic conductivity from the results of seepage-induced consolidation tests. Another point of importance is illustrated in Figure 4, which depicts hydraulic conductivity values determined for fresh water dredgings from the Maumee River by means of two field tests and six different types of laboratory tests; the lesson to be learned is that the entire band of a hundred or so laboratory-determined values provides little insight into the field values determined by pumping tests (one obvious explanation is that the field tests measured primarily the horizontal hydraulic conductivity, whereas the lab tests measured the vertical hydraulic conductivity).
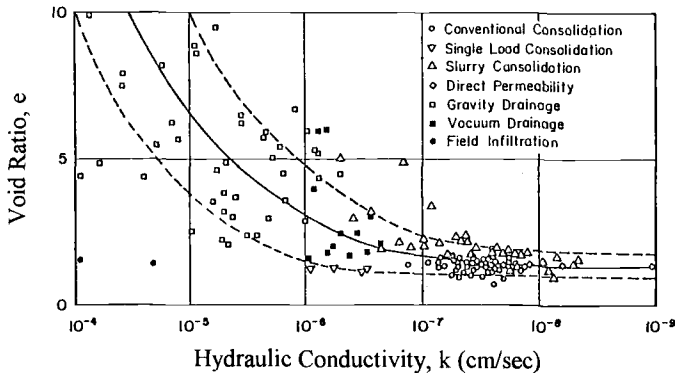


Figure 4 - *Hydraulic conductivity Data for Maumee River Dredged Materials (after Krizek and Salem, 1977)*

*Parameters for Classical Consolidation Theory*

The magnitude and rate of consolidation of some tailings can be predicted reasonably well by use of classical Terzaghi consolidation theory. For these cases the compression index, $C_c$, usually lies in the range from 0.1 to 0.3 (although values from 0.05 to 0.4 have been measured) and the coefficient of consolidation, $c_v$, may vary over several orders of magnitude. While these ranges are similar to those exhibited by many natural clays, the values for tailings usually manifest little consistency in their variation with void ratio, e. Guidelines for the estimation of $c_v$ and $C_c$ values may be obtained from Figure 5 (Vick, 1990) and Figure 6 (Krizek, Parmelee, Kay, and Elnaggar, 1971), respectively. The consolidation relationships in Figure 5 represent a variety of different tailings and convey an appreciation for the variability involved. Although the phosphatic clays show an essentially constant value for $c_v$ with large changes in void ratio, the extremely high void ratios suggest that a finite strain formulation utilizing a relationship of the form $\bar{\sigma} = f(e)$, instead of $c_v$, would be preferable. The compressibility data in Figure 6 were obtained from a variety of inorganic and organic clays and silty soils, and the indicated straight-line regression equation was chosen to best describe those data with an initial void ratio less than two.
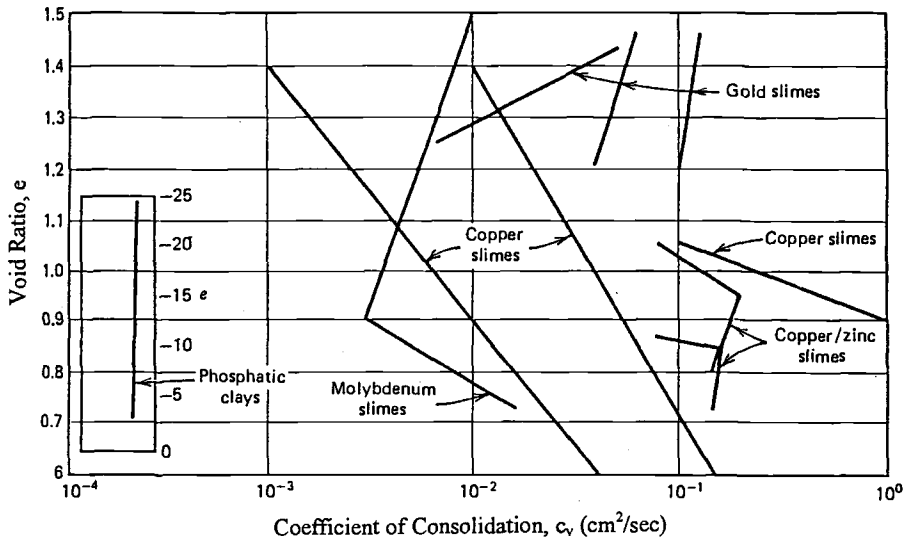


Figure 5 - *Variation in Coefficient of Consolidation with Void Ratio (after Vick, 1990)*
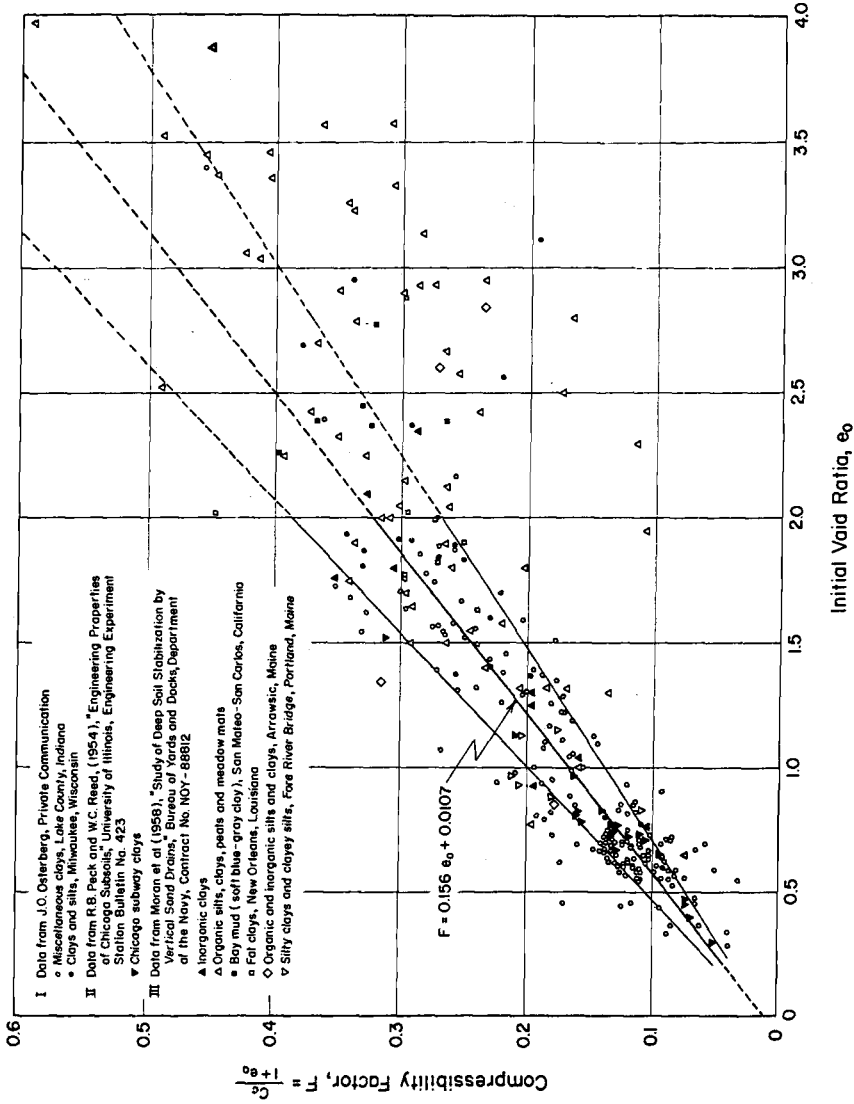
Figure 6 – *Compressibility Factor Versus Initial Void Ratio*
*(after Krizek, Parmelee, Kay, and Elnaggar, 1971)*

## Approaches to Solutions

The following sections identify and discuss briefly many of the concepts that have been used with success and that should be examined carefully when determining a solution for specific disposal problems involving high water content wastes. Only a few of the suggested ideas will usually be applicable in any particular situation, but this decision should not normally be made until each has been considered explicitly.

### Process Modification

When addressing a problem of waste disposal, often not considered in sufficient detail are the modifications that might be made in the process by which the waste is generated. This is especially true for geotechnical engineers because they are usually too quick to accept the wastes in whatever form the chemical or mechanical engineers in charge of the beneficiation process at the plant provide them. Oftentimes, however, a frank discussion by all concerned will reveal that some modification in the waste generation process at the plant will improve considerably the handling and disposal properties of the waste materials generated. For example, cyanide control is a major problem in ore deposits developed for precious metals, and increased emphasis is being placed on pretreatment and destruction of the cyanide prior to discharging the tailings into an impoundment. In some cases, chemicals can be added near the end point in the process to neutralize the waste or enhance sedimentation, vacuum filtration can decrease the water content, or perhaps flyash should not be removed because its presence in the waste can be beneficial (Krizek, Christopher, and Scherer, 1980; Krizek, Chu, and Atmatzidis, 1987).

### Dike Design

The design and construction of the dikes for an impoundment area usually comprises a substantial portion of the cost of the disposal operation. Accordingly, it is always desirable and economical to use the waste material, if possible, to construct the dikes. Although the waste materials are usually not ideal for this purpose, they have been used in many cases, and several excellent references, such as that by Vick (1990), are available to provide guidance. Surface impoundments can normally be categorized as water-retention dams and raised embankments. Water-retention dams are best suited for tailings impoundments with high water storage requirements; they are generally quite similar to conventional water storage structures, as indicated in Figure 7, and are usually constructed to their full height prior to the placement of tailings in the impoundment. Alternatively, raised embankment dams are staged over the life of the impoundment, beginning with a starter dike to contain the tailings for the first few years and then adding additional height on an as-needed basis. This scheme has significant advantages in distributing the costs over the life of the project (this is especially important in a start-up operation) and in providing flexibility in sizing the impoundment and choosing the materials (such as selected wastes from the mining operation itself) to construct subsequent stages. As depicted in Figure 8, the construction of raised embankments may be done by any of three methods: upstream, downstream, and centerline.
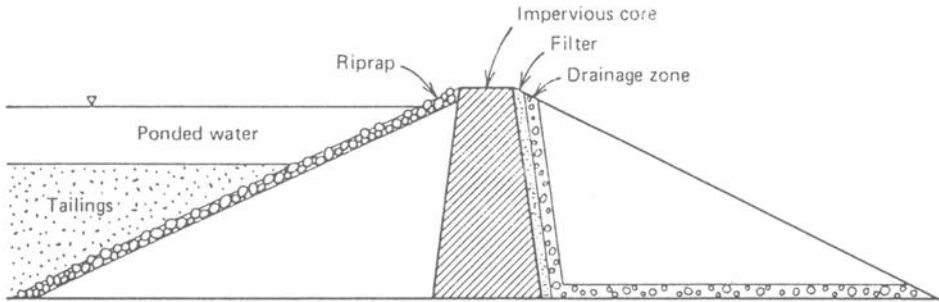
Figure 7 - *Water Retention Type Dam for Tailings Storage*
*(after Vick, 1990)*



(a) Upstream

(b) Downstream

(c) Centerline
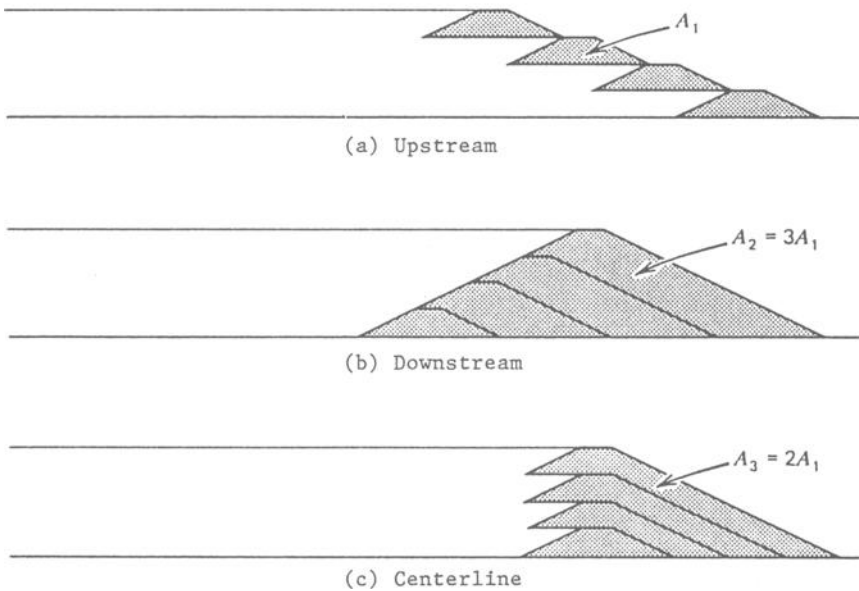
Figure 8 - *Types of Raised Embankment Dams*
*(after Vick, 1990)*

In the upstream method, the tailings are discharged from the crest of the starter dike to form a beach, which becomes the foundation for the second perimeter dike, and so forth. This method requires that the tailings form a reasonably competent foundation for the subsequent dikes, and on the order of 40% to 60% sand is needed in the tailings to achieve this goal; its advantages are cost and simplicity, and its disadvantages are water storage capacity, phreatic surface control, and seismic liquefaction susceptibility. The

downstream method begins with a starter dike and constructs subsequent raises by placing fill on the downstream slope of the previous raise. As such, impervious cores and internal drains can be easily incorporated to control the phreatic surface and allow the storage of large volumes of water. Control over the phreatic surface, together with better control over the construction process, renders the resulting dike more seismic resistant. The major disadvantages are the significantly larger volume of fill needed and the fact that the starter dike must be located to allow room for anticipated expansion. The centerline method is basically a compromise between the foregoing two methods, and as a result, it shares in their advantages and disadvantages. Of considerable importance, however, is that a dike constructed by the centerline method cannot be used for the permanent storage of large depths of water.

*Liner Design*

Liners are inherently high cost and are usually used only in situations involving high toxicity wastes and stringent groundwater protection requirements. Figure 9 shows the chemistry of some effluents for which liners might be considered to prevent contamination of the groundwater. Typical liners consist of clay or various geosynthetic membranes, but some wastes have a sufficiently low hydraulic conductivity to possibly serve as a liner material, thereby enhancing the economics of the disposal process. For use as a liner, the waste must have about 40% or 50% passing the No. 200 sieve, and cycloning must usually be used to separate this fraction from the overall tailings. In other cases the waste must be placed and compacted at or near optimum water content to serve effectively, and this usually precludes their use because it is difficult to adequately dewater them. In addition, some waste materials placed in such a condition are brittle, and the liner might crack and become ineffective with differential settlements.
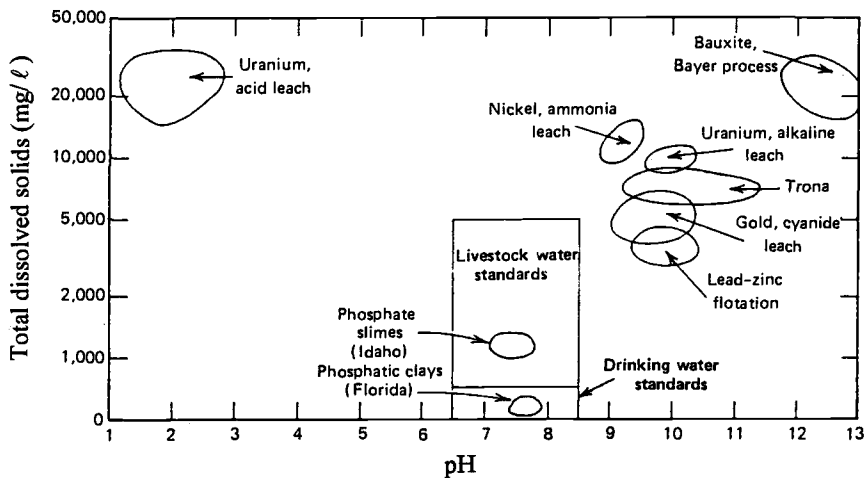


Figure 9 - *Chemistry of Some Typical Tailings Effluents*
*(after Vick, 1990)*

*Drainage Blanket*

Since the rate of dewatering is strongly dependent on the length of the drainage path for the escape of water, it may be highly advantageous in some special cases to install a drainage blanket and associated dewatering system at the bottom of an impoundment area prior to placing any wastes.  Many wastes contain significant quantities of sand which can be separated and used to construct such a drainage blanket. For the past two decades or so, a wide variety of geosynthetic materials (albeit rather expensive) has been available to serve as an underdrain system for an impoundment area, but little can be done to install geosynthetic drains after an area is partially filled, because the materials are too soft to traverse.  A partial vacuum in this drainage blanket would enhance the dewatering process considerably, especially during the early stages.

*Sedimentation*

When a low solids content waste is pumped into an impoundment area, the first physical process that occurs is sedimentation – presumably in conformance with Stoke's law or some modification thereof.  Accordingly, the particle size distribution of the solids in the suspension controls the rate of sedimentation.  In a conventional hydrometer test, a dispersing agent is usually added to the suspension to prevent flocculation.  However, such tests do not yield the proper particle size distribution for use in predicting the rate of sedimentation in the field because a dispersing agent is not normally added to the slurry. Alternatively, a flocculating agent may be added to the waste slurry at some point in the generation and disposal process to enhance flocculation, accelerate the settling rate, and clarify the effluent.

*Retention Time*

Very often the supernatant water from the sedimentation in an impoundment area flows over a weir into a water course or is collected via a drain system for reuse as process water.  The degree of clarity that is achieved in the supernatant water depends on the time available for the particles to settle from suspension, and the disposal area must be designed to provide a retention time commensurate with the water clarity desired. Sometimes this is handled by a successive series of ponds with each clarifying further the discharge from the preceding pond.  Too short retention times for an impoundment area will result in too many solids, as well as pollutants adhering to the solids, in the discharged supernatant water.  Guidelines for the design of impoundment facilities as solid-liquid separation systems have been presented by Krizek, Fitzpatrick, and Atmatzidis (1976).

*Filters to Maintain Water Quality*

Sometimes the discharged supernatant waters are passed through a filter to achieve further clarification.  In some situations large portions of the surrounding dikes can be designed as filter elements to enable the discharge of large quantities of

supernatant waters while maintaining the water quality.   For lower flows filter "cartridges" may be installed at the overflow weirs to accomplish this purpose, but they would have to be exchanged periodically to avoid excessive clogging and decreased flow. Krizek, Fitzpatrick, and Atmatzidis (1976) have developed criteria for designing such filter systems.

*Consolidation*

Although analytical models comprise the heart of most predictive techniques for the rate of settlement, the physical process to be simulated is often not adequately understood, and the complexity of the governing natural phenomena usually dictates the incorporation of several simplifying assumptions to achieve mathematical tractability. The major assumptions in conventional consolidation theory (namely, small strains, constant material properties, and no self-weight) are generally recognized as excessively restrictive for analyzing the large volume changes observed in slurried waste materials. The two most popular approaches to circumvent this restriction utilize either "incremental small strain" or "finite strain" formulations (Been and Sills, 1981; Schiffman, Pane and Gibson, 1984; Krizek and Somogyi, 1984; Toorman, 1996).

*Incremental Small Strain Models* - Incremental small strain models maintain the simplicity of the classical Terzaghi-type formulation and constitute a logical next step to extend its applicability.  The solution usually involves dividing a deposit into a series of layers, each with different material properties, and satisfying continuity at the interfaces between layers.   These models can handle nonuniform material properties (whether caused by dissimilar materials, self-weight, or other temporal or spatial variations in effective stress), but the need to continuously update both the material properties and the positions of the layers makes the solution computationally laborious.

*Finite Strain Models* - Finite strain formulations are usually based on the pioneering work of Gibson, England, and Hussey (1967) and result in nonlinear second-order partial differential equations.   Self-weight and material nonlinearities can be directly incorporated into the equations, which are usually developed in terms of material, rather than spatial, coordinates.   This formulation has significant mathematical advantages because it transforms a boundary value problem with a moving boundary whose location is unknown into one with a fixed known boundary (no filling) or one in which the boundary location is always known (during filling or accretion).

*Mathematical Techniques* – In the finite strain models, the equation describing the consolidation process is cast in terms of either void ratio or pore pressure.  The void ratio based models assume that both effective stress and hydraulic conductivity can be described as functions of void ratio, whereas the pore pressure based models assume that the void ratio depends on the effective stress and the hydraulic conductivity depends on the void ratio.   Explicit numerical techniques advance the solution from known (previously computed) values of the dependent variable and corresponding material properties, but stability and convergence criteria are often unattainable for nonlinear equations and can only be deduced after appropriate linearization of the equation.  On the other hand, implicit numerical techniques are computationally more efficient and unconditionally stable for linear equations, but criteria for their stability and convergence may be equally difficult to prove for highly nonlinear problems; in addition, a major

limitation for nonlinear problems is that the equations require material properties corresponding to unknown values of the dependent variable (i.e. at the "new" time step), so these must be either estimated or allowed to lag one time increment behind the solution.

*Validation* - To be accepted and used extensively, any theory must be validated in some way, and geotechnical centrifuge testing has provided one way to accomplish this objective with consolidation theories. Schiffman, Pane, and Gibson (1984) illustrate the comparative analytical ability of conventional consolidation theory and finite strain theory to describe the results from a series of tests on a remolded Georgia kaolin with $e_o = 2.86$ and $w_o = 110\%$ (2.5 times the liquid limit). This good agreement, together with similar results for tests on phosphate slimes at $e_o = 15$ (Scully, Schiffman, Olsen, and Ko, 1984) and other materials suggest that the results predicted from nonlinear finite strain consolidation theory are in good agreement with those measured in centrifuge tests. However, neither necessarily proves that field response will be accurately predicted by these techniques.

*Seepage-Induced Consolidation* - Because the changes in void ratio and hydraulic conductivity with effective stress are very large in the early stages of consolidation, the effect of seepage-induced consolidation can be important. In particular, seepage-induced consolidation makes it difficult, if not impossible, to measure the material properties in this region of low effective stresses, because the very process of applying a hydraulic gradient to measure hydraulic conductivity results in a varying effective stress and a resulting nonuniform void ratio in the direction of the gradient. To address this problem, several seepage-induced finite strain consolidation models have been developed recently (Imai, 1979; Huerta, Kriegsmann, and Krizek, 1988; Abu-Hehleh, Znidarcic, and Barnes, 1996; Fox and Baxter, 1997). Ideally, such a model can employ known or assumed material property relationships to determine the final thickness of a sedimented slurry subjected to a constant piezometric head, or alternatively the inverse solution can use the final settlement, steady-state flow data, and void ratio of the solids at the bottom of the laboratory sample or field layer to deduce hydraulic conductivity and compressibility relationships. One point of interest is that the hydraulic conductivity influences both the required time to reach a steady-state condition and the steady-state itself (i.e. the final height of the consolidated deposit depends on the variation of the hydraulic conductivity with the void ratio).

*Deviations from Primary Consolidation* – "Secondary" consolidation may be regarded as simply that portion of the settlement response that is not described by some appropriate theory of "primary" consolidation, and the deviation from the typically straight-line relationship between the volume change and the logarithm of time may be termed "tertiary" consolidation; however there is no implication that settlements due to secondary or tertiary consolidation are of negligible magnitude. Within the context of this definition, there would be no secondary or tertiary consolidation if a sufficiently comprehensive primary consolidation theory were available. Notwithstanding this idealized concept, the unavailability of the requisite comprehensive theory dictates that consolidation data be interpreted in accordance with the traditional concepts of primary and secondary consolidation, with any deviations from secondary being termed tertiary. Figure 10 (typical for eight specimens loaded for more than 200 days) shows clearly that fresh water dredged materials (Salem and Krizek, 1975) exhibit significant "tertiary"

consolidation. It can be seen in Figure 10 that a so-called "standard" primary-secondary response curve was measured for about a week, after which the slope of the e-log t curve increased substantially for about two months and then began to decrease. This behavior pattern was observed for both slurry and conventional consolidation tests. Similar response curves were discussed by Lo (1961).
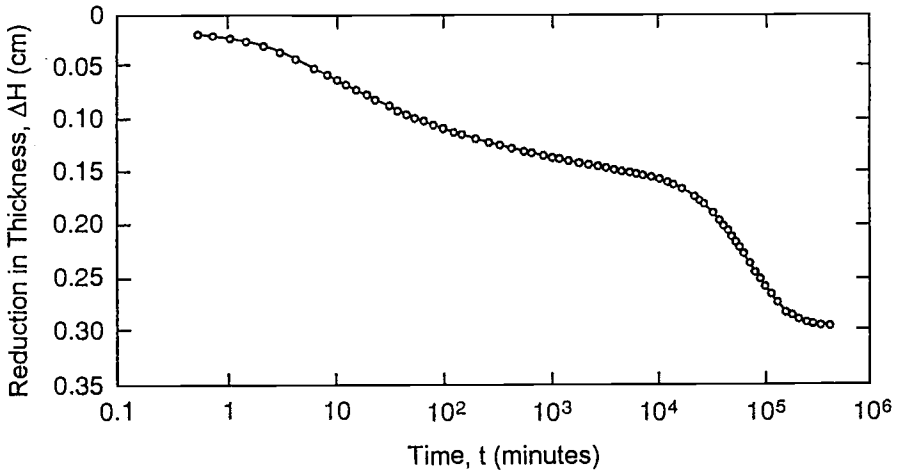


Figure 10 - *Consolidation Behavior of Fresh Water Dredged Material (after Salem and Krizek, 1975)*

*Thickened Discharge*

The thickened discharge method of tailings disposal originated from a concept advanced by Shields (1974) and developed by Robinsky (1979). The objective is to thicken the tailings-water mixture such that it behaves more like a viscous mud than a liquid slurry. Under such a condition the discharged material will form a conical pile with side slopes of a few percent, as illustrated in Figure 11, thereby allowing any free water to readily flow to the toe of the slope where it is collected and removed. Advantages of this method are the elimination (or significant reduction) of impoundment dams, reduction in pumping return water, reduction of seepage (because there is no decant pond), virtual elimination of embankment failure under static loading conditions, and simplification of the reclamation process. The cost savings realized by eliminating the impoundment dams may be largely offset by the higher costs for thickener construction and operation and the greater expenses associated with pumping. In many cases more surface area may be disturbed than for conventional impoundments, resulting in larger areas to be reclaimed. If not collected and diverted around the pile, runoff at the top of the slope may cause erosion and the transport of tailings. In addition, a dynamic excitation may cause a liquefaction flow slide in the lower (saturated) portions of the pile. Both liquefaction and runoff-handling problems become more severe if the thickened tailings are deposited on top of a conventional impoundment to augment its capacity.

This method of disposal is best suited for materials containing a reasonable sand fraction without a major proportion of clayey fines in relatively flat topography at sites close to the plant ( to minimize pumping costs) in areas of low seismicity.
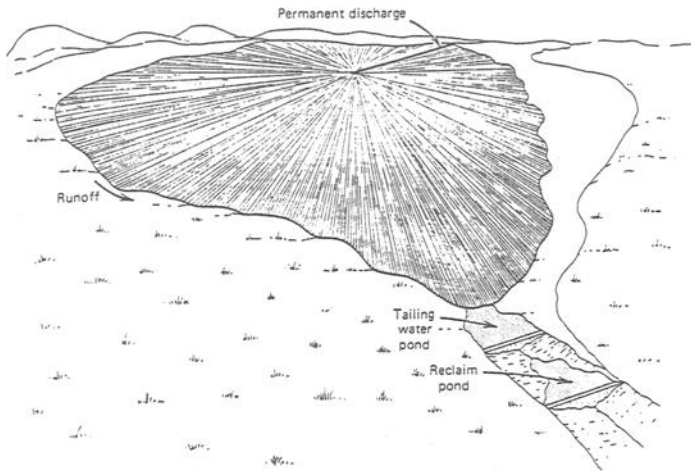


Figure 11 - *Thickened Discharge Disposal Method*
*(after Robinsky, 1979)*

*Dry Stacking*

Dry stacking is a modified version of the thickened discharge method described above and is suitable in areas where the evaporation rate is high. In one scenario a dike encircles the impoundment area, and a pipeline with discharge ports every few hundred feet rests on the dike. Disposal begins by opening one of the discharge ports and allowing the thickened slurry to form a "tongue" extending at a slight slope from the dike toward the center of the impoundment area. After the slurry "tongue" reaches a depth of perhaps one meter near the dike and extends a hundred meters or so toward the center of the area, the discharge port is closed, an adjacent discharge port is opened, and the process is repeated. This process continues for perhaps 30 or 40 discharge ports, each for a day or two, around the pipeline. By the time one cycle is completed, the "first tongue" of material deposited should ideally have desiccated to a rather low water content, at which time a "new tongue" of material is placed over the first, and so forth. The major limitation of this method is that the climate of the region must be such that each layer will dry sufficiently in the time available before an overlying layer is placed (Palmer and Krizek, 1987).

*Dry Disposal via Vacuum Filtration*

In an even more extreme case of reducing the water content of the waste at the plant, the dry disposal method endeavors to remove much of the water from the waste material before it is placed in an impoundment area. This is usually accomplished by vacuum filtration using a drum or belt, and the tailings come off the drum or belt as a relatively easily handled "dry cake." However, there is considerable controversy over the feasibility, advantages, and economics of vacuum filtration. The nature of the material will affect substantially the efficiency of the process, and it may not work at all for some materials with a high clay content. Since both capital and operating costs for vacuum filtration are very high, the method can usually be justified only when the filtration is an integral step in the ore processing operation, but not when it is a supplemental dewatering method added to conventional thickeners. If dewatered in this fashion, the tailings can usually be placed and compacted in a disposal area in essentially solid form, and reclamation can proceed concurrently. Although the tailings are in "solid" form when handled and placed, their water content is often around 20% to 30%, which will result in near saturation for some materials when placed at typical void ratios. Accordingly, the seepage from the saturated tailings may still be significant in the absence of liners or underlying natural materials of low hydraulic conductivity.

*Evaporation and Crust Formation*

The loss of water from the surface of a tailings pond is a two-stage process. In the first stage the conductivity of water is sufficiently large that water loss is controlled by the prevailing climatic conditions (radiation, air temperature, wind speed, humidity, etc.), and results are comparable to those measured in pan evaporation tests. This stage has been found (Brown and Thompson, 1977) to govern the response until the water content reaches a value slightly below the liquid limit. During the second stage, the converse is true, and evaporation losses are essentially independent of the environment. However, the presence of a water table near the surface may provide a sufficiently large supply of water to continuously rewet the surface and preclude the evaporative process from entering the second stage. In any case, when the overlying free water is decanted, evaporates, or drains through the layer into the underlying soil, the surface begins to desiccate and a crust is formed. The formation of a crust has both advantages and disadvantages. One of the advantages is that it provides, in some cases, a layer with adequate strength to support workers and equipment. A second advantage is an increase in the dry density with a resulting settlement of the surface and increase in the storage capacity of the impoundment. A major disadvantage of a crust is that it greatly inhibits subsequent evaporation because the partially saturated surface layer has a drastically reduced hydraulic conductivity. Nature often provides the first solution to this problem by the development of "alligator" cracking as shrinkage occurs in the desiccating crust; this provides drainage channels for the horizontal movement of water and additional surface area for evaporation. When attempting to analyze the volume change of a partially saturated medium, a dichotomy is encountered. Geotechnical engineers usually assume 100% saturation and a deforming medium, whereas soil scientists usually assume that flow takes place in a partially saturated medium with a rigid structure (no volume

change). This physical process of desiccation and crust formation was incorporated as an integral part of a mathematical model developed by Casteleiro, Krizek, and Edil (1981); solutions obtained from this model are able to (a) describe the water content distribution in the fill at any time after deposition, (b) predict the desiccation and consolidation behavior as a function of time, and (c) aid in evaluating different techniques for accelerating the dewatering process. An improved desiccation theory by Abu-Hejleh and Znidarcic (1995) includes, in addition to one-dimensional consolidation, desiccation under one-dimensional shrinkage, propagation of vertical cracks and tensile stress release, and desiccation under three-dimensional shrinkage. It has been found that slow evaporation rates form a thicker crust with more widely spaced cracks. In addition to evaporation, transpiration has an important effect on the dewatering process during the early stages of desiccation, but this effect tends to disappear as the water table approaches an equilibrium position.

*Agitation*

To overcome the impedance of a crust to the evaporation process and consequent dewatering of the wastes, various techniques have been utilized to agitate or break up the crust (Haliburton, 1977). Since it is usually difficult, if not impossible, for equipment with any substantial weight to traverse the soft sediments, disc-like or plow-like tools are often pulled across the surface by cables operated from the tops of the impoundment dams. However, even under the best of circumstances, this process enhances desiccation for only a few feet of depth and its cost-benefit relationship must be evaluated carefully. Another limitation is that the climate must have a favorable evaporation rate.

*Vegetation*

For some types of materials conducive to the growth of vegetation, near surface dewatering can be accomplished by transpiration through the leaves and associated root systems of appropriate vegetation. Plants transpire large quantities of water during the growing season; the rate of water loss may exceed that of free water evaporation and continue long after the surface has become dry. In favorable climates and for wastes with favorable composition (texture, fertility, and toxicity), the colonization of the site by volunteer vegetation or selected vegetation may occur by natural processes in a short period of time. However, if the waste is acidic or highly saline or contains high concentrations of heavy metals, the establishment of vegetation may be a lengthy, difficult, and costly process – and ultimately not justify the effort involved. As with agitation of the crust, dewatering by vegetation is limited in the depth of its influence (and evapotranspiration effects are much more complex to model than evaporation alone). However, vegetation can assimilate minerals and various organic toxic compounds, and much of this material can be removed by timely harvest. In the reclamation operation, those wastes incapable of sustaining vegetation must be covered with a layer of topsoil that is conducive to fostering vegetation (Vick, 1990).

*Surcharging*

Surcharging offers a time-tested procedure for accelerating the consolidation and dewatering process and increasing the rate of strength gain, but the low shear strength of many high water content waste materials usually makes it difficult to apply the surcharge without causing a stability failure and consequent mud wave. The use of geosynthetics can help considerably in preventing a mud wave, but extreme care must still be exercised in adding the surcharge slowly. The cost of the geosynthetic materials, the expense in applying and removing the surcharge, and the long times involved in the process preclude the use of this procedure except for special situations. The use of wicks to accelerate drainage can reduce substantially the time required, but there is usually a problem for the equipment to access the site; often a few feet of surcharge is necessary to form a "pad" on which the equipment can operate. If a drainage blanket or system of geosynthetic drains is installed at the bottom of the impoundment area, the dewatering process can be accelerated by applying a partial vacuum to the system which enables advantage to be taken of atmospheric pressure as a surcharge load. While generally functional in principle, cost often limits the use of this method.

*Spraying and Sandwiching*

Spraying involves using a floating pipeline equipped with spray nozzles to sprinkle sand tailings over the surface of the soft tailings (perhaps 10% to 15% solids). The sand slowly sinks through the tailings to form vertical channels (sand drains), which together with the added overburden, serve to relieve pore pressures and accelerate dewatering; the result is a drier and stronger upper layer to support additional thicknesses of sand. This operation can be alternated with layers of tailings to form a sand-tailings sandwich effect (Bromwell and Oxford, 1977).

*Electro-osmosis*

Many studies have been done to investigate the effectiveness and feasibility of electro-osmosis as a means of dewatering high water content materials. The first limitation is the relatively narrow range of materials (primarily silts) over which it is effective, and the second limitation is that, except for certain very special situations, the power consumption and associated cost are prohibitive. Even for one study where windmills were used to generate the electricity at a remote location, the use of electro-osmosis was not judged to be feasible.

*Storage Capacity*

The storage capacity of a given impoundment area depends to a large extent on the final dry density of the tailings placed within it; however, since it may require years to achieve the final dry density, a knowledge of the increase in dry density with time will aid in sizing the disposal area. Typical in-place dry densities of various tailings shortly after disposal range from 15 to 20 pcf (2.4 to 3.1 $kN/m^3$) for phosphate slimes and red mud to more than 100 pcf (15.7 $kN/m^3$) for taconite and copper tailings. One well

documented case history (Krizek and Salem, 1977) for the time rate of increase in dry density for fresh water dredgings placed in slurry form in four different impoundment areas over eight years and subjected to self-weight consolidation and desiccation (including evapotranspiration) is shown in Figure 12. The indicated increase of 4% per year in dry density is, of course, site and material specific and obviously cannot continue *ad infinitum*; however, the trend seems clear and well defined for at least 8 to 10 years.
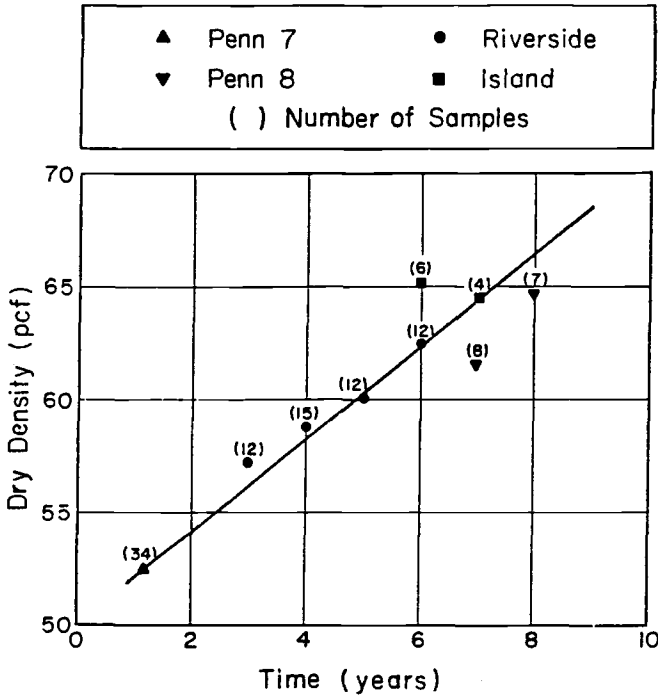


Figure 12 - *Increase in Dry Density as a Function of Time (after Krizek and Salem, 1977)*

*Reclamation*

Current environmental regulations dictate that virtually all disposal sites must be reclaimed. While most of the preceding discussion has dealt with aspects of the disposal process during the period when the wastes were being deposited, closure is not possible until the materials deposited are considered to be permanently stable and environmentally innocuous. Toward this end there are many cases where more effort has been expended on remedial groundwater and toxicological studies for abandoned deposits than was ever allotted in the original design and operation of the site; similarly, there are cases where the costs for permanent stabilization of abandoned tailings are orders of magnitude greater than the value of all the ore produced. However, because of the land areas disturbed and the varying (and sometimes unknown) toxicities of the wastes involved,

tailings impoundments usually provide the focal point for public opposition to mining projects. Since there have been few serious efforts at reclamation to date, there is little experience by which to judge the long-term success of such endeavors. Measures of success must be judged by the degree to which the following fundamental objectives are satisfied (Krizek and Atmatzidis, 1978; Vick, 1990):

- Long-term mass stability of the impoundment
- Long-term erosion stability
- Long-term prevention of environmental contamination
- Eventual return of the disturbed area to productive use

Typical costs to accomplish reclamation may range from $1000 to $5000 per acre, and government authorities commonly require the posting of a reclamation bond at the outset to ensure that appropriate reclamation efforts are carried out after termination of the disposal operation. While "productive use" is a generally accepted goal, the term means "different things to different people," and the specific definition influences considerably the manner in which the area is reclaimed. Generally, "productive use" is defined in the context of land use patterns that existed prior to the establishment of the disposal area.

## Summary

High water content wastes produced by a wide variety of mining and beneficiation processes are usually discharged hydraulically in to a diked impoundment area. Predicting the time-dependent large-deformation behavior of these sedimented high water content tailings subjected to self-weight consolidation and dessication is an extremely challenging problem that encompasses new developments in mathematical modelling, laboratory testing and associated interpretations, material property formulations, and engineering judgment. Standard analyses are elusive, and experience dictates a cautious approach to empirical extrapolations. Despite the sophistication that might be incorporated into a given model or the apparent preciseness of its formulation, it is likely that inadequate material property relationships and improper boundary conditions will prevent an accurate prediction of the field response. However, even a correct prediction does not necessarily validate the model or its input, because the complexity of the many factors involved allows the "right" overall behavior to be obtained by using a fortuitous combination of erroneous material properties, boundary conditions, and mathematical formulation. Because the analytical capability of many models exceeds our ability to specify correct boundary conditions and material properties, constantly improving computer technology is fostering a situation wherein we are undertaking "million-dollar solutions" to problems based on "a dollar's worth of data." Determining a solution to some particular problem will involve consideration of a broad range of alternatives and the decision must include a generous portion of engineering judgment.

## References

Abu-Hejleh, A. N. and Znidarcic, D., 1995, "Desiccation Theory for Soft Cohesive Soils," *Journal of Geotechnical Engineering*, ASCE, Vol. 121, No. 6, pp. 493-502.

Abu-Hejleh, A. N., Znidarcic, D., and Barnes, B. L., 1996, "Consolidation Characteristics of Phosphatic Clays," *Journal of Geotechnical Engineering*, ASCE, Vol. 122, No. 4, pp. 295-301.

Been, K. and Sills, G. C., 1981, "Self-Weight Consolidation of Soft Soils:    An Experimental and Theoretical Study," *Geotechnique*, Vol. 31, pp. 519-535.

Bromwell, L. G. and Oxford, T. P., 1977, "Waste Clay Dewatering and Disposal," *Proceedings of the ASCE Specialty Conference on Geotechnical Practice for Disposal of Solid Waste Materials*, Ann Arbor, MI, pp. 541-558.

Brown, K. W. and Thompson, L. J., 1977, "Feasibility Study of General Crust Management as a Technique for Increasing Capacity of Dredged Material Containment Areas, Technical Report D-77-17, U. S. Army Engineer Waterways Experiment Station, Vicksburg, MS.

Carrier, W. D., Bromwell, L. G., and Somogyi, F., 1983, "Design Capacity of Slurried Mineral Waste Ponds," *Journal of the Geotechnical Engineering Division*, ASCE, Vol. 109, No. GT5, pp. 699-716.

Casteleiro, M., Krizek, R. J., and Edil, T. B., 1981, "Mathematical Model for One-Dimensional Desiccation and Consolidation of Sedimented Soils," *International Journal for Numerical and Analytical Methods in Geomechanics*, Vol. 5, pp. 195-215.

Fox, P. J. and Baxter, C. P. D., 1997, "Consolidation Properties of Soil Slurries from the Hydraulic Consolidation Test," *Journal of the Geotechnical and Geoenvironmental Engineering*, ASCE, Vol. 123, No. 8, pp. 770-776.

Gibson, R. E., England, G. L., and Hussey, M. J., 1967, "The Theory of One-Dimensional Consolidation of Saturated Clays, I,. Finite Non-Linear Consolidation of Thin Homogeneous Layers," *Geotechnique*, Vol. 17, pp. 261-273.

Haliburton, T. A., 1977, "Development of Alternatives for Dewatering Dredged Material," *Proceedings of the ASCE Specialty Conference on Geotechnical Practice for Disposal of Solid Waste Materials*, Ann Arbor, MI, pp. 615-631.

Huerta, A., Kriegsmann, G. A., and Krizek, R. J., 1988, "Permeability and Compressibility of Slurries from Seepage-Induced Consolidation," *Journal of Geotechnical Engineering*, ASCE, Vol. 114, No. 5, pp. 614-627.

Imai, G., 1979, "Development of a New Consolidation Test Procedure Using Seepage Force," *Soils and Foundations*, Tokyo, Japan, Vol. 19, No. 3, pp. 45-60.

Krizek, R. J. and Atmatzidis, D. K., 1978, "Disposition of Dredged Material," Chapter 35 in *Reclamation of Drastically Disturbed Lands*, F. W. Schaller and P. Sutton, eds., American Society of Agronomy, pp. 629-644.

Krizek, R. J., Christopher, B. R., and Scherer, S.D., 1980, "Stabilization of Double Alkali Scrubber Sludges," *Journal of Civil Engineering Design*, Vol. 2, No. 3, pp. 279-304.

Krizek, R. J., Chu, S. C., and Atmatzidis, D. K., 1987, "Geotechnical Properties and Landfill Disposal of FGD Sludge," *Proceedings of the ASCE Specialty Conference on Geotechnical Practice for Waste Disposal*, Ann Arbor, MI, pp. 625-639.

Krizek, R. J., Fitzpatrick, J. A., and Atmatzidis, D. K., 1976, "Investigation of Effluent Filtering Systems for Dredged Material Confinement Facilities," Contract Report D-76-8, U. S. Army Engineer Waterways Experiment Station, Vicksburg, MS.

Krizek, R. J., Parmelee, R. A., Kay, J. N., and Elnaggar, H. A., 1971, Structural Analysis and Design of Pipe Culverts, National Cooperative Highway Research Program, Report 116, National Research Council, Washington, D. C.

Krizek, R. J. and Salem, A. M., 1977, "Field Performance of a Dredgings Disposal Area," *Proceedings of the ASCE Specialty Conference on Geotechnical Practice for Disposal of Solid Waste Materials*, Ann Arbor, MI, pp. 358-383.

Krizek, R. J. and Somogyi, F., 1984, "Perspectives on Modelling Consolidation of Dredged Materials," *Proceedings of the Symposium on Sedimentation-Consolidation Models: Prediction and Validation*, R. N. Yong and F. C. Townsend, Eds., ASCE, pp. 296-332.

Lo, K. Y., 1961, "Secondary Compression of Clays," *Journal of the Soil Mechanics and Foundations Division*, ASCE, Vol. 87, No. SM4, pp. 61-87.

Monte, J. L. and Krizek, R. J., 1976, "One Dimensional Mathematical Model for Large-Strain Consolidation," *Geotechnique*, Vol. 26, No. 3, pp. 495-510.

Palmer, B. and Krizek, R. J., 1987, "Thickened Slurry Disposal Method for Process Tailings," *Proceedings of the ASCE Specialty Conference on Geotechnical Practice for Waste Disposal*, Ann Arbor, MI, pp. 728-743

Robinsky, E., 1979, "Tailings Disposal by the Thickened Discharge Method for Improved Economy and Environmental Control," *Proceedings of the Second International Tailing Symposium*, G. Argall, Ed., Miller Freeman, San Francisco, CA, pp. 75-95.

Salem, A.M. and Krizek, R. J., 1975, "Secondary Compression of Maintenance Dredgings," *Proceedings of the Fifth Panamerican Conference on Soil Mechanics and Foundation Engineering*, Buenos Aires, Argentina.

Schiffman, R. L., Pane, V., and Gibson, R. E., 1984, "The Theory of One-Dimensional Consolidation of Clays, IX. An Overview of Nonlinear Finite Strain Sedimentation and Consolidation," *Proceedings of the Symposium on Sedimentation-Consolidation Models: Prediction and Validation*, R. N. Yong and F. C. Townsend, Eds., ASCE, New York, N.Y., pp. 296-332.

Scully, R. W., Schiffman, R. L., Olsen, H. W., and Ko, H-Y., 1984, "Validation of Consolidation Properties of Phosphatic Clay at Very High Void Ratios," *Proceedings of the Symposium on Sedimentation/Consolidation Models: Predictions and Validation*, R. N. Yong and F. C. Townsend, Eds., ASCE, pp. 158-181.

Sheeran, D. E. and Krizek, R. J., 1971, "Preparation of Homogeneous Soil Samples by Slurry Consolidation," *Journal of Materials*, American Society for Testing and Materials, Vol. 6, No. 2, pp. 356-373.

Shields, D., 1974, "Innovations in Tailings Disposal," *Proceedings of the First Symposium on Mine and Preparation Plant Refuse Disposal*, National Coal Association, pp. 86-90.

Somogyi, F. 1979, "Analysis and Prediction of Phosphatic Clay Consolidation: Implementation Package," Technical Report, Florida Phosphatic Clay Research Project, Lakeland, FL.

Taylor, M. J. and D'Appolonia, E., 1977, "Integrated Solutions to Tailings Disposal," *Proceedings of the ASCE Specialty Conference on Geotechnical Practice for Disposal of Solid Waste Materials*, Ann Arbor, MI, pp. 301-326.

Toorman, E. A., 1996, "Sedimentation and Self-Weight Consolidation: General Unifying Theory," *Geotechnique*, London, England, Vol. 46, No. 1, pp. 103-113.

Vick, S. G., 1990, "Planning, Design, and Analysis of Tailings Dams," BiTech Publishers, Ltd., Vancouver, B.C. Canada.

Znidarcic, D., 1982, *Laboratory Determination of Consolidation Properties of Cohesive Soil*, Doctoral Dissertation, University of Colorado, Boulder, CO.

Patrick J. Fox[1]

## CS4: A Large Strain Consolidation Model for Accreting Soil Layers

**Abstract:** This paper presents a piecewise-linear model, called CS4, for one-dimensional consolidation of an accreting soil layer. CS4 was developed using a fixed Eulerian coordinate system and general constitutive relationships defined by discrete data points. The model includes the effects of vertical strain, self-weight, and decreasing compressibility and hydraulic conductivity during the consolidation process. In addition, the rate of accretion and the initial void ratio of the accreting material can vary with time. The model is dimensionless such that solutions are independent of the final Lagrangian height of the layer and the absolute magnitude of the hydraulic conductivity of the material. Solutions obtained using CS4 for an example problem are essentially identical to available solutions based on material coordinates. Using CS4, dimensionless solution charts were prepared for the time required to fill a disposal pond in which material is accreting at a constant rate. The charts require only hand calculations and may be suitable for preliminary design purposes.

**Keywords:** consolidation, settlement, large strain, accreting soil layers, numerical modeling, solution chart

### Introduction and Background

The consolidation of an accreting soil layer (i.e., one to which material is added over time) is relevant to many geotechnical applications involving soft soils. High water content waste materials (e.g., dredgings, mine tailings, and slurries) are commonly sluiced into large ponds for temporary storage and dewatering or permanent disposal. The capacity of such ponds depends on the relative rates of accumulation and consolidation of the material. Sediment deposition in aquatic environments also involves the consolidation of an accreting soil layer. Depending on the deposition rate, soils may become underconsolidated as additional material is added, possibly leading to slope instability. Early solutions for this problem were limited to small strains (Gibson 1958). Finite strain models based on material coordinates have been presented by Schiffman and Cargill (1981), Koppula and Morgenstern (1982), and Schiffman *et al.* (1984). Yong and Ludwig (1984) presented a finite strain model using the piecewise-linear approach, in which all variables pertaining to problem geometry, material properties, fluid flow, and effective stress are updated at each time step with respect to a fixed Eulerian coordinate system. In all cases, solutions are obtained through numerical simulation. Such simulations require special computer programs and may be computationally intensive due to the large strains involved.

The physical process of soil accretion in an aquatic environment generally involves both sedimentation and self-weight consolidation effects. Three different models have been de-

---

[1] Associate Professor, Department of Civil and Environmental Engineering, University of California, Los Angeles, CA 90095.

veloped to represent this process: (i) unhindered settling of discrete particles, (ii) hindered settling where particle interactions become significant, and (iii) self-weight consolidation involving effective stresses and excess pore pressures. Although experimental evidence indicates that the void ratio corresponding to zero effective stress is not unique but rather depends on material, pore fluid chemistry, and initial water content (Been and Sills 1981, Imai 1981), several studies have considered self-weight consolidation to commence at a void ratio in the range of 4 to 8 (Monte and Krizek 1976, Bloomquist and Townsend 1984, Yong 1984). Finite strain consolidation models that ignore sedimentation effects have however been applied with success to problems involving initial void ratios ranging from 14 to 19 (Scully et al. 1984, Somogyi et al. 1984, McVay et al. 1986). The use of such models for materials with initial void ratios higher than approximately 20 to 25 may produce erroneous results (Bloomquist and Townsend 1984).

This paper presents a piecewise-linear numerical model, called CS4, for one-dimensional consolidation of an accreting soil layer. CS4 was adapted from a previous code, CS2 (Fox and Berles 1997), which models the consolidation of a soil layer subjected to surcharge loading. Like CS2, CS4 accounts for large strain, soil self-weight, the relative velocity of fluid and solid phases, and variable hydraulic conductivity and compressibility during the consolidation process. In addition, the rate of accretion and the initial void ratio of the accreting material can vary with time. CS4 does not account for sedimentation effects and thus may not accurately model the behavior of high void ratio materials during the early stages of deposition. The development of CS4 is first presented. Verification of the model is illustrated through a comparison of numerical solutions with those in the literature for an example problem. Finally, solution charts are presented for the time required to fill a disposal pond in which material is accreting at a constant rate.

## Model Description

### Geometry

The accreting soil layer is represented as a column of $R_j$ elements. The deposition process, which is typically continuous, is approximated by adding new elements to the column at specified time intervals. Figure 1 shows the geometry of the layer at time t, just after the addition of element $R_j$. The height of the layer is $H^t$ and the Lagrangian height is $H_L^t$. The Lagrangian height is the height of the layer if no consolidation were to occur. The material is assumed to be saturated, homogeneous with respect to constitutive relationships, and of wide lateral extent such that the problem can be treated as one-dimensional. A vertical Eulerian coordinate, z, and element coordinate, j, are defined as positive upward from a fixed datum plane coincident with the bottom of the layer.

Each $j^{th}$ element in the column has unit cross sectional area, a central node located at elevation $z_j^t$, and height $L_j^t$. The bottom boundary may be drained or undrained, whereas the top boundary is assumed to be drained with total head of $H^t$ (with respect to the datum). If the bottom boundary is drained, the total head at the bottom may be specified as $H^t$ or a constant value $H_b$. The initial height of each $j^{th}$ element is $L_{o,j}$ and the initial void ratio is $e_{o,j}$.

CS4 is written in dimensionless form using the following dimensionless quantities,

$$H_{Lf}^* = \frac{H_{Lf}}{H_{Lf}} = 1 \qquad (1)$$
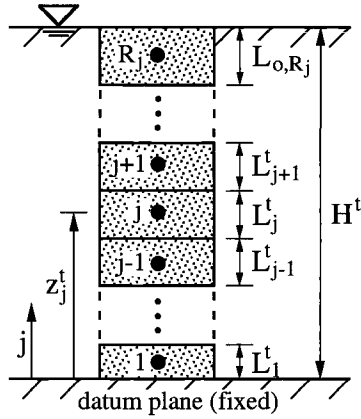
Figure 1 – *Configuration of elements for CS4 just after the addition of element $R_j$.*
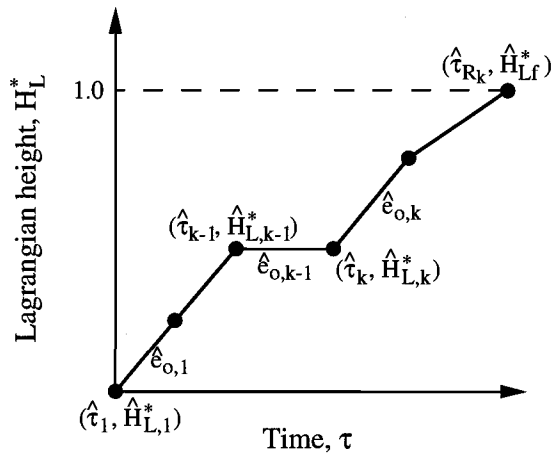


Figure 2 – *Lagrangian height and initial void ratio vs. time.*

$$H_L^{*\tau} = \frac{H_L^{\tau}}{H_{Lf}} \tag{2}$$

$$H^{*\tau} = \frac{H^{\tau}}{H_{Lf}} \tag{3}$$

$$L_{o,j}^{*} = \frac{L_{o,j}}{H_{Lf}} \qquad j = 1, 2, ..., R_j \tag{4}$$

$$L_j^{*\tau} = \frac{L_j^{\tau}}{H_{Lf}} \qquad j = 1, 2, ..., R_j \tag{5}$$

$$z_{o,j}^{*} = \frac{z_{o,j}}{H_{Lf}} \qquad j = 1, 2, ..., R_j \tag{6}$$

$$z_j^{*\tau} = \frac{z_j^{\tau}}{H_{Lf}} \qquad j = 1, 2, ..., R_j \tag{7}$$

$$\tau = \frac{k_r t}{H_{Lf}} \tag{8}$$

where $H_{Lf}$ is the final Lagrangian height of the layer and $k_r$ is the vertical hydraulic conductivity at arbitrary reference void ratio $e_r$. Thus, in CS4, the compressible layer has a final Lagrangian height of unity and all parameters are scaled accordingly.

*Rate of Accretion*

The rate of accretion is defined by $R_k$ ($\geq 2$) pairs of corresponding dimensionless Lagrangian height, $\hat{H}_L^{*}$, and dimensionless time, $\hat{\tau}$, (Figure 2) where,

$$\hat{H}_L^{*} = \frac{\hat{H}_L}{H_{Lf}} \tag{9}$$

$$\hat{\tau} = \frac{k_r \hat{t}}{H_{Lf}} \tag{10}$$

The overscript $^\wedge$ is used to distinguish the input values of Lagrangian height and time that define this relationship. The first data point ($\hat{\tau}_1$, $\hat{H}_{L,1}^{*}$) is assumed to be (0,0). The initial void ratio, $\hat{e}_{o,k}$, is assumed to be constant between any two data points in Figure 2. Essentially any desired filling history can be accommodated by CS4, including periods of quiescent consolidation (i.e., during which no material is added). The only restriction is that $\hat{H}_L^{*}$ must not decrease with increasing $\hat{\tau}$ (i.e., solid mass cannot be removed from the system).

*Constitutive Relationships*

Constitutive relationships for the compressible layer are shown in Figure 3. The compressibility curve (Figure 3a) is defined by $R_m$ ($\geq 2$) pairs of corresponding void ratio, $\hat{e}$, and dimensionless vertical effective stress, $\hat{\sigma}'^{*}$, where,
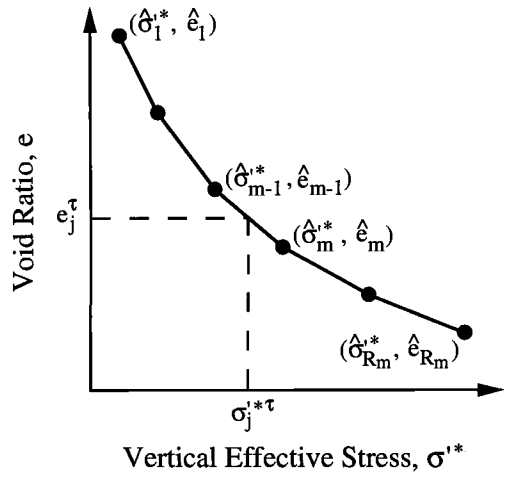
(a)
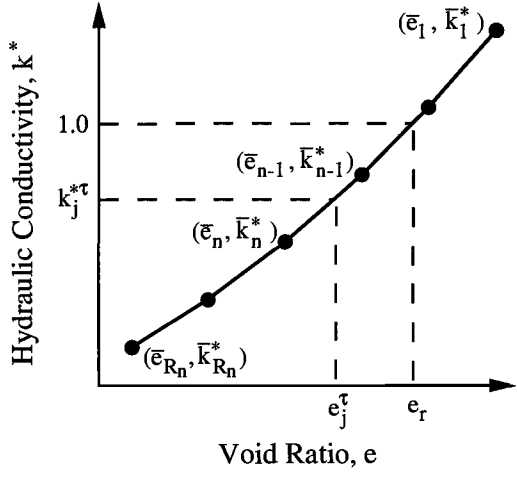


(b)

Figure 3 – *Soil constitutive relationships: (a) compressibility,*
*and (b) hydraulic conductivity.*

$$\hat{\sigma}'^{*} = \frac{\hat{\sigma}'}{H_{Lf}\gamma_w} \qquad (11)$$

and $\gamma_w$ is the unit weight of water (constant). The hydraulic conductivity relationship (Figure 3b) is defined by $R_n$ ($\geq 2$) pairs of corresponding void ratio, $\bar{e}$, and dimensionless vertical hydraulic conductivity, $\bar{k}^{*}$, where,

$$\bar{k}^{*} = \frac{\bar{k}}{k_r} \qquad (12)$$

The overscripts $^\wedge$ and $^-$ are used to distinguish the input values of void ratio, vertical effective stress, and vertical hydraulic conductivity that define these relationships. A one-to-one correspondence is assumed for each constitutive relationship in Figure 3. Thus, CS4 does not account for the effects of strain rate, secondary compression, or aging on the compressibility or hydraulic conductivity of the soil. The relationships can, however, take nearly any desired geometric form by choosing an appropriate number of data points. The only restriction is that $\hat{e}$ must continuously decrease with increasing $\hat{\sigma}'^{*}$ and $\bar{k}^{*}$ must continuously decrease with decreasing $\bar{e}$.

*Stress, Pore Pressure, Flow, and Settlement*

CS4 calculates stresses, pore pressure, fluid flow, and settlement in the same fashion as does CS2. Fox and Berles (1997) present detailed information on these aspects. To summarize, the dimensionless vertical total stress at node j, $\sigma_j^{*\tau}$, is computed from the self-weight of overlying elements as,

$$\sigma_j^{*\tau} = \frac{\sigma_j^{\tau}}{H_{Lf}\gamma_w} = \frac{L_j^{*\tau}\gamma_j^{*\tau}}{2} + \sum_{i=j+1}^{R_j} L_i^{*\tau}\gamma_i^{*\tau} \qquad j = 1, 2, ..., R_j \qquad (13)$$

where $\gamma_j^{*\tau}$ is the dimensionless saturated unit weight of element j,

$$\gamma_j^{*\tau} = \frac{\gamma_j^{\tau}}{\gamma_w} = \frac{G_s + e_j^{\tau}}{1 + e_j^{\tau}} \qquad j = 1, 2, ..., R_j \qquad (14)$$

and $e_j^{\tau}$ is the corresponding void ratio. The specific gravity of soil solids, $G_s$, is assumed to be constant for the entire layer and $e_j^{\tau}$ is taken as constant within each element for any given time increment.

Dimensionless vertical effective stress, $\sigma_j'^{*\tau}$, and dimensionless vertical hydraulic conductivity, $k_j^{*\tau}$, are computed for each node using $e_j^{\tau}$ and interpolating between data points in Figure 3. The dimensionless pore pressure, $u_j^{*\tau}$, is the difference between the total and effective stresses,

$$u_j^{*\tau} = \frac{u_j^{\tau}}{H_{Lf}\gamma_w} = \sigma_j^{*\tau} - \sigma_j'^{*\tau} \qquad j = 1, 2, ..., R_j \qquad (15)$$

Flow between adjacent elements is computed using the Darcy-Gersevanov law (Gersevanov 1934, Schiffman *et al.* 1985) which accounts for the relative motion of fluid and solid phases. The dimensionless relative discharge velocity (positive upward), $v_{rf,j}^{*\tau}$, between nodes j and j+1 is,

$$v_{rf,j}^{*\tau} = \frac{v_{rf,j}^{\tau}}{k_r} = -k_{s,j}^{*\tau}i_j^{\tau} \qquad j = 1, 2, ..., R_j\text{-}1 \qquad (16)$$

where the hydraulic gradient, $i_j^{\tau}$, is,

$$i_j^{\tau} = \frac{h_{j+1}^{*\tau} - h_j^{*\tau}}{z_{j+1}^{*\tau} - z_j^{*\tau}} \qquad j = 1, 2, ..., R_j\text{-}1 \qquad (17)$$

the dimensionless total head for node j, $h_j^{*\tau}$, is,

$$h_j^{*\tau} = \frac{h_j^{\tau}}{H_{Lf}} = z_j^{*\tau} + u_j^{*\tau} \qquad j = 1, 2, ..., R_j \qquad (18)$$

and the equivalent dimensionless series hydraulic conductivity, $k_{s,j}^{*\tau}$, between nodes j and j+1 is,

$$k_{s,j}^{*\tau} = \frac{k_{j+1}^{*\tau}k_j^{*\tau}\left(L_{j+1}^{*\tau} + L_j^{*\tau}\right)}{L_{j+1}^{*\tau}k_j^{*\tau} + L_j^{*\tau}k_{j+1}^{*\tau}} \qquad j = 1, 2, ..., R_j\text{-}1 \qquad (19)$$

Once the discharge velocities are known, new dimensionless element heights are computed as,

$$L_j^{*\tau+\Delta\tau} = L_j^{*\tau} - \left(v_{rf,j}^{*\tau} - v_{rf,j-1}^{*\tau}\right)\Delta\tau \qquad j = 2, 3, ..., R_j \qquad (20)$$

new void ratios are,

$$e_j^{\tau+\Delta\tau} = \frac{L_j^{*\tau+\Delta\tau}\left(1 + e_{o,j}\right)}{L_o^*} - 1 \qquad j = 1, 2, ..., R_j \qquad (21)$$

the new dimensionless height of the layer is,

$$H^{*\tau+\Delta\tau} = \sum_{j=1}^{R_j} L_j^{*\tau+\Delta\tau} \qquad (22)$$

and the new dimensionless settlement, $S^{*\tau+\Delta\tau}$, is,

$$S^{*\tau+\Delta\tau} = \frac{S^{\tau+\Delta\tau}}{H_{Lf}} = H_L^{*\tau+\Delta\tau} - H^{*\tau+\Delta\tau} \qquad (23)$$

where $S^{\tau+\Delta\tau}$ is the settlement of the layer at time $\tau+\Delta\tau$.

*Time Increment*

CS4 uses three criteria to calculate the dimensionless time increment, $\Delta\tau$. The first two criterion are similar to those presented by Fox and Berles (1997),

$$\Delta\tau_j = \frac{k_r\Delta t}{H_{Lf}} = \frac{\alpha a_{v,j}^{*\tau}\left(L_j^{*\tau}\right)^2}{k_j^{*\tau}\left(1+e_j^\tau\right)} \qquad j = 1, 2, ..., R_j \qquad (24)$$

$$\Delta\tau_j = \left|\frac{0.005L_j^{*\tau}}{\left(v_{rf,j}^{*\tau} - v_{rf,j-1}^{*\tau}\right)}\right| \qquad j = 2, 3, ..., R_j \qquad (25)$$

where $\alpha = 0.4$, $a_{v,j}^{*\tau}$ is the dimensionless coefficient of compressibility computed for $e_j^\tau$ from Figure 3a, and the vertical bars signify absolute value. Eq. 24 is needed for numerical stability of the explicit time integration method. Eq. 25 ensures that the change in element height for any time step is no larger than 0.5% of the current height. This criterion is needed to properly resolve large relative discharge velocities, such as when a new element is added to the system. CS4 also executes at least 20 time steps between the addition of any two elements to the system. Using these three criterion, CS4 finds the smallest value of $\Delta\tau$ at each time step, which is then used to advance the solution forward in time for all elements.

## CS4 Computer Program

The required input data for CS4 is the minimum number of elements $R_{j,min}$, data points for the accretion rate and initial void ratio, data points for the constitutive relationships, specific gravity of solids $G_s$, termination time $\tau_{final}$, and the bottom boundary drainage condition (and total head if necessary). As CS4 is cast in dimensionless form, the solution is independent of $H_{Lf}$ and $k_r$. The choice for $R_{j,min}$ depends on the desired solution accuracy and the acceptable computation time. Depending on the material properties of the layer, a value of $R_{j,min}$ between 25 and 100 usually gives satisfactory results.

After CS4 reads the input data, a schedule for addition of elements is determined. To do this, CS4 calculates $\tau$ and $L_o$ values such that: i) $R_j \geq R_{j,min}$, ii) at least one element is added to the layer between any two non-quiescent data points in Figure 2, and iii) elements are added at the middle of their respective time increments. An initial void ratio consistent with Figure 2 is also assigned to each element. Figure 4 shows two accretion schedules, corresponding to $R_{j,min} = 4$ and $R_{j,min} = 20$, produced by CS4 for a hypothetical example involving variable accretion rate.

To begin the main calculation loop, elevation and total stress are computed for each node. The effective stress, hydraulic conductivity, and coefficient of compressibility are then calculated for each element from the corresponding initial void ratio and the constitutive relationships. The distribution of total head is used to compute flow between contiguous elements and the vertical compression of each element is calculated from the net fluid outflow during time increment $\Delta\tau$. New element heights and void ratios are calculated, as well as the settlement of the layer. Elements are added to the column at the appropriate time intervals. Program execution terminates when $\tau \geq \tau_{final}$. If this condition is not satisfied, CS4 repeats the calculation sequence with new values of $e_j$, $L_j^*$, and $H^*$.
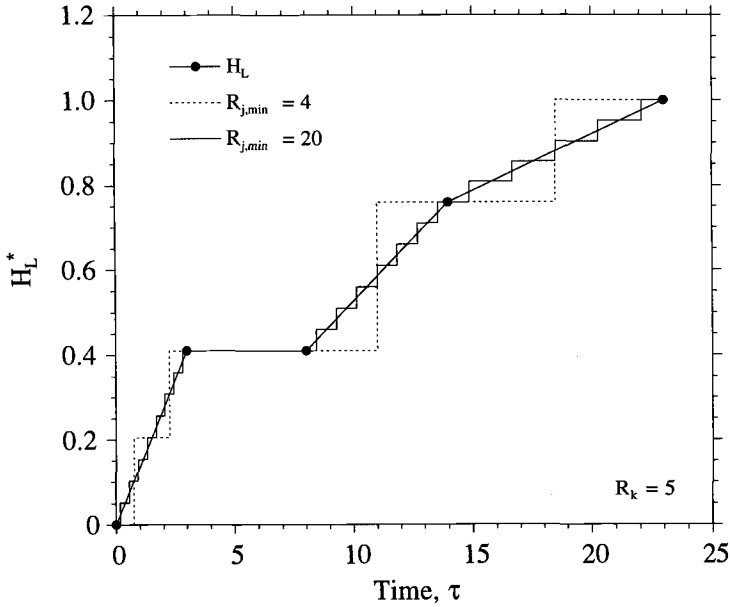
Figure 4 – *Examples of accretion schedules produced by CS4.*

## Model Verification

The performance of CS4 is illustrated for a problem described by Schiffman *et al.* (1984). Copper slimes are placed in a tailings impoundment at a void ratio of 1.3 and at constant rate for 3000 days. Thereafter, the tailings undergo quiescent consolidation. The Lagrangian height of the impoundment is 80 m, the bottom of the impoundment is impervious, and the water level is maintained at the top of the slimes. The slimes have $G_s$ = 2.6 and the following material properties,

$$e = 1.45 - 0.265 \log(\sigma'(\text{kPa}))$$ (26)

$$e = 5.34 + 0.56 \log(k(\text{m}/\text{s}))$$ (27)

Settlement of the slimes was computed using CS4 and $R_{j,min}$ = 100. Figure 5a shows the height and Lagrangian height of the slimes as a function of time and Figure 5b presents the distribution of pore pressure as a function of depth at 3000 days. The results obtained using CS4 are in very good agreement with those provided by Schiffman *et al.* (1984). Figure 5 indicates that simulation results produced using CS4 are essentially equivalent to those obtained using material coordinates. Fox and Berles (1997) present additional verification checks of the piecewise-linear approach for problems involving small strain, large strain, non-linear compressibility and hydraulic conductivity relationships, and material self weight.
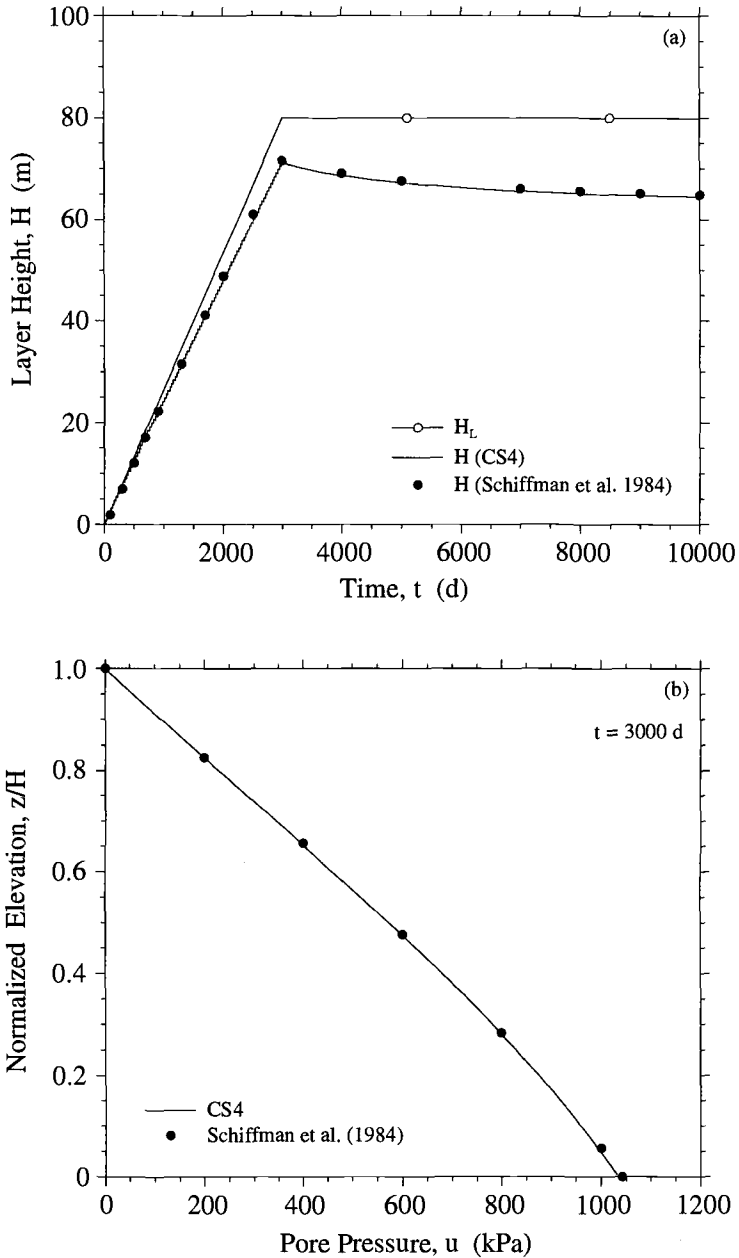
Figure 5 – *Numerical solutions for: (a) layer height vs. time, and (b) pore pressure vs. normalized elevation for an accreting layer of copper slimes (individual data points scaled from Figures 6 and 7 of Schiffman et al. (1984)).*

## Solution Charts

*Development of Chart Tables*

CS4 was used to prepare dimensionless solution charts similar to those presented by Fox (1999) for the consolidation of a homogeneous clay layer under a surcharge load. The charts are applicable for a soil layer accreting at constant rate, r, with a constant initial void ratio, $e_o$. The charts give the time, $t_f$, required for the layer to reach a given height, $H_f$. The material is assumed to have $G_s = 2.7$ and constitutive relationships of the following form,

$$e = A(\sigma')^B \qquad (28)$$

$$k = C(e)^D \qquad (29)$$

where A, B, C, and D are constants. Eqs. 28 and 29 have been widely used for studies of the consolidation of waste clays and other soft soils (Somogyi 1979, Carrier *et al.* 1983 (Eq. 28), Bloomquist and Townsend 1984, Krizek and Somogyi 1984, Somogyi *et al.* 1984, McVay *et al.* 1986, Huerta *et al.* 1988, Townsend *et al.* 1989 (Eq. 28), Townsend and McVay 1990, Abu-Hejleh *et al.* 1996 (Eq. 29)). Experimental data presented in several other studies further supports the general use of Eqs. 28 and 29 (Imai 1979, Pane *et al.* 1983, Znidarcic *et al.* 1986, Tan *et al.* 1988).

To prepare the solution charts, CS4 was modified to accommodate the specific constitutive relationships given by Eq. 28 and 29. Accordingly, the following dimensionless quantities are defined for the solution charts,

$$H^* = \frac{H}{H_f} \qquad (30)$$

$$\tau_f = \frac{rt_f}{H_f} \qquad (31)$$

$$\sigma'^* = \frac{\sigma'}{H_f \gamma_w} \qquad (32)$$

$$k^* = \frac{k}{r} \qquad (33)$$

$$A^* = A(H_f \gamma_w)^B \qquad (34)$$

$$C^* = \frac{C}{r} \qquad (35)$$

The constitutive relationships are then written in dimensionless form as,

$$e = A^*(\sigma'^*)^B \qquad (36)$$

$$k^* = C^*(e)^D \qquad (37)$$

All dimensionless quantities in CS4 were redefined to be consistent with Eqs. 30-37. Based on the above cited references and typical values for r and $H_f$, the following ranges of parameters were chosen for the charts: $e_o = 5, 10, 15, 20$; $A^* = 0.1$ to 10, B = -0.05, -0.15, -0.25, -0.35; $C^* = 1 \times 10^{-6}$ to $1 \times 10^{-2}$ (depending on D); and D = 3, 4, 5. The accreting layer is assumed to be single-drained (impervious base) or double-drained with both boundaries having total head $H^t$ (i.e., both boundaries hydraulically connected to a water table maintained at the top of the layer). A value of $R_{j,min} = 25$ was chosen to develop

the charts. Depending on material properties, more than 100 elements were needed to complete the simulations in most cases. The maximum number of required elements for one simulation was 297.

Solutions for $\tau_f$ are presented in the form of 8 chart tables in Figures 6 through 9. Each contour plot was created from 289 data points and thus the chart tables represent 27,744 solutions of the CS4 computer program. The charts include the effects of vertical strain, self-weight, and decreasing compressibility and hydraulic conductivity during the consolidation process.

Chart tables giving the required time for a single-drained accreting layer, $\tau_{f,SD}$, and a double-drained accreting layer, $\tau_{f,DD}$, with $e_o = 5$ are shown in Figure 6. Each table consists of twelve contour plots arranged into three rows and four columns. Each row corresponds to a constant value of D and each column corresponds to a constant value of B. Each row of charts has identical $C^*$ vs. $A^*$ (log-log) axes. Contours of constant $\tau_{f,SD}$ or $\tau_{f,DD}$ are drawn on each plot. Corresponding chart tables for $e_o = 10, 15,$ and 20 are shown in Figures 7, 8, and 9, respectively.

Figures 6-9 reveal consistent trends. In general, $\tau_f$ decreases with increasing $A^*$ and increases with increasing B, $C^*$, and D. The figures also show that $\tau_f$ increases with increasing $e_o$. A value of $\tau_f = 1$ corresponds to a case in which $H_f = H_{Lf}$ (i.e., the accreting layer as a whole does not consolidate or swell). Thus, values of $\tau_f < 1$ indicate swelling of the layer and values of $\tau_f > 1$ indicate consolidation of the layer. Layer swelling is indicated for low $e_o$ and high $A^*$. Appreciable swelling would be unlikely for an actual waste disposal pond due to surface desiccation and a lack of additional available water. Each chart contains a lower left region in which $\tau_f$ is largely independent of $A^*$ and an upper right region in which $\tau_f$ is largely independent of $C^*$. These trends reflect the relative importance of material compressibility, material hydraulic conductivity, final layer thickness, and accretion rate on the required time. For example, consider values of $\tau_{f,SD}$ corresponding to $e_o = 10, B = -0.15, D = 5,$ and $A^* = 2$ (Figure 7). If $C^* = 1 \times 10^{-6}, \tau_{f,SD} \approx 1$. The accretion rate is too large relative to the hydraulic conductivity for appreciable consolidation to occur in this case. As $C^*$ increases beyond $1 \times 10^{-5}$, appreciable consolidation of the layer can occur and $\tau_{f,SD}$ begins to increase accordingly. As $C^*$ continues to increase, the value of $\tau_f$ eventually becomes independent of $C^*$, reaching an ultimate value of 3. This corresponds to a case in which the hydraulic conductivity of the material is sufficiently high relative to the accretion rate that the material can fully consolidate as it is placed without generation of excess pore pressures.

*Example Problem*

An example problem is provided to illustrate the use of the solution charts. A disposal pond for waste clay is 12 m high and is filled at a constant rate of 0.1 m/d. The bottom of the pond is impervious. The clay has $G_s = 2.7$, $e_o = 15$, and the following material properties,

$$e = 7(\sigma'(kPa))^{-0.25} \tag{38}$$

$$k(m/s) = 3 \times 10^{-11}(e)^5 \tag{39}$$
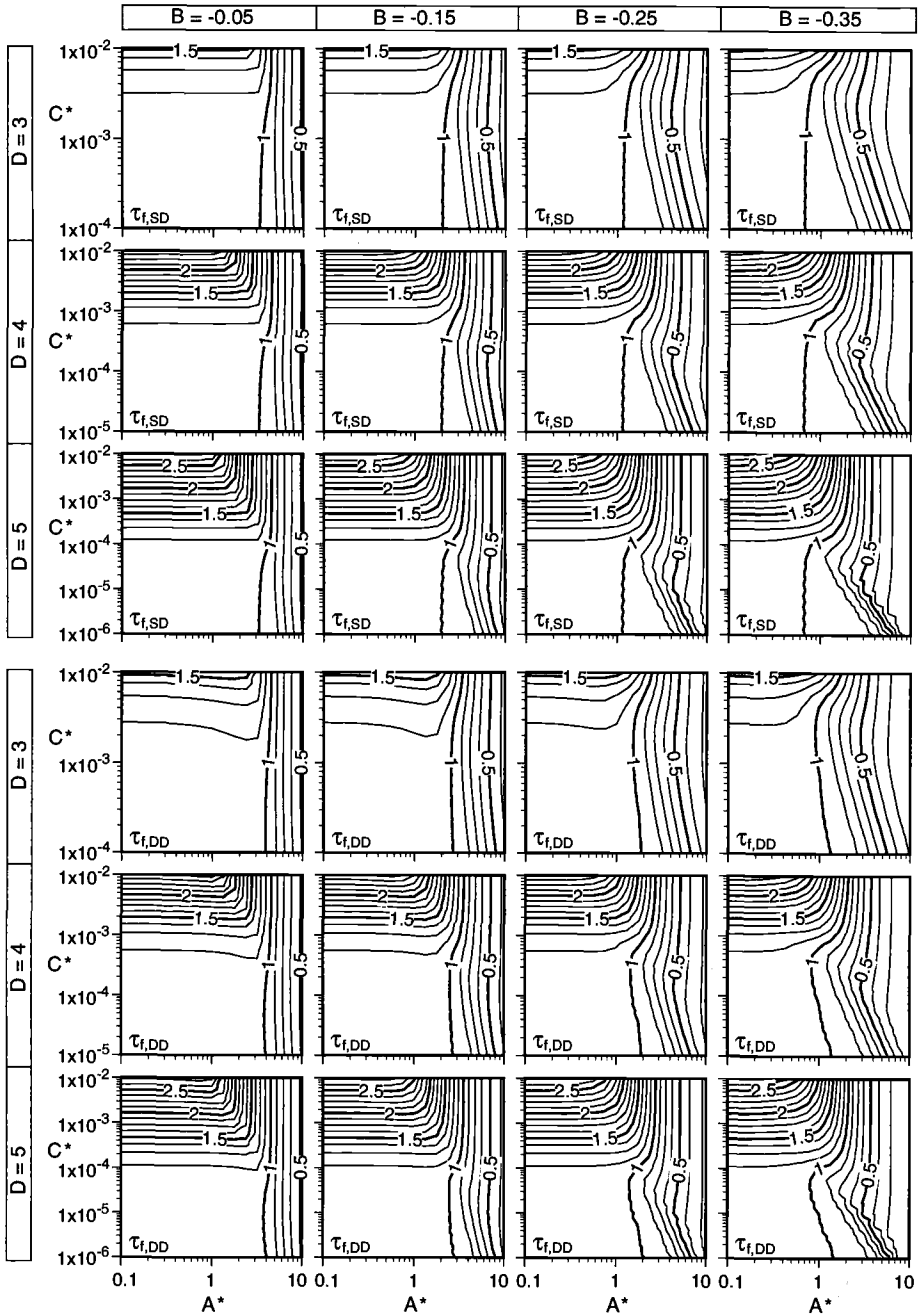
Figure 6 – *Chart tables for* $\tau_{f,SD}$ *and* $\tau_{f,DD}$, $e_o = 5$.
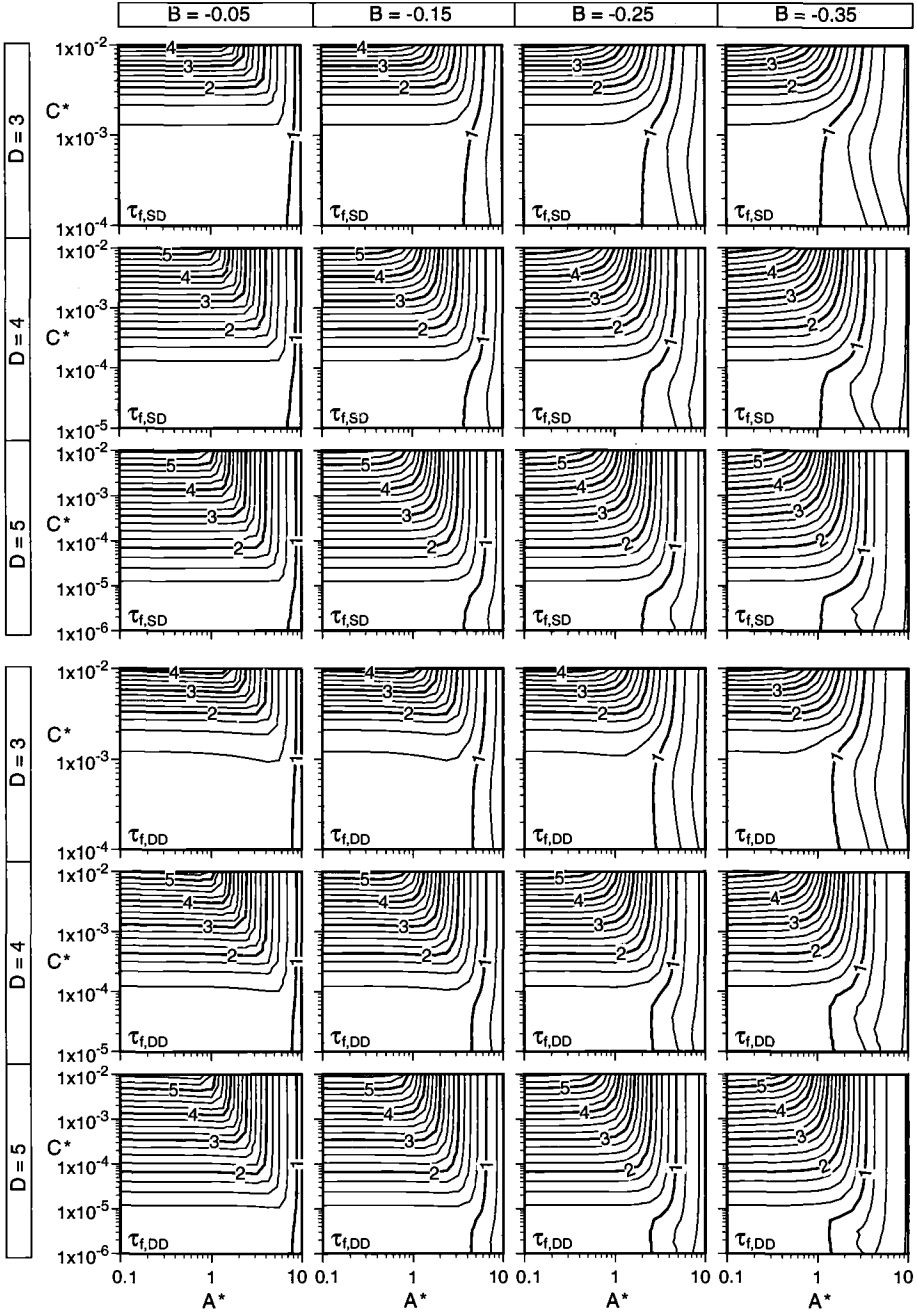
Figure 7 – Chart tables for $\tau_{f,SD}$ and $\tau_{f,DD}$, $e_o = 10$.
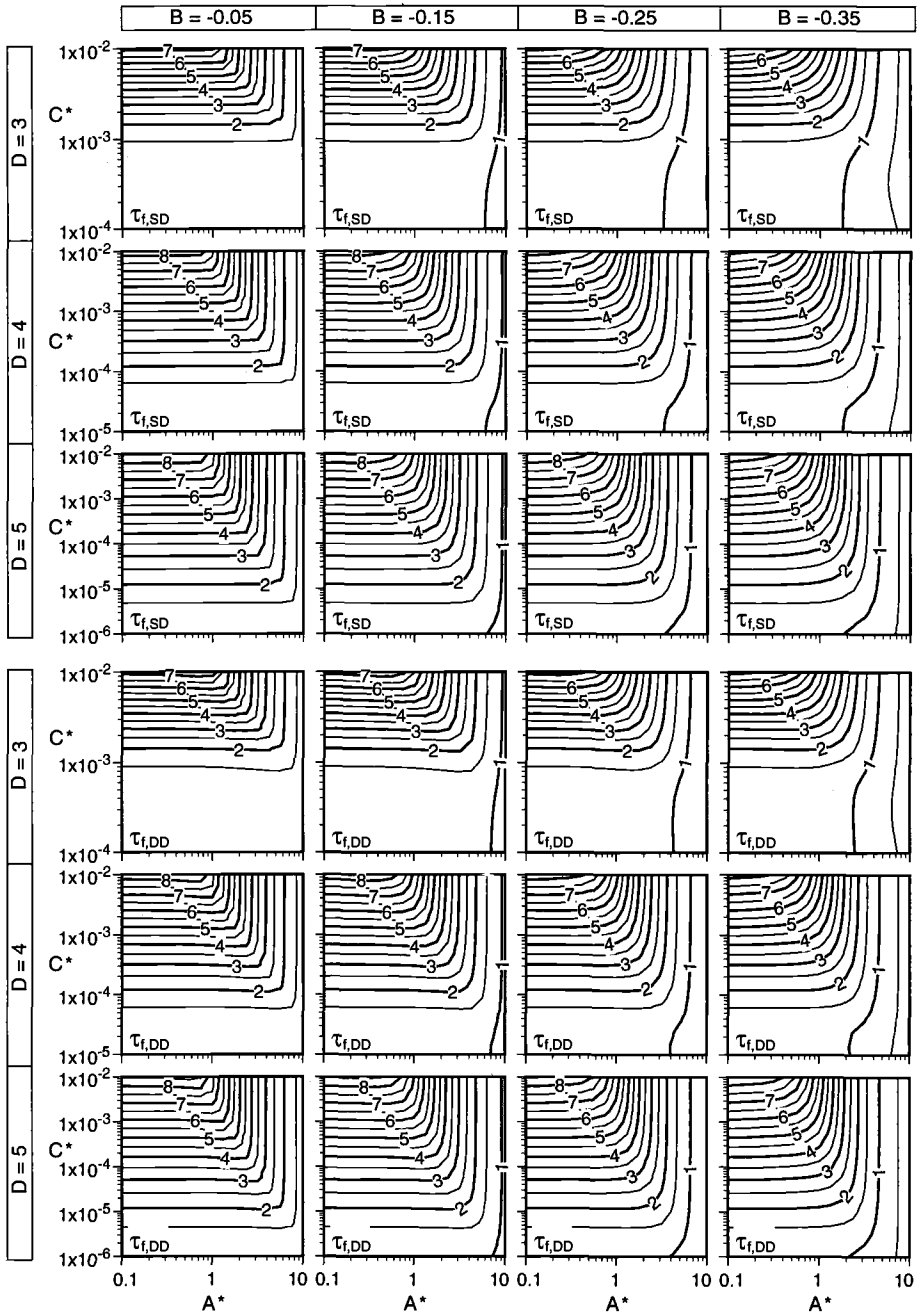
Figure 8 – *Chart tables for* $\tau_{f,SD}$ *and* $\tau_{f,DD}$, $e_o = 15$.
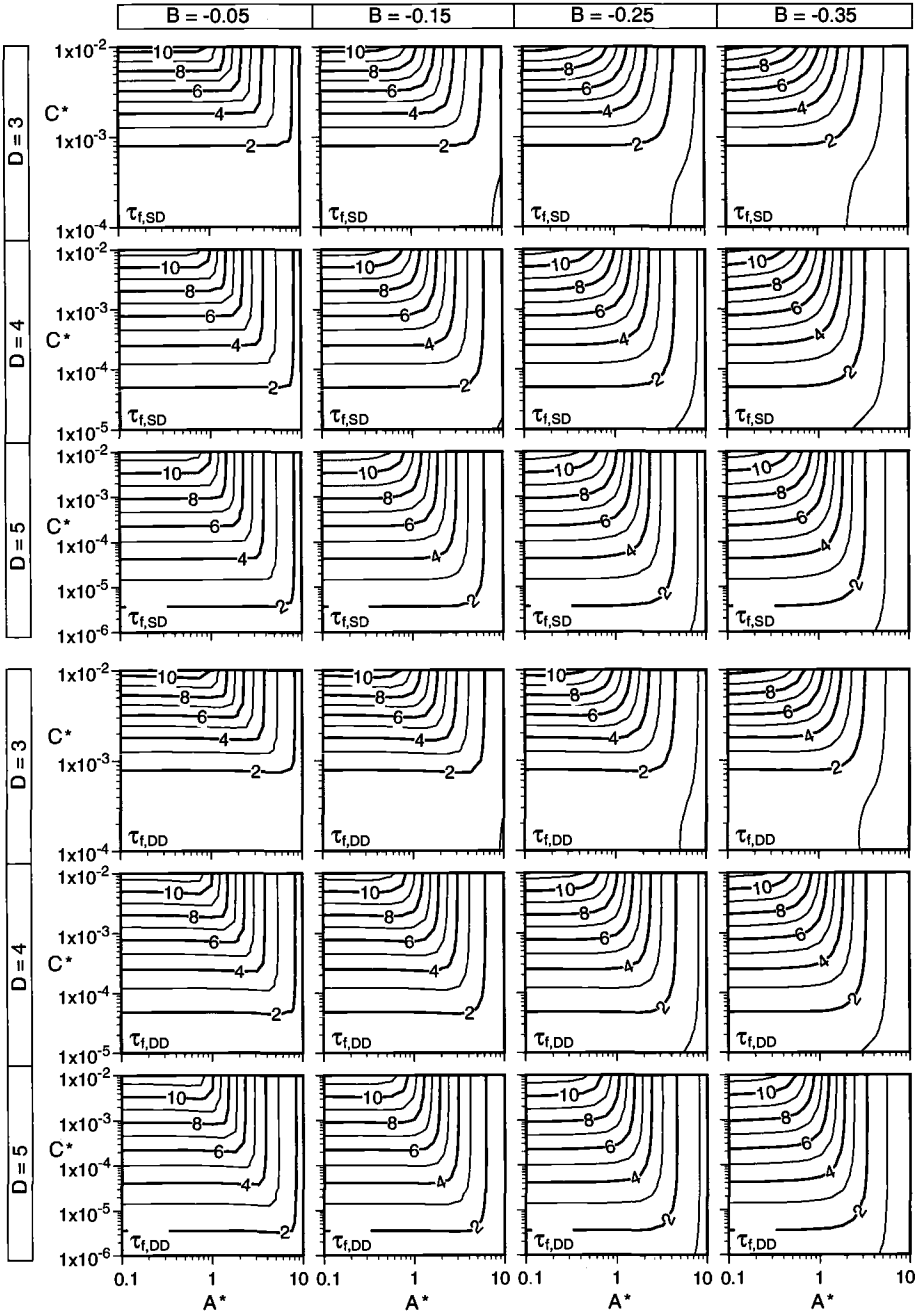
Figure 9 – *Chart tables for* $\tau_{f,SD}$ *and* $\tau_{f,DD}$, $e_o = 20$.

Specifying $H_f = 12$ m, $\gamma_w = 9.81$ kN/m$^3$, and r = $1.16 \times 10^{-6}$ m/s, the input parameters are $A^* = 2.1$, B = -0.25, $C^* = 2.6 \times 10^{-5}$, and D = 5. A value of $\tau_{f,SD} \approx 2.2$ is obtained from Figure 8. The corresponding value of $t_f$ = (2.2)(12 m)/(0.1 m/d) = 264 d. Thus, pond capacity would be exceeded in 264 days. Using the CS4 program directly, a value of $t_f$ = 267 d is obtained, which is very close to the chart estimate.

## Conclusions

CS4 is a dimensionless piecewise-linear model for consolidation of an accreting soil layer. CS4 accounts for large strain, self-weight, and variable hydraulic conductivity and compressibility during the consolidation process. Constitutive relationships for the material and relationships for accretion rate and initial void ratio versus time are defined using discrete data points, and as such can take nearly any desired form. CS4 uses a conventional Eulerian coordinate system in which node elevations are taken with respect to a fixed datum and all variables refer to the current configuration of the system. A comparison of solutions indicates that CS4 produces solutions equivalent to those obtained using material coordinates. CS4 does not account for particle sedimentation and thus may not accurately model the behavior of high void ratio materials during the early stages of deposition.

Using CS4, dimensionless solution charts were prepared for the time, $t_f$, required to fill a disposal pond in which material is accreting at a constant rate. The charts require only simple hand calculations and may be suitable for preliminary design purposes. To estimate $t_f$, a user must specify the final layer height, accretion rate, material parameters, initial void ratio, and boundary drainage conditions. An example problem indicates that chart solutions provide a very close approximation to solutions obtained directly from the CS4 program. The solution charts are based on several assumptions which may not be acceptable for some problems.

## Acknowledgments

## References

Abu-Hejleh, A. N., Znidarcic, D., and Barnes, B. L., 1996, "Consolidation Characteristics of Phosphatic Clays," *Journal of Geotechnical Engineering*, Vol. 122, No. 4, pp. 295-301.

Been, K. and Sills, G. C., 1981, "Self-Weight Consolidation of Soft Soils: An Experimental and Theoretical Study," *Geotechnique*, Vol. 31, No. 4, pp. 519-535.

Bloomquist, D. G. and Townsend, F. C., 1984, "Centrifugal Modeling of Phosphatic Clay Consolidation," *Proceedings, Symposium on Sedimentation/Consolidation Models: Prediction and Validation*, R. N. Yong and F. C. Townsend, Eds., San Francisco, ASCE, pp. 565-580.

Carrier, W. D., III, Bromwell, L. G., and Somogyi, F., 1983, "Design Capacity of Slurried Mineral Waste Ponds," *Journal of Geotechnical Engineering*, Vol. 109, No. 5, pp. 699-716.

Fox, P. J. and Berles, J. D., 1997, "CS2: A Piecewise-Linear Model for Large Strain Consolidation," *International Journal for Numerical and Analytical Methods in Geomechanics*, Vol. 21, No. 7, pp. 453-475.

Fox, P. J., 1999, "Solution Charts for Finite Strain Consolidation of Normally Consolidated Clays," *Journal of Geotechnical and Geoenvironmental Engineering*, Vol. 125, No. 10, in press.

Gersevanov, N. M., 1934, *Kinamika Mekhaniki Gruntov* (Foundations of Soil Mechanics), Gosstroiisdat, Moscow, U.S.S.R.

Gibson, R. E., 1958, "The Progress of Consolidation in a Clay Layer Increasing in Thickness with Time," *Geotechnique*, Vol. 8, No. 4, pp. 171-182.

Huerta, A., Kriegsmann, G. A., and Krizek, R. J., 1988, "Permeability and Compressibility of Slurries from Seepage-Induced Consolidation," *Journal of Geotechnical Engineering*, Vol. 114, No. 5, pp. 614-627.

Imai, G., 1979, "Development of a New Consolidation Test Procedure Using Seepage Force," *Soils and Foundations*, Vol. 19, No. 3, pp. 45-60.

Imai, G., 1981, "Experimental Studies on Sedimentation Mechanism and Sediment Formation of Clay Minerals," *Soils and Foundations*, Vol. 21, No. 1, pp. 7-20.

Koppula, S. D. and Morgenstern, N. R., 1982, "On the Consolidation of Sedimenting Clays," *Canadian Geotechnical Journal*, Vol. 19, No. 3, pp. 260-268.

Krizek, R. J. and Somogyi, F., 1984, "Perspectives on Modelling Consolidation of Dredged Materials," *Proceedings, Symposium on Sedimentation/Consolidation Models: Prediction and Validation*, R. N. Yong and F. C. Townsend, Eds., San Francisco, ASCE, pp. 296-332.

McVay, M., Townsend, F., and Bloomquist, D., 1986, "Quiescent Consolidation of Phosphatic Waste Clays," *Journal of Geotechnical Engineering*, Vol. 112, No. 11, pp. 1033-1049.

Monte, J. L. and Krizek, R. J., 1976, "One-Dimensional Mathematical Model for Large-Strain Consolidation," *Geotechnique*, Vol. 26, No. 3, pp. 495-510.

Pane, V., Croce, P., Znidarcic, D., Ko, H.-Y., Olsen, H. W., and Schiffman, R. L., 1983, "Effects of Consolidation on Permeability Measurements for Soft Clay," *Geotechnique*, Vol. 33, No. 1, pp. 67-72.

Schiffman, R. L. and Cargill, K. W., 1981, "Finite Strain Consolidation of Sedimenting Clay Deposits," *Proceedings, 10th International Conference on Soil Mechanics and Foundation Engineering*, Stockholm, Vol. 1, pp. 239-242.

Schiffman, R. L., Pane, V., and Gibson, R. E., 1984, "The Theory of One-Dimensional Consolidation of Saturated Clays. IV. An Overview of Nonlinear Finite Strain Sedimentation and Consolidation," *Proceedings, Symposium on Sedimentation/ Consolidation Models: Prediction and Validation*, R. N. Yong and F. C. Townsend, Eds., San Francisco, ASCE, pp. 1-29.

Schiffman, R. L., Pane, V., and Sunara, V., 1985, "Sedimentation and Consolidation," *Proceedings, Engineering Foundation Conference: Flocculation, Sedimentation, and Consolidation*, B. M. Moudgil and P. Somasundaran, Eds., Sea Island, Georgia, pp. 57-121.

Scully, R. W., Schiffman, R. L., Olsen, H. W., and Ko, H.-Y., 1984, "Validation of Consolidation Properties of Phosphatic Clay at Very High Void Ratios," *Proceedings, Symposium on Sedimentation/ Consolidation Models: Prediction and Validation*, R. N. Yong and F. C. Townsend, Eds., San Francisco, ASCE, pp. 158-181.

Somogyi, F., 1979, *Analysis and Prediction of Phosphatic Clay Consolidation: Implementation Package*, Technical Report, Florida Phosphatic Clay Research Project, Lakeland, Fla.

Somogyi, F., Carrier, W. D., III, Lawver, J. E., and Beckman, J. F., 1984, "Waste Phosphatic Clay Disposal in Mine Cuts," *Proceedings, Symposium on Sedimentation/ Consolidation Models: Prediction and Validation*, R. N. Yong and F. C. Townsend, Eds., San Francisco, ASCE, pp. 545-564.

Tan, S.-A., Tan, T.-S., Ting, L. C., Yong, K.-Y., Karunaratne, G.-P., and Lee, S.-L., 1988, "Determination of Consolidation Properties for Very Soft Clay," *Geotechnical Testing Journal*, Vol. 11, No. 4, pp. 233-240.

Townsend, F. C., McVay, M. C., Bloomquist, D. G., and McClimans, S. A., 1989, "Clay Waste Pond Reclamation by Sand/Clay Mix or Capping," *Journal of Geotechnical Engineering*, Vol. 115, No. 11, pp. 1647-1666.

Townsend, F. C. and McVay, M. C., 1990, "SOA: Large Strain Consolidation Predictions," *Journal of Geotechnical Engineering*, Vol. 116, No. 2, pp. 222-243.

Yong, R. N., 1984, "Particle Interaction and Stability of Suspended Solids," *Proceedings, Symposium on Sedimentation/Consolidation Models: Prediction and Validation*, R. N. Yong and F. C. Townsend, Eds., San Francisco, ASCE, pp. 30-59.

Yong, R. N. and Ludwig, C. A., 1984, "Large-Strain Consolidation Modelling of Land Subsidence," *Proceedings, Symposium on Geotechnical Aspects of Mass and Materials Transport*, Bangkok, pp. 14-29.

Znidarcic, D., Schiffman, R. L., Pane, V., Croce, P., Ko, H.-Y., and Olsen, H. W., 1986, "The Theory of One-Dimensional Consolidation of Saturated Clays: Part V, Constant Rate of Deformation Testing and Analysis," *Geotechnique*, Vol. 36, No. 2, pp. 227-237.

Peter J. Blommaart,[1] Peter The,[1] Jan Heemstra,[2] and Ruud J. Termaat[3]

**Determination of Effective Stresses and the Compressibility of Soil Using Different Codes of Practice and Soil Models in Finite Element Codes**

**Abstract:** Creep or secondary compression plays an important role in the deformation behavior of soft soils like peat and organic clay. For the determination of long term settlements several methods have been proposed and implemented in codes for the engineering practice. However, some of the methods used have been developed empirically. In this paper the effective stresses and the compressibility of soils are addressed for some practical cases using the methods mentioned and soil models in finite element codes. The conceptual differences in methods and calculation results are compared. A stress-strain-creep strain rate model is proposed (Plaxis Soft Soil Creep model) in which strain rates are coupled with stresses and strains. The proposed material creep model is based on the modified Cam-clay model, which has been extended with a viscoplastic formulation using a single creep parameter $\mu^*$. The compressibility parameters $\kappa^*$, $\lambda^*$ and $\mu^*$ used within the model can be determined by standard one-dimensional consolidation tests. Applying the different methods, the calculated settlements show differences in the ratio between the primary and secondary compression as well as the distribution in time of the excess pore pressures. For large settlements the introduction of the natural strain, defined as the strain related to the actual height instead of the initial height of the soil layer, gives a further improvement of the model proposed (*a-b-c* model).

**Keywords:** soft soil, compression, consolidation, creep

---

[1]Project Manager, Road and Hydraulic Engineering Division, Ministry of Transport, Public Works and Water Management, Delft, The Netherlands.
[2] Project Manager, GeoDelft, Delft, The Netherlands.
[3] Research Manager, Road and Hydraulic Engineering Division, Ministry of Transport, Public Works and Water Management, Delft, The Netherlands.

## Nomenclature

*Symbols*

| | |
|---|---|
| $C_c$, $C_s$, $C_\alpha$ | Compressibility parameters (Bjerrum), - |
| $K_0$ | Coefficient for lateral soil pressure at rest, - |
| M | Cam-clay critical state stress ratio (q/p'), - |
| N | Organic content, weight % |
| a, b, c | Compressibility parameters (*a-b-c* soil model), - |
| $c_k$ | Change of permeability = (log $k/k_0$) / $\Delta e$, - |
| $c_v$ | Coefficient of consolidation, $m^2$/s |
| e | Void ratio (ratio of pore volume to volume of solids, 1-v), - |
| h | Layer thickness, sample height, m |
| k | Permeability, m/day |
| p | Total stress, pressure, $kN/m^2$ |
| p' | Effective mean stress, effective pressure, $kN/m^2$ |
| $p_c$, $p_g$ | Preconsolidation pressure, $kN/m^2$ |
| q | Deviator stress, $kN/m^2$ |
| $r_p$, $r_s$ | Compression ratio's (BSI 1975), - |
| s | Settlement, compression, m |
| t | Time, day |
| v | Specific volume (ratio of total volume to volume of solids, 1+e), - |
| w | Natural water content, dry mass % |
| $w_L$ | Liquid limit, dry mass % |
| $w_P$ | Plastic limit, dry mass % |
| $\varepsilon_v$ | Vertical strain, - |
| $\varepsilon_{vol}$ | Volume strain, - |
| $\varepsilon^C$ | Linear (Cauchy) strain, - |
| $\varepsilon^H$ | Natural (Hencky) strain, - |
| $\phi'$ | Effective friction angle, ° |
| $\gamma_{nat}$ | Natural unit weight, $kN/m^3$ |
| $\kappa$, $\lambda$ | Compressibility parameters (Cam-clay model), - |
| $\kappa^*$, $\lambda^*$, $\mu^*$ | Compressibility parameters (Soft Soil Creep model), - |
| $\nu$ | Poisson's ratio, - |

*Prefix*

| | |
|---|---|
| $\Delta$ | Increment |

*Indices*

| | |
|---|---|
| 0 | Initial |

## Introduction

Secondary compression or creep are terms used for long term, time dependent deformation behavior of non-consolidated soils. The long term deformation behavior is especially of importance for peat and organic clay.

All deformation theories for soils, are based on effective stresses. Therefore it is evident that the effective stresses need to be determined accurately, in order to be able to determine the deformations accurately. The effective stress is usually determined as the total stress minus the pore pressure. The total stress is rather easily determined, but the determination of the pore pressure is more difficult. This problem will be addressed in this paper.

When all stresses and pore pressures are known, the deformation behavior can be determined, using one of many deformation theories. The most widely used deformation theory for settlements is Bjerrum's compression theory. This compression theory will be compared with more advanced soil models, used in finite element methods. An overview of the compression theories discussed in this paper is given in Figure 1.



|    Bjerrum    |    Cam clay    |    a-b-c    | Soft Soil Creep Model |
| :-----------: | :------------: | :---------: | :-------------------: |
|      (a)      |      (b)       |     (c)     |          (d)          |
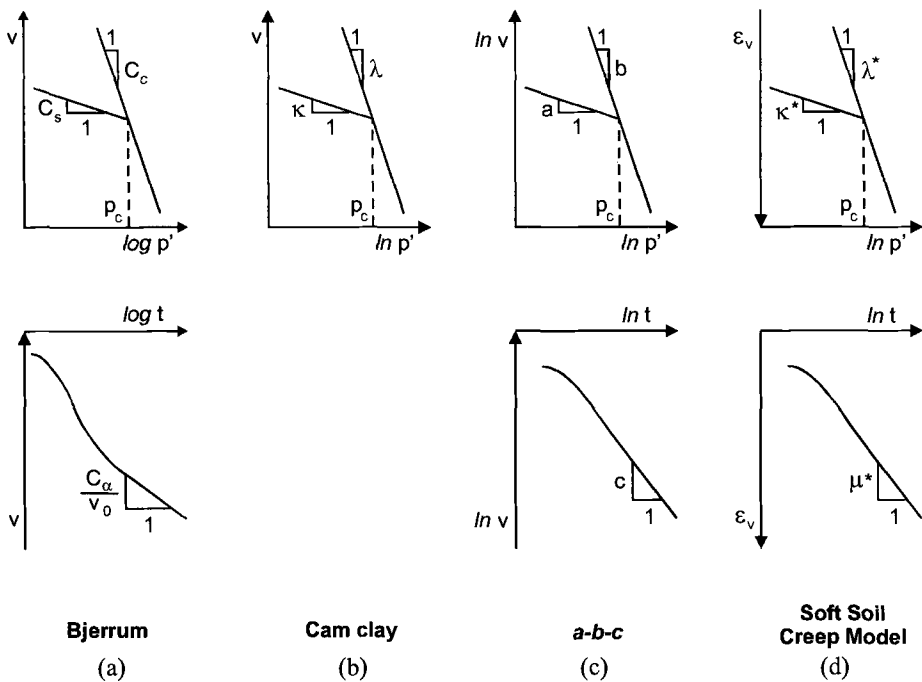
Figure 1 – *Overview of soil compression models*

All mentioned compression theories are compared for one-dimensional compression or settlement. Other aspects, such as multi-dimensional deformation behavior and strength, are not within the scope of this paper.

The mentioned compression theories are compared to see whether or not the calculated settlements are significantly different. In case the differences between all calculated settlements are small no additional recommendation have to be made for the engineering practice. This would make life simple for the geotechnical engineer. In case the differences are significant a national as well as an international discussion is needed to come to a recommendation for the use of a particular compression theory for the engineering practice. When comparing different theories two aspects have to be considered: current practice and theoretical correctness. In daily engineering practice the end-of-primary (EOP) approach (Mesri, Kwan Lo and Tao-Wei Feng 1994) based on Bjerrum's compression theory is widely used. The EOP approach however does not take into account a coupled analysis of consolidation, creep and large strains. Theoretically a coupled analysis of consolidation and creep in combination with the possibility of large strain analysis is preferable. Especially for soft soil consolidation and creep are dominant and large strains (> 30%) are no exception.

A calculation model needs input. For settlement calculations, the input consists of compressibility parameters, effective stresses and stress increments. For Bjerrum's compression theory the determination of the compressibility parameters is addressed in various national standards. Some of these standards are compared. For the other mentioned compression theories, no standards exist. The way of determining the compressibility parameters will be addressed in concept.

## Bjerrum's Compression Theory

Bjerrum's compression theory is described in (Bjerrum 1967) and in many publications afterwards and is widely used to calculate settlements. Because of the experience with Bjerrum's compression theory and its simplicity, it is a powerful tool to use in determining settlements. Yet, the theory does have some limitations, as will be discussed in this section.

Based on one-dimensional consolidation test results, Bjerrum assumed a linear relation between the specific volume v and the [10]logarithm of the effective stress p' (Figure 1a, top). For the time dependent component of the settlement after completion of the consolidation period, Bjerrum assumed a linear relation between the specific volume v and the [10]logarithm of time t (Figure 1b, bottom).

*Large Strains*

Observations show that the assumed linear relation between the specific volume v and the [10]logarithm of the effective stress p' (Figure 1a, top) is only valid for a limited strain range for soft soils. For large strain ranges the v - *log* p' relation is not linear but convex.

Bjerrum's compression theory describes compression in terms of linear or Cauchy strains $\varepsilon^C$, where linear strain is the ratio of compression or settlement s and the initial thickness of the soil sample or layer $h_0$:

$$\varepsilon^C = \frac{s}{h_0} = -\left(\frac{\Delta v}{v_0}\right) = -\left(\frac{v - v_0}{v_0}\right) = -\left(\frac{e - e_0}{1 + e_0}\right) \tag{1}$$

By describing compression in terms of linear strains $\varepsilon^C$ it is assumed that a relation exists between the linear strain $\varepsilon^C$ and the $^{10}$logarithm of the effective stress p' (Figure 1a). Observations show that the strain $\varepsilon$ is not only dependent of the effective stress level p', but also of the stress path and the actual state of the soil. Therefore it is proposed to use the incremental change of the layer thickness dh/h, the incremental change of the specific volume dv/v or the incremental change of the void ratio de/e for determining the compression. Especially for large strain ranges (> 30%) a relation between the actual incremental change of thickness of the soil layer dh/h and the effective stress p' is advocated by Butterfield (Butterfield 1979) and Den Haan (Den Haan 1994).

Settlements are no longer described in terms of linear (Cauchy) strains $\varepsilon^C$, but in terms of natural (Hencky) strains $\varepsilon^H$, where:

$$\varepsilon^H = -\int_{v_0}^{v}\frac{dv}{v} = -\ln\left(\frac{v}{v_0}\right) \tag{2}$$

For small strains the linear strain $\varepsilon^C$ and the natural strain $\varepsilon^H$ are related through:

$$\varepsilon^H = -\ln\left(1 - \varepsilon^C\right) \tag{3}$$

Calculated linear strains larger than 30% overestimate the expected real strain (Figure 2). Calculated linear strains can even be larger than 100% (Figure 2) for highly compressible soil close to the surface and a large load increment, like the construction of a road embankment on a peat layer. For natural strains as is illustrated in Figure 2 the 100% strain line is an asymptote.
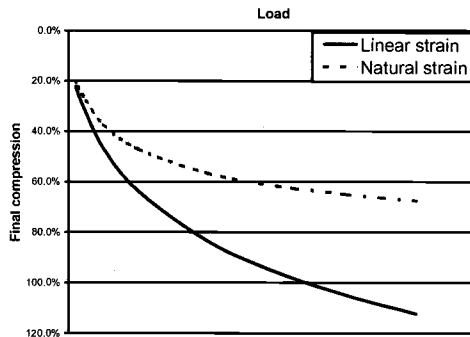


Figure 2 – *Linear (Cauchy) strain and natural (Hencky) strain*

*Time Dependency of Compression of Cohesive Soils*

During compression of cohesive soils, two time dependent phenomena can be observed: dissipation of excess pore pressure (consolidation) and secondary compression (creep). In Figure 3 both phenomena are visualized.
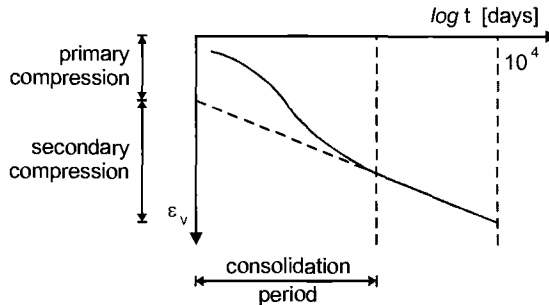


Figure 3 – *Time dependency of compression of cohesive soils*

Because of the presence and incompressibility of pore water and the limited permeability of the cohesive soil, pore water cannot be driven out instantly. Part of the applied load will initially be carried by the pore water, creating excess pore pressure. The drive for equilibrium will transport pore water from a region with excess pore pressures to a region with hydrostatic pore pressures. This process is called consolidation, and will take some time, depending on the permeability of the soil and the gradient in pore pressure. The primary compression will develop as a result of the consolidation process and will be completed when all excess pore pressure has been dissipated. The time at which all excess pore pressure has been dissipated is also called EOP (End Of Primary). The magnitude of the final primary compression and the secondary compression are covered by Bjerrum's compression theory. The consolidation process, however, is not covered. In order to determine the rate of one-dimensional consolidation Terzaghi's theory for one-dimensional consolidation has to be combined with Bjerrum's compression theory, especially for highly compressible soils in which the secondary compression is high. Two-dimensional consolidation is described by Biot (Biot 1940). One-dimensional consolidation, when using vertical drainage is described by Barron/Kjellman (Barron 1948) and Carillo (Carillo 1942).

Because of the uncoupled analysis of consolidation and secondary compression, it is not possible to make an accurate prediction of the time dependent development of the compression and pore pressures. This may be of interest when limited conditions are stated for the stability of an embankment during construction and directly thereafter and for residual settlements after construction and when applying staged constructions.

*Conclusions Concerning Bjerrum's Compression Theory*

Because of the extensive experience, Bjerrum's compression theory for calculating compression has proven its value and is especially useful for materials, which are not highly compressible. It is a reliable method for calculating strains no larger than 30%.

Bjerrum's compression theory also has some limitations: it is not reliable for calculating large strains (> 30%) and it does not offer a coupled analysis of consolidation and secondary compression, it is therefore not possible to accurately determine pore pressures.

**Standards for Determining the Bjerrum Compressibility Parameters from One-Dimensional Consolidation Tests**

The one-dimensional consolidation test or oedometer-test is widely used for the determination of consolidation and compressibility parameters. The test procedures and the calculation of the parameters are described in various national standards. Here the following standards are compared: the ASTM Standard Test Method for One-Dimensional Consolidation Properties of Soils D 2435-96 and ASTM Standard Test Method for One-Dimensional Swell or Settlement Potential of Cohesive Soils D 4546-96, the British Standards Institution BS 1377 – Test 17: Determination of the One-Dimensional Consolidation Properties (BSI 1975) and the Dutch Standards Institution NEN 5118: Geotechnics – Determination of the One-DimensionalConsolidation Properties of Soil (NNI 1991).

Table 1 – *Standards for one-dimensional consolidation tests and parameters described in those standards*

| Parameter | ASTM D 2435 | ASTM D 4546 | BS 1377 Test 17 | NEN 5118 |
|---|---|---|---|---|
| Primary compression (loading) | - | $C_c$ | $r_p$[1] | $C_c$ |
| Seconday compression (creep) | - | - | $r_s$[1] | $C_\alpha$ |
| Swell/recompression (unloading/reloading) | - | $C_s$ | - | - |
| Preconsolidation pressure | $p_c$ | - | - | $p_g$ |
| Coefficient of consolidation | $c_v$[1] | - | $c_v$[1] | $c_v$[1] |

[1] For each load increment

The apparatus and test procedure, described in each of these standards are similar. The interpretation of the test results varies from standard to standard. In Table 1 an overview is given of the different standards and the parameters described in those standards.

In ASTM Standard Test Method for One-Dimensional Swell or Settlement Potential of Cohesive Soils D 4546-96 the possibility is offered to apply an loading-/unloading/reloading schedule, in order to derive swell and/or recompression parameters. In ASTM Standard Test Method for One-Dimensional Swell or Settlement Potential of

Cohesive Soils D 4546-96 and the Dutch standard NEN 5118 (NNI 1991) the compressibility parameters are constants. In the British standard BS 1377 – Test 17 (BSI 1975) the compressibility parameters are stress related.

## Advanced Soil Models and Finite Element Methods

The various national standards do not include advanced deformation models or finite element methods. These models and methods, however, offer the way to a solution of the problems which arose in using Bjerrum's compression theory. Advanced soil models, like the Cam-clay soil model and finite element codes, such as CRISP and Plaxis, already exist for some time. With the ever increasing possibilities of desktop computers, the use of finite element methods came within everybody's grasp. All that is needed now is a suitable soil model, which covers all aspects of compression analyses.

## Cam-clay Soil Model

The first widely used soil model in finite element methods was the Mohr-Coulomb soil model. Most finite element codes for soil and rock include this soil model. The Mohr-Coulomb is not suitable for all cases. Therefore, the Cam-clay soil model was developed at the Cambridge university, United Kingdom. This soil model is able to model the real soil behavior more accurately, than the Mohr-Coulomb soil model.

The compressibility parameters of the Cam-clay soil model can be derived from an one-dimensional consolidation test, using a linear relation between the specific volume v and the natural logarithm of the effective stress p' (Figure 1b, top).

The Cam-clay soil model provides a good description of deformations, not only under compression, but also under deviatoric loading. Using the Cam-clay soil model in combination with a finite element method, it is possible to analyze multiple load steps. However, the model does not account for large strain analyses and time dependent deformation behavior.

Mitachi and Fukuda (Mitachi and Fukuda 1998) have investigated the applicability of the Cam-clay soil model as a constitutive relation for deformation behavior of highly compressible soils. The results are give in Figure 4.

For the analyses of the deformation behavior, Mitachi and Fukuda used the CRISP finite element code with the Cam-clay soil model. The top figure of Figure 4 shows a comparison of the Cam-clay soil model with the results of a consolidated undrained triaxial compression test on peat. The bottom figure of Figure 4 shows a comparison with the results of settlement measurements of an 2 m high embankment on peaty subsoil.

From the top figure of Figure 4 it can be concluded that it is very well possible to calculate the final settlement accurately using the Cam-clay soil model in a finite element analysis, provided the right choice of parameters is made. Therefore Mitachi and Fukuda conclude that the Cam-clay soil model is very well applicable as a constitutive relation for deformation behavior of highly compressible soils. From the bottom figure of Figure 4 it can also be concluded that the Cam-clay model is not able to calculate the deformation process in time accurately. The measurements are not in good agreement with one individual curve.
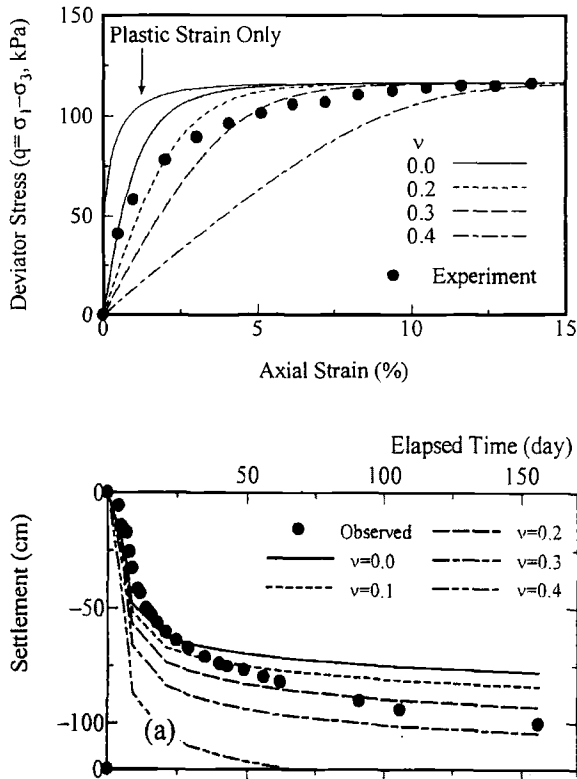
Figure 4 – *Comparison of measured deformation and the results of a parameter study using the Cam-clay soil model (Mitachi and Fukuda 1998)*

**a-b-c Soil Model**

Many investigators have worked on the development of a coupled analysis of consolidation and secondary compression or creep. Some based their research on Bjerrum's compression theory (Garlanger 1972, Szvaits-Nossan 1988, Lan 1992) and others on the use of isotaches (Šuklje 1957, Den Haan 1994).

Den Haan is developing the *a-b-c* soil model, based on the work of Šuklje (Šuklje 1957), Garlanger (Garlanger 1972) and Butterfield (Butterfield 1979). This soil model carries in it the possibility for analyzing large strains, multiple load steps and coupled consolidation and secondary compression and is also referred to as the $C_\alpha$-$C_c$ Isotache soil model.

The volume changes of clay and sand, on which Terzaghi and Bjerrum based there compression theory, are comparatively small in relation to the volume changes of peat and organic clay under compression. The linear relation between the specific volume v

and the $^{10}$logarithm of the effective stress p' is no longer valid for large deformations of highly compressible soils (Figure 5a). For large deformations, a linear relation between the specific volume v and the $^{10}$logarithm of the effective stress p' is physically impossible, because this may result in a strain of more than 100%. Butterfield (Butterfield 1979) and later Den Haan (Den Haan 1994) conclude that on an double logarithm scale, a linear relation exists between the natural logarithm of the specific volume v and the natural logarithm of the effective stress p' (Figure 5b).

From Figure 5c it can be concluded that a unique relation exists between the effective stress p', the strain rate $\dot{\varepsilon}$ and specific volume v (Figure 5c). At constant effective stress p' the specific volume v and hence the creep rate $\dot{\varepsilon}$ decrease. Lines with constant creep rate $\dot{\varepsilon}$ are called isotaches. The isotaches are equidistant for $\dot{\varepsilon}_{i+1} = x \cdot \dot{\varepsilon}_i$, where x is constant for all isotaches.



(a)                    (b)                    (c)                    (d)
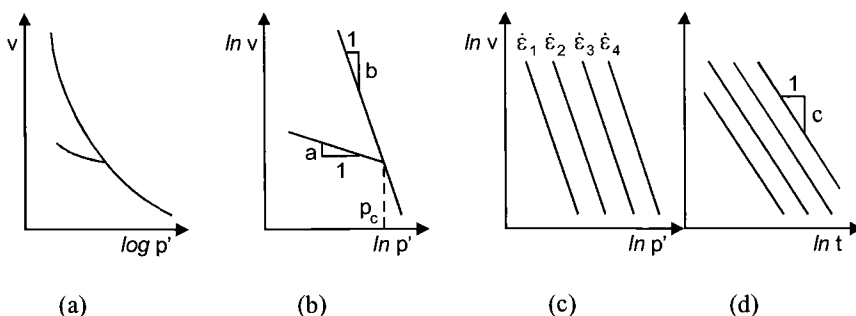
Figure 5 – *a-b-c soil model*

The exact formulation of the *a-b-c* soil model and the definition of the initial situation require further investigation. The *a-b-c* soil model, however, is potentially so powerful that some aspects of the theory are already implemented (Soft Soil Creep model).The Dutch Ministry of Transport, Public Works and Water Management will probably adopt the theory for further development and implementation into their guidelines, handbooks and standards.

## Soft Soil Ceep Model

*Theory*

The before mentioned compression theory of Bjerrum, the Cam-clay soil model and the *a-b-c* soil model all address the compressibility of soils. None of these models cover all aspects of compression, such as large strains, multiple load steps and coupled consolidation and secondary compression. For the combination we need a tool like the finite element method. The Soft Soil Creep model is developed especially for use in finite element models and covers all mentioned aspects of compression. The model is based on the modified Cam-clay soil model, extended with a viscoplastic component and combined with Biot's consolidation theory, to account for consolidation and time

dependent deformation behavior. The natural strains can be simulated, using the updated mesh option.

Where the Cam-clay soil model describes a linear relation between the specific volume v and the natural logarithm of the effective stress p', for the time independent part of the Soft Soil Creep model this relation is transformed to a linear relation between the volume strain $\varepsilon_{vol}$ and the natural logarithm of the effective stress p'. (Figure 1d, top). This is done for numerical reasons. For an one-dimensional consolidation test, the volume strain $\varepsilon_{vol}$ is equal to the vertical strain $\varepsilon_v$.

The viscoplastic component of the soft soil model is derived form the a-b-c soil model and describes a linear relation between the volume strain $\varepsilon_{vol}$ and the natural logarithm of time t ( Figure 1d, bottom).

The Soft Soil Creep model is implemented in version 7.1 of the Plaxis finite element code for soil and rock.

*Verification Using the Results of a One-Dimensional Consolidation Test*

A series of one-dimensional consolidation tests have been performed on clay according to the Dutch standard NEN 5118 (NNI 1991). The clay is supposed to be representative for Dutch soft clays.

The tested clay has the following characteristics: natural unit weight $\gamma_{nat}$ = 15.2 kN/m$^3$, initial sample height $h_0$ = 21 mm, natural water content w = 53%, liquid limit $w_L$ = 112.8%, plastic limit $w_P$ = 28.7%, organic content N = 9.5%, initial void ratio $e_0$ = 1.85, natural permeability k = 2.16 · 10$^{-8}$ m/d, permeability at beginning of test $k_0$ = 6.73 · 10$^{-5}$, change of permeability $c_k$ = 0.53, swelling index $\kappa^*$ = 0.01, compression index $\lambda^*$ = 0.08, creep index $\mu^*$ = 0.006. The parameters $e_0$, k, $k_0$, $c_k$, $\kappa^*$, $\lambda^*$, $\mu^*$ are derived from a one-dimensional consolidation test.
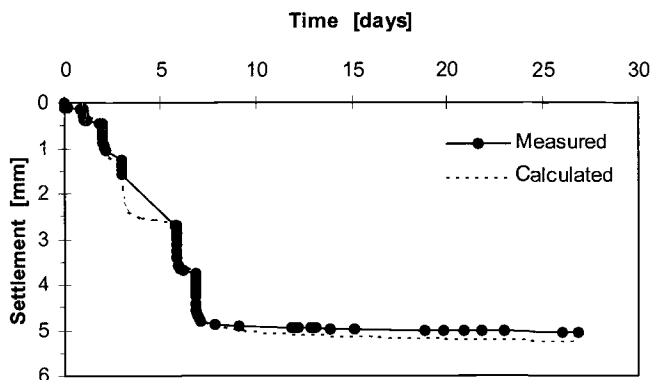


Figure 6 – *Comparison of one-dimensional consolidation test results and finite element analysis using the Soft Soil Creep model (The, Vermeer, and Termaat 1998)*

The tests consisted of a number of 7 load steps. The initial loading was 3.69 kN/m$^2$ and was doubled every 24 hours. The loading sequence was 3.69 - 7.38 - 14.77 - 29.53 - 59.07 - 118.13 - 236 kN/m$^2$. The last load step was maintained for a period of 20 days, in order to investigate the creep characteristics of the soil. In (The, Vermeer, and Termaat 1998) a back analysis of one of the tests is presented, using the Plaxis finite element code for soil and rock and the Soft Soil Creep model. The results are shown in Figure 6.

The results of the finite element analysis are in good agreement with the tests results. From Figure 6 it can be concluded, that the proposed Soft Soil Creep model can describe large strains, as well as coupled consolidation-secondary compression behavior and long term deformation behavior.

*The Vaasa Trial Embankment*

The back analysis of a laboratory test under controlled condition is all very well. But, a new method is not really put to the test, until it is used in a situation, outside the laboratory. In (Vepsälainen, Arkima, Lojander, and Näätänen 1991) a trial embankment near Vaasa, Finland, is presented. Figure 7a shows the layout of the embankment and Figure 7b shows the layout of the instrumentation.



(a)                                      (b)
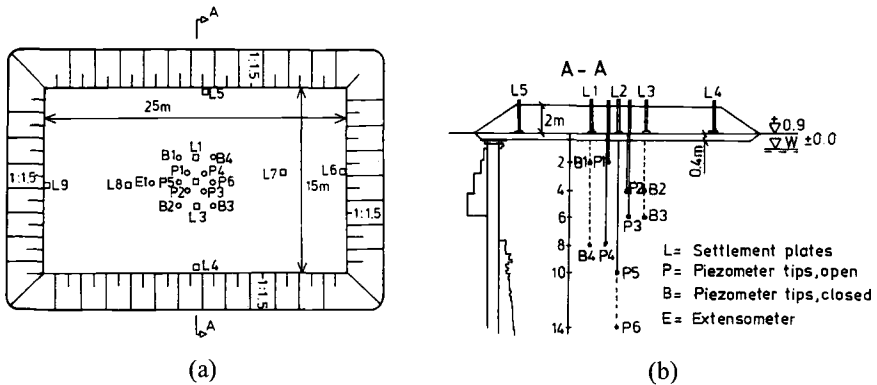
Figure 7 – *Geometry and instrumentation of the Vaasa trial embankment (Vepsälainen, Arkima, Lojander, and Näätänen 1991)*

The subsoil consists of more than 40 m of soft silty clay with high organic content and sulfur. The soil characteristics are given in Table 2. The clay can be considered near homogeneous. The ground water table is approximately 0.5 m below the original surface. Settlements at the base level of the embankment where measured, using settlement plates. Pore pressures were measured, using open and closed piezometer tips. The construction of the embankment took 3 days.

Table 2 – *Soil properties at the Vaasa trial embankment (Vepsälainen, Arkima, Lojander, and Näätänen 1991)*

| Depth [m] | $\gamma_{nat}$ [kN/m³] | $e_0$ [-] | k [m/day] | w [%] | $w_L$ [%] | $w_P$ [%] | $\nu$ [-] | $\kappa^*$ [-] | $\lambda^*$ [-] | $\mu^*$ [-] |
|---|---|---|---|---|---|---|---|---|---|---|
| 0.0-1.0 | 16.0 | 2.0 | $8.70 \cdot 10^{-5}$ | ≈43 | ≈15 | ≈53 | 0.22 | 0.006 | 0.065 | 0.009 |
| 1.0-3.5 | 14.0 | 2.0 | $8.70 \cdot 10^{-5}$ | ≈90 | ≈107 | ≈39 | 0.22 | 0.022 | 0.293 | 0.009 |
| 3.5-7.5 | 14.2 | 2.0 | $2.63 \cdot 10^{-5}$ | ≈89 | ≈103 | ≈33 | 0.15 | 0.029 | 0.325 | 0.014 |
| 7.5-10.5 | 14.7 | 2.0 | $1.33 \cdot 10^{-5}$ | ≈85 | ≈106 | ≈34 | 0.07 | 0.029 | 0.325 | 0.012 |
| 10.5-12.5 | 15.0 | 2.0 | $6.00 \cdot 10^{-6}$ | ≈79 | ≈105 | ≈35 | 0.08 | 0.029 | 0.325 | 0.014 |
| 12.5-30.0 | 16.0 | 2.0 | $1.17 \cdot 10^{-5}$ | ≈71 | ≈103 | ≈34 | 0.08 | 0.039 | 0.390 | 0.015 |

In (The, Vermeer, and Termaat 1998) a back analysis of the settlements and development of pore pressures has been presented, using the Plaxis finite element code for soil and rock and the Soft Soil Creep model. The results are shown in Figure 8.
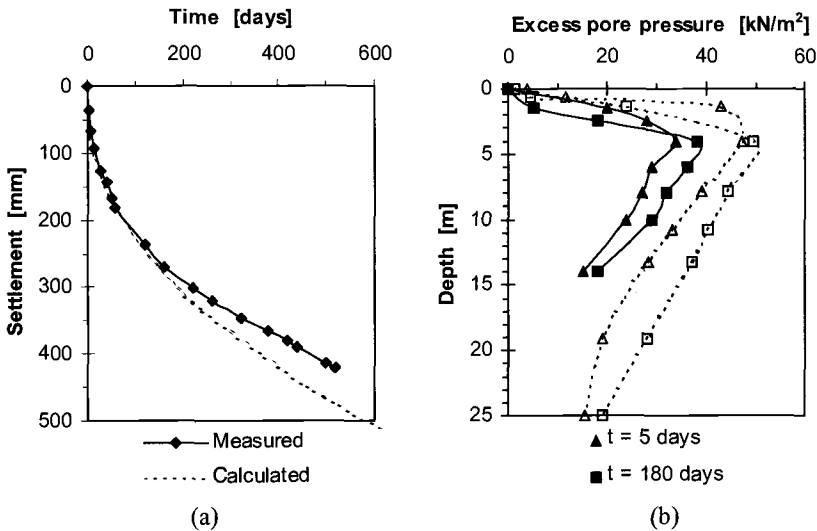
Figure 8 – *Comparison of in situ measurements and finite element analyses using the Soft Soil Creep model*

Figure 8a shows that the calculated settlement overestimates the measured settlement by 11%. Figure 8b shows that the calculated pore pressure overestimates the measured pore pressures by 12%. In geotechnical engineering practice, this is considered to be quite acceptable and even good.

The permeability of the subsoil is derived from one-dimensional consolidation tests. This is not considered to be the best way to determine permeability parameters. If

the permeability of the subsoil would have been determined with greater accuracy, it is expected that the results of the back analysis will be in even better agreement with the measurements.

## Conclusions

The basics of all mentioned compression theories are shown in Figure 1, based on the results of one-dimensional consolidation tests. In Table 3 the compressibility parameters of the different deformation theories are compared for small strains only.

Table 3 – *Comparison of the compressibility parameters for small strains*

| Bjerrum | Cam-clay | a-b-c ($C_\alpha$-$C_c$ Isotache) | Soft Soil Creep Model |
|---|---|---|---|
| (ASTM D 4546-96, BS 1377 – Test 17, NEN 5118) | | (CUR 1996, Heemstra and Deutekom 1994, Den Haan 1994) | (The, Vermeer, and Termaat 1998, CUR 1997) |
| $C_c$ | $\lambda \cdot ln10$ | $b \cdot (1 + e_0) \cdot ln10$ | $\lambda^* \cdot (1 + e_0) \cdot ln10$ |
| $C_s$ | $\kappa \cdot ln10$ | $a \cdot (1 + e_0) \cdot ln10$ | $\kappa^* \cdot (1 + e_0) \cdot ln10$ |
| $C_\alpha$ | - | $c \cdot (1 + e_0) \cdot ln10$ | $\mu^* \cdot (1 + e_0) \cdot ln10$ |

Using Bjerrum's compression theory as well as with the Cam-clay soil model it is possible to make rather accurate predictions of final settlements, as long as no highly compressible soil is considered. However, the settlement process until final settlement has been reached and the actual pore pressures cannot be accurately described by both soil models.

The principle of the *a-b-c* soil model has none of the limitations mentioned earlier; however, this soil model is still under development.

Viscoplasticity is modeled by the Soft Soil Creep model and implemented in the Plaxis finite element code for soil and rock. This Soft Soil Creep model is actually a combination of the modified Cam-clay soil model, Biot's consolidation theory and viscoplasticity, based on the *a-b-c* soil model. The Soft Soil Creep model has proven its usefulness in evaluating one-dimensional consolidation tests performed on Dutch soft clays and in evaluating the settlments of the Vaasa trial embankment on soft clay.

Implemented in a finite element code, this soil model offers a practical tool for everyday engineering practice for calculating long term deformation behavior of highly compressible soils.

## References

Barron, R. A., 1948, "Consolidation of Fine grained Soils by Drain Wells," *Transactions*, Vol. 113, Paper No. 2346, American Society of Civil Engineers, pp. 718-743.

Biot, M.A., 1940, *General Theory of Three-Dimensional Consolidation*, Colombia University, New York, United States of America.

Bjerrum, L., 1967, "Engineering Geology of Norwegian Normally-Consolidated Marine Clay as Related to Settlements of Buildings," *Géotechnique* **17**, No. 2., pp. 83-118

British Standards Institution (BSI), 1975, "Determination of the One-Dimensional Consolidation Properties," *Methods of Test for Soils for Civil Engineering Purposes, BS 1377 : 1975*, British Standards Institution, Milton Keynes, United Kingdom, pp. 92-99.

Butterfield, R., 1979, "A Natural Compression Law for Soils (an Advance on *e*-log p')", *Géotechnique* **29**, No. 4, pp. 469-480.

Carillo, N., 1942, "Simple Two and Three Dimensional Cases in the Theory of Consolidation of Soils," *Journal of Mathematical Physics*, Vol. 21, American Institute of Physics, pp. 1-5.

Centre for Civil Engineering Research and Codes (CUR), 1996, *Building on soft soils,* A.A. Balkema, Rotterdam, The Netherlands.

Centre for Civil Engineering Research and Codes (CUR), 1997, *Backgrounds on Numerical Modeling of Geotechnical Structures,* part 2, Centre for Civil Engineering Research and Codes, publication 191, Gouda, The Netherlands (in Dutch).

Den Haan, E. J., 1994, *Vertical Compression of Soils,* Ph. D. Thesis, Delft University Press, Delft, The Netherlands.

Dutch Standards Institution (NNI), 1991, *Geotechnics - Determination of the One-Dimensional Consolidation Properties of Soil*, NEN 5118, Dutch Standards Institution, Delft, The Netherlands (in Dutch).

Garlanger, J. E., 1972, "The Consolidation of Soils Exhibiting Creep under Constant Effective Stress," *Géotechnique* **22**, No. 1, pp. 71-78.

Heemstra, J., and Deutekom, J. R., 1994, "Compression, but Different: the Similarities Between the Koppejan Method and the Den Haan Method," *Road Building Workshop 1994*, part III, CROW, publication 82, Gouda, The Netherlands, pp. 1055-1066 (in Dutch).

Lan, L. T., 1992, *A model for One-Dimensional Compression of Peat*, Ph. D. Thesis, University of Wisconsin, United States of America.

Mesri, G., Kwan Lo D. O., and Tao-Wei Feng, June 1994, "Settlement of Embankments on Soft Clays," *Geotechnical Special Publication*, No. 40, Vol. 1, Yeung, A. T., and Félio, G. Y., Eds., American Society of Civil Engineers, pp. 8-56.

Mitachi, T., and Fukuda, F., October 1998, "Applicability of Cam-clay Model as a Constitutive Relation for Consolidation-Deformation Coupled Three Dimensional FE Analysis for Highly Organic Soft Ground," *Proceedings of the International Symposium on Problematic Soils*, Vol. 1, E. Yanagisawa, N. Moroto, and T. Mitachi, Eds., A.A. Balkema, Rotterdam, The Netherlands, pp. 65-68.

Šuklje, L., August 1957, "The Analysis of the Consolidation Process by the Isotaches Method," *Proceedings of the Fourth International Conference on Soil Mechanics and Foundation Engineering*, Vol. I, Div. 1-3a, Butterworths Scientific Publications, London, United Kingdom.

Szvaits-Nossan, V., 1988, *Intrinsic Time Behavior of Cohesive Soil During Consolidation*, Ph. D. Thesis, University of Colorado.

The, B. H. P. A. M., Vermeer, P. A., and Termaat, R. J., October 1998, "A Viscoplastic Creep Model for the Engineering Practice," *Proceedings of the International Symposium on Problematic Soils*, Vol. 1, E. Yanagisawa, N. Moroto, and T. Mitachi, Eds., A.A. Balkema, Rotterdam, The Netherlands, pp. 657-660.

Vepsälainen, P., Arkima, O., Lojander, M., Näätänen, A., 1991, "The Trial Embankments in Vaasa and Paimio, Finland," *Proceedings of the X$^{th}$ European Conference on Soil Mechanics and Foundation Engineering*, Vol. II, A.A. Balkema, Rotterdam, The Netherlands, pp. 633-640.

I. R. McDermott,[1] A. D. King,[2] C. M. T. Woodworth-Lynas,[3] and P. LeFeuvre[2]

**Dewatering Structures in High Water Content Materials**

**Abstract:** This paper describes the behaviour of soft soils created by the rapid deposition of a sediment slurry and the mechanisms by which pore fluid escapes from the consolidating bed. Such rapid deposition occurs as a result of dumping dredge spoils at sea or in the case of disposing of mine tailings in settling ponds. Soft soils may experience a variety of natural deformations during consolidation. Consolidation-related structures are commonly observed in settling column experiments, geotechnical centrifuge tests and in the field. This paper deals with the specific class of soft-sediment intrusive and extrusive dewatering structures called respectively pillars and boils (or sediment volcanoes) that form spontaneously through self-weight consolidation. Dewatering structures were formed during self-weight consolidation centrifuge experiments of a naturally-occurring marine sediment under the influence of high "$g$" conditions. A description of the phenomenon is given, describing the geometry and nature of the dewatering structures observed, and highlights some of the soil physical properties and depositional conditions which appear to control the formation of the structures. This phenomenon is believed to have relevance to dredge spoil and mine tailing disposal, and to the safe handling and disposal of polluted high water content soil-like wastes.

**Keywords:** consolidation, centrifuge, dewatering structures, soft soils, sediment, dredge spoils, mine tailings, grain size, pore fluid

---

[1] Director Geophysics, C-CORE, Memorial University of Newfoundland, St. John's, Newfoundland, Canada, A1B 3X5.

[2] Research Engineer, C-CORE, Memorial University of Newfoundland, St. John's, Newfoundland, Canada, A1B 3X5.

[3] President, PETRA International, Cupids, Newfoundland, Canada, A0A 2B0.

64

## Introduction

Soft soils are broadly defined as those with high water contents that have very low shear strength and exhibit large strains during consolidation. Examples of such soils include mine tailings, marine sediments and dredge spoils. Consolidation theories that are used to predict the behaviour of soft soils during self-weight consolidation all make the same basic assumption: pore water which is expelled during the consolidation process migrates uniformly through the soil mass under the influence of excess pore pressure gradients. The phenomenon of flow channeling has been noted in the field, during laboratory settling column experiments and during geotechnical centrifuge self-weight consolidation experiments. These, so called, dewatering structures are localized macrostructural features resulting from preferential flow paths or flow channeling. Figure 1 shows such a structure, as seen through the wall of a glass cylinder, formed in a Speswhite kaolin clay slurry undergoing self-weight consolidation under normal laboratory conditions. When dewatering structures are observed then the assumption of uniform pore fluid migration may not always be appropriate when attempting to apply existing consolidation theories to self-weight consolidation.

The process of flow channeling during self-weight consolidation results in the formation of boils on the surface of the soil. Dyer (1986) explains that during self-weight consolidation the escaping pore water can cause "piping" within the bed and that pore fluid, instead of escaping uniformly upwards, travels sideways towards regions of higher permeability. Such "tributary-like" migration to a common focal point within the soil then triggers fluidization and creates the vertical conduits. These conduits emerge at the surface according to Dyer (1986), "as small fairly evenly spaced holes." Such extrusive dewatering structures are known as boils or sediment volcanoes. The development of sediment volcanoes has also been reported in settling column experiments by Been



Figure 1 - *A Dewatering Structure (Highlighted) in Speswhite Kaolin Clay*

(1980) who observed that the dewatering structures in his experiments appeared as several pipes, 1-2 mm in diameter, rising almost vertically through the mud. He described how the water flow entrains the surrounding soil particles and carries them upwards so

that the soil is in a quick (i.e. liquified) condition in a localised area around the channel. Been describes how, at the sediment/water interface the dewatering structure "appears as if a volcano is erupting there, with the soil deposited in a cone around the pipe outlet."

Been (1980), Elder (1985) and McDermott (1992) document some of the conditions which govern the formation of dewatering structures and regulate consolidation behaviour. Elder describes a critical initial slurry density of approximately 1.130 kg/m$^3$ (void ratio of 12) for Combwich mud. If the deposited slurry has a density below this critical value, the soil will exist initially as a suspension with pore pressures equal to the total vertical stress and with no effective stresses present. With increasing time, a denser sediment layer, in which effective stresses are greater than zero, will accumulate upwards from the base. Been (1980) noted that during its consolidation such a soil bed exhibits a unique void ratio - effective stress relationship; has considerable soil particle segregation and that dewatering structures are present. If a soil slurry is deposited above this critical density, Elder (1985) observed that no suspension phase occurs and surface density increases slowly with time. There is a near immediate increase in effective stress with no significant compression. This resulted in quite different consolidation behaviour in which different elements within the same soil mass followed different consolidation paths. A non-unique void ratio/effective stress relationship was evident. This meant that potentially any value of void ratio could be associated with a wide range of effective stress. This behaviour is indicative of time dependent compression or creep (Elder 1985). Elder and Sills (1984) described this phenomenon as being the result of collapsing soil structure, with the flocs either breaking down or rearranging themselves such that a smaller rise in effective stress resulted. Significantly, this change in consolidation behaviour resulted in practically no soil particle segregation and no visible dewatering structures. Similar soil behaviour was observed by McDermott (1992) in a series of settling column experiments on Irish Sea sediments.

The dewatering structures observed during self-weight consolidation of soft soils appear to be similar, at least in general outward appearance, to a variety of water release structures observed in a variety of geological settings. Dewatering structures are commonly observed preserved in sedimentary rocks (Johnson 1977; Mount 1993). Lowe (1975) identifies a variety of processes which result in the formation of water escape structures in natural sediments. Dewatering structures have also been observed during the construction of dikes (Neumann-Mahlkau 1975).

## Dewatering Structures Observed During Centrifuge Modelling

A number of studies have used geotechnical centrifuges to model the self-weight consolidation of soft soils. Mikasa and Takada (1984) used a 3 metre diameter centrifuge in Osaka, Japan to determine the self weight consolidation characteristics of dredged material and to determine its suitability as raw material for the construction of artificial islands. The consolidation behaviour of phosphate mine tailings material has also been modelled in geotechnical centrifuges (Bloomquist and Townsend 1984, Scully et al. 1984). The self-weight consolidation behaviour of gold mine tailings has also been

modelled in the geotechnical centrifuge at the University of Western Australia (Stone et al. 1994). The consolidation behaviour of kaolinite clay was modelled using the geotechnical centrifuge at the University of Colorado (Croce et al. 1984) and the centrifuge scaling laws were verified.

Although there are a number of accounts of geotechnical centrifuge use to model self-weight consolidation of soft-soils, there has been no discussion of the formation of dewatering structures. Dewatering structures have often been observed during centrifuge modelling in the 5.5 metre radius geotechnical centrifuge at C-CORE. Dewatering structures were also observed during self-weight consolidation tests in a small bench-top centrifuge with a radius of less than 0.5 metres (McDermott and King, 1998). To date, the majority of centrifuge self-weight consolidation tests carried out at C-CORE have involved the use of kaolin clay. Kaolin clay slurries which undergo self-weight consolidation in either the geotechnical or benchtop centrifuge form prominent
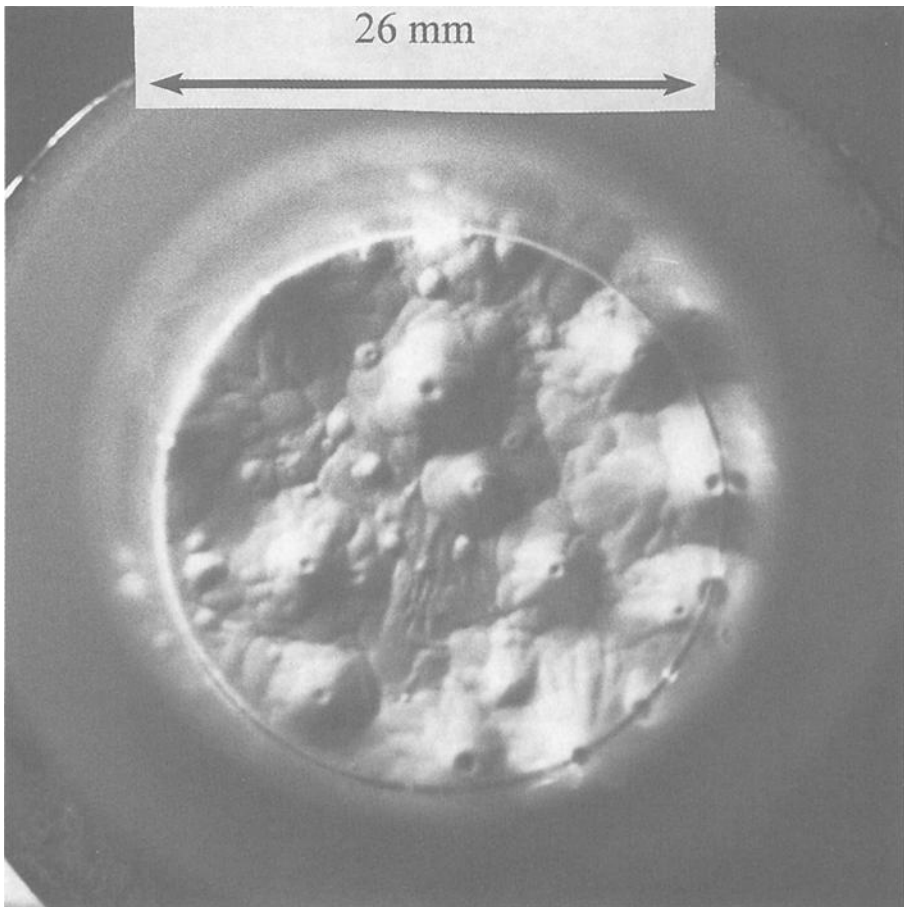


Figure 2 - *Boils on the Surface of a Speswhite Kaolin Clay Sample*

dewatering structures on the surface. Figure 2 shows typical boils formed on the surface of a kaolin clay slurry consolidated by self-weight in the bench-top centrifuge. This sample had an initial water content of 100%, an initial height of 98 mm and was consolidated under a mean acceleration of 750 g's. Surface settlement was monitored during testing and indicated that 100% primary consolidation was achieved within 4 hours of starting the test. During this time the sample strain was approximately 35%. Similar structures were observed during self-weight consolidation experiments in C-CORE's geotechnical centrifuge, although these experiments were conducted at lower g-levels (around 100 g) and, to date, have been carried out with kaolin slurries with initial water contents of 500%. Post-test analysis of kaolin samples has not revealed any discernable internal structure associated with the boils on the sample surfaces.

## Dewatering Structures Observed in Combwich Mud

One material which was tested using the bench-top centrifuge was Combwich mud, a marine sediment from the coast of England. The bench-top centrifuge, described by McDermott and King (1998), is a simple device which is often used for preliminary testing and evaluation of self-weight consolidation characteristics in readiness for large scale geotechnical centrifuge testing. For testing purposes a slurry of Combwich mud with a water content of 115% was made up. Two samples were used in the bench-top centrifuge experiment. The samples required approximately 7 hours to consolidate under a mean acceleration of 750 g. During this time the sample heights decreased from an average of 99 mm to 71 mm. The dewatering structures observed on the surface of the specimen differed somewhat from those observed on kaolin clay specimens, and were less numerous and less prominent (i.e. had fewer vertical and horizontal extents). They resembled shallow pockmarks on the surface of the sample, rather than the mounds visible on the surface of kaolin samples (Figure 2). Part of the routine post-test analysis of samples tested in the bench-top centrifuge was to slice the sample into thin sections to allow the variation of water content over the height of sample to be determined. During this process, using the first sample, it was observed that the sample did not have uniform colouration. A number of distinct beige coloured "spots"(perhaps a millimetre or two in diameter) were observed within each of the sections. Furthermore, these "spots" appeared to be continuous from slice to slice. It was realized that the spots represented sectioned dewatering structures and that to trace and reconstruct the paths of these dewatering "channels" might prove a worthwhile exercise.

It became obvious that cutting wet samples with a thin blade caused undesirable disruption of the sample surface and that a different technique was required in order to trace the dewatering channels. It was found that the dewatering structures could be maintained by drying the sample and then removing very thin layers using a high speed grinding wheel. As each layer was removed a photograph was taken for analysis. The thickness of the layer removed was determined by comparing successive measurements of total sample height. The average thickness removed for each layer was 2 millimetres. It should be noted that when the sample was dried there was some shrinkage. The

original height was 71 millimetres and the dried height was 65 millimetres. The original diameter was 26 millimetres and dried diameters varied from 22.4 millimetres at the bottom to 17.8 millimetres at the top.

The photographs of the various sample sections were transferred onto CD-ROM. The images were imported into an image processing software package, filtered and inverted so that the previously light coloured channels were converted to black areas on a white background. The images were then saved and imported into MATLAB® where a program, written specifically for the task, determined the position of each flow channel after correcting it for sample shrinkage during drying. An additional routine was written to display this data in a 3-dimensional format, shown in Figure 3. A colour animated Graphics Interchange Format (GIF) bitmap version of this image is also available from the authors upon request. This animation



Figure 3 - *Reconstructed Dewatering Structure Paths*

assists in the visualization of the dewatering structures. There was a certain degree of subjective judgement required in order to connect the individual points into three-dimensional channel structures and the figure represents the "best fit." There are seven distinct structures in the sample as illustrated in Figure 3. There is no obvious pattern to the distribution of the dewatering structures or the surface boils being randomly distributed throughout the sample. The structures show the convoluted nature of the channels. Some channels bifurcate and merge together again, higher in the sample column, while others are single conduits.

**Grain Size Analysis**

The mechanism by which the dewatering structures form is not known, but it was thought that a close examination of the grain size distribution of the consolidated sample could yield some insight into the process. Prior to centrifuge testing, the homogeneous Combwich mud slurry was a light brown colour. After testing, three distinct zones of

colouration were to be observed in the sample: Zone 1, forming a 10 mm layer at the top
of the sample, had a dark brown colouration;  Zone 2, making up the bulk of the
remaining sample, had the same colour as the original slurry; Zone 3 , representing the
dewatering structures, had a distinctly beige colouration.

It was thought that the darker (Zone 1) material on the top of the sample was
transported or flushed to the top of the sample (possibly at the time of deposition) and
would consist of smaller grain sizes, while the beige coloured (Zone 3) material left in the
channels would be a coarser material.  This would be consistent with  observations by
Lowe (1975)  of grain size segregation due to dewatering structure formation.  In the
upper portion of the dried sample it was difficult to determine the position of the channels
because there was no beige (Zone 3) material visible within the individual channels. This
would also seem to support the conclusion that the beige material, observed in  channels
deeper in the sample, was coarser material left behind when the fluid moving through the
channel transported the smaller, darker particles to the top of the sample.

These conclusions are supported by results from grain size analysis. The small amount
of material required the use of a Sedigraph 5100 Particle Size Analyzer. The Sedigraph
was used to determine the grain size distribution of the original sediment, the material
transported to the top of the sample, the material in the channels within the soil sample
and the material surrounding the channels.  Results are shown in Figure 4. First, it should
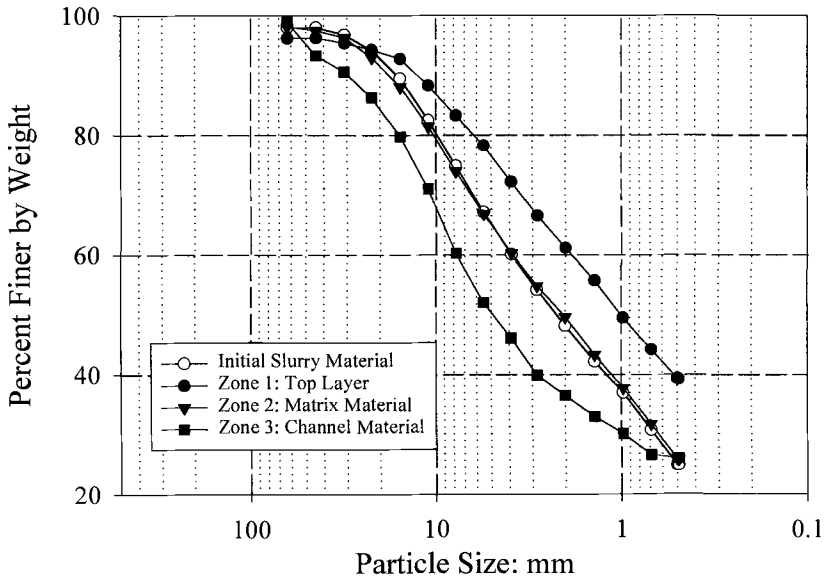


Figure 4 - *Grain Size Curve for Combwich Mud Sample*

be noted that the grain size distribution of the matrix material (Zone 2) surrounding the channels and the initial slurry material is virtually identical. This indicates that very little, if any, of the fines transported to the surface originated from the soil matrix between the flow channels. Secondly, the contrast between the material in the channels and on the surface is obvious proving that the conclusion of transport of fines to the surface is correct.

## Conclusions

The dewatering structures observed within the Combwich mud sample were visible by virtue of the fact that there was a marked difference in both grain size and colour between the channels and the surrounding matrix. The variation in colour provided sufficient contrast that the channels could be easily traced through the sample. These structures were distinct and appeared to be of a fairly consistent spatial density throughout the height of the sample. The number of dewatering structures within a material may be estimated to a reasonable degree of accuracy by a simple count of the number of sediment volcanoes at the surface. The density of the Combwich mud ($1408$ kg/m$^3$) was greater than the $1130$ kg/m$^3$ critical density reported by Elder (1985). Elder had reported that no dewatering structures were evident in Combwich mud settling column experiments above this critical density. This difference suggests that either increased stress levels or higher gradients, created in this case by the enhanced g-level, induces the formation of dewatering structures at higher initial densities. This phenomenon in itself is worthy of further investigation.

Previous work with kaolin clay in the bench-top centrifuge has indicated that its permeability and compressibility can be determined with a reasonable degree of accuracy based on its behaviour during self-weight consolidation (McDermott and King 1998). Significant formation of dewatering structures can be observed during these tests suggesting that their formation does not drastically alter the consolidation characteristics of the sample.

There are a number of engineering implications associated with dewatering structures. Probably the most important feature is the transport of fines to the surface of samples by the formation of dewatering structures observed during 1-g column tests and in the field. Fine grain cohesive materials are known to be effective natural sequestering agents for pollutants such as hydrocarbons, polychlorinated biphenyls (PCBs) and heavy metals. Dewatering structures result in the accumulation of finer material at the surface and hence could lead to the preferential concentration of pollutants at the surface. In some cases this may be desirable, allowing the pollutants to be easily treated or removed during site remediation. In other cases it may be preferable to keep the pollutants dispersed throughout the deposit. An example of this would be a case in which these dewatering structures led to the concentration of pollutants at the surface of contaminated dredge spoil mounds which had been mass dumped at sea, or in mine tails holding ponds. This is an undesirable condition since pollutants may be resuspended and possibly introduced into the overlying water column by a variety of mechanisms. These mechanisms include

the action of water currents or waves and, in the case of dredge spoil mounds, surface slumping.

Darcy's Law, which states that the velocity of the flow of water through a soil is directly proportional to the hydraulic gradient, is assumed to be valid for commonly used one dimensional finite strain consolidation theories such as that of Gibson et al (1967). Dewatering structures may be the reason why this assumption appears to be true for soft soils  and why large strain models, such as that of Gibson's et al, have been so successful in modelling their self-weight consolidation behaviour.

A more extensive investigation, than reported here, is needed in order to explore the dewatering structure phenomenon. This investigation should identify the soil properties and associated environmental factors which govern the formation of de-watering structures. Further investigations into the implications of the phenomenon in terms of environmental engineering would be particularly beneficial for reasons described above.

*Acknowledgments*

**References**

Been, K., 1980,  *Stress Strain Behaviour of a Cohesive Soil Deposited Under Water,*
        PhD. Thesis, University of Oxford.

Bloomquist D. G. and Townsend F. C., 1984, "Centrifuge Modelling of Phosphatic Clay
        Consolidation," *Proceedings, Symposium on Sedimentation/Consolidation
        Models: Prediction and Validation,* pp. 565-580.

Croce P., Pane V., Znidarčić, D., Ko H. Y., Olsen H. W. and Schiffman R. L., 1984,
        "Evaluation of consolidation theories by centrifuge modelling," *Proceedings of
        International Conference on Applications of Centrifuge Modelling to
        Geotechnical Design,*  pp. 381-396.

Dyer, K. R., 1986,  *Coastal and Estuarine Sediment Dynamics,*  John Wiley and Sons,
        Chichester.

Elder, D. McG., 1985, *Stress Strain and Strength Behaviour of Very Soft Soil Sediment*, PhD. Thesis, University of Oxford.

Elder, D. McG. and Sills, G. C., 1984, *Time and Stress Dependent Compression in Soft Sediments*, University of Oxford Soil Mechanics Report No. SM048/84.

Gibson, R. E., England, G. L. and Hussey, M. J. L., 1967, "The Theory of One Dimensional Consolidation of Saturated Clays," *Geotechnique*, Vol. 17, pp. 261-273.

Johnson, H. D., 1977, "Sedimentation and Water Escape Structures in some Late Precambrian Shallow Marine Sandstones from Finnmark, North Norway," *Sedimentology*, Vol. 24, pp. 389-411.

Lowe, D. R., 1975, "Water Escape Structures in Coarse Grained Sediments," *Sedimentology*, Vol. 22, pp. 157-204.

McDermott, I. R. and King, A. D., 1998, "Use of a Bench-Top Centrifuge to Assess Consolidation Parameters," *Proceedings of the Fifth International Conference on Tailings and Mine Waste '98*, Fort Collins, Colorado, 26-28 January, pp. 281-288.

McDermott, I. R., 1992, *Seismo-Acoustic Investigations of Consolidation Phenomena*, PhD Thesis, University of Wales.

Mikasa M. and Takada N., 1984, "Selfweight Consolidation of Very Soft Clay by Centrifuge," *Proceedings, Symposium on Sedimentation/Consolidation Models: Prediction and Validation*, pp. 121-141.

Mount, J. F., 1993, "Formation of Fluidization Pipes during Liquefaction; Examples from the Uratanna Formation (Lower Cambrian), South Australia," *Sedimentology*, Vol. 40, pp. 1027-1037.

Neumann-Mahlkau, P., 1975, "Recent Sand Volcanoes in the Sand of a Dyke Under Construction," *Sedimentology*, Vol. 23, pp. 421-425.

Scully R. W., Schiffman R. L., Olson H. W., and Ko H., 1984, "Validation of Consolidation Properties of Phosphatic Clay at Very High Void Ratios," *Proceedings, Symposium on Sedimentation/Consolidation Models: Prediction and Validation*, pp. 158-181.

Stone K. J. L., Randolph M. F., Toh S. and Sales A. A., 1994, "Evaluation of Consolidation Behaviour of Mine Tailings," *Journal of Geotechnical Engineering*, Vol. 120, No. 3, pp. 473-490.

Arieh Klein[1] and Robert W. Sarsby[2]

**Problems in Defining the Geotechnical Behaviour of Wastewater Sludges**

---

**Abstract:** Wastewater sludge can be viewed as a geotechnical material from the moment it is placed on the ground, as landfill, lagoons or capping layers for landfill. Wastewater, or sewage sludges show unpredictable behaviour owing to the floccular nature of the 'solid' part of the material, and because of the high bonding, or adsorption, of the liquid phase within and around these flocs.

The authors have carried out a series of tests, including consolidation and shear strength tests, in order to attempt to characterise the geotechnical engineering and consolidation behaviour of these sludges. The great influence of the gaseous phase is discussed, both in the light of the test results, and with reference to published descriptions of sludge behaviour in an actual slip of lagooned wastewater sludge.

A model for the consolidation behaviour of lagooned wastewater sludge is postulated, based on published descriptions of pore fluid distribution within the floccular structure of sludges. This model has to take into account the different solid, liquid and gas phases in the sludges, the compressibility of both the 'solid' phase (the sludge flocs) and the liquid phase (the viscous pore fluid). Simplifications are necessary for the model to be useful in explaining test and field observations and in predicting future behaviour.

**Keywords:** wastewater, sewage, sludges, flocs, consolidation, shear strength, gaseous phase, pore pressure

**Introduction**

Wastewater, or sewage sludge is a by-product of the wastewater treatment process, and as such is essentially a man-made material. Therefore, such a medium should

---

[1]Geotechnical and Geoenvironmental Consultant, 49/4 Einstein St., Haifa, 34602, Israel.
[2]Professor of Geotechnical Engineering, Faculty of Technology, Built Environment, Bolton Institute, Deane Road, Bolton BL3 5AB, England.

be amenable to engineering behaviour analysis and prediction, in a similar manner to other soft, fibrous materials encountered in Civil Engineering.

However, in reality, wastewater sludges show unpredictable engineering behaviour, which can be attributed to a number of causes. Firstly, the engineering process for treating and dewatering the raw wastewater involves, in most plants, the addition of flocculating agents, which affect the final structure of the wastewater sludge. Secondly there is a problem of ongoing or re-activated decomposition of the organic content of the sludge – especially if it is disturbed, warmed or aerated. Thirdly the nature and composition of the pore fluid is likely to change with time. This pore fluid is far from being water, and is in reality a viscous fluid with a tendency to set like a gel.

Claydon et al. (1997) described in detail the failure of a wastewater sludge tip or lagoon in Deighton, Yorkshire (North England), which occurred in February, 1992. Approximately 250,000 $m^3$ of material suddenly and without warning, moved a distance of up to 100 m., from a tip which contained about 750,000 $m^3$. The resulting investigation revealed that industrial and wastewater sludges had been placed in the lagoon for a period of up to ninety years. During this period a mixture of pressed sludge cake and hardcore (builders rubble, etc.) had been placed in an effort to increase the stiffness, or strength of the stored material. However it must be noted that the tip was not formally engineered and the fill was placed in a haphazard manner.

Immediately after the failure, the material which flowed from the tip was found to consist of extensive areas of soft black sludge, with a consistency similar to semi-liquid peat, which would not support the weight of a person together with pools of dark coloured liquid leachate and rafts (up to 3 m. thick) of stronger material comprising discarded excavated subsoil, demolition rubble and other debris. Significantly, Claydon et el. (1997) also reported that immediately after the slip occurred, gas bubbles could be seen emanating from liquid filled pockets and that a strong unpleasant odour was noticeable. It was stated that the mechanism of failure was almost certainly a result of the surcharging of soft normally consolidated sludge by the dense clay/rubble/sludge cake capping. This surcharging, together with other factors (such as deterioration of engineering properties due to ongoing sludge decomposition and decreasing effective stresses due to gas generation) triggered a slip of the front face of the tip. Movement of the retaining bund allowed mobilisation of the very soft sludge and the development of the large scale undrained flow slide. The authors also noted that gas pressures of up to 35 kPa were noted at certain of the boreholes/gas monitoring wells. Analysis of the survey of the conditions and the soil/sludge profile at Deighton, leads one to the conclusion that the sludge, even at depths of 9 m. or more, remained microbiologically active in the lagoon for up to ninety years.

Within Britain there are thousands of lagoons containing wastewater sludge (just like the one at Deighton) which have the potential to create significant environmental pollution. These lagoons have not been engineered and their stability is uncertain. Furthermore the stability of these lagoons is unlikely to improve with time because of the poor consolidation settling properties of the sludges, continued input of liquid (rainwater) into the sludge, and  leakage from the sites. In order to determine the stability of these lagoons and develop remediation programmes it is necessary to quantify the engineering properties of these wastewater sludges. This is the overall objective of the Authors' work

on wastewater sludges; specific objectives are to elucidate the consolidation behaviour and shear strength characteristics of these extremely soft, fibrous materials.

## Background

Vesilind and Martel (1990) postulated a classification for the viscous pore liquid, or pore water distribution in sludges, involving four types of liquid, dependent on the freedom of the liquid molecules to move in the sludge suspension, and on their degree of association with the sludge solids (see Figure 1). In this model, 'free water' was defined as the liquid not associated with the sludge solids, moving independently of the solids and surrounding the sludge flocs. Liquid trapped within the floc structure, travelling with the floc or held by capillary forces between the particles inside the floc, was defined as 'interstitial water'. When the flocs are broken up, by mechanical or other means, then at least some of the interstitial water becomes free water. The third category postulated was that of liquid associated with individual particles within the floc. These liquid molecules are held to the particles by surface forces, and the liquid is known as 'surface water'. The authors stated that this liquid cannot be removed by mechanical means. Finally, the authors defined 'bound water'. The molecules of liquid in bound water are chemically bound to the sludge particles and the authors suggested that they can only be released by the thermochemical destruction of the particles.
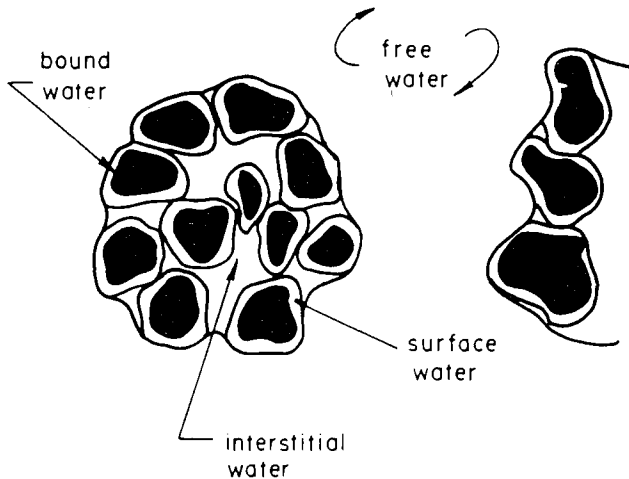


Figure 1 – *Postulated Pore Liquid Distribution in Sludge Flocs*

It has been known for some time that bacterial activity affects the engineering behaviour of soils and sands. For example, Gupta and Swartzendruber (1962) described the effect of bacterial activity on the hydraulic conductivity of quartz sand, even when boiled deionized water was used for the tests at room temperature. They found that at a

level of over 400,000 bacteria per gram, there was a drastic reduction in the hydraulic conductivity of the sand. This effect was found to be localised near the water inlet end of the permeameter cell, and the effect was eliminated when 0.1% phenol (a well-known anti-bacterial agent) was added to the water, and reasonably well eliminated if the flow system was kept at a temperature just above freezing. Gupta and Swartzendruber (1962) discussed the fact that the mechanism by which bacteria decrease the hydraulic conductivity is unclear. They stated that the critical threshold bacterial number of 400,000/g. would only occupy 0.00031% of the total void volume of the sand, thereby ruling out the direct effects of the bacterial bodies on the conductivity, unless they were strategically located at grain contacts throughout the sand, so that the relatively few organisms could seal off whole pores. No information has been found on research work into the effect of bacterial activity on the geotechnical behaviour of wastewater sludge, and the Authors of this paper believe that the topic has not been studied before.

A number of attempts have been made to develop a unified theory of sedimentation and consolidation (Schiffman, et al., 1985, Toorman, 1996), generally of clay materials. Schiffman, et al. (1985), proposed a descriptive model for the process of flocculation/sedimentation/consolidation, based on the work of Imai (1981), which postulated a boundary between the upper settling zone and the sediment as 'the birth place of the new sediment'. In this model all of the sediment thus formed undergoes self-weight consolidation and finally approaches an equilibrium state. In another section of this paper, Schiffman, et al. (1985) stated that it appears that there is also a thin transition zone separating the settling and consolidation zones where the effective stresses are non-zero, but do not follow the classical Terzaghi equation. Interestingly, in another related paper on nonlinear finite strain sedimentation and consolidation (Schiffman, et al., 1984), the authors stated that atmospheric pressure affected the pore liquid pressure values obtained in analysing the sedimentation/consolidation behaviour of a slimes, or tailings, settling impoundment, and if this was not taken into account, this could lead to 'negative' pore water pressures.

Wastewater sludge may be compared to non-preloaded (non-consolidated) cohesive soils with a high content of organic components. For soft cohesive soils Hvorslev (1960) has suggested an exponential relation between water content $w$ and undrained shear strength $C_u$ such that if $Cu_0$ is the undrained shear strength at initial water content $w_0$:

$$C_u = Cu_0 . e^{[\gamma_s (w_0 - w) / (\gamma_w. C_c)]} \qquad (1)$$

where

$\gamma_s$ = unit weight of solids
$\gamma_w$ = unit weight of water
$C_c$ = compressibility

In a German investigation of 70 different sludges, approximately 65% of the samples had a shear strength less than $10kN/m^2$ when the dry solids content was 35% (Loll, 1990). Although it was observed that the shear strength often increases as the dry solids

content increases the investigators found it impossible to prove a unified relationship. On the other hand for dewatered sludge Koenig and Kay (1996) observed a relationship between shear strength and total solids of the form:

$$S_u = A \cdot e^{-m/TS} \tag{2}$$

where

$S_u$ = undrained shear strength (kN/m$^2$)
$TS$ = proportion (by weight) of total solids
$A,m$ = sludge specific contents
        The value of $m$ was approximately 0.5 but $A$ was found to be very sludge specific with a wide range of 35.6 to 119.8.

## Laboratory Tests

*Sludge Properties*

        In the authors' research (Klein, 1995), a number of samples from two wastewater sludge lagoons in the north of England, were placed in 254 mm. diameter Rowe hydraulic consolidation cells (Figure 2), and subjected to very low vertical effective pressures, ranging from 2 to 10 kN/m$^2$. The initial void ratios of the samples ranged from 7.85 to 10.27, while the particle densities were between 1.74 and 1.77 Mg/m$^3$. One lagoon contained sludge from the Bolton wastewater treatment plant, with an approximate age of at least 17 years; the second lagoon contained sludge and industrial and chemical waste from the Eccles wastewater treatment plant, in Manchester, with an age of possibly up to thirty years.
        The results of laboratory tests carried out on the sludge samples are summarised in (Table 1). According to Landva et al. (1983) the ash content test results show that the sludges can be classified as organic soils, or alternatively as peaty muck. In the present authors' opinion, these sludges differ from organic soils in their geotechnical behaviour, owing to the different type of fibre present, and because the pore liquid is viscous and more akin to a soft gel than water.

Table 1 – *Summary of Laboratory Test Results*

| Sample source | Initial moisture content | Fines content (<0.063 mm) | Organic content (440°C) | Fibre content | PH | Initial dry solids content |
|---|---|---|---|---|---|---|
| Bolton | 580% | 87.2% | 51% | 6.5% | 6.96 | 15% |
| Eccles | 450% | 82.1% | 55% | 16% | - | 18% |
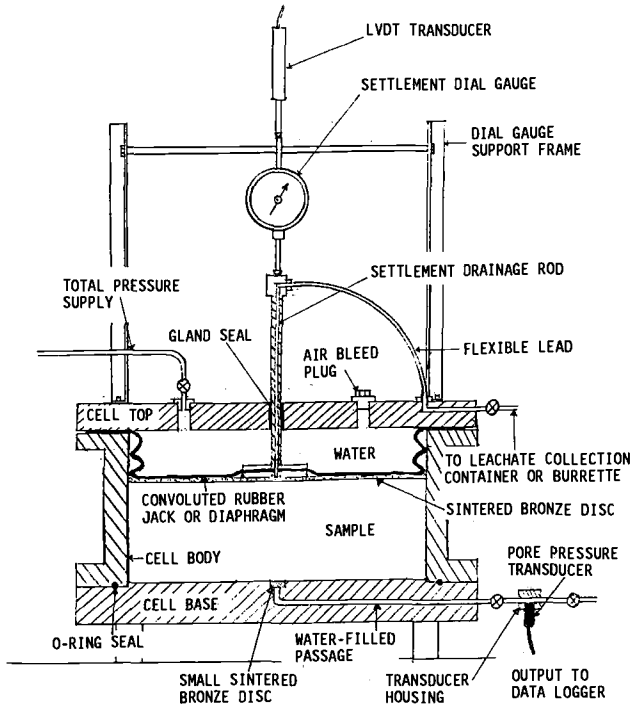
Figure 2– *Schematic Layout of Rowe Hydraulic Consolidation Cell*

*Consolidation Tests*

Two samples from each lagoon were consolidated in the Rowe cells, with initial sample heights ranging from 85 to 101 mm. The samples were step-loaded, with each step taking two months or more, so that secondary consolidation behaviour could be investigated. The results of the first loading increment from each cell are summarised in (Table 2).

When sludge from the Bolton lagoon was placed in a Rowe cell (Cell no. 2), and loaded with an effective pressure of 2 kN/m$^2$, the authors found that after initial settlement of 14.5 mm., the sample expanded and the dial gauge showed upward movement of over 19 mm. (see Figure 3). As the investigation into this phenomenon proceeded, it became clear that this was caused by microbial activity, which created a gaseous phase in the cell, or possibly expanded an existing gaseous phase. An enquiry to Yorkshire Water plc elicited the response that all bacteria in such lagoons should become inactive within 15 years[3]. However, all the samples tested over a period of at least six months exhibited gas

---

[3] Claydon, J.R., 1993, Private communication.

'generation' behaviour, with consolidation proceeding somewhat similar to the Terzaghi model, whilst the expulsion of liquid from the samples ceased within the first third of the time period of each load increment (which was at least two months for each increment). The gas which built up in each sample was in fact released slowly via the connecting tube to the leachate collection container, which was used to collect expelled pore liquid in the earlier stages of the test.
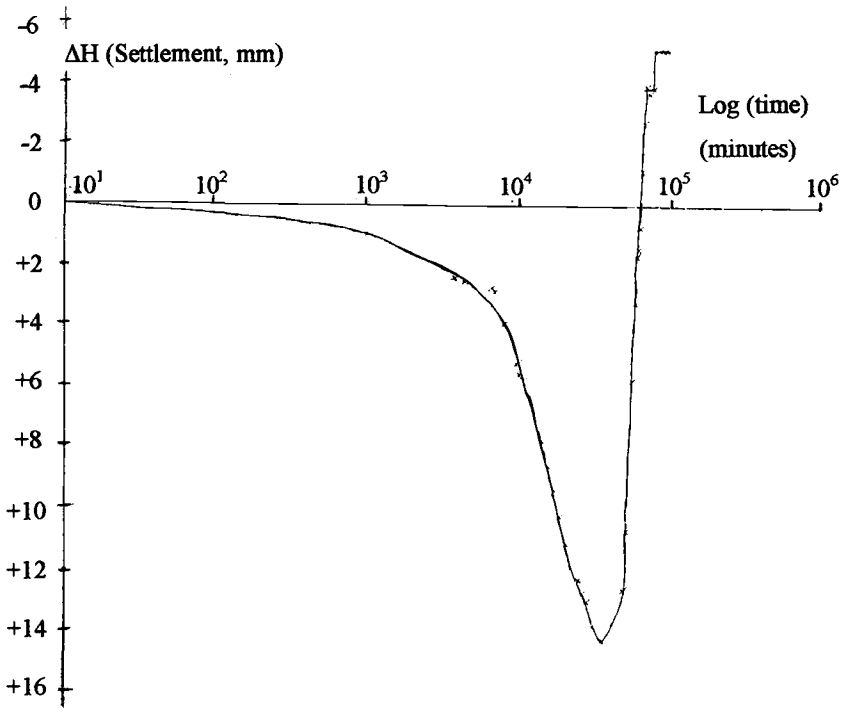


Figure 3 – *Consolidation Curve of Sample of Bolton Wastewater Sludge*

The presence of gas was directly detected at the end of each loading increment, by the use of a Draeger pump, which detected methane and carbon dioxide within the Rowe cells, both in the Bolton and Eccles wastewater sludge samples. This indicates that the microbes were digesting the sludge in anaerobic conditions. Similar gas generation was seen immediately after the slip at Deighton (Claydon, et al., 1997), in lagooned wastewater sludge up to 90 years old.

Another central feature of the results obtained in the authors' research (Klein, 1995) was that pore liquid pressure dissipation did not follow the traditional Terzaghi consolidation theory, in that the values of the pore liquid pressures in the samples tested were not related to the consolidation behaviour of the samples, as shown for example in Figure 4.

Table 2 – *Summary of Consolidation Test Results*

| Sample source | Cell no. | $\Delta p'$ (kN/m²) | Initial voids ratio $e_0$ | Final voids ratio $e$ | $C_v$ (log t method) (m²/year) | $C_\alpha$ | $\frac{C_\alpha}{C_c}$ | Cohesion $C_u$ (kN/m²) |
|---|---|---|---|---|---|---|---|---|
| Bolton | 1 | 10.0 | 10.27 | 7.49 | 0.075 | 0.032 | 0.0047 | 2.61 |
| Bolton | 2 | 2.0 | 10.27 | 10.76 | 0.041 | - | - | 1.90 |
| Eccles | 3 | 2.0 | 7.85 | 6.91 | 0.35 | 0.168 | 0.0187 | 2.1 |
| Eccles | 4 | 2.5 | 7.85 | 6.04 | 0.45 | 0.065 | 0.0072 | 3.6 |

where

$\Delta p'$ = pressure increment (kN/m²)
$C_v$ = coefficient of vertical consolidation (log t method) (m²/year)
$C_\alpha$ = coefficient of secondary consolidation
$C_c$ = compression index

Terzaghi's theory is based on the assumption that the excess pore water, or pore liquid pressure dissipates as consolidation of the sample takes place, with complete dissipation of the excess pore liquid pressure occurring at the end of the primary consolidation phase. Figure 4 shows that in the case of this wastewater sludge sample (Eccles, cell no. 3), the excess pore liquid pressure dissipated very slowly indeed (the effective pressure increment being 2 kN/m²), reducing from 3.93 kN/m² to 2.86 kN/m² in the first 30,000 minutes of consolidation and thereafter slowly increasing to around 4 kN/m² after some 100,000 minutes from the start of consolidation, well into the secondary consolidation phase. The consolidation curve of this sample is shown in Figure 5.
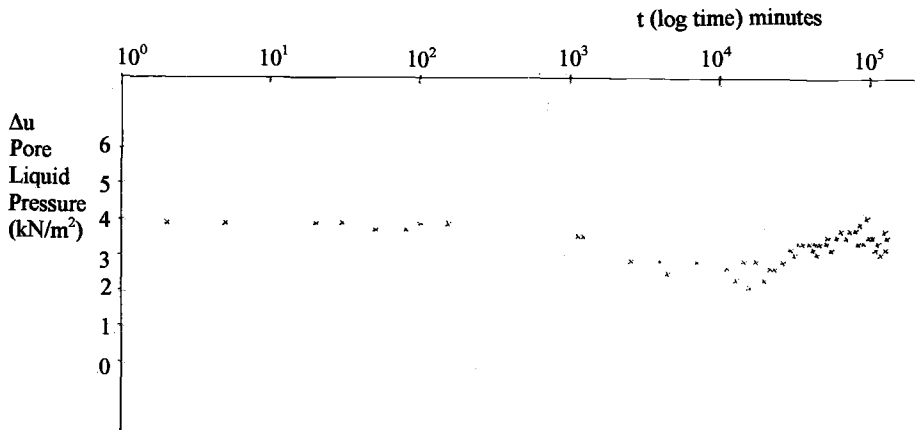


Figure 4 – *Eccles Wastewater Sludge Sample – Pore Liquid Pressure Behaviour*
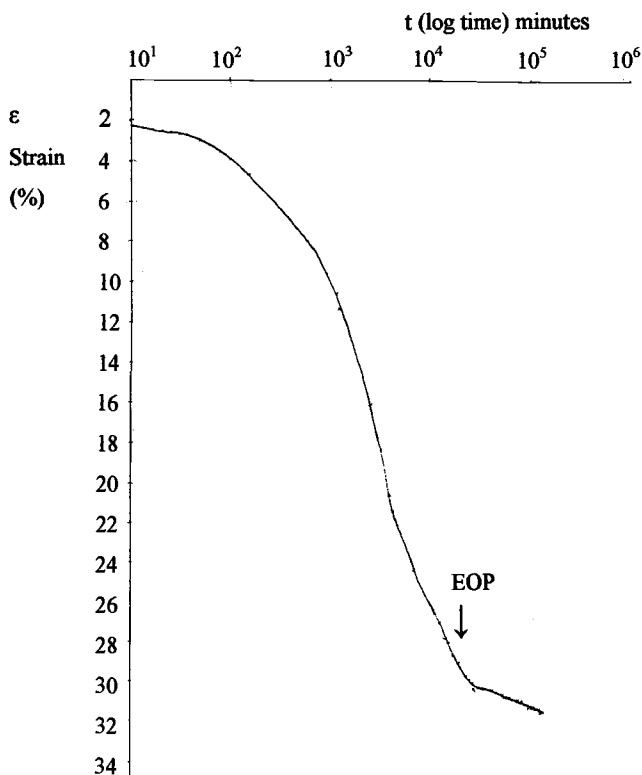
Figure 5 - *Consolidation Curve of Sample of Eccles Wastewater Sludge*

In the authors' opinion, this was the result of at least the following effects:

(a) The microstructure of the sludge particles consisted of fibrous flocs (see Vesilind and Martell, 1990), which contained within themselves a significant percentage of the total pore liquid/gas. During the consolidation process, some of this 'interstitial' pore liquid crossed the floc boundary, and became either surface liquid or free liquid. When taken together with the undoubted presence of gas within at least the free liquid, as a result of microbial activity in the sludge, one can see that the ability to take meaningful measurements of the pore liquid pressure became very doubtful indeed.

(b) It is unclear whether the testing apparatus used for measuring pore liquid pressures, really did measure these, or whether the values obtained were the result of measuring other parameters, such as the level of the clogging of the filter paper covering the pore pressure measurement drain in the laboratory apparatus.

(c) The changes in the ambient atmospheric pressure caused changes in the pore liquid pressures within the samples in the laboratory. This effect is similar to that noted by Schiffman et al. (1985). The low effective pressure increments ($2 - 10$ kN/m$^2$) were in fact very close in magnitude to the changes in atmospheric pressure in the laboratory, and it was necessary to correlate, and correct, the pore pressure readings

against a high-precision, certified barometer (Fortin) situated nearby. The graph in Figure 4 shows the corrected pore pressure readings for a sample of Eccles wastewater sludge.

*Shear Strength Tests*

Lagoons are usually used to store large volumes of wastewater sludge for relatively long periods of time (Frost et al., 1980). Most lagoons have been constructed simply by excavating a suitable void space and using the extracted material to build up banks surrounding the lagoon to increase its volume, i.e. there has been no proper engineering of these embankments. In the long term the stability of the thickened sludge mass in the lagoons is a cause for concern. Thickened sludge retains a thixotropic nature for very long periods, especially when several metres depth are deposited. Although surface drying may proceed to the point where a dry crust forms sufficient to support vegetation the mass of waste may remain unstable and pose a danger to both humans and animals venturing onto the surface, and remain completely unsuitable for reclamation to any useful purposes. To safeguard the environment the stability of these lagoons must be assessed and this requires information on the shear strength behaviour of the sludge after deposition, which requires both undrained and effective stress parameters.

Of all methods used to measure undrained shear strength, the laboratory vane appears to be the most suitable one for application to wastewater sludge because of the very low strength of the material and the problems of what exactly is the pore pressure. There are other methods to infer the shear strength of weak 'soils', such as the falling-cone, however the calibration of this method with respect to wastewater sludge is not known.

An exponential relationship between undrained cohesion and bulk density was proposed by Voss (1993) following a study of the development of shear strength in wastewater sludges placed in mono-disposal landfill sites. A vane test was used for field measurements of immediate undrained shear strength. The resultant empirical relationship was:

$$C_u = 2.09 * 10^{-8} * e^{17.5} \rho \qquad\qquad (3)$$

where

$e$ = voids ratio,
$\rho$ = bulk density (in Mg/m$^3$)

Equation (3) gives a reasonable representation of the shear strengths (of very high moisture content, weak sludges) measured by the authors of this paper – their data from laboratory shear vane tests on 'fresh' sludge are included in Figure 6 together with values from Voss' extensive testing of landfilled wastewater sludge.

The vane test was used to assess the strength of 'fresh', soft sludge and since it was saturated the undrained friction angle was assumed to be zero, because although the pore fluid was viscous it did not have real gel strength. Voss (1993) also conducted drained triaxial tests on 'old', compressed sludge. The effective friction angle recorded by

Voss (1993) was highly variable ($\phi'$ from 2.5° to 35°) and the effective cohesion was relatively low (c' ranging from 0 to 10 kN/m$^2$) so that even though the sludge was highly fibrous the fibres did not 'mat' together, like peat, to give high tensile strength, because the fibres were short in length (unlike in the case of organic soils or paper sludge) and because they were not pressed together. Thus the fibres were not really in intimate contact with each other and were separated by the viscous pore fluid.

Shear strength (kN/m$^2$)
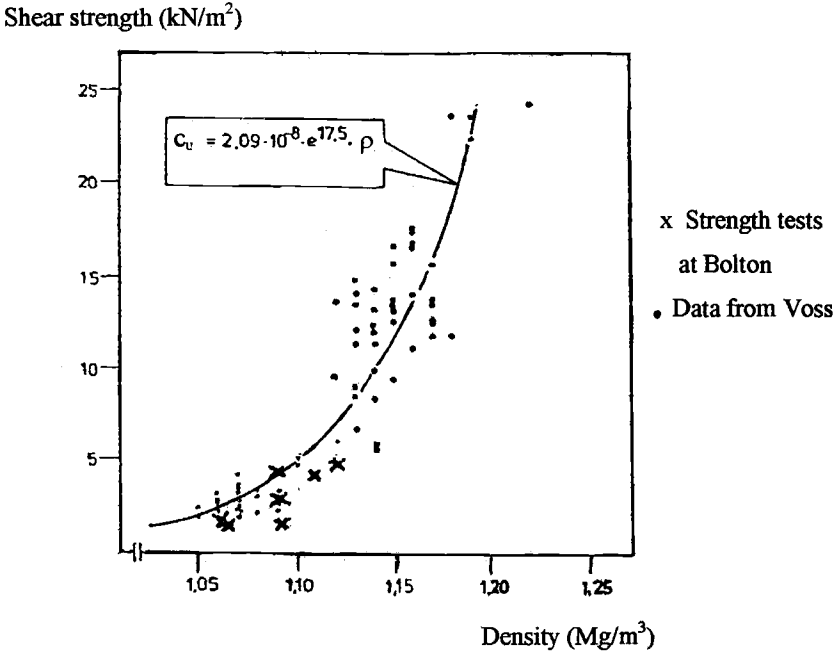


Figure 6 – *Laboratory Vane Shear Strength of Wastewater Sludges*

The values of $e^{-m/TS}$ in equation (2) for lagooned wastewater sludge will be close to unity; thus this equation predicts undrained shear strengths of between 30 – 120 kN/m$^2$. This range of values is typical for well dewatered sludges as tested by Koenig and Kay (1996), but it is unrealistic for lagooned wastewater sludge. On the other hand, equation (3) predicts shear strengths in the general range of 1 to 50 kN/m$^2$ as bulk density moves from 1.0 to 1.25 Mg/m$^3$. This range of shear strengths and bulk densities is much more in keeping with the characteristics of lagooned wastewater sludge. Bulk unit weight is a better indicator of the shear strength behaviour than just water content or fibre/solid ratio because it encompasses the effects of both voids ratio (its pore fluid has essentially zero shear strength) and fibre/solids content (the fibres will provide little frictional shear strength).

**Conclusion**

Wastewater sludge, after being placed on the ground in landfill or lagoons, can be viewed as a geotechnical material; as such there is an urgent need to understand its' consolidation and shear strength behaviour. A major slip occurred in early 1992 at Deighton in northern England in just such lagooned wastewater sludge.

The authors carried out a series of consolidation tests on lagooned wastewater sludge, from Bolton and Eccles in the north of England, in Rowe hydraulic consolidation cells (Klein, 1995). These tests established that gas was generated anaerobically in samples of wastewater sludge through microbial activity, throughout almost the whole length of the consolidation process in the laboratory. This conclusion was supported by eye-witness accounts of gas generation in decades-old wastewater sludge contributing to the tip failure at Deighton (Claydon et al., 1997).

Additionally, the excess pore liquid pressure in the samples of wastewater sludge tested by the authors (Klein, 1995) did not dissipate in accordance with the traditional Terzaghi consolidation theory. In fact, in one sample the gas caused the sludge to expand, forcing the dial gauge upward (see Figure 3). In other samples, the excess pore liquid pressure slowly reduced, but then began to increase back to its' original value (see Figure 4). This activity took place well into the secondary consolidation phase, where according to traditional theory the excess pore pressure has dissipated completely.

Using the model for pore fluid distribution suggested by Vesilind and Martel (1990), this generation of gas from within the sludge samples can be postulated as the slow release of interstitial or bound liquid/gas across the floc surface, taking place as part of the ongoing consolidation of the sludge mass, which in turn releases free or surface liquid/gas into the surrounding media, whether in the laboratory or in the field. Further, one can postulate on the basis of this model that secondary consolidation in wastewater sludges and sludge-like material, most notably in peats, involves this ongoing, slow release of interstitial or bound liquid/gas from within the sludge flocs (the 'solid' phase of the sludge mass).

Further development of such a model for the consolidation behaviour of wastewater sludges will need to take account of the microstructure of the sludge flocs, the interaction between them and the free and bound pore fluid, with treatment of the pore fluid as a viscous fluid or possibly even as a thixotropic gel. Both the 'solid' phase (the sludge flocs) and the liquid phase (the viscous pore fluid) can be seen to be compressible. This is in contrast to one of Terzaghi's central assumptions in his theory of consolidation, that of the incompressibility of the solid phase. Additionally, the compressibility of both the sludge flocs and the viscous pore fluid leads one to question whether the coefficient of permeability can be assumed to be constant during the consolidation of lagooned wastewater sludges.

Wastewater sludge can be classified on the basis of ash content tests as an organic soil (Landva et al., 1983). However, it is clear that these sludges differ from organic soils in their geotechnical behaviour, principally because the type of fibre present in the sludges is very different from that found in organic soils, and because the pore liquid in wastewater sludges is viscous and more akin to a soft gel than water.

Thickened lagooned wastewater sludge retains a thixotropic nature for very long periods of time in the field, especially when several metres depth of sludge are deposited. Laboratory vane tests carried out by the authors on sludge samples showed very low undrained shear strengths, in the range of 1.9 to 3.6 $kN/m^2$. These data are in reasonable agreement with results of field vane tests carried out on landfilled wastewater sludge reported by Voss (1993), and shown in Figure 6. Bulk unit weight seems to be a better indicator of the shear strength behaviour of soft, lagooned wastewater sludge than just water content or fibre/solid ratio, since it encompasses the effects of both voids ratio (the viscous pore fluid has essentially zero shear strength) and fibre/solids content (the fibres will provide little frictional shear strength).

## References

Claydon, J.R., Eadie, H.S., and Harding, C., 1997, "Deighton Tip - Failure, Investigation and Remedial Works", *Proceedings of the Nineteenth Congress of the International Commission on Large Dams*, Florence, pp. 233-245.

Frost, R., Powlesland, C., Hall, J.E., Nixon, S.C. and Young, C.P., 1980, "Review of Sludge Treatment and Disposal Techniques", Report No PRD 2306-M/1, HMIP/WRc.

Gupta, R.P. and Swartzendruber, D., 1962, "Flow-Associated Reduction in the Hydraulic Conductivity of Quartz Sand", *Soil Science Society Proceedings*, pp. 6-10.

Hvorslev, M.J., 1960, "Physical Components of the Shear Strength of Saturated Clays", *ASCE Research Conference on the Shear Strength of Cohesive Soils*, Boulder, Colorado.

Imai, G., 1980, "Settling behaviour of Clay Suspensions", *Soils and Foundations*, Vol. 20, No. 1, pp. 7-20.

Klein, A., 1995, "The Geotechnical Properties of Sewage Sludges", thesis submitted in partial fulfilment of the requirements for Master's degree, Bolton Institute, Bolton, UK.

Koenig, A. and Kay, J.N., 1996, "The Geotechnical Characterisation of Dewatered Sludge from Wastewater Treatment Plants", *3rd International Conference on Environmental Geotechnology*, San Diego.

Landva, A.O., Korpijaakko, E.O. and Pheeney, P.E., 1983, "Geotechnical Classification of Peats and Organic Soils", *Testing of Peats and Organic Soils, ASTM STP 820*, P.M. Jarrett, Ed., American Society for Testing and Materials, West Conshohocken, PA, pp. 37-51.

Loll, U., 1990, "Sludge Treatment - State of the Art and Development in Sludge Recycling", in *Klarschlammebehandlung - stand und entwicklung*, EF, Berlin.

Schiffman, R.L., Pane, V. and Gibson, R.E., 1984, "The Theory of One-Dimensional Consolidation of Saturated Clays IV. An Overview of Nonlinear Finite Strain Sedimentation and Consolidation", *Proceedings, Symposium on Sedimentation/Consolidation Models: Prediction and Validation*, ed. by R.N. Yong and F.C. Townsend, ASCE, New York, NY, pp. 1-29.

Schiffman, R.L., Pane, V. and Sunara, V., 1985, "Sedimentation and Consolidation", *Flocculation, Sedimentation and Consolidation*, ed. by B.M. Mougdil and P. Somasundaran, pp. 57-121.

Toorman, E.A., 1996, "Sedimentation and Self-Weight Consolidation: General Unifying Theory", *Geotechnique*, Vol. 46, No. 1, pp. 103-113.

Vesilind, P.A. and Martell, C.J., 1990, "Freezing of Water and Wastewater Sludges", *Journal of Environmental Engineering*, Vol. 116, No. 5, pp. 854-862.

Voss, T., 1993, "Contribution to the Strength Development of Sludges in Mono-Disposal Sites", Doctoral thesis, Kassel University.

# Laboratory Investigations

Craig H. Benson[1] and Xiaodong Wang[2]

**Hydraulic Conductivity Assessment of Hydraulic Barriers Constructed with Paper Sludge**

**Abstract:** Paper sludges are being used with increasing frequency for construction of hydraulic barrier layers in landfill final covers because they often have substantial clay content and relatively low hydraulic conductivity. This paper addresses the assessment of the hydraulic conductivity of paper sludges using data obtained from a series of laboratory and field tests conducted on two barrier layers constructed with paper sludge that were part of final cover test sections. Field hydraulic conductivities were measured using sealed double-ring infiltrometers (SDRIs) and two-stage borehole permeameters (TSBs). Laboratory tests were conducted in flexible-wall permeameters on undisturbed specimens collected as blocks and in thin-wall sampling tubes as well as remolded specimens. The in-service hydraulic conductivity, computed from water balance data, was also available for comparison. Analysis of the data shows that similar hydraulic conductivities are measured in large field tests and on small laboratory specimens regardless of whether the specimens are undisturbed or remolded. Based on the analysis, recommendations are made regarding the need for field testing, laboratory and field test methods, and sampling techniques.

**Keywords:** paper sludge, barrier layers, hydraulic conductivity, sealed double-ring infiltrometers, two-stage borehole permeameters, effective stress, sampling, gas

## Introduction

Wastewater treatment plants operated by the paper industry generate large quantities of paper sludge each year. Paper sludges are soft and fibrous soil-like materials having high water content (150-300%). They are composed of fibrous organic material remaining from pulping, clay minerals (predominantly kaolinite), and other inert solids (Kraus et al. 1997). In recent years, the paper industry has been investigating applications in which paper sludge can be beneficially used. Applications include agronomic

---

[1]Associate Professor, Dept. of Civil & Environmental Engineering, University of Wisconsin-Madison, Madison, WI 53706, chbenson@facstaff.wisc.edu

[2]Geotech. Lab. Mgr., Dept. of Civil & Environmental Engineering, University of Wisconsin-Madison, Madison, WI 53706, wang1@cae.wisc.edu

amendments (e.g., admix to topsoil layers), lightweight backfill (after firing to harden the sludge), and hydraulic barrier layers in landfill final covers.  Hydraulic barriers are of interest because paper sludges often have high clay content and relatively low hydraulic conductivity, and can be obtained and placed at lower cost than compacted clay (NCASI 1989, Genthe 1993, Zimmie et al. 1993, Floess et al. 1995, Moo-Young and Zimmie 1996, Kraus et al. 1997).

Use of paper sludges for constructing barrier layers has lead to many questions regarding how to assess the in situ hydraulic conductivity of paper sludge, including the following.

- Are large-scale field tests necessary to adequately assess macroscopic features affecting field hydraulic conductivity?
- Or, are laboratory hydraulic conductivity tests conducted on small (71 mm) specimens collected in sampling tubes adequate?
- How should specimens be sampled if laboratory tests are conducted?  Should thin-wall sampling tubes be used or should block samples be carved?
- Must special care or procedures be used when conducting field or laboratory hydraulic conductivity tests on paper sludge?

This paper addresses these questions using data from field and laboratory hydraulic conductivity tests conducted by the authors on two test plots simulating landfill final covers.  Both test plots contained a barrier layer constructed with paper sludge.


## Background: Test Plots for the NCASI Final Cover Study

A field study investigating the use of paper sludges for constructing barrier layers for landfill final covers was conducted by he National Council of the Paper Industry for Air and Stream Improvement (NCASI).  The results of this study are described in detail by Maltby and Eppstein (1994). Four test plots simulating final covers were constructed and instrumented in November 1987, and two of these test plots contained barrier layers constructed with paper sludge.  Only data from the test plots containing paper sludge are described in this paper.  Results from the other test plots can be found in Maltby and Eppstein (1994) and Benson and Wang (1996). A schematic of the test plot design is shown in Fig. 1.

One of the barrier layers was constructed with a combined sludge, composed of primary sludge from clarification of raw wastewater and biological sludge from an activated sludge treatment plant.  The other test section contained a barrier layer constructed with primary sludge. The barrier layers were compacted in two lifts 300 mm thick, which yielded a total thickness of 600 mm.  The sludges were compacted at their natural water contents (i.e., water content after processing at the treatment plant) to a dry unit weight comparable to that achieved with standard Proctor effort.  Other details of the construction can be found in NCASI (1990) and Maltby and Eppstein (1994).
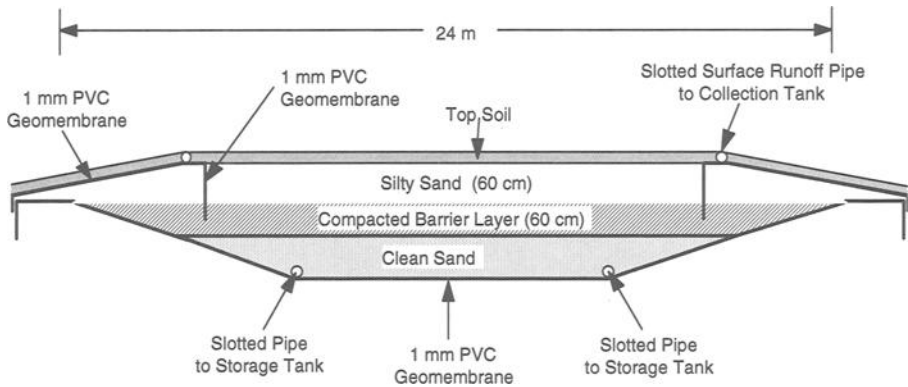
FIG. 1 -- *Schematic of test plot.*

The test plots were monitored for nearly eight years. During this period, data describing the water balance (surface runoff, soil water storage, and percolation) and meteorology were collected continuously. Maltby and Eppstein (1994) provide a summary of the data. The percolation data are of particular interest because these data provide an assessment of the actual in-service hydraulic conductivity of the barrier layers, as reported in Kraus et al. (1997).

When the test plots were decommissioned in Summer 1995, the surficial soils overlying the barrier layers (Fig. 1) were stripped away. The authors then conducted field hydraulic conductivity tests on the barrier layers as well as laboratory tests on specimens collected while installing the field equipment. Field hydraulic conductivity tests were conducted with sealed double-ring infiltrometers (SDRIs) and two-stage borehole permeameters (TSBs). Laboratory tests were conducted in flexible-wall permeameters on specimens collected in thin-wall sampling tubes, as large block specimens, and on remolded specimens prepared in the laboratory.

## Field Test Methods

### SDRI Tests

An SDRI consists of two concentric water-filled rings (Fig. 2). The outer ring is open to the atmosphere; it is used to apply driving head and acts as a buffer to ensure streamlines beneath the inner ring are vertical. The inner ring is sealed, and is used to measure the volume of water infiltrating into the underlying medium. A flexible plastic bag is used to measure the amount of water flowing from the inner ring. Plastic tubing connects the inner ring and the plastic bag. Tensiometers, which measure matric suction, are used to monitor depth of the wetting front during infiltration. A meter stick installed in the outer ring is used to measure the depth of ponded water.
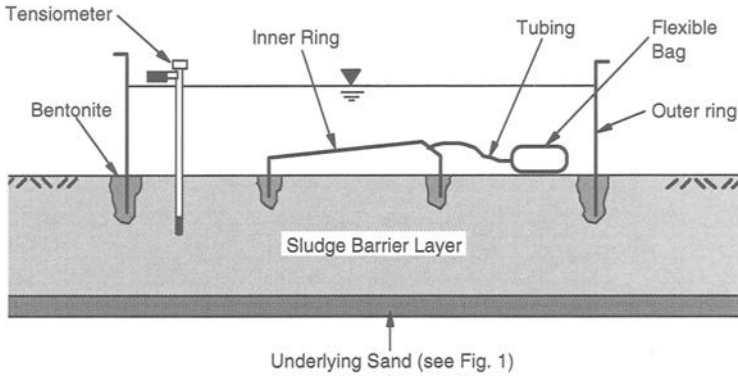
FIG. 2 -- *Schematic of sealed double-ring infiltrometer.*

The SDRIs were installed following procedures described in ASTM D 5093, *Standard Test Method for Field Measurement of Infiltration Rate Using a Double-Ring Infiltrometer with a Sealed-Inner Ring.* The outer rings were 2.4 m wide and the inner rings were 0.9 m wide. Trenches for the inner rings were excavated by hand (depth = 100 to 150 mm) to avoid disturbance of the sludge and then were filled with a fully hydrated bentonite grout. The inner rings were pushed directly into the grout, and then the grout was smeared around the outside edges of the rings to provide a tight seal. The outer trenches were excavated with shovels and filled with bentonite grout before inserting the outer ring. Five tensiometers were installed between the inner and outer rings of each SDRI at depths of 75, 150, 230, 300, and 380 mm. Holes for the tensiometers were drilled using an auger having a diameter slightly smaller than the tensiometer tip. A bentonite seal was placed around the shaft of each tensiometer near the surface of the barrier layer.

Data were collected from the SDRIs for 51 days. Data collection consisted of weighing the 1-liter plastic bags attached to the inner rings, recording depth of water in the outer rings, recording matric suctions displayed on the tensiometers, and measuring water temperatures. Infiltration rate (I) was determined using:

$$I = \frac{\Delta W}{A \; \Delta t \; \gamma_w} \tag{1}$$

where $\Delta W$ is the change in weight of the plastic bag in an interval of time $\Delta t$, A is the cross-sectional area of the inner ring, and $\gamma_w$ is the unit weight of water. Hydraulic conductivity (K) was computed from infiltration rate using the Green-Ampt formulation:

$$K = \frac{I}{i} \tag{2}$$

where i is the hydraulic gradient, which is computed by (Daniel 1989, Trautwein and Boutwell 1994):

$$i = \frac{D_p + D_f + H_s}{D_f} \tag{3}$$

In Eq. 3, $D_f$ is the depth to the wetting front, $D_p$ is the depth of ponding, and $H_s$ is the suction head at the wetting front. During the entire test period, matric suctions were negligible because heavy rains had saturated the barrier layers. Thus, in this analysis, $H_s$ was assumed to be zero and $D_f$ was assumed to 60 cm (barrier layer thickness).

Hydraulic conductivities computed from the SDRIs fluctuated wildly during the two weeks of field testing (Fig. 3) because gas from biological decomposition collected in the inner ring. The inner ring "burped" whenever the vent valve was opened, and gas having a strong sulfur odor was emitted. To remedy this problem, a 25-mm-diameter vent tube open to the atmosphere was installed at the upper-most point on the inner ring. The vent tube extended above the water level so that gas could readily flow out of the inner ring while water could not enter. Adding the vent tube essentially "unsealed" the SDRI. Nevertheless, the data obtained subsequently appeared reasonable.
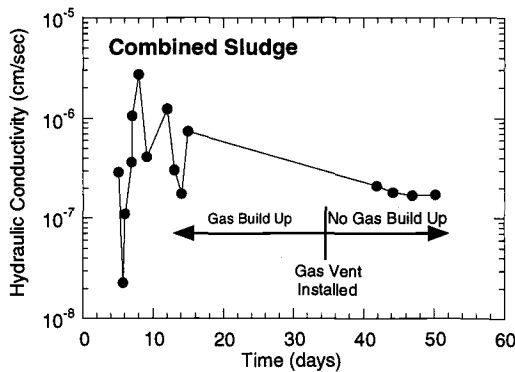


FIG. 3 -- *Hydraulic conductivities obtained from SDRI on combined sludge before and after installation of gas vent.*

*TSB Tests*

The TSB test is a two-stage falling-head infiltration test. A schematic of a TSB is shown in Fig. 4. The TSB consists of a casing grouted in a borehole and a standpipe affixed to the top of the casing. Water flows out of the casing and into the media being tested, which results in a drop in the water level in the standpipe. In Stage 1, the base of the casing is placed flush against the soil and a falling-head test is conducted. In Stage 2, the borehole is extended beneath the base of the casing, and another falling-head test is conducted. From these two stages, two "apparent" conductivities are obtained, $K_1$ and $K_2$. These apparent conductivities are related to, but do not equal, the horizontal and

vertical hydraulic conductivities, $K_h$ and $K_v$. The relationship between $K_1$, $K_2$, $K_h$, and $K_v$ is described subsequently.
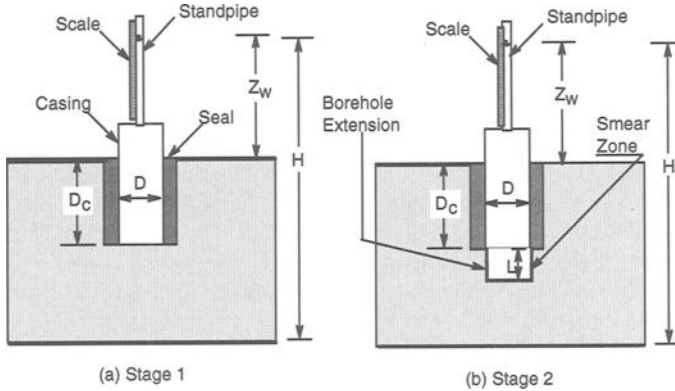


FIG. 4 -- *Schematic of Stage 1 (a) and Stage 2 (b) of a TSB test.*

The TSBs were installed following methods described in Boutwell (1992), which are essentially identical to the methods in the newly approved ASTM method for TSB testing. The TSBs were installed outside the confines of the SDRI tests. The base of Stage 1 was placed at a depth of 200 mm (near mid-depth of the barrier layer) and the borehole extensions were 100 mm long. Holes for all of the TSBs were excavated by hand and the annulus of each TSB was backfilled using a bentonite grout.

Data from the TSBs were collected for 40 days. In the middle of this period, Stage 1 was terminated, the boreholes were extended, and Stage 2 was conducted. The boreholes were extended using a bucket auger similar to the auger described in Boutwell (1992). After the boreholes were extended, their walls and base were scraped by hand to ensure smear did not exist.

The data were analyzed following the procedure described in Trautwein and Boutwell (1994). The generalized apparent conductivity $K_i$ ($i = 1$ or 2) for Stages 1 and 2 is formulated as:

$$K_i = \frac{RG_i \ln(H_1/H_2)}{t_2 - t_1} \qquad (4)$$

where R is the temperature correction described in ASTM D 5084 (*Standard Test Method for Measurement of Hydraulic Conductivity of Saturated Porous Materials Using a Flexible Wall Permeameter*), $H_1$ is the head H (Fig. 4) at time $t_1$, $H_2$ is the head at time $t_2$, and $G_i(m)$ ($i = 1$ or 2) are geometric constants for each stage:

$$G_1(m) = \frac{pd^2}{11md} \left[ 1 + a\left( \frac{D}{4mb_l} \right) \right] \qquad (5a)$$

$$G_2(m) = \frac{d^2}{16 L f m^2}(2 \ln U_1 + a \ln U_s + p \ln U_3) \tag{5b}$$

In Eqs. 5, $m = (K_h/K_v)^{1/2}$, d is the inside diameter of the standpipe, D is the inside diameter of the casing, a is a constant (=1 for impermeable base, =0 for semi-infinite medium, and = -1 for a permeable base), L is the length of the borehole extension, $b_1$ thickness of the barrier layer, and p is the smear ratio (defined as $K_h/K_s$, where $K_s$ is the hydraulic conductivity of the smear zone, Fig. 4). For all tests, p was assumed to be 1 (no smear) and a was -1 (permeable base). The functions $U_1$, $U_2$, and $U_3$, and f in Eqs. 5 are:

$$U_1 = \frac{mL}{D+2T} + \sqrt{1+\left(\frac{mL}{D+2T}\right)^2} \tag{6a}$$

$$U_2 = \frac{\frac{4mb_2}{D} + \frac{mL}{D} + \sqrt{1 + \left(\frac{4mb_2}{D} + \frac{mL}{D}\right)^2}}{\frac{4mb_2}{D} - \frac{mL}{D} + \sqrt{1 + \left(\frac{4mb_2}{D} - \frac{mL}{D}\right)^2}} \tag{6b}$$

$$U_3 = \frac{\left[\frac{mL}{D} + \sqrt{1+\left(\frac{mL}{D}\right)^2}\right]}{U_1} \tag{6c}$$

$$f = 1 - 0.5623 \exp\left(\frac{-\pi L}{2D}\right) \tag{6d}$$

In Eqs. 6, $b_2 = b_1 - L/2$ and T is the thickness of the smear zone (Fig. 4). For all tests, T was set to 0 (no smear). The variable m is unknown and must be determined by solving:

$$\frac{K_2}{K_1} = \frac{G_1(m)G_2(1)}{G_1(1)G_2(m)} \tag{7}$$

using $K_1$ and $K_2$ measured during Stages 1 and 2. The *Solver* function in Microsoft Excel® was used to obtain m. Then $K_v$ and $K_h$ were computed as:

$$K_v = \frac{K_1 G_1(m)}{G_1(1)} \tag{8a}$$

$$K_h = m^2 K_v \tag{8b}$$

*Problems with Excessive Head*

Testing with the TSBs showed that the head would drop very rapidly upon refilling the standpipe, but then would slow down dramatically once the water level in the standpipe was within about 150 mm of the top of the casing. The rapid drop in head is evident in the $K_1$ data shown in Fig. 5, which were obtained from a TSB installed in the primary sludge barrier layer. The rapid drop in head (or $K_1$) observed in the TSB tests has also been observed when testing compacted clay barriers, and is attributed to "hydraulic fracturing" caused by near zero effective stress at the bottom of the borehole.
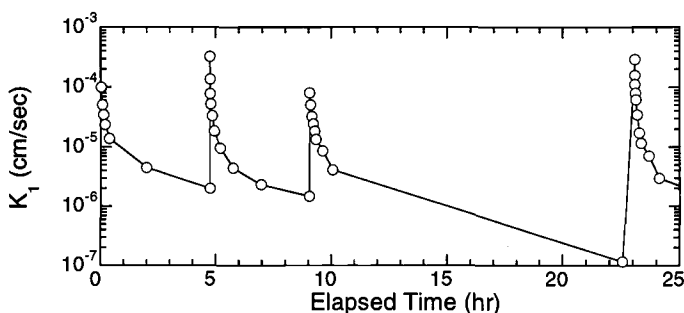


FIG. 5 -- *Apparent conductivity $K_1$ showing anomalies due to excessive head.*

To avoid this problem when testing compacted clays, the water level relative to the ground surface ($Z_w$ in Fig. 4) is usually maintained less than twice the depth of casing embedment ($D_c$ in Fig. 4). This rule-of-thumb was initially applied when testing the sludge, but data such as that shown in Fig. 5 demonstrated that the rule-of-thumb was inappropriate because of the low unit weight ($<10$ kN/m$^3$) of paper sludge, which is about one-half the typical unit weight of compacted clay. A more appropriate guideline for paper sludge is to maintain $Z_w < D_c$, which was 200 mm for the TSBs installed in the sludge. This water level elevation corresponds closely to the elevation at which the rapid drop in head ceased, and reasonable $K_1$ measurements were obtained. Thus, subsequent tests were conducted with very low water levels, i.e., $Z_w < 200$ mm.

## Sampling and Laboratory Methods

Hydraulic conductivity tests were conducted in the laboratory on undisturbed and remolded specimens collected from the sludge barrier layers. Undisturbed specimens were collected in thin-wall sampling tubes and as carved blocks.

*Sampling Methods*

The fibers in paper sludge preclude pressing thin-wall tubes during sampling. Strength provided by the fibers causes the sludge to resist shearing and compress ahead of

the tube, causing disturbance. Thus, a method similar to that described in Moo-Young and Zimmie (1995) was used to obtain samples in 71-mm-diameter sampling tubes. The tubes were displaced into the sludge using a series of blows by a "Corps of Engineers" 4.5 kg drop hammer (Fig. 6) instead of the conventional slow, steady push. The blows shear fibers in the sludge, allowing the sample to enter the tube in a relatively undisturbed state. The tubes were removed from the sludge using a shovel.



FIG. 6 -- *Sampling combined sludge in tubes using 4.5 kg drop hammer.*

Specimens removed as blocks were trimmed by hand into PVC rings following procedures described in Benson et al. (1995). The rings had a diameter and height of 400 mm. Once the sludge was contained within the ring, excess sludge was trimmed away and the ends of the ring were sealed with polyethylene affixed with duct tape.

*Remolded Specimens*

Remolded specimens were prepared by compacting trimmings leftover from trimming the block specimens. The specimens were compacted using the standard Proctor procedure (ASTM D 698, *Standard Test Method for Laboratory Compaction Characteristics of Soil Using Standard Effort*) at their existing water content. These water contents were comparable to the water content at which the sludges were placed. The dry unit weights of these specimens ranged between 3 and 4 $kN/m^3$, which is consistent with dry unit weights reported for these sludges by Kraus et al. (1997).

*Testing Method*

All specimens were permeated in flexible-wall permeameters using the falling-headwater rising-tailwater method described in ASTM D 5084. The tube specimens were

tested at a diameter of 71 mm and the block specimens were tested at a diameter of 300 mm. All specimens had an aspect ratio (height/diameter) of approximately one. The ends of the specimens were scarified prior to testing to eliminate smear developed during trimming.

The specimens were initially isotropically consolidated to an effective stress of 5 kPa to approximate the effective stress existing during field testing. No backpressure was applied to simulate the field-saturated condition. Afterwards, a hydraulic gradient of 6 was applied. After equilibrium was achieved during permeation at 5 kPa, the specimens were consolidated to higher effective stress and subsequently re-permeated.

*Gas Control*

As with the SDRI tests, gas generated by biological activity proved to be problematic during laboratory testing. Initial indications of gas problems were reversal of flow in the influent burette, large fluctuations in hydraulic conductivity and outflow-to-inflow ratio, very high or negative outflow-to-inflow ratios, and bubbles appearing in the water lines near the cap and pedestal in the permeameter. Gas flushed from the lines had a strong sulfur odor, confirming that biological activity was the source of the gas.

Three methods were attempted to eliminate the gas bubbles: back pressure, daily flushing, and permeation at cool temperatures. Back pressures up to 560 kPa were tried to limit the formation of gas bubbles. However, back pressuring appeared to have no impact on gas generation. Daily flushing proved more successful. Flushing consisted of running water through the influent and effluent lines each day to eliminate any gas bubbles. Typical results obtained from flushing tests are shown in Fig. 7. The hydraulic conductivity and outflow-to-inflow ratio became essentially steady once flushing began.
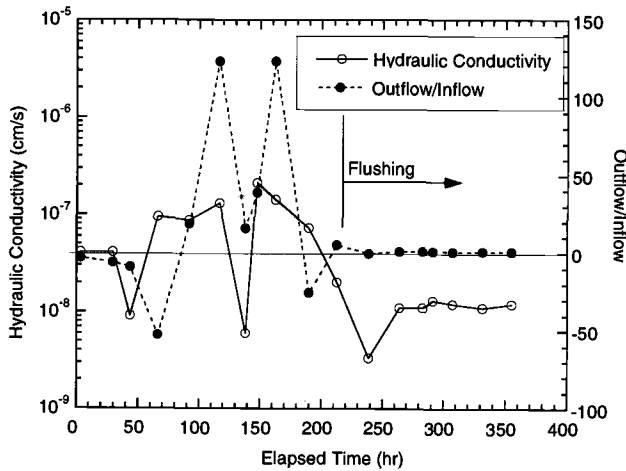


FIG. 7 -- *Typical hydraulic conductivity and outflow/inflow data before and after daily flushing.*

Although daily flushing was successful, it was also tedious and time consuming. Thus, additional tests were conducted with the permeameter placed in a refrigerator operating at 4°C. The hydraulic conductivity data were adjusted to correspond to conditions at 20°C using Eq. 5 and Table 1 in ASTM D 5084. Results obtained from tests conducted in the refrigerator were similar to those shown in Fig. 7; i.e., testing at 4°C eliminated the fluctuations caused by gas. Because of its simplicity, refrigeration is now the authors' method of choice for testing paper sludges provided the number of tests to conduct is not too large.

## Results of Field and Laboratory Hydraulic Conductivity Tests

Tables 1 and 2 contain summaries of all hydraulic conductivities measured in the study. Reliable data for both stages were obtained from three TSBs installed in the combined sludge, and only one TSB in the primary sludge. Leaks in the casing seal were the primary reason for the unreliable data. These leaks were caused by improper installation by an inexperienced installer and are not characteristic of TSB testing in sludge. For all TSBs, $K_1$ and $K_2$ were practically the same, indicating that the hydraulic conductivity was nearly isotropic. Thus, for brevity only $K_v$ is reported in Tables 1 and 2. A complete summary of the data can be found in Benson and Wang (1996).

Table 1 -- *Results of Hydraulic Conductivity Tests-Primary Sludge.*

| Field or Laboratory | Sample or Test Type | Test No. | Effective Stress (kPa) | K (cm/sec) |
|---|---|---|---|---|
| Laboratory | Tube | TP-1 | 5 | $4.1 \times 10^{-7}$ |
| Laboratory | Tube | TP-2 | 5 | $6.3 \times 10^{-7}$ |
| Laboratory | Tube | TP-3 | 5 | $5.6 \times 10^{-7}$ |
| Laboratory | Tube | TP-4 | 5 | $6.7 \times 10^{-7}$ |
| Laboratory | Tube | TP-1 | 30 | $2.2 \times 10^{-7}$ |
| Laboratory | Tube | TP-2 | 30 | $8.4 \times 10^{-8}$ |
| Laboratory | Tube | TP-3 | 30 | $4.5 \times 10^{-8}$ |
| Laboratory | Tube | TP-4 | 30 | $5.6 \times 10^{-8}$ |
| Laboratory | Tube | TP-1 | 60 | $1.0 \times 10^{-8}$ |
| Laboratory | Tube | TP-2 | 60 | $2.4 \times 10^{-8}$ |
| Laboratory | Tube | TP-3 | 60 | $2.7 \times 10^{-8}$ |
| Laboratory | Tube | TP-4 | 60 | $1.5 \times 10^{-8}$ |
| Laboratory | Block | BP-1 | 5 | $5.3 \times 10^{-7}$ |
| Laboratory | Block | BP-1 | 18 | $8.1 \times 10^{-8}$ |
| Laboratory | Block | BP-1 | 30 | $2.7 \times 10^{-8}$ |
| Laboratory | Block | BP-1 | 60 | $1.7 \times 10^{-8}$ |
| Laboratory | Remolded | RP1 | 5 | $6.2 \times 10^{-7}$ |
| Laboratory | Remolded | RP2 | 20 | $5.1 \times 10^{-8}$ |
| Laboratory | Remolded | RP3 | 40 | $2.9 \times 10^{-8}$ |
| Laboratory | Remolded | RP4 | 60 | $1.3 \times 10^{-8}$ |
| Field | TSB | TC | 5 | $8.3 \times 10^{-7}$ |
| Field | SDRI | SP | 5 | $6.5 \times 10^{-7}$ |

Kraus et al. (1997) report in-service field hydraulic conductivities that were computed from the percolation data in Maltby and Eppstein (1994). These field hydraulic conductivities were computed using percolation rates recorded when the barrier layers were saturated following rainfall and snowmelt. Under such conditions, nearly all of the head loss occurs in the barrier layer and the hydraulic gradient is approximately one. The in-service field hydraulic conductivities determined in this manner by Kraus et al. (1997) are $2x10^{-7}$ cm/s (primary sludge) and $4x10^{-8}$ cm/s (combined sludge). The in-service effective stress was approximately 18 kPa. This effective stress is higher than the effective stress during field hydraulic conductivity testing because of the overburden pressure provided by the soil layers above the barrier layer (Fig. 1).

Table 2 -- *Results of Hydraulic Conductivity Tests-Combined Sludge.*

| Field or Laboratory | Sample or Test Type | Test No. | Effective Stress (kPa) | K (cm/sec) |
|---|---|---|---|---|
| Laboratory | Tube | TC-1 | 5 | $3.1 \times 10^{-7}$ |
| Laboratory | Tube | TC-1 | 30 | $2.4 \times 10^{-8}$ |
| Laboratory | Tube | TC-2 | 30 | $3.8 \times 10^{-8}$ |
| Laboratory | Tube | TC-3 | 30 | $4.2 \times 10^{-8}$ |
| Laboratory | Tube | TC-4 | 30 | $1.7 \times 10^{-8}$ |
| Laboratory | Tube | TC-1 | 60 | $1.4 \times 10^{-8}$ |
| Laboratory | Tube | TC-2 | 60 | $2.1 \times 10^{-8}$ |
| Laboratory | Tube | TC-3 | 60 | $2.4 \times 10^{-8}$ |
| Laboratory | Tube | TC-4 | 60 | $1.1 \times 10^{-8}$ |
| Laboratory | Block | BC-1 | 5 | $2.6 \times 10^{-7}$ |
| Laboratory | Block | BC-1 | 18 | $4.6 \times 10^{-8}$ |
| Laboratory | Block | BC-1 | 30 | $1.9 \times 10^{-8}$ |
| Laboratory | Block | BC-1 | 60 | $9.9 \times 10^{-9}$ |
| Laboratory | Remolded | RC1 | 5 | $2.4 \times 10^{-7}$ |
| Laboratory | Remolded | RC2 | 20 | $4.0 \times 10^{-8}$ |
| Laboratory | Remolded | RC3 | 40 | $2.3 \times 10^{-8}$ |
| Laboratory | Remolded | RC4 | 60 | $1.5 \times 10^{-8}$ |
| Field | TSB | TCA | 5 | $2.2 \times 10^{-7}$ |
| Field | TSB | TCB | 5 | $2.5 \times 10^{-7}$ |
| Field | TSB | TCC | 5 | $1.5 \times 10^{-7}$ |
| Field | SDRI | SC | 5 | $1.7 \times 10^{-7}$ |

Comparison of the laboratory and the field data in Table 1 or 2 at similar effective stress shows that the hydraulic conductivities obtained using large-scale field methods and laboratory tests on small-scale specimens are similar. This is more clearly shown in Fig. 8, where hydraulic conductivity is graphed as a function of effective stress. Moreover, hydraulic conductivities of the remolded specimens are similar to those measured on undisturbed sludge in the field and the laboratory. The similarity of the hydraulic conductivities suggests that the sludge has similar fabric at small and large scales and in the in-service, undisturbed, and remolded states. The fabric is similar because the sludge is very soft when placed, and thus deforms and compresses readily when placed during construction. As a result, micropores control flow and these pores are adequately sampled in large and small-scale tests.
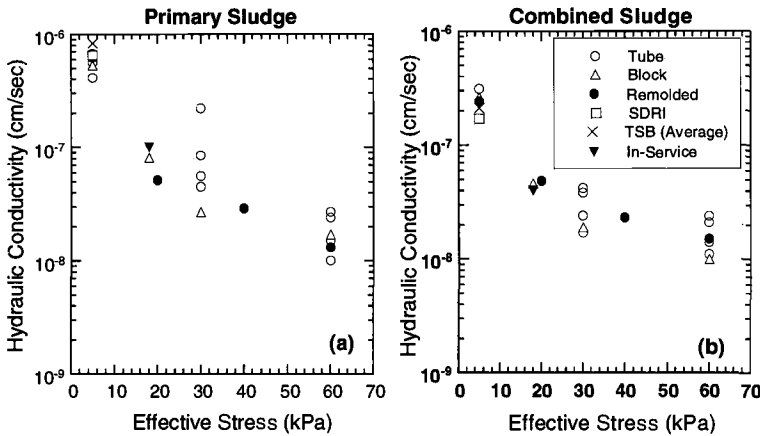
FIG. 8 -- *Hydraulic conductivity vs. effective stress: (a) primary and (b) combined.*

The absence of macroscopic features was confirmed by conducting a dye tracer study once the SDRI tests were complete. The inner rings were removed and Rhodamine WT dye was added to the water in the outer rings at a concentration of 2000 mg/L. The dye and concentration were selected based on a preliminary laboratory study comparing the effectiveness of several dyes (Benson and Wang 1996). The preliminary study showed that the purple Rhodamine WT readily marked flow paths in the white or gray colored sludge. Photographs of transects through the dyed sludges are shown in Fig. 9. The purple dye is at the surface (appears dark gray to black in black and white print). None of the dye penetrated more than 40 mm into either sludge.
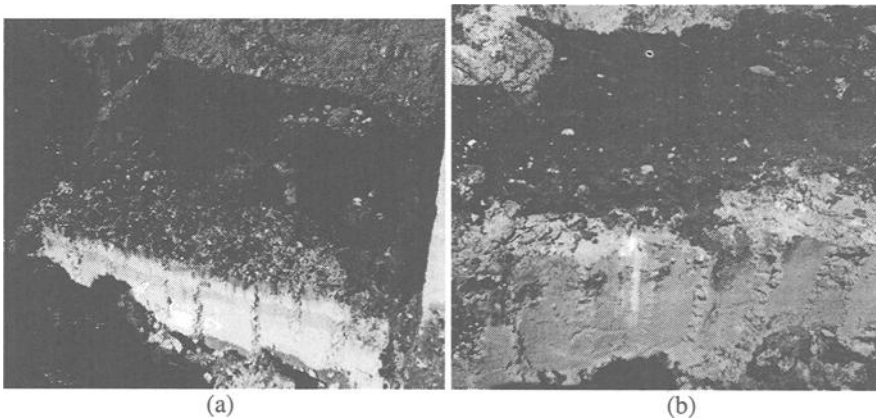


FIG. 9 -- *Photographs of transects through primary (a) and combined (b) sludge after permeation with dye.*

Hydraulic conductivities of the specimens obtained as blocks and with thin-wall sampling tubes are also similar when compared at the same effective stress. Their similarity suggests that disturbance during tube sampling using the 4.5 kg drop hammer is minimal or unimportant. Also, the remolded specimens had similar hydraulic conductivities as the specimens removed as blocks and in tubes, which suggests that methods commonly used for pre-construction testing yield hydraulic conductivities representative of the as-constructed field condition.

The sensitivity of hydraulic conductivity to effective stress is also evident in Fig. 8. Moo-Young and Zimmie (1996) report similar sensitivity. Because the sludge is soft, it compresses significantly under small loads and accordingly the hydraulic conductivity decreases. Thus, effective stresses anticipated in the field must be applied when testing sludge. Otherwise, misleading results may be obtained. The importance of applying the appropriate effective stress was particularly evident in a project on which the authors recently consulted. Pre-construction hydraulic conductivity testing of sludge being considered for use in a barrier layer for a landfill cap was performed at an effective stress of 80 kPa, even though the effective stress anticipated in the field was 25 kPa. Results of the pre-construction tests indicated that the sludge would have a hydraulic conductivity of approximately $1 \times 10^{-8}$ cm/sec, far below the maximum hydraulic conductivity of $1 \times 10^{-7}$ cm/sec prescribed by the regulatory agency. However, tests conducted at 25 kPa on specimens collected from a test section constructed prior to full-scale construction showed that the hydraulic conductivity of the sludge was approximately $2 \times 10^{-7}$ cm/sec. Fortunately the project engineer had the foresight to conduct the tests on the test section prior to full-scale construction. Had these tests not been conducted, costly corrective action may have been required.

**Implications for Hydraulic Conductivity Assessments**

The results of this study have several important implications for assessing the hydraulic conductivity of barrier layers constructed with paper sludge. These implications are summarized as follows.

*1. Large-Scale Field Hydraulic Conductivity Testing*

Large-scale field tests are not necessary for assessing the field hydraulic conductivity of barrier layers constructed with paper sludge. Because paper sludges are soft and compressible, they do not contain macropores that cause large discrepancies between measurements of hydraulic conductivity at large and small scales. As a result, conventional small-scale tests (71-mm-diameter) are satisfactory for assessing the hydraulic conductivity of paper sludges.

If field hydraulic conductivity tests are conducted, precautions must be made for venting gas caused by biological activity. Also, to obtain reliable hydraulic conductivity measurements, heads must be maintained at low levels when conducting TSB tests on paper sludge. The authors recommend that the water level in TSB standpipes be no higher than the depth of embedment of the casing.

## 2. Laboratory Testing

Laboratory hydraulic conductivity tests on paper sludge can be conducted using the same methods employed for testing compacted clays (e.g., ASTM D 5084). However, as with field tests, precautions must be taken to prevent gas formation or to flush gas bubbles from the permeameter. Tests conducted at low temperatures that minimize biological activity (e.g., $4^\circ C$) are recommended because of their simplicity. However, the temperature should be greater than $0^\circ C$ to prevent freezing and corrections must be made to report hydraulic conductivities at temperatures representative of field conditions.

Laboratory tests on paper sludges should always be conducted at effective stresses representative of the field condition. The engineer in charge of the project should state the stresses to be applied during laboratory testing. Laboratory personnel who receive paper sludge samples without instructions regarding the effective stress should obtain the appropriate stress from the engineer before conducting the tests.

## 3. Sample Collection

Samples for hydraulic conductivity testing can be obtained using conventional 71-mm-diameter thin wall sampling tubes. However, the tubes should be inserted using a method that will shear the fibers, such as the method described in Moo-Young and Zimmie (1996) or using the 4.5-kg hammer described in this paper. Collecting block specimens is not necessary.

## 4. Pre-Construction Testing

Pre-construction testing of paper sludges can be performed using conventional methods employed for compacted clays. Specimens can be prepared in compaction molds using methods such as ASTM D 698. However, because the sludge is soft and nearly saturated when received, the compactive effort may need to be reduced to obtain a competent test specimen.

These recommendations are based on the authors' experience to date on testing paper sludges. As more experience is gained and more data become available, these recommendations may change. The authors are currently initiating an in-depth study regarding laboratory protocols for hydraulic conductivity testing of paper sludges. Recommendations from this study will be made available in future publications.

## References

Benson, C., Chamberlain, E., Erickson, E., and Wang, X., 1995, "Assessing Frost Damage in Compacted Clay Liners," *Geotechnical Testing Journal*, Vol. 18, No. 3, ASTM, Philadelphia, pp. 324-333.

Benson, C. and Wang, X., 1996, Field Hydraulic Conductivity Assessment of the NCASI Final Cover Test Plots, Environmental Geotechnics Report 96-9, Dept. of Civil and Environmental Engineering, University of Wisconsin-Madison.

Boutwell, G., 1992, "The STEI Two-Stage Borehole Field Permeability Test," Geotechnical Division Seminar, Houston Branch, ASCE, Houston, TX.

Daniel, D., 1989, In Situ Hydraulic Conductivity Tests for Compacted Clay," *Journal of Geotechnical Engineering*, ASCE, Vol. 115, No. 9, pp. 1205-1227.

Floess, C., Smith, R., and Hitchcock, K., 1995, "Capping with Fiber Clay," *Civil Engineering*, ASCE, pp. 62-63.

Genthe, D., 1993, "Shear Strength of Two Pulp and Paper Mill Sludges with Low Solids Content," MS Thesis, University of Wisconsin-Madison, Madison, WI.

Kraus, J., Benson, C., Maltby, V., and Wang, X., 1997, "Field and Laboratory Hydraulic Conductivity of Compacted Papermill Sludges," *Journal of Geotechnical and Geoenvironmental Engineering*, ASCE, Vol.123, No. 7, pp. 654-662.

Maltby, V., and Eppstein, L., 1994, "A Field-Scale Study of the Use of Paper Industry Sludges as Hydraulic Barriers in Landfill Cover Systems," *Hydraulic Conductivity and Waste Contaminant Transport in Soils, ASTM STP 1142*, American Society for Testing and Materials, Philadelphia, pp. 546-558.

Moo-Young, H. and Zimmie, T., 1995, "Quality assurance and Quality Control Laboratory and In Situ Testing of Paper Mill Sludges used as Landfill Covers," *Proc. Eleventh Annual Waste Testing and Quality Assurance Symposium*, United States Environmental Protection Agency, Washington, D.C., pp. 668-684.

Moo-Young, H. and Zimmie, T., 1996, "Geotechnical properties of paper mill sludges for use in landfill covers, *Journal of Geotechnical and Geoenvironmental Engineering*, ASCE, Vol. 122, No. 9, pp. 768-776.

NCASI, 1989, "Experience with and Laboratory Studies of the Use of Pulp and Paper Mill Solid Wastes in Landfill Cover Systems," *Technical Bulletin No. 559*, National Council of the Pulp and Paper Industry for Air and Stream Improvement, New York, NY.

NCASI, 1990, "A Field Study of the Use of Paper Industry Sludges in Landfill Cover Systems: First Progress Report," *Technical Bulletin No. 595*, National Council of the Paper Industry for Air and Stream Improvement, New York, NY.

Trautwein, S., and Boutwell, G., 1994, "In-Situ Hydraulic Conductivity Tests for Compacted Soil Liners and Caps," *Hydraulic Conductivity and Waste Contaminant Transport in Soils, ASTM STP 1142*, American Society for Testing and Materials, Philadelphia, pp. 184-227.

Zimmie, T., Moo-Young, H., and La Plante, K., 1993, "The Use of Waste Paper Sludge for Landfill Cover Material," *Green '93: Waste Disposal by Landfill, An International Symposium on Geotechnics Related to the Environment*, Bolton Institute, Bolton, UK, Vol. 2, pp. 11-19.

Horace K. Moo-Young,[1] Marc J. Gallagher,[2] Amanda Amadon,[3] Jennifer Polaski,[3] and Michael Wolfe[3]

**Use of Paper Clay as a Barrier for Treatment of Contaminated Ground Water**

**Abstract:**

As Superfund approaches its twentieth anniversary, it has become clear that many commonly employed ground water remediation methods have not been successful. Active methods such as "pump and treat" have been shown to be effective only during operational time frames, and once discontinued, contaminants often reach pre-treatment levels. As a result, governmental agencies and the industry are looking to containment of pollution as a better long-term solution. The research presented here begins to take containment to the next level, by offering a treatment component through passive remediation. The objective of the current research was to determine the feasibility of utilizing paper mill sludge, a wastewater treatment residual, as a sorbent of heavy metals in water.

If it is found that paper sludge (herein referred to as paper clay) is an effective sorbent of heavy metals, future use may include slurry walls or other containment layers, which are in contact with metal contaminated solutions. In such a system, the pollution will be both contained, and slowly remediated with little external energy or maintenance. To assess the feasibility of paper clay as a sorbent material, sequential batch tests were conducted.

**Keywords:** paper clay, paper sludge, papermill wastes, heavy metals, reactive barrier, passive treatment, wastewater treatment residual, and slurry wall

[1]Assistant Professor, Lehigh University, 13 East Packer Avenue, Bethlehem, PA 18015.
[2]Project Engineer, Langan Engineering and Environmental Services, One Penn Center, 1617 JFK Boulevard, Suite 889, Philadelphia, PA 19103.
[3]Undergraduate Research Assistant, Lehigh University, 13 E. Packer Ave., Bethlehem, PA 18015.

## Introduction

Since the earliest civilizations, ground water has been polluted with both natural and man-made substances, as well as materials which are naturally present in water as trace elements, but which become toxic at high concentrations. Prime examples of this case are heavy metals such as cadmium, lead, mercury and zinc, which can enter the environment at elevated levels from smelting plants, metal plating industries, mine tailings and battery production, etc. Whatever the source, an unacceptable environmental condition is created which cost governments and industry billions of dollars each year for clean-up efforts.

Current remediation methods, including pump and treat and electrokinetics, are generally energy and maintenance intensive, and have been found to produce only limited long-term success (Suthersan 1997, Ward et al. 1997). A wide range of factors can affect the long term success and cost of a remediation project, including composition of the contaminant, permeability and composition of the soil matrix, geologic setting and hydraulic characteristics of the area (Gallagher 1998). Many sites have been subjected to extensive clean-up efforts only to fail to reach United States Environmental Protection Agency (EPA) drinking water standards and/or see contaminant levels return to pre-treatment levels after the remediation efforts are discontinued (Ward et al. 1997, Suthersan 1997). Therefore, research and development of technologies, which stress in-situ containment and/or treatment, are being promoted by both the EPA and industry. This approach will limit the migration of a contaminant while providing relatively inexpensive remediation (Moo-Young and Gallagher 1997).

## Passive Remediation System

Slurry walls have been widely used as passive vertical barriers to control the horizontal flow of ground water, and therefore limit the migration of a contaminant through the subsurface. Soil-bentonite is the most commonly used slurry wall material. In this technique a trench is excavated and backfilled with a mixture of bentonite and water to form the barrier. However, these barriers are nothing more than a large containment system, which require another component to actually remove the contaminant from the ground. Most systems have employed pump and treat methods once the contaminant plume has been contained by the slurry wall, thereby incurring some of the same problems of standard pump and treat systems. Cutoff walls can also require substantial initial expenditures with the cost of raw sodium bentonite in the range of $70-100/ton ($0.07-0.11 /kg)(excluding shipping, handling and construction costs). On a large site, the cost can quickly multiply. Therefore, the search is for a technique which will both contain, and remove contaminants with relatively little energy input; can be constructed of an inexpensive material; and can be left in place for extended periods of time.

Perhaps the most intriguing of the new passive technologies is reactive barriers. The concept behind reactive barriers is to utilize the natural hydraulic gradient, which causes ground water to flow, to drive the contaminant(s) through an in situ structure. The

structure would contain a reactive material to remove or alter the contaminant(s) present in the ground water (Benner et al. 1997, Blowes et al. 1995, Gallagher 1998, O'Hannesin and Gillham 1998, Puls et al. 1998, Starr and Cherry 1994). By constructing the slurry wall with material, which can both limit the flow of water, and react with the contaminant of concern, the slurry wall can achieve both containment, and attenuation of the contaminants as the ground water slowly passes through the barrier system. Finally, if the reactive material utilized in the barrier is either a waste product, or a material that is easily manufactured, the costs of the system can be dramatically reduced. Figure 1 shows a conceptual layout of a reactive semi-permeable barrier.

**Objectives**

The current study looked at the use of a waste material, paper clay, to remove heavy metal ions from aqueous solution, with the eventual goal of utilizing the paper clay in a reactive barrier setting. Paper clay is generated during wastewater treatment processes at a rate of approximately $11 \times 10^9$ kg per year in the United States alone (Springer 1986, Gregg et al. 1997). By diverting this material from the waste stream, a significant saving in landfill space can be realized. Further, by avoiding landfill tipping fees, the paper clay should be provided as a low or no cost barrier material to the remediation project.

Paper clay generally contains organic fibers and tissues (lignin and pulp), clay fillers, and trace components (resins, starch, etc. added to produce specific paper products). Paper clay has several properties, which make their use in reactive barriers very promising. They can be compacted to very low permeability ($10^{-9}$ m/sec to $10^{-11}$ m/sec) and have a high organic content, which may act as a potential carbon source for heavy metal sorption and attenuation (Moo-Young and Zimmie 1996, Kraus et al. 1997,
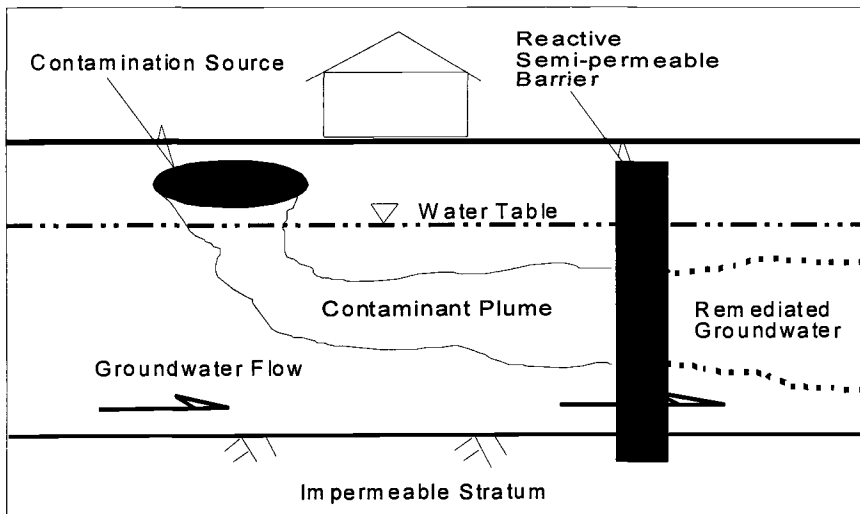


Figure 1 - *Conceptual Cross-Section Layout of a Reactive Barrier*

Moo-Young and Gallagher 1997, Gallagher 1998). Further, the paper clays generally have a high water content (150% or greater) and a low initial solids content (15-20%), which compares favorably to the common bentonite slurry material (5-15% solids) before the addition of soil (Moo-Young and Gallagher 1997).

To determine if paper clay can attenuate heavy metals from aqueous solution, isotherms need to be developed relating the amount of contaminant adsorbed to the quantity of sorbent material and contaminant present. In this study, sequential batch equilibrium testing was conducted on paper clay and aqueous solutions containing heavy metal ions (cadmium, chromium, copper, lead and zinc) to determine the sorption isotherm for each metal. The isotherm models were then utilized to predict the behavior of a paper sludge barrier exposed to heavy metal contaminated ground water. Several index and geotechnical tests were also performed including grain size distribution, Atterberg limits, specific gravity, compaction, and hydraulic conductivity testing.

## Materials

The paper clay utilized in this testing program was obtained from Ponderosa Fibers of Pennsylvania (PFP), located in Northampton, Pennsylvania. It was used in an as-received state for all testing, unless otherwise noted. The water content of the two bulk grab samples provided by PFP was approximately 150% as per ASTM Standard Test Method for Moisture, Ash, and Organic Matter of Peat and Other Organic Soils (D 2974). The paper clay was dried at a temperature of 70° C to avoid the burning off of organics. PFP is a recycling paper mill that utilizes a filter press to dewater their paper clay. Ponderosa Fibers' paper clay is approximately 50% kaolinite clay and 50% organics.

## Procedures

### Geotechnical Testing

All geotechnical engineering tests were performed as per the relevant ASTM procedure as follows. The reader is directed to the appropriate standard for further detail:

1. Specific Gravity -    ASTM D854
2. Particle Size Analysis -   ASTM D422
3. Compaction (Proctor) Tests -  ASTM D698
4. Hydraulic Conductivity -   ASTM D5084.

### Batch Equilibrium Sorption Testing

Batch equilibrium testing (batch tests) is utilized to obtain the equilibrium sorption capacity of a given sorbent for an individual sorbate (Roy et al. 1991, Kershaw 1996, Gallagher 1998). Batch testing data was used to develop equilibrium isotherms, which describe the sorption capacity of a given sorbate, exposed to various concentration of a contaminant.

A series of batch tests were conducted on PFP paper clay utilizing Environmental Protection Agency (EPA) procedures developed by Roy et al. (1991). The heavy metals tested were cadmium, chromium, copper, lead and zinc, at concentrations ranging from 5 to 1000 mg/L.

Batch tests are normally conducted on reactive mixture suspensions prepared with air dried soil and distilled-deionized water mixed with a specific amount of dissolved contaminant in a sealed container (Roy et al. 1991). Due to the nature of paper clays however, the material cannot be allowed to dry beyond a critical point to maintain the desired hydraulic and moisture-density characteristics (Moo-Young and Zimmie 1996). Further, the study aimed at testing "as-received" material to ensure constructability if employed in field applications. Therefore, the paper clay was tested as received from the Ponderosa Fiber's facility. Once the mixture is added, the container is then agitated until equilibrium occurs. Equilibrium time is defined as a change of less than 5% between successive 24 hour measurements and was determined experimentally for each sorbent/sorbate system by conducting multiple test runs and testing the concentration of the solution at various times (Roy et al. 1991, Gallagher 1998).

The equilibrium concentration of the contaminant is obtained from measurements of the liquid phase ions following centrifuge separation of the liquid from the solids. This value is compared to the initial concentration of the contaminant, and used for construction of the adsorption isotherm. The mass balance relationship used to determine the amount of contaminant sorbed to the soil surface is as follows:

$$q_{batch} = \frac{(C_o - C_{eq})(V - m/\rho)}{m} \qquad (1)$$

where:
$q_{batch}$ = sorption capacity of the solid for the solvent (mg/g)
$C_o$ = initial contaminant concentration (mg/L)
$C_{eq}$ = equilibrium contaminant concentration in solution at the end of test (mg/L)
$V$ = total volume of the batch reactor (L)
$m$ = mass of sorbent placed in reactor (g)
$\rho$ = mass concentration of the sorbent (g/L).

Plotting the sorption capacity of the sorbent ($q_{batch}$), versus the equilibrium concentration ($C_{eq}$) defines the sorption isotherm for the system. Three commonly used sorption models were fitted to the sorption data produced by the batch tests: the linear sorption isotherm, the Freundlich sorption isotherm, and the Langmuir sorption isotherm. These are described in the following equations (Roy et al. 1991).

Linear sorption isotherm
$$q_{batch} = KC_{eq} \qquad (2)$$

Freundlich sorption isotherm
$$q_{batch} = K_f C_{eq}^{(1/n)} \qquad (3)$$

Langmuir sorption isotherm

$$q_{batch} = \frac{K_L M C_{eq}}{1 + K_L C_{eq}}$$
(4)

where:

K   = partition coefficient (L/kg)
$K_f$   = Freundlich isotherm empirical constant $((L^{1/n} mg^{(1-1/n)})/g)$
n   = empirical constant (dimensionless)
$K_L$   = Langmuir equilibrium isotherm empirical constant (L/kg)
M   = empirical constant (mg/g)
$C_s$   = saturation concentration constant of sorbate in water (mg/L).

By linearizing Equations 2, 3, and 4, a least square regression analysis can be performed on data to determine which isotherm best models the observed reactions. Three useful pieces of information are provided by the adsorption isotherms:
1.  The adsorption magnitude of the contaminant.
2.  The development of an equilibrium capacity to provide a basis for preliminary estimate for how much contaminant is sorbed.
3.  The adsorptive capacity changes relative to contaminant concentrations.

*Chemical Analysis*

Analysis of heavy metals was conducted using the EPA procedures for batch studies developed by Roy et al. (1991) in the geotechnical and environmental laboratories at Lehigh University in Bethlehem, Pennsylvania. Heavy metal concentrations were determined using a Perkin Elmer AAnalyst 100 Atomic Adsorption Spectrometer (AA). The detection limit for the AA technique ranges from 0.5 to 5 parts per million (ppm) utilizing the flame technique (e.g. Cd = 0.5 ppm, $Cr_{total}$ = 1 ppm, Cu and Zn = 0.2 ppm, and Pb = 5 ppm) and from 5 to 10 parts per billion (ppb) utilizing the graphite technique.

**Results**

*Geotechnical Testing*

Specific gravity tests were conducted on the paper clay used in this study. Slight modifications were made to apply the procedure to paper clay (Moo-Young and Zimmie 1996). An aspirator was used to remove the entrapped air from the sample. Boiling the sample was avoided to reduce possible thermal reactions from occurring and giving poor results. The sludge samples were taken at their natural water content and soaked in water for an hour before pulverization, since upon drying, the sludge samples formed flocs, developed a coarse texture, and are not easily pulverized. The specific gravity of PFP paper clay was 1.76, which compares favorably with the results from other researchers (Moo-Young and Zimmie 1996, Kraus et al. 1997).

A grain size distribution test was performed on the samples. The testing of paper clay material was difficult to perform and interpret. According to ASTM Test Method for Particle Size Analysis (D 422), a representative sample should be air dried and well

pulverized prior to sieving. However, in this study, the goal was to evaluate the "as-received" characteristics of the paper clay. Therefore, the paper clay material was not pulverized prior to sieving to estimate the as received size distribution of the clods. This yielded a distribution of the clods (which naturally form in the paper clay sample) rather than individual particles-sizes. Previous research has indicated that for compacted clay barriers the size of clay clods has a strong influence on the hydraulic conductivity of compacted clay (Benson and Daniel 1990). Since paper clay is 50% kaolinite clay, the clod size may impact hydraulic conductivity.

Figure 2 shows the clod distribution curve for the paper clay in three physical conditions: oven dried, as-received water content, and hand crushed at the initial water content. In this study, the paper clay clod size ranged from 19 to 2 mm, 2 to 0.425 mm, and 19 to 0.15 mm for the as-received, hand crushed, and oven dried samples, respectively. In the study conducted by Benson and Daniel (1990), there was an increase of several orders of magnitude in the hydraulic conductivity of compacted clay caused by clod size. Similar to compacted clays during compaction, the clods in paper clay must be broken down mechanically as small as possible to reduce the effects of the clods on hydraulic conductivity. Moo-Young and Zimmie (1997) suggested the use of several passes of a low ground-pressure dozer to compact paper clay.

The moisture-density relationship was determined using the ASTM Test Method for Laboratory Compaction Characteristics of Soil Using Standard Effort (D 698). The paper clay sample yielded a maximum dry density of approximately 30 lbs/ft$^3$ (4.6
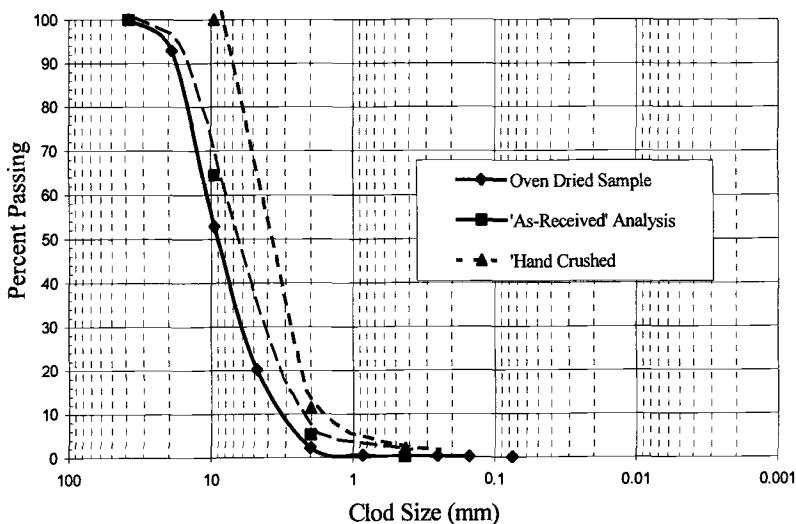


Figure 2- *Clod-Size Distribution Curve for Paper Clay*

kN/m$^3$) at 140% water content.  A maximum dry density ranging from 38 to 55 lbs/ft$^3$ (6 to 8.6 kN/m$^3$) at an optimum moisture content between 40 and 60% have been reported for paper clay (Moo-Young and Zimmie 1996, Kraus, et al. 1997).  Figure 3 shows the moisture-density relationship for paper clay.

Hydraulic conductivity tests were conducted on paper clay samples compacted at the optimum moisture content.  Previous research has indicated the maximum hydraulic conductivity of paper clay occurs at or near the optimum moisture content (Moo-Young and Zimmie 1996).  The samples were saturated and allowed to consolidate under a low confining stress of 5-psi (34.5 kPa).  The test revealed that the paper clay compacted at a water content of 140% has a hydraulic conductivity of approximately 5x10$^{-9}$ m/sec for a hydraulic gradient of 20.

Past research has shown that samples compacted at or near the optimum moisture content should have hydraulic conductivities between 10$^{-7}$ and 10$^{-9}$ m/sec (Zimmie et al. 1995, Kraus et al. 1997, Moo-Young 1997).  Moreover, it should be noted that the hydraulic conductivity of the paper clay will decrease as the moisture content increase above the optimum moisture content.  The minimum hydraulic conductivity for paper clay is typically achieved 50 to 100% wet of the optimum moisture content (Moo-Young and Zimmie 1996).  The obtained value indicates this the paper clay may serve as an effective hydraulic barrier and treatment zone provided adequate retention time of the contaminated water within the slurry wall is provided.
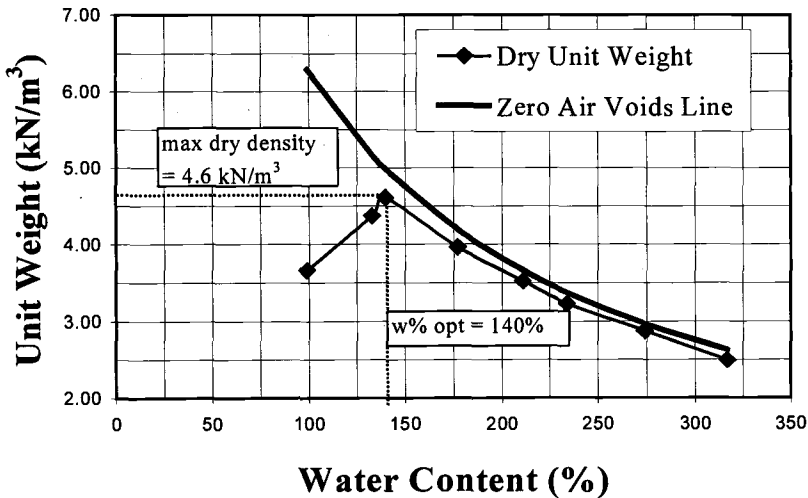


Figure 3- *Moisture-Density Relationship for Paper Clay*

*Batch Testing and Isotherm Development*

As mentioned, equilibrium batch testing was used to develop sorption isotherms for each of the sorbent/contaminant systems. It was generally found that the paper clay was able to sorb a portion of the heavy metal ions from solution. Table 1 summarizes the isotherm model which best predicted the observed reactions for the paper clay. Each of the equations listed in Table 1 is the model, which best fit the batch test data points when plotted as sorption capacity versus equilibrium concentration. Figure 4 shows the linear isotherm models for various contaminants and the paper clay. The linear isotherm models are shown since they will be used in the modeling section of the paper.

## Mathematical Modeling of a Reactive Barrier

*Procedure*

The data obtained through batch reaction testing was utilized to model the transport of a contaminant through a reactive barrier. In this study, the advection-dispersion-adsorption equation was utilized for modeling contaminant flow. The conditions and equations outlined by Evans et al. (1997) were utilized for later comparison to other sorption material.

The effluent concentration passing though a barrier is predicted with the advection-dispersion-adsorption equation defined as (Evans et al. 1997, Shackelford 1997):

$$C'e(T) = 0.5 erfc\left[\left(\frac{P}{4R_dT}\right)^{0.5}(R_d - T)\right] + 0.5e^P erfc\left[\left(\frac{P}{4R_dT}\right)^{0.5}(R_d + T)\right] \tag{5}$$

where:
$C_e'$ = dimensionless effluent concentration, $C_e/C_o$
$C_e$ = effluent concentration (mg/l)
$C_o$ = influent concentration (mg/l)
$T$ = number of pore volumes passed though the bed, $vt/L$
$t$ = time
$L$ = length of bed (barrier thickness) (m)
$P$ = Peclet number, $vL/D_x$
$D_x$ = hydrodynamic dispersion (m²/s)
$R_d$ = retardation factor
$erfc$ = complementary error function.

In Equation 5, several other factors must be defined for calculation:

$$R_d = 1 + \frac{\rho K_d}{n} \tag{6}$$

Table 1-*Summary of Isotherm Models for Paper Clay*

| Contaminant | Model | Model Equation | $r^2$ value |
|---|---|---|---|
| Cadmium | $L_m$ | $X = 0.525C_{eq}/(1+0.0172C_{eq})$ | 0.90 |
| Chromium | L | $X = 0.0041C_{eq}$ | 0.90 |
| Copper | F | $X = 0.1192C_{eq}^{0.574}$ | 0.97 |
| Lead | F | $X = 0.3857C_{eq}^{0.524}$ | 0.96 |
| Zinc | $L_m$ | $X = -0.950C_{eq}/(1-1.384C_{eq})$ | 0.85 |

$X = mg/g$; $C_{eq} = mg/L$ or ppm
L = Linear Isotherm Model; F = Freundlich Isotherm Model; $L_m$ = Langmuir Isotherm Model
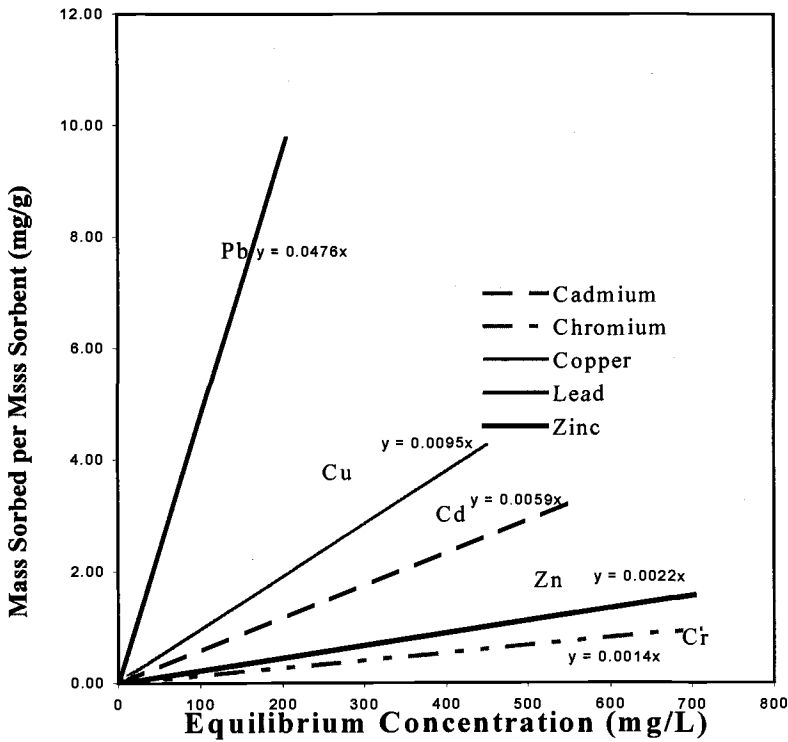


Figure 4-*Linear Sorption Isotherms for Paper Clay*

$$\rho = (1 - n)\rho_s \tag{7}$$

$$D_x = D_m + 1.75\, d\, v \tag{8}$$

where

$\rho$ = average bed density (mg/L)

$K_d$ = linear partitioning coefficient (slope of linear isotherm) (L/mg)

$\rho_s$ = density of solids (sorbent material) (mg/L)

n = porosity

$D_m$ = Diffusion coefficient ($5 \times 10^{-6}$ m$^2$/s)

d = grain size (50 micron for kaolinite clay)

v = velocity (m/s)

As can be concluded by the use of $K_d$, the partition coefficient, this model is only valid for contaminant concentrations, which fall within the linear range of the sorption isotherm. For many of the systems studied here, this limits the use of this model to low concentrations, generally under 100 mg/L.

Equation 5 is used to calculate the dimensionless effluent concentration, $C_e$', for a variety of elapsed times. By plotting $C_e$' versus time, a breakthrough curve is developed to estimate the time required to reach a point where the effluent concentration exceeds established limits. Once the effluent reaches an unacceptable level, the sorbent material would have to be replaced, or an alternate remediation method employed.

*Mathematical Modeling Results*

The final step in the study was to predict the effectiveness of a reactive barrier constructed of paper clay material, for the removal of heavy metals from a ground water environment. As mentioned, Equation 5 was used for this task, following the same methods outlined by Evans et al. (1997). For each of the systems, a partitioning coefficient was determined (slope of the linear portion of the $C_{eq}$ versus $q_{batch}$ plots). Retardation factors were then calculated with Equation 6 (see Table 2). Using the calculated retardation factor, the experimentally determined hydraulic conductivity, and assumed hydraulic gradient of 1, wall thickness of 1 m and an estimated diffusion coefficient of $5 \times 10^{-6}$ cm$^2$/sec, Equation 5 was used to model the flow of a heavy metal plume through a paper clay barrier. Table 3 shows the estimated breakthrough time (5%

Table 2-*Estimated Retardation Coefficients and Partitioning Coefficient*

| Metal | Paper Clay $K_d$ | Retardation Coefficient |
|---|---|---|
| Cadmium | 94 L/kg | 67 |
| Chromium | 3 L/kg | 3.2 |
| Copper | 32 L/kg | 23 |
| Lead | 124 L/kg | 88 |
| Zinc | 16 L/kg | 12 |

Table 3-*Estimated Breakthrough Times in Years*

| Metal | Paper Clay | | |
|---|---|---|---|
| | $K=10^{-8}$ m/sec | $k=10^{-9}$ m/sec | $k=10^{-10}$ m/sec |
| Cadmium | 92 | 350 | 523 |
| Chromium | 4.5 | 18 | 27 |
| Copper | 33 | 110 | 190 |
| Lead | 110 | 490 | 700 |
| Zinc | 17 | 63 | 95 |

Breakthrough defined as 5% of initial influent concentration detected in effluent

of the original concentration) for the paper clay. As can be seen in Table 3, paper clay barriers may serve as an effective containment/remediation system given suitable conditions.

## Comparison of Paper Clay to Other Adsorption Barriers

The paper clay results were compared to the study conducted by Evans et al. (1997), which examined the use of sand-bentonite slurry wall materials to sorb heavy metals. In comparing the results in this study to the results obtained by Evans et al. (1997), paper clay has a higher sorption capacity for lead and cadmium than sand-bentonite mixtures tested contaminants. On the other hand, paper clay has a lower adsorption capacity than the soil-bentonite mixes for zinc solutions. The concentrations, which were tested by Evans et al. (1997), were generally below 15 to 20 ppm, so no conclusions can be drawn regarding performance at the higher contaminant concentration levels tested by the author.

Since paper clay is typically 50% kaolinite clay (and 50% organics), the expected adsorption capacity should be low. The increase adsorption capacity of paper clay in comparison to kaolinite may be a result of its organic constituents. It may be postulated that the organic fibers and tissues may act as an electron acceptor in oxidation and reduction reactions, and may act as a carbon source to support microbial growth. Further research is required to support this hypothesis.

Previous research in the adsorption of heavy metals to organic materials may aid in understanding the increase in adsorption capacity of paper clay in comparison to kaolinite. Despite rather extensive research, the environmental engineering community has not reached a common conclusion as to the mechanisms causing metal and organic adsorption (McKay 1996). Naturally occurring peat has been used for the treatment of wastewater for over 20 years. In fact, the use of peats for the removal of heavy metals such as copper, zinc, lead, and mercury have been studied since 1939 (McKay 1996). Peat consists primarily of lignin, cellulose and humic acids, and should represent papermill wastes to a certain degree. Provided flow rates are low and the quantity of water to be treated is small, peat has been shown to be a very effective adsorbent of metals (McKay 1996). According to McKay (1996), there has not been a clear

conclusion as to whether metal adsorption is a result of exchange reactions (positive metal ions are electrostatically attracted to negatively charged sorbent surface), or chemical adsorption (metal forms strong bonds to the sorbent material).

Most researchers have agreed on a few items however. First, the uptake of metal ions by peat is very rapid. Second, that adsorption capacity of the peat is directly related to the pH of the solution. The optimal range for adsorption capacity has been found to lie between pH of 3.5 and 6.5 (McKay 1996). If the pH drops below 3.5, the hydrogen ions strip metals from the peat causing a leaching effect. At pH above 8.5, the peat itself is not very stable. Batch tests conducted on the paper clay at various contaminants were typically at the higher end (i.e., 6.5) of this pH range. Finally, it has also been found that the larger the specific surface area of the adsorbing material, the greater the sorption capacity.

The sorption of heavy metals from aqueous solution by organic plant matter was studied by Roy et al. (1993). In this study, the authors utilized green algae and crushed rice hulls to determine the sorption ability of arsenic, cadmium, cobalt, chromium, lead, strontium, nickel and zinc. They undertook the work because even through the exact sorption mechanism is not understood, it has been found that many different types of biomass have the ability to adsorb heavy metal ions though chelation (Roy et al. 1993). While the study did not present maximum sorption capacities of the rice hulls and algae, they did state that the sorbents were able to remove over 90% of all the metal species tested. They also found that equilibrium of the systems was reached quickly (under one hour) and that the sorption was not affected by having multiple metal ions present, simultaneously. This last point is in contradiction to the peat sorption studies.

Another project focused on the use of cattails as a sorbent material for heavy metals in an aqueous solution. This study, conducted at the University of Toronto, found that crushed cattail leaves were an effective adsorbent of lead, cadmium, and mercury (Krichnan et al. 1988).

## Conclusions

Overall, the research appears to show promise for the use of paper clay as a sorbent material. The ability to utilize this waste stream in ground water remediation projects is attractive from environmental, economic, and social viewpoints. Initial batch tests show that paper clay may provide an adequate sorbent to retard the movement of contaminants in the subsurface. In comparison with kaolinite clay, paper sludge has a greater affinity to adsorb certain heavy metals. The high organic content of paper clay may have contributed to its greater affinity to adsorb the contaminant.

## Acknowledgement

## References

Benson, C. H. and Daniel, D. E., 1990, "Influence of Clods on Hydraulic Conductivity of Compacted Clay," *Journal of Geotechnical Engineering*, American Society of Civil Engineering, Vol. 116, No. 12, pp. 1811-1830.

Benner, S. G., Blowes, D. W., and Ptacek, C. J., 1997, "A Full-Scale Porous Reactive Barrier for Prevention of Acid Mine Drainage," *Ground Water Monitoring and Remediation*, Vol. 17, No. 4, pp. 99-109.

Blowes, D. W., Ptacek, C. J., Cherry, J. A., Gillham, R. W., and Robertson, W. D., 1995, "Passive Remediation of Ground Water Using In Situ Treatment Curtains," *Geoenvironmental 2000*, Geotechnical Special Publication No. 46, Yalcin B. Acar and David E. Daniel Eds., American Society of Civil Engineering, Reston, VA, pp. 1588-1607.

Evans, J., Adams, T. and Prince, M. J., 1997, "Metal Attenuation in Minerally-Enhanced Slurry Walls," *Conference Proceedings for the International Containment Technology Conference*, Florida State, Tallahassee, pp. 679-687.

Gallagher, M. A., 1998, *The Use of Paper Mill Wastes for Heavy Metal Removal from Ground water*, Masters Thesis, Lehigh University, Bethlehem, Pennslyvania.

Gregg, J. J., Zander, A. K. and Theis, T. L., 1997, "Fate of Trace Elements in Energy Recovery from Recycled Paper Sludge," *TAPPI Journal*, Vol. 80, No. 9, p. 157-162.

Kershaw, D. S., 1996, *BTEX Removal From Ground water Using Ground Tire Rubber*, M.S. Thesis, Department of Civil and Environmental Engineering, Lehigh University, Bethlehem, Pennsylvania.

Kraus, J. F., Benson, C. H., Van Maltby, C. and Wang, X., 1997, "Laboratory and Field Hydraulic Conductivity of Three Compacted Paper Mill Sludges," *Journal of Geotechnical and Geoenvironmental Engineering*, American Society of Civil Engineering, Vol. 123, No. 7, p. 654-662.

Krichnan, S. S., Cancilla, A. and Jervis, R. E., 1988, "Waste Water Treatment for Heavy Metal Toxins Using Plant and Hair as Adsorbents," *The Science of the Total Environment*, Vol. 68, p. 267-273.

McKay, G., 1996, *Use of Adsorbents for the Removal of Pollutants from Wastewaters*, CRC Press, Boca Raton, Florida.

Moo-Young, H. K., and Gallagher, M., 1997, "Determination of the Adsorption Capacity of Paper Sludge for Use as a Reactive Barrier," *First International Workshop on the Use of Paper Industry Sludges in Environmental Geotechnology and*

*Construction,* J. Saarela and T. F. Zimmie, Eds., Suomen Ymparistokeskus, Helsinki, pp. 73-80.

Moo-Young, H. K., and Zimmie, T., 1996, "Geotechnical Engineering Properties of Paper Mill Sludges for Use in Landfill Covers," *Journal of Geotechnical Engineering*, American Society of Civil Engineering, Vol. 122, No. 9, p. 768-776.

Moo-Young, H. K. and Zimmie, T. F., 1997, "Utilizing a Paper Sludge Barrier Layer in a Municipal Landfill Cover in New York," *Testing Soils Mixed with Waste or Recycled Materials, ASTM STP 1275,* Mark A. Wasemiller and Keith Hoddinott Eds., American Society for Testing and Materials, West Conshohocken, PA, pp. 125-140.

O'Hannesin, S. F. and Gillham, R. W., 1998, "Long-Term Performance of an In Situ 'Iron Wall' for Remediation of VOC," *Ground Water*, Vol. 36, No. 1, pp. 164-170.

Puls, R. W., Blowes, D. W., and Gillham, R. W., (1998), "Emplacement Verification and Long-Term Performance Monitoring of Permeable Reactive Barrier at the USCG Support Center, Elizabeth, North Carolina," *International Association of Hydrological Science*, No. 250, pp. 459-466.

Roy, D., Greenlaw, P. N. and Shane, B. S., 1993, "Adsorption of Heavy Metals by Green Algae and Ground Rice Hulls," *Journal of Environmental Science and Health – Part A, Environmental Science and Engineering*, Vol. 28, No. 1, p. 37-50.

Roy, W. R., Krapac, I. G., Chou, S. F. J. and Griffin, R. A., 1991, *Batch-Type Procedures for Estimating Soil Adsorption of Chemicals*, U.S. Environmental Protection Agency Technical Resource Document, Washington, D. C., Doc. No. EPA/530-SW-87-006-F.

Shackelford, C. D., 1997, "Modeling and Analysis in Environmental Geotechnics: An Overview of Practical Applications," *Environmental Geotechnics*, M. Kamon, Ed., A.A. Balkema, Rotterdam, Vol. 3, pp. 1375-1404.

Springer, A. M., 1986, *Industrial Environmental Control – Pulp and Paper Industry*, John Wiley and Sons, New York, New York.

Starr, R. C. and Cherry, J. A., 1994, In Situ Remediation of Contaminated Ground water: The Funnel and Gate System, *Ground Water*, Vol. 32, No. 6, pp. 958-967.

Suthersan, S.S. 1997, *Remediation Engineering Design Concepts*, CRC Publishers, Boca Raton, Florida.

Ward, C. H., Cherry, J. A. and Scalf, M. R., 1997, *Subsurface Restoration*, Ann Arbor Press, Inc., Chelsea, Michigan

Masashi Kamon,[1] Takeshi Katsumi,[2] and Kaku Watanabe[3]

## Heavy-Metal Leaching from Cement Stabilized Waste Sludge

**Abstract:** The purpose of this paper is (1) to review the current Japanese status on the contamination of sediments, (2) to evaluate the leaching characteristics from cement stabilized sludge containing heavy metals, and (3) to discuss some factors affecting the leaching characteristics. Waste sludge is discharged from dredging works in harbors, lakes and rivers. Waste sludge has a high water content and is often contaminated with toxic substances. The reuse of treated sludge in geotechnical applications should be encouraged if the sludge can be sufficiently treated to minimize adverse environmental impact.

Column and batch leaching tests are conducted on the cement stabilized sludge containing heavy metals (lead and chromium). The batch test is in accordance with the Japanese regulatory requirement. The column leaching test is performed to account for hydraulic conductivity. The accumulated mass of heavy metal leached from a stabilized sludge with a unit thickness (1 m) per unit area (1 m$^2$) under a one-dimensional vertical seepage flow with a unit hydraulic gradient (i = 1) is calculated from the column test results in order to discuss the environmental impact when the stabilized sludge is reused in geotechnical applications. When the contaminated sludge with high water content (300%) is directly stabilized, significant leaching occurs. For instance, in 0.8 year, a total of 300 mg/m$^2$ of Cr leached from 1 m thick stabilized soil, and 2 g/m$^2$ of Pb leached. When sludge is stabilized after the dewatering to a water content of 80%, the mass leaching is substantially reduced due to the lower hydraulic conductivity of the stabilized soil. For example, cumulative mass leaching is expected to be approximately 1 g/m$^2$ in 200 years for Pb, and less than 50 mg for Cr mass in 300 years. However, if the stabilized sludge is crushed, subjected to drying, or exposed to acid, higher quantities of Pb and Cr are expected to leach. In conclusion, the contaminated sludge can be used as earthen material if it is stabilized properly, that is, with low water content, without exposure to acid and drying, and without being crushed.

**Keywords:** soil stabilization, heavy metal, leaching, sludge, hydraulic conductivity, chromium, lead, geo-environmental impact

[1] Professor, Disaster Prevention Research Institute (DPRI), Kyoto University, Uji, Kyoto 611 0011, Japan.

[2] Research Associate, Disaster Prevention Research Institute (DPRI), Kyoto University, Uji, Kyoto 611 0011, Japan.

[3] Graduate Student, Department of Civil Engineering, Kyoto University, Sakyo, Kyoto 606 8501, Japan (Currently, Civil Engineer, Toda Construction Co. Ltd., Japan).

123

## Introduction

Contamination of bottom sediments in seas, lakes and rivers is a major environmental issue, and has also been becoming an important geotechnical challenge for Japan in recent years. Contaminated sludge requires proper treatment to minimize its environmental impact. Typically, contaminated sludges are landfilled following some treatment process. However, available capacity of landfill space is limited in Japan. The reuse of treated sludge in geotechnical applications is encouraged provided the sludge can be sufficiently treated to minimize adverse environmental impact and attain an excellent engineering property. Cement stabilization, whether independently applied or associated with dehydration treatment, is considered an effective treatment method for such sludge materials.

When considering the geotechnical application of treated sludge, the potential environmental impact should be assessed. It has been pointed out that there is a need to develop an appropriate method for evaluating the environmental impact of reused waste materials, including soils to be abandoned (e.g. Kamon 1998, Edil and Benson 1998, Hartlén et al. 1997, Sakai et al. 1996). A mass basis method to evaluate the environmental impact arisen by the leaching from the stabilized soil or waste containing heavy metals is proposed (Shackelford and Glade 1997, Kamon and Katsumi 1999). Kamon and Katsumi (1999) also claim that the current Japanese regulatory method to evaluate the toxicity of waste may not represent the in situ condition of the stabilized recycled materials such as stabilized sludge. In addition, there is a need to discuss the environmental impact of recycling treated sludge materials with respect to the treatment process. Of particular importance is whether the waste sludge with high water content should be directly solidified or be dehydrated prior to the solidification. Also, the leaching characteristics following pulverizeing the soil, exposure to acid, and drying should be assessed.

In this paper, the effects of the treatment process and condition affecting the leaching characteristics of cement stabilized sludge are discussed. First, current Japanese regulations governing contaminated bottom sediments, treatment technology, and possible geotechnical application for waste sludge are reviewed. Second, effect of dehydration treatment prior to cement stabilization is assessed from laboratory column leaching tests on stabilized Cr- and Pb-soil. Finally, some aspects affecting the leaching characteristics, namely crushing, drying, and acid exposure, are discussed.

## Background –Japanese Status–

*Contamination of Sediments*

Contamination of sediments in sea, lakes and rivers has been a major environmental issue in Japan. In some cases, it even impacted human health, such as Minamata disease which inflicted people who had fishes in Minamata Bay where the bottom sediments were heavily contaminated with mercury.

Toxic substances designated by the following regulations: "Environmental Standard for Soil (Environmental Agency Notification No. 46)" which designates 10 types of heavy metals and related chemicals (cadmium, cyanide, phosphorus, lead, hexavalent chromium, arsenic, mercury, alkyl mercury, PCB and copper) and 15 organic chemicals (dichloromethan, carbon tetrachloride, 1,2-dichloroethan, 1,1-dichloroethylen, cis-1,2-dichloroethylene, 1,1,1-trichloroethane, 1,1,2-trichloroethane, trichloroethylene, tetrachloroethylene, 1,3-dichloropropene, ciulam, cymagin, ciobenkalb, benzene, and

selenium), and "Law for the Prevention of Marine Pollution" which adds 7 more chemicals (zinc, fluoride, beryllium, chromium, nickel, vanadium, and total organic chemicals) to the ones designated by the "Environmental Standard for Soil." The chemicals designated by "Provisional Standard for Treatment and Disposal of Deposits" are identical except copper is excluded.

Site investigation focuses primarily on mercury and PCB, although there are many chemicals designated by the regulation and considered to be present in contaminated sludge. Nakajima (1998) documents mercury concentrations from 47 sites that were above the regulatory requirement, and estimates that 8,500,000 $m^3$ Hg-contaminated sludge, including 2,500,000 $m^3$ sludge from Minamata Bay, has been treated and disposed. Also, sediments from 88 sites were above the regulatory requirement for PCB.

Table 1–*Selected Bottom Sediment Removal Projects in Japan*

| Port | Work period | Pollutant | Volume of dredging (*1,000 $m^3$) | Removal standard | Disposal method |
|------|-------------|-----------|-----------------------------------|------------------|-----------------|
| Tokyo | 1972-81 | Organics | 2,400 | 6 points or more in the overall, Ignition loss, COD, and sulfides | Reclamation by totally sealed grab buckets and special pumps |
| Yokohama | 1973-79 | Organics | 691 | same as above | Reclamation by ordinary grab buckets |
| Nagoya | 1972-81 | Mercury, Organics | 729 | 25 ppm Hg; 15% Ignition loss | Reclamation by ordinary grab buckets |
| Yokkaichi | 1974-79 | Mercury, Oils | 2,200 | 6 ppm Hg; 4,000 ppm Oils | Reclamation by special pumps |
| Osaka | 1973-81 | Organics | 1,645 | 15% Ignition loss | Reclamation by special pumps |
| Kita-Kyusyu | 1972-81 | Mercury, Organics | 3,300 | 30 ppm Hg | Reclamation by totally sealed grab buckets |
| Tagonoura | 1972-80 | PCBs, Organics | 1,720 | 10 ppm PCBs | (1) Reclamation by pump; (2) Dredging by ordinary grab buckets, solidification and reclamation |
| Mizushima | 1972-80 | Oils | 813 | 1,500 ppm Oils | |
| Minamata | 1975-87 | Mercury | 1,675 | 25 ppm Hg | |
| Takamatsu | 1980 | PCBs, Organics | 397 | Undecided | |
| Omuta | 1973-79 | Cadmium, Mercury | 536 | 25 ppm Hg; 200 ppm Cd | (1) Reclamation by special pumps; (2) Earth covering |
| Mikawa | 1973-75 | Organics | 50 | 16 mg/g COD; 10% Ignition loss; 1 mg/g Sulfides | Reclamation by totally sealed grab buckets |
| Sakata | 1974-75 | Mercury | 71 | 28 ppm Hg | Reclamation by special pumps |

The remediation work has been completed for 84 of these sites which corresponds to 6,800,000 $m^3$ sludge treatment, from which 6,200,000 $m^3$ of sludge is from 5 sites. In addition, 1,200,000 $m^3$ sludge in 19 sites have been treated for lead, cadmium, copper, arsenic, chromium, and petroleum contamination.

*Treatment Technology*

Technology for the treatment and disposal of contaminated waste sludge or bottom sediment from seas, rivers and/or lakes has been developed for the pollution control as a total system combining treatment and disposal processes. The former is dredging, dehydration, drying, solidification of waste sludge and spill water treatment, and the later is land reclamation. Recent focus has been on in situ treatment because of the lack of reclamation site, as summarized by Kamon et al. (1998b). Therefore, alternative technologies such as reuse, recycling, and sand covering are required because of their environmental friendliness.

Table 1 summarizes the treatment projects which have been undertaken in ports and harbors and inland seas in Japan. The mercury-contaminated sludge in Minamata Bay, the cause of Minamata disease, and the PCBs-contaminated pulp sludge in Tagonoura Port were the first attempts of waste sludge treatment.

Solidification techniques are used for two purposes. One is to strengthen the high water content sludge and the other is to immobilize the heavy metals and other toxic substances. After solidified, these sludges can be landfilled.

The current focus of waste sludge treatment in Japan is stabilizing organic sludges which consists mainly of clay and silt with organic matter and nutrients. It is, however, limited to the non-toxic waste sludges. Toxic or harmful sludges are contained in the controlled disposal sites.

*Geotechnical Application of Sludge and Environmental Regulation*

The sediments from harbor, lakes and rivers may be treated in a manner similar to the methods for improving the waste sludge discharged from construction works. Following treatment, they may be reused in geotechnical applications. Several methods which have been proposed to treat the waste sludge from construction works are reviewed by Kawachi et al. (1996). Among them, solidification treatment is preferred. Cement might work well for the raw sludge, but solidification combined with dehydration is effective from the viewpoint of volume reduction and rapid treatment (Kamon and Katsumi 1994; Kamon et al. 1998a).

For geotechnical applications, classification according to the Japanese Ministry of Construction can be applied. According to properties of the soil (e.g. unconfined compressive strength), soils are classified into 5 levels, namely 1st-, 2nd-, 3rd- and 4th-class-soils and sludge. The materials classified as level 4 or higher may be used as earthen materials, such as embankment construction.

To evaluate the toxicity of soil and/or waste, Japanese regulations require a batch leaching test (elution test) be performed. The required procedure is as follows; (1) crush the sample into particles, (2) mix the sample with de-ionized water to achieve L/S (liquid per solid ratio in a weight basis) = 10, (3) adjust the sample pH to 5.8-6.3 (e.g. add HCl if necessary), (4) stir the solid-liquid mixture for 6 hours, (5) filter the solid from the mixture (0.00045 mm mesh), and (6) determine the concentration of specific chemicals in the liquid. Allowable concentrations of several inorganic chemicals are listed in Table 2.

Table 2—*Judgment Criterion, Environmental Standard and Effluent Standard in Japan*

| Substance | Toxicity of Waste (mg/L) | Environmental Standard for Soil (mg/L) | Environmental Standard of Drinking Water (mg/L) |
|---|---|---|---|
| Alkyl mercury compound | Not detected | Not detected | Not detected |
| Mercury or a comp. thereof | 0.005 | 0.0005 | 0.0005 |
| Cadmium or a comp. thereof | 0.3 | 0.01 | 0.01 |
| Lead or a compound thereof | 0.3 | 0.01 | 0.05 |
| Organic phosphorus comp. | 1 | - | - |
| Hexavalent chromium comp. | 1.5 | 0.05 | 0.05 |
| Arsenic or a comp. thereof | 0.3 | 0.01 | 0.01 |
| Cyanide compound | 1 | Not detected | Not detected |
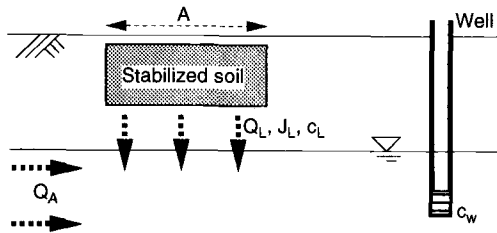


$Q_A$: Flow rate of aquifer
$Q_L$: Flow rate of seepage from the stabilized soil
$J_L$: Mass flux of the heavy metal in the seepage
$c_L$: Concentration of the heavy metal in the seepage
A: Area of the stabilized soil
$c_w$: Concentration of the heavy metal in the downstream aquifer

$$c_w = J_L \, A \, / \, ( \, Q_L + Q_A \, ) \quad < \text{Environmental criterion}$$

Figure 1—*Senario for Mass Based Environmental Impact Assessment of Stabilized Contaminated Soil (after Kamon and Katsumi 1999)*

However, inherent deference in the properties of stabilized soils from unstabilized soils is not accounted for by this method. Also, concentration basis evaluation might not be appropriate, even leaching of large quantity of chemicals may result in more amount of low concentrated water due to dilution effect. Kamon and Katsumi (1999) propose a mass basis method for evaluating leaching from the stabilized soil containing heavy metal which accounts for the hydraulic conductivity. Figure 1 shows a schematic scenario for this method.

**Materials Used**

For the following experiments, alluvial clay (LL = 63.7%, PL = 28.7% , $G_s$ = 2.67, $D_{max}$ = 0.425 mm) obtained from a 10 m depth at a construction site located in Higashi-Osaka City, Osaka Prefecture was used. The soil was air-dried to approximately 60%

water content, then mixed with the de-ionized water containing dissolved $K_2Cr_2O_7$ or $PbNO_3$ until a target water content (80% or 300%) and target mass (10 mg or 100 mg) of Cr or Pb per 1 kg dry soil was achieved. Then, various amounts of cement were added to the Cr- and Pb-contaminated soils aged for at least 24 hours. Samples were mixed for 10 minutes, and placed in the molds where they were cured for the period of 7 or 28 days.

Seven-day unconfined compressive strengths of the stabilized mixtures are 40-60 kPa for the sludge with 300% water content and 9% cement addition, 160 kPa for 300% water content and 18 % cement addition, 30-60 kPa for 80% water content and 5% cement addition, and 110-170 kPa for 80% water content and 15% cement addition. According to the criteria of the Japanese Ministry of Construction, the stabilized Cr- and Pb-soil may be used for geotechnical applications.

## Effect of Water Content on Leaching Characteristics

The effect of water content on leaching characteristics is required when deciding if a waste sludge should be dehydrated prior to the solidification.

### High Water Content Sludge

Column leaching tests were conducted using a rigid wall permeameter on the stabilized Cr- and Pb-soil with 300% water content. Test specimens were 5.0 cm tall and 5.1 cm in diameter. An upward hydraulic gradient of 3.6 was applied through the sample which was cured for either 7 or 28 days. Deionized water was used as the influent.
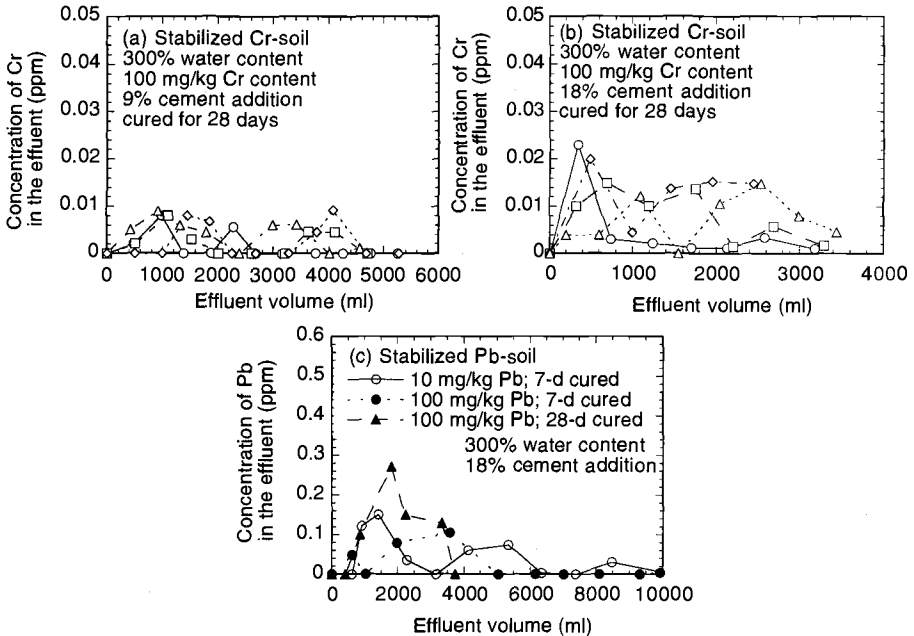


Figure 2—*Concentration of Cr and Pb in the Effluent*

Effluent from the specimen was collected periodically, and pH and heavy metals concentration were measured.

Changes in concentration of Cr or Pb leaching from the stabilized sludge versus effluent volume are shown in Figure 2. Values of the Cr concentrations are scattered, but the range of the Cr concentration is 0 to 0.01 ppm for sludge stabilized with 9% cement addition, and 0 to 0.02 ppm for the sludge stabilized with 18% cement. Also, the leaching concentrations under several different conditions (10 mg/kg Cr content, 7 days curing prior to the leaching test, etc.) reported by Watanabe (1998) indicate that the initial Cr content, curing period before the leaching test, and the cement additive content do not have a clear effect on leaching characteristics, and Cr concentration values are always below 0.025 ppm. The Pb concentrations are also scattered, and it is hard to derive some tendency from these results. However, when Cr and Pb concentrations are compared to the regulatory standards presented in Table 2, Cr concentrations are below the Environmental Standards for both soil and drinking water (both 0.05 mg/L), while Pb concentrations exceed the regulatory level for soil and drinking water (0.01 and 0.05 mg/L respectively).

Values of pH and hydraulic conductivity are shown in Figure 3. The pH values are steady at between 12 and 13 for the stabilized Cr-soil, and decrease slightly over time for the stabilized Pb-soil. Hydraulic conductivity is in the range of $2 \times 10^{-6}$ to $3 \times 10^{-5}$ cm/s.

The leaching performance of Cr and Pb are discussed by Kamon and Katsumi (1999). $Cr_2O_7^{2-}$ in $K_2Cr_2O_7$ may change to $CrO_4^{2-}$ under the high pH condition. $CrO_4^{2-}$ may exist in the immovable water layer (Stern layer) of the clay particles with other cations and water molecules, or in the diffuse layer of clay particles. Adsorption of $CrO_4^{2-}$ on the clay particle surface could be low relative to cations because of its net negative charge. Thus, it is likely that $CrO_4^{2-}$ is immobilized in the cement hydrated products. $CrO_4^{2-}$ is immobilized by tri-sulfate and mono-sulfate hydrated products, because it might replaces $SO_4^{2-}$ (e.g. Kujala 1989). For Pb, $Pb(OH)_2$ precipitates at weak alkali conditions, while a soluble complex ion $(Pb(OH)_4^{2-})$ is formed at a strong alkali condition (pH>11). The experimental results are consistent with this theory. The pH decreases slightly, and the concentration of Pb approaches to zero during permeation.

Because the results of column leaching tests are not a direct measure of the in situ performance, it is necessary to make some translation to consider in situ conditions. Figure 4 presents the results calculated using a mass based approach proposed by Kamon
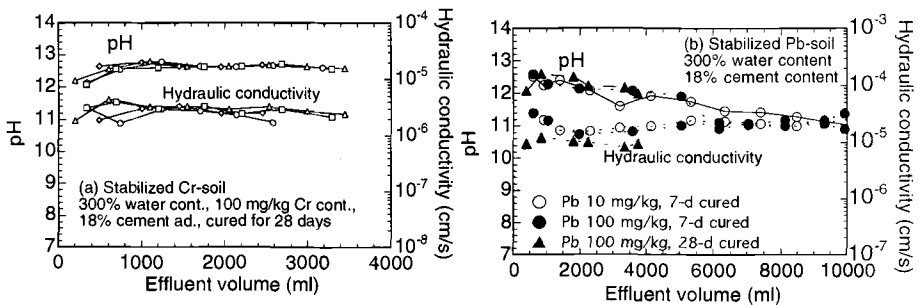


Figure 3–*Hydraulic Conductivity and pH of Effluent from Column Leaching Tests of the Stabilized Soil Containing Cr and Pb*
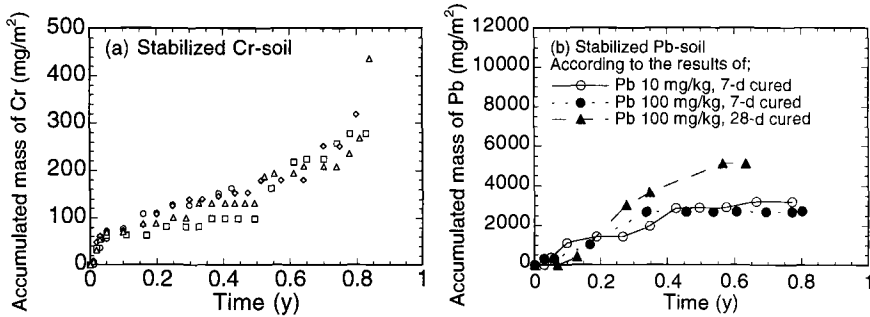
Figure 4—*Cumulative Mass of Cr or Pb Leaching from 1 m Thick Stabilized Soil for a Supposed Period*

and Katsumi (1999). Herein, one-dimensional, vertical seepage through the stabilized soils under a unit hydraulic gradient ($i = 1$) is assumed to estimate the time required to obtain seepage in the field which is equivalent to the quantity of effluent obtained from the laboratory column tests. Accumulated mass leachate per unit area ($1 \text{ m}^2$) from a 1 m thick stabilized soil is calculated from the experimental results (Figures 2 (b) and (c)). As shown in Figure 4, the volume of effluent obtained from laboratory tests corresponds to less than 1 year period of seepage in the field because of the high hydraulic conductivity. The accumulated mass of Cr leached from 1 m thick stabilized soil for 0.8 year is about 300 mg/m$^2$ (0.29% of the total mass of Cr added to the soil), whereas the mass of Pb under a similar condition is greater than 2 g/m$^2$ (2.0% of the total mass of Pb added to the soil).

*Reduced Water Content Sludge*

An example of change in total mass and volume of the sludge due to the direct solidification and the dehydration-solidification treatment is shown in Figure 5. Herein, it is assumed that the original water content of 300% is reduced to 80% by the dehydration treatment prior to solidification. The final volume of the stabilized sludge should decrease
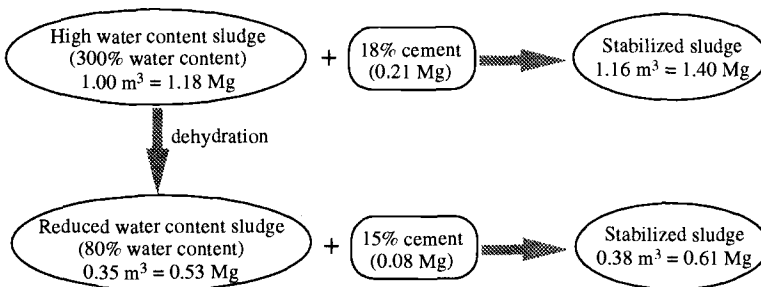


Figure 5—*Mass and Volume of the Sludge Stabilized with and without prior Dehydration Process*
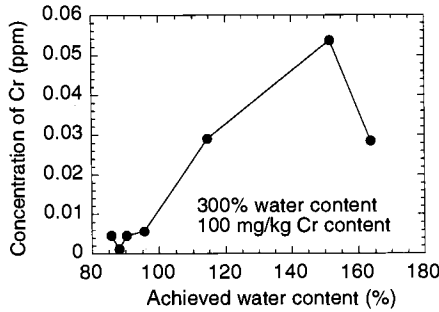
Figure 6–*Concentration of Cr in the Water Dehydrated from Cr-Soil*
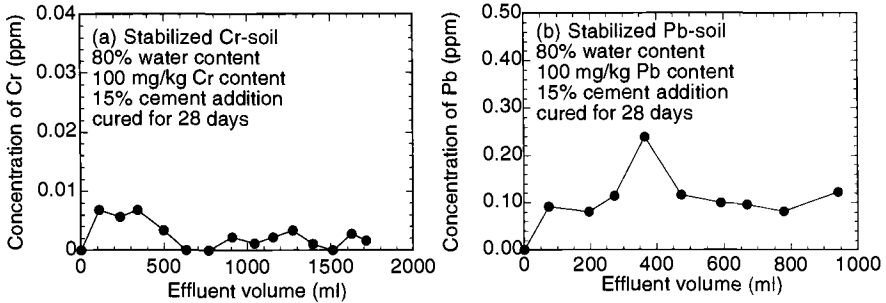


Figure 7–*Concentration of Cr or Pb in the Effluent from the Stabilized Soil (after Kamon and Katsumi 1999)*

from 1.0 m³ to approximately 0.4 m³ due to the dehydration.

Heavy metal content in the dehydrated water is also important. The Cr concentration in the water dehydrated from a sludge sample with an initial Cr concentration of 100 mg/kg is shown in Figure 6. A centrifugal force was used to dehydrate sludge. The Cr concentration of the effluent decreases as more water is drawn from the sample. This may occur because Cr is present with the clay particles so that when a stronger centrifugal force is applied less particles remain in the dehydrated water. In addition, the concentration levels of Cr are below the regulatory requirement for drinking water (0.05 mg/L). Thus the dehydrated water could be freely released.

Results of the leaching characteristics from the reduced water content sludge (80% water content) using a flexible permeameter have been reported by Kamon and Katsumi (1999). The results shown in Figure 7 indicate that the both Cr and Pb concentrations are in a similar range to concentrations obtained from the high water content sludge (300%) (Figure 2). However, since hydraulic conductivity values are significantly lower ($10^{-8}$ cm/s), the accumulated mass per unit area (1 m²) leached from the 1 m thick stabilized soil under a unit hydraulic gradient (i = 1) is lower than the mass from the high water content sludge. As shown in Figure 8, the cumulative mass of Pb is approximately 1 g in 200 years (5 mg in 1 year), and less than 50 mg Cr mass for over 300 years. These values are only 0.72% and 0.036% of the total mass of Pb and Cr added to the soil respectively.
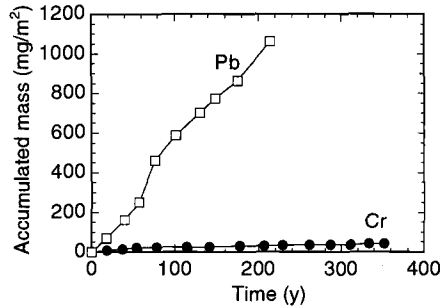
Figure 8–*Culumative Mass Leaching from 1 m Thick Stabilized Soil for a Supposed Period (after Kamon and Katsumi 1999)*

In conclusion, dehydration prior to solidification results in lower mass leaching from the stabilized sludge and low concentration of dehydrated water.

## Factors Affecting Leaching Characteristics

*Crushing*

It is likely that stabilized sludge would be crushed prior to the recycling. Also, the stabilized sludge might have in situ cracks. Therefore, the leaching characteristics were evaluated on crushed specimens of stabilized-sludge. The sludge with 80% water content stabilized using 5% cement that was cured for 7 days, was crushed to particles finer than 9.5 mm. The aggregate was then compacted and cured in the mold. All the specimens prepared according to this procedure had unconfined compressive strengths higher than 150 kPa, which indicates the crushed stabilized-sludge may be used in some geotechnical applications.

Figure 9 shows the results of the column leaching test on three specimens cured for 21 days after crushed. Although there are some spikes higher than 0.02 ppm at early stages of testing, the concentrations of Cr in the effluent are in the range of 0-0.02 ppm. These concentrations are similar to the results from uncrushed specimens. Hydraulic conductivity, however, is about two order magnitude larger ($10^{-6}$ cm/s) than uncrushed specimens. As a result, the estimated cumulative mass leached from 1 m thick crushed stabilized soil per 1 $m^2$ area is 100 mg for 2 years. Also, it should be noticed that pH values of one specimen decreased to less than 10 after 2000 ml of permeation. Deterioration of cement reacted products could occur under the low pH condition and might result in the additional leaching.

The comparison of concentration of leached Pb between the case that crushed clods were left for 21 days without compaction and the case that the crushed clods were compacted immediately after crushed is shown in Figure 10. Significantly more Pb leached from the sample which was not immediately compacted. This may be due to the longer contact time of crushed clods to the air which results in the higher leaching amount of heavy metals. As a result, it is recommended stabilized soil be compacted immediately after crushing.
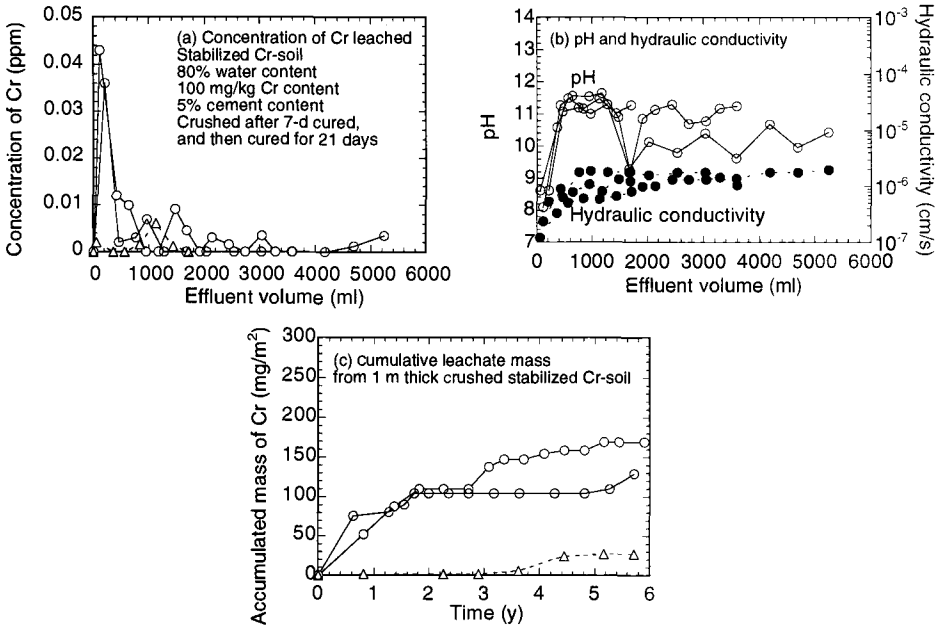
Figure 9–*Column Leaching Test Results and Cumulative Leachate Mass on the Crushed Stabilized Cr-Soil*
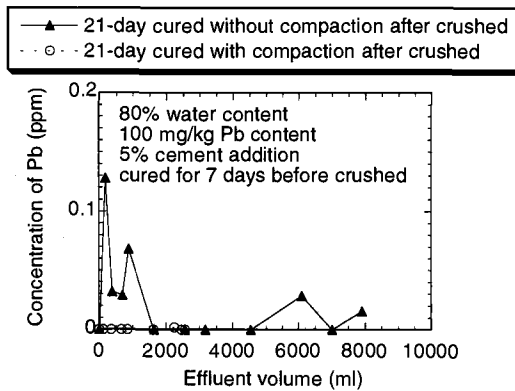


Figure 10–*Concentration of Pb Leaching from the Crushed Stabilized Pb-Soil*

## Drying

A series of batch leaching tests were conducted to evaluate whether the drying process has an effect on leaching characteristics. The stabilized and cured sludge containing 100 mg/kg Cr was crushed into the clods under 2 mm diameter, air-dried at 20
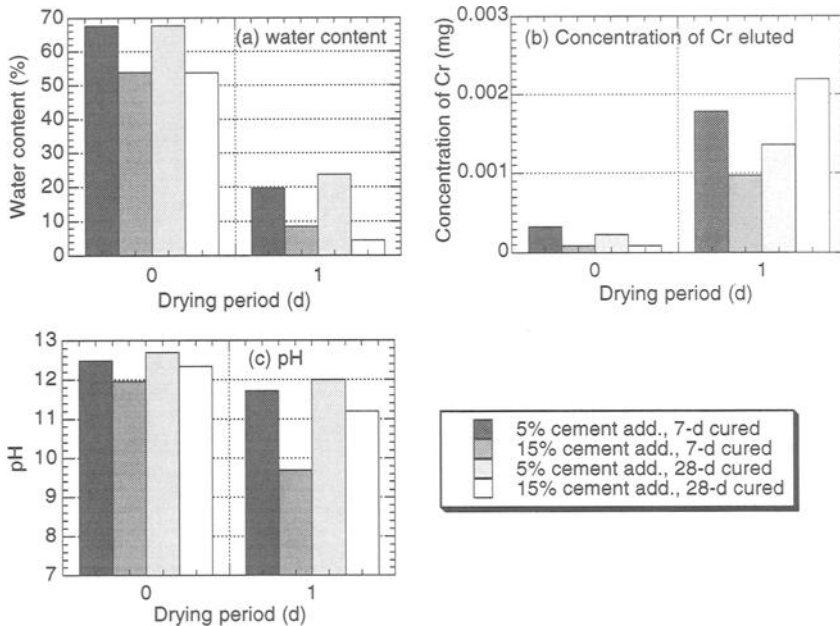
Figure 11–*Effect of Drying prior to the Elution on the Stabilized Soil Containing 100 mg/kg Cr*

degree Celsius, mixed with water to a liquid per solid ratio (L/S) of 10 ml/g, stirred for 6 hours, and then filtered.

The drying process significantly reduced the water content and substantially decreased the pH (Figure 11). Water contents decrease from 50-70% to 5-25%, and pH values decrease from 12-12.5 to 9.5-12. As a result, concentrations of leached Cr increase significantly for all testing conditions, and increased by almost one order of magnitude above specimens without the drying process. Thus, drying stabilized soil increases heavy metal leaching.

*Acid*

Effect of pH of eluted water on the leaching characteristics is of great importance. For the experiment, the stabilized soil was crushed into clods under 5 mm diameter, and mixed with water under L/S = 100. Also, $HNO_3$ was added to the solid-liquid mixture to maintain a pH of 7 or 4. The Cr concentration of the liquid obtained from filtration of the mixture was measured. The solids obtained after the filtration were subjected again to the elution test in the same manner.

In the case of pH = 7, the concentrations of leached Cr are almost 0.01 ppm for the first elution and less than 0.001 ppm for the second elution (Figure 12). The values for the first elution are the same values as the results from column leaching tests. Low pH liquid (pH = 4) results in the significantly higher concentration of leached Cr for both first and second elution. The negative effect of acid on the stabilized soil has been reported by
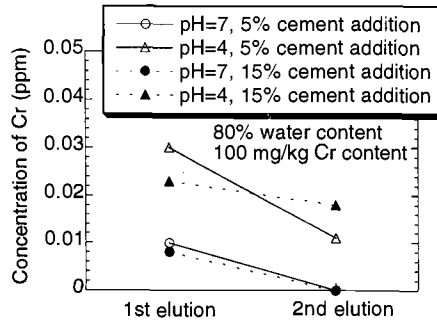
Figure 12–*Effect of pH on the Leaching of Cr*

Kamon et al. (1996). Acid deteriorates cement products and is believed to significantly increase the mobility of heavy metals.

## Conclusions

The following conclusions are drawn:
(1) Japanese regulations for contaminated bottom sediments are reviewed. The application of treatment technologies to several projects are summarized. Deficiencies in the regulatory requirement for evaluating the environmental impact of contaminated sludge, in particular to its reuse for geotechnical applications are pointed out.
(2) The column leaching test results on stabilized Cr- and Pb-soil with 300% water content indicate that the heavy metal leaching from the high water content sludge is significant on a mass per unit volume basis when hydraulic conductivity is taken into account.
(3) According to the column leaching test on stabilized Cr- and Pb-soil with 80% water content, the low hydraulic conductivity results in little mass leaching. Furthermore, the water dehydrated from the 300% water content sludge is below the environmental standards for heavy metals.
(4) Some factors affecting the leaching characteristics were evaluated. Crushing, drying and acid exposure all increase the mobility of heavy metals in stabilized sludge.

## Acknowledgment

## References

Edil, T. B. and Benson, C. H., 1998, "Geotechnics of Industrial By-Products," *Recycled Materials in Geotechnical Applications, Geotechnical Special Publication No. 71,* C. Vipulanandan & D. J. Elton, eds., ASCE, pp. 1-18.

Hartlén, J., Carling, M. and Nagasaka, Y., 1997, "Recycling or Reuse of Waste
    Materials in Geotechnical Applications," *Environmental Geotechnics,* M. Kamon, ed.,
    Balkema, Vol.3, pp.1493-1513.

Kamon, M., 1998, "Re-Use of By-Products," *Environmental Geotechnics,* P. S. Seco e
    Pinto, ed., Balkema, Vol.4, pp.1279-1292.

Kamon, M. and Katsumi, T., 1994, "Utilization of Waste Slurry from Construction
    Works," *Proceedings of the Thirteenth International Conference on Soil Mechanics
    and Foundation Engineering,* Oxford & IBH Publishing Co., Vol.4, pp.1613-1616.

Kamon, M. and Katsumi, T., 1999, "Evaluating Environmental Impact of Stabilized Soil
    Containing Heavy Metal," *Proceedings of the Eleventh Asian Regional Conference on
    Soil Mechanics and Geotechnical Engineering,* Balkema *(in press).*

Kamon, M., Ying, C. and Katsumi, T., 1996, "Effect of Acid Rain on Lime and Cement
    Stabilized Soils," *Soils and Foundations,* Japanese Geotechnical Society, Vol.36,
    No.4, pp.91-99.

Kamon, M., Katsumi, T., and Inui, T., 1998a, "Dehydration-Solidification Treatment
    and Geotechnical Utilization of Waste Sludge from Construction Works,"
    *Environmental Geotechnics,* P. S. Seco e Pinto, ed., Balkema, Vol.2, pp.603-608.

Kamon, M., van Roekel, G., and Blümel, W., 1998b, "Assessment of Geo-
    Environmental Hazards from Dredged Materials," *Environmental Geotechnics,* P. S.
    Seco e Pinto, ed., Balkema, Vol.3, pp.1057-1074.

Kawachi, T., Katsumi, T., Tran Duc, P. O., and Yamada, M., 1996, "Treatment and
    Utilization of Waste Sludge/Slurry from Construction Works in Japan,"
    *Environmental Geotechnics,* M. Kamon, ed., Balkema, Vol.2, pp.767-772.

Kujala, K., 1989, "Stabilization of Harmful Wastes and Muds," *Proceedings of the
    Second International Symposium on Environmental Geotechnology,* Shanghai, Vol.1,
    pp.540-548.

Nakajima, Y. 1998, "Status and Countermeasure of Sediment Contamination," *Hedoro,*
    Japan Sediments Management Association, No.71, pp.28-43 *(in Japanese).*

Sakai, S., Mizutani, S., and Takatsuki, H., 1996, "Leaching Tests for Waste Materials,"
    *Waste Management Research,* Japan Society for Waste Management Experts, Vol.7,
    No.5, pp.383-393 *(in Japanese).*

Shackelford, C. D. and Glade, M. J., 1997, "Analytical Mass Leaching Model for
    Contaminated Soil and Soil Stabilized Waste," *Ground Water,* Vol.35, No.2, pp.233-
    242.

Watanabe, K., 1998, *Immobilization and Leaching Characteristics of Stabilized Heavy
    Metal-Contaminated Soils,* Masters thesis, Department of Civil Engineering, Kyoto
    University *(in Japanese).*

J. L. Hanson,[1] T. B. Edil,[2] and N. Yesiller[3]

**Thermal Properties of High Water Content Materials**

---

**Abstract:** Fundamental thermal properties of various high water content materials were determined using a number of thermal testing methods. Tests were conducted on peat soils, solid wastes, industrial sludge, and bentonite slurries. Thermal conductivity, heat capacity, and thermal diffusivity were determined. The thermal conductivity of the materials was determined using a needle probe method. The volumetric heat capacity of the materials was determined using a dual probe method. These values were used together to obtain thermal diffusivity. Analytical methods are also used to determine heat capacity and thermal diffusivity. The theory for determination of thermal parameters using the various methods is presented. Experimental methods were determined to be effective at measuring thermal properties of high water content materials. Thermal parameters are dependent on material composition and structure. Heat capacity and thermal diffusivity are greatly affected by water content because of the high heat capacity of water compared with air and solids. A comparison is made between experimental and analytical methods used to determine thermal parameters. Good agreement was observed between experimental and analytical methods. Results of thermal tests have applications in the prediction of heat transfer through soils, sludges, and wastes.

**Keywords:** thermal properties, peat, bentonite slurry, thermal conductivity, thermal diffusivity, heat capacity, specific heat, solid waste, sludge

## Introduction

Heat transfer in high water content materials is caused by both natural and man-made thermal gradients. Natural thermal gradients are caused by seasonal temperature cycles, waste decomposition, and geothermal activity. Man-made thermal gradients are produced by manufacturing and energy producing facilities, soft ground improvement methods (including thermal precompression of peat and soil freezing), and environmental remediation techniques (including thermal bioremediation and soil vitrification). Analysis of thermal properties of high water content materials including organic soils and wastes is

---

[1] Assistant Professor, Department of Civil Engineering, Lawrence Technological University, 21000 W. Ten Mile Rd., Southfield, MI 48075.

[2] Professor, Department of Civil and Environmental Engineering, University of Wisconsin, 1415 Engineering Dr., Madison, WI 53706.

[3] Assistant Professor, Department of Civil and Environmental Engineering, Wayne State University, 5050 Anthony Wayne Dr., Detroit, MI 48202.

required to determine temperatures near heat sources, assess efficiency of ground improvement techniques, and optimize operation of landfills as bioreactors.

Thermal properties of various high water content materials were determined in this study. Probe methods (needle probe thermal conductivity method and specific heat dual probe method) were used. A description of applicable thermal properties, theory of the probe methods, and results of laboratory and field measurements are presented. A comparison of methods for determining thermal properties is also presented.

## Background

The two major parameters needed to quantify heat transfer are the rate of heat flow through a medium (thermal conductivity, $k_t$), and the ease with which a medium can be heated (mass heat capacity, $c$, or volumetric heat capacity, $C$). Mass heat capacity is also known as specific heat. The effectiveness at which a medium gains heat content (thermal diffusivity, $\alpha$) is a composite parameter of $k_t$ and $C$ (Andersland and Ladanyi 1994). Thermal conductivity can be defined as the amount of heat passing through a unit area over a unit time under the effect of a unit thermal gradient. Heat capacity can be defined as the amount of heat required to change the temperature of a material by one degree Kelvin. This can be quantified on a unit-mass or a unit-volume basis. A low heat capacity corresponds to a relatively large temperature change for a given amount of heat application. Thermal diffusivity is defined as the quotient of thermal conductivity, $k_t$, and volumetric heat capacity, $C$ (Equation 1). Volumetric heat capacity, $C$, is the product of mass heat capacity, $c$ and density of material, $\rho$.

$$\alpha = \frac{k_t}{C} = \frac{k_t}{c\rho} \qquad (1)$$

where:
$\alpha$ = thermal diffusivity (m$^2$/s)
$k_t$ = thermal conductivity (W/m·°C)
$C$ = volumetric heat capacity (kJ/m$^3$·°C)
$c$ = mass heat capacity (kJ/kg·°C)
$\rho$ = mass density (kg/m$^3$)

Thermal diffusivity is a composite parameter that indicates how fast temperature change occurs in a material subjected to a thermal gradient. A material that has a high thermal diffusivity experiences an increase in temperature faster than a complementary material that has a low thermal diffusivity (Andersland and Anderson 1978). Table 1 shows the thermal properties of various materials that make up soil. The difference in the thermal properties of the materials in Table 1 indicate the importance of soil composition on the thermal properties of soils.

Thermal properties of soil are dependent on material composition, fabric or packing arrangement, water content, and temperature. For a porous material at a given dry density, thermal conductivity increases with increasing moisture content. For a given moisture content, thermal conductivity increases with increasing dry density. The composition of porous material also has an effect on the magnitude of the thermal conductivity (e.g. organic vs. inorganic constituents, Table 1). Thermal conductivity increases with increasing temperature. Reasons for this include an increase in the thermal conductivity of the individual components of the porous material, an increase in moisture migration, and improvement of particle contact bonds with increasing temperature (Farouki 1981).

Table 1 - *Thermal Properties for Various Soil Constituents*

| Material | Density $\rho$ (kg/m$^3$) | Heat Capacity $c$ (kJ/kg·°C) | Thermal Conductivity $k_t$ (W/m·°C) | Thermal Diffusivity $\alpha$ (m$^2$/s x10$^{-7}$) | Source[a] |
|---|---|---|---|---|---|
| Many Soil Minerals* | 2600 | 0.73 | 2.90 | 15 | (2) |
| Water | 981 | 4.19 | 0.60 | 1.42 | (2) |
| Soil Organic Matter* | 1275 | 1.93 | 0.25 | 1.0 | (2) |
| Air | 1.2 | 1.00 | 0.03 | 0.210 | (1) |

\* Approximate average values
[a] (1) Lunardini 1985; (2) De Vries 1966

The fundamental thermal properties (thermal conductivity, heat capacity, and thermal diffusivity) can be determined using probe devices. Thermal conductivity is determined using a single probe method and heat capacity and thermal diffusivity are determined using a dual probe method. ASTM Test Method for Determination of Thermal Conductivity of Soil and Soft Rock by Thermal Needle Probe Procedure (D 5334) involves placing a thermal needle probe into the soil and monitoring the transient heating effects. The probe has both heating and temperature sensing capabilities. The heat energy applied to the soil is monitored by means of a voltage application through a calibrated resistor. The temperature is measured with a thermocouple positioned at the midpoint of the probe. By comparing the amount of heat energy applied to the needle to the resulting temperature increase, the amount of heat transferred to the surrounding material can be deduced.

The thermal needle probe method has proven to be a reliable and straightforward means of obtaining the thermal conductivity of soils. Mitchell and Kao (1978) concluded that the thermal needle probe was the most effective means of determining thermal conductivity of soils. The thermal needle probe has been adapted for field (Slusarchuk and Foulger 1973, Goodrich 1986). For field applications, the diameter and length of the probe are increased. The aspect ratio of length to diameter of a common laboratory probe is 95 (120 mm length, 1.27 mm diameter). The aspect ratio of the field probe is 35 (330 mm length, 9.5 mm diameter).

The dual probe method has been developed for an accurate determination of heat capacity of soils (Bristow et al. 1994). An apparatus which consists of two closely spaced, small probes is used in this method. One of the probes provides a short duration heat pulse and the other probe monitors temperature at a nearby location. By monitoring the maximum temperature rise at a known distance from the heat source, the heat capacity of the material can be determined. The dual probe method allows for direct calculations of thermal diffusivity and volumetric heat capacity. Using these values and the density of the material, the thermal conductivity can be calculated.

## Experimental Methods for Determination of Thermal Properties

Thermal conductivity is determined using ASTM D 5334. Volumetric heat capacity is determined using the Dual Probe Method (Bristow et al. 1993, 1994). Thermal diffusivity is determined using the results of these two tests. The methods and theory required to determine thermal parameters using these tests is briefly described.

*Needle Probe Method*

The needle thermal conductivity probe consists of a stainless steel tube (hypodermic needle) that contains a heating element and a thermocouple which are both connected to a datalogger. Specifications of the probe used in the test program are: length: 120 mm; diameter: 1.27 mm; resistance: 151 ohms (resistance includes reference resistor); resistivity: 1141 ohm/m; heating voltage: 4.4 V (supplies approximately 1W/m). A schematic of the thermal conductivity probe used in the test program is presented in Figure 1.
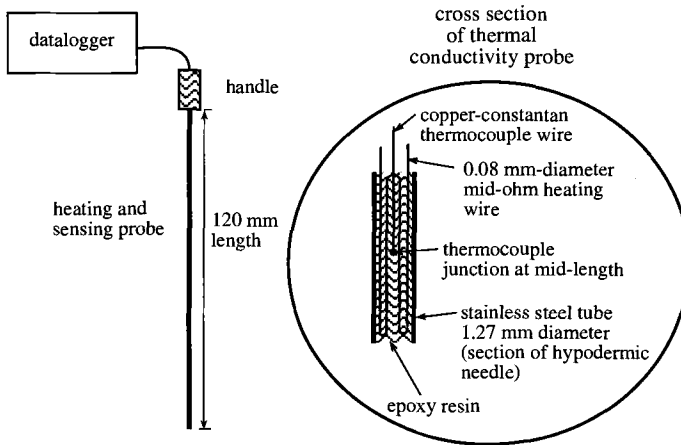


Figure 1 - *Schematic of Thermal Conductivity Probe*

The test is conducted by applying a heating current to the probe and monitoring temperature at the midpoint of the probe for a duration of 1-2 minutes. The interpretation of the needle probe method is based in the theory of an infinite line source of heat within an infinite homogeneous medium. The rate of temperature rise along the linear heat source is monitored. The temperature at any radius, $r$, from the linear heat source is given by Carslaw and Jaeger (1959) as:

$$T = \frac{q}{4\pi k_t} E_i\left(-\frac{r^2}{4\alpha t}\right) \qquad (2)$$

where:
$T$ = temperature (°C)
$q$ = power input (W/m)
$k_t$ = thermal conductivity (W/m·°C)
$E_i$ = exponential integral
$r$ = radial distance from line heat source (m)
$\alpha$ = thermal diffusivity (m$^2$/s)
$t$ = time (s)

For small values of the last term (small $r$, large $t$), the exponential integral can be approximated by a logarithm function (Slusarchuk and Foulger 1973). A straight line is obtained when this function is plotted as temperature rise vs. logarithm of time for a given

distance from the heat source.  The slope of this line represents thermal conductivity of the material and is calculated as follows:

$$k_t = \frac{q}{4\pi(T_2 - T_1)} \ln\left(\frac{t_2}{t_1}\right)$$     (3)

where:

$k_t$ = thermal conductivity (W/m·°C)
$q$ = power input (W/m)
$T_1$ = temperature (°C) at time, $t_1$ (s)
$T_2$ = temperature (°C) at time, $t_2$ (s)

Typical experimental test results for the needle probe method are presented in Figure 2.  The linear portion of the data in Figure 2 represents the steady state portion of the test.  Data obtained before the linear portion of the curve represents transient conditions of the probe itself heating and should be neglected for curve-fitting procedures.  Data beyond the linear portion results from edge and end effects and should also be neglected. A shallow slope of the line indicates that the heat produced along the length of the probe is transferred more effectively into the surrounding medium resulting in a high thermal conductivity (Hanson 1996).
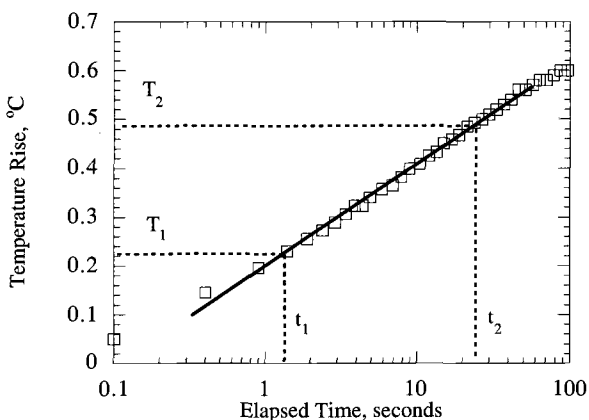


Figure 2 - *Typical Response of Thermal Conductivity Probe*

*Dual Probe Method*

The Dual Probe Method is used for the determination of heat capacity.  The apparatus consists of two small stainless steel tubes of the same diameter and length, placed parallel to each other at a spacing of approximately 6 mm.  The length of the probes is 30 mm and the diameter is 0.90 mm.  One probe contains a heating element and the other probe contains a thermocouple.  The heater has a resistivity of 1141.5 Ω/m.  The thermocouple is made of Copper-Constantan (Type T).  A schematic of the dual probe used in the test program is presented in Figure 3.
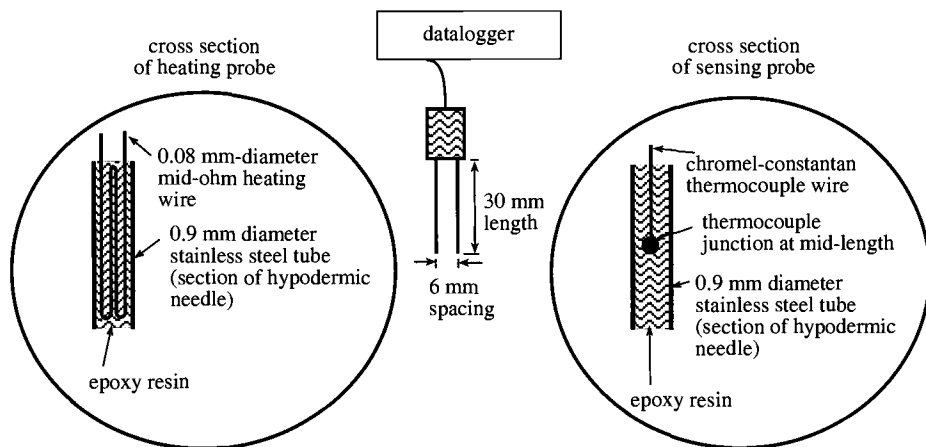
Figure 3 - *Schematic of Specific Heat Dual Probe*

Power is supplied to the heating probe for an 8 second heating interval. The power supplied to the heating probe and resulting temperature rise at the sensing probe is monitored for 80 seconds. Maximum temperature rise and power input are used to compute heat capacity using Equation 4 (Campbell et al. 1991). The magnitude of the peak temperature change is inversely proportional to heat capacity.

$$C = \rho c = \frac{q}{e \, \pi r_m^2 \Delta T_m} \tag{4}$$

where:

$\rho$  = mass density (kg/m$^3$)
$c$  = mass heat capacity (kJ/kg·°C)
$q$  = power supplied to probe (W/m)
$C$  = volumetric heat capacity (kJ/m$^3$·°C)
$e$  = base of the system of natural logarithms
$r_m$  = fixed distance from heating probe (probe spacing) (m)
$\Delta T_m$  = maximum temperature rise (°C)

Typical response of the specific heat dual probe is presented in Figure 4. Both the magnitude of the peak and the time required to reach the peak temperature indicate the thermal behavior of the material being tested.
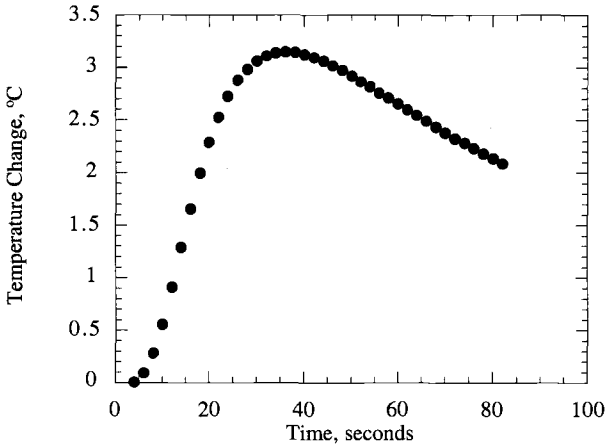
Figure 4 - *Typical Response of Specific Heat Dual Probe*

## Indirect Methods for Determination of Thermal Properties

Indirect and analytical methods can be used to estimate thermal properties. Heat capacity can be approximated by summing components of composite materials. Also, ground temperature data with depth can be used, together with an idealized analytical solution, to approximate thermal diffusivity of subsurface materials.

### *Theory for Summing Components of Heat Capacity*

Common values for heat capacity for various materials are presented by Andersland and Ladanyi (1994), Carslaw and Jaeger (1959), and De Vries (1966). The heat capacity of a composite material can be calculated by the summation of the individual components of volumetric heat capacity (Equation 5). Values from Table 1, together with weight-volume relationships, can be used to approximate heat capacity of soils and slurries. Equation 5 can be adapted to reflect other constituents of geomaterials (Andersland and Ladanyi 1994). The accuracy of equation 5 is limited by the accuracy of weight-volume relationships and the volumetric heat capacity of the various constituents of the material. Errors in these parameters will be reflected in the overall volumetric heat capacity determined using Equation 5.

$$\rho C \cong \rho_w C_w \theta + \rho_b C_m \qquad (5)$$

where:

$\rho$ = overall mass density (kg/m$^3$)
$C$ = overall volumetric heat capacity (kJ/m$^3\cdot$°C)
$\rho_w$ = mass density of water (kg/m$^3$)
$C_w$ = volumetric heat capacity of water (kJ/m$^3\cdot$°C)
$\theta$ = volumetric water content
$\rho_b$ = bulk density of soil minerals (kg/m$^3$)
$C_m$ = volumetric heat capacity of soil minerals (kJ/m$^3\cdot$°C)

*Approximation of Thermal Diffusivity from Field Temperatures*

Thermal diffusivity of soils can be estimated by monitoring amplitude decrement and phase lag of the ground surface temperature wave with depth. Infinite half-space conductive heat transfer theories are used to back calculate values of thermal diffusivity (Lundy 1981). Uniform soil conditions are assumed between two depths of temperature measurements. A schematic plot of temperature vs. time at two depths is presented in Figure 5. Equation 6 is used to estimate thermal diffusivity based on amplitude decrement.
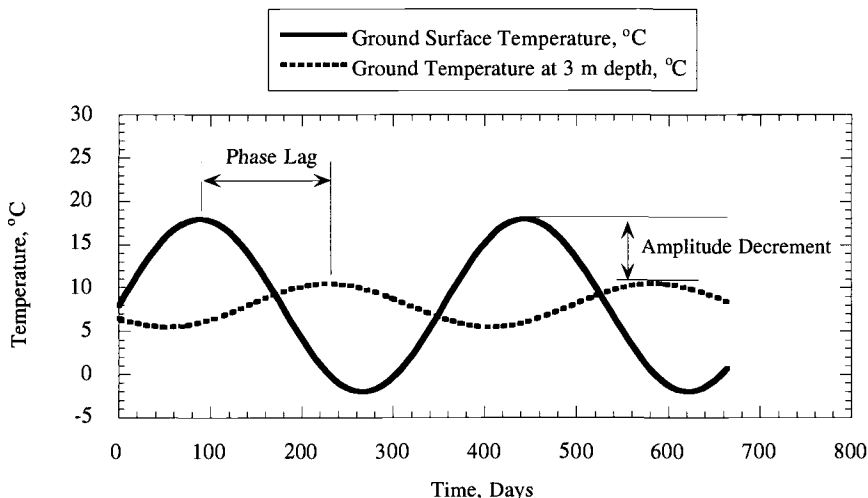


Figure 5 - *Schematic Plot of Phase Lag and Amplitude Decrement*

$$A_x = A_s e^{-x\sqrt{\frac{\pi}{365\alpha}}}$$ (6)

where:

$A_x$ = amplitude of ground temperature wave at $x$ (°C)
$A_s$ = amplitude of ground temperature wave at surface (°C)
$x$ = depth below surface (m)
$\alpha$ = thermal diffusivity (m²/day)
$e$ = base of the system of natural logarithms

Phase lag measurements of the seasonal ground temperature wave can also be used to estimate the thermal diffusivity in the field (Lundy 1981). At various depths, the peak of the temperature wave will occur at different times due phase lag of the wave. This phase lag can be used to calculate thermal diffusivity using Equation 7. Annual peak to peak temperatures are used to determine phase lag.

$$L = \frac{1}{2}\sqrt{\frac{365}{\pi\alpha}}$$ (7)

where:

$L$ = time lag (days)
$\alpha$ = thermal diffusivity (m²/day)

## Materials Tested for Thermal Property Determination

Thermal property testing was conducted on high water content organic soils, municipal solid waste, industrial sludge, and bentonite slurries. The organic soils were obtained from a National Science Foundation/Federal Highway Administration Thermal Precompression field test site in Middleton, Wisconsin (Hanson 1995). The municipal solid waste and industrial sludge were obtained from Sauk Trail Hills Landfill in Canton, Michigan. Bentonite slurries (both chip and powder) were prepared in the laboratory at various water contents.

The two organic soils tested for this program are a fibrous peat and a sedimentary peat. The physical properties of the two soils are presented in Table 2.

Table 2 - *Properties of Fibrous and Sedimentary Peat*

| Physical Property | Fibrous Peat | Sedimentary Peat |
|---|---|---|
| Specific Gravity[1] | 1.7 | 1.7 |
| Initial Void Ratio | 10 ± 2 | 7.4 ± 1 |
| Water Content[2] | 500-700% | 430-520% |
| Organic Content[2] | 88-95% | 58-65% |
| Fiber Content[3] | 30-60% | 20-30% |
| Wet Unit Weight (kN/m³) | 10 ± 0.4 | 10.3 ± 0.2 |
| Dry Unit Weight (kN/m³) | 1.25-1.88 | 1.6-2.0 |
| Von Post Classification[4] | H3 | H6 |
| pH[5] | 5.04 ± 0.02 | 6.06 ± 0.03 |

[1] ASTM Test Method for Specific Gravity of Soils (D 845)
[2] ASTM Test Methods for Moisture, Ash, and Organic Matter of Peat and Other Organic Soils    (D 2974)
[3] ASTM Test Method for the Laboratory Determination of the Fiber Content of Peat Samples by Dry Mass (D 1997)
[4] ASTM Test Method for Estimating the Degree of Humification of Peat and Other Organic Soils (Visual/Manual Method) (D 5715)
[5] ASTM Test Method for pH of Peat Materials (D 2976)

Peat samples were obtained using 75 mm diameter Shelby tubes. The brown fibrous peat consists of porous fibers interwoven in a horizontal plane that results in a structurally anisotropic fabric (Fox 1992). The individual fibers of the fibrous peat are characterized by roots and limbs. A block sample of fibrous peat was also used for thermal property testing. The greenish-brown sedimentary peat is characterized by highly decomposed plant remains which resemble grass and leaves. Fibers of sedimentary peat are much softer and more easily torn apart than the fibers of fibrous peat. The sedimentary peat is more uniformly decomposed in appearance and consistency than the fibrous peat. The fabric of both peats is affected by layering in the horizontal plane.

The municipal solid waste (MSW) is quite variable in nature depending on waste stream and sampling location. Field tests were conducted to include the macro-effects and

spatial variability of the MSW. Main components of the MSW include paper, food, clothing, organic yard waste materials, and shredded wood daily cover material. Water contents of the MSW tested ranged from 16% to 38%.

The industrial sludge is a waste product of the automobile industry and has gravimetric moisture content, w = 50%, bulk specific gravity, $G_s$ = 1.6, and pH = 12.5. The consistency of the sludge is primarily granular with some separate highly plastic (tar-like) components.

The bentonite mixtures were made using Wyoming bentonite. The powder and chips were obtained from Bariod Drilling Fluids, Inc.®[4]. The bentonite slurry from powder was prepared by mixing water with 2%, 5%, and 10% bentonite by weight. The bentonite powder slurries were prepared in 20 L containers. The bentonite chips were approximately 6 mm diameter angular particles. The bentonite chips/water mixture was prepared to model a seal used for backfilling a borehole at a water content of 50%. The bentonite chips were placed dry in a 5 L cylinder and allowed to hydrate for 30 days before testing. The resulting mixture had a unit weight of approximately 14 kN/m³. The specific gravity of the bentonite chips and bentonite powder was 2.6.

## Results and Discussion

Thermal conductivity and volumetric heat capacity were determined using the needle probe method and dual probe method, respectively. The results of the thermal probe testing program are presented in Table 3. The variable structure and composition of the materials result in scatter in the thermal property data. The uncertainty in thermal conductivity and heat capacity are reported as Two-Sigma error corresponding to a 95% confidence interval (Table 3). Any uncertainty in thermal conductivity and heat capacity affect the calculation of thermal diffusivity. The uncertainty in thermal diffusivity was calculated using an adaptation of Taylor's Theorem on the propagation of uncertainty (Beckwith and Marangoni 1990). The uncertainty of the thermal diffusivity, $\alpha$ can be expressed as is shown in Equation 8.

$$u_\alpha = \sqrt{\left(u_{k_t}\frac{\partial\alpha}{\partial k_t}\right)^2 + \left(u_c\frac{\partial\alpha}{\partial C}\right)^2}$$

(8)

where:

$u_\alpha$ = the overall uncertainty in thermal diffusivity
$u_{k_t}$ = discrete uncertainty in thermal conductivity, $k_t$
$u_C$ = discrete uncertainty in volumetric heat capacity, $C$

The results of the tests indicate that the thermal conductivity of peat is lower than the thermal conductivity of typical soils (sands and silts). The large void ratios of the organic soils prevent effective transfer of heat through the soil. The fibrous peat has a higher thermal conductivity than the sedimentary peat. This can be attributed to the presence of a structural skeleton in the fibrous peat. The heat capacity of the peats is higher than that of sands and silts. The high water content of peats controls the heating process.

A block sample of fibrous peat was used to investigate the spatial variability of thermal parameters. The size of the block was approximately 250 mm x 300 mm x 500 mm. Thermal probes were inserted both vertically and horizontally into the block sample.

---

[4] Baroid Drilling Fluids, Inc., Denver, Colorado.

The values obtained from the block sample were all in good agreement. All thermal parameters determined from the block sample were within the range of values obtained from the Shelby tube samples. No evidence of anisotropic behavior was apparent from the block sample tests. The testing of the block sample also indicated that scaling effects between Shelby tube samples and block samples were negligible. The variability associated with placement of the probes within the larger block sample was similar to the variability of results from Shelby tube samples.

The thermal properties of the MSW are the most variable of any of the materials tested. This is due to the nonuniform composition of the waste materials. Most values of thermal conductivity measured for the MSW were quite low and compared to values for air. This is due to the large void ratio of the waste materials that is occupied by air.

Table 3 - *Thermal Properties from Experimental Program*

| Soil Type | Thermal Conductivity (W/m·°C) | Heat Capacity (MJ/m$^3$·°C) | Thermal Diffusivity (m$^2$/s x10$^{-7}$) |
|---|---|---|---|
| Fibrous Peat | 0.71 ±0.3 | 3.9 ±0.4 | 1.8 ±0.2 |
| Sedimentary Peat | 0.57 ±0.1 | 3.7 ±0.2 | 1.5 ±0.1 |
| MSW | 0.01-0.7 | 0.8-10 | 0.2-0.7 |
| Industrial Sludge | 0.4 ±0.2 | 2.4 ±0.2 | 0.22 ±0.1 |
| Bentonite Slurry, 10% solids | 0.75 ±0.1 | 4.3 ±0.1 | 1.9 ±0.2 |
| Bentonite Slurry, 5% solids | 0.72 ±0.2 | 3.6 ±0.1 | 1.9 ±0.2 |
| Bentonite Chips/Water Mixture | 0.95 ±0.1 | 2.5 ±0.3 | 4.0 ±0.5 |
| Silt Topsoil* | 1.3 ±0.1 | 2.5 ±0.1 | 5.3 ±0.2 |
| Sand Fill* | 1.4 ±0.25 | 1.8 ±0.3 | 7.8 ±1.0 |

*values provided for reference; (Hanson 1996)

Variation was observed in the thermal properties of the industrial sludge can be attributed to high spatial variability and the presence of distinct immiscible phases in the material. Results were dependent on placement of the probes within the material. The sludge was less conductive than the peats and slurries. The sludge had a relatively low thermal diffusivity.

The thermal properties of the three typical bentonite slurries (2%, 5%, and 10% solids content) were determined. The thermal properties of the 5% solids and 10% solids bentonite slurries are similar. Results from the 2% solids bentonite slurry are inconsistent with the other results and are not reported in Table 3. Convective heat transfer in the low solids content slurry may be responsible for the inconsistent trends.

The bentonite chips/water mixture, at a substantially higher solids content, has a higher thermal conductivity than the slurries. The high solids content of the bentonite chips/water mixture allows for more effective heat transfer than the bentonite powder slurries. The bentonite chips/water mixture, however, is less conductive than silts and sands due to the relatively low dry density.

Thermal diffusivity is a composite parameter of thermal conductivity and heat capacity. Results of the tests indicate that of these materials, inorganic soils (including bentonite chips/water mixture) have the highest thermal diffusivity. The lowest values of thermal diffusivity were obtained for the MSW and industrial sludge. The highest water

content materials (peats and bentonite slurries) had diffusivity values approaching that for water.

Problems were encountered in using the probes in the field. The most important problem was interference of large particles during insertion of the probes. Many trials were required to successfully insert the thermal conductivity probe into the ground. Proper placement of the specific heat dual probe (maintaining a constant distance between the probes) was difficult due to the interference of materials within the waste.

## Comparison of Thermal Properties Test Methods

A comparison was made between the experimental and indirect methods used to determine thermal parameters. An analysis was conducted to compare volumetric heat capacity determined using the dual probe method to the determination using summation of components of the materials and published values of heat capacity of the material components. In the summation method, water content, organic content, and degree of saturation were used in the estimation of heat capacity. A summary of this comparison is presented in Table 4. The volumetric heat capacity for fibrous peat, sedimentary peat, and bentonite slurries are in good agreement with those measured using the dual probe. This is due to the high volumetric water content of these materials. Discrepancy exists between the two methods due to structural variability (predominant in the peats and bentonite chips/water mixture) and potential for convective flow (in the relatively low viscosity bentonite slurries). Comparisons for MSW and industrial sludge are not included in Table 4 because published values of volumetric heat capacity are not available for all the components of these materials.

Table 4 - *Comparison of Volumetric Heat Capacity Determinations*

| Material | Dual Probe (MJ/m$^3$·°C) | Summing Components (MJ/m$^3$·°C) |
|---|---|---|
| Fibrous Peat | 3.9 ±0.4 | 3.8 |
| Sedimentary Peat | 3.7 ±0.2 | 3.8 |
| Bentonite Slurry, 10% solids | 4.3 ±0.1 | 3.8 |
| Bentonite Slurry, 5% solids | 3.6 ±0.1 | 4.0 |
| Bentonite Chips/Water Mixture | 2.5 ±0.3 | 1.8 |

Thermal diffusivity was determined using experimental methods and inferred from theoretical amplitude decrement and phase lag of the ground surface temperature wave with depth. The maximum seasonal amplitude was monitored at various depths at the Middleton field site. Temperatures at various depths (1.5 m, 3.2 m, and 4.5 m) were recorded for 5 years at an unheated reference site and used for this analysis. Damping envelopes were graphically fit around the ground temperature data to estimate temperature decrement with depth. The maximum amplitude analysis is presented in Figure 6 (Hanson 1996).

Temperature data collected at the three depths at the field site are shown on this graph. The maximum temperature fluctuation amplitudes at the various depths are identified using this graph. The two peat layers are combined for this analysis because of limited temperature data with depth. Experimental values of thermal diffusivity are obtained from the probe methods. Experimental values for the two peats are averaged. Table 5 summarizes the comparison of analytical prediction of thermal diffusivity to experimental results. The analytical results were obtained using Equations 6 and 7. Good agreement is observed between analytical prediction and the thermal probe methods. A

benefit of the analytical method is that a larger volume of material is represented, thus including macro-effects of the soil structure. However, drawbacks of the method include the necessity for long-term temperature monitoring and complications due to extreme seasonal weather conditions and layering of different soils.
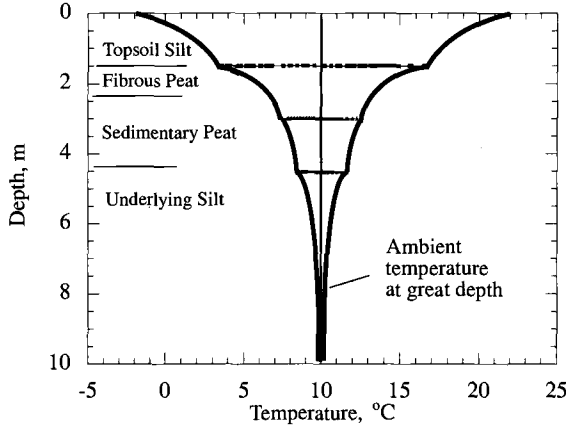


Figure 6 - *Estimation of Approximate Damping Envelope*

Table 5 - *Thermal Diffusivity of Peat*

| Method | Thermal Diffusivity $(m^2/s \times 10^{-7})$ |
|---|---|
| Laboratory thermal probes | 1.7 ±0.8 |
| Inferred from amplitude decrement | 1.5 - 2.9 |
| Inferred from phase lag | 1.3 - 1.9 |

## Conclusions

The needle probe thermal conductivity method and specific heat dual probe method are effective techniques for determining thermal properties of high water content materials. High water content materials are inherently spatially variable and ranges of parameters are possible within a material type. Thermal parameters are affected by material composition and structure. Heat capacity and thermal diffusivity are greatly affected by water content because of the high heat capacity of water compared to air and solids.

The results of the testing program indicate that the thermal conductivity of peat is lower than the thermal conductivity of typical soils (sands and silts). The large void ratios of the peats prevent the effective transfer of heat through the soil. The heat capacity of the peats is higher than that of sands and silts. This is due to the high water content of the these materials. The high water content of peats controls the thermal parameters.

The thermal properties of the MSW are the most variable of any of the materials tested. This is due to the nonuniform composition of the waste materials. Most values of thermal conductivity measured for the MSW were quite low and compared to values for air. This is due to the large void ratio of the waste materials that is occupied by air. A large

variation in heat capacity was also observed for the MSW. Variation was observed in the thermal conductivity of the industrial sludge that can be attributed to high spatial variability and the presence of distinct immiscible phases in the material. Heat capacity of the sludge compares to published values for organic soil materials.

The two bentonite slurries (5% and 10% solids content) displayed similar results. The bentonite slurries have a thermal conductivity similar to the peats and a heat capacity similar to water. The bentonite chips/water mixture that contains a substantially higher solids content has a higher thermal conductivity than the slurries and peats. The bentonite chips/water mixture allows for more effective heat transfer. The bentonite chips/water mixture, however, is less conductive than silts and sands. The heat capacity of the bentonite chips/water mixture was similar to the heat capacity of soil.

Results of the tests indicate that of these materials, inorganic soils (including bentonite chips/water mixture) have the highest thermal diffusivity. The lowest values of thermal diffusivity were obtained for the MSW and industrial sludge. The highest water content materials (peats and bentonite slurries) had diffusivity values approaching values associated with water.

Similar results were obtained for thermal diffusivity determined using analytical methods (summing components, phase lag, and amplitude decrement) and experimental methods (needle and dual probe methods). Indirect methods for determining thermal diffusivity compare well to experimental methods. The methods using field temperature data provide assessment of a large volume of material and in-situ conditions. However, for most applications, these methods may not be practical due to complications in the analysis and due to the extensive ground temperature monitoring required. Summing components of volumetric heat capacity is a simple method; however, it requires identification of material components and knowledge of the volumetric heat capacity of the individual components.

## Acknowledgment

## References

Andersland, O. B. and Anderson, D. M., 1978, *Geotechnical Engineering for Cold Regions*, McGraw-Hill Inc.

Andersland, O. B. and Ladanyi, B., (1994). *An Introduction to Frozen Ground Engineering,* Chapman and Hall, New York.

Beckwith, T. G. and Marangoni, R. D., 1990, *Fundamentals of Mechanical Measurements, Fourth Edition,* Addison-Wesley, New York.

Bristow, K. L., Campbell, G. S., and Calissendorff, K., 1993, "Test of a Heat Pulse Probe for Measuring Changes in Soil Water Content," *Soil Science American Journal,* Vol. 57, pp. 930-934.

Bristow, K. L., Kluitenberg, G. J., and Horton, R., 1994, "Measurement of Soil
    Thermal Properties with a Dual-Probe Heat-Pulse Technique," *Soil Science
    American Journal*, Vol. 58, pp. 1288-1294.

Campbell, G. S., Calissendorff, K., and Williams, J. H., 1991, "Probe for Measuring
    Soil Specific Heat Using a Heat Pulse Method," *Soil Science American Journal*, Vol.
    55, pp. 291-293.

Carslaw, H. S. and Jaeger, J. C., 1947, *Conduction of Heat in Solids*, Oxford.

De Vries, D. A., 1966, *Physics of Plant Environment, 2nd Ed.*, W. R. Van Wijk.
    Amsterdam: North-Holland.

Farouki, O. T., 1981, *Thermal Properties of Soils*, Cold Regions Research and
    Engineering Laboratory Report 82-8, U.S. Army Corps of Engineers, Hanover,
    New Jersey.

Fox, P. J., 1992, "An Analysis of One-Dimensional Creep of Peat," Ph.D. Thesis,
    University of Wisconsin-Madison, Department of Civil and Environmental
    Engineering, Madison, Wisconsin.

Goodrich, L. E., 1986, "Field Measurements of Thermal Conductivity," *Canadian
    Geotechnical Journal*, Vol. 23, pp. 51-59.

Hanson, J. L., 1995, "Field Demonstration of Thermal Precompression of Peat,"
    *Proceedings 43rd Annual Geotechnical Engineering Conference*, Feb. 3, 1995,
    Minneapolis, Minnesota, pp. 1-16.

Hanson, J. L., 1996, "Thermal Precompression of Peat," Ph.D. Thesis, University of
    Wisconsin-Madison, Department of Civil and Environmental Engineering, Madison,
    Wisconsin.

Lunardini, V. J., 1985, *Heat Transfer in Cold Climates*, U.S. Army Cold Regions
    Research and Engineering Laboratory, Hanover, NH; Van Nostrand Reinhold
    Company, New York.

Lundy, K., 1981, *Regional Analysis of Ground and Above-Ground Climate*, Oak Ridge
    National Laboratory, Oak Ridge, Tennessee.

Mitchell, J. K. and Kao, T. C., 1978, "Measurement of Soil Thermal Resistivity," *Journal
    of the Geotechnical Engineering Division*, ASCE, Vol. 104, No. 5, pp. 1307-1320.

Slusarchuk, W. A. and Foulger, P. H., 1973, *Development and Calibration of a Thermal
    Conductivity Probe Apparatus for use in the Field and Laboratory*. Technical Paper
    No. 388 of the Division of Building Research, Ottawa.

Thomas A. Bennert,[1] M. H. Maher,[2] Farhad Jafari,[3] and Nenad Gucunski[2]

**Use of Dredged Sediments from Newark Harbor for Geotechnical Applications**

---

**Abstract:** Under the Joint Dredging Plan for the Port of New York and New Jersey, New Jersey has committed to using stabilized dredged material for beneficial reuse. Under the short-term planning (1997 –2000), an annual average of 1.39 million cubic meters of dredged material must be used. Laboratory tests were conducted to investigate the geotechnical properties of the Newark Harbor dredged sediments stabilized with portland cement. The material properties and strength characteristics were investigated using soil characterization, California Bearing Ratio, unconfined compression, unconsolidated undrained and consolidated undrained triaxial compression, and resilient modulus tests. Currently, portland cement stabilized dredged material is being placed as a subgrade layer for a future parking lot. Cone penetration testing was conducted on the material to evaluate the in-situ density of the deeper, compacted layers. Nuclear density tests were also conducted to verify compaction of the material. Correlations between the two in situ tests were developed to analyze the two-meter-deep structural fill.

**Keywords:** dredged sediments, beneficial reuse, laboratory tests, subgrade, Newark Harbor, cone penetration, nuclear density test

## Introduction

On October 7, 1996, a joint dredging plan was developed for the Port of New York and New Jersey region. The main objectives of the plan were to:
- furnish a coordinated and comprehensive method on managing dredged material;
- provide procedures to identify short term (1997 - 2000) disposal requirements while developing procedures for long term (2000 - 2025) disposal requirements;

---

[1]Graduate Student, Dept. of Civil and Environmental Eng., Rutgers University, 623 Bowser Road, Piscataway, NJ 08854-8014
[2]Chairman and Associate Professor, respectively, Dept. of Civil and Environmental Eng., Rutgers University, 623 Bowser Road, Piscataway, NJ 08854-8014
[3]Field Engineer, Sadat Associates, Inc., 116 Village Blvd., Princeton, NJ 08543

- abolish contaminants from their origin; and
- remediate areas where levels of contamination have affected the dredged material.

Currently under the short-term plan, the region is expected to dredge approximately 16,100,000 cubic meters of material. Under the new joint plan, only 9,100,000 cubic meters are allocated for ocean disposal. The remaining 6,900,000 cubic meters must be stabilized and an appropriate end use for placement found. Disposal alternatives which provide a viable option include subaqueous pits (Wakeman et al. 1996), confined disposal facilities, upland disposal and possible beneficial reuse (USACE 1991).

In New Jersey alone, 4,200,000 cubic meters of Category II/III are appropriated for the development of beneficial uses under the short-term plan. Category II sediments demonstrate no toxicity, but have a potential for bioaccumulation. Category III sediments fail acute toxicity testing or pose a threat of significant bioaccumulation. State sponsored transportation projects must utilize 1,600,000 cubic meters of the material. The remaining material, inclusive of all categories, will be utilized for upland beneficial reuses, such as landfill cover/closure, hazardous site remediation, and for various other construction projects (Joint Dredging Plan 1996).

Recent laboratory research and case studies over the past decade have shown that the use of cementitious additives, such as portland cement, cement kiln dust, quicklime, and lime kiln dust, can stabilize and solidify soils and marine sediments containing unacceptable levels of constituents (MacKay and Emery 1994, Chang et al. 1996, Dermatas and Meng, 1996, Lin et al. 1996). Once stabilized, these sediments are usually contained in a lined and capped site for permanent disposal. However, with the surplus of contaminated marine sediments to be dredged in the New York/New Jersey region, other end uses or beneficial uses need to be evaluated.

## Laboratory Testing

Vaghar et al. (1997) conducted laboratory tests on portland cement stabilized dredged sediments from the Boston Harbor and concluded that the shear strength of the material was suitable for use as a structural fill. To determine if Newark Harbor stabilized dredged sediment could be used in geotechnical applications, a rigorous laboratory program was employed. The program provided material properties and strength characteristic tests including:

- time for solidification of treated dredged sediments;
- physical characteristics, such as Atterberg limits (liquid, plastic, and shrinkage limit), grain size analysis, moisture-density, and specific gravity; and
- shear strength properties (UU and CU triaxial, unconfined compression, California Bearing Ratio and resilient modulus tests)

Portland cement was added to the dredged sediment on a percentage basis of the wet mass of the dredged sediment. The mix proportion was selected to model the current field admixture, which was 8% portland cement by wet mass. The dredged sediment and portland cement was mixed in the laboratory with the aid of a blade mixer. After mixing, the material was allowed to air dry at room temperature. Samples were periodically taken to measure the solidification of the mixture.

Material characteristics and strength parameters determined from the series of laboratory tests were used in the construction and design of the field application, discussed later in the paper.

The basis of using 8 % portland cement is from field experience. Using less than 8 % for stabilization purposes makes placement and compaction of the material time consuming, as the drying process becomes longer. On the other hand, using higher percentages of portland cement would not be economically feasible. Also, higher percentages of cement tend to form hardened fragments of cement during the winter stockpiling months. These hardened fragments make the excavation and placement difficult. Still, depending on the type of project, the percentage of cement added to raw dredge can be adjusted.

*Solidification of the Treated Material*

A critical factor in the placement of the treated dredged sediment is the solidification of the material. Solidification is the process of eliminating excess water from a soil mass by hydration with an addition of a setting agent. This process is especially important when considering workability, placement costs and manageability of the treated material in the field.

Raw dredged sediment typically has an initial moisture content of 195 %. Immediately after the addition of 8 % portland cement, the moisture content drops to 143 %. Figure 1 illustrates the time dependency of the solidification of the treated dredged material, measured from a two hundred pound laboratory sample. As shown in the figure, the sample takes approximately thirty days to reach a moisture content of 52 %, which is the moisture content at 90 % of the maximum dry unit weight under a modified compactive effort.

Determination of field solidification, however, is highly dependent on weather and site conditions. To accelerate solidification, normal field procedures include aeration by continual disking and rotation of moist material to ensure even drying.

*Identification and Classification*

After the mixing of the treated dredged sediment was complete, the material was classified based on the Standard Test Method for Liquid Limit, Plastic Limit, and Plasticity Index of Soils (ASTM D 4318), Standard Test Method for Shrinkage Factors of Soils by the Mercury Method (ASTM D 427), Standard Test Method for Specific Gravity of Soils (ASTM D 854), and the Standard Test Method for Particle-Size Analysis of Soils (ASTM D 422). The results of these tests are shown in Tables 1 and 2, respectively.

*Strength Parameters*

Since New Jersey State sponsored transportation projects must utilize 1,600,000 cubic meters of the material, the strength parameters were centered around the design of a roadway embankment. For analysis, strength parameters for the slope stability, as
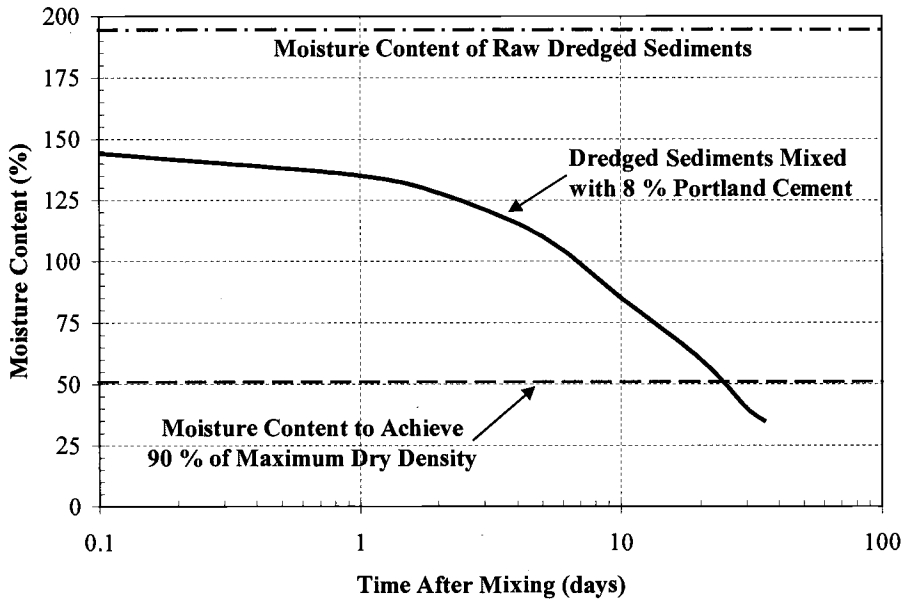
Figure 1 – *Laboratory Solidification of Treated Dredged Sediment*

Table 1 – *Specific Gravity, Atterburg and Shrinkage Limits*

| Liquid Limit | Plastic Limit | Shrinkage Limit | Specific Gravity | Classification |
|---|---|---|---|---|
| 104 | 61 | 66 | 2.65 | Elastic Silt (MH) |

Table 2 – *Grain-Size Characteristics*

| > 7.62 cm | Gravel | Sand | Silt | Clay |
|---|---|---|---|---|
| 0.0 % | 0.3 % | 9.7 % | 87.2 % | 2.8 % |

well as the roadway integrity had to be evaluated. All tests were conducted above the optimum moisture content and at 90 % of the maximum dry density for the modified compaction effort (Figure 2).
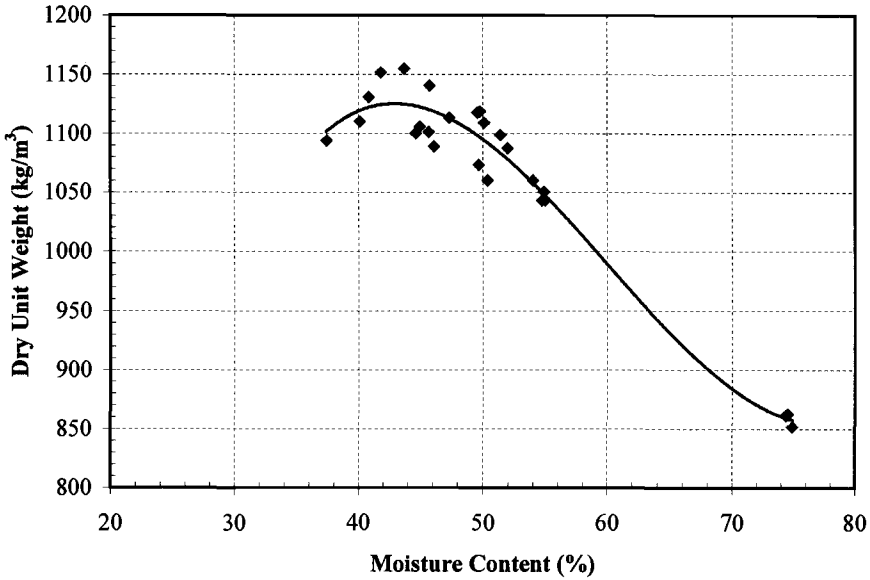
Figure 2 – *Moisture-Density Relationship for Treated Dredged Sediments*

*Shear Strength*

　　　To determine a factor of safety for a slope with a given subsurface profile, shear strength parameters of the treated dredge sediments were needed. Unconsolidated undrained (UU), consolidated undrained (CU) triaxial, and unconfined compression (UC) tests were conducted. The UU triaxial test recreates a condition where loading occurs so rapidly that no drainage in the embankment is allowed. This would simulate the condition experienced at the end of the construction phase. Immediately after construction, the induced pore pressure is maximum and no consolidation of the soil has taken place. However, with time, consolidation will take place, the void ratio will decrease, the water content will decrease, and the strength of the embankment material will increase. The CU triaxial test represents the condition where the material has somehow become saturated and was allowed to consolidate under its own weight. Then, a load is suddenly applied, not allowing dissipation of pore water from the newly developed saturated condition.

　　　The triaxial tests were conducted at confining pressures of 20.7, 34.5, 41.4, and 55.2, 68.95, and 137.9 kPa. The compacted density of the samples were conducted above the optimum moisture content and at 90 % of maximum dry density from the modified compaction effort (Figure 2). The samples were compacted under the method specified by AASHTO TP46-94 for Type II soils. This method, originally used for resilient modulus testing, allows for repeatability and an identical compaction method for triaxial and resilient modulus tests. The results of the testing are shown in Figure 3.
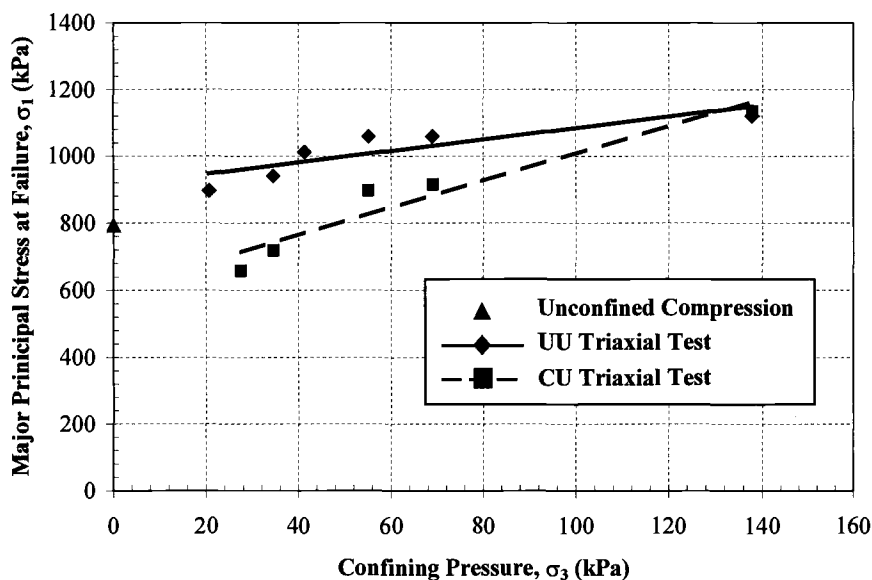
Figure 3 – *Shear Strength Behavior of Treated Dredged Sediment*

*Resilient Modulus (M$_r$) and California Bearing Ratio (CBR)*

Resilient modulus (M$_r$), also known as cyclic triaxial testing, was conducted to subject the treated material to an impulse type repeated loading, representative of moving wheel loads (National Stone Association 1993). M$_r$ is an index that describes the nonlinear stress-strain behavior of soils under repeated loads. Resilient modulus is defined as the ratio of cyclic deviator stress to the magnitude of recoverable strain for a given cycle. AASHTO's TP46-94 for M$_r$ testing provides two different testing protocols for soils designated to the base/subbase or the subgrade of roadways. However, since the treated material has a high fines content, to limit the possibility of heaving and frost susceptibility, the material should be kept under the frost line. Therefore, only testing for the subgrade condition was conducted. Results of the test are shown in Figure 4. The M$_r$ value was also compared to local New Jersey subgrade soils tested under the same test protocol for deviator stresses of 13.79, 41.37, and 68.59 kPa, respectively (Table 3). The subgrade soils are from existing pavement systems located under New Jersey roadways. For all deviator stresses shown in the table, the treated dredge sediment samples achieved a higher resilient modulus value than the local New Jersey subgrade soils.

The CBR value for the treated material was determined to be 17. This is well within the range of values (7 – 20) that AASHTO considers being a fair material for a subbase, and a good material for a subgrade (Bowles 1992).
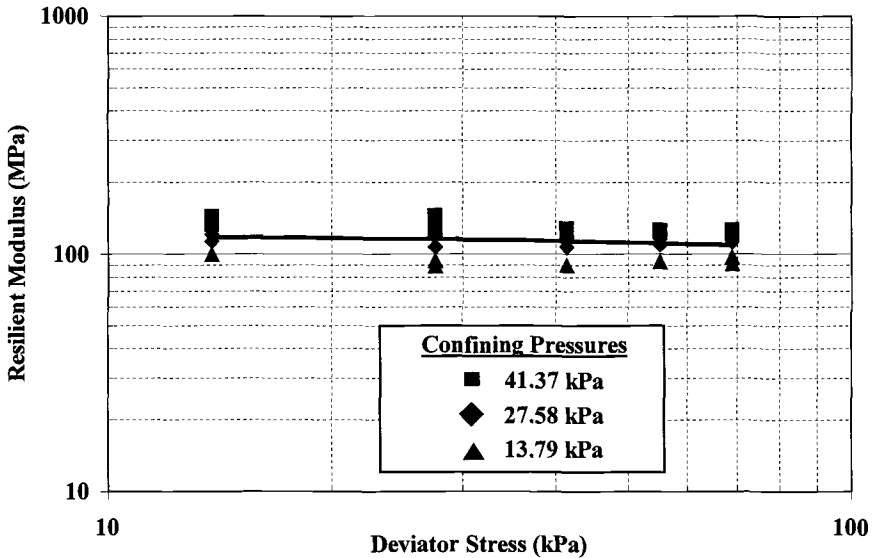
Figure 4 – *Subgrade Resilient Modulus Data for Treated Dredged Sediments*

Table 3 – *Comparison of Resilient Modulus Values for Treated Dredged Sediments and Local New Jersey Subgrade Soils*

| | Resilient Modulus Values Deviator Stress | | |
|---|---|---|---|
| Soil Type | 13.79 kPa | 41.37 kPa | 68.59 kPa |
| Treated Dredge Sediment | 117.43 MPa | 110.86 MPa | 107.96 MPa |
| Silty Sand[1] (Route 206) | 87.79 MPa | 66.87 MPa | 59 MPa |
| Sand with Silt[1] (Route 23) | 85.6 MPa | 73.81 MPa | 68.94 MPa |
| Sand with Silt[1] (Route 46) | 86.9 MPa | 69.81 MPa | 63.13 MPa |

[1] Samples compacted by modified proctor at optimum moisture content

**Field Application**

*Orion Site, Elizabeth, NJ*

The Orion Site in Elizabeth, NJ was among the first sites ever to receive treated dredge sediments as a structural fill. The site was formally a landfill where municipal waste was discharged for a ten-year period, ending in 1972. The New Jersey Department of Environmental Protection (NJDEP) allowed the site to receive treated dredge sediments as a structural fill under the parking areas of a developing shopping mall.

The development project itself is one of the models in the Environmental Protection Agency's (EPA) Brownfields Redevelopment Initiative. This involves taking contaminated sites and engineering a remediation process that would allow the site to be beneficially developed.

Approximately 460,000 m$^3$ of treated dredge material was placed from April 1996 to October 1998 to an average depth of 2 meters. The material was placed and compacted to a dry density greater than 1015 kg/m$^3$ with a corresponding moisture content less than 50 %. Compacted lifts of 0.3 meters were continually verified using a nuclear density gage. However, due to weather conditions causing wet-dry and freeze-thaw cycling of the material, not to mention the possible seepage of water into deeper layers from rain, a full-depth verification of the material was necessary. To accomplish this, cone penetration testing (CPT) was conducted on the compacted material throughout the site.

CPT tests were conducted in conjunction with a nuclear density gage to evaluate the in-situ density of the treated fill to its full depth. The correlation for the first 0.3 meters of material is shown in Figure 5. Equation (1) and (2) are the linear regression best-fit equations for the wet density and dry density, respectively. To determine the corresponding moisture content for the nuclear density test, samples were taken back to the laboratory. The one drawback of this procedure was that the initial 0.5 meters of the treated fill material may have under gone wet-dry and freeze-thaw cycling. This would cause lower density correlation values in the deeper layers then expected.

$$\gamma_m \cong 68.2(q_C) + 1450.1 \qquad\qquad (1)$$

$$\gamma_d = 43.4(q_C) + 899.4 \qquad\qquad (2)$$

where

$\gamma_m$ = wet in-situ density (kg/m$^3$)
$\gamma_d$ = dry in-situ density (kg/m$^3$)
$q_C$ = tip resistance (MPa)

To analyze the deeper layers with respect to the top 0.3 meters, the tip resistance was normalized with respect to initial 0.3 meters, which is where the nuclear density
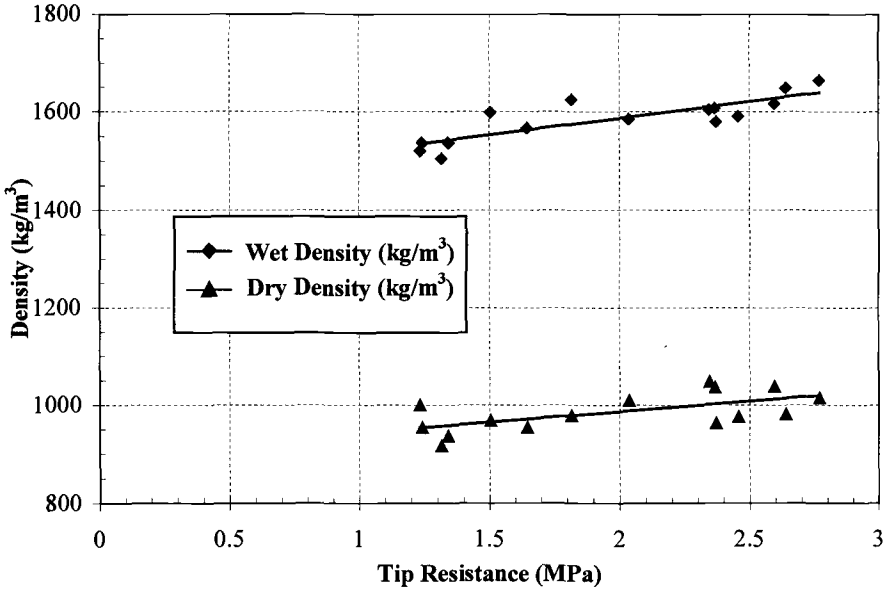
*Figure 5 – Correlation between Tip Resistance and Nuclear Density Gage Density Values for the First 0.3 Meters*

measurements were taken. Previous literature only provides correction factors for the normalization of the tip resistance for deeper layers (Robertson and Campanella, 1985). So, to accomplish the normalization, two methods were utilized. The first normalization of tip resistance method used was that suggested by Wroth (1984,1988). This method suggests normalizing the tip resistance using the following parameter:

$$Q_t = \frac{q_t - \sigma_V}{\sigma_V{'}} \qquad (3)$$

where

$Q_t$ = normalized tip resistance
$q_t$ = tip resistance corrected for pore pressure
$\sigma_V$ = overburden stress at cone tip
$\sigma_V{'}$ = effective overburden stress at cone tip

However, since the water table was far below the structural fill, the effective overburden stress equaled the overburden stress.

To effectively conduct the density analysis using this type of normalization, the normalized tip resistance must first be divided by the average normalized tip resistance for the first 0.3 meters to form a ratio factor, $R_q$. This value, $R_q$, is essentially a percentage of the tip resistance to the average tip resistance within the first 0.3 meters. Once $R_q$ is determined, it is then multiplied by the tip resistance values below the first 0.3 meters to form the a corrected tip resistance.

The second method evaluated, utilized the methodology for the correction of SPT blow-count values (Liao and Whitman 1986). However, the equation for the tip resistance correction factor utilized in this study was:

$$C_q = \sqrt{\frac{\sigma_{V0.3m}}{\sigma_V}} \qquad (4)$$

where

$C_q$ = correction factor for the tip resistance

$\sigma_{V0.3m}$ = average overburden stress for the first 0.3 meters

$\sigma_V$ = overburden stress at cone tip

A comparison of the two methods, and the actual tip resistance for a typical test is shown in Figure 6. As shown in the figure, the $R_q(q_t)$ is highly influenced by the relatively low overburden pressures, when compared to the much larger tip resistance. On the other hand, the $C_q(q_t)$ value tends to produce a flatter profile, corresponding to a more uniform material.

Once these two parameters are known, $R_q(q_t)$ and $C_q(q_t)$, they can be inserted into the linear regression equation derived for the relationship between the cone tip resistance and the nuclear density values for the first 0.3 meters. A comparison of this is shown in Figure 7. As shown in the figure, the $R_q(q_t)$ density values are again highly variable, while the $C_q(q_t)$ density values seem to depict a more uniform material, compacted under approximately the same method and conditions.

When compared to back-dated compaction logs, both methods seemed to overestimate the density, with the $C_q(q_t)$ method being the more accurate. However, the compared density tests were conducted at a time when treated dredge material had not been placed over the tested layer. Not to mention, during the time period the structural fill was placed and compacted, significantly more hydration could have taken place, creating a harder medium. Unfortunately, to determine the actual density of the deeper layers, excavating and measuring the density or using a cone penetrometer with the capability of measuring the in-situ density (Tjelta et al 1985), would be needed.

The placement and compaction of treated dredge sediments has not occurred since September 1998. As of that time, the material has performed satisfactorily. The mall is scheduled to open in the fall of 1999.

**Tip Resistance, q$_C$ (MPa)**
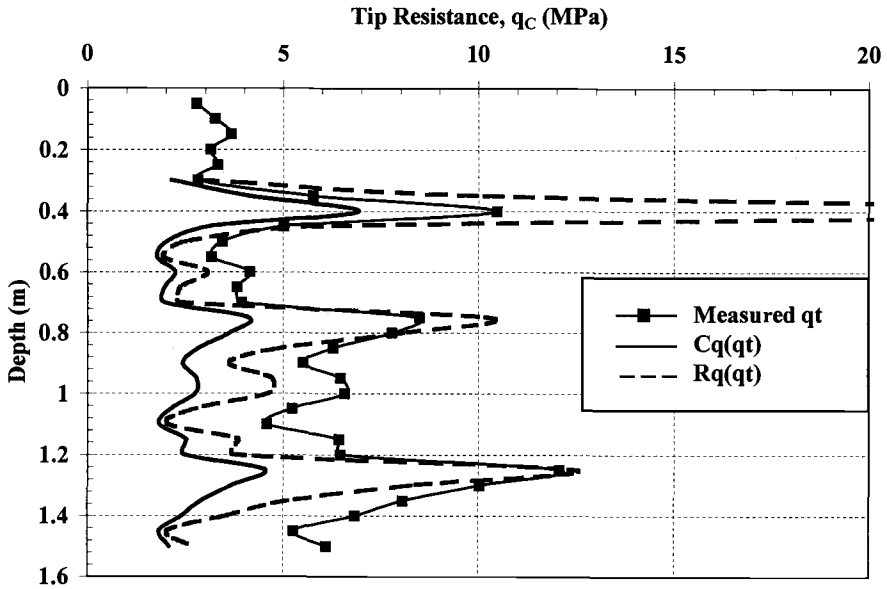


Figure 6 – *Comparison of Tip Resistance Corrected for In Situ Density Determination*

**In Situ Density (kg/m$^3$)**
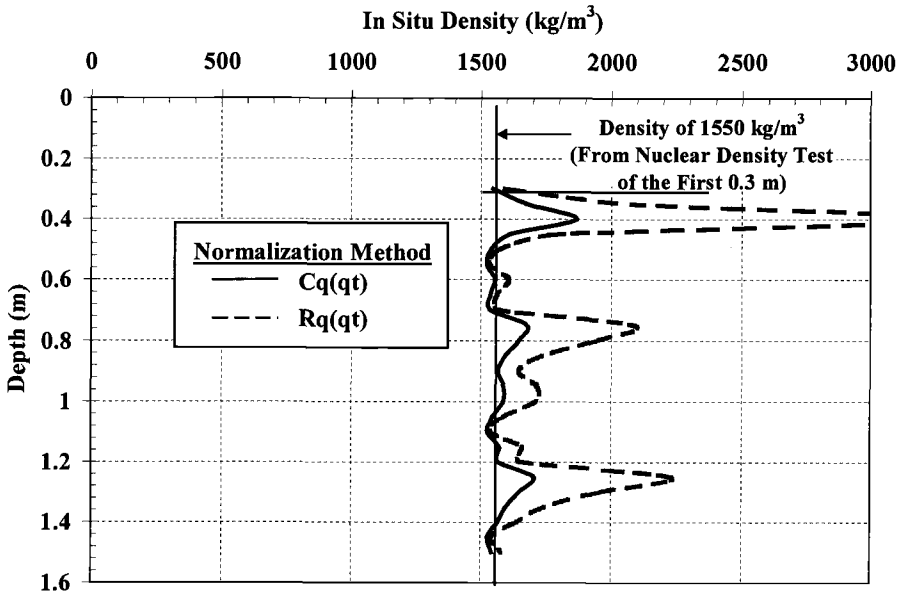


Figure 7 – *Comparison of Methods Used to Analyze the In Situ Density of Compacted, Treated Dredge Sediments*

## Conclusions

Laboratory and field testing of treated dredge sediment was conducted to evaluate the usefulness of this material in geotechnical applications. From this study, the following conclusions can be made:

1. The utilization of portland cement stabilized dredge material as a structural fill is a viable solution for the disposal of contaminated dredge sediments.

2. The raw dredge sediment can be used as structural fill after being mixed with approximately 8 % portland cement. Strength characteristics measured in the laboratory showed that the amended material would have sufficient strength to support the traffic load in parking areas.

3. The satisfactory behavior of treated dredge sediment under cyclic loading will make the material a good candidate for use as structural fill for roadway embankments.

4. The cone penetrometer can be used to provide a reasonable estimate of the in-situ density, provided a correlation can be developed between the tip resistance and the measured density of the soil.

## References

Bowles, J. E., 1992, *Engineering Properties of Soils and Their Measurement*, 4th Edition, McGraw-Hill, New York.

Chang, D., Liao, W., and Chen, S., 1996, "Effectiveness of Various Sludge Stabilization and Solidification Methods," *Transportation Research Record*, n1546, pp. 41-52.

Dermatas, D. and Meng, X., 1996, "Stabilization/Solidification (S/S) of Heavy Metal Contaminated Soils by Means of a Quicklime-Based Treatment Approach," *Stabilization and Solidification of Hazardous, Radioactive, and Mixed Wastes: 3rd Volume, ASTM STP 1240*, T. M. Gilliam and C. C. Wiles, Eds., American Society for Testing and Materials, West Conshohocken, PA, pp. 499-513.

*Joint Dredging Plan for the Port of New York and New Jersey*, October 7, 1996.

Liao, S. S. C. and Whitman, R. V., 1986, "Overburden Correction Factors for SPT in Sand," *Journal of Geotechnical Engineering*, Vol. 112, No. 3, pp. 373-377.

Lin, S. L., Cross, W. H., Chain, E. S. K., Lai, J. S., Giabbai, M., and Hung, C. H., 1996, "Stabilization and Solidification of Contaminated Soils," *Journal of Hazardous Materials*, Vol. 48, No. 1-3, pp. 95-110.

MacKay, M. and Emery, J., 1994, "Stabilization and Solidification of Contaminated Soils and Sludges Using Cementitious Systems: Selected Case Histories," *Transportation Research Record*, n1458, pp. 67-72.

National Stone Association, 1993, *The Aggregate Handbook*, National Stone Association, Washington, D. C.

Robertson, P. K. and Campanella, R. G., 1985, "Liquefaction Potential of Sands Using the CPT," *Journal of Geotechnical Engineering*, Vol. 111, No. 3, pp. 384-403.

Tjelta, T. I., Tieges, A. W. W., Smits, F. P., Geise, J. M., and Lunne, T., 1985, "In-Situ Density Measurements by Nuclear Backscatter for an Offshore Soil Investigation," *Proceedings of the Offshore Technology Conference*, Paper No. 4917.

US Army Corps of Engineers (USACE), 1991, "Use of Subaqueous Borrow Pits for Disposal of Dredged Material From the Port of New York – New Jersey," *Final Supplemental Environmental Impact Statement,* New York District, New York.

Vaghar, S., Donovan, J., Dobosz, K., and Clary, J., 1997, "Treatment and Stabilization of Dredged Harbor Bottom Sediments; Central Artery/Tunnel Project, Boston, Massachusetts," *Dredging and Management of Dredged Material, ASCE Geotechnical Special Publication No. 65*, American Society of Civil Engineers, New York, pp. 105-121.

Wakeman, T., Knoesal, E., Dunlop, P., and Knutson, L., 1996, "Dredged Material Disposal in Subaqueous Pits," *Northeastern Geology and Environmental Sciences,* Vol. 18, No. 4, pp. 286-291.

Wroth, C. P., 1984, "The Interpretation of In-Situ Soil Test," 24th Rankine Lecture, *Geotechnique*, Vol. 34, No. 4, pp. 449-489.

Wroth, C. P., 1988, "Penetration Testing – A More Rigorous Approach to Interpretation," *Proceedings of the International Symposium on Penetration Testing, ISOPT-1*, Vol. 1, pp. 303-311.

Ian R. McDermott,[1] Shawn J. Hurley,[2] Anthony D. King,[2] and Steven J. Smyth[2]

## Development of an Instrumented Settling Column for Use in a Geotechnical Centrifuge

**Abstract:** A geophysically and geotechnically instrumented settling column is used in conjunction with a geotechnical centrifuge, to monitor changing physical properties during the self-weight consolidation of a kaolin clay slurry. The column was equipped to monitor changes in excess pore pressure, bulk density and compressional wave velocity. The kaolin sample discussed in this paper was subject to an acceleration field of 100 g. The sample achieved 100% primary consolidation within 3 hours, excess pore pressures dissipating in a manner similar to that reported for 1 g settling column experiments. During this time the sample settled from a 0.865 m thick suspension to a 0.150 m thick soil deposit. The compressional wave velocity and density data, collected at one point in the sample, provided insight into the development of the soil during the centrifugation process. These data showed that below 1200 $kg/m^3$ the sample behaved as a suspension, which is comparable to the results of other researchers and consistent with suspension theory. Above this density, the experimental data indicates that the sample begins to develop a fabric and, as a consequence, the compressional wave velocity increases to values greater than those predicted by suspension theory. There are some issues which need to be resolved through further data analysis or centrifuge tests, but the principle aim of the experiment was successfully achieved. That is to demonstrate that the instrumented settling column for use in geotechnical centrifuge is an extremely useful technology for evaluating soft soil properties and behaviour in a time efficient and cost effective manner.

**Keywords:** self-weight consolidation, centrifuge, instrumented settling column, excess pore pressure, bulk density, compressional wave velocity, kaolin clay

[1]Director Geophysics, C-CORE, Memorial University of Newfoundland, St. John's, Newfoundland, Canada A1B 3X5
[2]Research Engineer, C-CORE, Memorial University of Newfoundland, St. John's, Newfoundland, Canada A1B 3X5

## Introduction

Interest in the behaviour of soft soils stems from their relevance to the dredging, waste disposal and mining industries. Increasingly stringent environmental legislation has called for modified practice in the handling and containment of contaminated soft soils. This has increased the demand for knowledge about soft soil properties and behaviour. Soft soils are characterized by their high water contents, low strengths, and large strains during the primary consolidation phase of their development. These characteristics make the task of recovering good quality soft soil samples for laboratory testing virtually impossible. This has resulted in a shift away from more traditional soils testing methods to such techniques as settling column tests.

This paper describes the use of an instrumented settling column which is used in conjunction with a geotechnical centrifuge to study consolidation phenomena associated with a sample of Speswhite kaolin clay. Speswhite kaolin clay was selected because its properties are well documented and because comparative data sets are available. The motivation of the experiment described in this paper was to demonstrate how geophysical and geotechnical measurements, which can be readily employed in situ, can be used to characterize the physical behaviour of soft soils and to provide insight into the mechanism of soft soil consolidation phenomena.

## Background

Soft soil consolidation behaviour is best modelled using large strain theories. Laboratory self-weight consolidation settling column experiments have been used for over two decades to study characteristics of surface settlement, bulk density profiles and excess pore pressure dissipation in soft soils (Been and Sills 1981, Elder and Sills 1984, Tan et al. 1988, McDermott 1991, Suthaker and Scott 1994). In some cases these data are used to calculate other characterizing parameters such as vertical effective stress and permeability (Been and Sills 1981, Elder and Sills 1984). Undrained shear strength using shear vanes (Bowden 1988) and small strain shear stiffness ($G_{max}$) using shear wave measurements (McDermott 1991), have also been used in settling column experiments. These experiments showed that increasingly higher strengths and stiffness are observed with increasing time and at constant effective stress, which demonstrate that certain soft soils are subject to thixotropic effects. In contrast to the vane measurements, the S-wave measurements proved to be a powerful non-destructive tool and clearly identified the time scale and magnitude of the thixotropic behaviour of the soil (McDermott 1992). Urick and Hampton (whose results are conveniently summarized in Ogushwitz 1985) carried out laboratory experiments to measure compressional wave (p-wave) velocity in kaolinite suspensions. These data indicate that the p-wave velocity versus bulk density curve follows a quadratic relationship the minimum of which is dependant on the relative density of the solid/fluid constituents. There is evidence to

suggest that this minimum is coincident with the point in time when the slurry is first able to sustain the transmission of S-waves, and hence to the time when a continuous soil fabric has been formed (McDermott 1992). It is the combination of these geotechnical and geophysical measurements which are providing such a useful insight into soft soil properties and show that they are governed by a complex interaction of sedimentation and consolidation processes.

Despite the large advances made using settling column experiments, the studies have become restrictive owing to the limited stress levels that can be applied to the soil samples, and because of the time required for completion of primary consolidation (a process which can take many months or even years). In an effort to enhance primary consolidation in soft soils, a number of researchers (Mikasa and Takada 1984, Miyake and Akamoto 1988, Kita et al. 1992, McDermott and King 1998) have chosen to use centrifuge model tests. These researchers have demonstrated that the large strain theories, used in the 1-g self-weight experiments, remain valid for the centrifuge models. The potential for centrifuge modelling of self-weight consolidation processes is far greater than that so far explored and much is to be learnt, as was demonstrated in the 1-g settling column experiments, by instrumenting centrifuge settling columns with a suite of measurement sensors.

This paper describes the use of a geophysically and geotechnically instrumented settling column which has been designed for use in a geotechnical centrifuge. The objective of the experiment described here, was to determine how the compressional wave velocity and bulk density changed as a kaolin slurry developed to form a consolidating soft soil bed under self-weight in a geotechnical centrifuge. The experiment was designed to observe these changes until the end of primary consolidation. The purpose of this was: to compare the experimental centrifuge results with available 1-g settling column data by way of validating the use of the centrifuge to model normal soft soil behaviour; to provide soft soil kaolin properties, particularly geophysical properties, for future research; and to use these data to gain some insight into the processes of soft soil development. The self-weight consolidation behaviour of kaolin clay had already been modelled using the geotechnical centrifuge at the University of Colorado (Croce et al. 1984) and the centrifuge scaling laws were verified at that time.

**Theoretical Considerations**

The equation for the velocity of compressional waves propagating through an infinite, homogeneous, isotropic and elastic medium is obtained from the solution of the wave equation:

$$V_p = \sqrt{\frac{B + \frac{4}{3}G}{\rho}} \tag{1}$$

where
$V_p$ = compressional wave velocity within the medium
$B$ = bulk modulus of the medium
$G$ = shear modulus of the medium
$\rho$ = bulk density of the medium

The above assumptions are assumed valid for small strain compressional waves propagating through soft soil.
Wood's equation (Hamilton 1971) was derived from the above expression for the special case of compressional waves propagating through a suspension. Wood's equation has the form:

$$V_{sus} = \sqrt{\frac{B_{sus}}{\rho_{sus}}} = \sqrt{\frac{1}{(\eta C_w + (1-\eta)C_s)(\eta \rho_w + (1-\eta)\rho_s)}} \qquad (2)$$

where
$V_{sus}$ = compressional wave velocity through the suspension
$B_{sus}$ = bulk density of the suspension
$\rho_{sus}$ = bulk density of the suspension
$C_w$ = fluid compressibility
$C_s$ = solid compressibility
$\rho_w$ = fluid density
$\rho_s$ = solids density
$\eta$ = porosity of the suspension

Wood's equation is applicable for soils with no rigidity (i.e. suspensions) and represents a lower limit for the velocity of compressional waves in a fluid saturated soft soil.

## Experimental Apparatus

### The Geotechnical Centrifuge

The Acutronic 680-2 centrifuge at the C-CORE Centrifuge Centre is capable of testing models at accelerations of up to 200 g and has a radius of 5.5 m to the surface of the swinging platform. The C-CORE centrifuge has a maximum payload capacity of 220 g-tonnes, reducing to 130 g-tonnes at 200 g due to the increased self-weight of the platform. Maximum payload size is 1.1 m high by 1.4 m long and 1.1 m wide. The platform and the payload are balanced by a 20.2 tonne mass counterweight, the position of which is adjusted to compensate for different test packages. Sliprings located on the centrifuge hub allow power to be supplied to test packages, control of experimental apparatus and data acquisition.

*The Instrumented Settling Column Apparatus*

The settling column consists of a 1000 mm long-PVC pipe, with an internal diameter of 241 mm and a wall thickness of 14 mm. The top and bottom of the column is sealed with steel plates of 25 mm thickness and the entire assembly is held together using four steel tie rods. The lower 615 mm of the column is reinforced with steel bands to resist the high hydrostatic pressures generated within the column while in flight. Two pieces of ABS conduit, each with a nominal diameter and wall thickness of 38 mm and 6 mm respectively, extend the full length of the column and are fixed to opposing sides of the inner wall of the column. During centrifuge experiments these pipes contain the gamma ray bulk density source and detector as described in more detail below. The column is constructed so that an assortment of geophysical and geotechnical transducers can be used during the centrifuge experiments. In this experiment the column was equipped to measure excess pore pressure dissipation, bulk density and p-wave velocity, but shear wave velocity and electrical resistivity can also be measured. Figure 1 shows a section through the column showing the relative positions of the measurement transducers.
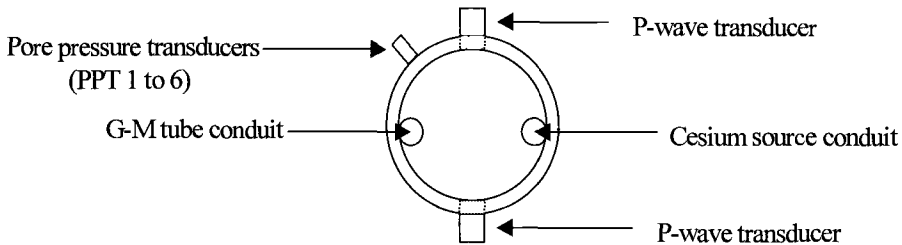


Figure 1: *Top View - Cross Section of the Instrumented Settling Column*

*Measurement of Excess Pore Pressure Dissipation*

Measurements of pore pressure were made using six Druck pressure transducers (type PDCR 81with pressure ratings ranging from 0.1 MPa to 1.4 MPa) mounted at various elevations in the column wall. Pore pressures were measured during the centrifugation process using a digital data acquisition system mounted in the hub of the centrifuge. These data were transferred out of the centrifuge chamber via slip ring couplings. The output voltage of the pore pressure transducers were converted into pore pressures using a previously derived calibration equation. Pore pressures were measured to an accuracy of better than ±0.3%.
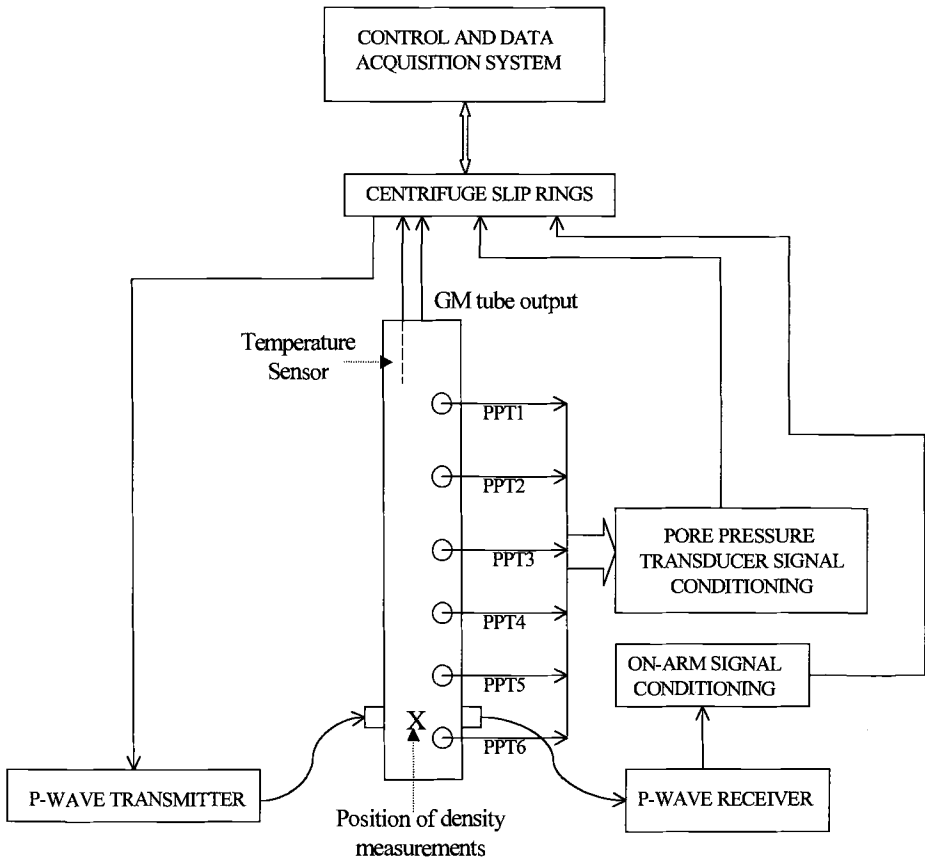
Figure 2: *Schematic of the Centrifuge Settling Column Apparatus*

*Bulk Density Measurement*

Bulk density of the soil specimen was measured at discrete time intervals during the centrifuge test at an elevation of 0.950 m from the top of the column. Bulk density was determined by measuring the degree to which a collimated beam of gamma rays was attenuated when passing through the soil specimen. The bulk density measurement apparatus consisted of a gamma ray source, detector and rate meter. The gamma ray source was a 111 M Bq Cesium-137 source which was encapsulated within a lead slug

with dimensions of 25 mm diameter and 50 mm in height.  The lead slug had a 3 mm diameter epoxy filled port which allowed a collimated beam of gamma rays to be emitted. The gamma ray detector was a LND 7121 Geiger-Muller (GM) tube which was connected to a Ludlum, Model 3 Radiation Survey or rate meter with which gamma count rate was monitored. During the centrifuge test the gamma ray source and detector were fixed in the column sidewall conduits (Figure 2).  During the experiment, gamma ionization events were counted, using the counter rate meter, over a given period of time. The gamma count was recorded manually.  The count rate (in counts per minute) was later converted to values of bulk density using water content measurements of pre-test and post-test sub-sampled soil specimens in combination with a previously obtained calibration equation. Density was measured to an accuracy of better than $\pm1.4\%$ using this technique.

*Compressional Wave (p-wave) Velocity*

    Compressional wave velocity in the soil was determined using a pair of p-wave transducers. Each transducer was fabricated in-house and comprises an epoxy resin transmission front face, Sensor Technology Ltd. BM532 250 kHz piezoelectric disc elements, backed by a pressure release and sound absorption material. This assembly was encapsulated within a threaded  PVC housing which was screwed into the column side wall against an O-ring seal which prevented leakage during centrifuge testing. The transmitting and receiving p-wave transducers were positioned opposite each other and at an elevation of 0.950 m from the base of the column. This was at the same elevation but at right angles to the bulk density source and detector. The p-wave transducers were mounted flush against the inside of the column so that the p-waves propagated over a distance of 0.241 m.
    The transmitting p-wave transducer was energized using the leading edge of a 20 volt amplitude square wave in a pulse excitation fashion. On energizing, a  compressional wave was generated in the soil and propagated across the column and was detected by the opposing receiving transducer. The transit time for these p-waves to travel the known path length across the column yielded the compressional wave velocity in the soil. The transit time for the wave to propagate a known distance across the column was determined by measuring the time delay between the transmit pulse and the onset of the p-wave. Compressional wave velocity was measured to better than $\pm0.4\%$ accuracy using this approach.
    The compressional waveforms were collected at discrete time intervals during the centrifuge tests and collected in parallel with the bulk density data. The received waveforms were  amplified and sent out through the centrifuge slip rings for display on a Tektronix TDS420 digitizing oscilloscope. To improve signal-to-noise ratio of the waveforms, 50 waveforms were signal averaged prior to being displayed and stored on a PC.

## Experimental Procedure

### Soil Preparation

A Speswhite kaolin clay slurry was prepared for the test. The soil was produced by mixing a Speswhite kaolin clay powder with deionized water overnight. The initial bulk density of the slurry was 1110 kg/m$^3$. The slurry was siphoned into the test package in a manner devised to minimize gas entrainment. At the beginning of the test, the slurry had a thickness of 0.865 m.

### The Centrifuge Test

The settling column apparatus was installed in the centrifuge and filled with water. The apparatus was then tested at 100-g to ensure integrity of the package and to obtain base hydrostatic pressure, density and p-wave velocity readings in the water. Temperature of the water was also recorded during the test. These readings were later used later in data analysis. The water was removed from the column and the kaolin slurry immediately siphoned into the column.

Centrifuge rotation began 10 minutes after depositing the kaolin slurry into the column. The experiment was carried out in an acceleration field of 100 gravities. The first pore pressure readings, bulk density counts and p-wave waveforms were recorded in-flight when the apparatus had reached test conditions. This was 22 minutes after deposition. Variations of soil temperature were recorded using a temperature probe. All measurements were repeated at convenient intervals during the test. During the centrifugation process the kaolin settled from its initial suspension to form a consolidating bed. The centrifuge test was terminated when the kaolin soil had attained 100% primary consolidation. The overlying water was syphoned off. Sub-samples of the kaolin were taken for water content analysis from the top, middle and towards the base of the soil. The sub-sample taken from the near the base of the sample was consistent with the elevation of the p-wave and density measurements.

## Results and Data Analysis

### Kaolin Clay Properties

The Speswhite kaolin clay has a liquid limit of 66%, a plastic limit of 36% and its solid component has a specific gravity of 2.61. This material has a particle size distribution such that 77% of the soil is clay fraction ($\leq$2 µm) and 100% of the soil

particles are finer than 9.5 μm.

The initial slurry water content was 580%. The water contents at the end of the test at elevations 0.85 m, 0.90 m and 0.95 m, from the top of the column, were 120%, 74% and 59% respectively.

*Excess Pore Pressure*

The variation in acceleration field between the upper most (PPT1) and lower most (PPT6) pore pressure transducer was 15% (see Figure 2). The pore pressure data has been corrected to remove this variation such that the data is representative of a uniform acceleration field of 100 g. The excess pore pressures in the sample were determined by subtracting the appropriate (100 g) hydrostatic pressure from the observed pore pressure measurements. Profiles of excess pore pressure observed during consolidation of the kaolin sample are shown in Figure 3. The experimental technique does not allow measurement of an excess pore pressure profile immediately after the slurry's introduction into the column at test conditions. The excess pore pressure distribution has therefore been calculated for the hypothetical case of a uniform slurry of 1100 kg/m$^3$, 0.865 m thick, in an acceleration field of 100 g (0 minutes in Figure 3). The resulting
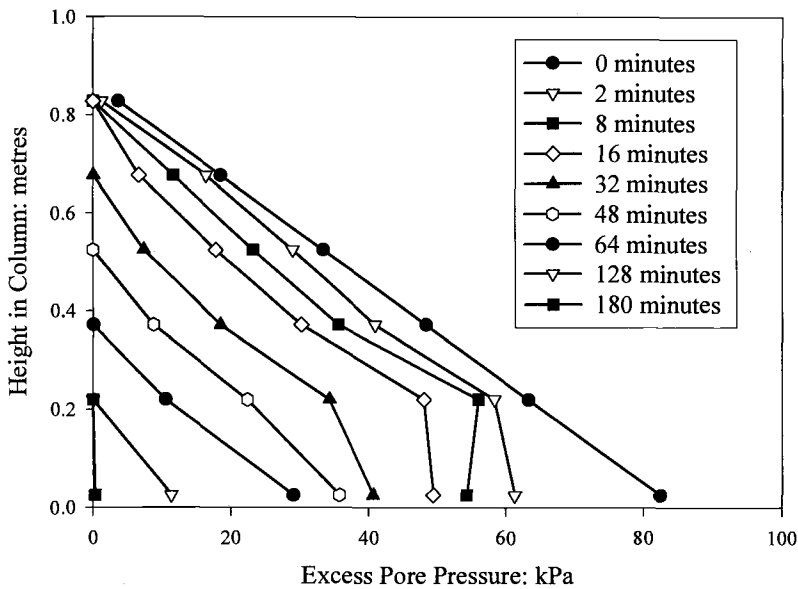


Figure 3 - *Excess Pore Pressure Dissipation*

triangular distribution represents the maximum possible value of excess pore pressure within the column under test conditions. The observed excess pore pressures are shown to decrease with time. The dissipation is at first most rapid at the base of column indicating that consolidation proceeds upwards from the base. The excess pore pressures have completely dissipated after 180 minutes.

*Settlement*

The soil surface settlement has been determined from the measured initial and final settlement heights and at intervening heights by using the time at which the pore pressure transducer registered zero excess pore pressure. The initial and final thickness of the sample was 0.865 m and 0.150 m respectively. The degree of settlement versus square root time is shown in Figure 4. This figure does not show any detail of the soil settling out of suspension since this would have commenced during the spin-up to test acceleration. The data shown here represents a soft soil consolidation curve.
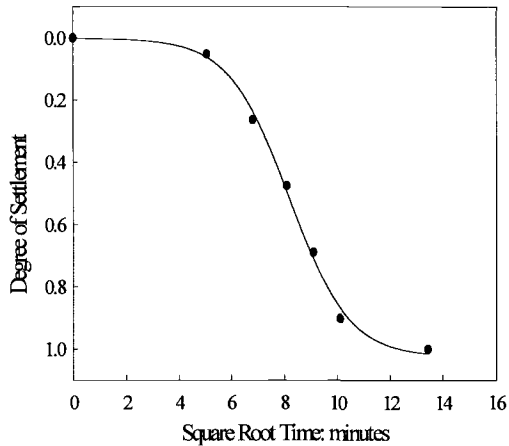


Figure 4 - *Degree of Settlement versus Square Root Time*

*Bulk Density Results*

The count rate was converted to values of bulk density using a combination of the pre-test and post-test water content measurements (at the same elevation as the gamma source and detector), and a previously determined calibration equation obtained in a series of kaolin slurries. It was not possible to monitor variations in background radiation within the centrifuge chamber during the experiment so no correction has been applied for this. Figure 5 shows the variation of bulk density with time. The bulk density results show a relatively rapid increase in bulk density from the initial slurry density of 1100

kg/m³ to 1580 kg/m³ within the first hour. Within the remaining two hours of the test, the bulk density increases steadily to a maximum density of around 1650 kg/m³. Density readings at the beginning of the test show slightly lower densities than the initial slurry density. This is thought to be due to variations in background radiation.
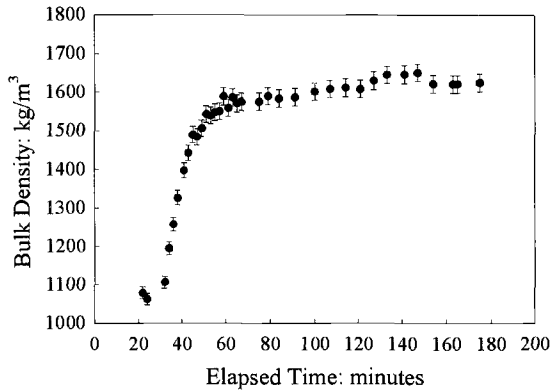


Figure 5 - *Variation in Bulk Density with Time*

*Compressional Wave Velocity Analysis*

The compressional waveforms collected during the test, both in water and in the kaolin sample, were analysed so as to obtain compressional wave first arrival or onset times. These preliminary p-wave velocities were uncorrected for variations in temperature. The change in sound velocity due to variations in water/ sediment temperature is well known and can be calculated from a standard equation (Clay and Medwin 1977, Schumway 1958). Using a standard equation (Clay and Medwin 1977) all the p-wave velocities were corrected to a standard temperature of 20°C. In order that a useful comparison could be made between the data obtained in this experiment and those of Urick and Hampton (from Ogushwitz 1985), and that of Wood's equation, the p-wave velocity in the kaolin was normalized using the sound velocity measured in water at 100g in an earlier test. These normalized values were then plotted against measured bulk density values to produce, Figure 6.

In reviewing Figure 6, it will be noted that there are far fewer data points at the lower densities than at higher densities. The main reason for this being that the kaolin clay settled and consolidated so quickly at the beginning of the test, reaching a density of 1400 kg/m³ after just 21 minutes, that only seven measurements were obtained in this early portion of the test. For 60% of the duration of the test, the p-wave velocity in the kaolin were less than that of water. Only when the density had reached a value of 1630 kg/m³ did the velocity increase to greater than that of water.

The data shows the quadratic relationship between p-wave velocity and bulk density. A best fit curve to these data gives an equation of the form:

$$\frac{Vp}{Vw} = 2.063 \times 10^{-7}\rho^2 - 5.143 \times 10^{-4}\rho + 1.335 \qquad (3)$$
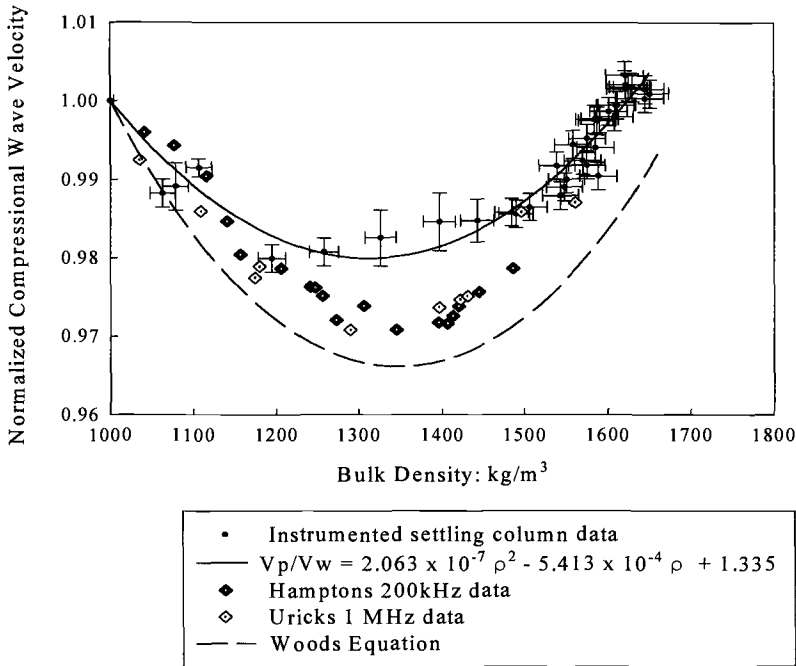
Figure 6 - *Normalized Compressional Wave Velocity versus Bulk Density*

where
$Vp$ = p-wave velocity in the kaolin soil
$V_w$ = p-wave velocity in water
$\rho$   = bulk density of the kaolin soil

This best fit equation indicates a minimum at 1311 kg/m³. This minimum occurs 16 minutes into the test. This coincides with a degree of consolidation of about 25%.

Wood's equation, Equation 2, has also been plotted on Figure 6. This curve has been generated using a compressibility of water of $4.55 \times 10^{-10}$ Pa⁻¹ and a compressibility of kaolinite grains of $2.3 \times 10^{-11}$ Pa⁻¹ (Ogushwitz 1985). Values of 1000 kg/m³ and 2610 kg/m³ were used for the density of water and kaolin grains respectively. In the early stage of the test, at densities below 1200 kg/m³, the experimental velocity data is close to that given by Woods "boundary" equation. These data agree well with Urick and Hampton's data, also shown on Figure 6. This would indicate that the kaolin specimen is behaving as if it were a suspension. The p-wave velocities collected at densities above 1200 kg/m³ deviate from that of Hampton and Wood's equation and, for the most part, from that of Urick's data also. These data lead to the conclusion that the kaolin is developing a soil fabric. As a soil develops from a suspension to a consolidating soil bed, a soil fabric is

created. This results in a non-zero shear modulus and a frame bulk modulus. Since these two parameters influence p-wave velocity (Equation 1), velocity increases to values higher than that predicted by the Wood's equation.

Somewhat perplexing, however,  is the fact that Wood's equation appears to be converging at higher densities with the experimental data. It is thought that this is a reflection on Wood's Equation being inappropriate for high density soils (i.e. > 1500 kg/m$^3$) rather than any problem with the experimental data. To investigate this, a sample of 1500 kg/m$^3$ Speswhite kaolin clay was mixed after the centrifuge test and was found to have the consistency of an emulsion rather than a true suspension. This sample was left to stand, undisturbed in the laboratory for a period of six hours at which time it was found to be able to support the transmission of shear waves. This indicates that the sample had developed a rigid fabric. Kaolin-water mixtures of less than 1400 kg/m$^3$  require much longer to show evidence of fabric formation.

Another item requiring consideration is Urick's two data points, at the higher densities, which coincide with the centrifuge experimental data. This might be explained by the difficulty of obtaining kaolin suspensions at these densities, as described above, or it could be due to velocity dispersion effects within the soil. The later possibility will be investigated and reported in future papers.

## Conclusions

This experiment established that it is possible to monitor excess pore pressure dissipation, changes in bulk density, and to generate and detect compressional waves in a consolidating soft soil in a geotechnical centrifuge at high acceleration levels. The excess pore pressure profiles measured during this experiment showed the same trends as those observed in settling columns used under normal gravitational conditions (for example Been and Sills 1981 and Tan et al. 1988). The increased stress level that can be applied to the soil using the geotechnical centrifuge means that the instrumented settling column can be used to extend the study of soft soil self-weight consolidation phenomena.  Increased stress levels are consistent with increased burial depth within the soil deposit. This makes the settling column and centrifuge apparatus an attractive technology for evaluating consolidation properties and behaviour of large scale waste disposal sites and fine tailing settling ponds.

The bulk density measurement apparatus described here requires refinement. A priority for future tests will be the addition of a second Geiger-Muller tube to monitor background radiation. This will allow the influence of background radiation to be removed from the density measurements made in the soil. The system described in this experiment allows the measurement of bulk density at a single elevation within the soil bed. As a result of the success of this experiment, C-CORE intend to install a bulk density profiling system within the coming year. This will yield valuable information concerning the way in which bulk density profiles change during the consolidation process. Such profiles, used in conjunction with the excess pore pressure measurements, will be used to monitor changes in effective stress and permeability during self-weight

consolidation.

Compressional wave velocity is not a measurement that is commonly adopted for geotechnical tests. However the author's feel that it has a place in both laboratory and field geotechnics, particularly in work which involves soft soils. As shown here, the p-wave velocity yields some insight into the behaviour of soft soils. The difference in magnitude of p-wave velocities propagating through a soft soil as compared to a suspension at the same density, is an indicator of the developing soil framework. Used in combination with shear wave velocity measurements they could provide a means of evaluating the developing frame bulk modulus and shear modulus. Shear waves have already been measured, using the settling column, in a centrifuge self-weight consolidation test of kaolin clay (King et al. 1996). This then represents the next stage of the work being undertaken by the authors. In addition, the centrifuge and settling column are already being employed to characterize the consolidation behaviour of mine tailings, building upon previous work carried out in this area by such researchers as Bloomquist and Townsend 1984, and Stone et al. 1994.

The comparison of the centrifuge results with those carried out in normal gravitational conditions indicates the technique is promising as a way of accurately modelling the natural behaviour of soft soils. It is hoped that by continuing this line of research, that industry will be encouraged to use centrifuge technology for the routine evaluation of soft soil self-weight consolidation behaviour and properties. The technique is thought to be of potential benefit to the dredging, waste disposal and mining industries in particular.

*Acknowledgements*

## References

Been, K. and Sills, G. C., 1981, " Self-Weight Consolidation of Soft Soils: An Experimental and Theoretical Study," *Geotechnique*, Vol. 31, No. 4, pp. 519-535.

Bloomquist, D. G. and Townsend, F. C. 1984, "Centrifuge Modelling of Phosphatic Clay Consolidation," *Proc. Symp. on Sedimentation/Consolidation Models: Prediction and Validation*, San Francisco, pp. 565-580.

Bowden, R. K., 1988, *Compression Behaviour and Shear Strength Characteristics of a*

*Naturally Silty Clay Sedimented in the Laboratory*,  D.Phil. Thesis, Oxford University.

Clay, C. S. and Medwin, H., 1977, *Acoustical Oceanography: Principles and Applications*, John Wiley and Sons, Chichester, pp. 3.

Croce, P., Pane, V., Znidarcic, D., Ko H.Y., Olsen, H. W., and Schiffman, R. L., 1984, "Evaluation of Consolidation Theories by Centrifuge Modelling," *Proc. International Conference on Applications of Centrifuge Modelling to Geotechnical Design*, pp. 381-396.

Elder, D. McG. and Sills, G. C., 1984, "Time and Stress Dependent Compression in Soft Sediments", *ASCE Symp. on Prediction and Validation of Consolidation*, San Francisco.

Hamilton, E. L, 1971, "Elastic Properties of Marine Sediments," *Journal of Geophysics Research*, 76, 2, pp.579-604.

King, A. D., McDermott, I. R., Hurley, S. J., and Smyth, S. J., 1996. "In-Flight Shear Wave Measurements in a Soft Cohesive Soil Undergoing Self-Weight Consolidation in C-CORE's Geotechnical Centrifuge", *49th Canadian Geotechnical Conf.*, St. John's, pp. 497-504.

Kita, K., Shibata, T., Yashima, A., and Kobayashi, S., 1992,  "Measurement of Shear Wave Velocities in a Centrifuge", *Soils and Foundations*, 32 (2), Japan. Soc. of Soil Mech. and Foundation Eng. pp. 134-140.

McDermott, I. R., 1991, "A Laboratory Method to Investigate Shear Waves in a Soft Soil Consolidating under Self-Weight", *Shear Waves in Marine Sediments*, J.M. Hovem, M. Richardson and R. Stoll (Eds.), Kluwer Academic Publishers, pp. 103-110.

McDermott, I. R., 1992. *Seismo-Acoustic Investigations of Consolidation Phenomena*, Ph.D. Thesis, University of Wales.

McDermott, I. R. and King, A. D, 1998, "Use of a Bench-Top Centrifuge to Assess Consolidation Parameters", *Tailings and Mine Waste '98*. Balkema Press., Rotterdam, pp. 281-288.

Mikasa, M. and Takada, N., 1984, "Self-Weight Consolidation of Very Soft Clay by Centrifuge", *Proc. Sedimentation/Consolidation Models: Prediction and Validation*, San Francisco, pp. 121-141.

Miyake, M. and Akamoto,H., 1988, "Filling and Quiescent Consolidation Including Sedimentation of Dredged Marine Clays", *Centrifuge 88*, Corte, J.F. (ed.),  A.A. Balkema, Pub., pp.163-170.

Ogushwitz, P. R.,  1985, "Applicability of the Biot Theory.II.  Suspensions", *Journal of the Acoustic Society of America*, 77, pp. 441-451.

Schumway, G., 1958, "Sound Velocity vs. Temperature in Water Saturated Sediments", *Geophysics*, Vol. 23, No.3, pp. 494-505.

Stone, K. J. L., Randolph, M. F., Toh, S. and Sales, A. A., 1994, "Evaluation of Consolidation of Mine Tailings, *Journal of Geotechnical Engineering*, ASCE, Vol. 120, No. 3, pp. 473-490.

Suthaker, S. and  Scott, D., 1994, "Large Scale Consolidation Testing of Oil Sand Fine Tails",  *1st Int. Congress on Environmental Geotechnics*, Edmonton, pp. 557-562.

Tan. S. A., Tan, T. S., Ting, L. C., Yong, K. Y., Karunaratne,G. P., and Lee, S. L., 1988, "Determination of Consolidation Properties for Very Soft Clay," *Geotechnical Testing Journal, ASTM GTJODJ, Vol. 11, No. 4, pp. 233-240.*

David Cazaux[1] and Gérard Didier[2]

**Estimation of the Quantity of Liquid Exuded by a Loaded Sludgy or Pasty Waste**

**Abstract:** In the disposal of sludgy or pasty wastes, the liquid contained in a loaded waste will exude. The quantity of liquid exuded will be a function of initial water content, waste consistency, applied stress and time. In order to determine the amount of liquid, we have designed a new oedometer was designed to perform consolidation tests on large dimension specimens ($\varnothing$ 250 mm, height $\leq$ 60 mm). Several tests on three types of waste have been performed. Settlement and amount of exuded liquid from both upper and lower drainage interfaces has been measured under different normal stresses and initial water contents. The hydraulic conductivity was also measured. To estimate the exuding potential of a given waste, a method to determine the amount of extractable liquid ($q_f$) for an infinite time is proposed. This method presents the advantage of considerably reducing the required time for consolidation tests. Given the density and height of a sludgy layer located at a given depth, the paper shows that it is possible to determine the total amount of liquid that will be expected at large times.

**Keywords:** sludge, waste, consolidation, hydraulic conductivity, settlement

**Introduction**

Disposal of sludges from industrial processes, mining operations or water treatment is increasing and sometimes requires geotechnical considerations within a more general environmental interest (Barden and Berry 1965). Our study consists of research to find simple ways of enabling us to determine consolidation parameters of pasty or sludgy wastes in order to estimate the liquid quantity that can exude under a self-weight or imposed loading conditions. Most of the solid and liquid materials which constitute of sludgy wastes are, by definition, heterogeneous phases. Generally, the liquid is not only composed of water but of a multi-element solution. The leaching potential of a sludge is a very important parameter when the material is received on the site for the knowledge of water balance within the landfill. By considering this leaching potential, we can select either the storage area or the more adapted drainage system to the material. The

---

[1] Project Manager, URGC Geotechnique, INSA Lyon, 20 avenue Albert Einstein, 69621 Villeurbanne, France

[2] Professor, URGC Geotechnique, INSA Lyon, 20 avenue Albert Einstein, 69621 Villeurbanne, France

contribution of sludges to the water balance of a landfill can be very important and should be considered more accurately to avoid saturation of drainage installation.

Some modifications have been made to conventional devices to optimize the representative scale of laboratory testing. The literature generally describes small scale testing, except for some authors who performed large oedometric tests (Barden and Berry 1965, Davis and Raymond 1971, Imai 1979, Rowe and Barden 1966, Znidarcic and Schiffman 1982). The specimen geometry, pore pressure and hydraulic conductivity are parameters that can be followed simultaneously. The oedometer that we developed is mainly adapted to high moisture content soils and sludges. In the same way viscosity and cohesion of the specimen are measured (Untung 1990). The analysis of consolidation is made by conventional measurement of the gradual reduction of volume of the fully saturated sludge by the drainage of liquid. One-dimesionnal consolidation data have been analyzed by different methods that can be found in the literature, such as Casagrande, Asaoka or Taylor (cited by Untung 1990).

**Test procedure and apparatus**

The new oedometer has an internal diameter of 250 mm with a piston that allows various heights of specimen, from 10 to 60 mm (Figure 1). Measurement of settlement is made with LVDT and the measurement of pore pressure with an electronic pressure transducer. Two stainless porous discs provide drainage of both faces of the specimen. Stress is applied via a piston driven by an oil pressure system. The hydraulic properties of the sludge are measured using a falling-head or constant-head devices connected to the cell. Many series of tests have been performed on various sludges. Two main loading procedures have been adopted: step-loading (between 50 and 800 kPa) or direct loading (200, 400 and 800 kPa). Loading schedules are described in table 1. Undrained cohesion has been measured using a vane shear test method after specimens have been previously consolidated to loading specifications. Viscosity has been also measured with a synchroelectric viscosimeter type "Brookfield" on another fraction of same pre-consolidated specimens.

Table 1 – *Loading Schedule for Step or Direct Procedure*

| Sludge | Step-loading | Direct loading |
|--------|--------------|----------------|
| B1 | Load is doubled every 24 hours from 50 to 800 kPa | Each load for 24 hours 200, 400 and 800 kPa |
| B2 | Load is doubled every 24 hours from 50 to 800 kPa | Each load for 24 hours 200, 400 and 800 kPa |
| B3 | Load is doubled every 24 hours from 200 to 800 kPa | Each load for 24 hours 200, 400, 600, 800 kPa |

**Samples**

The three sludges tested in this paper have been provided to us after previous treatment and under different conditions. Sample B1 is a mining sludge generated from the washing of glacial coarse tills. This yellow material was initially filtered and has average natural moisture of 53%. Sludge B2 was generated from the biological treatment of industrial wastewater; its initial moisture is about 800%. Its organic matter content is about 50% and the analysis of dry matter shows a high content of heavy metals (mainly Cu, Zn, Cr, Ni). The material was initially treated by a series of chemical processes (Lime, Sodium hydroxide, Sulfuric acid,...) and physical processes (centrifugation). The third sample, called B3, came from the treatment of residual industrial water and possesses an average moisture content of 136%. The sludge was initially treated with hydrochloric acid or lime and filtered. The main physical characteristics of the three samples are presented in Table 2.
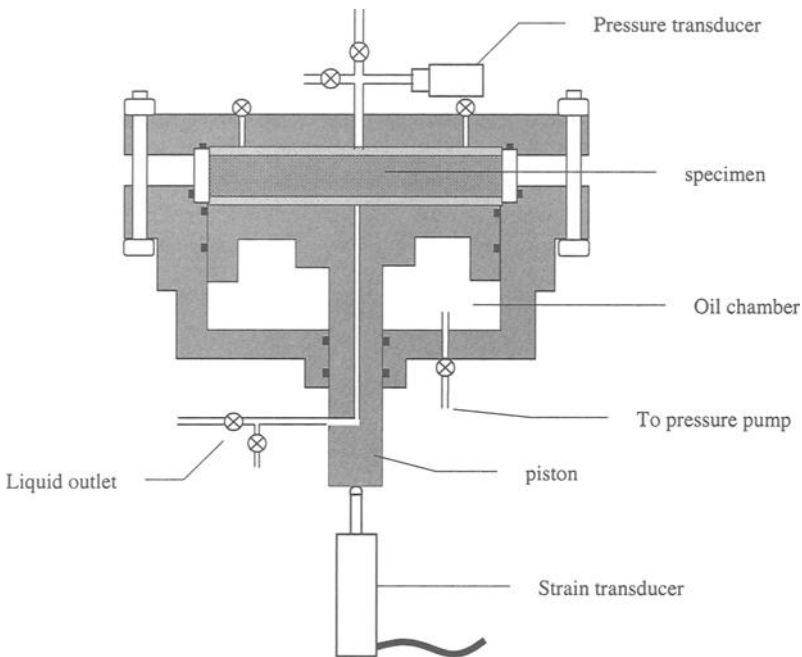


Figure 1 - *Consolidation cell for measurement of settlement and hydraulic properties of sludge specimen of 250-mm diameter*

Table 2 - *Main Physical Characteristics of the Three Tested Sludges*

|  | B1 | B2 | B3 |
|---|---|---|---|
| Specific gravity of solid grains | 2.79 | 1.57 | 2.16 |
| Average moisture (%) | 53 | 785 | 136 |
| Liquidity limit (%) | 30.1 | - | 55.8 |
| Plasticity limit (%) | 17.6 | - | 31.4 |
| Specific    surface    $(m^2/g)$ estimated    from    Methylene blue | 8.37 | - | 12.56 |

## Consolidation Curve

Casagrande's method and the hyperbolic method (Figure 2) allows determining the different stages of consolidation (Tan and al. 1991, Untung 1990). Examples of the evolution of settlement versus time are given for sludge B1 (figure 3). Comparison of $t_{100}$ values (time necessary to reach 100% of primary consolidation) shows that both graphical methods give lower results than measured values (Figure 4). Moreover, the results show that the values estimated from Casagrande's and hyperbolic methods are quite similar although slope contrast is not always well observed with the hyperbolic method.

Evolution of void ratio is calculated from values of settlement versus time. The following formula is used:

$$e_t = \frac{(H_{ini} - h_t - h_g)}{h_g} \tag{1}$$

where, $e_t$ is the void ratio at time $t$, $H_{ini}$, initial specimen height, $h_t$ settlement at time $t$, $h_s$ height of solids calculated from:

$$h_s = \frac{W_g}{(\gamma_s F)} \tag{2}$$

where, $W_g$ is the grains weight, $\gamma_s$, volumetric weight of solid grains, $F$ is the specimen area. The variation of void ratio versus logarithm of stress is a linear function for the B3 sludge. For B1 and B2 sludges, the linear function begins at 200 kPa.

Values of compression index, $C_c$, and swelling index, $C_s$, are determined from the compression curves. The average values are given in Table 3.

Table 3- *Average Values of Compression Index $C_c$ and Swelling Index $C_s$*

|  | $C_c$ | $C_s$ |
|---|---|---|
| Sludge B1 | 0.332 - 0.337 | 0.018 |
| Sludge B2 | 3.730 | 0.539 |
| Sludge B3 | 0.767 - 0.783 | 0.043 |
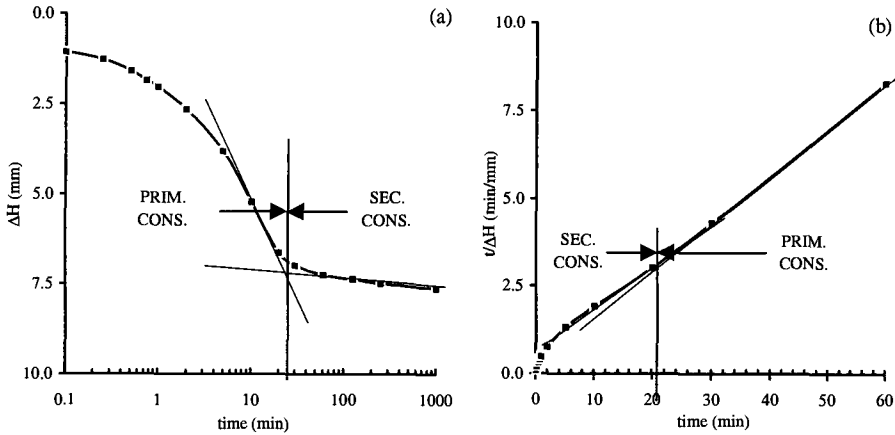


Figure 2 - *Determination of $t_{100}$ of primary consolidation by (a) Casagrande's method and (b) hyperbolic method*
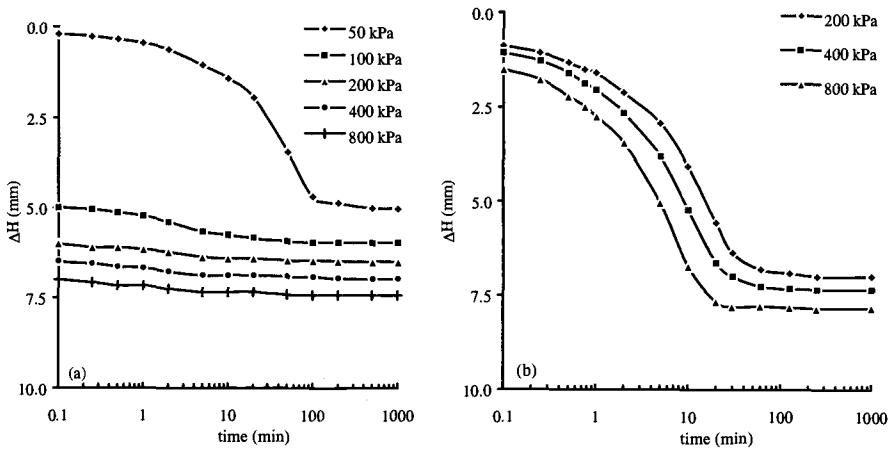


Figure 3 - *(a) Evolution of settlement for five loading steps versus time for sludge B1 ($H_{ini}$ = 20.2 mm, w = 55.1 %). (b) Evolution of settlement versus time for three direct loading tests of sludge B1 ($H_{ini}$ = 20.2 mm, w = 55 to 57 %)*
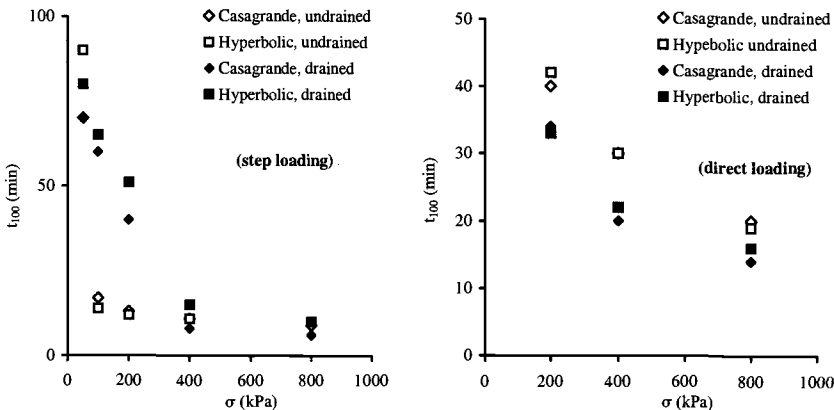
Figure 4 - *Values of $t_{100}$ versus vertical stress for step loading and direct loading tests either with drained or undrained conditions , calculated from graphical methods and experimental measurement – sludge B1*

## Settlement

In the current study, settlement is used to estimate the quantity of liquid that can exude from a loaded waste. Settlement of a material can be described by three stages: immediate settlement, primary settlement and final settlement.

### Immediate Settlement

The immediate settlement corresponds to the settlement observed within the first 15 seconds after loading. This settlement directly depends on the applied load, the initial moisture content and viscosity of material solid phase. Initial settlement is all the greater since hydraulic conductivity and loading stress are higher. The relationship between immediate settlement and moisture content is linear as is settlement versus log $\sigma$ (Untung 1990).

### Primary Settlement and Secondary Settlement

Primary settlement results from the dissipation of excess pore pressure. The rate depends on the hydraulic conductivity, which varies greatly for sludges. The liquid doesn't exude anymore beyond primary settlement for sludges B1 and B3. For B2 sludge, liquid goes on exuding from the waste because of a long secondary settlement. The secondary settlement corresponds to ongoing rearrangement of particles within the specimen.

*Final Settlement Value*

Final settlement is assumed to be the settlement at infinite time. The value of final settlement allows determination of the maximum quantity of liquid that the waste is able to exude under loading. Final value can be estimated by a hyperbolic method that consists in plotting $t/H$ versus $t$ (Tan and al. 1991, Untung 1990). Examples of the good fitting of hyperbolic law is showed Figure 5. For each test, we obtained two linear regions, both of them corresponding to primary and secondary settlement, respectively. For the latter, the equation is:

$$\frac{t}{\Delta H} = at + b \qquad (3)$$

where $a = 1/S_f$ and $S_f$ is the value of final settlement.

Final settlement is assumed to vary linearly with moisture content and the initial height of the specimen whatever the drainage conditions either by one face or both faces of specimen (Figure 6).
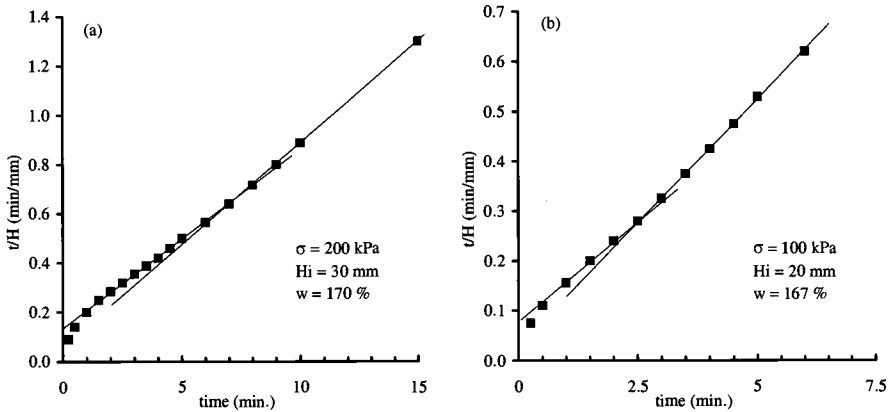


Figure 5 – *Example of fitting of Hyperbolic Law for two tests performed on sludge B1*
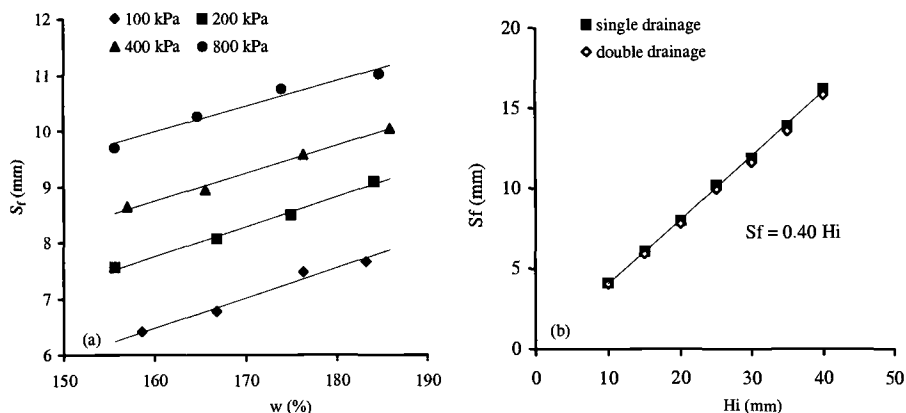
Figure 6 - *Evolution of final settlement $S_f$ versus (a) moisture content w for various stresses and (b) initial specimen height $H_i$ — sludge B3 -*

## Pore Pressure

The pore pressure is measured either with open drainage or closed drainage. In both cases, we determine the maximum value of $u$ reached for a given loading. When drainage is open, the evolution of pore pressure shows three distinct stages: a short stage where $u$ increases rapidly to a maximum value, a stage where $u$ remains constant (especially for the first loading stage or a direct loading), and a stage where $u$ decreases until equal atmospheric pressure is reached. When the drainage remains closed, the settlement appears immediately and after about one minute $u$ reaches a maximum value equal to the applied stress. This value is greater than for open drainage. This settlement is due to air-water compressibility when the material is not fully saturated. When drainage is opened, $u$ decreases rapidly and remains constant before decreasing in a manner similar to the drained case. It appears that the decrease of pore pressure is more rapid when the stress is high. For the undrained case, the maximum pore pressure $u_{max}$ is equal to the applied stress. When bottom drainage is open, $u_{max}$ is lower than the applied load and increases with load and specimen height. Figure 7 shows $u_{max}$ is a linear function of applied stress either in drained or undrained conditions for sludges B1 and B3.

## Coefficient of Consolidation $c_v$

The main methods used to determine $c_v$ are graphical methods and are proposed in the literature like Casagrande, Taylor, Asaoka, Sridharan or Prakash (Untung 1990). For such highly compressible materials, Casagrande's method requires a longer time to obtain the $t_{100}$ value. Taylor's was difficult to apply because of perturbation during early stages of the tests. Both other methods apply quite well to the three samples but show problems in the case of very rapid settlement.
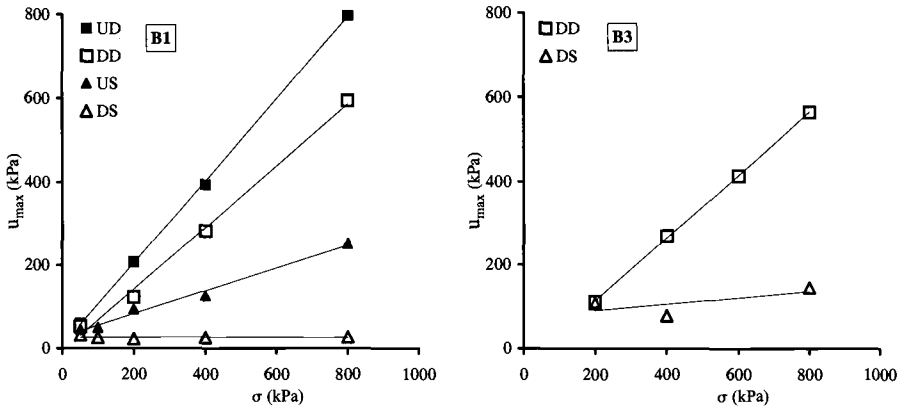
Figure 7 - *Maximum pore pressure $u_{max}$ versus stress for undrained (U) and drained (D) conditions and for step loading (S) and direct loading (D) – sludge B1 and B3*

## Hydraulic Conductivity

Hydraulic conductivity $k$ can be indirectly estimated from the coefficient of consolidation $C_v$ but we have chosen to make a direct measurement of hydraulic conductivity with a constant hydraulic head in the consolidation cell. Table 4 gives the range of values of $k$ determined from direct measurement and $c_v$ for the three sludges.

It seems that the smaller the hydraulic head is, the lower the hydraulic conductivity. For sludge B3, we can observe a deviation of Darcy's law especially with low hydraulic gradient as described by Hansbo (1960). The maximum deviation of Darcy's law is about 12% of the average value of $k$ measured under hydraulic head from 5 to 40 cm. Hydraulic conductivity of sludge B2 was impossible to measure in the cell because of its organic character (generating gases) and its very low permeability. Figure 8 compares experimental hydraulic conductivity to graphical determination from $C_v$ calculated from the four indirect methods. When drainage is closed, pore pressure is always higher than for drained conditions. Because of higher pore pressures induced by undrained loading, the quite homogeneous repartition of these pore pressures leads to a more permeable matrix, until the end of the test. The measurement of hydraulic conductivity must be realised with low hydraulic head to avoid further consolidation and creation of flowpaths. The compressibility data measured by both direct and step loading are in close agreement as shown by Figure 9a (Fox and Baxter 1997, Untung 1990). Figure 9b shows the *log k* versus *e* relationship measured for each test for both procedures of loading. Except for low stress values (< 200 kPa) corresponding to a void ratio of 0.75 or greater, the measured hydraulic conductivity does not vary much.

Table 4- *Comparison of the Hydraulic Conductivity Determined Experimentally ($k_{exp}$) or Theoretically ($k_{th}$) from $C_v$ Coefficient*

|  | $k_{exp}$ (m/s) | $k_{th}$ (m/s) |
|---|---|---|
| Sludge B1 | $2 \times 10^{-8}$ to $6 \times 10^{-10}$ | $4 \times 10^{-9}$ to $8 \times 10^{-10}$ |
| Sludge B2 | $< 5 \times 10^{-10}$ | $4 \times 10^{-9}$ to $2 \times 10^{-12}$ |
| Sludge B3 | $2 \times 10^{-8}$ to $7 \times 10^{-10}$ | $2 \times 10^{-8}$ to $8 \times 10^{-10}$ |
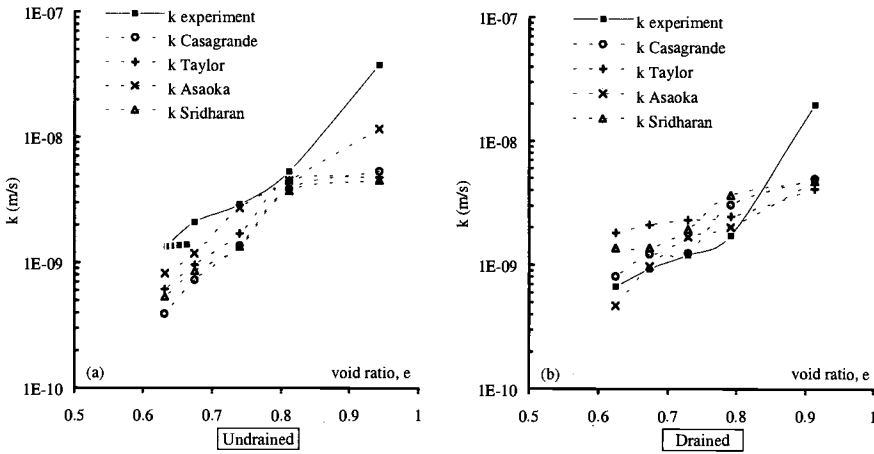


Figure 8- *Evolution of experimental hydraulic conductivity during step loading and comparison with theoretical estimations, in (a) undrained conditions and (b) drained conditions*
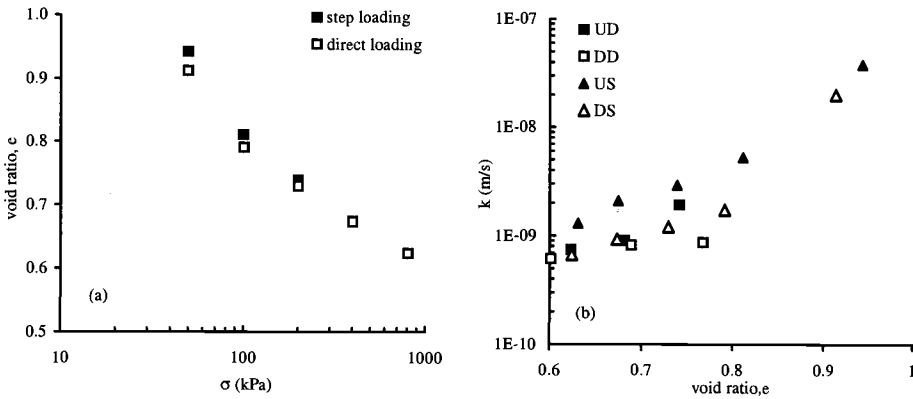


Figure 9 - *Comparison of specimen properties obtained from step loading and direct loading consolidation tests – sludge B1- (a) e versus log σ, (b) log k versus e*

**Study of Exuded Liquid**

*Mass of Exuded Liquid*

We are focused now on following the quantity of liquid that can exude during 24 hours. Initial saturation ratios of sludges are about 96-98%. Figure 10a shows the evolution of exuded liquid mass $M$ from the sludge B2. The mass of liquid exuded from the lower face ($M_{lo}$) is greater than from the upper face ($M_{up}$). This difference appears especially during the primary consolidation stage and is due to the difference of the pore pressure between upper and lower face of the specimen. The greater the stress applied, the lower the difference is between $M_{up}$ and $M_{lo}$. We have also shown by varying the specimen's height that the linear relation between the mass of exuded liquid and H is in close agreement (Figure 10b).

For the three materials, evolution of the liquid mass is directly related to the settlement. The final mass of liquid $M_f$ can be estimated from final settlement determined by a hyperbolic method applied to consolidation data as seen above.

$$Mf \approx Am \cdot Sf \cdot A \tag{4}$$

In this equation, $Am$ is a coefficient depending on the saturation degree and volumetric weight of the liquid. For a fully saturated material with a liquid whose $\gamma$ is close to $\gamma_{water}$, $Am$ becomes close to 1 and final mass equal to final settlement by specimen area, $A$. $Am$ defines the deviation from Mass-Settlement relation due to air escape for unsaturated materials. The higher is the saturation degree, the closer to 1 is $Am$. Experimental values of $Am$ vary from 1.004 to 1.043 for B2 and 0.983 to 1.048 for B3.

*Parametric Analysis*

A formula will be useful to estimate the quantity of liquid that can exude from sludge or a pasty waste after natural or artificial loading. The moisture content and the stress are the parameters we introduced in the relation. The quantity of liquid is expressed in term of liquid mass per unit of sludge mass. Consequently, $q_f$ is the ratio of $M_f$ to the initial mass of sludge and is related to the moisture content as shown by Figure 10a; the expression of $q_f$ is:

$$qf = A \cdot w + B \tag{5}$$

On Figure 11b, we can see that for four initial moisture contents, a relation exists between $q_f$ and the stress. This relation is linear in a semi-logarithm plot of $\sigma$. So we can write the following equation:

$$qf = C \cdot \log \sigma + D \tag{6}$$

For the results of the sludge B3 (Figure 11a and 10b), the values of the parameters $A$, $B$, $C$ and $D$ are given in the Table 5. $C$ and $D$ vary linearly with the moisture content of the sludge (Figure 12). Although linear relation can be found between $C$ and $w$, the variation of $C$ is quite low over the range of moistures measured. As shown in Figure 10b, relationship between $q$ and $\sigma$ can be fitted with the same slope whatever moisture content. We can find experimental relations between $C$, $D$ and $w$ that are introduced in equation 6:

$$q_f = (-0.152 \cdot w + 170) \log \sigma + 3.07 \cdot w - 533 \qquad (7)$$

The quantity of liquid $Q$ that a layer of height $hi$ could exude per unit area should be estimated by:

$$Q_{fi} = \gamma \cdot h_i \cdot q_{fi} \qquad (8)$$

where $\gamma$ is the unit weight of the unloaded sludge. If we consider a layer $H$ of homogeneous sludge characterized by $w$ and $\gamma$, loaded by a uniform stress $\sigma$, the total amount of liquid exuded could be calculated by:

$$Q_f(w, H) = \sum_{i=0}^{i=n} \gamma \cdot h_i \cdot q_f(w, \sigma_i) \cdot F \qquad (9)$$

The layer $H$ is decomposed in $n$ unit layers $h_i$ where a stress $\sigma_i$ is taken in the middle of the layer.
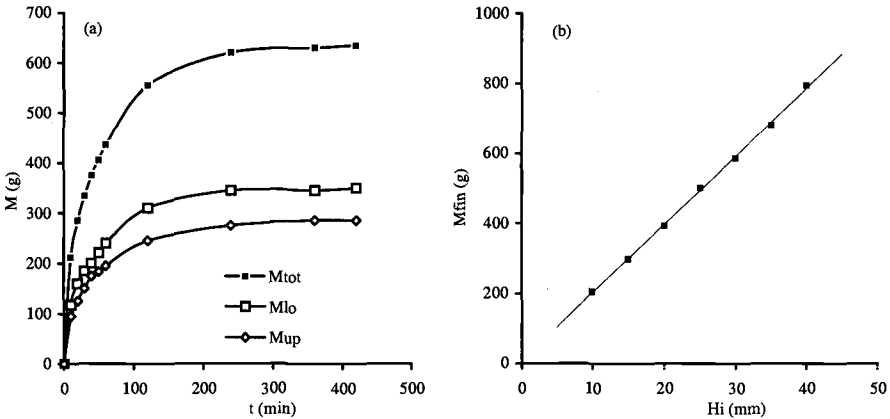


Figure 10 - (a) Evolution of exuded liquid mass versus time – sludge B3 ($\sigma = 200$ kPa, w=780 %) and (b) linear variation of $M_{fin}$ versus specimen height for sludge B2

Table 5- *Typical Values of A, B, C and D Parameters for B3 Sludge*

| σ (kPa) | A | B | w (%) | C | D |
|---------|------|--------|-------|-------|-------|
| 100 | 3.00 | -238.5 | 157 | 145.7 | -48.8 |
| 200 | 3.03 | -193.3 | 165 | 144.9 | -32.0 |
| 400 | 2.99 | -151.7 | 175 | 143.2 | 1.73 |
| 800 | 2.84 | -79.4 | 185 | 141.9 | 34.47 |
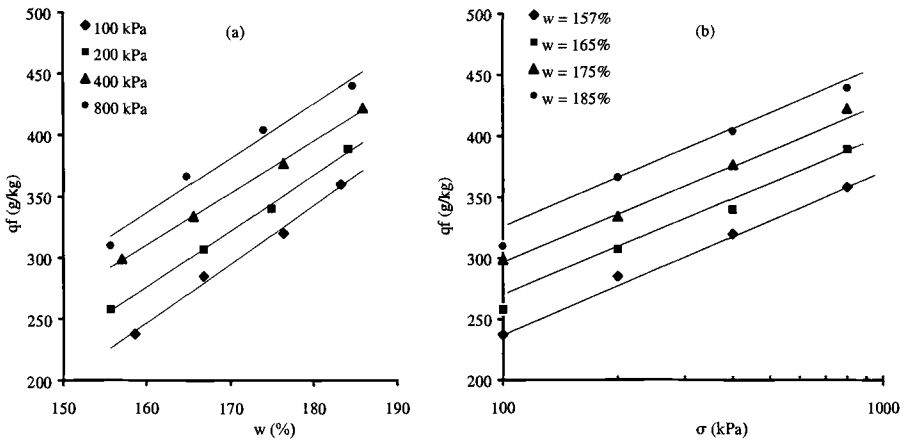


Figure 11 - *Evolution of the quantity of exuded liquid versus moisture content and stress showing linear relationships between $q_{fin}$ and w, and between $q_{fin}$ and s – sludge B3*
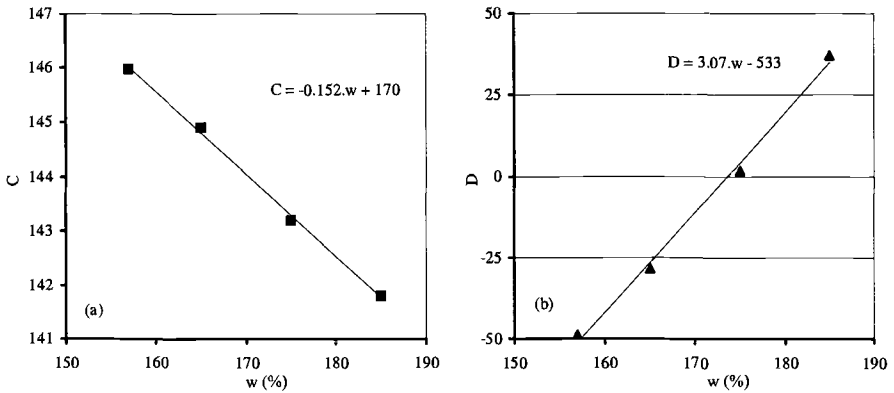


Figure 12 - *Experimental relations between C and D parameters versus moisture content*

**Summary and conclusions**

In order to determine the quantity of liquid that will be exuded when waste is loaded, we have developed a new testing device for large-scale laboratory tests (Ø 250 mm). One of the goal of this study was to have a big specimen to be able to extrapolate laboratory data to field configurations. This limits the important and dangerous scale effect that can be sometimes observed with small laboratory tests (conventional oedometer for example). We showed that the settlement under a known load is independent of the loading procedure for this type of material (step or direct loading). To reduce the duration of the tests, drainage should be permitted on both faces of the specimen. For sludges with very high moisture content (Sr > 98%), the potential quantity of liquid that could exude under a given load can be determined either by weighing the fluid exudes from both outlet ports or by the measurement of settlement versus time. We also showed that it is possible to estimate the settlement at an infinite time $S_f$ by plotting the hyperbolic relation between $\Delta H$ and $t$ ($t/\Delta h$ versus $t$). In the same way, the final mass of exuded liquid could be estimated from the final settlement (equation 4).

It is important to notice that this method has the advantage of reducing the duration of testing because of the larger amplitude of phenomenon due to large-scale specimen (250 mm diameter by a minimum of 20 mm height). It simply consists in determining the settlement and the mass of exuded liquid from the line obtained in the secondary compression stage. Whatever the type of sludge, the variation of exuded liquid mass (see equation 7) is a linear function of moisture content and logarithm of applied load.

**References**

Barden, L. and Berry, P.L., 1965, "Consolidation of normally consolidated clays", *Soil Mechanics and Foundation Division*, Vol. 91, No. SM5., pp. 15-35.

Davis, E.H. and Raymond, G.P., 1971, "Non linear consolidation and the effect of layer depth", *Proceedings of the first Australia-New Zealand Conference of Geomechanics*, Melbourne, pp. 105-111.

Fox, P.J. and Baxter, D.P., 1997, "Consolidation properties of soil slurries from hydraulic consolidation test", *Journal of Geotechnical and Geoenvironmental Engineering*, Vol. 123, No. 8, pp.770-776.

Hansbo, S., 1960, "Consolidation of clay with special reference to influence of vertical sans drains", *Swedish Geotechnical Institute Proc.*, No. 18, 159 p.

Imai, G., 1979, "Development of a new consolidation test procedure using seepage forces", *Soils and Foundations*, Tokyo, Vol. 19, No. 3, pp. 45-60.

Rowe, P.W. and Barden, L., 1966, "A new consolidation cell", *Geotechnique*, Vol.16, No. 2.

Tan, T.-S., Inoue T. and Lee S.-L., 1991, "Hyperbolic method for consolidation analysis", *Journal of Geotechnical Engineering*, Vol. 117, No. 11., pp. 1723-1730.

Untung, D., 1990, "Etude de la consolidation des déchets boueux ou pateux", thèse de doctorat de l'INSA de Lyon, 182 p.

Znidarcic, D. and Schiffman, R.L., 1982, "On Terzaghi's concept of Consolidation", *Geotechnique*, Vol. 32, No. 4, pp. 684-689.

Masashi Kawamura[1] and Yoshio Kasai[2]

**Methods to Determine the Saturated Surface-Dry Condition of Soils**

---

**Abstract:** When cement is mixed with water and wet soils to stabilize the ground, the exact amount of water available for cement hydration must be known in order to assure the resulting strength of the hardened body.

This study proposes an accurate method of determining the saturated surface-dry condition of soil by which rational mixture designs are made possible. Though soil moisture conditions related to engineering properties such as liquid limit, plastic limit and shrinkage limit can be determined in terms of pF, the saturated surface-dry condition of soil has been neither defined nor determined.

The proposed method is to dry natural wet soils under constant drying conditions and estimate the saturated surface-dry condition of soils from changes in the drying rate with respect to soil moisture ratio, and can be verified by pF measurement.

**Keywords:** cement treated soils, water-cement ratio, saturated surface-dry condition of soil, drying rate, pF

## Introduction

When manufacturing treated soils by mixing of cohesive soil, sand, cement and water, control of water-cement ratio of the slurry on the basis of saturated surface-dry condition of soil is required because no water transfer between cement and soil occurs under the saturated surface-dry condition. This paper proposes two methods capable of evaluating the moisture ratio of soils at the saturated surface-dry condition .

Available water for cement hydration in the treated soil has been determined in the following manners:

(1) Adding the amount of mixing water to that of the soil moisture (Japanese Geotechnical Society 1980), and

(2) Soil moisture is divided into adsorbed water and free water, and only the latter is added to the mixing water (Kida et al. 1977).

Taking into account the saturated surface-dry condition of soil, we established simple relationships between treated soil strength and mix parameters such as water-cement ratio, cement content, cement-soil ratio and soil-sand ratio (Kawamura and Kasai 1990a).

---

[1] Professor, Faculty of Building Engineering, College of Industrial Technology, Nihon University, 1-2-1 Izumi-cho, Narashino-shi, Chiba 275-8575.

[2] Emeritus professor, College of Industrial Technology, Nihon University, 1-2-1 Izumi-cho, Narashino-shi, Chiba 275-8575.

This has made the practical mixture design of the treated soil possible, and the use of super-plasticizers (Hiraishi et al. 1992 ), blast-furnace slags and fly-ash (Kawamura and Kasai 1990b, Kawamura and Kasai 1991, Kawamura and Kasai 1992) were also examined, resulting in the development of bamboo reinforced cement treated soil constructions (Kawamura et al. 1993). Because the strength of the treated soils depends largely on the water-cement ratio, we would show our



Figure 1-*Moisture Condition of Soil*

definition of the saturated surface-dry condition of soils and introduce testing methods capable of evaluating the saturated surface-dry condition of soils.

## Concept of the Saturated Surface-Dry Condition of Soils

We assumed that the moisture conditions of soil can be classified as absolute dry, air dry, saturated surface-dry and wet conditions similar to the classification for aggregates in concrete technology. We further defined that absorption as the difference in an amount of moisture between absolute dry and saturated surface-dry conditions and free surface water as that between saturated surface-dry and saturated conditions. The boundary between absorption and free water was estimated by a constant rate drying of the free water from wet to saturated surface-dry conditions.

These moisture conditions are illustrated in Figure 1.

In the saturated surface-dry condition of soil moisture, the followings were assumed;

(1) The concept of saturated surface-dry condition is applicable not only to sand, as used in concrete technology, but also to soils and can be determined as a definite moisture ratio for each type of soil.

(2) The boundary between saturated surface-dry condition and saturated condition can be represented as an inflection point observed in a constant rate drying process of free water from wet soils.

## Principles of Measuring the Saturated Surface-Dry Condition by Drying Rate Method and pF Method

*Drying Rate Method*

When soils in a natural moisture condition are subjected to drying under constant ambient conditions, relationship between moisture ratio of the soil and the drying rate changes as follows. When free water exists on the surface of soil particles, a constant rate period can be seen at the beginning of drying, while the drying rate decreases associated with the evaporation of water resulting in the exposure of soil particle surfaces. Subsequently, the drying rate further decreases passing through an inflection point and reaches an equilibrium moisture ratio where the drying rate becomes zero. Typical drying experiments are shown in Figure 2.
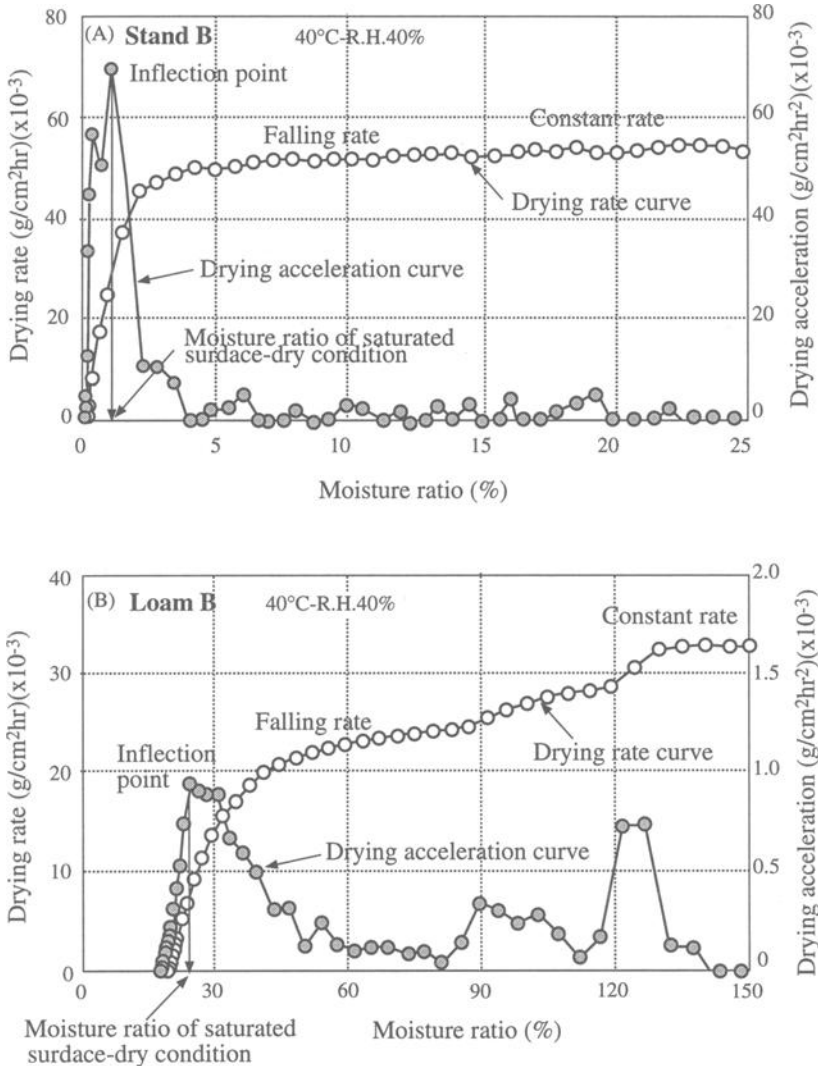
Figure-2 *Drying Rate and Drying Acceleration Curves from Wet to Equilibrium Conditions*

   If we draw moisture ratio versus drying acceleration curve, the time derivative of the drying rate, the drying acceleration increases as the drying proceeds, shows maximum at the inflection point and becomes zero at equilibrium moisture ratio.

   Specimens used for the drying experiments in Figure 2 are Sand B and Loam B. Sand B had a single-grained structure and smooth surfaces with a specific surface area of 0.01 to 0.001 $m^2/g$ (Handbook of Soil Engineerig 1982), while Loam B contained many

fine-grained and flattened fractions. Soil particles generally form cluster structure with a specific surface area from 1 to 200 m$^2$/g depending on the minerals included. Because of the structural difference, cohesive soils have larger moisture content than sand and are capable of supplying water to the drying front for a longer period. When in the falling rate drying period, Sand B dries out rapidly while cohesive soils have longer falling rate drying period and dries slowly.

From the time-moisture loss curves obtained for granular materials under constant temperature and humidity conditions, we can find an inflection point moisture ratio on the drying acceleration curve, the derivative of drying rate, which is nearly identical with the moisture ratio of the saturated surface-dry condition



Figure-3 *Water Retention of Soil and Methods of pF Measurement*

determined by the conventional flow cone method and centrifugal method.

We took the moisture ratio at the inflection point, where moisture ratio versus drying acceleration curve shows maximum, as the saturated surface-dry condition.

*pF Method*

A well-known pF is the energy difference between soil moisture and the free bulk water, and expressed as the common logarithm of the water head in cm. Moisture retention curve is a relationship between soil moisture ratio and pF value where characteristic moisture ratios such as the liquid limit, the plastic limit and the plant wilting point are arranged at pF values of 1.5, 3.0 and 4.2 respectively. When a sand and a soil with different moisture ratio are in contact, we can know the direction of moisture transport only by comparing their pF values.

We thought it possible to find the saturated surface-dry condition of soils somewhere in the moisture retention curve under drying. Because the single method to determine pF in the whole range, from 0 to 7, is not available, several methods have to be applied separately according to the targeted pF values as shown in Figure 3. Because we found that the saturated surface-dry condition of soils was less than pF 3.0 in the preceding experiments, a water activity meter (a commercially available Aw meter) was used.

**Specimens**

Soils used in this experiment were Sand A, Sand B, Loam A, Loam B, Silty clay , Marine clay and Kuroboku. Physical properties test and chemical analysis of these soils were made according to the Handbook (Handbook of Soil Engineerig 1982). Main crystalline phases were determined by X-ray diffraction, and organic components and pH were analyzed. The results are shown in Table 1.

Sand A from Fujigawa river in Sizuoka Prefecture was recognized to have typical river sand properties with the density of 2.68 g/cm$^3$ and was used after screened by the 2.0 mm sieve.

Sand B from Toyoura in Yamaguchi Prefecture has been used in concrete technology to prepare standard cement mortar specimens for strength test and is specified in the JIS R
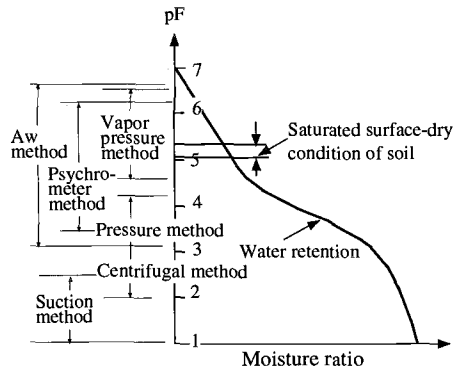
Table 1–*Physical Properties and Granular Composition of Cohesive Soils and Sands*

| Specimen | Moisture ratio (%) | Specific surface area(m²/g) | Density (g/m³) | Liquid limit (%) | Plastic limit (%) | Plasticity index | Granular composition(%) | | | Organic comp. (%) | Ig.loss (%) | pH |
|---|---|---|---|---|---|---|---|---|---|---|---|---|
| | | | | | | | Sand | Silt | Clay | | | |
| Sand A | — | 0.003 | 2.68 | Np | Np | Np | 89.0 | 11.0 | 0 | — | — | — |
| Sand B | — | 0.01 | 2.64 | Np | Np | Np | 99.0 | 1.0 | 0 | — | — | — |
| Loam A | 98.0 | 178.4 | 2.95 | 77.4 | 55.8 | 21.6 | 42.0 | 20.0 | 38.0 | 3.75 | 23.0 | 5.3 |
| Loam B | 102.0 | 90.9 | 2.88 | 70.3 | 50.4 | 19.1 | 61.0 | 25.0 | 14.0 | 2.17 | 19.9 | 5.8 |
| Silty clay | 32.6 | 18.4 | 2.62 | 41.1 | 23.4 | 17.7 | 18.0 | 40.0 | 42.0 | 2.01 | 8.4 | 7.2 |
| Marine clay | 28.2 | 18.3 | 2.69 | 42.8 | 25.5 | 17.3 | 32.0 | 40.0 | 28.0 | 1.97 | 6.2 | 4.0 |
| Kuroboku | 32.3 | 105.0 | 2.43 | 78.0 | 42.8 | 35.2 | 16.0 | 34.0 | 50.0 | 24.70 | 30.3 | 6.0 |

5201 - Test of Physical Properties of Cement. It was used with residue of 1 % at 300 μm sieve and more than 95 % at 106 μm sieve.

Loam A was a Kanto loam with dominant particle diameter of approximately 10 to 30 μm having smaller particles of 50 to 80 μm between them. Main mineral components were quartz, halloysite and montmorillonite. Organic components was 3.75 %, ignition loss was 23.0 % and pH was 5.3.

Loam B was a Kanto loam with dominant particle diameter of approximately 100 to 200 μm having smaller particles than 100 μm. Main mineral components were quartz, halloysite and montmorillonite. Organic components was 2.17 %, ignition loss was 19.9 % and pH was 5.8.

Silty clay was gray-green in color with dominant particle diameter of approximately 30 to 300 μm. Main mineral components were quartz, plagioclase and feldspar. Organic components was 2.01 % and alkali component was larger than any other specimen soils.

Marine clay was gray-brown in color with dominant particle diameter of approximately 200 to 300 μm having smaller particles of 20 to 80 μm between them. The color turned grey after drying and inside of a large particle was dark brown. Main mineral components were quartz, feldspar and montmorillonite. Organic components was not found and pH was 4.0.

Kuroboku was dark brown in color with dominant particle diameter of approximately 20 to 40 μm. Considerable plant roots were mixed in. Main mineral components were quartz, feldspar and montmorillonite. Organic components and ignition loss were the largest among specimens and pH was 6.0.

**Drying Conditions of Soils**

Before applying the drying rate method, test conditions such as thickness of soil specimen, ambient temperature and relative humidity must be determined. Preliminary drying experiments were carried out to find optimum drying conditions.
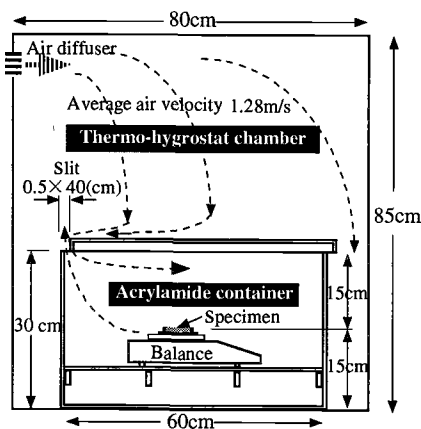


Figure-4 *Apparatus for Drying Rate Method*

*Apparatus*

Moisture conditioning apparatus was 60 cm wide, 80 cm deep and 85 cm high constant temperature-humidity chamber as shown in Figure 4. Temperature can be varied from -20 to 100 °C and relative humidity from 30 to 98 %. Average air flow in the chamber was 1.28 m/s.

In the center of the chamber, acrylamide box of 40 cm wide, 60 cm deep and 30 cm high was set, in which electronic balance of 1 mg resolution was placed to have a specimen holder at the midpoint of the height of the box. Loss of mass due to evaporation of moisture from the specimen holder was continuously monitored.

*Equilibrium Moisture Ratio*

When a wet soil is subjected to drying, loss of mass shows rapid decrease at the beginning and subsequent changes are normally slow, and it takes very long time to reach the equilibrium moisture ratio. In our experiment, the equilibrium moisture ratio was defined as a moisture ratio when the rate of weight loss reaches less than 0.01 % in one hour. Loam A specimen, for example, with a moisture ratio of 86% and 5 cm in thickness took 26 hours to reach the 0.01 % criteria and the equilibrium moisture ratio was 19.0 %.

*Thickness of Soil Specimens*

Effect of specimen thickness on drying rate was examined using Loam A with an initial moisture ratio of 63.0 %, and is shown in Figure 5. The drying acceleration curve, the derivative of the drying rate, was drawn with data reduced to that obtained in every one hour. In the relationship between moisture ratio and drying acceleration shown in Figure 5, the moisture ratios at each peaks were not so different by thickness of specimen, and ranged from 30.0 to 35.7 % with a deviation of ±2.5%. Though thinner specimen may be easier to dry, dimensions of φ69-5 mm was selected taking into account the necessary amount to determine moisture ratio of soil (10-30 g with maximum grain size of 2 mm) and ease of mounting the soil specimen.

*Drying Temperature*

Drying rate is also affected by temperature. Loam A with an initial moisture
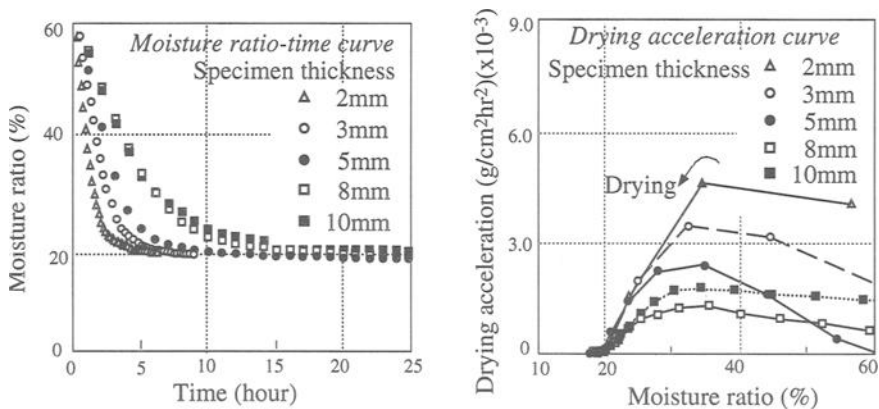


Figure-5 *Effect of Specimen Thickness on drying rate*

content of 86 % was subjected to drying under temperatures of 20, 30, 40 and 50 °C and relative humidity of 40 %. As shown in Figure 6, the apparent equilibrium moisture ratio became smaller and the height of drying acceleration peaks increased with the increase of temperature. The moisture ratios showing the peak varied considerably from 30.8 % to 35.7 % with a deviation of 4.9 % under a temperature range of 20 to 50 °C. Taking into account the shortening of drying and thermal effects on the soil, drying temperature of 40°C was selected because it is rapid enough but has less thermal effect than 50 °C.

*Relative Humidity*

Loam A with an initial moisture content of 86 % was subjected to drying under relative humidities of 35, 40, 45 and 50 % and temperature of 40 °C. In the relationship between moisture ratio and drying rate shown in Figure 7, the apparent equilibrium moisture ratio became smaller and the height of drying acceleration peaks increased with
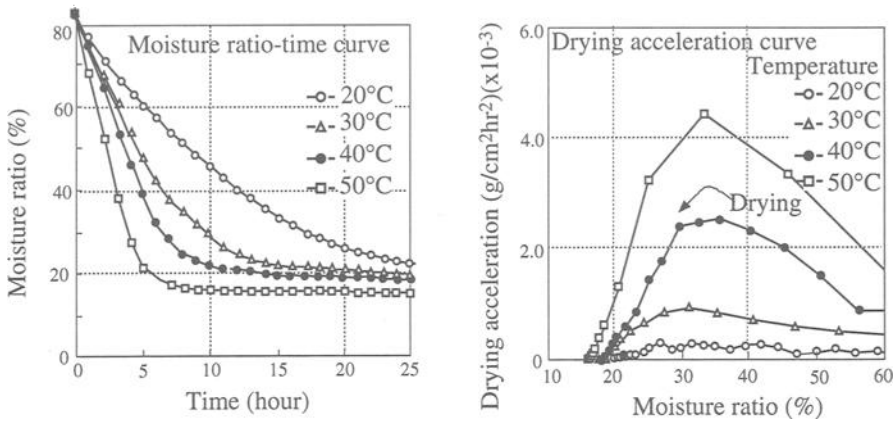


Figure-6  *Effect of Temperature on Drying Rate*
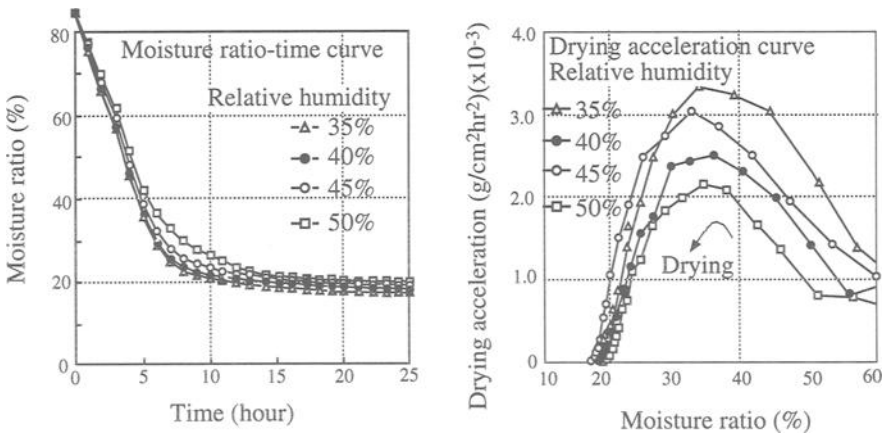


Figure-7  *Effect of Relative Humidity on Drying Rate*
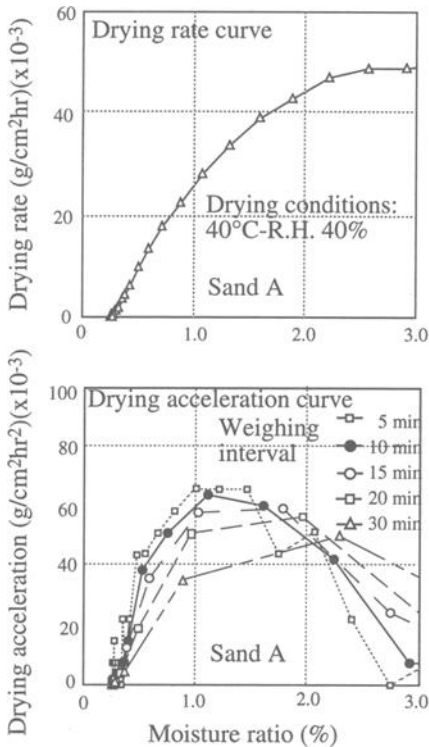
Figure-8  *Effect of Weighing Interval on the Drying Acceleration of Sand*
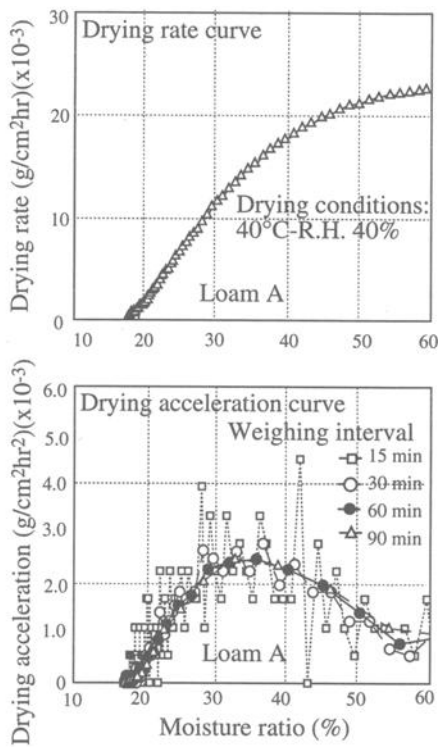
Figure-9  *Effect of Weighing Interval on the Drying Acceleration of Cohesive Soil*

the decrease of relative humidity. The moisture ratios showing the peak varied from 33.4 % to 35.7 % with a deviation of 2.3% under a relative humidity range of 35 to 50 %. Because the control of very low relative humidity was rather difficult, drying relative humidity of 40 % was selected.

*Interval of Weight-Loss Measurement*

        Effect of the interval of weight-loss measurement on the drying acceleration curve was examined because the result of numerical differentiation is affected by the increment, and is shown in Figure 8 for sand and in Figure 9 for cohesive soil. The original drying rate - moisture ratio curve of sand was obtained using Sand A with an interval of measurement of 5 minutes. With changes of the interval of weight-loss measurement from 5, 10 and 15 minutes, peaks in the drying acceleration curve changed from 1.0-1.5%, 1.1 % and 1.8 % respectively. Because the initial moisture ratio and the specific surface area of sand is comparatively smaller than that of soil, change of drying acceleration curve is very sharp. In order not to miss the abrupt change, interval of weight-loss measurement of 10 minutes was selected for sands.

        The original drying rate - moisture ratio curve of soil was obtained using Loam A with a interval of measurement of 15 minutes. With changes of the interval of weight-loss

measurement from 15, 30, 60 and 90 minutes in calculation, peaks in the drying acceleration curve changed from 42.0%, 37.5 %, 35.7 % and 32.9 % respectively. When the interval was as small as 15 or 30 minutes, considerable scatter was observed in the drying acceleration curve leading to a doubtful estimation of the saturated surface-dry condition. However the interval was as long as 90 minutes, some important physical-engineering information may be missed. We selected the interval of 60 minutes as a compatible solution for soils.

## Evaluation of Saturated Surface-Dry Condition by Drying Rate Method and pF Method

*Drying Rate Method*

   Procedure of the drying rate method is as follows:

   (1) Spread approximately 30 g of soil specimen, conditioned in wet but not sticky, in a mortar.

   (2) Fill an evaporation pan of 60 mm in diameter and 5 mm in thickness with the soil and flatten the top. Resulting amount of specimen is 10-12 g.

   (3) Measure an initial weight of the specimen $m_i$ and dry at temperature of 40°C and relative humidity of 40 % in a thermo-hygrostat chamber.

   (4) Measure weight changes regularly by an electronic balance, and when the specimen is in equilibrium with the humidity inside of the chamber, dry the specimen at 100-110 °C to obtain the moisture ratio.

   (5) Calculate drying rate $V$ (g/cm²hr) and drying acceleration $G$ (g/cm²hr²) by the equations (1) and (2).

   (6) Draw drying acceleration curve with the set of data of drying rates and corresponding moisture ratios.

$$V=\{[m_i-m_{(i+\alpha)}]/A\}/[h_i-h_{(i+\alpha)}] \qquad (1)$$

$$G=[V_i-V_{(i+\alpha)}]/\alpha \qquad (2)$$

where $m_i$ and $m_{(i+\alpha)}$ are masses of the specimen at respective times $h_i$ and $h_{(i+\alpha)}$ in gram, $\alpha$ is an interval of measurement in hour and $A$ is the area of the specimen surface exposed to dry air. $V_i$ and $V_{(i+\alpha)}$ are drying rates at a time $h_i$ and a $h_{(i+\alpha)}$ in g/cm²hr.

*pF Method*

   The water activity meter comprised a specimen chamber and a controller. Measurement was made first by sealing a specimen in the specimen chamber waiting for an equilibrium between soil moisture and water vapor pressure in the chamber, and finally an established relative pressure in the chamber was read. This water activity value, $Aw$, can be transformed into a *pF* value by the following formula [10],

$$pF=log_{10}(-\Delta\mu)=log_{10}[-RTln(Aw)] \qquad (3)$$

where $\Delta\mu$ is the chemical potential of the water expressed as the water pressure head in cm $H_2O$. Substituting the gas constant of water vapor $R = 461.5$ *J/kgK*, absolute temperature $T = 293$ *K* and introducing a transformation constant 10.2 to convert energy $J$ per $kg$ of water into water pressure head in cm, we have
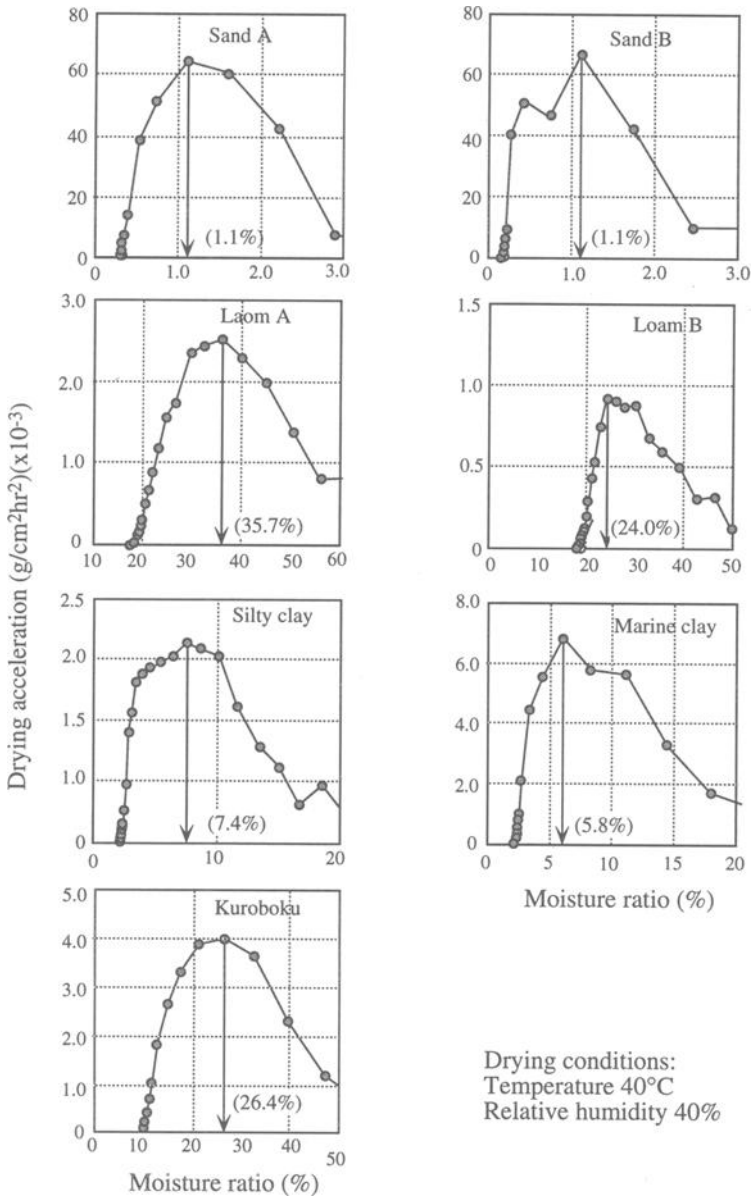
Figure-10 *Moisture Ratio and Drying Acceleration*

$$pF=log_{10}[-1379237(Aw)]  \tag{4}$$

Procedure of the pF method is as follows.

(1) Weigh a 20-30 g of specimen and introduce to the specimen chamber immediately. Read water activity value when in equilibrium.
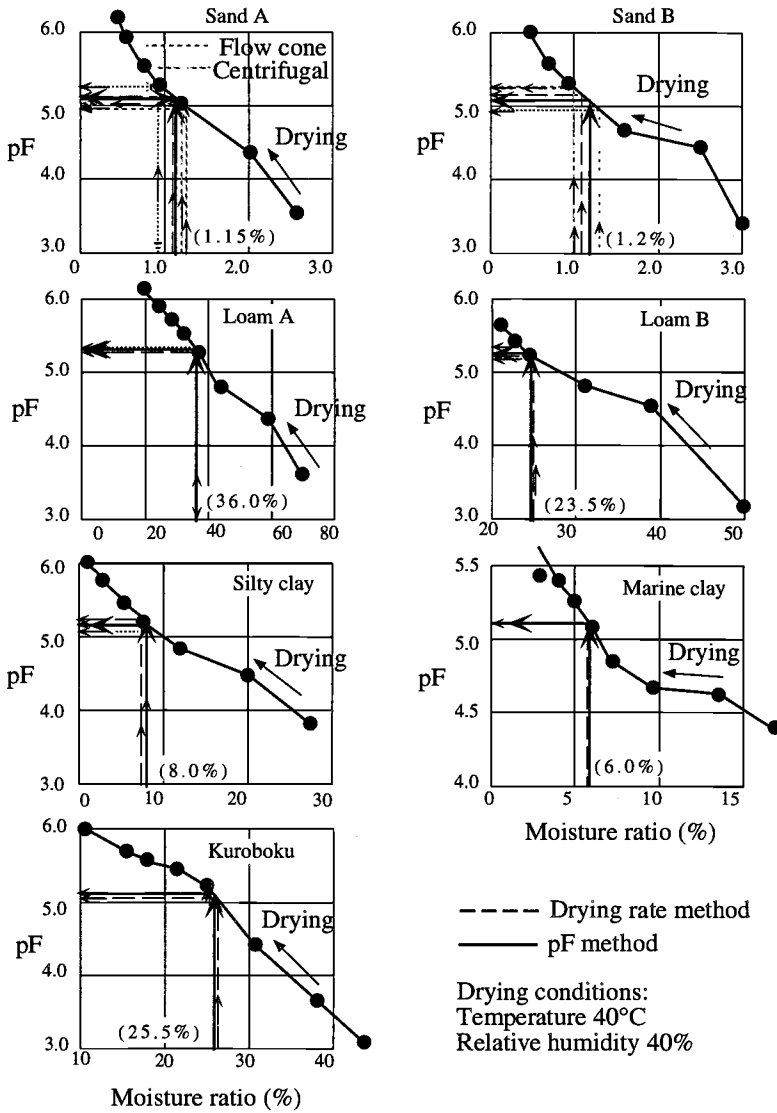


Figure-11 *Moisture Ratio and pF*

(2) Move the soil specimen to a drying chamber conditioned to temperature of 40 °C and relative humidity of 40% to reduce moisture ratio.

(3) Repeat pF measurement and subsequent drying for 7 to 8 times.

(4) When the specimen is in equilibrium with the humidity inside of the chamber, dry the specimen at 100-110 °C to obtain the moisture ratio.

(5) Draw water retention curve with the set of data of pF values and corresponding moisture ratios.

## Results and Discussions

The drying acceleration curves of all specimens are shown in Figure 10 with data of relevant portion in determining the saturated surface-dry condition. The moisture ratios giving the saturated surface-dry condition were different with each other; 1.1 % for Sand A, 1.1 % for Sand B, 35.7 % for Loam A, 24.0 % for Loam B, 7.4 % for Silty clay, 5.8 % for Marine clay and 26.4 % for Kuroboku.

Results of determination of the saturated surface-dry condition by drying rate method, flow cone method and centrifugal method (3500G-20 minutes) are compared in Table 2. Because of the coagulative nature of the cohesive soil, the flow cone method was unable to be applied, and the centrifugal method was found to be inadequate for cohesive soils because it takes long time and large power to expel water inside of the soil particles.

Table 2–*Results of Determination of Saturated Surface-Dry Conditions*

| Specimen | Drying rate method | pF | Flow cone | Centri fugal |
|---|---|---|---|---|
| Sand A | 1.1 | 5.1 | 1.3 | 1.2 |
| Sand B | 1.1 | 5.1 | 1.0 | 1.0 |
| Loam A | 35.7 | 5.3 | — | — |
| Loam B | 24.0 | 5.2 | — | — |
| Silty clay | 7.4 | 5.2 | — | — |
| Marine clay | 5.8 | 5.1 | — | — |
| Kuroboku | 26.4 | 5.1 | — | — |

Unit: moisture ratio in %

As shown in Table 2, moisture ratio of sand at the saturated surface-dry condition determined by the drying rate method were slightly smaller than that determined by flow cone method and centrifugal method, but the agreement was so well that the drying rate method can be applicable either to an evaluation of the saturated surface-dry condition of fine aggregate. For cohesive soils, on the other hand, neither flow cone method nor centrifugal method was applicable by the above reasons.

Water retention curves of the specimens are shown in Figure 11 with data of relevant portion in determining the saturated surface-dry condition. All pF values read from the moisture ratios at the saturated surface-dry condition of each soil specimens fell into a range from 5.1 to 5.3. Sands with coarse grain whose saturated surface-dry moisture ratios ranging from 0.9 to 1.3 and cohesive soils with large saturated surface-dry moisture ratios of 34.0 to 36.0 like Loam A or with small saturated surface-dry moisture ratios of 7.4 to 9.0 like Silty clay, had nearly the same pF value of 5.1 to 5.3. When the saturated surface-dry condition of a soil is unknown, determination of a moisture ratio of pF 5.1 - 5.3 can give a solution.

## Conclusions

New methods capable of evaluating the saturated surface-dry condition of soil were presented to control treated soils made of cohesive soil, sand and cement. Major findings are as follows:

(1) The saturated surface-dry condition did exist in soil as in sand and can be determined both by drying rate method and pF method.

(2) On executing the drying rate method, recommended conditions are specimen thickness of 5 mm, drying temperature of 40 °C, relative humidity of 40 % and measuring intervals of loss of mass of 10 minutes for sands and 60 minutes for soils. Measurement should continue until the moisture ratio of specimen reaches the equilibrium moisture ratio.

(3) On executing pF method, the saturated-surface dry condition can be estimated by finding a moisture ratio of pF 5.1-5.3.

(4) The saturated surface-dry conditions measured by the drying method were 1.1 (5.1) % for Sand A, 1.1 (5.1) % for Sand B, 35.7 (5.1) % for Loam A, 24.0 (5.3) % for Loam B, 7.4 (5.2) % for Silty clay, 5.8 (5.2) % for Marine clay and 26.4 (5.1) % for Kuroboku. Numbers in parentheses are the pF values corresponding to the moisture ratios of the saturated surface-dry condition.

## References

*Handbook of Soil Engineerig,* 1982, pp. 21-27.

Hiraishi, S., Mizuno, Y., Kawamura, M., and Kasai, Y., 1992, "Hydration Heat, Setting and Strength of Soil-Cement Concrete with Various Types of Superplasticizer," *Preprint of Annual Meeting of Cement Association of Japan*, No.46, pp. 874-879.

Japanese Geotechnical Society, 1990, *Test Methods of Soil Properties.*

Kawamura, M. and Kasai, Y., 1990a, "Strength of Soil-Cement Concrete with Different Ratios of Soil-Sand, Cement-Water and Cement-(Soil+Sand)," *Preprint of Annual Meeting of Cement Association of Japan,* No.44, pp. 720-725.

Kawamura, M. and Kasai, Y., 1990b, "Strength and Density of Cement Treated Soil based on the Concept of Saturated-Surface Dry Condition," *Preprint of Annual Meeting of AIJ- B,* pp. 1617-1618.

Kawamura, M. and Kasai, Y., 1991, "Strength and Density of Cement Treated Soil based on the Concept of Saturated-Surface Dry Condition Using BFS and Fly-Ash," *Preprint of Annual Meeting of AIJ- B*, pp. 1021-1022.

Kawamura, M. and Kasai, Y., 1992, "Strength and Density of Cement Treated Soil Using Verious type of Soils" *Preprint of Annual Meeting of Cement Association of Japan*, No.46, pp. 932-937.

Kawamura, M., Kawai, T., Xu, J., and Kasai, Y., 1993, "Mixture Proportion and Strength of Cement Treated Soils - Bamboo Reinforced Cement Treated Soil Construction Method", *Preprint of Annual Meeting of AIJ- B*, pp. 1231-1232.

Kida, D., Sumida, M., and Kubo, H., 1977, "Study on the Cementation of Soils, Part 3 Application of pF Moisture to the Relationship Between Strength of Hardened Body and Water-cement Ratio", *Technical Report of Technical Research Laboratory of Taisei Corporation*, No.14, pp. 104-108.

Tuncer B. Edil[1] and Xiaodong Wang[2]

Shear Strength and $K_o$ of Peats and Organic Soils

**Abstract**: Peats and organic soils are encountered in many geographical areas and because of their organic solids and high water content they exhibit mechanical properties somewhat different than the customary behavior of inorganic clays. Shear strength and coefficient of earth pressure at-rest are two mechanical properties that are commonly required in design of embankments and other structures over such soils. Various investigators have studied these properties of peats and organic soils and the reported results indicate important differences in behavior from inorganic soils both qualitatively and quantitatively. Because of the capacity of these materials to retain high water contents, they are generally weak in their natural states but significant strength gain is achievable with consolidation. The presence of fibers induces both some anisotropy and internal reinforcement. These effects are reflected in strength parameters and lateral earth pressure transfer. Using peat and organic soil samples from sites in Minnesota and Wisconsin, undrained strength, effective strength and coefficient of earth pressure at-rest behavior are investigated and comparisons are made with other reports of these properties to arrive at general behavioral trends.

**Keywords**: peat, organic soil, shear strength, earth pressure at-rest, fibers

Introduction

Peats and organic soils are encountered in many geographical areas and because of their organic solids and high water content, they exhibit mechanical properties somewhat different than the customary behavior of inorganic clays. Shear strength and coefficient of earth pressure at-rest are two mechanical properties that are commonly required in design of embankments and other structures over such soils. Shear strength is a fundamental property required in the analysis of construction projects over peat and organic soils and it generally has a limiting low value for such soils. Shear strength is a concern both during construction for supporting construction equipment as well as at the end of construction in

_____

[1]Professor, Dept. of Civil & Environ Engr., Univ. of Wisconsin-Madison, Madison, WI 53706.
[2]Assoc. Instr. Tech, Dept. of Civil & Environ Engr., Univ. of Wisconsin-Madison, Madison, WI 53706.

supporting the structure.  Construction of heavy structures and bridges is often resolved by using piles to bypass the soft soils.  For light structures covering large areas such as warehouses, shopping centers and similar single-story buildings, column loads can be supported on deep foundations; however, construction of a structural floor to prevent differential settlements often renders such an approach expensive and uneconomical. Construction of highway embankments or bridge approaches presents even greater challenges since conventional deep foundations often are not very economical. Furthermore, such earthen structures can tolerate much greater magnitudes of settlement especially if it is not differential settlement.  Initial stability of fill construction is the most critical problem due to rather low undrained shear strengths of peats and organic soils in their normally consolidated state.  Stage-construction and/or use of geosynthetics typically solve the stability issues.  Of course, ground improvement techniques such as preloading and deep in situ mixing improve both the resistance to compression as well as the strength. Use of geosynthetics has simply revolutionized construction over soft ground.  Unlike stage loading, construction can proceed without waiting by use of geogrids and geotextiles.   Tensile reinforcement increases embankment stiffness and reduces shear stress and strain magnitudes and plastic deformations.

Design of fills and structures over organic ground requires an understanding of shear strength and state of stress of such materials.  In this paper, the shear strength and coefficient of earth pressure at-rest for peats and organic soils are presented.

## Background

Various investigators have studied these properties of peats and organic soils and the reported results indicate important differences in behavior from inorganic soils both qualitatively and quantitatively.  Because of the capacity of these materials to retain high water contents, they are generally weak in their natural states but significant strength gain is achievable with consolidation.  Presence of fibers induces both some anisotropy and internal reinforcement.  These effects are reflected in strength parameters and lateral earth pressure transfer.

Adams (1965) reported that the behavior of the peat was exclusively frictional in character, with a friction angle of 48° and also measured a coefficient of earth pressure at-rest, $K_o$ as low as 0.18, and found that preconsolidation and anisotropic consolidation had little effect on the strength parameters.  Subsequently, other researchers also reported similar findings regarding the shear strength of peat being essentially frictional with high friction angles and relatively small cohesion intercepts (0 to 6 kPa).  In a series of anisotropically consolidated undrained triaxial compression tests performed on a range of peats from highly fibrous to amorphous, Edil and Dhowian (1981) reported both the effective strength parameters as well as $K_o$.  In a comprehensive paper, Landva and La Rochelle (1983) delineated the importance of internal reinforcement provided by fibers in fibrous peats and explained the rather high effective friction angles reported by various investigators.  They concluded that the shearing resistance would vary depending on the orientation of the failure plane relative to the general alignment of the fibers.  For instance, in triaxial tests the failure plane would intersect the generally horizontal plane of fibers and

mobilize the fiber pullout resistance along the failure plane, giving rise to high friction angles. On the other hand, in a ring shear test performed on a fibrous peat where fibers align in the direction of the applied horizontal stress, their contribution to shearing resistance would be minimal. They showed that fiber reinforcement would account up to $16°$ of the measured friction angle in the triaxial compression test depending on fiber content with zero contribution for amorphous peats.

It is interesting that both the undrained shear strength and the effective strength parameters of many peats and organic soils increase with increasing water content or decreasing unit weight (Den Haan 1997). This seemingly counter intuitive behavior is attributed to the fiber effects and the fact that fiber content, in general, increases with increasing water content and decreasing unit weight.

In North America, it is common practice to use undrained shear strength and a total stress analysis in assessing the end-of-construction stability of embankments. Undrained strength is expressed as a normalized strength, i.e., ratio of undrained strength to vertical effective stress. Peat undrained strength is typically determined by vane shear in the field and by unconfined and consolidated undrained triaxial compression tests in the laboratory. Plate load, screw plate and cone penetration tests in the field and ring or direct shear tests in the laboratory have been used to a much lesser extent. Presence of fibers and their varying interaction within the shearing mode imposed by the particular testing procedure creates difficulties in assessing the true operating strength value under a proposed embankment.

In Europe, use of drained strength with estimated pore pressures is more common for stability analyses because drained parameters are considered to be more fundamental and less variable than undrained strength points. Both approaches have their share of difficulties when applied to peats.

Presence of fibers modify our concepts of strength behavior in several ways:

- It can provide effective stress where there is none and it induces anisotropy. This is fine as long as the shear test induces a shear plane that is representative of the field shear mode. For instance, a triaxial compression shear plane would not represent a horizontal sliding surface. Direct, ring and simple shear tests and triaxial extension test have been shown to give lower strength than triaxial compression tests because of the fiber orientation (typically horizontal) relative to the shear plane. The reduction due to this effect could be 25% (Lechowicz 1994).

- It results in reduced $K_0$ values compared to clays. The measurements of $K_0$ on peats indicated values in the range of 0.3 to 0.5 depending on fiber content and quality (Edil and Dhowian 1981, Termaat and Topolnicki 1994).

- Shear resistance continues to develop at high strains without a significant peak behavior.

In the case of clays, undrained strength ratio, $c_u/\sigma_v'$ is considered to be a constant for normally consolidated clays and vary with overconsolidation ratio. Recently, it has been reported that the strength ratio is not constant in the normally consolidated range for organic soils and amorphous peats but varies with stress level (Lechowicz 1994) in a range from 0.43 to 0.49. In another research project employing anisotropically consolidated undrained triaxial compression tests on three different peats covering a range of fiber contents, $c_u/\sigma_v'$ varied from 0.62 to 0.75 (Dhowian 1978). Den Haan (1997)

reports similarly high $c_u/\sigma_v$' for organic soils from different sources in the range of 0.54 to 0.78 and Farrell (1997) reports a lower bound of 0.45 for Irish organic soils. These $c_u/\sigma_v$' values appear unusually high compared to the typical values for inorganic clays, i.e., 0.20 to 0.25.

Correction of isotropically consolidated undrained triaxial compression data from $\sigma_3$ to $\sigma_v$ becomes important because of low $K_o$ values for peats and organic soils. For instance, this correction would reduce undrained strength ratio from 0.45 to 0.24 for $K_o =$ 0.3. If one adds the effect of fiber-induced anisotropy and unavailability of the assumed shear resistance on certain shear surface orientations in the field like near horizontal planes, this ratio gets even lower. This effect was reported to be 25% reduction for peats from other locations (Lechowicz 1994). These considerations may result in very low values of undrained strength ratios to work with and it is not clear that they are true in the field. There is need for an improved understanding in this area. One redeeming aspect of peat shear strength behavior is that there is no pronounced expectation of strength loss at high strains as is the case with some inorganic clay soils.

## Peats and Organic Soils Tested

The origin, physical composition, and important index properties of the soils in the University of Wisconsin-Madison (UW) database are summarized in Table 1. The samples are from different locations and cover a range of peats and to a lesser extent organic soils. The soils from Hoyt Lakes, Minnesota were already consolidated in the field by a significant vertical load that was applied gradually over the years. Therefore, the behavior of these soils under relatively high consolidation stresses was needed. The other soils were surficial materials consolidated under self-weight; therefore, their response under low consolidation stresses was of interest.

Table 1. *Characteristics of Soils Tested in the University of Wisconsin-Madison*

| Source of Sample | Description | Water Content | Unit Weight | Organic Content | Fiber Content | Specific Gravity |
|---|---|---|---|---|---|---|
| | | % | kN/m³ | % | % | |
| Middleton, WI | Fibrous Peat | 500 - 600 | 9.1 - 10.1 | 83 - 95 | 64 | 1.40 - 1.70 |
| Middleton, WI | Amorph. Peat | 430 - 520 | 10.3 | 58 - 65 | 20 - 30 | 1.60-1.90 |
| Portage, WI | Fibrous Peat | 600 | 9.6 | 81 | 31 | 1.72 |
| Fond du Lac, WI | Amorph. Peat | 240 | 10.2 | 60 | 20 | 1.94 |
| Nine Springs, WI | Fibrous Peat | 450 - 655 | 9.8 | 74 - 84 | 75 - 92 | 1.62 - 1.85 |
| USH 12, Middleton, WI | Fibrous Peat | 157 - 165 | 12.9 | - | - | - |
| USH 12/18, Cambridge, WI | Fibrous Peat | 361 | - | 66 | - | 1.82 |
| USH 12/18, Cambridge, WI | Organic Soil | 321 | - | 10 | - | 2.56 |
| STH 29, Shawano, WI | Fibrous Peat | 250 - 516 | 9.6 - 12.1 | 35 - 66 | - | 1.82 – 2.23 |
| STH 29, Shawano. WI | Organic Soil | 125 - 367 | 18.4 | 6 - 10 | - | 2.55 |
| Hoyt Lakes, MN | Fibrous Peat | 270 - 470 | 10.4 | 50 - 85 | 36 - 76 | 1.59-1.70 |
| Hoyt Lakes. MN | Organic Soil | 50 - 100 | 12.5 | 3 | - | 2.47-2.63 |
| Richfield, MN | Amorph. Peat | 175 - 300 | 11.6 | 31 - 37 | 37 - 45 | 2.02 |
| Richfield. MN | Organic Soil | 150 - 160 | - | 25 | - | 2.29 |

## Test Methods

Three types of tests were performed. The isotropically and anisotropically consolidated undrained triaxial compression (CIUTC or CKUTC)) tests were performed in accordance with ASTM Test method for Consolidated-Undrained Triaxial Compression Test on Cohesive Soils (D 4767). When large deformations were expected under the planned consolidation stresses, samples were consolidated initially in the sampling tubes under a vertical stress approximately equal to the isotropic consolidation stress planned in the triaxial test. After this step, the samples were extruded from the tube, trimmed to size (35.6 mm in diameter and 75 mm in height), and installed in the triaxial cell and were subjected to the isotropic consolidation stress. This resulted in additional consolidation of the samples to the final desired stress but with relatively small additional dimensional change. The remainder of the test followed the standard CU test procedure. The axial loading rate was 0.061 mm/min giving an approximate rate of strain equal to 0.086% per minute. Excess pore pressures were monitored during undrained shear.

Direct shear tests were performed again on samples pre-consolidated in the tube as described above. They were subsequently trimmed into a direct shear ring of 635 mm in diameter, re-consolidated to the final desired consolidation pressure, and subjected to slow drained shear. To assure drained conditions, a horizontal displacement rate of 0.0032 mm/min was maintained.

$K_0$ measurements were made in a specially constructed $K_0$ consolidation cell. Edil and Alanazy (1992) describe the detailed construction of this cell. A LabView routine was written to control the test and acquire the test data. Figure 1 shows the test setup and the data acquisition system. The details of the $K_0$ cell are shown in Figure 2. The cell with the dimensions of a conventional consolidation ring (63.5 mm in diameter and 25.4 mm high) consists of a hallowed ring fitted with strain gages. The thinned wall has a thickness of 1 mm. A sealed outer ring creates a lateral pressure chamber around the thinned ring. Air pressure is applied in this chamber to maintain the lateral displacement of the thin wall during vertical stress application to a minimum. The LabView control system was able to keep radial strains equal or less than $2 \times 10^{-6}$. The tests are presented and discussed along with similar data obtained from the literature under two topical headings.
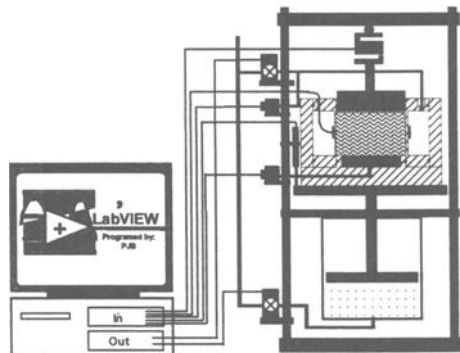


FIG. 1 – $K_o$ Test Setup
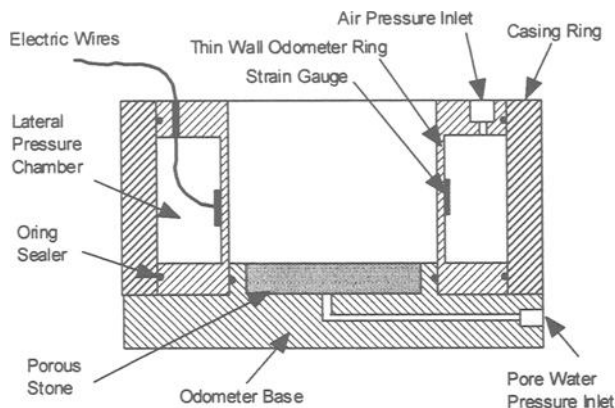
FIG. 2 – $K_o$ Consolidation Cell

## $K_o$ Behavior

$K_o$ represents the one-dimensional lateral earth pressure coefficient under confined conditions in which no lateral strain is permitted, in other words, at-rest condition. Several reports of laboratory measurements of $K_o$ are available in the literature. Table 2 provides a listing of $K_o$ values measured at the University of Wisconsin along with those reported in the literature. In the earlier UW study, a honed stainless steel semi-rigid confining tube (72.5-mm ID, 250 mm in height, and 2 mm in thickness) that was fitted with strain gages at three levels mounted outside of the tube was used in measuring $K_o$ (Edil and Dhowian 1981). The advantage of the $K_o$-test tube was that it accommodated large vertical strains due to consolidation for a significant range of vertical stresses, i.e., up to 800 kPa. Its disadvantage was potential for significant side friction and lateral deformation even though they were determined to be within acceptable limits in that study. The tests in the current study were performed using the $K_o$ cell shown in Figure 1. The main disadvantage of the cell for peats is the difficulty to conduct the test at progressing vertical stresses due to rapid shortening of the specimen. Therefore, the $K_o$ values determined in the current study correspond to relatively low vertical stresses (less than 100 kPa) except for Hoyt Lakes sample #11, which was precompressed in the sampling tube before trimming and placement into the cell. Thus, it was possible to use higher vertical stresses for sample #11.

The $K_o$ data presented in Table 2 are plotted in Figure 3 as a function of loss on ignition (LOI), i.e., organic content. Figure 3 does not reveal a trend with respect to LOI; however, it is clear that the average $K_o$ for amorphous peats (0.53) is higher than the average value for fibrous peats (0.34). This distinction confirms the early inference by Edil and Dhowian (1981) based on few data points as observed later by Stinnette (1998). It is remarkable that the data are from peats from widely varying areas and generated using a variety of equipment. The scatter of the data can be attributed to differences in

Table 2. *K$_o$ Database*

| Sample Designation | Description | Water Content (%) | Specific Gravity, Gs | Organic Content (%) | Coefficient of Earth Pressure at Rest | Reference |
|---|---|---|---|---|---|---|
| Middleton | Fibrous Peat | 510 | 1.41 | 88 | 0.31 | Edil & Dhowian, 1981 |
| Portage | Fibrous Peat | 600 | 1.72 | 81 | 0.30 | Edil & Dhowian, 1981 |
| Fond du Lac | Amorph. Peat | 240 | 1.94 | 60 | 0.53 | Edil & Dhowian, 1981 |
| Middleton (R2-7) | Fibrous Peat | 624 | 1.48 | 91 | 0.50 | |
| Middleton (B2-6) | Fibrous Peat | 446 | 1.48 | 83 | 0.29 | |
| Middleton (B3-2) | Amorph. Peat | 321 | 1.58 | 57 | 0.50 | |
| Hoyt Lakes (#1) | Fibrous Peat | 304 | 1.75 | 50 | 0.37 | |
| Hoyt Lakes (#11) | Fibrous Peat | 244 | 1.52 | 78 | 0.22 | |
| The Netherlands | Fibrous Peat | 500 | - | 67 | 0.40 | Krieg & Goldscheider, 1994 |
| The Netherlands #1 | Fibrous Peat | 669 | 1.52 | 66 | 0.38 | Termaat & Topolnicky, 1994 |
| The Netherlands #2 | Fibrous Peat | | | 74 | 0.29 | Termaat & Topolnicky, 1994 |
| The Netherlands #3 | Fibrous Peat | | | 84 | 0.38 | Termaat & Topolnicky, 1994 |
| The Netherlands #4 | Fibrous Peat | | | 66 | 0.26 | Termaat & Topolnicky, 1994 |
| The Netherlands #5 | Fibrous Peat | | | 72 | 0.37 | Termaat & Topolnicky, 1994 |
| Indiana #1 | Amorph. Peat | - | - | 27 | 0.52 | Joseph, 1985 |
| Indiana #2 | Amorph. Peat | - | - | 38 | 0.54 | Joseph, 1985 |
| Indiana #3 | Amorph. Peat | - | - | 60 | 0.52 | Joseph, 1985 |
| Japan | Fibrous Peat | 507 | 1.76 | 58 | 0.36 | Kanmuri, 1998 |
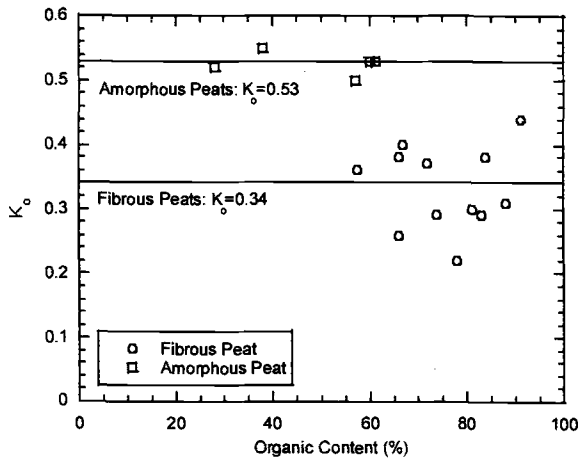


FIG. 3 – *K$_o$ versus Organic Content*

fiber content/quality as well as natural variability associated with data from different sources. Unfortunately, routine measurement of fiber content as part of peat testing is not an established tradition to allow an investigation of fiber content effects at this time other than making a qualitative observation.

The $K_o$ data presented above pertains to normally loaded specimens. During unloading, $K_o$ becomes greater than those during loading, as would be expected of overconsolidated soils. Schmidt (1952) proposed the following formula to relate $K_{o(rb)}$ (during rebound) to $K_{o(nc)}$ (during normal loading):

$$K_{o(rb)}=K_{o(nc)}(OCR)^\alpha \tag{1}$$

where OCR is the overconsolidation ratio (the ratio of the maximum past stress to the current stress) and $\alpha$ is an empirical coefficient. Several values have been proposed for $\alpha$ including sin $\phi$' (Mayne and Kulhawy 1982) based on an extensive review of inorganic soils. Another commonly used value for $\alpha$ is 0.5 for inorganic soils. Similar data for peats and organic soils are limited. Kanmuri et al. (1998) report a value of 0.5 for $\alpha$ for a fibrous peat based on numerous tests in a $K_o$-consolidation triaxial apparatus. Edil and Dhowian (1981) reported much lower values for $\alpha$ (0.09 to 0.18) for a range of peats. However, their tests were in a $K_o$-test tube and they were concerned about the elastic rebound response of the tube wall influencing their data during unloading.

**Shear Strength Behavior**

Early research on peat strength indicates some confusion as to whether peat should be treated as a frictional material like sand or cohesive like clay. Commonly, surficial peats are encountered as submerged surficial deposits. Because of their low unit weight and submergence, such deposits develop very low vertical effective stresses for consolidation and the associated peats exhibit high porosities and hydraulic conductivities comparable to those of fine sand or silty sand (Dhowian and Edil 1980). Such a material can be expected to behave "drained" like sand when subjected to shear loading. However, with consolidation porosity decreases rapidly and hydraulic conductivity becomes comparable to that of a clay. For example, time for end of primary consolidation as defined by full dissipation of the base pore pressure in a singly-drained consolidation test on Middleton peat increased 10 times under the second load increment from about 2 min to 20 min and to 200 min after several load increments. There is a rapid transition immediately from a well-drained material to an "undrained" material. In the following sections both the drained and undrained strength behavior are presented. The discussion pertains to normally loaded organic deposits.

*Effective Friction Angle*

Effective friction angle of peats is typically determined in consolidated undrained (CU) triaxial compression tests and occasionally in drained direct, ring or simple shear

tests.   Drained triaxial tests are seldom performed due to gross change in specimen dimensions and shape during the test.  The use of CU test requires measurement of pore pressures  during  the  test  to  derive  the  effective  strength  parameters.    Normally consolidated peats exhibit zero or small effective cohesion and generally high effective friction angles.  Tables 3 and 4 summarize the shear strength data for variety of peats and organic soils available to the authors (designated as the University of Wisconsin, i.e., UW data) and those obtained from the published literature (designated as the Literature data), respectively.   The tests are mostly CU triaxial compression tests with either isotropic consolidation (ICUTC) or anisotropic consolidation (KCUTC).  The consolidation stress reported in Tables 3 and 4 are the minor principal consolidation stress ($\sigma'_{3c}$) for the ICUTC tests and the major principal consolidation stress ($\sigma'_{1c}$) for the KCUTC tests. Yamaguchi et al. (1985) reported that anisotropic fabric of fibrous peat remains after isotropic consolidation.   Therefore, the results from both types of tests were treated together.
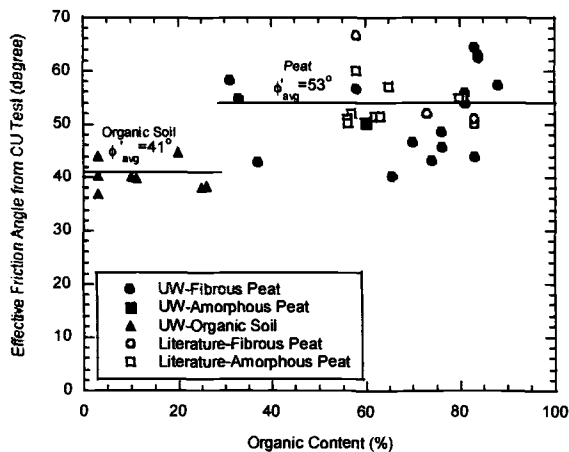


FIG. 4 – *Effective Friction Angle versus Organic Content*

Figure 4 gives the reported effective friction angle as a function of organic content. In this figure, those materials with an organic content less than approximately 25% are called organic soils.   The UW data and the data from the literature show no distinct differences and together indicate no direct dependency of friction angle on organic content once there is enough organic material, i.e., more than 25% to designate the material "peat."  The fibrous and the amorphous peats show no perceptible differences.  Fiber content measurements were available except for only a few of the samples; therefore, these designations are based on visual observations or on reports (for those obtained from the literature).   There is significant dispersion of the data with most of the data falling between 40° and 60°.  The average effective angle of friction is 53° for the peats and

Table 3. *UW Strength Database for Peats and Organic Soils*

| Source of Samples | Description | Water Content (%) | Organic Content (%) | Test Type | Consolidation Stress* (kPa) | Normalized Undrained Strength | Effective Friction Angle** (°) |
|---|---|---|---|---|---|---|---|
| Nine Springs | Fibrous Peat | 562 | 74 | ICUTC | 12 | 0.62 | 30.8 |
| | | 589 | 76 | ICUTC | 19 | 0.75 | 48.6 |
| | | 626 | 81 | ICUTC | 24 | 0.69 | 55.9 |
| | | 616 | 84 | ICUTC | 32 | | 62.5 |
| | | 655 | 83 | ICUTC | 48 | 0.66 | 64.3 |
| | | 562 | 74 | ICUTC | 19 | 0.70 | 43.2 |
| | | 589 | 76 | ICUTC | 41 | 0.55 | 45.6 |
| | | 626 | 81 | ICUTC | 29 | 0.71 | 54.2 |
| | | 616 | 84 | ICUTC | 55 | 0.61 | 63.0 |
| Richfield | Fibrous Peat | 181 | 31 | ICUTC | 17 | | 58.3 |
| | | 175 | 37 | ICUTC | 69 | 0.58 | 42.9 |
| | Organic Soil | 166 | 25 | ICUTC | 34 | 0.74 | 38.1 |
| | | 153 | 25 | ICUTC | 69 | 0.57 | 38.2 |
| Hoyt Lakes #1 | Fibrous Peat | | 70 | ICUTC | 34 | 0.60 | 46.6 |
| | | | 58 | ICUTC | 103 | 0.62 | 56.7 |
| | | | 88 | ICUTC | 517 | 0.56 | |
| | | | 83 | ICUTC | 862 | 0.55 | 43.9 (37) |
| | Organic Soil | | 3 | ICUTC | 69 | 0.54 | 43.8 (37) |
| | | | 3 | ICUTC | 345 | 0.51 | 40.3 |
| | | | 3 | ICUTC | 690 | 0.42 | 36.8 |
| | | | 20 | ICUTC | 690 | 0.55 | 44.7 |
| | | | 9 | ICUTC | 1035 | 0.44 | |
| Hoyt Lakes #2 | Fibrous Peat | | | ICUTC | 96 | | 48 (23.7) |
| | | | | ICUTC | 192 | 0.63 | 46 |
| | | | | ICUTC | 383 | 0.50 | 37 |
| USH 12 | Fibrous Peat | 165 | | ICUTC | 69 | 0.70 | 51 |
| | | 157 | | ICUTC | 207 | 0.60 | |
| USH 12/18 | Fibrous Peat | 361 | 66 | ICUTC | 59 | 0.55 | 40.3 |
| | Organic Soil | 321 | 10 | ICUTC | 59 | 0.64 | 39.8 |
| STH 29 | Fibrous Peat | 374 | 33 | ICUTC | 958 | 0.61 | 55 |
| | Organic Soil | 217 | | ICUTC | 479 | 0.62 | 47 |
| | | | | ICUTC | 958 | 0.45 | |
| | | | | ICUTC | 1916 | 0.43 | |
| | | | 10 | ICUTC | 479 | 0.44 | 40 |
| | | | 10 | ICUTC | 958 | 0.41 | |
| Middleton | Fibrous Peat | | 88 | KCUTC | 120 | 0.75 | 57.4 |
| | | | | KCUTC | 180 | | |
| | | | | KCUTC | 400 | | |
| Portage | Fibrous Peat | | 81 | KCUTC | 200 | 0.69 | 53.8 |
| | | | | KCUTC | 100 | | |
| | | | | KCUTC | 50 | | |
| Fond du Lac | Amorph. Peat | | 60 | KCUTC | 100 | 0.62 | 50.2 |
| | | | | KCUTC | 200 | | |

*Consolidation stress is $\sigma'_{3c}$ for ICUTC and $\sigma'_{1c}$ for KCUTC
**Friction angle in parenthesis is from direct or simple shear test

Table 4. *Peat Strength Database from the Literature*

| Source of Samples | Description | Water Content (%) | Organic Content (%) | Test Type | Consolidation Stress* (kPa) | Normalized Undrained Strength | Effective Friction Angle**(°) | Reference |
|---|---|---|---|---|---|---|---|---|
| Ohmiya City, Japan | Fibrous Peat | | 73 | ICUTC | 99 | 0.52 | 52 | Yamaguchi et al. 1985 |
| | | | 73 | ICUTC | 101 | 0.51 | | |
| | | | 73 | ICUTC | 98 | 0.54 | | |
| | | | 71 | ICUTC | 100 | 0.50 | | |
| | | | 71 | ICUTC | 200 | 0.50 | | |
| | | | 71 | ICUTC | 100 | 0.50 | | |
| | | | 71 | ICUTC | 200 | 0.63 | | |
| | | | 71 | ICUTC | 300 | 0.63 | | |
| Sacramento-San Joaquin, CA, USA | Fibrous Peat | 146-783 | 42-72 | ICUTC | | 0.6 | | Tillis et al. 1992 |
| Japan | Amorphous Peat | | 57 | ICUTC | | 0.54 | 52 | Tsushima et al. 1977 from Yamaguchi et al 1985 |
| | | | 58 | ICUTC | | 0.52 | 60 | |
| Japan | Amorphous Peat | | 56-67 | ICUTC | | 0.63 | | Oikawa et al. 1980 from Yamaguchi et al 1985 |
| Raheenmore, Irland | Amorphous Peat | 800-900 | 80 | ICUTC | | 0.5 | 55 (38) | Farrell&Hebib 1998 |
| Akita City, Japan | Amorphous Peat | 560-680 | 60-70 | ICUTC | | 0.54 | 57 | Tsushima&Mitachi 1998 |
| France | | | >30 | ICUTC | | 0.5 | | Magnan 1994 |
| Kamedago, Japan | Fibrous Peat | | 58 | KCUTC | 19.6 | 0.61 | 66.5 | Kanmuri 1998 |
| | | | 58 | KCUTC | 39.2 | 0.61 | | |
| | | | 58 | KCUTC | 58.8 | 0.61 | | |
| Canada | Fibrous Peat | 375-400 | 78-88 | KCUTC | | 0.59 | 50 | Adams 1962 from Yamaguchi et al 1985 |
| | | 375-401 | 78-89 | KCUTC | | | 51 | |
| Canada | Fibrous Peat | 200-600 | | KCUTC | | | 48 | Adams 1965 from Yamaguchi et al 1985 |
| Japan | Amorphous Peat | | 57-67 | KCUTC | | | 51.5 | Tsushima et al. 1977 from Yamaguchi et al 1985 |
| | | | 57-68 | KCUTC | | | 51.5 | |
| Japan | Amorphous Peat | | 56 | KCUTC | | | 51.1 | Tsushima et al. 1982 from Yamaguchi et al 1985 |
| | | | 56 | KCUTC | | | 50.2 | |
| Antoniny, Poland | Amorphous Peat | 250 | | KCUTC | | 0.48 | | Lechovicz 1994 |
| | | 100 | | KCUTC | | 0.43 | | |
| Raheenmore, Irland | Amorphous Peat | 800-900 | 80 | KCUTC | | 0.6 | | Farrell&Hebib 1998 |

*Consolidation stress is $\sigma'_{3c}$ for ICUTC and $\sigma'_{1c}$ for KCIT
**Friction angle in parentheisi is from direct o simple shear test

clearly above the average angle of 41° for the organic soils. These averages include all the friction values listed in Tables 3 and 4 including the ones without a reported organic content.

There is clear evidence that peats have extraordinarily high effective friction angles based on CU triaxial compression tests compared to most inorganic soils. However, it is not clear, how much of it is due to high pore pressures measured during the tests that artificially give a sense of lower effective normal stresses for the shear resistance sustained by fiber reinforcement. The question is how much of this high measurable friction angle can be counted on to operate in the field in an effective stress analysis. There are not many direct shear, ring shear or direct simple shear data available. Such data were available only in four such cases with only one of them by the authors (Tables 3 and 4). The effective friction angles averaged 33° when tested in this manner compared to 48° in the corresponding triaxial compression tests. Landva and LaRochelle (1983) also reported 32° for a fibrous peat based on extensive ring shear testing compared to immeasurably high friction angles from a triaxial compression test on the same material. Yamaguchi et al (1985) and Farrell and Hebib (1998) report lower friction angles in triaxial extension tests compared to triaxial compression tests.

*Normalized Undrained Strength*

Normalized undrained strength with consolidation pressure is a very useful way of expressing the undrained behavior. For normally consolidated deposits, undrained strength ratio provides a means of estimating strength increase with depth. Alternatively, for staged construction or preloading, it allows a means of estimating strength gain because of consolidation when it is expressed incrementally, i.e., $\Delta c_u / \Delta \sigma_v$. Lechowicz (1994) showed that this latter ratio is not constant for normally consolidated peats and organic soil unlike inorganic clays and depends on the magnitude of consolidation stress applied relative to the original effective overburden stress. Figure 5 shows normalized undrained strength as a function of consolidation stress for both ICUTC and KCTC tests using the peat data (both fibrous and amorphous) given in Tables 3 and 4. The UW and the literature data were again very similar and therefore not distinguished in Figure 5. The data from the ICUTC are indistinguishable from the KCUTC data in the manner they are expressed, respectively, in term of $\sigma'_{3c}$ and $\sigma'_{1c}$. While there is a greater dispersion of the data at low consolidation pressures, there is not a trend with respect to increasing consolidation stress and the undrained strength ratio can be taken to be constant. While this may be true for strength increase with depth, it may not hold for incremental strengthening estimations due to staged consolidation.

Figure 6 presents normalized undrained strength ($c_u/\sigma'_{3c}$ or $c_u/\sigma'_{1c}$) as a function of organic content for all peats and organic soils given in Tables 3 and 4. Again, the UW data and the data from the literature showed no distinct differences and are plotted together. The data indicate no direct dependency of normalized undrained strength on organic content. The fibrous and the amorphous peats show no perceptible differences and give an average normalized undrained strength of 0.59 with most of the data falling

between 0.5 and 0.7.  The organic soils, especially those with an organic content less than 20%, seem to have lower normalized undrained strength compared to the peats.
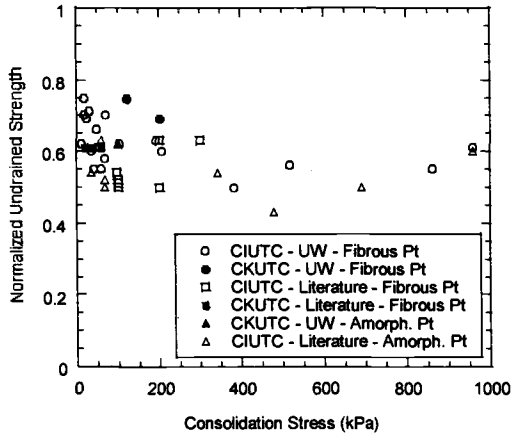


FIG. 5 – *Normalized Undrained Strength versus Consolidation Stress*
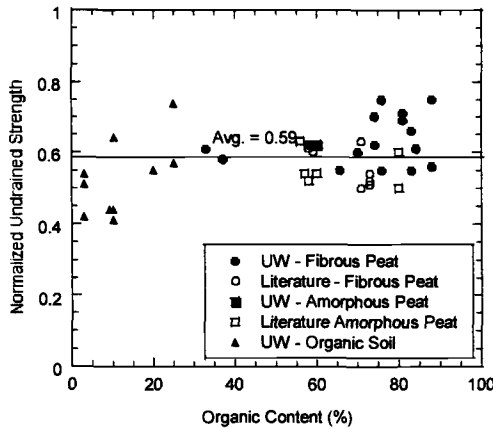


FIG. 6 – *Normalized Undrained Strength versus Organic Content*

  Normalized undrained strength can be obtained from vane shear in the field.  Data from two highway sites in Wisconsin were available.  Field vane normalized undrained strength is given as a function of organic content in Figure 7.  The data shows much greater dispersion than in the laboratory tests but similar trends with respect to organic content and type of peat.  The data for peats vary between 0.5 and 1.5.  Landva and La

Rochelle (1983) reported similarly high vane strengths compared to ring shear strengths. They attributed it to the peculiarities of vane shear when applied in a fibrous material.
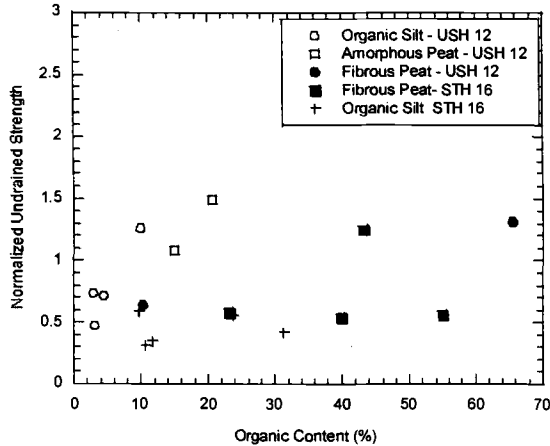


FIG. 7 – *Normalized Undrained Strength from Field Vane Shear Test vs Organic Content*

## Conclusions

Based on an interpretation of the data generated by the authors as well as those reported in the literature regarding lateral earth pressure and strength testing of peats and organic soils, the following conclusions and guidelines are advanced. These interpretations are limited to the data available herein and may be subject to change, as more data become available. However, the database is one of the most extensive on organic materials to date.

1. Coefficient of earth pressure at-rest ($K_o$) for normally consolidated peats are typically lower than for inorganic soils. It does not depend on organic content but depends on fiber content. Broadly, it can be taken equal to 0.49 for amorphous peats and 0.33 for fibrous peats.

2. Effective angle of friction ($\phi'$) for normally consolidated peats, as determined from consolidated undrained triaxial compression tests, does not appear to depend on organic content or type of peat. It varies between 40° to 60° with an average value of 53°. It is lower for organic soils (~ 41°). Effective cohesion is, in general, small for peats.

3. Normalized undrained strength ($c_u/\sigma'_{3c}$ or $c_u/\sigma'_{1c}$) for normally consolidated peats, as determined from isotropically or anisotropically consolidated undrained triaxial compression tests, does not appear to depend on organic content, type of peat, or type or level of consolidation (isotropic or anisotropic). It varies between 0.5 and 0.7 with an average value of 0.59. It seems to be lower for organic soils. Normalized

undrained strength ($c_u/\sigma'_v$) from field tests confirm the same independence from organic content or type of peat but give generally higher values.

4.  Review of strength data implies a shift in behavior as organic content increases from about 20 to 25% to higher values. Therefore, an upper classification border can be proposed for organic soils at 20 to 25% loss on ignition on the basis of geotechnical considerations.

The data reported herein are somewhat dispersed. This is probably due to a number of factors such as wide geographic distribution of sample sources, test equipment, test operators as well inherent variability of peats and organic soils including their degree of humification. It was not possible to delineate the effect of fiber content clearly for lack of data. It is possible in the wide dispersion of the data there is a fiber content dependency. It is strongly recommended that water content (ASTM Test Methods for Moisture, Ash, and Organic Matter of Peat and Other Organic Soils, D 2974), organic content (D 2974), fiber content (ASTM Test Method for Laboratory Determination of Fiber Content of Peat Samples by Dry Mass, D 1997) and degree of humification (ASTM Test Method for Estimating the Degree of Humification of Peat and Other Organic Soils (Visual/Manual Method), D 5715) tests be performed and reported routinely on all organic soils tested for strength, compressibility, hydraulic conductivity or other engineering properties. This is the equivalent of Atterberg limit tests for inorganic soils.

The properties of peats and organic soils presented above are based on laboratory investigations. Their applicability directly in the field is not clearly understood and is beyond the scope of this paper.

## Acknowledgments

## References

Adams, J.I., 1962, "Laboratory Compression Test on Peat," *Ontario Hydro Research News, Third Quarter*, pp. 35-40.

Adams, J.I., 1965, "The Engineering Behavior of a Canadian Muskeg," *Proceedongs, 6th International conference on Soil Mechanics and Foundation Engineering*, Vol. 1, pp. 3-7.

Den Haan, E.J., 1997, "An Overview of the Mechanical Behavior of Peats and Organic Soils and Some Appropriate Construction Techniques," *Proceedings, Conference on Recent Advances in Soft Soil Engineering*, Vol. 1, Huat & Bahia, Eds., Kuching, Sarawak, Malaysia, pp. 17-45.

Farrell, E.R., 1997, "Some Experiences in the Design and Performance of Roads and Road Embankments on Organic Soils and Peats," *Proceedings, Conference on Recent Advances in Soft Soil Engineering,* Vol. 1, Huat & Bahia, Eds., Kuching, Sarawak, Malaysia, pp. 66-84.

Dhowian, A. W., 1978, "Consolidation Effects on Properties of Highly Compressive Soils-Peats," *Ph.D, Thesis,* Department of Civil Engineering, the University at Madison.

Dhowian A. W. and Edil, T. B. 1980, "Consolidation Behavior of Peats," *ASTM Geotechnical Testing Journal,* 3 (3), pp. 105-114.

Edil, T. B. and Alanazy, A. S., 1992, "Lateral Swelling Pressures," *Proceedings, 7th International Conference on Expansive Soils,* Dallas, TX, pp. 227-232.

Edil, T. B. and Dhowian, A. W., 1981, "At-rest Lateral Pressure of Peat Soils," *Journal of Geotechnical Engineering,* Vol. 107, No. GT2, pp. 201-217.

Farrell, E. R. and Hebib, S., 1998, "The Determination of the Geotechnical Parameters of Organic Soils," *Problematic Soil,* Yanagisawa, Moroto & Mitachi, Eds., Balkema, Rotterdam, pp. 33-37.

Joseph, P. G., 1985, "Behavior of Mucks and Amorphous Peats as Embankment Foundations, *Interim Report,* Joint Highway Research Project, FHWA/IN/JHRP-85/16, Purdue University.

Kanmuri, H., Kato, M., Suzuki, O., and Hirose, E., 1998, "Shear Strength of Ko Consolidated Undrained Peat," *Problematic Soil,* Yanagisawa, Moroto & Mitachi, Eds., Balkema, Rotterdam, pp. 25-29.

Krieg, S. and Goldscheider, M., 1994, "Some Results About the Development of $K_0$ During One-dimensional Creep of Peat," *Proceedings, International Workshop on Advances in Understanding and Modelling the Mechanical Behaviour of Peat,* Den Haan, Termaat & Edil, Eds., Balkema, Rotterdam, pp. 71-76.

Landva, A.O. and La Rochelle, P., 1983, "Compressibility and Shear Characteristics of Radforth Peats," *Testing of Peats and Organic Soils, ASTM STP 820,* Jarrett, Ed., American Society for Testing and Materials, pp. 157-191.

Lechowicz, Z., 1994, "An Evaluation of the Increase in Shear Strength of Organic Soils," *Proceedings, International Workshop on Advances in Understanding and Modelling the Mechanical Behaviour of Peat,* Den Haan, Termaat & Edil, Eds., Balkema, Rotterdam, pp. 167-180.

Magnan, J. P., "Construction on Peat: State of the Art in France," *Proceedings, International Workshop on Advances in Understanding and Modelling the Mechanical Behaviour of Peat*, Den Haan, Termaat & Edil, Eds., Balkema, Rotterdam, pp. 369-380.

Mayne, P.W. and Kulhawy, H.F., 1982, "$K_0$-OCR Relationship in Soils," *ASCE Journal of Geotechnical Engineering*, Vol. 108, No. GT6, pp. 851-872.

Oikawa, H. and Miyakawa, I., 1980, "Undrained Shear Characteristics of Peat," *Journal of Japanese Society of Soil Mechanics and Foundation Engineering*, Vol.20, No.3, pp. 92-100 (in Japanese).

Schmidt, B., 1967, "Lateral Stresses in UniaxialStrain," *Danish Geotechnical Institute Bulletin*, No. 23, pp. 5-12.

Stinnette, P. 1998, "Prediction of Field Compressibility from Laboratory Consolidation Tests of Peats and Organic Soils," *Geotechnical Testing Journal*, Vol. 21, No. 4, pp. 297-306.

Termaat, R. and Topolnicki, M., 1994, "Biaxial Tests with Natural and Artificial Peat," *Proceedings, International Workshop on Advances in Understanding and Modelling the Mechanical Behaviour of Peat*, Den Haan, Termaat & Edil, Eds., Balkema, Rotterdam, pp. 241-252.

Tillis, R. K., Meyer, M. R. and Hultgren, E. M., 1992, "Performance of Test Fill Constructed on Soft Peat," *Proceedings, Stability and Performance of Slopes and Embankments-II, ASCE GSP 31*, Seed & Boulanger, Eds.,Vol. 1, pp. 775-787.

Tsushima, M., Miyakawa, I. and Iwasaki, T., 1977, "Some Investigation on Shear Strength of Organic Soil," *Journal of Japanese Society of Soil Mechanics and Foundation Engineering*, No. 235, pp. 13-18 (in Japanese).

Tsushima, M. and Oikawa, H., 1982, "Shear Strength and Dilatancy of Peat," *Journal of Japanese Society of Soil Mechanics and Foundation Engineering*, Vol. 22, No. 2, pp. 133-141 (in Japanese).

Tsushima, M. and Mitachi, T., 1998, "Method for Predicting in-situ Undrained Strength of Highly Organic Soil Based on the Value of Suction and Unconfined Compressive Strength," *Problematic Soil*, Yanagisawa, Moroto & Mitachi, Eds., Balkema, Rotterdam, pp. 11-15.

Yamaguchi, H., Ohira, Y., Kogure, K., and Mori, S., 1985, "Undrained Shear Characteristics of Normally Consolidated Peat Under Triaxial Compression and Extension Conditions," *Soils and Foundations*, Vol. 25, No. 3, pp. 1-18.

Francesco Colleselli,[1] Giampaolo Cortellazzo,[2] and Simonetta Cola[2]

**Laboratory Testing of Italian Peaty Soils**

**Abstract:** This paper presents laboratory findings in peats from two different Italian sites; the tested peats are typical of superficial deposits near the Northern Adriatic Coast. Standard and special laboratory tests were carried out on undisturbed soil cores. In particular, oedometer tests in standard and in Rowe cell with measurement of pore pressure, adopting different load increment ratio and load permanence, were performed. The compression characteristics ($C_c$, $C_\alpha$) and the difficulties involved in reliably determining the end of primary consolidation and evaluating the permeability were investigated. Since one peat is normal-consolidated and the other is over-consolidated, a different behavior was expected and is described. The data are also compared with those in the literature.

**Keywords:** peat, consolidation, permeability, primary consolidation, secondary compression

**Introduction**

Peats are considered difficult foundation soils because they exhibit unusual compression behavior, different from the conventional one of clays. In fact, these soils have a high compressibility with a significant secondary compression stage, which is not constant with the logarithm of time in some cases. Moreover, peaty soils have a short duration of primary consolidation due to their high initial permeability. In fact, the initial permeability of peats is 100 - 1000 times that of soft clays and silts and the coefficient of consolidation is 10 - 100 times greater. Other particular characteristics are high in situ

---

[1] Professor, Università degli Studi di Brescia, Dipartimento di Ingegneria Civile, Via Branze 27, 25100 Brescia, Italia.
[2] Doctor, Università degli Studi di Padova, Dipartimento di Ingegneria Idraulica, Marittima e Geotecnica, Via Ognissanti 39, 35129 Padova, Italia.

void ratios, high values of compression index ($C_c$) and secondary compression index ($C_\alpha$), about ten times greater than those of the clayey soils.

The analysis of the behavior of peat materials presents difficulties when the conventional methods are adopted. In order to improve the Terzaghi theory and better reproduce the behavior of peats, two different hypotheses were suggested, e.g. the Hypothesis A (Mesri and Choi 1985) according to which secondary compression begins after primary consolidation has ended, and Hypothesis B (Kabbaj et al. 1988) according to which secondary compression is simultaneous with primary consolidation. The results of research fail to clarify which theory is the most realistic one, probably due to difficulties relating to the great variability in the characteristics of peat.

Moreover the observation of many one-dimensional compression tests suggested that the ratio $C_\alpha/C_c$ is constant for any time, effective stress and void ratio during secondary compression (Mesri and Godlewski 1977) with a range of $0.06 \pm 0.01$, the highest values of $C_\alpha/C_c$ ratio among geotechnical materials. However other authors (Fox and Edil 1992) do not agree on the application of $C_\alpha/C_c$ concept to fibrous peats.

This paper presents laboratory findings in peats from two different Italian sites and compares these with data in the literature. Our main aim was to investigate the compression characteristics ($C_c$, $C_\alpha$) and the difficulties involved in reliably determining the end of primary consolidation and evaluating the permeability.

Since one peat is normal-consolidated and the other is over-consolidated, a different behavior was expected and is described.

## Description of the Peats

The peaty soils used in the study were collected from two different sites in the north-east of Italy, one near Adria in the Po delta area; the other at Correzzola in an area between the Adige and Bacchiglione Rivers near the "Canale dei Cuori". In both sites the peat deposits are superficial and stretch for many square kilometers with a thickness of 2-3 meters. The area samples were taken at a depth between -3.0 and -6.0 m in Adria and between -1.5 and -2.1 m in Correzzola.

Eight samples of Adria peat (Adria-1) and 3 samples of Correzzola peat (Correzzola), were collected at more or less the same level at each site and stored in a humid room until the time of testing. A thin wall tube sampler suitable to collect samples with a diameter of 0.22 m and a height of 0.80 m was used to minimize the soil disturbance. Three additional samples had previously been taken at the Adria site and tested in the laboratory (Adria-2).

The principal characteristics of the three peaty soils are shown in Table 1.

The Adria-1 peat has an average natural water content (w) of 375%, an average organic content ($O_c$) of 72%, an average in-situ void ratio (e) of 5.74, a specific gravity of solids ($G_S$) of 1.56, a fiber content of about 25% and a pH of about 6.9, with a Von Post classification (Landva and Pheeney 1980) $H_6$-$B_2$-$F_3$-$R_{1-2}$-$W_0$-$N_3$-$A_1$-$P_1$-$pH_{0-L}$.

The Adria-2 samples, on the other hand, have an average natural water content of 280%, an average in-situ void ratio of 4.70, a specific gravity of solids of 1.47, a fiber

content greater than 75% and a pH of about 4.5, with a Von Post classification $H_{3-4}$-$B_2$-$F_{1-2}$-$R_{2-1}$-$W_0$-$N_3$-$A_1$-$P_1$-$pH_L$. Consolidation tests carried out before and during this study have indicated that both kinds of Adria peat are over-consolidated, with an effective pre-consolidation stress of about 100 kPa, so the over-consolidation ratio is about 1.5.

The Correzzola peat has an average natural water content of 690%, an average organic content of 71%, an average in-situ void ratio of 10.5 and a specific gravity of solids of 1.53. The pH is about 4.6 and the fiber content is about 25%. The Von Post classification is $H_5$-$B_3$-$F_2$-$R_2$-$W_0$-$N_3$-$A_0$-$P_1$-$pH_L$. Consolidation tests carried out during the study have indicated that it is normal-consolidated with an effective pre-consolidation stress of about 15 kPa.

**Testing Program**

For the Adria-1 and Adria-2 peats, a total of 9 multiple loading stage standard oedometer tests with a load increment ratio (LIR) of 1.0 were performed. Special oedometer tests using different LIRs were also carried out; three of these involved a single load increment and four had two load stages at 50 - 200 kPa and 100 - 200 kPa. For the Correzzola peat 2 multiple loading stage standard oedometer tests with a LIR of 1.0, an oedometer test with two load stages at 50 - 200 kPa and another one at 100 - 200 kPa were performed. Different load increment times were adopted, ranging from 1 day for the standard oedometric test to more than 8 months for the single load oedometric tests.

Two different devices were used, i.e. a 70.5 mm diameter standard oedometric consolidation cell and a 75.5 mm Rowe cell with pore pressure measurement at the base of the specimens. Room temperature was kept at 20.0° ± 2.0° during testing.

Table 2 summarizes the complete testing program, concerning duration of loading, load increment ratio and characteristics of the specimens.

Table 1 - *Soil characteristics*

| Site | $C_u$[1], kPa | $\gamma$[2], kN/m$^3$ | W[3], % | $O_c$[4], % | $G_s$[5] | pH[6] |
|---|---|---|---|---|---|---|
| Adria-1 | 90 - 160 | 10.3 - 10.7 | 330 - 421 | 68 - 75 | 1.55 - 1.58 | 6.5 - 7.2 |
| Adria-2 | 90 - 170 | 8.8 - 11.7 | 226 - 427 | 65 - 84 | 1.42 - 1.52 | 4.1 - 4.2 |
| Correzzola | 20 - 110 | 10.3 - 10.8 | 606 - 790 | 70 - 72 | 1.46 - 1.60 | 4.0 - 5.1 |

[1] ASTM Test Method for Laboratory Miniature Vane Shear Test for Satured Fine-Grained Clayey Soil (D4648-94)
[2] ASTM Test Method for Bulk Density of Peat and Peat Products (D4531-86)
[3] ASTM Test Method for Laboratory Determination of Water (Moisture) Content of Soil and Rock (D2216-92)
[4] ASTM Test Method for Moisture, Ash, and Organic Matter of Peat and Other Organic Soils (D2974-87)
[5] BS1377 - 1990 Determination of the specific gravity of soil particles. Test 6(B). Method for fine-grained soils
[6] ASTM Test Method for pH of Peat Materials (D2976-71)

Table 2 - *Testing program*

| Test No. | Load duration | LIR | Device | Initial w % | $e_0$ |
|---|---|---|---|---|---|
| Adria-1 | | | | | |
| E2-1 | 1 day | 1 | Std. oed. Cell | 334 | 5.15 |
| E2-2 | 2 months | 4, 3 | Std. oed. Cell | 358 | 5.60 |
| E2-3 | 2 months | 9, 1 | Std. oed. Cell | 357 | 5.47 |
| E2-4 | 2 months | 19 | Std. oed. Cell | 357 | 5.33 |
| E2-5 | 1 week | 1 | Rowe cell | 364 | 5.58 |
| I7-1 | 1 day | 1 | Std. oed. Cell | 418 | 6.49 |
| I7-2 | 2 months | 4, 3 | Std. oed. Cell | 421 | 6.44 |
| I7-3 | 2 months | 9, 1 | Std. oed. Cell | 395 | 5.87 |
| Adria-2 | | | | | |
| A1 | 2 days | 1 | Std. oed. Cell | 226 | 4.98 |
| A2 | 2 weeks | 1 | Std. oed. Cell | 269 | 4.60 |
| A3 | 1 week | 1 | Rowe cell | 285 | 4.94 |
| A4 | 1 week | 1 | Rowe cell | 282 | 4.36 |
| A5 | 8 months | 19 | Std. oed. Cell | 271 | 4.23 |
| A6 | 8 months | 9 | Std. oed. Cell | 243 | 4.09 |
| B1 | 1 week | 1 | Rowe cell | 290 | 3.52 |
| B2 | 1 week | 1 | Rowe cell | 427 | 6.62 |
| Correzzola | | | | | |
| S3-1 | 1 day | 1 | Std. oed. Cell | 790 | 11.84 |
| S3-2 | 2 months | 4, 3 | Std. oed. Cell | 715 | 10.51 |
| S3-3 | 2 months | 9, 1 | Std. oed. Cell | 740 | 10.90 |
| S3-4 | 1 week | 1 | Rowe cell | 696 | 10.25 |

## Long-Term Behavior

Figure 1 shows the settlement in log time of the three different peats for the single load increment from 10 kPa to 100 kPa. The Adria-1 and Correzzola peats usually show a curve with a clear primary consolidation and secondary compression; the slope of the latter changes with time, but the variation is relatively small. Instead the Adria-2 peat has a low primary compression, usually merging with the secondary compression. In this case, the secondary compression slope variation is clearly evident after a week of loading and a tertiary compression range can be defined (Dhowian and Edil 1980).

Since the organic content of the test specimens is essentially similar, the different long-term behavior can be attributed to the different fiber content of the three peats. In fact, the Adria-2 peat has the highest fiber content and shows the greatest tertiary settlement.
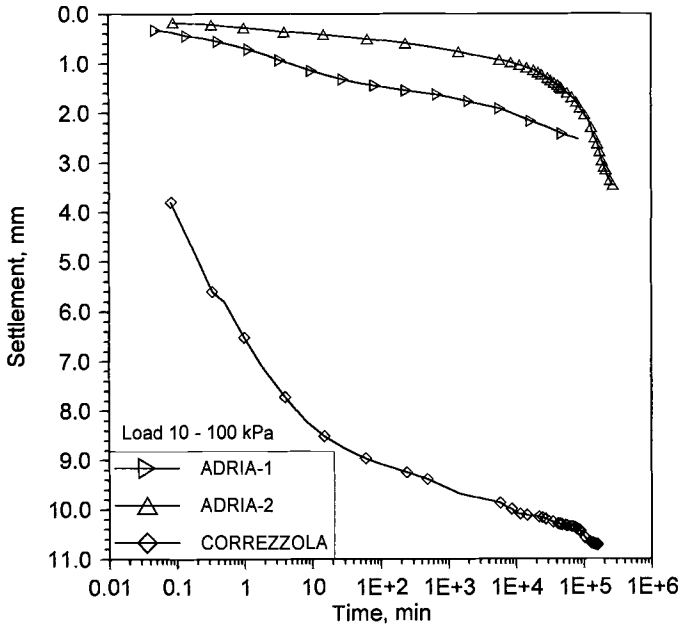
Figure 1 - *Typical settlement - time curves for Adria-1, Adria-2 and Correzzola peats*

## Load Increment Ratio Effects

Figure 2 compares the void ratio variation in log time for specimens of the E2 sample loaded at 200 kPa under the same drainage condition, but with a different load increment ratio. In particular, the time of the end of primary consolidation (EOP) is almost equal for the two specimens loaded with an LIR = 1.0. The EOP time diminishes in the tests carried out with an LIR greater than 1.0. The inflection point is more marked in the curves for higher LIRs. The secondary coefficient is quite similar for all the tests, so it is probably independent of the LIR imposed.

## Evaluation of the End of Primary Compression

Figures 3, 4 and 5 show some sample settlement-time curves; the data are plotted with log time and square root time axes. In Figures 4 and 5 the pore pressure dissipation is also reported. Where possible, the EOP time was estimated using the Casagrande ($t_{pC}$) and Taylor ($t_{pT}$) methods and at 95% of the pore pressure dissipation ($t_{pU}$).
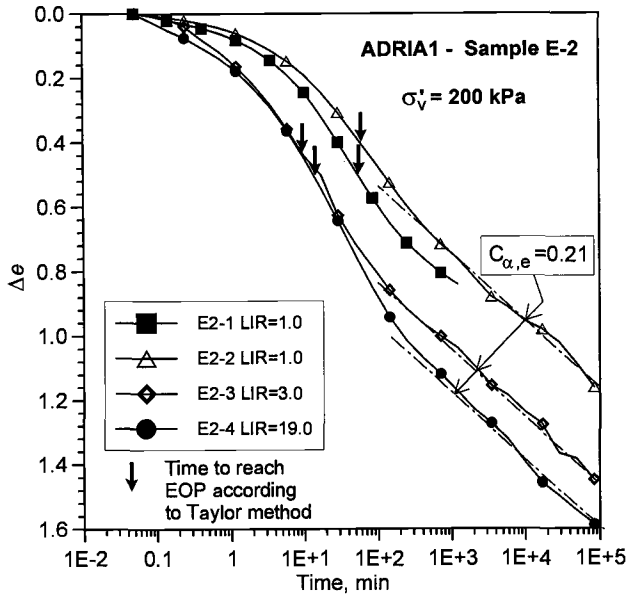
Figure 2 - *Effects on settlement behavior with different load increment ratio for E2 samples*
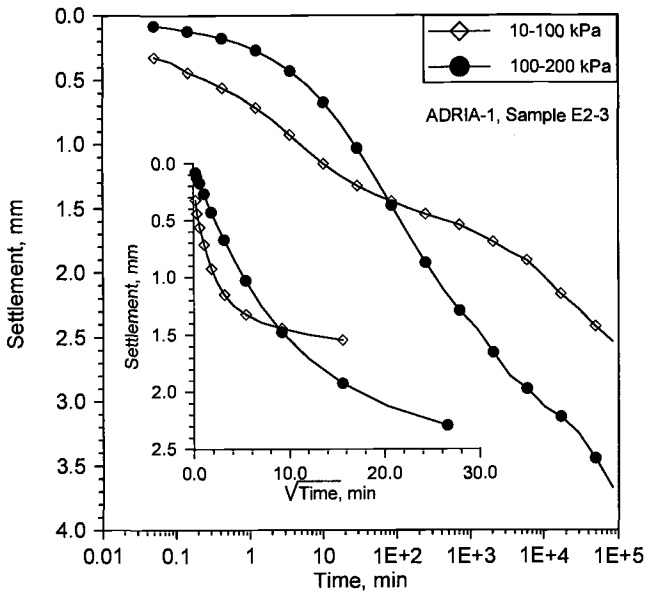


Figure 3 - *Typical settlement - time curves for Adria-1 peat*
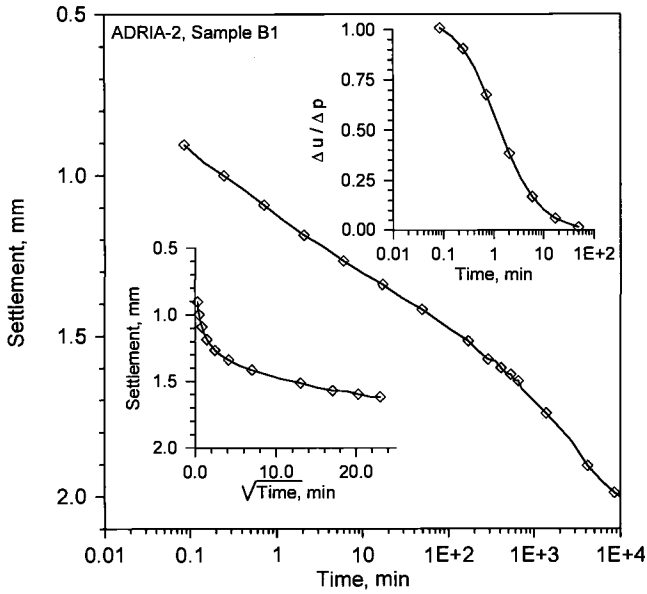
Figure 4 - *Typical settlement and pore pressure dissipation in time curves for Adria-2 peat*
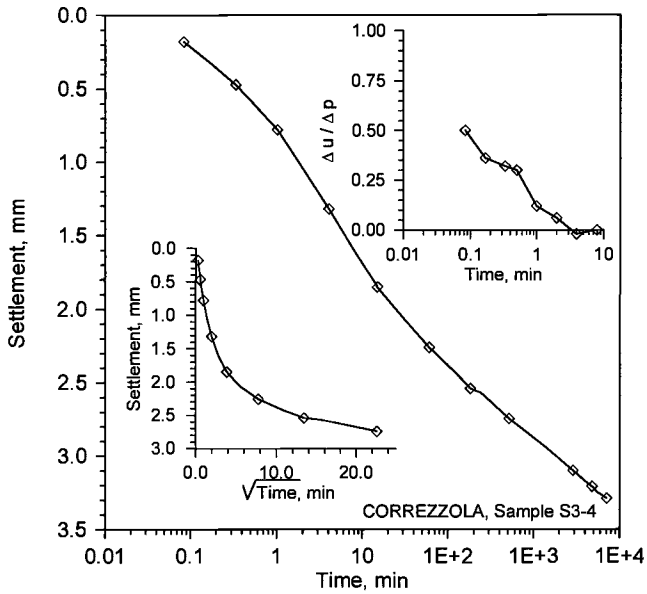


Figure 5 - *Typical settlement and pore pressure dissipation in time curves for Correzzola peat*

The Taylor method can be applied in each case, whereas the Casagrande method cannot be used when primary consolidation is not clearly identified, i.e. for the Adria-2 samples (Figure 4), for some of the Correzzola samples, and in the load range lower than pre-consolidation pressure. The determination of EOP on the basis of pore pressure dissipation is theoretically correct, but in some tests the dissipation was so fast that the measurements were probably not reliable.

The $t_{pC}$ and $t_{pT}$ values change with the applied load level (Figure 3) and with the load duration for the same load. The former method finds a greater EOP time than the latter. Moreover, they do not change in the same way, so the $t_{pC}/t_{pT}$ ratio (Figure 6) varies and is related to load duration. The variation in the ratio is greater than reported elsewhere in the literature (Ladd 1973). In fact, for Adria peats the values range between 2.0 and 10.0 and are greater in the long-term tests. For Correzzola peat, the variation is between 1.5 and 5.0 and in this case the lower values are associated with the long-term tests.

Some previously-collected data on Adria-2 peat show a $t_{pU}/t_{pT}$ ratio varying between 1.0 and 20.0, but the same trend was not identified for Adria-1 and Correzzola peats. However, the change in void ratio related to this different $t_p$ evaluation is lower than 15% (Colleselli and Cortellazzo 1998).

The data in the following paragraphs were obtained using the Taylor method.
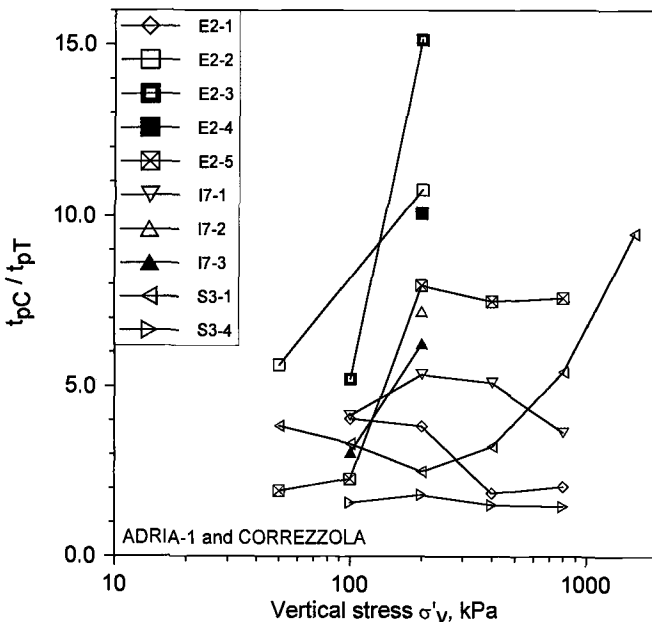


Figure 6 - $t_{pC}/t_{pT}$ ratio versus $\sigma$ for Adria-1 and Correzzola peats

## $C_\alpha/C_c$ Ratio

Figures 7 and 8 show the $e$ - log $\sigma'_v$ curves for the three peats evaluated at different loading times ($t_{pT}$, 10 $t_{pT}$, 100 $t_{pT}$). The slope of the curves changes with stress and with the elapsed time, but there are some differences. The Adria-1 and Adria-2 curves have the same shape, but the shifting among the curves evaluated at longer times is relatively constant for Adria-1 and tends to increase for Adria-2.

For the Adria peats, $C_c$ increases with increasing effective stress values in the range between 100 kPa and 400 kPa, then decreases; a similar variation in $C_c$ values was found by Mesri et al. (1997) for stress levels greater than twice the consolidation pressure. For the normal-consolidated Correzzola peat, $C_c$ decreases with stress at a constant rate. At any given stress, $C_c$ varies with the elapsed loading time, particularly for the Adria-2 peat. $C_\alpha$ also changes with the same trend as $C_c$.

In Figures 9 and 10, the $C_c$ and $C_\alpha$ data are determined for different elapsed loading times on the basis of Taylor's $t_{pT}$ using the procedure described by Mesri and Godlewski (1977). The results for $t_{pT}$ and 10 $t_{pT}$ values are relatively scattered ($R^2 = 0.91 - 0.93$ for Adria and $R^2 = 0.73 - 0.75$ for Correzzola). The $C_\alpha$ values for $t_p$ are higher than for longer loading times, probably due to an inaccurate determination of the primary consolidation time when the Taylor method is used.

However, the $C_\alpha$ values determined at 1000 $t_{pT}$ for the two tests on Adria-1 peat are clearly higher than for lower $t_{pT}$, highlighting a probable tertiary stage in the compression.
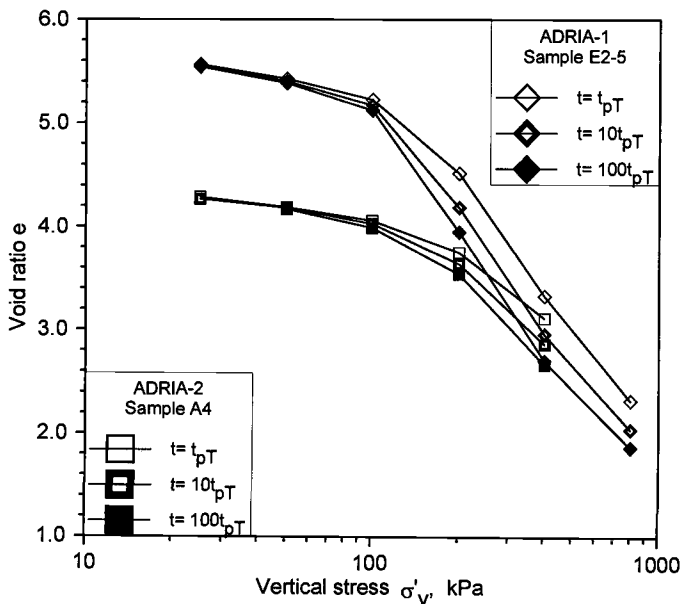


Figure 7 - $e$ - log $\sigma'_v$ curves for Adria-1 and Adria-2 Rowe tests

The $C_\alpha/C_c$ ratio versus void ratio was also investigated (Figures 11 and 12). For both peats, the ratio is substantially constant and about 0.04 - 0.06 when evaluated at 10 $t_{pT}$. The data evaluated at $t_{pT}$ show higher values and greater scattering; in fact they range between 0.06 - 0.10. These findings can also be attributed to the inaccurate determination of time to reach EOP.

## Permeability Coefficient

The permeability of the two peats was measured directly in the Rowe cell (PT-R) and in the triaxial cell (PT-Tx) and determined indirectly using the equation ($k = c_v\, m_v\, \gamma_w$ ; where $c_v$ = coefficient of consolidation, $m_v$ = coefficient of volume compressibility and $\gamma_w$ = unit weight of water).

In Figures 13 and 14, the data are compared with the octahedric stress and void ratio respectively. In Figure 13, the octahedric stress has been used to adapt the stress level of the various tests. In particular, in the equation for octahedric stress, $p'=(\sigma'_v + 2\, k_o\, \sigma'_v)/3$, the coefficient at rest $k_o$ has been assumed equal to 0.27 as determined with some anisotropic triaxial tests performed on these soils. The permeability coefficient changes from $10^{-6}$ m/s to $10^{-11}$ m/s as the applied load increases. The trend of the curves is fairly similar for all the tests. However, especially for Adria peat, the values at a fixed stress vary by about one order of magnitude, corresponding to the different tests. The permeability values measured in the Rowe cell differ from calculated values by at least
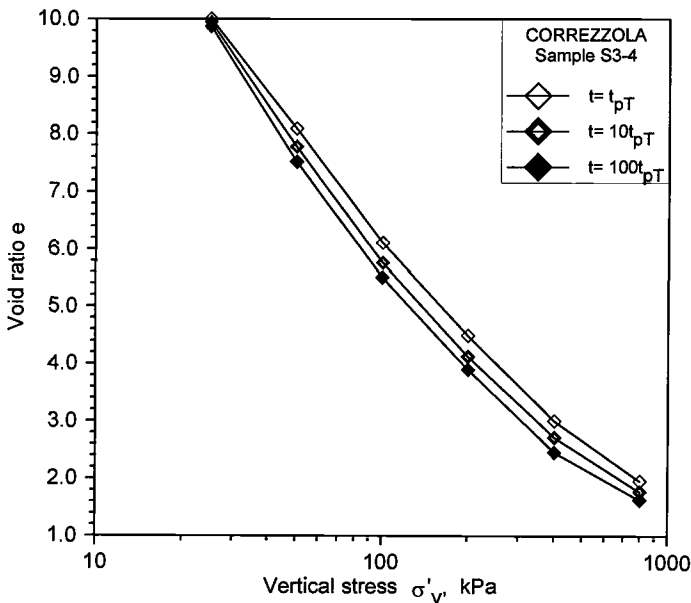


Figure 8 - e - log $\sigma'_v$ curves for Correzzola Rowe test
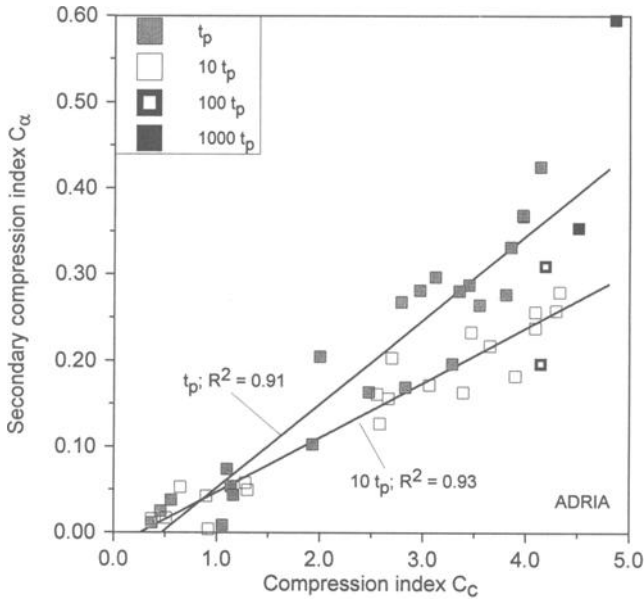
Figure 9 - $C_\alpha$ versus $C_c$ for Adria-1 and Adria-2 peats
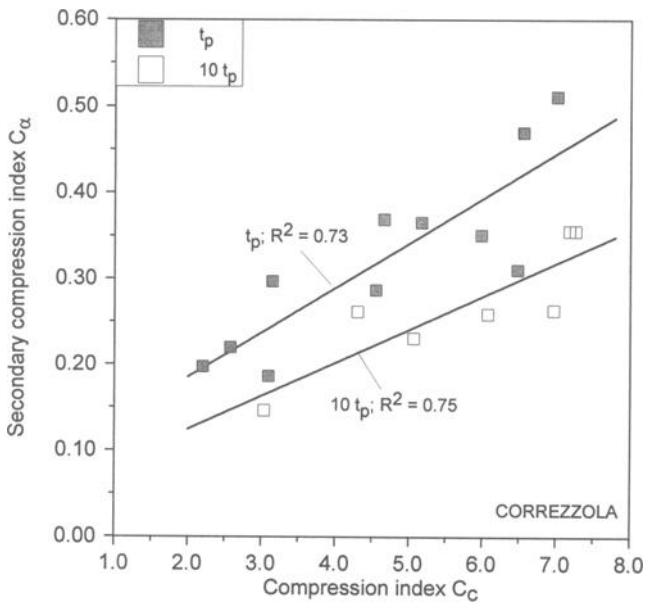


Figure 10 - $C_\alpha$ versus $C_c$ for Correzzola peat
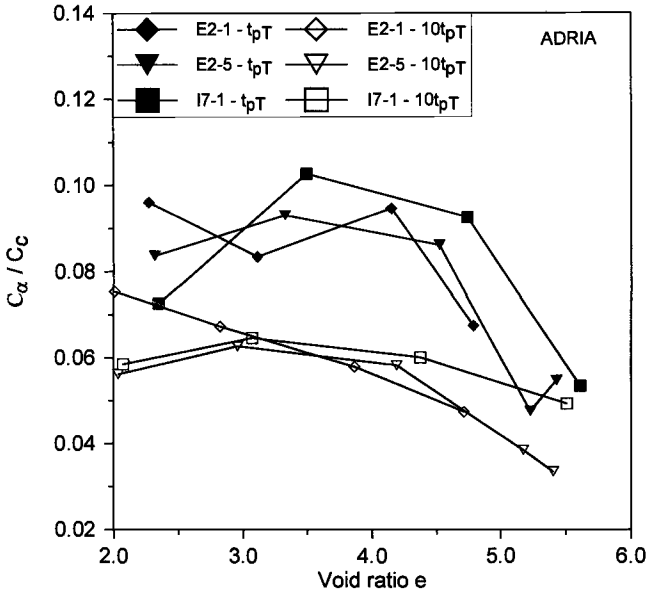
Figure 11 - $C_\alpha / C_c$ versus e for Adria-1 peat
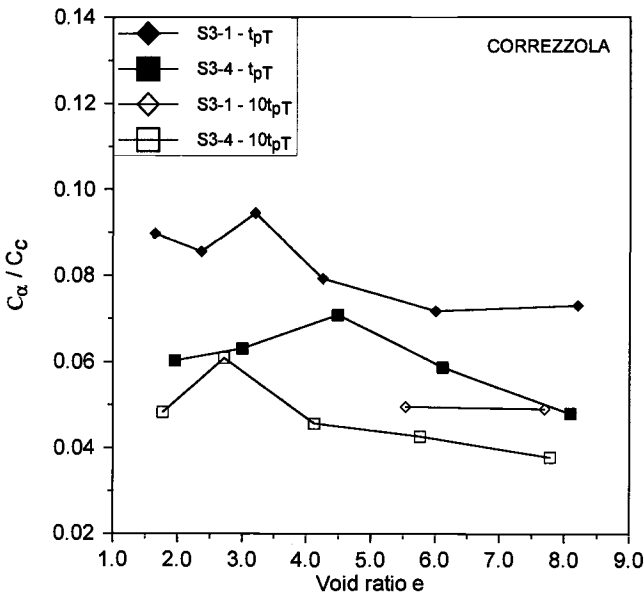


Figure 12 - $C_\alpha / C_c$ versus e for Correzzola peat
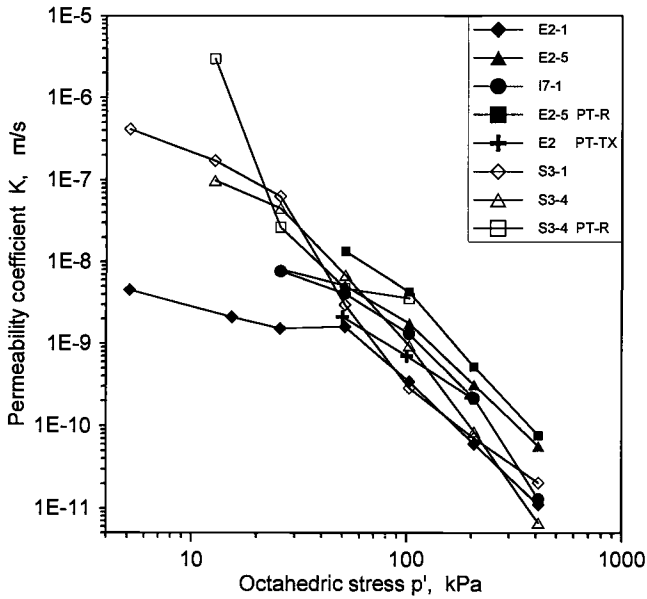
Figure 13 - *Permeability coefficient versus octahedric stress*
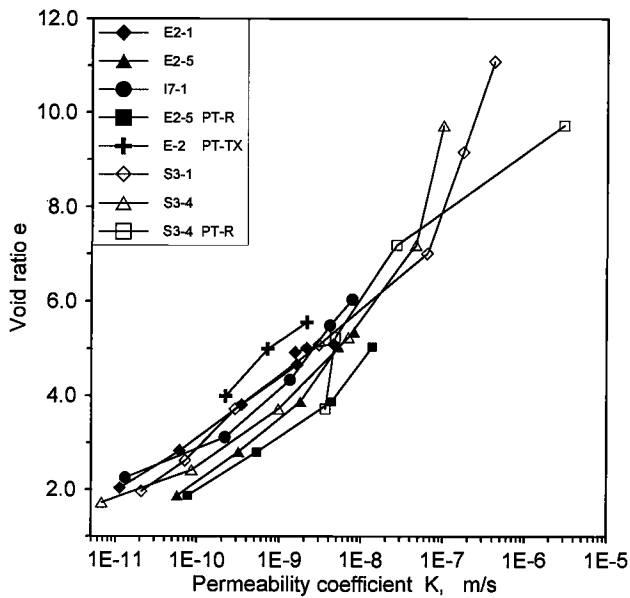


Figure 14 - *Permeability coefficient versus void ratio*

about 100% and the difference decreases with load level. The permeability measured in the triaxial cell for Adria peat is lower than was measured in the Rowe cell and comparable with the other tests. Since the Correzzola peat has a higher initial void ratio, the permeability related to low loads is greater than for the Adria peat, but at comparable void ratios the permeability of the two peats is quite similar.

Tavenas et al. (1983) established an empirical correlation between the log k and $e$ data for soft clay and silt deposits, with values of $C_k = \Delta e/\Delta \log k$ close to $e_o/2$. Mesri et al. (1997) determined a $C_k$ value of $e_o/4$ for peaty soils. In Figure 14 the permeability data of the Adria and Correzzola peats are plotted together versus void ratio; the $C_k$ ranges between 1.2 - 1.6 and 2.6 - 2.7 for Adria and Correzzola, respectively. The $C_k/e_o$ ratio is therefore between 0.22 and 0.28, which is consistent with Mesri's results.

## Conclusions

Peats from two different sites were tested to identify their compressibility and permeability characteristics. Both peats are classified as sapric, but one is over-consolidated and the other is normal-consolidated. Findings were also compared with previous data obtained using a fabric peat collected at the first site.

The different long-term behavior detected is attributable to the different fiber content of the peats, with a more marked tertiary compression stage for the fibrous peat.

The time of the end of primary consolidation changes depending on the method used (Taylor, Casagrande and pore pressure measurement). Each method has its drawbacks: the pore pressure measurement time is sometimes very short, the Taylor method can be applied to all load increments, but the time determined is often shorter than the one found with pore dissipation; the Casagrande method is difficult to apply to over-consolidated soils and the EOP time is often different from $t_{pU}$.

The $C_c/C_\alpha$ ratio is usually confined between 0.05 - 0.08, but the uncertainty connected to the evaluation of $t_p$ causes a greater scattering in the values related to $t_p$.

Permeability diminishes considerably with increasing load, and the $C_k/e_o$ ratio is about 0.25, consistent with results in the literature for these materials.

## Acknowledgments

## References

Colleselli, F. and Cortellazzo, G., 1998, "Laboratoring Testing of an Italian Peaty Soil", *International Symposium on Problematic Soils - IS-TOHOKU '98*, Sendai.

Dhowian, A. W., and Edil, T. B., 1980, "Consolidation Behavior of Peats", *ASTM Geotchnical Testing Journal*, Vol. 3, No. 3, pp. 105-114.

Fox, P. J., Edil, T. B., and Lan, L. T., 1992, "$C_\alpha/C_c$ Concept Applied to Compression of Peat", *Journal of Geotechnical Engineering*, ASCE, Vol. 118, No. 8, pp. 1256-1263.

Kabbaj, M., Tavenas, F., and Leroueil, S., 1988, "In Situ and Laboratory Stress-Strain Relationships", *Geotechnique*, Vol. 100, No.1, pp. 38-83.

Ladd, C. C., 1973, *Estimating Settlement of Structures Supported on Cohesive Soils*, MIT Soils Pubblication No. 272, 99 pp.

Landva, A. O. and Pheeney, P. E., 1980, "Peat Fabric and Structure", *Canadian Geotechnical Journal*, Vol. 17, No. 3, pp. 416-435.

Mesri, G., 1986, "Discussion of Post Construction Settlement of an Expressway Built on Peat by Precompression", *Canadian Geotechnical Journal*, Vol. 23, No. 3, pp. 403-407.

Mesri, G. and Choi Y. K., 1985, "The Uniqueness of End-of-Primary (EOP) Void Ratio Effective Stress Relationship. *Proceedings of 11th International Conference on Soil Mechanics and Foundation Engineering*, Vol. 2, pp. 587-590.

Mesri, G. and Godlewski, P. M., 1977, "Time- and Stress-Compressibility Interrelation-ship", *Journal of Geotechnical Engineering*, ASCE, Vol. 105, No. 1, pp. 106-113.

Mesri, G., Stark, T. D., Ajlouni, M. A., and Chen, C. S., 1997, "Secondary Compression of Peat With or Without Surcharging", *Journal of Geotechnical and Geoenvironmental Engineering*, ASCE, Vol. 123, No. 5, pp. 411-421.

Tavenas, F., Jean, P., Leblond, P., and Leroueil, S., 1983, "The Permeability of Natural Soft Clays. Part II: Permeability Characteristics", *Canadian Geotechnical Journal*, Vol. 20, No. 4, pp. 645-660.

# Field Performance

Ian R. McDermott[1] and Gilliane C. Sills[2]

**In-Situ Measurement of Small Strain Shear Stiffness of High Water Content Contaminated Dredge Spoils**

**Abstract:** Two intrusive in-situ measurement systems, the C-CORE Shear Wave Profiling System and the Oxford University Densimeter, were used to carry out in-situ profiles of bulk density and shear wave velocity in contaminated dredge spoils. The spoils have high water content and, at the time of the survey, exhibited densities in the range of 1160 kg/m³ to 1302 kg/m³ and undrained shear strengths in the range of zero to 2.7 kPa, in the uppermost 3.85 metres of the deposit. The objective of using the above technologies was to provide a profile of in-situ small strain shear stiffness of the deposit through the combination of the bulk density and shear wave velocity measurements.

Small strain shear stiffness values were calculated to produce a profile 3.85 metres deep within the deposit. These data revealed much information about the in-situ conditions of the deposit. The upper 1.00 metre was unable to support the transmission of shear waves and therefore was assumed to have zero shear stiffness. This upper region represented the most recent deposit in this area of the repository and it is likely that this material had had insufficient time to develop a continuous, soil matrix. These zero stiffness measurements were coincident with the zero undrained shear strength measured using a shear vane apparatus. Beneath this surface layer, three other distinct layers were found based on the small strain shear stiffness measurements. The maximum value of stiffness, which was measured at the bottom of the profile, was 129 kPa ± 3 kPa. There was some evidence to suggest that shear wave amplitude and velocity were affected by gas contained within the sediment. Close correlation between shear velocity and stiffness and that of undrained shear strength was found in the upper region of the deposit.

**Keywords:** in-situ measurement, small strain shear stiffness, bulk density, undrained shear strength, dredge spoils, soft soil

[1]Director, Geophysics at C-CORE, Memorial University of Newfoundland, St. John's, Newfoundland, Canada A1B 3X5.
[2]University Lecturer, Department of Engineering Science, University of Oxford, Oxford, United Kingdom, OX1 3PJ.

243

## Introduction

The Slufter is a 260ha storage depot for contaminated dredge material from the Rhine delta. The material is removed from the delta using trailing suction hopper dredges. The dredged material is pumped via a hydraulic pipeline into the Slufter. In the Slufter, the dredge material is spread under water, over a large area using a discharge pipe equipped with a diffuser. This provides an even spread of discharge material and helps to reduce the turbidity around the discharge opening. An echo sounder record across the Slufter displays a bed which has a terraced appearance, the result of sequential deposition of dredged material. The cost of building the Slufter was $75 million  and it is designed to contain 150 million m³ contaminated dredge spoils.

The contaminated sediments located in the Slufter are monitored on a regular basis by the Port of Rotterdam authorities for variation in geotechnical properties. This paper describes the activities of a joint C-CORE/Oxford University team at the site to profile in-situ bulk density and shear wave velocity with the ultimate objective of determining the small strain shear stiffness profile of the dredge spoil located within the Slufter basin. To achieve this, two intrusive in-situ measurement systems  were used at the site: the C-CORE Shear Wave Profiling System (SWPS) and the Oxford University Densimeter, which is designed to profile  bulk density. Although other shear wave measurements systems have been reported in the literature (Barbagelata et al 1991, Campenella and Davies 1994) these have been designed for use in much stiffer soils. The SWPS and Densimeter are specifically designed for profiling soft soil properties such as might be found in waste disposal sites. A brief description of the systems is given below. Shear vane measurements were carried out at the site at the same time but not by the C-CORE/ Oxford University team. These data are presented here courtesy of the Dutch Ministry of Transport, Public Works and Water Management as a comparative data set.

## Theoretical Considerations

For an elastic, isotropic, homogeneous and unbounded material, the small strain shear stiffness, henceforth referred to as shear stiffness, is related to the shear wave velocity and the bulk density by the equation:

$$G_{max} = V_s^2 \times \rho \qquad (1)$$

where
$G_{max}$ = small strain shear stiffness
$V_s$    = shear wave velocity
$\rho$     = bulk density

Shear stiffness is therefore an interpreted parameter, since it is based on a number of assumptions. In a liquid saturated sediment these assumptions are presumed valid in the horizontal plane for small strain shear waves.

There is considerable evidence that shear stiffness magnitude is dependent on strain level, with significantly higher values being measured at small strains in apparatus such as the resonant column (Doroudian and Vucetic 1995). The value calculated from the shear wave velocities described herein would be expected to be an appropriate value for small strains (strains < $10^{-6}$ ), this has been confirmed by Dyvik and Madshus (1985), who showed a close linear correlation between shear modulus measured in the resonant column with that determined using shear wave bender elements.

**Instrumentation**

*Shear Wave Profiling System and Measurement*

Measurements of shear wave velocity and amplitude were determined using a Shear Wave Profiling System (SWPS). This comprises a transmission probe and data acquisition hardware. The transmission probe consists of a single pair of transmit/receive shear wave transducers. These shear wave transducers consist of a pair of piezo-electric bender elements encapsulated in a thin insulating epoxy resin coating. The shear wave transducers, having a dimension of 20 mm x 28 mm x 4 mm, are operated in cantilever mode (that is, clamped at one end whilst the other end was free to vibrate) orientated vertically as shown in Figure 1. In water the transducers have a resonant frequency of 1.5 kHz ± 3 Hz. The spacing between the transmitting and receiving transducers was a fixed distance of 200 mm.

The data acquisition system comprises a pulse excitation unit, signal conditioning hardware including a 60 dB amplifier, a bandpass filter and a signal averaging unit, and a Tektronix TDS420 digital oscilloscope which was used to display the waveforms.

In operation, the transmission probe is lowered into the sediment and held stationary during the measurement procedure. The transducer is energized in a pulse excitation fashion using the rising edge of 20 V square wave such that a small strain amplitude, horizontally polarized, shear wave is generated in the soil. The transit time for the shear waves to travel the known path length (200 mm) between the transmitting and receiving transducers yields the velocity in the sediment. It should be pointed out that the measurement and interpretation of shear waves using bender elements has recently received much discussion in the literature (Viggiani and Atkinson 1995, Jovičić et al 1996, Nakagawa et al 1996, and Arulnathan et al 1998). Based on Jovičić et al (1996) findings, the shear waveforms recorded by the SWPS, generated by a square wave excitation voltage, were interpreted using the transit time associated with the first reversal point ("peak travel time") of the waveform. This interpretation is in agreement with that used by Dyvik and Madshus (1985) according to Jovičić et al (1996). Shear wave velocity can be measured to an accuracy of ± 1% to ± 4%, depending on the stiffness of the
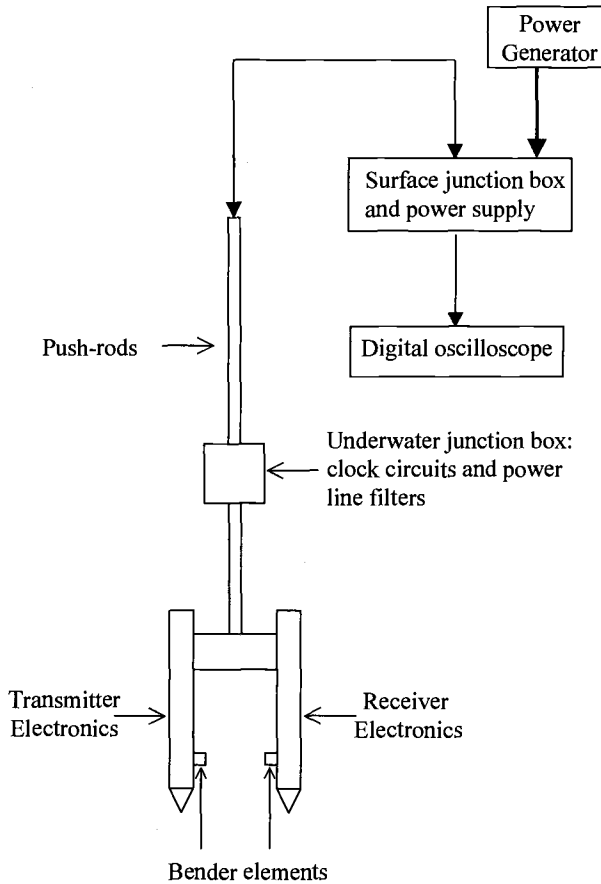
Figure 1- *Schematic of the Shear Wave Profiling System*

deposit, using this technique.

Relative changes in amplitude can also be monitored using the SWPS. The oscilloscope was used to measure the amplitude of the received shear waveform. This was achieved by centering the received waveform about zero and measuring the maximum positive deviation from zero of the wave on the oscilloscope.

*Bulk Density Measurement*

The bulk density measurement system is described in detail in Parker et al. (1975); the main points are dealt with here. The in-situ bulk density is determined using a gamma ray transmission probe which links the bulk density of a sediment with the degree of gamma

ray attenuation. This probe consists of a collimated 3 millicurie Ba[133] point source and a detector comprising a NaI crystal, a photomultiplier assembly and counter ratemeter. The source and detector are held a fixed distance 150mm apart. The probe is calibrated by placing it in three or four uniform soil slurries of known density to obtain the calibration constants $N_0$ and $k$ in the equation linking the count rate $N$ obtained from the photomultiplier with the bulk density $\rho$:

$$N = N_0 \exp(-k\rho) \tag{2}$$

The accuracy of density measurement depends on the speed with which the probe is lowered, and the variability of the soil, since the measured value is obtained by a rolling integration. Typical values of accuracy during a slow continuous deployment are around $\pm 20$ kg/m$^3$.

In the Slufter, the Densimeter was lowered slowly and steadily for about 1 m at a time, and then was held stationary for 30 seconds or more to obtain a more accurate reading. This allowed the accuracy of the continuous profiles to be assessed.

**Field Procedure**

Measurements were made from a mobile operational platform which was secured, during the profiling procedure, to a fixed concrete measurement platform located in the northern sector of the Slufter. The platform was equipped with a hydraulic push-frame to which the Densimeter and SWPS transmission probe were attached using standard Fugro push-rods. The units were then pushed into the Slufter deposit. The depth of penetration was measured directly from the push-frame to an estimated accuracy of $\pm 0.01$ metres.

The bulk density, shear wave velocity/amplitude and shear strength measurements were made in a series of profiles located in a straight line with 5 m separation between each of the profiles 1, 2 and 3, and 3 m between profiles 3 and 4. Profiles 1 and 2 comprise bulk density profiles logged in a continual manner as the densimeter was lowered to a depth of 2.00 m and 3.88 m respectively in the bed. Profile 3 involved measuring velocity and amplitude at 0.2 metre intervals within the bed to a depth of 5.45 metres. Measurements of in-situ undrained peak and remoulded shear strength (Profile 4) were made at intervals of 0.25 metres to a depth of 4.55 m within the deposit with an in-situ vane.

**Results and Data Analysis**

The densimeter count rate profiles were converted to bulk density using the calibration equation established in the laboratory. The resulting bulk density profiles for Profile 1 and 2 are shown in Figure 2a. The values obtained from the stationary readings coincided

with the output from the continuous profiles at those levels, providing confidence in the structural detail visible in the profiles. Shear wave amplitudes obtained in Profile 3, shown in Figure 2c, also shows considerable variation along the length of the profile.

The shear wave velocity was calculated using the travel time associated with the first reversal point ($t_p$) of the recorded shear waveform and the travel path distance (x) using Equation 3. Because the SWPS generates horizontally polarized shear waves, the shear wave velocity computed using Equation 3 is appropriate for horizontal shear. It should be pointed out that vertically polarized shear waves may have a different velocity at the same location in the soil, however this has yet to be established in such soft soils as reported here.

$$V_S = \frac{x}{t_p}$$    (3)

The resulting velocity profile is shown in Figure 2b.

The shear wave velocity and bulk density data were used to compute a shear stiffness profile for the deposit using Equation 1. Again this must be considered to be a horizontal shear stiffness for reasons described above. Data from Profile 3 and bulk density values, from the same elevation in the bed as the shear wave data, from Profile 2 were used for the computation. The resulting profile is shown in Figure 3a. The undrained and remoulded shear strength profiles are also shown in Figure 3b.
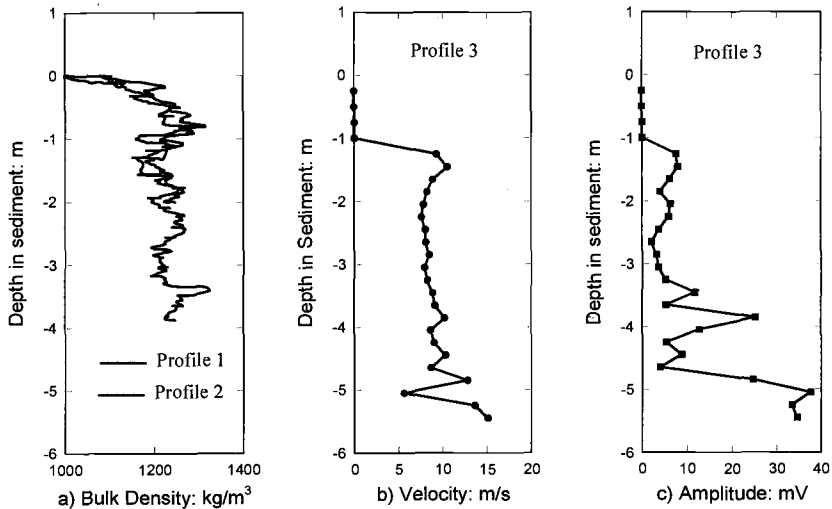


Figure 2 - *Bulk Density, Shear Wave Velocity and Relative Amplitude Profiles*
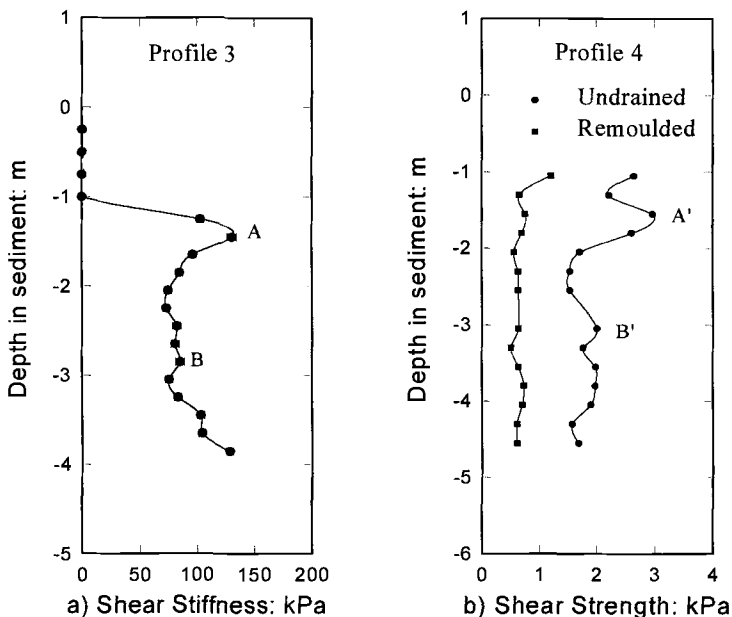
Figure 3 - *Profiles of Small Strain Shear Stiffness and Undrained Shear Strength*

## Interpretation of Results

The density profiles of Figure 2a show considerable similarity and therefore it is reasonable to assume that Profile 3 would have a similar density profile and it is upon this assumption that the following data interpretation is based.

*In the depth range between the bed surface and a depth of 1.00 m,* the density increased from that of the overlying water to around 1280 kg/m$^3$. Despite this increase, shear waves could not be transmitted through the sediment bed. This suggested that the deposit had virtually zero stiffness in this region and could therefore be considered a fluid. This interpretation was reinforced by differential piezometer measurements in this layer which suggested that the pore water pressures were very high, close to the values of total stress obtained by integrating beneath the density profile. The shear vane was also unable to provide a value of undrained shear strength in this upper part of the deposit (Opstal, 1998).[3]

*In the depth range 1.25 m to 1.85 m within the sediment bed,* shear waves were

---

[3] Opstal, A. Th. P. J., 1998, personal communication.

observed and shear wave velocity recorded. Shear wave velocity ranged from 10.5 m/s ± 0.3 m/s to 8.2 m/s ± 0.3 m/s in this region. The density dropped a little from the highest value that occurred around 1 m, which may indicate the presence of some gas. This is consistent with the gas release which was evident during the profiling procedure at all profile locations.  If this is indeed the explanation, it appears that there was not sufficient gas to prevent the passage of the shear waves. The shear stiffness takes on a range of values from 131 kPa ± 3 kPa to 84 kPa ± 3 kPa. The high value of shear stiffness (labelled A in Figure 3), having a magnitude of 131 kPa at 1.45 m, is reflected in the undrained peak shear strength measurements (A' in Figure 3). A maximum value of 3.0 kPa at a depth of 1.50 m was recorded. The difference in depths of the peak values are a reflection of the different measurement intervals used in each of the measurement techniques, and due to the profiles being offset by 3 m. The properties of this region are distinct from materials above and below and so it is concluded that this is a distinct layer of 0.6 m thickness.

*In the depth range 2.05 m to 3.25 m* the shear wave amplitude was reduced to very small values, between 2.2 and 3.6 mV, making identification of the shear waveform onset very difficult. As a consequence shear stiffness was determined, less accurately, by using the corrected travel time of the peak. The shear stiffness ranges from 73 kPa ± 4 kPa to 85 kPa ± 4 kPa. Again, the shear vane test results reflect similar trends in this region. For example, the small peak and trough (labelled B and B' in Figure 3) are obvious in both the shear stiffness and undrained shear strength results.

*In the depth range of 3.45 m to 5.45 m* the shear velocity increases from 8.6 ± 0.3 m/s to 15.1 ± 0.2 m/s. Shear wave velocity and amplitude are erratic in this region which suggests that the probe could have been moving in and out of gas lenses/pockets as it was pushed into the bed.  The shear wave velocity gradient has a positive trend in this region of the bed. The increasing shear wave velocity is probably indicative of a more stable and competent material at depth. Below a depth of 5.05 m the shear wave amplitude is considerably larger than that measured in overlying sediments, with  magnitudes in excess of 30 mV. Depths of 3.85 m and 3.88 m represent the maximum depths profiled for shear stiffness and bulk density respectively. The shear stiffness  profile increases from a value of 103 ± 3 kPa at 3.25 m to a value of 129 ± 3 kPa at a depth of 3.85 m. In this region the undrained shear strength profile fails to reflect the trend shown in the shear stiffness measurements: instead the profile reveals  uniform shear strength  with depth with a mean value of 1.8 kPa (standard deviation of 0.2 kPa).

To conclude this section, a summary figure is presented (Figure 4) illustrating the 4 distinct layers and the associated mean physical properties.

**Discussion**

The Slufter disposal site represents a particularly challenging site due to its complex and recent depositional history. Measurements of in-situ bulk density and shear wave velocity have been used  to demonstrate how a profile of small strain shear stiffness can be obtained in a soft soil deposit and, have shown that it provides a useful means of characterizing soft sediments. Concerns over the validity of the assumptions discussed in the "Theoretical Considerations" section, regarding the isotropy and homogeneity of soft

soils which may contain organics or gas, are justified. The presence of gas in the sediments presents a three phase media (solid/liquid/gas) which is compositionally and behaviourally very complex. The gas can have a significant effect on the storage capacity of a disposal site such as the Slufter, and on the shear strength of the sediment bed. The gassy soil can be modelled as a two-phase material consisting of saturated soil surrounding discrete gas voids, as discussed in Sills et al (1991). Such a model has been used by Wichman (1999) to describe the effects of the gas on the consolidation of the bed.

The two measurements of shear stiffness and shear strength can be expected to be linked, since the consolidation process that increases one also increases the other. For soft normally consolidated soils which are nevertheless stiffer than those in the Slufter, the ratio $G/s_u$ typically lies in the range 50 to 150, where $G$ is obtained as the secant modulus at 50% of the strain associated with yield in a triaxial test. It is therefore valuable to compare the profiles of stiffness and strength in the Slufter. However, before doing this, it is useful to make a number of observations regarding the two data sets. The shear vane test, a static test, involves a relative rotational movement of a cylindrical volume of sediment and the surrounding material. On the other hand, shear stiffness, derived from a dynamic test, is an interpreted parameter from the measurement of the transmission of small strain shear waves (shear wave velocity) combined with bulk density in the sediment. It is well documented for much stiffer soils that dynamic measurements of elastic moduli are several magnitudes higher than those given by static measurement techniques (Lambe and Whitman 1979). There is mounting evidence that this remains true for softer soils also (Theilen and Pecher 1991, McDermott 1998). It might therefore be expected

-------------------------------------- 0 m
**Layer 1**
Fluid Mud Layer
Thickness:1.25 m
Stiffness: zero
Shear strength: zero
Mean density: 1188 kg/m³
------------------------------------------- 1.00 m
------------------------------------------- 1.25 m
**Layer 2**
Thickness:0.6 m
Mean density: 1213 kg/m³
Mean stiffness: 104 kPa
Mean shear strength: 2.5 kPa
------------------------------------------- 1.85 m
------------------------------------------- 2.05 m
**Layer 3**
Thickness: 1.20 m
Mean density: 1231 kg/m³
Mean stiffness: 79 kPa
Mean shear strength: 1.7 kPa
------------------------------------------- 3.25 m
------------------------------------------- 3.45 m
**Layer 4**
Mean density: 1252 kg/m³
Mean stiffness: 112 kPa
Mean shear strength: 1.8 kPa
------------------------------------------- 3.88 m

Figure 4 - *Interpretation Summary*

that the $G/s_u$ ratio for the Slufter muds obtained from the small strain stiffness measurements would be higher than the soft soil range quoted above, but this is not in fact the case. In layers two and three, the ratio of the mean values is around 40, and it reaches 70 in layer four. Reviewing Figure 3, it is clear that there is considerable similarity between the patterns of the stiffness and strength results. The upper metre of the deposit registered zero stiffness (Figure 3) and zero shear strength.[3] Immediately below this region lay two more distinct layers which display similar trends in the stiffness and  undrained shear strength profiles. It is only in the last layer, Layer 4, that the trends differ.  The explanation may lie in the fact that the shear velocity and density are both more local measurements than that of shear strength, which is inevitably averaged over the height of the vane.  The high value of shear stiffness just above the 4 m depth is mainly due to the isolated high velocity and amplitude of shear wave signal recorded at this level, and it may be that this represents a thin stiffer layer.

The work described above has led C-CORE, with the assistance of Oxford University, to develop  an in-situ Soil Stiffness Probe for the profiling of density and stiffness in soft soil deposits. The technology is now being used in various soft soil applications (McDermott 1998, McDermott and English 1997).

**References**

Arulnathan, R., Boulanger, R. W., Riemer, M. F., June 1998, "Analysis of Bender Element Tests," *Geotechnical Testing Journal,* GTJODJ, Vol 21, No 2, pp. 120-131.

Barbagelata, A., Richardson, M., Miaschi, B., Muzi, E., Guerrini, P., Troiano, L. and Akal, T., 1991, *"ISSAMS: an In Situ Sediment Acoustic Measurement System,"* Shear Waves in Marine Sediments, J. M. Hovem, M. D. Richardson and R. D. Stoll, Eds., Kluwer Academic Publishers, Dordrecht, The Netherlands, pp. 305-312.

Campanella, R. G. and Davies, M. P., 1994, "The Seismic Piezocone: A Practical Site Investigation Tool," *Geophysical Characterization of Sites,* International Society for Soil Mechanics and Foundation Engineering Technical Committee # 10, R. D. Woods, Ed., International Science Publisher, New York, pp. 49-55.

Deibel, I. K., Zwakhals, J. W. and Opstal A. Th. P., 1996, "Nine Years Experience in Filling a Large Disposal Site with Dredged Material," *Characterization And Treatment of Sludge CATS III*, Oostende, Belgium, pp.219-231.

Doroudian, M. and Vucetic, M., 1995, "A Direct Simple Shear Device for Measuring Small Strain Behavior," *Geotechnical Testing Journal*, ASTM, Vol. 18, No. 1, pp. 69-85.

Dyvik, R. and Madshus, C., 1985, "Laboratory Measurement of $G_{max}$ using Bender Elements," In *Advances in the Art of Testing Soils Under Cyclic Load Conditions*, American Society for Civil Engineering, Vijay Kholsa, Ed., New York, pp. 186-196.

Lambe, T. W. and Whitman, R. V., 1979, *Soil Mechanics, SI Version*, John Wiley and Sons, Chichester, pp. 154-155.

Jovičić, V., Croop, M. R., and Simić, M., 1996, "Objective Criteria for Determining $G_{max}$ for Bender Element Tests," *Geotechnique*, Vol. 46, No. 2, pp. 357-362.

McDermott, I. R., 1998, "An Investigation into the Correlation between the Sediment Parameters Influencing Depth of Mine Penetration and the Small Strain Shear Stiffness of Marine Sediments," Contract Report for the Defence Research Establishment Atlantic DREA CR 98/409.

McDermott, I. R., 1997, "The Use of Shear Wave Transmission as a Non-Destructive Tool to Assess Soft Soil Stiffness in Dredging Applications," In *Modern Geophysics in Engineering Geology*, Geological Society Engineering Geology Special Publication No. 12, McCann, D. M., Eddleston, M., Fenning, P. J. & Reeves, G. M., Eds., pp. 347-353.

McDermott, I. R. and English, G. E., 1997, "Geophysical Characterization of Contaminated Muddy Sediments," *Proceedings 19th Canadian Waste Management Conference*, St. John's, Newfoundland, Canada. Session 13, Theme 5, paper 3.

Nakagawa, K., Soga, S. and Mitchell, J. K., April 1996, "Pulse Transmission System for Measuring Wave Propagation in Soils," *Journal of Geotechnical Engineering*, ASCE, Vol. 122, No. 4, pp. 302-308.

Parker, W. R., Sills, G. C. and Paske, R. E. A., 1975, "*In Situ* Nuclear Density Measurements in Dredging Practice and Control," *First International Symposium on Dredging Technology*, 17-19 September, University of Kent at Cantebury, England, Paper 3, pp. 25-42.

Sills, G. C., Wheeler, S. J., Thomas, S. D. and Gardner, T. N., 1991, "The Behaviour of Offshore Soils Containing Gas Bubbles," *Geotechnique*, Vol 41, No 2, pp. 227-241.

Theilen, F. R. and Pecher, I. A., 1991, "Assessment of Shear Strength of the Sea Bottom from Shear Wave Velocity Measurement on Box Cores and *In Situ*," In *Shear Waves in Marine Sediments*, J.M. Hovem, Richardson, M.D. and Stoll, R.D., Eds., Kluwer Academic Publishers (Netherlands), pp. 67-74.

Viggiani, G. and Atkinson, J. H., 1995, "Interpretation of Bender Element Tests," *Geotechnique*, Vol. 45, No. 1, pp. 149-154.

Wichman, B. G. H. M., 1999, "A Finite Strain Theory for Gassy Sludge," accepted for publication in *Géotechnique*.

Juan D. Quiroz[1] and Thomas F. Zimmie[2]

**Field Shear Strength Performance of Two Paper Mill Sludge Landfill Covers**

---

**Abstract:** Field vane tests were conducted on paper sludge landfill covers located in Montague and Hubbardston, Massachusetts, to measure the in-situ undrained shear strength. These landfill covers used the same type of sludge for the barrier layer, and the basic cover designs were similar. The Hubbardston Landfill closure was completed in 1993 (the barrier layer has consolidated) and the Montague Landfill closure was constructed from 1993 to 1998. Therefore, the field vane results can be directly compared and the effects of consolidation can be evaluated. The range of undrained shear strength and water content for landfill covers constructed with Erving paper sludge was between 55 kPa to 12 kPa and 100% to 180%, respectively. The undrained shear strength of the paper sludge layer increased as the water content decreased, and the undrained shear strength generally increases due to consolidation. The field vane test is a rapid and economical method for determining the in-situ shear strength.

**Keywords:** paper sludge, landfill covers, slope stability, field vane tests, shear strength

**Introduction**

The use of paper mill sludge in landfill cover systems has provided a means for recycling the residuals from the paper making process. Although, paper sludge is a non-conventional construction material, the successful completion of a number of landfill closures using paper sludge has sparked an international interest for this technology. Currently, the United States, several countries within the European Community, Canada, and South Africa are investigating the feasibility of using paper sludge as landfill cover barrier material.

From an economical standpoint, the main advantage of using paper sludge in landfill covers is that the landfill owner and the paper mill owner have the potential to save money. The landfill owner (often a municipality) saves the cost of buying clay since the paper sludge is offered at little or no cost, and the paper mill saves the cost of

---

[1] Graduate Research Assistant, Civil Engineering Department, Rensselaer Polytechnic Institute, 110 8th St., Troy, NY 12180-3590.
[2] Professor, Civil Engineering Department, Rensselaer Polytechnic Institute, 110 8th St., Troy, NY 12180-3590.

disposal, or saves valuable volume in their own monofill.  This win-win situation has
resulted in typical savings between $50,000 to $120,000 per hectare.

Several researchers (Pepin 1984, NCASI 1989, Aloisi and Atkinson 1990, Zimmie
et al. 1995, Moo-Young and Zimmie 1996, Kraus et al. 1997, NCASI 1997) have
investigated the geotechnical properties associated with paper sludges used as hydraulic
barriers.  Most of this research has focused on hydraulic conductivity.  Paper sludges
can be characterized as having high water contents, high organic contents, high
compressibilities and low shear strengths.

The integrity of a landfill cover depends on a number of factors.  Hydraulic
conductivity is usually the main design criterion for hydraulic barriers.  However, shear
strength and slope stability are also primary considerations for design and construction.
To date little data exists on the shear strength of paper mill sludge landfill covers.

In this paper, the results of field vane tests performed on the paper sludge landfill
covers of the towns of Montague and Hubbardston, MA are presented.  The paper
sludge used by the two landfill closures was provided by Erving Paper Mills, Inc.  A
testing program was developed to measure the in-situ undrained shear strength of the
Erving paper sludge after some slope instabilities occurred at the Montague Landfill.
The purpose of this paper is to identify the low shear strength ranges and unique shear
strength behavior associated with paper sludges.  In addition, factors that affect the
undrained shear strength behavior of paper mill sludge landfill covers will be discussed,
i.e., high settlement strains due to consolidation, and general cross section design
aspects.

## Landfill Characteristics and Construction History

### Hubbardston Landfill

The Hubbardston Landfill closure was completed in 1993.  The footprint of this
landfill is about 1.7 hectares and the side slopes are about 25%.  The typical cross
section of the landfill cover system is shown in Figure 1.  Moo-Young and Zimmie
(1996) presented data from this landfill with respect to hydraulic conductivity and
consolidation.  Figure 2 shows the in-situ time settlement curve of the Hubbardston
Landfill.  After about two years, the rate of settlement was significantly reduced
indicating that the paper sludge barrier layer had undergone significant consolidation.
During this two year period, the hydraulic conductivity of a particular section of the
landfill decreased from about $1 \times 10^{-9}$ m/s to about $4 \times 10^{-10}$ m/s, a decrease of about a
half an order of magnitude.  The water content also decreased from about 160% to 90%.
Moo-Young and Zimmie (1996) directly attributed the decrease in hydraulic
conductivity and water content to consolidation.

### Montague Landfill

The Montague Landfill has a footprint of 5.7 hectares and side slopes about 25%.
The typical cross section of this landfill cover system is similar to that shown in Figure
1 for the Hubbardston Landfill.  Most of the landfill closure occurred during two main
construction periods.  The first was from 1993 to 1994, when a one hectare section was

constructed. During this time, minor slope instabilities were noticed in the form of slight bulges and slumping. In these cases, the paper sludge was replaced. The second construction period was between late 1996 to early 1998 (slightly over a year in time), when the landfill closure was completed. During mid and late July 1997, several slope failures occurred immediately after construction of the cover system. The types of failure during this period ranged from slight bulges on the side slopes to a 0.2 hectare area that experienced movements of up to 1.5 m. These failures prompted the subsequent field vane testing investigation presented herein. The paper sludge in the failed areas (which corresponded to a large percentage of the recently completed area at the time) was removed and replaced by new production sludge in late 1997.
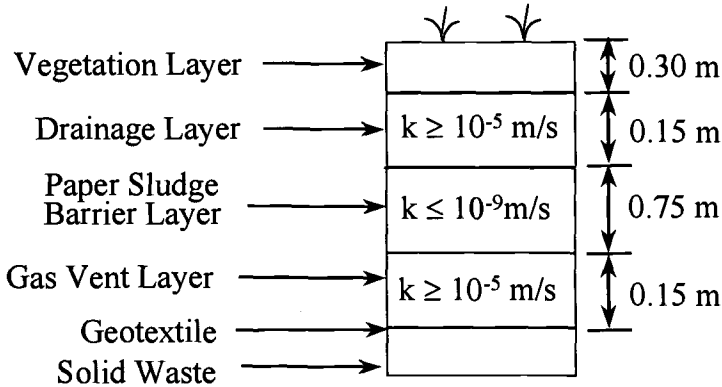


Figure 1 – *Landfill Cover Cross Section for Hubbardston and Montague Landfills.*
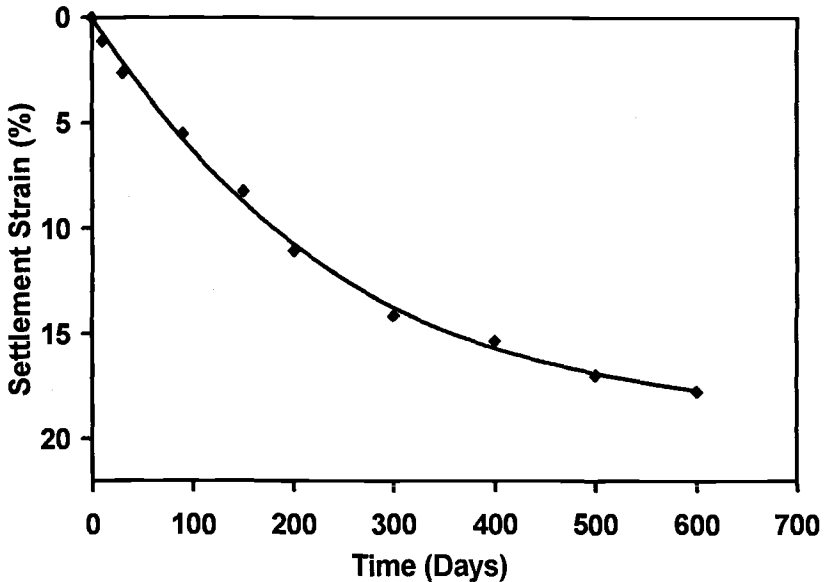


Figure 2 – *Time Settlement Curve (after Moo-Young and Zimmie (1996)).*

### Geotechnical Properties of Erving Paper Mill Sludge

The paper sludge in the Montague and Hubbardston landfill covers was provided by Erving Paper Mills, Inc. which is a recycling paper plant. The wastewater treatment plant receives about 96% of the influent from the paper mill and about 4% from the Town of Erving. This paper sludge is a blended primary and secondary sludge with an organic content of about 50%. Kaolin clay which is used to create a smooth finish for paper is the fixed solids. The sludge has a high percentage of tissues and fibers.

The geotechnical properties of the Erving paper sludge are presented in Table 1. These properties are determined from sludge produced during normal operations. The geotechnical properties of the Erving sludges are in a different range compared to compacted clays. Compacted clays used for hydraulic barriers typically have water contents less than 30% and compression indices between 0.2 to 0.4 (Lambe and Whitman 1969). The Atterberg limits for the sludge are very high and should be viewed with caution. Atterberg limits were designed for fine-grained materials, however, paper sludge is about 50% organics. In addition, Atterberg limits are difficult to measure due to the fibrous nature of the sludge. LaPlante (1993), Moo-Young (1996) and Kraus et al. (1997) concluded that Atterberg limits for paper sludge are questionable.

Table 1 – *Geotechnical Properties of Erving Paper Mill Sludge (after Zimmie and Moo-Young (1996)).*

| Water Content (%) | Organic Content (%) | Specific Gravity ($G_S$) | Plastic Limit (%) | Liquid Limit (%) | Plasticity Index | Compression Index ($C_C$) |
|---|---|---|---|---|---|---|
| 150-250 | 45-50 | 1.88-1.96 | 94 | 285 | 191 | 1.24 |
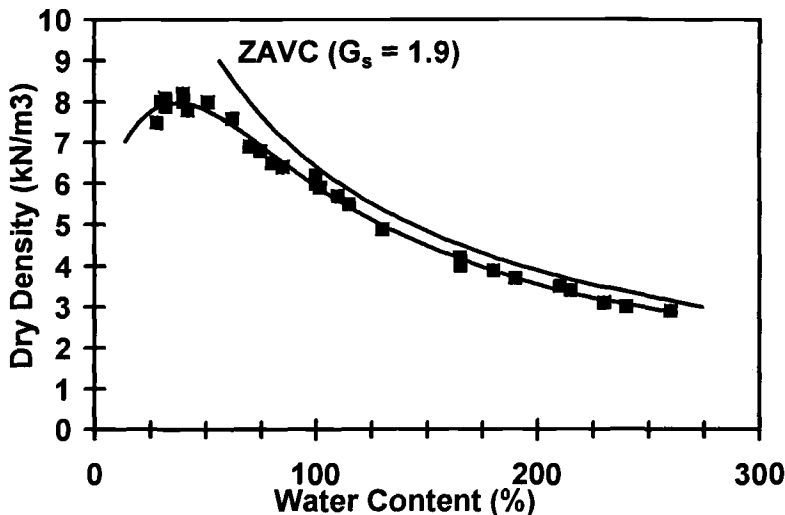


Figure 3 – *Standard Proctor Curve (after Zimmie et al. 1995).*
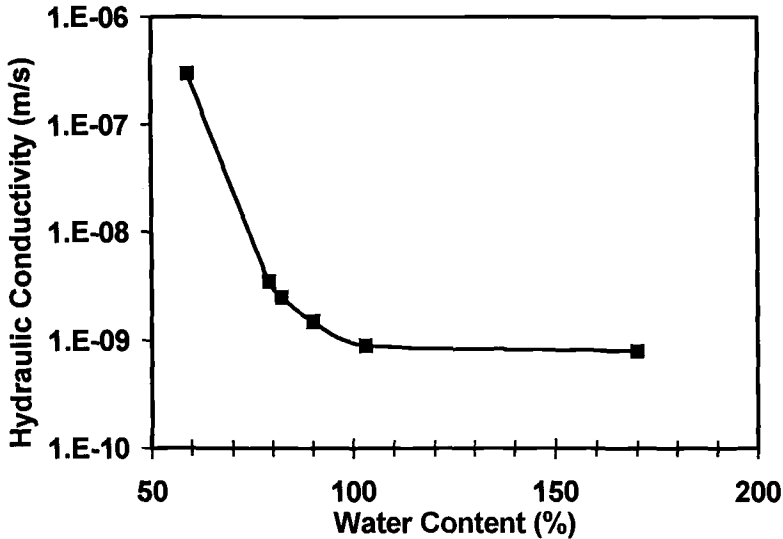
Figure 4 – *Hydraulic Conductivity versus Water Content Relationship (after Zimmie et al. 1995).*

Figures 3 and 4 present the standard Proctor curve and hydraulic conductivity vs. water content curve for the Erving paper mill sludge, respectively. Figure 4 shows the large range of water contents at which a hydraulic conductivity of less than $10^{-9}$ m/s can be achieved. These water contents are about 50% wet of optimum water content or higher (see Figure 3). The dry densities of the paper sludge are quite low, below 10 $kN/m^3$, whereas compacted clays typically have dry densities greater than 15 $kN/m^3$ and are compacted several percent wet of optimum in covers and liners.

**Field Vane Testing Procedure**

The sampling process for obtaining undisturbed samples for laboratory testing may impose a large degree of sample disturbance, a common problem with highly organic and fibrous soils. Thus, an in-situ test procedure was used. The field vane test method was used to eliminate or minimize the sample disturbance problem and measure the peak in-situ undrained shear strength of the paper sludge landfill covers. Quiroz and Zimmie (1998) describe the testing procedure using a hand-held field vane. The procedure for testing the paper sludge layer is in accordance with ASTM Test Method for Field Vane Shear Test in Cohesive Soil (D-2573) guidelines where applicable. The method presented by Flaate (1966) was also used as a guide. Remolded undrained shear strength values were not measured. A Geonor hand-held field vane that used a standard tapered vane and a calibrated Torqueleader torque wrench for soft soils was utilized for testing (see Figure 5). The test method can be summarized as follows:
1. Insert the vane directly into the paper sludge if the layer is exposed. If the layer is covered, a post-hole digger is used to excavate a hole about 15 cm to

20 cm in diameter into the paper sludge, then the vane is inserted into the paper sludge.  The depth of the test typically ranges between 30 cm and 90 cm.

2. Once the desired depth is reached, the vane is torqued and the peak undrained shear strength is measured directly.

3. A water content sample is retrieved so that the shear strength can be correlated to water content.
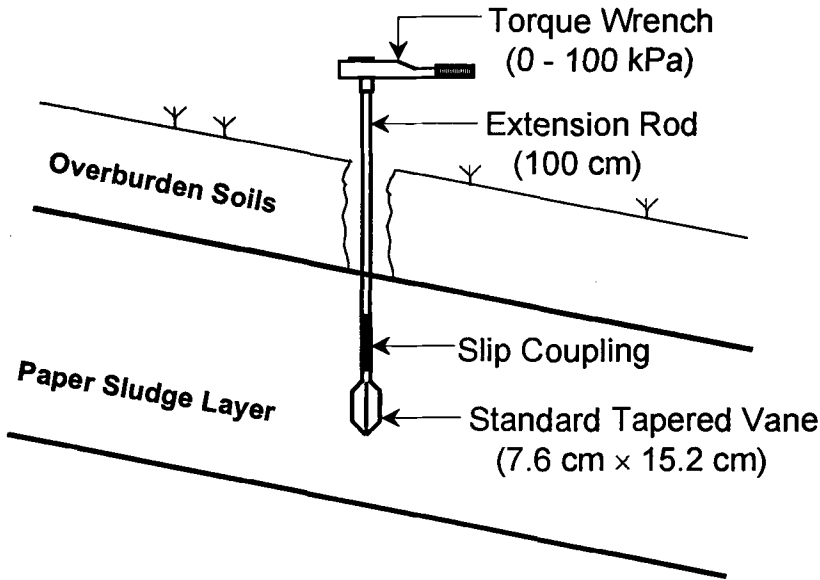


Figure 5 – *Field Vane and Test Set-Up.*

The tests can be easily performed on level ground as well as on the side slopes of the landfill.  Test times vary from 10 to 15 minutes, including excavation.  This test is simple and fast, so many tests can be performed in a short period of time.

**Results and Discussion**

*Montague Landfill*

Three testing rounds were conducted at the Montague Landfill.  The first and second testing rounds were conducted during July 1997 after each slope failure incident. The third testing round was conducted during April 1998, three months after completion of the landfill closure.  Field vane tests were also conducted in the section of the landfill that was completed in 1993, which had sufficient time to consolidate.

Quiroz and Zimmie (1998) presented the data for the first and second testing rounds (Figure 6).  These data correspond to undrained shear strength values measured for stable slopes.  The behavior is similar to that for typical normally consolidated clays,

that is, as the water content decreases the undrained shear strength increases. The ranges of undrained shear strengths and corresponding water contents is 36 kPa to 12 kPa and 120% to 180%, respectively. An average value of 23 kPa for the undrained shear strength is observed from Figure 6.
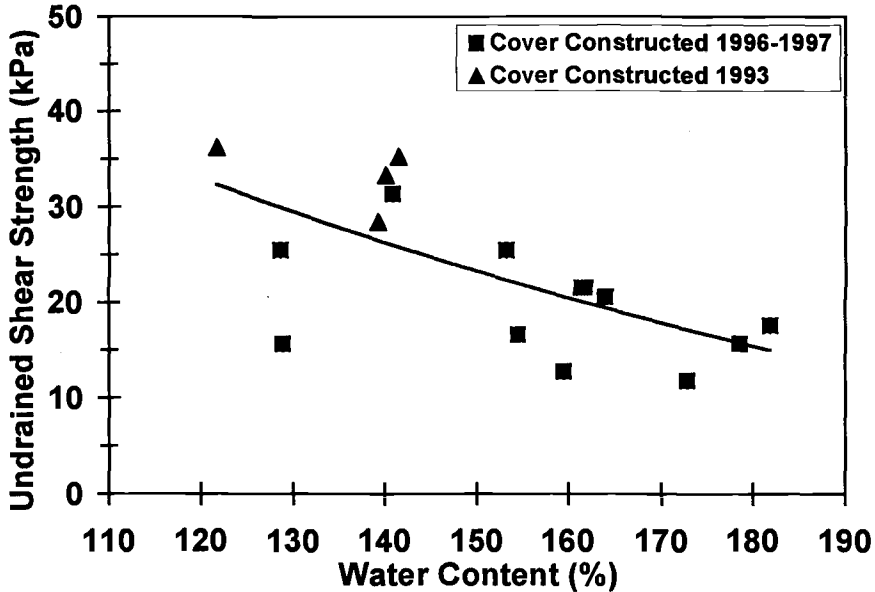


Figure 6 – *Undrained Shear Strength versus Water Content Curve for Montague Landfill, Test Rounds 1 and 2 (after Quiroz and Zimmie (1998)).*

Shear strengths measured in the section of the landfill completed in 1993 had considerably lower water contents, between 120% to 140%, and higher undrained shear strengths, from 28 kPa to 36 kPa (see Figure 6). The initial range of water contents for this area was between 140% and 180%, indicating that a decrease in water content occurred due to consolidation of the barrier layer.

Field vane tests performed on the failed sections of the landfill yielded undrained shear strengths less than 10 kPa with correspondingly high water contents. Stable sections of the landfill consistently had undrained shear strengths higher than 10 kPa. Thus, by observation, any slope area that measured higher than 10 kPa to 15 kPa was stable. Also, from a practical standpoint, a shear strength of less than 10 kPa is difficult to measure accurately. With paper sludge strengths less than 10 kPa, an average person sinks in the sludge under his own weight, and the operation of low pressure compaction equipment is difficult.

The field vane investigations suggested that the slope instabilities were caused by the high water contents of the paper sludge. If the water content is too high the undrained shear strength approaches critical values. For design this implies that an

upper bound for working water contents should be established for slope stability purposes.

A third testing round was conducted to evaluate the undrained shear strength of the newly completed sections that had previously failed and of the stable sections of the landfill. The results of the third testing round are presented in Figure 7. The range of undrained shear strength values was between 45 kPa to 15 kPa and the range of water contents varied between 105% to 175%. An average value of 28 kPa for undrained shear strength can be observed from Figure 7. Two additional tests were performed on the section of the landfill completed during 1993. These shear strengths were high (29 kPa and 37 kPa) and the water contents were moderate (154% and 140%, respectively). For the third testing round, the shear strength vs. water content trend is not as clear as that shown in Figure 6. This may be due to several factors such as a change in the quality of the paper sludge produced at the paper mill, consolidation effects that have occurred between testing rounds, and a difference in field compaction for the newly constructed sections. However, the important point is that the undrained shear strength and water content ranges for stable slopes for the third testing round are not very different from those of the first and second testing rounds.
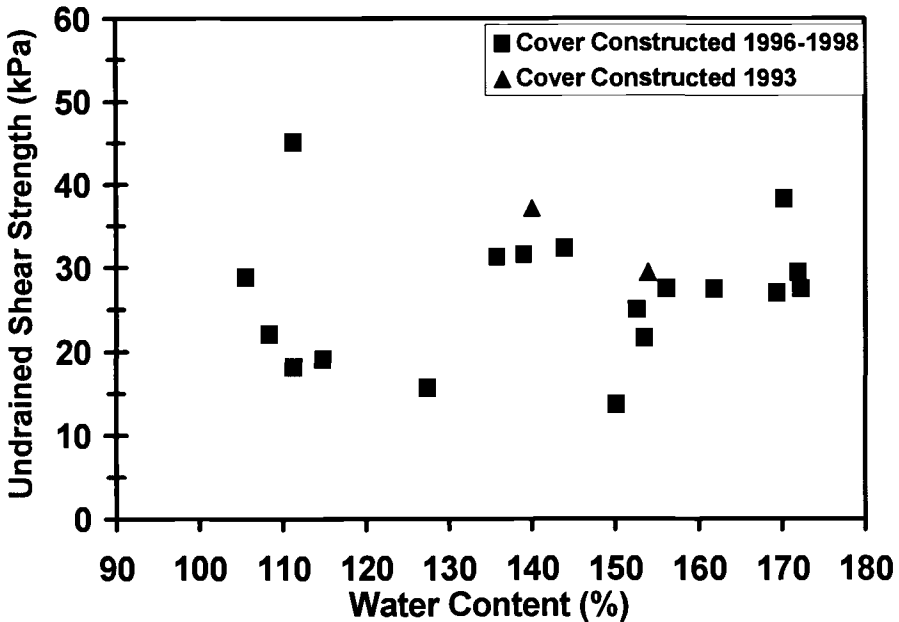


Figure 7 – *Undrained Shear Strength versus Water Content Curve for Montague Landfill, Testing Round 3.*

*Hubbardston Landfill*

Seven field vane tests were conducted during February 1998 on the Hubbardston Landfill and the results are shown in Figure 8. This landfill was completed in 1993 and as shown in Figure 1 the settlement rate has slowed considerably. Therefore, these values represent the undrained shear strength after consolidation of the paper sludge barrier. Even though the paper sludge layer is essentially consolidated, a large range of water contents exists. This is as expected, since there was also a wide range of initially high water contents measured, some greater than 200%. The range of undrained shear strengths and the corresponding range of water contents shown in Figure 8 is between 55 kPa to 14 kPa and 96% to 170%, respectively. The average value is 37 kPa which is higher than the average values determined for the Montague Landfill.
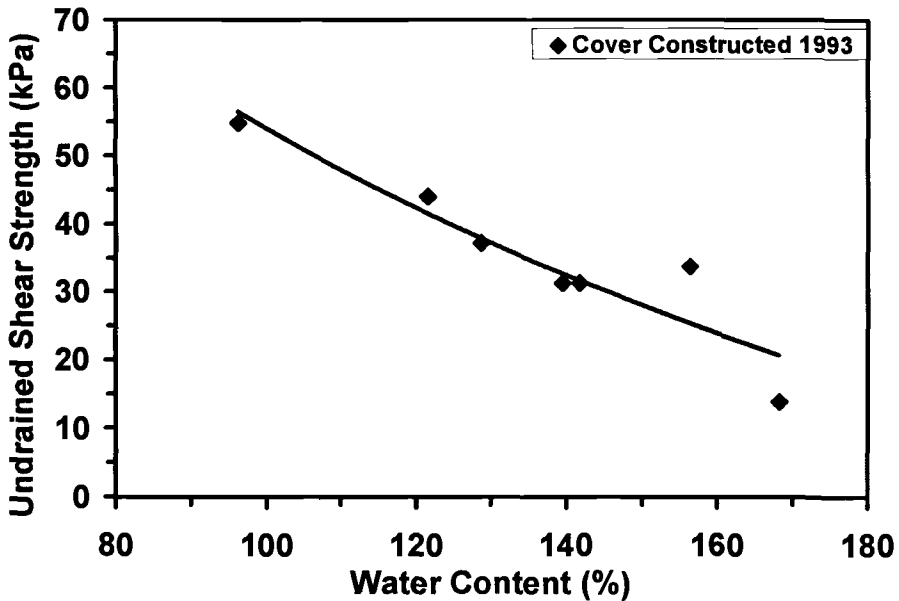


Figure 8 – *Undrained Shear Strength versus Water Content Curve for Hubbardston Landfill.*

*Factors Affecting Slope Stability of Paper Mill Sludge Landfill Covers*

There are several factors to consider in the design of paper sludge landfill covers. Design considerations include hydraulic conductivity, shear strength for slope stability, cross section design and constructability (Zimmie and Moo-Young 1995, Quiroz and Zimmie 1998b).

The high compression indices associated with paper sludge play an important role in the stability of paper sludge landfill covers. The settlement strains for paper sludge landfill covers are about 20% to 35% (Zimmie et al. 1994, Zimmie et al. 1995, NCASI 1997) even for the low overburden pressures in landfill cover systems. This settlement is much higher than the typical 2% to 3% for compacted clays. For this reason, the thickness of the paper sludge barrier layer is often about one meter thick or greater. During the settlement period large reductions in void ratio occur which decrease water content and hydraulic conductivity, and increase undrained shear strength. This trend was previously observed by Moo-Young and Zimmie (1996), and is illustrated by the data in Figures 6 and 8.

The landfill cover cross section design is important relative to the stability of the paper sludge slopes. An example of a properly designed cross section is shown in Figure 1. A drainage layer above and below the barrier layer is used to promote consolidation by allowing any excess pore water to drain freely. These drainage layers create a double drainage condition which has an important effect on the time rate of settlement of the paper sludge layer. Basic consolidation theory indicates that it takes four times longer for a soil layer to consolidate under single drainage conditions. This is an important consideration, especially when the rate of change in paper sludge properties (such as hydraulic conductivity and undrained shear strength) depends largely on consolidation.

## Summary

Field vane tests were conducted on two paper sludge landfill covers located in Hubbardston and Montague, Massachusetts (USA). The Hubbardston Landfill closure was completed in 1993 while the construction period for the Montague Landfill closure was from 1993 to 1998. The intent of the field studies was to evaluate the undrained shear strength and identify the relative ranges of shear strength for paper sludge hydraulic barriers. The same paper sludge was used for both landfill covers and the basic cover design were also similar. Thus, these field vane test results included the effects of consolidation.

For the first and second testing rounds of the Montague Landfill the range of undrained shear strengths and corresponding water contents was 36 kPa to 12 kPa and 120% to 180%, respectively. A trend of increasing undrained shear strength and decreasing water content was observed in the data. For the third testing round of the Montague Landfill the range of undrained shear strengths was between 45 kPa to 15 kPa and the range of water contents varied between 105% to 175%. The values of shear strength that corresponded to the section of the Montague Landfill completed in 1993 had lower water contents, between 120% to 154%, and higher undrained shear strengths, from 28 kPa to 37 kPa.

For the Hubbardston Landfill, the range of undrained shear strengths and the corresponding range of water contents was between 55 kPa to 14 kPa and 96% to 170%, respectively. A trend of increasing undrained shear strength and decreasing water content was reflected in the data.

Figure 9 shows a summary plot for the field vane tests performed on the Montague and Hubbardston Landfills. The overall range of undrained shear strengths and water

contents for Erving paper sludge landfill covers is between 55 kPa to 12 kPa and 96% to 180%, respectively. The field vane test is an excellent method to evaluate the in-situ shear strength for paper sludge landfill covers. The advantage of this test is its simplicity, economic feasibility and short test times.
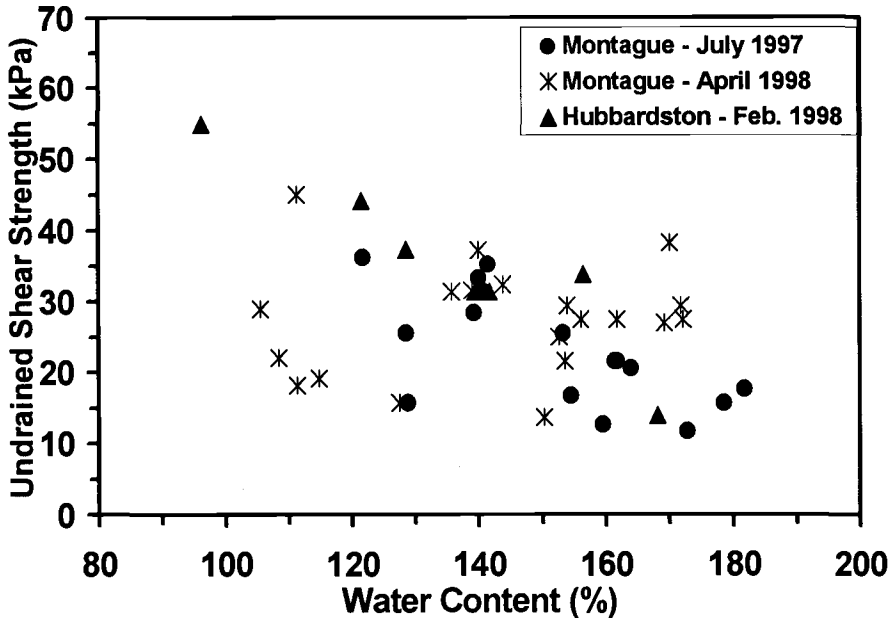


Figure 9 – *Summary Plot of the Field Vane Tests Performed on Erving Paper Mill Sludge Landfill Covers.*

## References

Aloisi, W. and Atkinson, D. S., Evaluation of Paper Mill Sludge for Landfill Cover Capping Material, Report Prepared for the Town of Erving, MA by Tighe and Bond Consulting Engineering, Westfield, MA, 1990.

Flaate, K, 1966, "Factors Influencing the Results of Vane Tests," *Canadian Geotechnical Journal*, Vol. 3, No. 1, pp. 18-31.

Kraus, J. F., Benson, C. H., Maltby, C. V. and Wang, X., 1997, "Laboratory and Field Hydraulic Conductivity of Three Compacted Paper Mill Sludges," *Journal of Geotechnical and Geoenvironmental Engineering*, ASCE, Vol. 123, No. 7, pp. 654-662.

Lambe, T. W. and Whitman, R. V., 1969, *Soil Mechanics.* John Wiley and Sons, Inc., New York, NY.

LaPlante, K., 1993, "Geotechnical Investigation of Several Paper Mill Sludges for Use in Landfill Covers," *M.S. Thesis.* Rensselaer Polytechnic Institute, Troy, NY.

Moo-Young, H. K. and Zimmie, T. F., 1996, "Geotechnical Properties of Paper Mill Sludges for Use in Landfill Covers," *Journal of Geotechnical Engineering,* ASCE, Vol. 122, No. 9, pp. 768-776.

National Council of the Paper Industry for Air and Stream Improvement, 1989, "Experience with and Laboratory Studies of the Use of Pulp and Paper Mill Solid Waste in Landfill Cover Systems," *NCASI Tech. Bulletin No. 559,* NCASI, New York, NY.

NCASI, 1997, "A Field Scale Study of the Use of Paper Industry Sludges in Landfill Cover Systems: Final Report," *NCASI Tech. Bulletin No. 750,* NCASI, New York, NY.

Pepin, R. G., 1984, "The Use of Paper Mill Sludge as a Landfill Cap," *Proceedings, 1983 NCASI Northeast Regional Meeting,* NCASI, New York, NY.

Quiroz, J. D. and Zimmie, T. F., 1998, "Field Vane Tests and Shear Strength of a Paper Sludge Landfill Cover," *Proceedings, Third International Congress on Environmental Geotechnics,* P. Seco e Pinto, ed., Lisbon, Portugal, pp. 275-279.

Quiroz, J. D. and Zimmie, T. F., 1998b, "Paper Mill Sludge Landfill Cover Construction," *Recycled Materials in Geotechnical Applications, Geotechnical Special Publication No. 79,* C. Vipulandanan and D. J. Elton, eds., ASCE, Reston, VA, pp. 19-36.

Zimmie, T. F., Mahmud, M. B. and De, A., 1994, "Simulation of Long Term Performance of Landfill Covers," *Proceedings, Centrifuge 94,* C. F. Leung, F. H. Lee and T. S. Tan, eds., Balkema, Rotterdam, pp. 375-380.

Zimmie, T. F. and Moo-Young, H., 1995, "Hydraulic Conductivity of Paper Sludges Used for Landfill Covers," *Geoenvironment 2000, Geotechnical Special Publication No. 46,* Y. Acar and D. Daniel, eds., ASCE, New York, NY, pp. 932-946.

Zimmie, T. F., Moo-Young, H. K. and LaPlante, K., 1995, "The Use of Waste Paper Sludge for Landfill Cover Material," *Green '93: Waste Disposal by Landfill; Symposium on Geotechnics Related to the Environment,* R. W. Sarsby, ed., Balkema, Rotterdam, pp. 487-495.

Ahmad N. Hussein

**The Behavior of Trial Embankments in Malaysia**

---

**Abstract:** The behavior of four trial embankments located on the west coast of Peninsular Malaysia are described. The trial embankments were located in Kuala Perlis (2 embankments), Juru, and Muar. Two construction rates were used for the construction of the embankments. A slow construction rate was used for three embankments (Kuala Perlis north embankment, Juru, and Muar) while a rapidly construction rate was used for the Kuala Perlis south embankment. No ground improvement methods were used to accelerate consolidation of the embankments. Behavior of the embankments was monitored using settlement gauges, standpipe and pneumatic piezometers, inclinometers, and heave markers. Comparison with trial embankments from temperate regions is also described.

**Keywords:** trial embankments, behavior, soft ground, Peninsular Malaysia, geotechnical instrumentation

Due to the rapid development occurring in Malaysia, more and more unsuitable land, namely soft soil and peat areas is being developed. Therefore the need to understand the field performance of embankments on soft soil deposits in tropical regions is important, as it will enable designers to back analyze and evaluate geotechnical parameters used in the design. This can lead to more economical and better embankment designs in the future. Four embankments from three trail sites located on the west coast of Peninsular Malaysia were chosen for comparison in this study.

**Location of the Trial Sites**

Data obtained from three trial embankment sites were chosen for comparison. Two trial embankments namely the north and south embankments were located at Kuala

---

Senior Geotechnical Engineer, Road Design Unit, Roads Branch, Public Works Department, Malaysia, Jalan Sultan Salahuddin, 50582 Kuala Lumpur, Malaysia.

267

Perlis (Perlis), while the other two trial embankments were located in Juru (Penang) and Muar (Johore). The locations of the trial sites are shown in Fig.1.
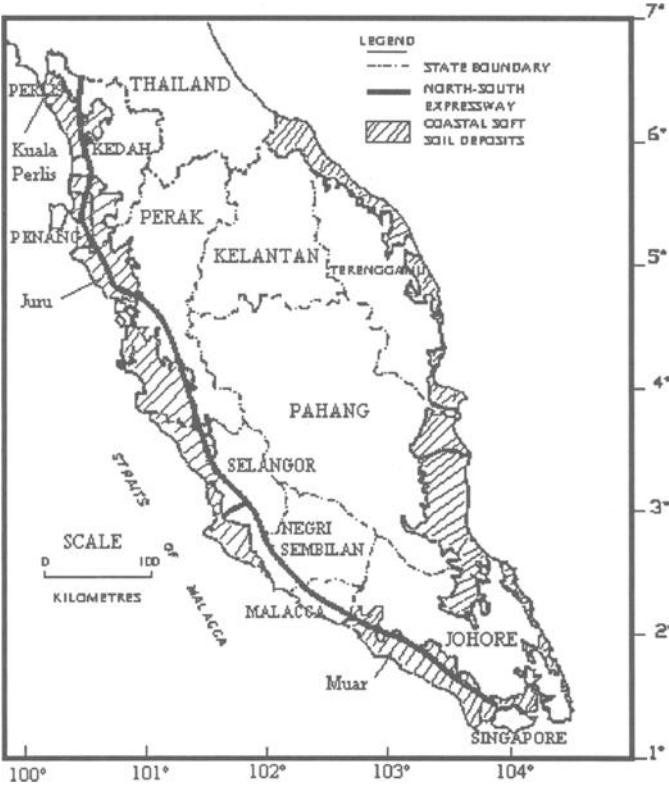


Fig.1- *Locations of the Trial Sites*

## Geotechnical Properties of the Trial Sites

A summary of the geotechnical properties of the subsoil at the three trial sites obtained from both field and laboratory tests is shown in Table 1 and Fig. 2. It can be seen that the geotechnical properties of the three trial sites are generally quite similar. Larger values are observed at the top and these values then gradually decrease with depth. Hussein (1995), Hussein et al. (1996), and MHA (1989) have described the geotechnical properties of each site in detail.

Table 1 – *Subsoil Geotechnical Properties of the Three Trial Sites*

| Soil Properties | Kuala Perlis | Juru | Muar |
|---|---|---|---|
| Thickness of Soft Soil Layer (m) | 13 | 14 | 15 |
| Liquid Limit (%) | 120-50 | 130-40 | 100-40 |
| Plastic Limit (%) | 20-40 | 20-45 | 20-40 |
| Moisture Content (%) | 70-130 | 60-130 | 50-120 |
| Unit Weight (kN/m$^3$) | 13-17 | 14-19 | 14-17 |
| Liquidity Index | 0.5-2 | 0.5-1.5 | 1-2 |
| Preconsolidation Pressure (kPa) | 30-70 | 20-100 | 20-110 |
| Overconsolidation Ratio | 1-3 | 1.5-5 | 0.9-1.9 |
| Void Ratio | 2-3 | 1-3 | 1.4-3 |
| Compression Index ($C_c$) | 1-2 | 0.5-2.5 | 0.5-2.2 |
| Undrained Shear Strength (kPa) | 10-35 | 8-35 | 8-30 |
| Sensitivity | 3-5 | 3-7 | 2-7 |
| Specific Gravity | 2.5-2.8 | 2.35-2.75 | - |
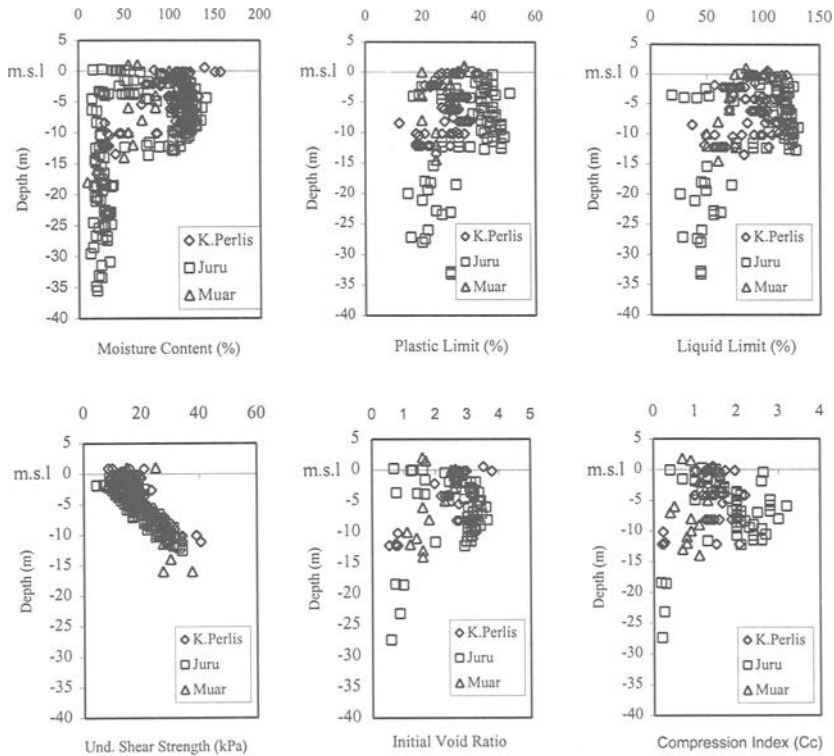


Fig. 2 – *Geotechnical Properties of the Trial Sites*

**Details of Construction Sequence, Cross-Sections, and Instrumentation**

A cross-section of each trial embankment is shown in Fig. 3. Two types of trial embankments were constructed at Kuala Perlis. The first is the south embankment, which was rapidly constructed with stabilizing berms at 2-m height and side slopes of 1:1.5. The second is the north embankment, which was slowly constructed in about one year. Both embankments have dimensions of 90 m in length and 60 m in width.

The Juru trial control embankment was slowly constructed in about 150 days with dimensions of 100 m in length and 56 m in width and a finished height of 4 m. The embankment was constructed in stages with a stabilizing berm at 2 m height and with side slopes of 1:1.5.

For Muar, although 13 trial embankments were constructed, only the behavior of the 3 m control embankment was analyzed as it has about the same finished height of fill as well as it was constructed without the use of any ground improvement methods. The Muar control trial embankment is 3 m in height and was slowly constructed in 287 days. Three rest periods were taken during the whole construction period at 18 to 35 days, 52 to 140 days, and 168 to 280 days. These rest periods were as a result of problems that occurred during the construction of an adjacent embankment. The 3 m Muar trial control embankment has dimensions of 50 m in length by 32 m in width and side slopes of 1:2 but no berms.

Figure 3 also shows the instrumentation layout for each embankment. The type of instruments that were installed includes settlement plates, pneumatic and standpipe piezometers, inclinometers, and heave markers. A hydrostatic profile gauge was also used for the Juru embankment and deep settlement gauges were used for the Muar embankment.


**Behavior of the Trial Embankments**

This section compares field measurements for the trial embankments in order to understand the general behavior of embankments on Peninsular Malaysia soft soil deposits. Detailed behavior of each embankment has already been described by Hussein and McGown (1996, 1998) for the Kuala Perlis embankments, Albakri et al. (1990) and Ramli et al. (1991) for the Juru embankment, and Malaysian Highway Authority (1989) for the Muar embankment


*Settlement*

Figure 4 shows the height of fill and settlement with time at the center of the embankment for the four embankments. It can be seen that the total settlement at the center of each embankment generally increases as the height of fill increases. The rate of settlement then decreases with time after construction was completed. It can be observed that there are some differences in the trend and magnitude of the total settlement between the four embankments. The total settlement of the four embankments at 700 days ranges from 0.9 m for the Kuala Perlis south embankment to
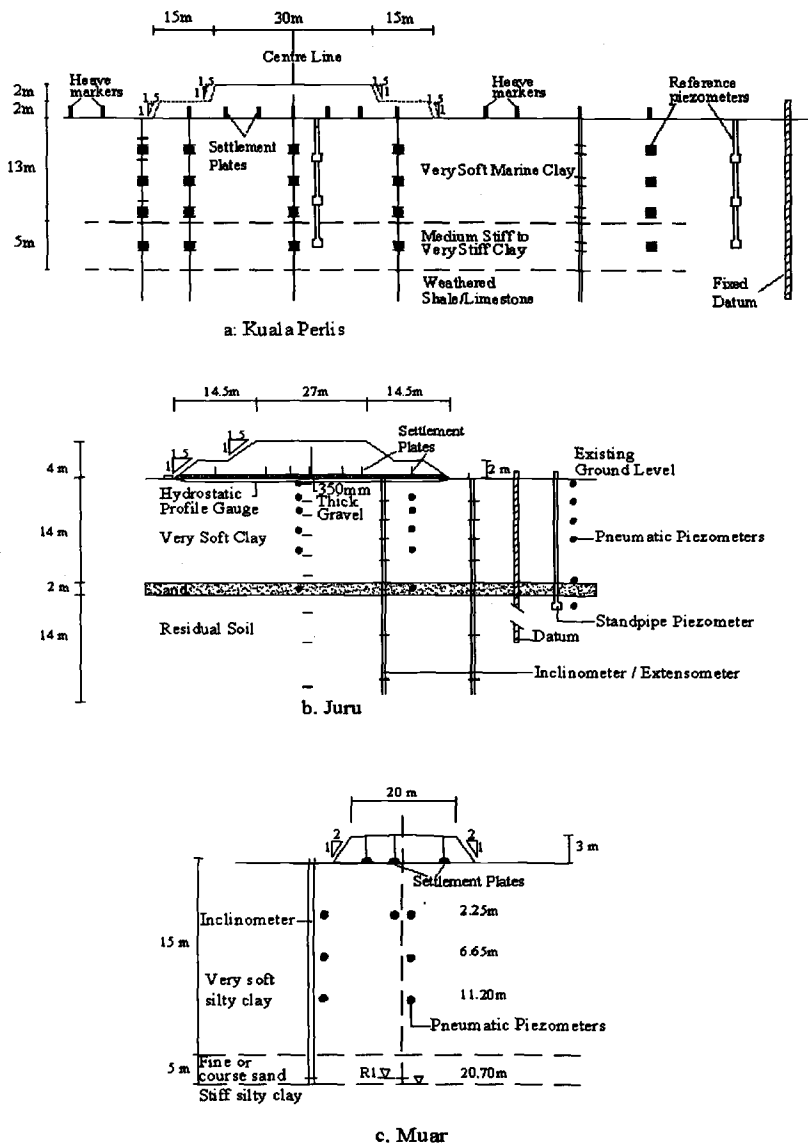
Fig. 3 – Cross-Section and Instrumentation Layout of the Trial Embankments

about 1.5 m for the Kuala Perlis north embankment. These differences can be attributed to the construction methods and the rate of construction, the duration of rest periods

taken during the construction of the trial embankment, and the final height of the fill material constructed.
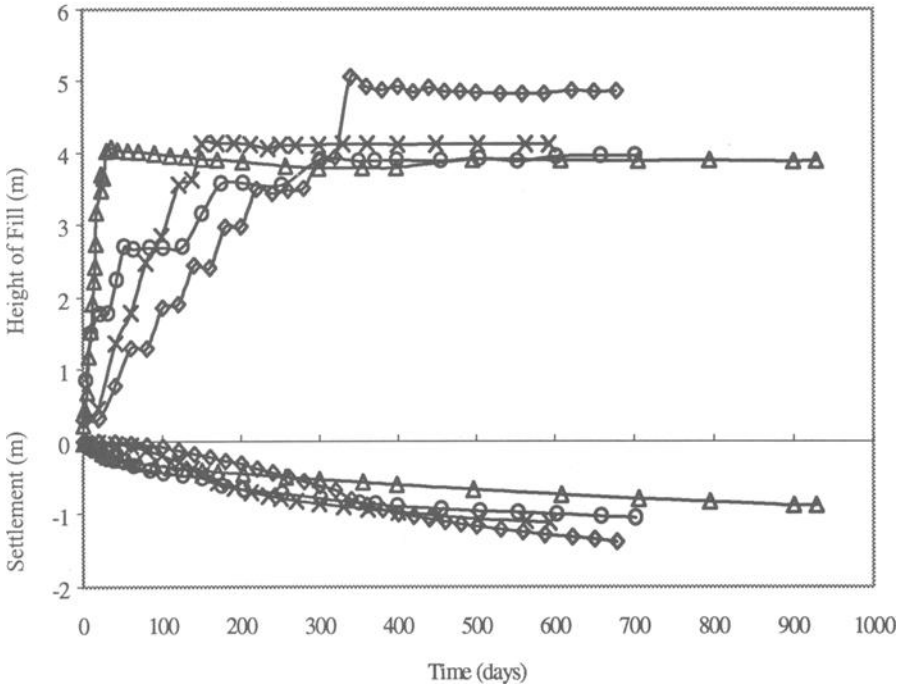


Fig. 4 – *Settlement vs. Time*

*Excess Pore Pressure Distribution*

Excess pore pressures at the center of the four embankments are shown in Fig. 5. All four trial embankments show an increase in excess pore pressures during construction with little dissipation of excess pore pressure thereafter. In general, it can be said there are similiarities between the trends and magnitudes of excess pore pressures with time obtained from Kuala Perlis trial embankment (58 to 78 kPa) and those obtained from Juru and Muar (49 to 68 kPa), although some notable differences exist. These differences again can be due to the type of construction method used, the duration of rest periods taken during the construction, and the presence and depth of ground water table. James (1970), Mesri and Choi (1979), and Mitchell (1986) have described the slow dissipation of excess pore pressure after construction period. These authors attributed this behavior to large decreases in hydraulic conductivity or to changes in soil structure during consolidation. The simulation of pore pressure

dissipation for the Kuala Perlis south embankment using a two-dimensional consolidation model (Kon 2DN) overestimated the field excess pore pressure dissipation (Hussein 1995). However, large-strain consolidation simulations using a modified version of Kon 2DN (TWOCON) gave some reasonable predictions of excess pore pressure dissipation (Rahadian 1995).
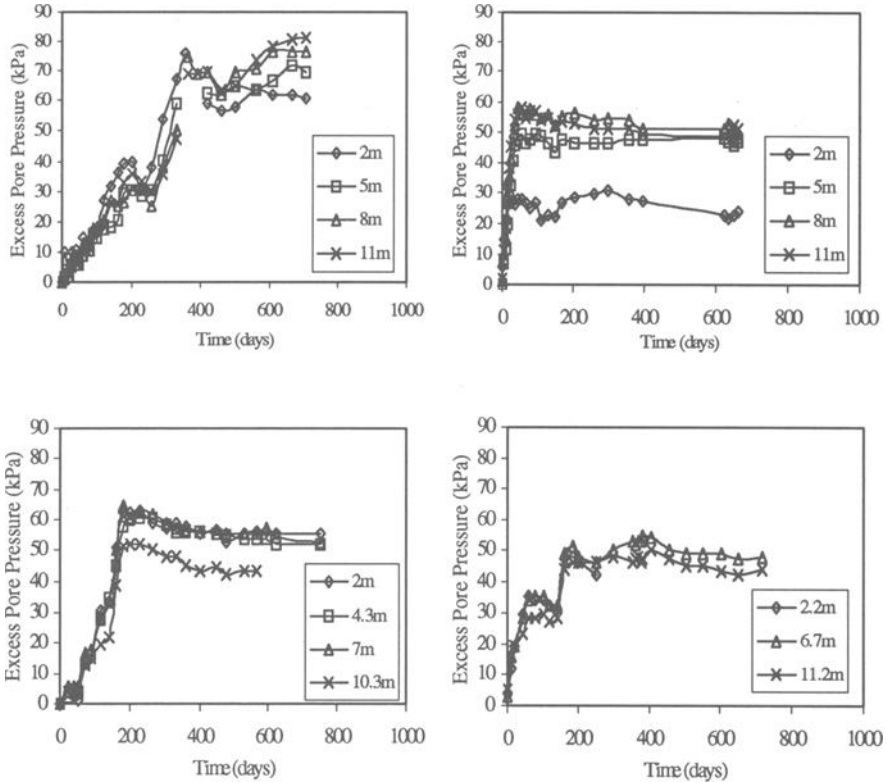


Fig. 5 – *Excess Pore Pressure vs. Time*

*Lateral Displacement*

Figure 6 shows lateral displacements of subsoil obtained from inclinometers located at 1-2 m from the edges of the embankments at various times. In general, the amount of lateral displacement that occurred in the four embankments increased with time although some differences in the rate of the magnitude of lateral displacement at different time periods are observed. The lateral displacement at 370 days ranges from 0.2 m for the Kuala Perlis and Muar embankments to 0.4 m for the Juru embankment.

Readings were only taken up to 700 days except for the Kuala Perlis south embankment and Juru embankment where readings were stopped after 370 days due to vandalism to the inclinometer.
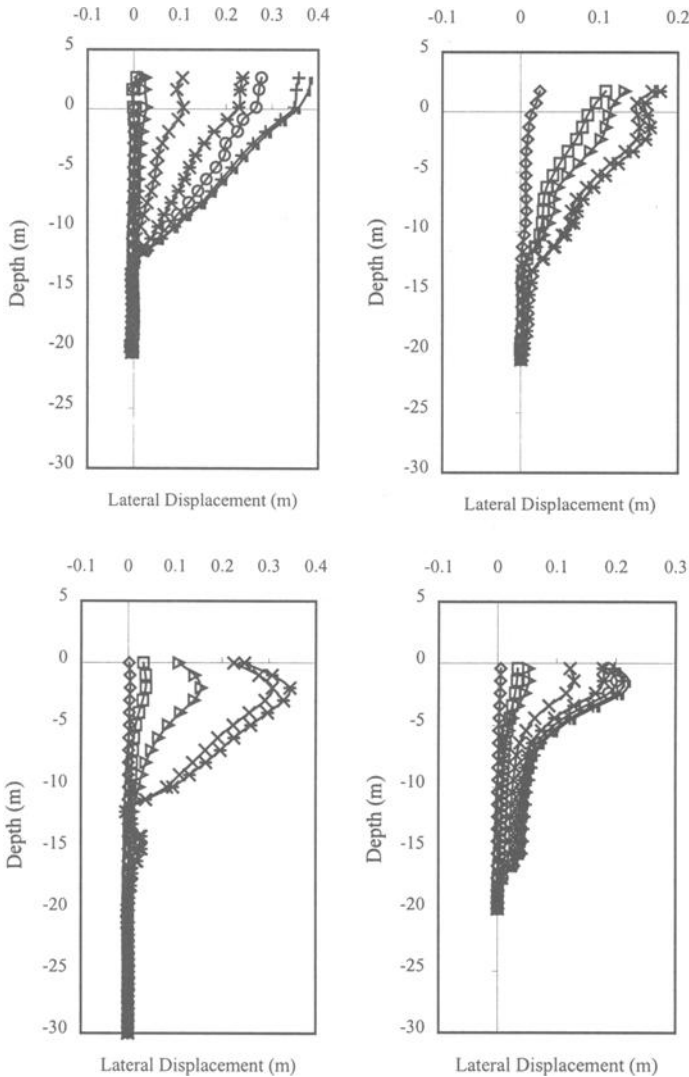


Fig. 6 - *Lateral Displacement vs. Time*

Figure 7 shows the relationship between maximum lateral displacement and height of fill. It is observed that lateral displacement increases with the height of fill up to the end of construction and then remains almost constant thereafter.
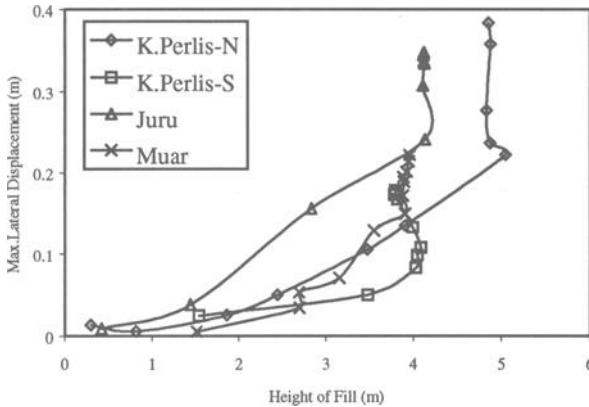


Fig. 7–*Maximum Lateral Displacement vs. Height of Fill*

*Volume Displaced*

Figure 8 shows the increase in volume displaced vertically and laterally by the four trial embankments. All the data obtained from the four trial embankments show that the volume displaced laterally is generally smaller than the volume displaced vertically. The Juru trial embankment has the largest displaced lateral volume which ranges from 13% to 37% of the vertical volume, while the values for Kuala Perlis and Muar are 3-15% and 0.5%-15%, respectively, of the vertical volume.
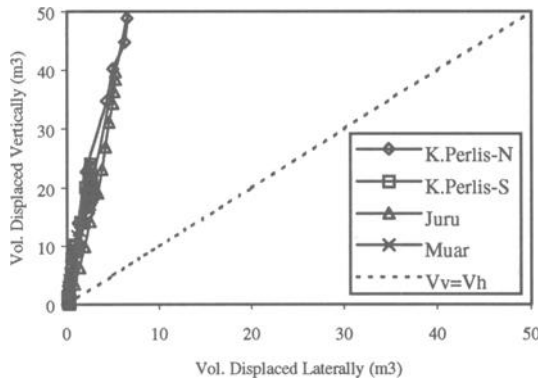


Fig. 8-*Vertical and Lateral Volume Displacements*

## Comparison with Trial Embankments from Temperate Regions

Figure 9 shows the relationship between the ratio of the vertical and lateral volume displaced and the height of fill for four trial embankments in Peninsular Malaysia, as well as three embankments that were constructed in temperate regions. The three embankments are the St.Alban test fill B in Canada, (Tavenas et al. 1974), the I-95 trial embankment in U.S.A., (Poulos 1972), and the Over Causeway By-Pass in the United Kingdom, (Symons and Murray 1975). It can be seen that the ratio of vertical to lateral volume displaced in Peninsular Malaysia is higher than corresponding values obtained from temperate regions, although more data is needed for a detailed comparison to be carried out.
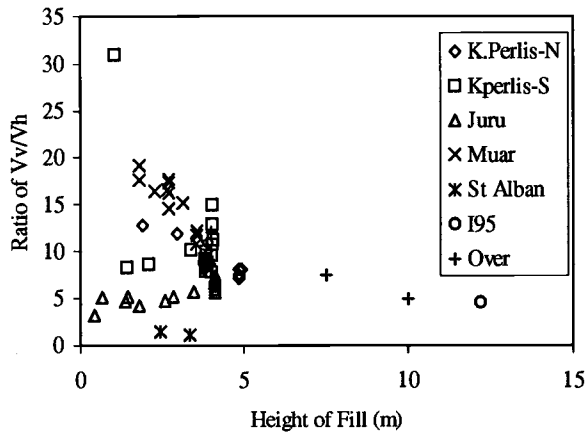


Fig. 9–*Ratio of Vv/Vh vs. Height of Fill*

## Conclusions

1.  The field behavior of four trial embankments was found to be quite similar to each other although slight differences do occur. The differences are attributed to the method and rate of construction used, final height of fill and the rest periods taken during construction.
2.  The field behavior of the four embankments could be used as a guide in understanding the general field behavior of embankments constructed on Peninsular Malaysia coastal soft soil deposits. The field behavior of the embankments shows that although large settlement occurs, there seems to be little excess pore pressure dissipation with time and also small lateral displacement. This could be associated with reduction in permeability and some change in soil structure during consolidation; however, the actual cause is unknown and further study is necessary.

3. The ratio between the volume displacement vertically ($\Delta V_v$) and the volume displaced horizontally ($\Delta V_h$) with height of fill shows that the $\Delta V_v/\Delta V_h$ ratio is higher for embankments in Peninsular Malaysia than in the Temperate Regions. More data are needed in order to establish a definitive relationship.

## References

Albakri, W. H., Othman, K., How, K. T., and Chan, P. C., 1990, "Vertical Drain Embankment Trial at Sungei Juru," *Seminar on Geotechnical Aspects of the North-South Expressway*, Kuala Lumpur, pp. 195-205.

Hussein, A. N., 1995, "The Formation, Properties and Behavior of Coastal Soft Soil Deposits at Perlis and Other Sites in Peninsular Malaysia," *University of Strathclyde*, Glasgow, Ph.D. Thesis, Vols. 1 and 2.

Hussein, A. N., McGown, A., and Nik Hassan, N. R., 1996, "Geotechnical Characteristics of Coastal Soft Soil Deposits at Perlis, Malaysia," *Twelfth Southeast Asian Geotechnical Conference*, Kuala Lumpur, Vol.1, pp. 113-119.

Hussein, A. N. and McGown A., 1996, "The Performance of A Rapidly Constructed Embankment at Perlis," *2nd Malaysian Road Conference*, Kuala Lumpur, pp. 41-49.

Hussein, A. N. and McGown, A., 1998, "The Behavior of Two Trial Embankments at Perlis, With Different Rates of Construction," *The Fourth International Conference on Case Histories in Geotechnical Engineering*, St Louis, USA, Paper No. 2.22.

James, P. M., 1970, "The Behavior of a Soft Recent Sediment Under Embankment Loadings," *Quarterly Journal of Engineering Geology*, Vol. 3, pp. 41-53.

Malaysian Highway Authority, 1989, "Factual Report on the Performance of the 13th Trial Embankments," *Proceedings of the International Symposium on Malaysian Marine Clays*, R.R.Hudson, C.T.Toh and S.F.Chan, Eds., Malaysian Highway Authority, Vols. 1 and 2.

Mesri, G. and Choi, Y.K., 1979, " Excess Pore Water Pressure During Consolidation," *Sixth Asian Regional Conference on Soil Mechanics and Foundation Engineering*, Vol. 1, pp 151-154.

Mitchell, J.K., 1986, "Practical Problems from Suprising Soil Behaviour", the Twentieth Karl Terzaghi Lecture, *Journal of Geotechnical Engineering*, ASCE, Vol.112, No.2, pp. 259-289.

Mohammad, R., Nicholls, R. A., Albakri, W. H., Dobie, M. J. D., and Othman, K., 1991, "Vertical Drains Trial at Juru, Malaysia: Performance During Construction," *Ninth Asian Regional Conference on Soil Mechanics and Foundations Engineering*, Bangkok, pp. 509-515.

Poulos, H. G., 1972, "Observed and Predicted Behavior of Two Embankments on Clay", *Geotechnical Engineering*, Vol.13, pp. 1-19.

Rahadian, H., 1995, "Analysis of the Consolidation Behavior of a Tropical Soft Water-Laid Soil," *University of Strathclyde,* Glasgow, Ph.D. Thesis, Vols. 1 and 2.

Symons, L. F. and Murray, R. T., 1975, "Embankments on Soft Foundations: Settlement and Stability Study at Over Causeway By-Pass", *Transport and Road Research Laboratory*, Report No. 675, 14 pp.

Tavenas, F. A, Chapeau, C., La Rochelle, P. and Roy, M., 1974, "Immediate Settlements of Three Test Embankments on Champlain Clay", *Canadian Geotechnical Journal*, Vol.14, pp. 109-141.

Toyoshige Mohri,[1] Ryoichi Fukagawa,[2] Kazuyoshi Tateyama,[3] Kunio Mori,[4] and N. Ochieng Ambassah[2]

## Slurry Dewatering System with Planetary Rotation Chambers

**Abstract:**

A new dewatering system for slurry has been developed with the aim of realization of efficient mud-water treatment. In the system, centrifugal force is employed for the purpose of densification of mud and for separation of mud particles from water. In this research, an original idea has been developed for discharge of the dewatered mud. This made it possible to achieve a continuous dewatering process without the use of any filtering device. Furthermore the proposed dewatering system neither requires a high initial cost nor a high maintenance cost. Consequently, the system will achieve a higher cost performance in comparison with conventional systems. In this paper, the mechanism of the dewatering process in the new system is explained. The applicability of the system is discussed based on the results of the experiments carried out with a trial machine on four kinds of slurry materials. In addition, a miniature centrifugal testing apparatus was used for experiments on three kinds of clays. We believe that the system will highly contribute in the improvement of our environmental conditions.

**Keywords:** dewatering system, slurry, centrifugal force, laboratory test

[1]President, Horyo Sangyo Co. Ltd., 3-4-10 Mitsuya-naka, Yodogawa, Osaka, Japan,
[2]Professor and post graduate student, respectively, Civil Engineering Department, Ritsumeikan University, 1-1-1 Noji-higashi, Kusatsu, Shiga, Japan,
[3]Associate Professor, Civil System Engineering Division, Kyoto University, Yoshida-honmachi, Sakyo, Kyoto, Japan,
[4]Manager, Research and Development Division, Kumagai-gumi Co. Ltd., 2-1 Tsukudo-cho, Shinjyuku, Tokyo, Japan.

**Introduction**

As a result of construction work, a large amount of surplus soil is discharged from the construction sites. Lots of resources (time and money) are required in order to deal with the surplus soil. When dealing with high water content soils, e.g. the slurry used in shield tunneling works, the situation becomes worse. Moreover, it is very important for engineers to treat such soils, e.g. in river and lake bed, so as to recreate a clean environment. The dewatering technique is essential for this purpose. In the past in order to dewater the slurry, a large size of filter press type or a single-drum type dewatering devices etc. have been used [1]. In the former process, slurry is added into a folding cloth and consolidated by applying high pressure from both ends of the folding cloth. Although this method can give highly dewatered soils, the treatment needs long time for the consolidation. Besides, there is need for frequent maintenance of the folding cloth. In the latter case (also known as the decanter type), the slurry is densified in the fast rotating single drum which is set on a floor sideways. However, to achieve high efficiency, extremely high rotation speed has to be employed. Consequently, these processes are generally very large and expensive [2]. As such a compact and better cost performance type dewatering system is strongly desired in many sites in Japan.

**A new Dewatering System of Slurry**

*Structures*

The new dewatering system proposed in this paper has been mainly manufactured from mild steel. It consists of a large stationary chamber. Inside this chamber there is the inner structure. The inner structure is composed of smaller chambers (i.e. dewatering chambers) capable of slowly rotating on their own about their axes (the minor axis/axes), Figure 1. It is in these smaller chambers that dewatering by centrifugal force takes place. The inner structure revolves at high speed about its axis (the central axis). The system also consists of a pump unit to supply slurry into the dewatering chambers. Roughly, the specifications of the proposed system, which were used in the trial machine, are shown in Table 1. It is possible to fabricate a practical machine based on the same system with a dewatering capacity of 5.0 m³/hr at a reasonable cost of about 80,000 US dollars (1 US\$ ≒ 120 Japanese Yen).

*Dewatering Process*

*Supply of Slurry* - Slurry is supplied into the system through the bottom part of
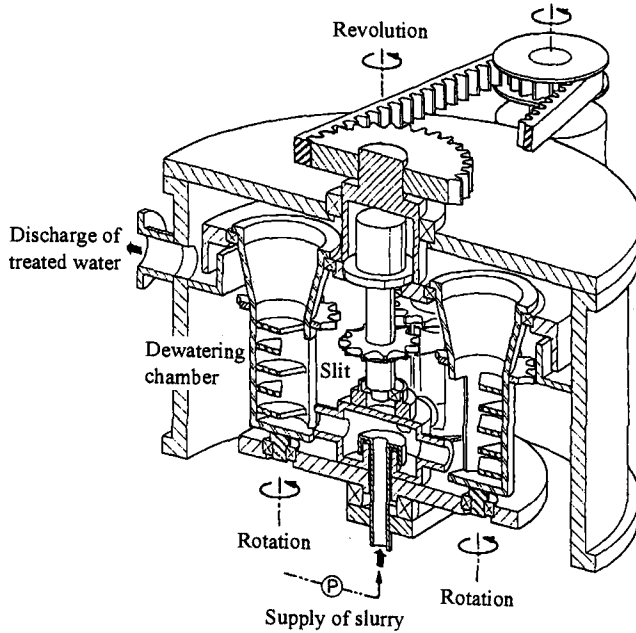
Figure 1 - *A new Dewatering Device Using Planetary Rotation Chambers*

Table 1 - *Specifications for a Model Dewatering System*

| Diameter of main chamber (mm) | 1,350 | Maximum revolution speed (rad/s) | 89.3 |
|---|---|---|---|
| Height of main chamber (mm) | 1,071 | Maximum revolutional acceleration ($\times$g) | 300 |
| Total weight (kN) | 11.8 | Rotation speed (rad/s) | 0.21 |
| Volume of dewatering chamber (m$^3$) | 0.009$\times$4 | Dewatering capacity (m$^3$/hr) | 0.5 |

the chamber by means of the pump unit.   The pumped slurry is injected into the dewatering chambers through the slit on the wall of the dewatering chambers (see Figure 2(a)).  During this stage, the inner structure revolves very fast whereas individual dewatering chambers do not revolve about their own (minor) axes.   The operation of the system is described by the flow diagram in Figure 3.

     *Dewatering with Centrifugal Movement* - During the rotation of the inner structure, as a result of centrifugal force, slurry in the dewatering chambers moves away from the central axis of rotation.  During this stage, the dewatering chambers themselves

(a) Supply of soils

(b) Densification                    (c) Discharge of dewatered soils
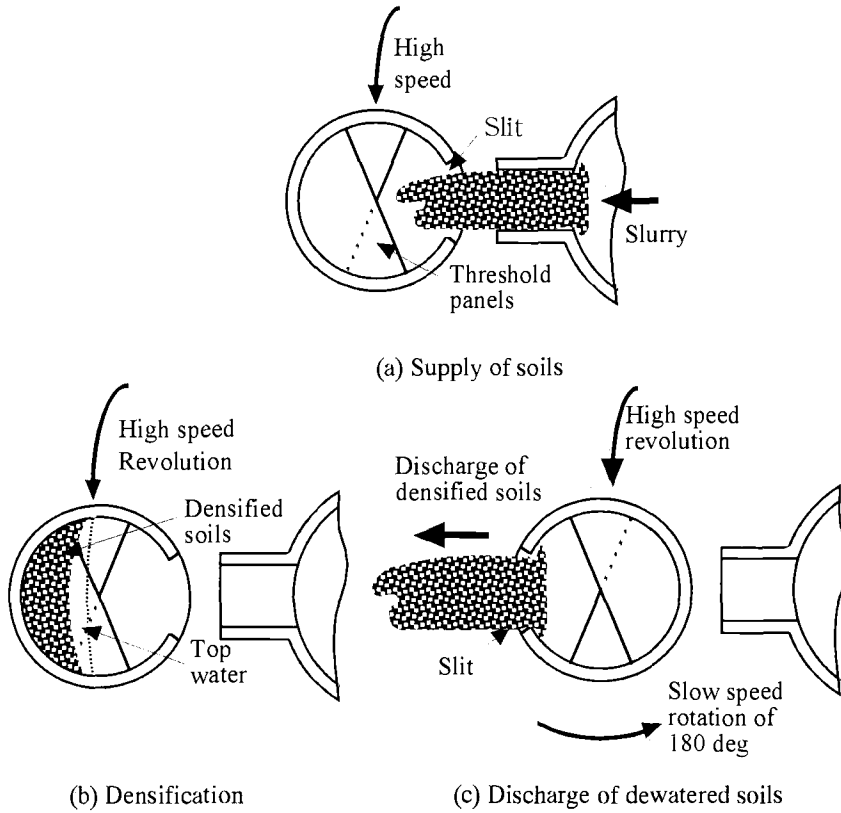
Figure 2 - *Dewatering Procedure*

don't rotate about their own axes. Thus, within the dewatering chambers, slurry will mainly lie along the wall of the outer half with the most dense mixture (densified soil) being farthest away from the central axis, and the less dense mixture (mainly water) lying above the dense mixture, closer to the central axis. This process causes separation of water from the densified mixture, Figure 2(b).

*Discharge of Dewatered Soil and Treated Water* - Within the small chambers there are threshold panels, shown in Figures 2 and 4. As the inner structure revolves, these panels trap the densified mixture. Water, on the other hand, depending on such factors as rotation speed, position of the panels, amount of slurry etc. can move over the panels and out at the top of the dewatering chambers. After most of the water has left the dewatering chamber, densified soils are discharged by rotating the small chambers through 180 deg, about the minor axis, Figure 2(c). In so doing, the slurry supply slit will be positioned just behind the densified soil. The densified mixture flows through the slit, splashing onto the inner side of the large chamber, where it accumulates. The
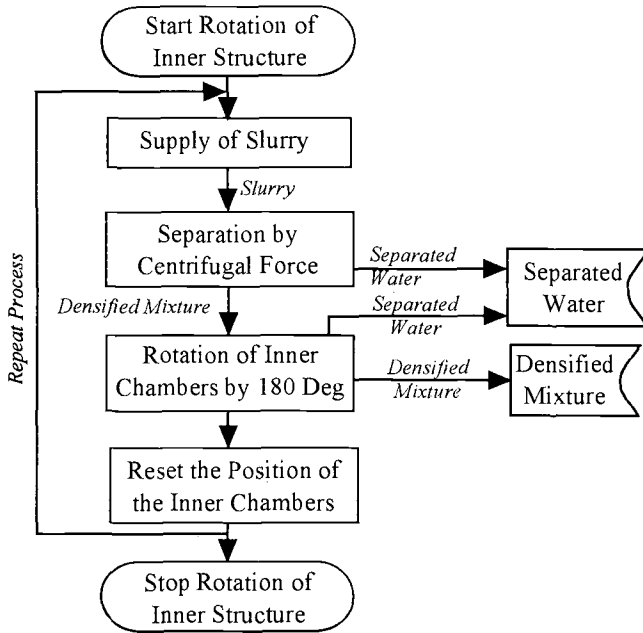
Figure 3 - *Flow Chart of Test Procedure*
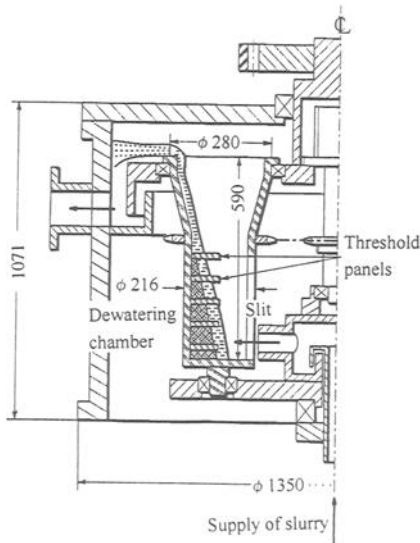


Figure 4 - *Inner Structure of Dewatering Chamber*

accumulated soil gradually drops to the bottom of the large chamber due to its own weight.

## Performances of the New Dewatering System

### Test Procedures

   *Test Conditions of the Dewatering System* - When carrying out tests on the dewatering system, some working conditions have to be fixed. The conditions are:
1) The revolution speed of the inner structure is 84 rad/s (i.e. an operational speed of about 800 r.p.m.). This approximately corresponds to 282g (where g is the gravitational acceleration),
2) The rotation time cycle of each small chamber in total is 60 seconds,
3) The time required for densification is 150 seconds.
The test time cycle used in the tests is shown in Figure 5.
   *Test Samples* - Four kinds of samples were used in the experiments, i.e. Masado A (decomposed weathered granite), Masado B, Kaolin Clay and Silica Sand. Masado is naturally and widely distributed in western Japan. The density of the soil particles of these samples are 2.56, 2.58, 2.61 and 2.54 respectively and the particle size distribution of each material, determined experimentally, is displayed in Figure 6. Tests were basically carried out on three kinds of specimens: the original slurry, the dewatered soil and the separated water. Water content and suspended solids (SS) were the most
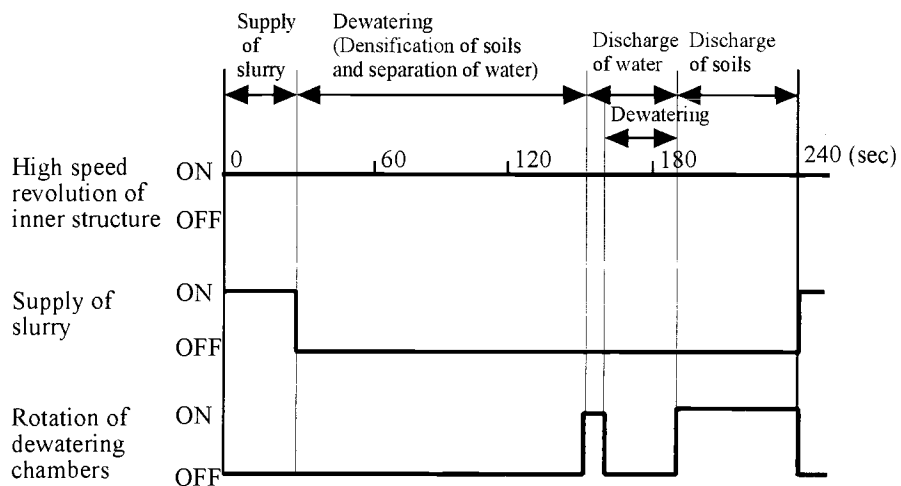


Figure 5 - *Test Time Cycle*

important factors in judging the effectiveness of the new system. SS was calculated from the following equation, based on the Standard Methods for the Examination of Water and Wastewater (American Public Health Association):

$$SS = \frac{m_b}{(m_a - m_b) + \dfrac{m_b}{\rho_s}}$$

where

$m_a$: the weight of wet sample
$m_b$: the weight of dry sample
$\rho_s$: the density of soil particles.
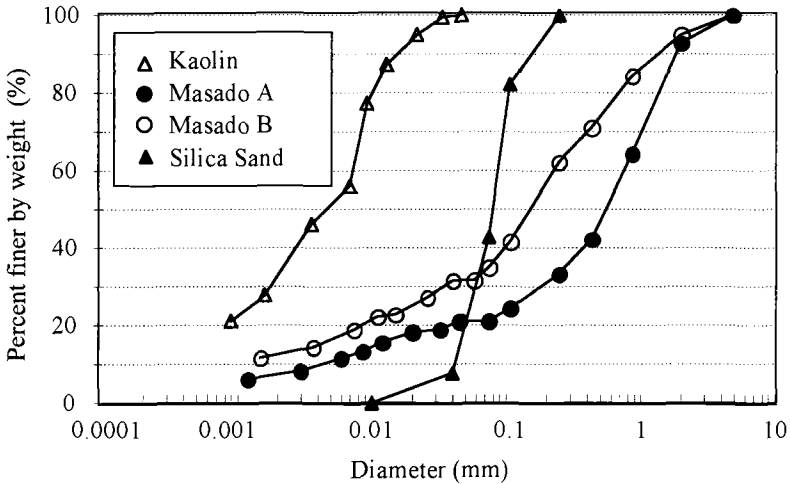


Figure 6 - *Particle Size Distribution of Tested Samples*

**Efficiency of the Dewatering Process**

The efficiency of the dewatering process can be determined by measuring the water content of the dewatered soils and the suspended solids of the separated water.

*Water Contents of Dewatered Soils*

Figure 7 shows the result of the dewatering process. Significant dewatering
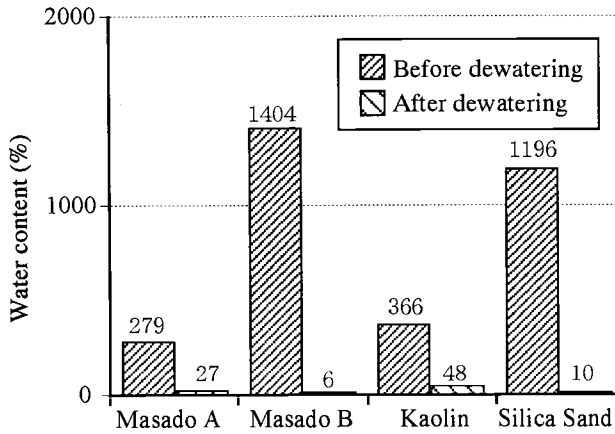
Figure 7 - *Improvement of Water Content of Dewatered Soils by Use of New Dewatering System*

impact was observed for each material. From the results, it can be seen that the newly proposed system had a great effect in improving dewatering process. Dewatering effect on Kaolin was slightly less than it was on the other materials. This is because the Kaolin contains a lot of fine particles in comparison with the other materials. Subsequently, in the following section, the effect of the fine particles will be discussed.

*Suspended Solids in Separated Water*

Figure 8 shows the change in suspended solids (SS) after performing the dewatering process. The overall tendency was almost the same as in Figure 7. The dewatering effect was remarkable on all the materials except for Kaolin. As mentioned above, Kaolin contains a large amount of very fine particles, which were difficult to treat within a reasonable time period.

**Countermeasures for Clayey Soils**

*Additional Tests Using a Small Centrifugal Testing Device*

Additional tests were carried out to investigate the effect of centrifugal force and
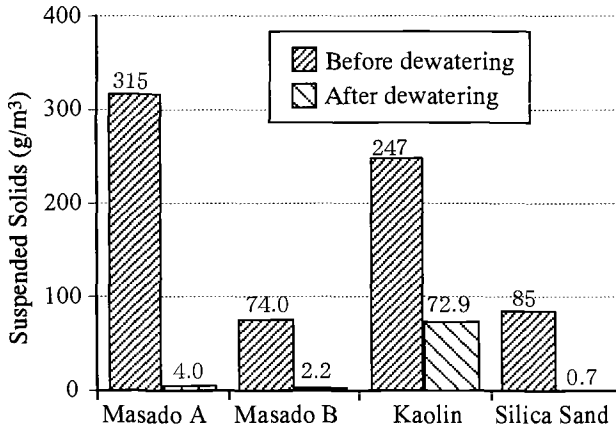
Figure 8 - *Improvement of SS of Separated Water by Use of New Dewatering System*

operation time, specifically for soils having very fine particles. A small size centrifugal testing device (H-11NA, made by Kokusan Co. Ltd.) was used. The schematic view of the apparatus is shown in Figure 9. This device can yield a maximum speed of 420 rad/s (4000 r.p.m.), which is about 2000 g. The operation time can be adjusted accordingly. Samples were put into a 15 $cm^3$ glass test tube, and the test tubes into a disk. The disk, with 8 test tubes, was set into a fast rotation. After rotation, under fixed operation time, samples of clay and top (separated) water having fine particles were taken in order to measure the water content of the dewatered soils and SS of the separated water, respectively. Three kinds of samples were tested, that is Kasaoka Clay, Kaolin and lakebed soil from Biwako-lake, the largest lake in Japan. The density of the soil particles of these samples are 2.70, 2.61 and 2.53 respectively and the particle size distribution of each material is displayed in Figure 10. For each type of clay, the initial water content of the test slurry was adjusted to 300 %.



(a) Top view                    (b) Front view
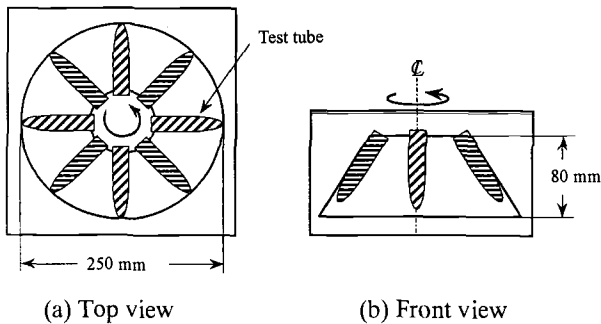
Figure 9 - *Miniature Centrifuge Testing Apparatus*
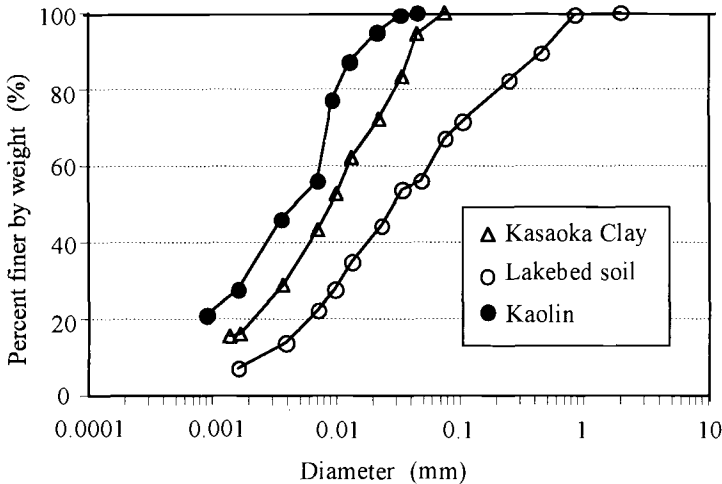
Figure 10 - *Particle Size Distribution of Tested Clay Samples*

*Effect of Centrifugal Force*

*Dewatered Soils* - Figure 11 shows the effect of centrifugal force on the water content of the dewatered Kaolin. The water contents used in Figures 11 and 12 are the average values obtained from the dewatered samples. The operation times used in the series of tests were: 60, 120 and 180 seconds. It can be observed that the relationship between the water content and the centrifugal force is inversely linear. However, beyond a revolution rate of 262.5 rad/s (2500 r.p.m.), the influence of the centrifugal force on the water content decreases. Figure 12 shows the effect of centrifugal force on three kinds of dewatered soils. It can be concluded that an increase in centrifugal force is effective for each material. Further, the overall patterns of the relationship between the water content and the revolution rate are similar. Since the newly proposed system is operated at a speed of 282 g, higher centrifugal force can be used in order to improve the dewatering properties.

*Separated Water* - Figure 13 shows the effect of the centrifugal force on SS (Suspended Solids) in the case of Kaolin. The effect of centrifugal force was also remarkable, although the influence gradually decreases as the centrifugal force increases. Kasaoka clay also showed similar results. Figure 14 shows the results obtained from the lakebed soil sample. Since the separated water from the lakebed soil sample was much purer than that obtained with the other soils, that means that the content of fine particles was less. It seems to be difficult to improve the effectiveness by increasing the centrifugal force especially below 2 $g/m^3$ of SS. Probably it would be very difficult to densify very fine negatively charged particles by means of centrifugal forces.
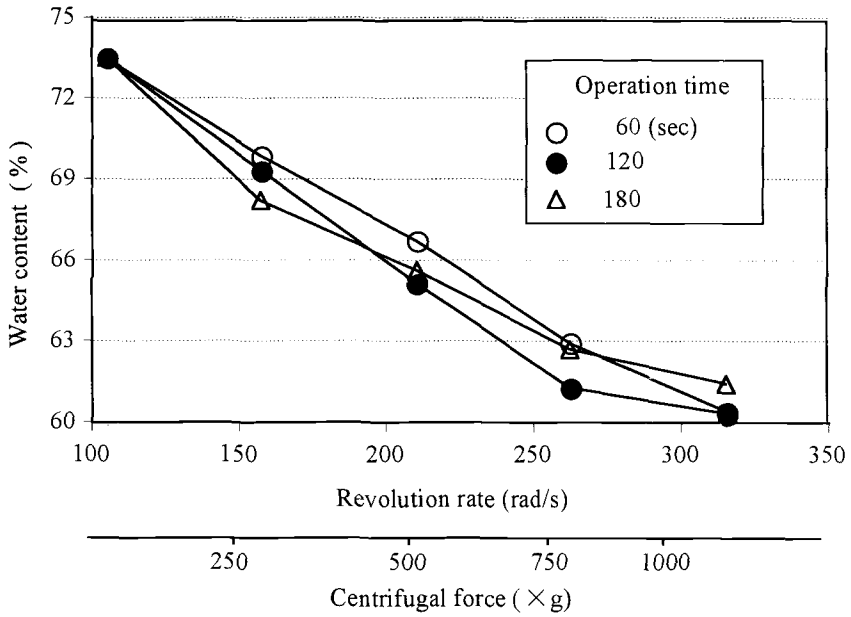
Figure 11 - *Effect of Centrifugal Force on Dewatered Kaolin*
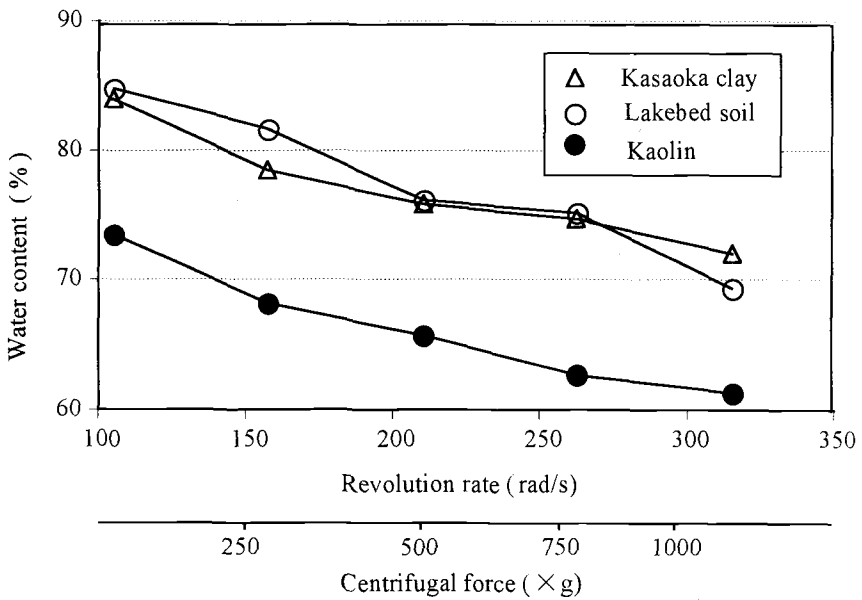


Figure 12 - *Effect of Centrifugal Force on Dewatered Soils*
*(Operation Time is 180 Seconds)*
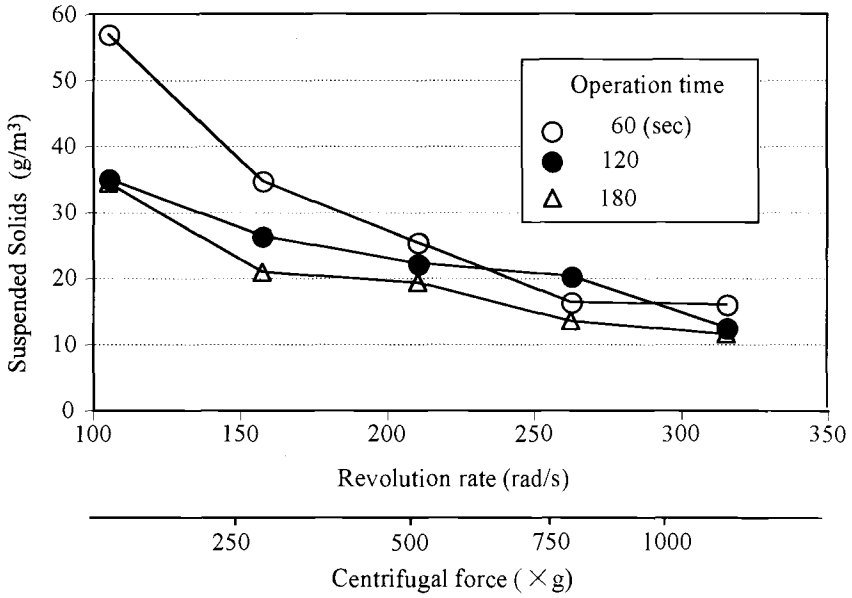
Figure 13 - *Effect of Centrifugal Force on Separated Water of Kaolin*
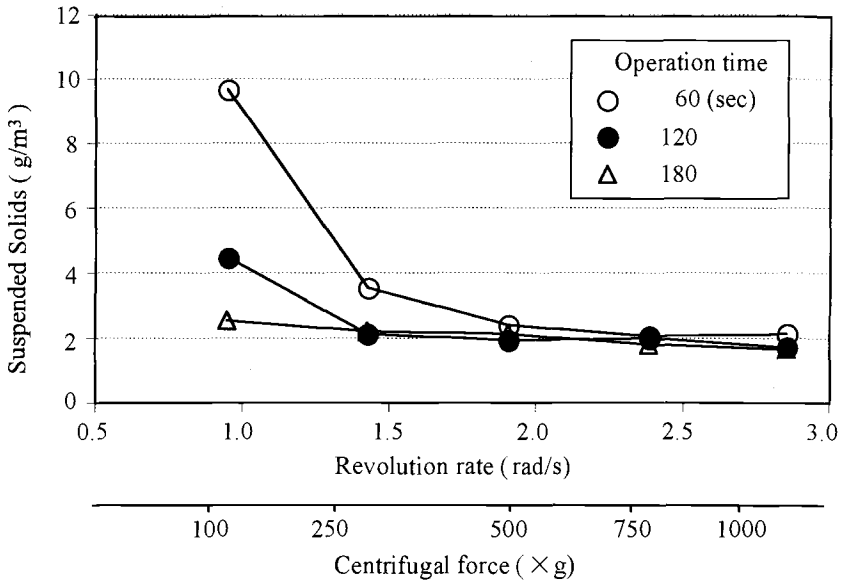


Figure 14 - *Effect of Centrifugal Force on Separated Water of Lakebed Soil*

Accordingly, the existence of a critical size of fine clay particles which can be densified by centrifugal dewatering system can be expected.

*Effect of Operation Time*

*Dewatered Soils* - Figure 15 shows the variation of operation time with the water content of the dewatered Kaolin. The measured water contents in this figure are the average values from the soil sample in the test tubes. The operation time in this series of tests was 60, 120 and 180 seconds. The effect of operation time wasn't apparent. The other two materials also exhibited similar results. These results suggest that operation time is not as important as the centrifugal force in dewatering process.
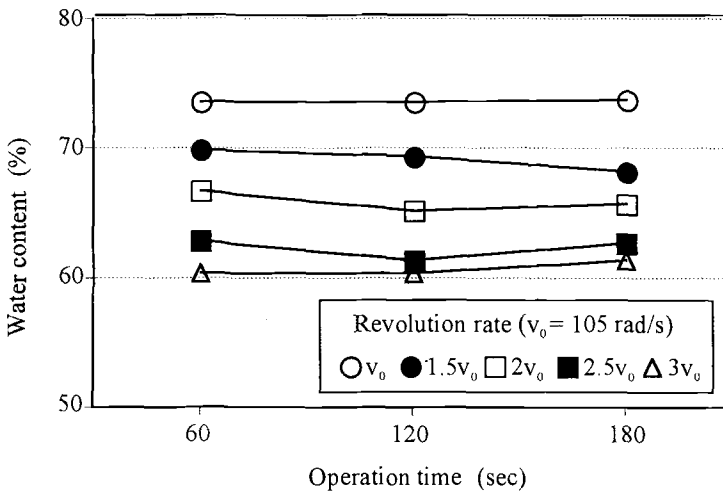


Figure 15 - *Effect of Operation Time on Dewatered Soil of Kaolin*

*Separated Water* - Figure 16 shows the effect of operation time on SS of separated water from the Kaolin sample. Although the effectiveness slightly decreases as the operation time increases, it can be concluded that increasing the operation time is to some extent effective in purifying the top separated water. This is important since the cleanliness of the separated water is the most important criteria in many cases.
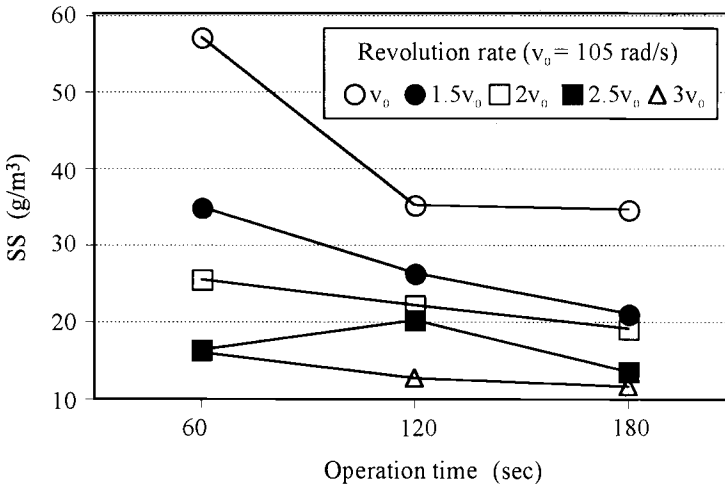
Figure 16 - *Effect of Operation Time on Separated Water of Kaolin*

## Conclusions

The main conclusions obtained from this study are as follows:

(1) A new dewatering system for slurry with planetary rotation chambers was developed. The slurry is first injected into four small chambers. The soil material in the slurry is then condensed by means of centrifugal force, due to fast revolution of the inner structure. At the final stage of dewatering, the small chambers are rotated slowly and the condensed soil material is discharged from the small chambers through the slit on the side of the chambers.

(2) The effectiveness of the new dewatering system was confirmed through dewatering experiments. These were carried out using four kinds of slurry made from Masado A and B clays, Kaolin Clay and Silica Sand. The new device showed successful results for every material tested except for Kaolin, which contains a large amount of very fine particles.

(3) A small size centrifugal testing device was employed to investigate the viability of the new dewatering system for clayey soils. From the results, the effect of centrifugal force was evident. On the other hand, the operation time had no significant effect in improving dewatering properties. It was not easy to densify the clay samples containing a large amount of very fine negatively charged soil particles by use of the centrifugal-type dewatering system.

Abdelmalek Bouazza,[1] Jayantha Kodikara,[2] and Roger Parker[3]

On the Use of Sand Washing Slimes for Waste Containment

**Abstract:** Sand mining has long been practiced in the southeast sand belt of Melbourne to obtain clean sand for use in construction. The material remaining after the sand extraction, which generally exists in a sludge or slurry form, is commonly referred to as slimes. Since the late 1960s most of the abandoned sand mining pits have been used for waste disposal. Due to the unique hydrogeology of the region, the use of slime cut-off walls has become an essential consideration in the design of waste containment facilities in abandoned sand mining pits. One technique to isolate the landfills from adjoining shallow aquifers is to construct cut-off walls using hydraulically placed slimes from sand mining (fines washed from the sand). This involves placing wet sand washing slimes mixed with clean fill to achieve a low permeability slurry curtain around the landfill walls. Another alternative successfully used is the use of a sidewall liner in which there is a combination of compacted refuse bales and slimes. This paper presents and discusses various facets linked to this innovative method for using slimes in waste containment systems.

**Keywords:** cut off wall, landfill, liner, permeability, slimes, strength,

Introduction

The southeastern part of Melbourne is often termed the "sandbelt" because of its extensive deposits of sand. The sand in this area can be up to 80 m thick and comprise three tertiary units; the Eocene Werribee formation, the Miocene Fyansford formation and the Pliocene Black Rock sandstone and Red Bluff sands or Brighton group. Most of the extraction occurs in the Red Bluff sands and to a lesser extent the Black Rock sandstone. The Red Bluff sands are comprised of clays, sandy clays, clayey and silty sands, sands and occasional silt. The clayey and silty sands are the most dominant (Chandler 1992)

---

[1] Senior Lecturer, Department of Civil Engineering, Monash University, Clayton, Victoria, Vic. 3168, Australia

[2] Senior Lecturer, School of Built Environment, Victoria University of Technology, Melbourne 8001, Australia.

[3] Principal, Golder Associates Pty. Ltd., Hawthorn, Victoria, Vic. 3122, Australia.

293

The mining operation is traditionally carried out by using a high-pressure water jet to erode the sand and convert it into a slurry. The slurry is then pumped to a sand washing plant. The material remaining after the sand extraction, which generally exists in a sludge or slurry form, is commonly referred to as slimes or mud by the local sand mining industry. The slimes consist mainly of clay, which has been washed from the extracted sand and fine sand particles.

It is estimated that there are at least five million cubic meters of slimes located in the sandbelt area, mostly in the form of deep (up to 18 m) ponds. Since the late 1960s, abandoned sand mining pits in the region have been used as landfills, with a goal of obtaining the double benefit of waste disposal and land rehabilitation of marginal areas. This trend is increasing with the ever higher demand for new landfill space (although the regulatory pressure for higher standards of waste containment is resulting in most new sites being developed for selective disposal, i.e. inert waste). Many of the sand mining companies are either actively participating in landfills operations or selling void space to landfill operators.

One of the characteristics of the region is the fact that most landfills are buried below natural groundwater level in permeable sand formations. During sand mining, the watertable, normally located less than 5 m below ground level, is lowered as much as 40 m. Following cessation of mining and commencement of landfilling, watertable recovery creates a water saturated landfill from which leachate migrates in the direction of the regional groundwater flow. Groundwater monitoring data revealed evidence of leachate contaminated groundwater close to those landfills (Hancock et al. 1994). Over the last decade, the issue of ground and ground water protection has come under increased public scrutiny. Currently, most of the modern waste containment facilities are constructed according to the principle of having liner barriers composed of clayey soils or composite systems (geotextile and/or geomembrane, and clayey soils) in order to minimize leachate migration out of waste containment systems. However, these types of barriers are not always used in landfills in the southeast region due to different constraints such as difficulty of dewatering large slime volumes and topography. A solution that has been identified is the use of the slimes as part of the lining system and/or as cut-off walls (slimes curtain wall). This not only can create further void space for the landfill but it can also provide an effective means of reducing the impacts of landfill leachate on groundwater.

The present paper discusses the geotechnical properties of sand washing slimes and their implications on the design of containment barriers in the southeastern part of Melbourne.

## Geotechnical Characterization of Sand Washing Slimes

*Basic Geotechnical Properties*

The basic geotechnical properties of sand washing slimes can vary depending on the geologic origin and nature of the sand deposit as well as on the mechanical processes

involved in sand washing.  The geologic origin would determine the nature and the composition of the sand deposit thereby influencing the composition of the resulting slimes.  The sand washing process also influences the properties of the slimes through parameters such as the efficiency of the washing plant, and the location of the slimes in relation to the discharge point.

Table 1 shows a summary of some basic geotechnical properties of slimes obtained from 14 different locations in the southeastern region of Melbourne.  The sand deposits in this region are mainly of lacustrine and fluviatile origin and commonly comprised of poorly sorted clayey silty sands.  Although other classifications may sometimes apply, commonly the slimes can be classified as clays of high plasticity (CH) under the Unified System.  The natural water content and the dry density of the slimes will depend on how much drying and consolidation have taken place from the initial slurry stage.

Table 1-*Basic Geotechnical Properties of Slimes (Hancock et al. 1994)*

| Water content  (%) | | 136 to 533 |
|---|---|---|
| Particle size distribution | Sand (%) | 2 to 20 |
| | Silt (%) | 3 to 33 |
| | Clay (%) | 47 to 95 |
| | Organic (%) | 0 to 10 |
| Atterberg limits | Plastic limit (%) | 27 to 32 |
| | Liquid limit (%) | 44.5 to 72 |
| | Plasticity index (%) | 18 to 40 |
| | Linear shrinkage (%) | 6 to 20 |
| Dry density (kg/m$^3$) | | 1200 to 1600 |
| Specific gravity | | ~2.6 |

*Chemical and Mineralogical Composition*

Similar to geotechnical properties, the slimes exhibit a wide variation in chemical composition as well.  Table 2 shows the chemical composition and properties of slimes obtained from one given site.  As can be seen, $SiO_2$ dominates the chemical composition of the slimes, this is also reflected in the mineralogical composition, which comprises predominantly kaolinite, quartz and to a lesser extent pyrite.  However, Hancock et al. (1994) have reported that the slimes they have tested from this region contained both kaolinite and illite in the clay fractions.  As shown in Table 2, the concentrations of trace elements are generally low with exception to arsenic.

Hancock et al. (1994) have examined the cation exchange and adsorption of slimes using laboratory batch techniques.  Their work has shown that slimes display a substantial attenuation capacity in the form of cation adsorption.  For instance, linear isotherms, as described by the Freundlich equation, have been proposed for $Na^+$, $K^+$ and $NH_4^+$ with respective distribution coefficients, $K_d$, (or cation exchange coefficients) of

Table 2-*Chemical Properties of Slimes (Yuen and Styles 1995)*

| Chemical component | % | Trace element | (ppm) |
|---|---|---|---|
| $SiO_2$ | 54.53 | Cl | 141 |
| $Al_2O_3$ | 16.39 | Cr | 147 |
| $Fe_2O_3$ | 10.75 | Ba | 117 |
| $SO_3$ | 15.42 | Sc | 17 |
| MnO | 0.01 | Ce | 93 |
| MgO | 0.28 | Nd | 41 |
| CaO | 0.15 | V | 576 |
| $Na_2O$ | 0.13 | Co | 36 |
| $K_2O$ | 0.5 | Cu | 34 |
| $P_2O_3$ | 0.06 | Zn | 126 |
| $TiO_2$ | 0.68 | Ni | 91 |
| | | Ga | 13 |
| | | Zr | 252 |
| | | Y | 25 |
| | | Sr | 23 |
| | | Rb | 30 |
| | | Nb | 33 |
| | | Th | 27 |
| | | Pb | 33 |
| | | As | 1048 |
| | | Mo | 15 |
| | | U | 7 |
| Mineralogy (mineral in the order of predominance) | kaolinite, quartz, pyrite | pH of Slimes Suspension pH of Pore Water | 2.7 to 3.9 3.7 |

0.0018 to 0.0024, 0.0038 to 0.0045 and 0.0039 to 0.0044 $m^3$/kg. Their results indicate that slimes have a strong ability to adsorb $K^+$ and $NH_4^+$, with a lesser ability to adsorb $Na^+$. This behavior was attributed to the predominant presence of kaolinite and illite minerals in the clay fraction as well as to the presence of organic matter that increases the effective negative charge available in exchange sites. Hancock et al. (1994) also indicated that the magnitudes of $K_d$ obtained for slimes are similar in magnitudes to those reported in the literature for kaolinite soils that contain some hydrous mica (illite). The low pH waters observed in the slimes are mainly caused by the oxidation of pyrites. Salinities are reported to be in excess of 4000 mg/L in terms of total dissolved solids. Hancock et al. (1994) have also indicated that the effective cation exchange capacity (ECEC) of slimes increased substantially with the increase of pH and solution ionic strength. For instance, increasing of solution ionic strength from 0.02 mol/L and increasing pH from 3 to 8 has increased the ECEC of slimes from 6 cmol(+)/kg to 26 cmol(+)/kg. This behaviour was attributed mainly to increase of negatively charged exchange sites in kaolinite and in organic matter with the increase of solution pH. If the slimes are to be used as landfill liners, this behaviour poses important implications because municipal landfill leachate

can also change from being acidic to becoming alkaline with time.

*Shear Strength*

    The shear strength of slimes is predominantly a function of the void ratio. Because the slimes are generally saturated, shear strength is directly linked to water content. Reported shear strength values for the slimes vary over a wide range, even at the same void ratio. This variation may be attributed to the variation in mineralogical composition of slimes as well as to the influences of the testing technique. The vane shear and triaxial testing have been commonly performed for shear strength determination. Both these tests may fail to provide accurate answers when the slimes are of high water contents, for example when the water content is in excess of the liquid limit. The consistency of slimes can vary from almost zero shear strength to that of very soft to firm soil. Figure 1 shows a relationship between water content ($w$) and the undrained shear strength ($c_u$) as determined from laboratory vane shear tests on slimes. According to the critical state theory for soils, the relationship of $\log_e (c_u)$ vs $w$ should be linear (Wroth and Wood 1978). It is, however, difficult to establish the conformance of slimes to this aspect of the critical state on the basis of limited data available.
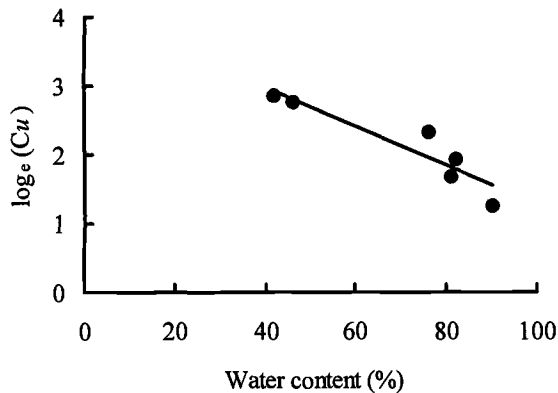


Figure 1-*Shear Strength-Water Content Relationship ( $\log_e c_u$ against w) For Slimes (Based on Yuen and Styles, 1995)*

    Viscous and thixotropic properties generally govern the very low shear strength that slimes display in slurry stage. These properties are important for slurry distribution via pipelines, and for providing short-term stability if the slimes are to be used as cut-off

walls. On the basis of laboratory results using a rotational concentric cylinder viscometer, Yuen and Styles (1995) reported that the slimes slurries featured an initial yield shear stress before displaying a linear viscous behavior. This form of shear behavior may be explained by Bingham plastic model for quantitative analyses of slimes slurries (Blight and Bentel 1983). They reported approximately an eight-fold increase in shear strength or yield stress (32 Pa to 250 Pa) when the water content was reduced from 180% to 110%. As can be seen from Figure 1, when the slimes are dried to lower water contents below the liquid limit (which is 59% for the slimes used in these tests), larger gains in shear strengths are possible. However, the slimes did not display significant thixtropic properties (i.e. significant gain in shear strength) when allowed to rest up to about a day from the agitated state (Yuen and Styles 1995). The insignificant thixotropy displayed by slimes slurries may be attributed to their particle size distribution and mineralogy, in particular, the high sand and silt content and the lack of smectite type minerals.

*Compressibility and Drying*

Limited studies were undertaken on the compressibility of sand washing slimes. Similar to the shear strength, the compressibility also depends on the state of drying of slimes. Traditional oedometer tests performed on slimes indicate that compression index, $C_c$, varies between 0.2 to 0.3 (Soilmech 1981). The slimes may also display a pre-consolidation pressure reflecting the initial drying state of the undisturbed slimes. Studies on the creep or secondary consolidation characteristics of slimes are not readily available.

The drying rate of sand washing slimes is an important issue, particularly if a landfill barrier is to be constructed by compacting dried slimes. Field tests of slimes drying have been undertaken over about three months duration (Golder Associates 1993). The tests included drying of slimes slurries in three trial pits. The dimensions, *length* x *width* x *height*, of the three pits, were: Pit 1, 2 m x 2.3 m x 1.6m; Pits 2 and 3, 12 m x 2.3 m x 0.8 m; Pit 4, 3.4m x 2.3 m x 0.8 m. All the pits were constructed of baled refuse blocks, each measuring, 1.68 m in length, 1.14 m in width and 0.81 m in height. Pits 1, 2 and 3 were filled with slimes slurries in layers after each layer has dried and formed a crust. In Pit 1, however, a 100 mm thick sand layer was placed to accelerate the drying of slimes after one month in which two layers of slimes (each 200 mm thick) were placed. The final layer of slimes in Pit 1 included dried slimes obtained from a separate drying bed. Pit 4 was constructed by placing dredged slimes in a single layer of 800 mm thickness. The initial water content of slimes slurry at placement varied from layer to layer, but mainly was roughly in the order of twice the liquid limit (~ 120%).

The drying behavior of slimes is generally similar to other slurries such as mine tailings. The initial phase of drying causes the slimes to shrink one-dimensionally and the formation of a surface crust, which eventually fractures into polygonal blocks of varying size. The surface crust limited the evaporation rates from the surface and maintained the underlying slimes in a relatively wet state. The water content of underlying wet slimes was found to be lower than the liquid limit by varying degrees.

The loss of water must have occurred through surface evaporation up to crust formation and through lateral drainage into the bales. After three months from their initial placement, the slimes have not gained sufficient shear strength to permit walking over the pit surfaces. The cracks appeared to have occurred only within the surface crust zone. It is not clear, however, to what extent these cracks affected the progressive drying of underlying wet slimes. In Pit 1, however, the addition of sand appeared to have influenced drying of slimes indicating lower water contents and a general increase of vane shear strength with depth. A similar trend was not clear in other pits, which did not have intermediate sand layers. After the three-month duration, the average vane shear strength of the tests performed in Pit 1 to Pit 3 was found to be about 6.4 kPa with a standard deviation of 5.5 kPa. When the bales were removed from a longitudinal side of Pit 1 and Pit 2, the slimes slumped because of the low shear strength.

Potential shrinkage of the slimes was another important issue, which needed to be addressed. This was assessed by conducting a shrinkage test based on the Australian Standards (AS1289.C4.1). The linear shrinkage of the slimes was found to vary between 6 to 20% indicating that the slimes can display a low to high shrinkage potential. This raises the issue that design and construction procedures should take into account the potential drying and cracking of the slimes. However, the field drying tests indicated that drying is predominantly limited to the formation of a surface crust with extensive cracking. In the event of field construction, the surficial crack of a given layer would be filled when the next wet slimes layer is deposited. The field and laboratory tests also indicated that drying from water leakage from wall sides was also limited due to the formation of filter cakes. Nevertheless, it is prudent to examine the potential for drying and subsequent cracking on site specific basis.

*Hydraulic Properties*

The observed slow drying rates and the high clay content suggest that the hydraulic conductivity of slimes is low. However, as can be seen from Table 3, their hydraulic conductivity will depend on the water content of the slimes. The results shown in Table 3 were mainly estimated from laboratory tests using rigid wall falling head tests on remoulded slimes. Undisturbed samples can also be obtained for slimes with water contents less than the liquid limit. Tube samples were obtained from the exposed walls of trial slimes pits described in the previous section. The flexible wall permeability testing conducted on these samples has yielded hydraulic conductivities in the range of $2.1 \times 10^{-10}$ m/s to $7.8 \times 10^{-11}$ m/s. The initial water content of these samples varied between 54.6% to 39.7% but a clear relationship between the water content and the hydraulic conductivity was not evident.

For slimes and slime slurries with water content above the liquid limit, the hydraulic conductivity will be governed by the formation of a filter cake at the effluent end. Yuen and Styles (1995) studied the formation of filter cakes on a poorly-graded medium to coarse sand and on a well-graded gravelly slit/sand mixture. The filtration tests of 24 hours duration were carried out in 250 mm diameter pressure cells. The experimental set up included the filtration of 90 mm thick slurry layer on top of a 50 mm thick sand or gravelly slit/sand mixture, the bottom of which was open to the atmosphere through a

porous stone. The top of the slurry was subjected to a regulated air pressure (30 kPa and 210 kPa).

Table 3-*Expected Range of Hydraulic Conductivity Of Slimes (Yuen and Styles 1995)*

| Consistency of sample | Expected k value (m/s) |
|---|---|
| Slimes with water content close to liquid limit | $10^{-9}$ to $10^{-10}$ |
| Slimes with water content slightly above liquid limit | $10^{-8}$ to $10^{-9}$ |
| Slimes slurry with water content between 115% to 180% | $10^{-7}$ to $10^{-8}$ |

The results of these tests are shown in Table 4. It can be seen that no time dependence filter cakes were formed on both soil types, thickness of the filter cake was greater when the filtration was done with higher pressure. Also, the filter cake invaded into a greater depth in gravelly silt/sand mixture than in clean sand. The ability of slime slurries to form filter cakes, however, is not as strong as that of bentonite slurries. This is mainly because of the mineralogical composition of the slimes containing minerals that are not conducive to forming relatively impermeable and stable filter cakes under low confining pressures.

Table 4-*Properties of Filter Cake Formation In Slime Slurries (Yuen and Sytles 1995)*

| Soil type | Applied pressure (kPa) | Initial slurry w.c. (%) | Filter cake hydraulic conductivity (m/s) x $10^{-9}$ | Cake thickness (mm) | Cake water content (%) | Depth of invasion zone (mm) |
|---|---|---|---|---|---|---|
| Clean sand | 210 | 115 | 1.63 | 23 | 57 | 1 |
| | | 150 | 1.05 | 19 | 56 | 2 |
| | | 180 | 7.43 | 23 | 69 | 1 |
| | 30 | 115 | 1.1 | 15 | 72 | 1 |
| | | 150 | 6.07 | 21 | 76 | 1 |
| | | 180 | 3.16 | 22 | 86 | 1 |
| Gravelly silt/sand | 210 | 115 | 7.55 | 20 | 63 | 1 to 3 |
| | | 150 | 3.41 | 21 | 68 | 1 to 10 |
| | | 180 | 1.30 | 22 | 74 | 2 to 3 |
| | 30 | 115 | 3.33 | 10 | 73 | 3 to 5 |
| | | 150 | 2.14 | 10 | 78 | 1 to 10 |
| | | 180 | 1.62 | 3 | 78 | 2 to 3 |

*Chemical Compatibility*

Chemical compatibility is also an important issue if the slimes are to be used as landfill liners or cut off walls. Since the clay fraction of slimes contains predominantly

kaolinite minerals, it can be argued that the slimes should be relatively compatible with typical landfill leachates. The limited test data available on this issue also appear to support this argument. However, the main issue to consider in chemical compatibility of slimes is the long-term stability of kaolinite under a low pH environment that is normally present in the slimes (Mitchell 1976). Furthermore, one has to be cautious of the possibility of mineral transformations that could take place under certain chemical environments. For example, it may be possible for illite to transform into more reactive vermiculite if the interlayer $K^+$ ions in illite are leached out by leachates that are predominantly acidic (Kodikara and Rahman 1997). It may be necessary to evaluate the implications of these reactions in relation to the long-term stability of the slimes.

**Slimes as cut off wall or liner barriers**

*Constructional Aspect*

   One leachate management technique identified for landfills designed in the abandoned sand quarries is the use of slime curtain walls. Since slimes have low strength, it is necessary to consider appropriate methods of construction to ensure that local shear failure does not occur. These methods should ensure continuity of the slimes against the compacted refuse. Decomposition and compaction of the refuse will generate horizontal stresses in the slime curtain wall.   However, little is known on the interaction behavior of a given structure and the horizontal pressure due to domestic wastes (Syllwasschy and Jessberger 1998; Bouazza and Seidel 1999).
   An attempt has been made to asses the effect of compaction on the slime curtain. The effect of horizontal stresses due to the vertical settlement of the refuse is not addressed since it is a long term effect rather than a short term effect. The method of estimation of compaction stresses proposed by Ingold (1979) and Filz and Duncan (1992) are both applicable to compaction of granular materials next to a rigid, non-yielding retaining wall. These methods indicate that higher horizontal stresses are developed close to the surface during compaction. During the construction of the wall barrier, the development of such stresses may cause waste deforming and breaking into the slime wall. This possibility was asseessed by applying the relatively simple Ingold (1979) method. Owing to the yielding nature of the slimes wall, this method overestimates the stresses generated by compaction, these stresses would in any case dissipate when the wastes deform into the liner. This procedure was qualitatively used to examine the possibility of the wastes breaking into the slime wall during construction.
   The following parameters were used in the computations: slimes wet unit weight = 15.50 kN/m$^3$; slimes shear strength = 3 kPa. For the domestic waste, the parameters are much more difficult to assess. The unit weight is difficult to determine because of variabilities in composition, method of placement, compactive effort employed during placement of the waste, induced aging, depth, volume of daily soil cover and local moisture content. Numerous values are reported in the literature. Based on the work of Watts & Charles (1990) and Fassett et al. (1994) it was estimated that the unit weight to be 10 kN/m$^3$ for refuse with good compaction.  The waste was assumed to be purely

cohesionless and the friction angle was determined ($\phi$=38°) from the chart proposed by
Manassero et al. (1996). This assumption is of course limited since the behaviour of
domestic waste can also be of a frictionless type or a c-$\phi$ type depending on the vertical
stress level (Manassero et al. 1996; Bouazza and Seidel 1999).

Figure 2 shows the variation of the different pressures for at-rest conditions. The
horizontal pressure exerted by the slimes, assuming that slimes are in hydrostatic
conditions, is also plotted in Figure 2. The compaction stresses in the refuse exceed the
resisting pressure of the slimes in the top two meters only. For depths greater than 2
meters, slimes will exert higher pressures and refuse will densify (the settlement and the
biodegradation process will also contribute to that densification), resulting in eventual
equalisation of pressures. In any case, compaction equipment should not operate
immediately adjacent to the slimes and operating conditions must be established to ensure
that damage does not occur to the side wall liner once the liner is in place.
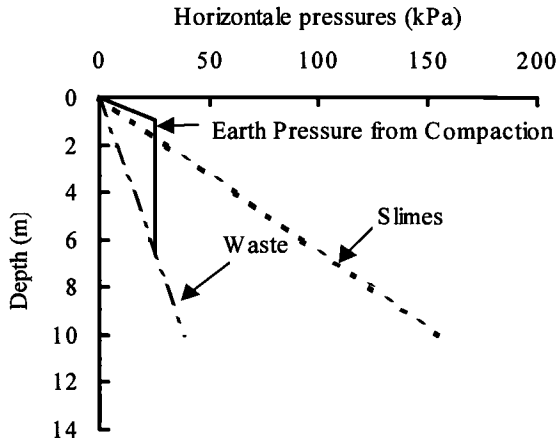


Figure 2-*Variation Of Horizontal Stresses*

A technique was developed specifically to enable greater control of the placement of
the slimes and in particular to ensure that the design thickness of the slime walls could be
maintained. The method consists of a combination of compacted refuse bales and slimes
as illustrated in Figure 3. The major points outlining the sequence of construction
consists of placing a bale wall to form a trench of 2.5 m width for the slimes. The bales
can be placed as a single width or wider depending on the number of bales available.

Refuse should be placed up to the top of bales. If a single width of bales is used, the
refuse should be placed and compacted before any slimes are placed. This is to limit
subsequent movement of bales into the slimes during compaction. If compaction is to be
performed against the bales after placement of slimes it will be necessary to provide some
lateral restraint, either by forming a wide platform of bales or pin the bales. Slimes are
added into the trench in layers of about 0.2 m, allowing drying between successive lifts

(Figure 3a). For the next lift of refuse, the bale wall is extended and the process is repeated (Figure 3b).

Development of the slimes curtain in this manner has already commenced. However, quality control data was not available at the time of preparation of this paper to enable comments on the performance of the wall. It should also be noted that a leachate management system has been put in place to minimize leachate migration out of the landfill. Discussion of this is beyond the scope of this paper.
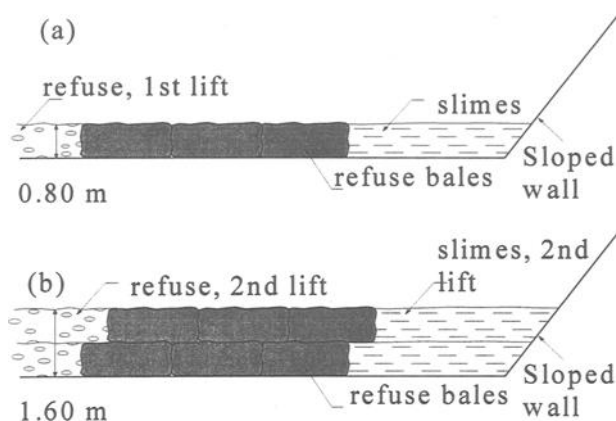


Figure 3-*Slime Curtain Wall*

Another technique to isolate landfills from adjoining shallow aquifers is described by Hancock et al. (1994). The technique involves placing wet sand washing slimes (50 to 60%) mixed with clean fill (inert waste) to achieve a low permeability (in the order of 2 x $10^{-8}$ m/s) slurry curtain around the landfill walls as shown in Figure 4. This technique is based on the filter cake formation as discussed earlier. However, further field trials should be performed in order to verify this technique. A filter cake may not form in coarse grained materials around large size particles and can result in mixes containing large voids.

Another concept developed for a landfill liner and cover system was based on using the on-site materials to provide lining and capping barriers. Combination of cement treatment and drying of the slimes, and the excavation of fine sand from the base of the pit, provided enough material to construct the 1 m thick compacted liner (Figure 5). Two mix proportions of, 30/65/5 and 40/55/5 (slimes/sand/cement), produced acceptable hydraulic conductivity and strength.
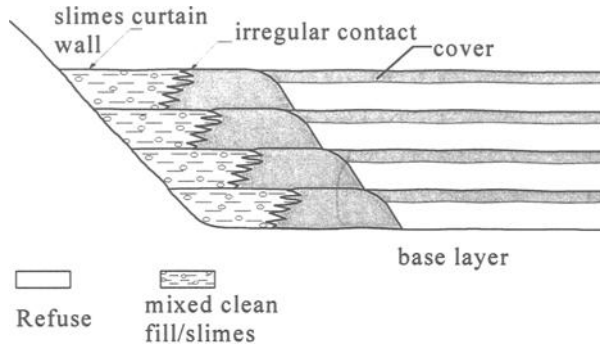
Figure 4-*Slime Curtain Wall* (from Cavey 1993)
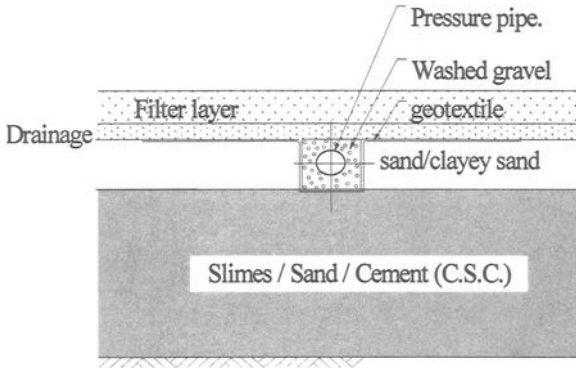


Figure 5-*Bottom Liner Cross Section At The Hampton Park Landfill (Seddon and Bateman 1994)*

**Conclusions**

This paper highlight a site-specific lining technique adopted by practitioners for landfilling of pits created by commercial sand mining operations. The high-water-content slimes generated after sand washing are used to construct slime curtains abutting to the pit walls to act as side-liners. Special techniques were needed to construct the liners at steep angles. The construction techniques developed included the use of baled

refuse to create a stable void to hold slimes, mixing of slimes slurry with inert wastes to create stable lining material, and modification of dried slimes by mixing with sand and cement. Geotechnical and physico-chemical characteristics of slimes were examined as part of the design process of slime curtains. They indicated that slimes strength will depend heavily on the water content, have hydraulic conductivities as low as $10^{-10}$ m/s at water content near the liquid limit, and exhibit significant attenuation capacity by cation adsorption. Field tests also revealed that drying of slime slurries are time consuming. Hence, special methods to facilitate drainage of slime slurries would be necessary if the slimes are to be dried prior to using as a lining material. Overall, slimes lining technology in Melbourne has been useful in not only developing acceptable lining conditions for municipal waste landfills in the sand pits, but also it enabled the rehabilitation of dangerous sites by reusing a waste product.

*Acknowledgments*

## References

Blight, G.E. and Bentel, G.M., 1983, "The behaviour of mine tailings during hydraulic deposition", *Journal of the South African Institute of Mining and Metallurgy*.

Bouazza, A. and Seidel, J.P., 1999, "Foundation design on municipal solid waste", *Proceedings 8th Australia-New Zealand Conference on Geomechanics*, Institute of Engineers of Australia, Vol.1, pp. 235-241.

Cavey, B.W. 1993, "*Slimes and clay liners in landfills*". Final year project. Monash University, Department of Civil Engineering, Melbourne, Australia.

Chandler, K.R.,1992, "Brighton group-engineering properties*", Proceedings Seminar On Engineering Geology of Melbourne*, Balkema, Rotterdam, pp.197-203.

Fassett, J.B., Leonardo, G..A. and Repetto, P.C., 1994, "Geotechnical properties of municipal solid wastes and their use in landfill design", *Proceedings Waste Technical Conference*, Charleston, SC.

Filz, G.M. and Duncan, 1992, "*An experimental and analytical study of earth loads on rigid retaining walls*", Research Report, Virginia Polytechnic Inst. And State University, VA, USA.

Golder Associates Pty Ltd., 1993, "*Hydrogeological and engineering review – proposed Fraser road No. 2 landfill, Clayton Victoria*", (unpublished report).

Hancock, J.S., Phillips, I.R. and Othman, M.,1994, "Use of sand washing slimes for leachate containment in landfills", *Proceedings 2nd National Hazardous and Solid Waste Convention*, AWWA, Melbourne, pp. 257-266.

Ingold, T.S, 1979, "The effects of compaction on retaining walls", *Geotechnique*, vol.29, No3, pp. 265-283.

Kodikara, J. and Rahman, F.,1997, "Clay hydraulic conductivity and permeant electrolyte concentration", *Proceedings 1st Australia-New Zealand Conference on Environmental Geotechnics*, Balkema, Rotterdam, pp. 257-263.

Manassero, M., Van Impe, W.F. and Bouazza, A.,1996, "Waste disposal and containment", *Proceedings 2nd International Congress on Environmental Geotechnics*, Balkema, Rotterdam, Vol. 3, pp.1425-1474.

Mitchell, J.K., 1976, *Fundamentals of soil behaviour*, Series in Geotechnical Engineering, John Wiley & Sons, New York.

Soilmech, 1981, *Report on site investigation for reclamation of slimes pit for rubbish tip for Oakleigh Council*, (unpublished report).

Seddon, K.D., and Bateman, C.S., 1994, "The concept design and development plan of a 10 million $m^3$ MSW landfill at sand pit in S.E. Melbourne", *Proceedings 2nd National Hazardous and Solid Waste Convention*, AWWA, pp. 498-505.

Syllwasschy, O. and Jessberger, H.L., 1998, "Horizontal earth pressure in municipal solid waste landfills. *Proceedings 3rd International Congress on Environmental Geotechnics*, Balkema, Rotterdam, vol.1, pp.163-168.

Watts, K.S. and Charles, J.A., 1990, "Settlement of recently placed domestic refuse landfills", *Proceedings Institution of Civil Engineering*, London, Vol. 8, No 1, pp. 971-993.

Wroth, C.P. and Wood, D.M., 1978, "The correlation of index properties with some basic engineering properties of soils", *Canadian Geotechnical Journal*, vol. 15, No2, pp. 137-145.

Yuen, S.T.S. and Styles, J.R., 1995, "Use of sand washing slimes as landfills liner material", *Australian Civil Engineering Transactions*, vol. CE37, No3, pp. 201-209.

# Case Histories

Ahmet H. Aydilek,[1] Tuncer B. Edil,[1] and Patrick J. Fox[2]

**Consolidation Characteristics of Wastewater Sludge**

---

**Abstract:** Capping is a cost-effective remediation method for soft contaminated sludge. The Madison Metropolitan Sewerage District evaluated different remediation alternatives to treat its polychlorinated biphenyl (PCB) contaminated sludge and the U.S. EPA agreed to permit capping as the method of remediation. Design of the cap required knowledge of the consolidation behavior of the sludge. In order to analyze this behavior, a series of consolidation tests was performed. The laboratory testing program included three large-scale consolidation tests and four conventional oedometer tests. Consolidation settlement of the sludge was observed in two field test cells capped with a wood chip/soil mixture which was reinforced with a woven geotextile. Instrumentation of the test cells included settlement plates, surface survey markers, and piezometers at different depths in the sludge. Laboratory and field observations were compared with results from conventional consolidation theory and a nonlinear finite-strain (large strain) numerical model (CS2). Conventional theory exhibited some limitations in analyzing the results and underpredicted the time for completion of consolidation. However, the large strain model more accurately predicted the behavior observed in both the laboratory and the field.

**Keywords:** sludge, consolidation, hydraulic conductivity, compressibility, large strain, capping, covers.

## Introduction

Construction of an engineered cover or capping system is an efficient and economical component of many in situ containment strategies for contaminated sludges and other high water content waste materials. Considerable evidence has been provided in recent studies (Grefe 1989, Zeman 1994) that containment of soft sediments and papermill sludges by capping, including subaqueous capping, may provide a cost-effective solution.

---

[1] Graduate Research Assistant and Professor, respectively, Dept. of Civil and Envir. Engr., University of Wisconsin, Madison, WI 53706

[2] Associate Professor, Dept. of Civil and Envir. Engr., University of California, Los Angeles, CA 90095

309

The Madison Metropolitan Sewerage District (MMSD) generates sludge as part of its water treatment process. This sludge has been disposed in lagoons and subsequently retrieved as fertilizer for application on farmlands.  Some of the sludge contained polychlorinated biphenyls (PCBs) at concentrations above the allowable limit (50 mg/kg) and was banned from land application. The main objective of capping was to isolate the sludge and support the growth of a vegetative cover, thus minimizing exposure to potential ecological receptors. The U.S. EPA has approved this concept of capping as the method of remediation for the lagoons.

A cap constructed over a high water content sludge is subject to considerable settlement that needs to be assessed at the design stage.  This paper presents the settlement behavior of MMSD wastewater sludge.  Small and large-scale laboratory consolidation tests were conducted and field observations were made for two test cells capped with a wood chip/soil mixture. Field and laboratory results were evaluated using two consolidation models, conventional (infinitesimal strain) theory and nonlinear finite strain (large strain) theory.

## Experimental Work

### Sludge Characteristics

Sludge samples were obtained from a test cell in Lagoon #2A of the MMSD Nine Springs Wastewater Treatment Plant in Madison, Wisconsin USA.  The samples had an average water content of 305%, corresponding to a solids content (weight of solids as percentage of total weight) of 25%.  The sludge did not exhibit plasticity.  The solid phase of the sludge contained 22-30% fines (<0.075 mm) as determined by wash sieving. The sludge had a mean specific gravity of 1.85 and an organic content of 25%.

### Laboratory Consolidation Tests

Large-scale consolidation tests were performed using a slurry consolidometer (203 mm in diameter) similar to that described by Sheeran and Krizek (1971) (Figure 1). Small-scale oedometer (63 mm in diameter) tests (ASTM D2435) were also performed on four specimens trimmed from a consolidated block generated at the end of one large-scale consolidation test.  Preliminary test results indicated that gas generated in the sludge impedes the consolidation process (Aydilek 1996).  The effect was not noticeable in the oedometer tests due to the small specimen size.  However, this effect was evident from the initial settlement readings of the slurry consolidometer tests.  In order to eliminate this problem, a backpressure of 345 kPa was applied to the sludge specimens during testing. Before placement of the sludge in the slurry consolidometers, a woven slit-film polypropylene geotextile (mass per unit area = 203 g/m$^2$) was placed over the bottom porous stone to prevent clogging with fine particles.  This also facilitated the separation of the consolidated block from the lower stone after testing.  The same geotextile was also placed on top of the sludge prior to testing.

Three large-scale consolidation tests were performed.  The first two were conducted using a single small vertical stress increment (9.65 kPa) which was comparable to the

vertical stress expected in the field due to the cap. In these tests, the load was maintained constant on the specimen after the end of consolidation to observe secondary compression. Consolidation was considered to be complete when excess pore pressure at the base of a specimen decreased below the measurement limit (1 kPa). The third test was initiated at a higher vertical stress (15.2 kPa) and continued incrementally to a final stress of 123 kPa with a load-increment-ratio (LIR) of one. Each loading stage was terminated at the end of consolidation, also determined by pore pressure measurements at the base of the specimen. Settlement was measured using a long-stroke dial gage and a potentiometer because of the large deformations. In general, both devices gave comparable results. After each load increment, a hydraulic conductivity test was performed with flow moving from top to bottom of the sludge specimen. Outflow was collected at the base of the specimen (see Figure 1). The hydraulic gradient was smaller than 3 in each test to minimize seepage-induced consolidation. The main objective of the large-scale testing was to determine the large strains caused by small stress increments.
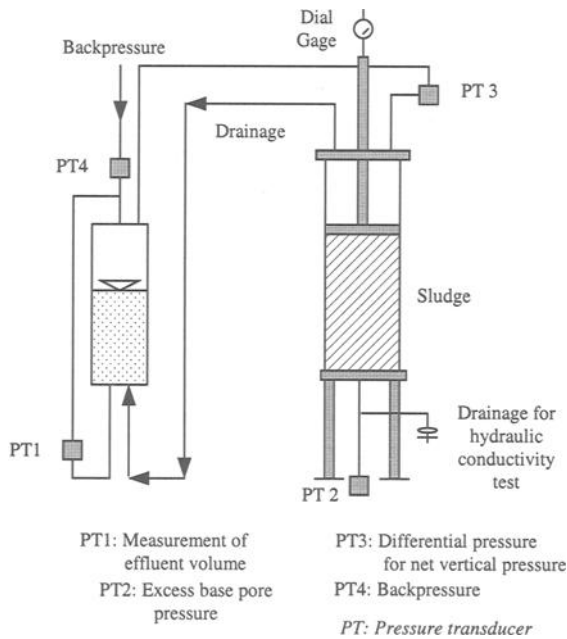


Figure 1- *Large-scale consolidation test*

Sludge specimens for the small-scale oedometer tests were obtained from the consolidated block of a single-increment large-scale consolidation test (Large-scale test 1). They were loaded incrementally in the oedometer cell to a maximum consolidation stress of 50 kPa using a load increment duration (LID) of 24 hours and a LIR of one. Backpressure was not applied to the specimens and no hydraulic conductivity tests were

conducted between load increments. Drainage was provided at the top of the specimens and base pore pressures were monitored with a pressure transducer. Table 1 provides a summary of the laboratory consolidation test program.

Table 1 – *Summary of laboratory testing program.*

| Test No.* | Initial water content, $w_o$ (%) | Initial void ratio, $e_o$ | Vertical effective stress, $\sigma'$ (kPa) | Final void ratio, $e_f$ | Final strain (%) |
|---|---|---|---|---|---|
| S1 | 306 | 5.66 | 6.25, 12.5, 25, 50 | 3.98 | 4.3, 8.4, 15, 25 |
| S2 | 284 | 5.25 | 6.25, 12.5, 25, 50 | 3.30 | 7, 12.8, 21, 31 |
| S3 | 256 | 4.74 | 6.25, 12.5, 25, 50 | 3.14 | 4, 8.8, 16.8, 28 |
| S4 | 230 | 4.26 | 6.25, 12.5, 25, 50 | 2.72 | 5.5, 12, 19.4, 29 |
| L1 | 367 | 6.77 | 9.65 | 4.97 | 24 |
| L2 | 302 | 5.57 | 9.65 | 4.39 | 18 |
| L3 | 389 | 7.18 | 15.2, 30.4, 60.8, 123 | 4.14 | 19.7, 26.4, 30.8, 37 |

*S = small-scale oedometer test, L= Large-scale consolidation test

## Results of Laboratory Tests

*Large-Scale Consolidation Tests*

Vertical strains for the first stress increment of the large-scale tests were much larger than those observed in the small-scale tests (Table 1) because of higher initial water contents. Test L1 continued for 100 days under constant vertical stress to observe the secondary compression behavior (Figure 2). It is interesting to note that a tertiary compression behavior, as reported for peats and dredgings (Edil and Dhowian 1979, Krizek and Salem 1974) was also observed for the MMSD wastewater sludge. The
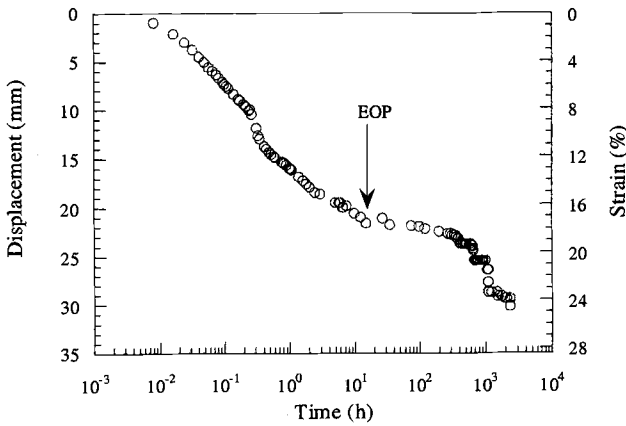


Figure 2 – *Displacement versus time for large-scale test 1*

coefficient of secondary compression $(C_\alpha)$ observed after the end of primary consolidation (EOP), but prior to tertiary, was 0.062. The sharp increase of $C_\alpha$ observed after 500 hours may be due to decomposition of organic matter in the sludge (Fox et al. 1999).

Plots of void ratio versus stress for the large-scale consolidation tests did not show a consistent relationship due to the different initial void ratio $(e_o)$ for each test. Figure 3a shows a plot of void ratio change $(\Delta e)$ from the initial value versus stress. The measurements obtained in field tests are also shown for comparison. The decrease in $\Delta e$ with increasing stress is given by the following approximation:

$$\Delta e = 1.402\log(\sigma') - 0.058 \qquad (1)$$

where $\sigma'$ is vertical effective stress (kPa).

The coefficient of compressibility $(a_v = -de/d\sigma')$ is plotted versus $\sigma'$ in Figure 3(b). Except for the first stress increment in the large-scale test, $a_v$ values are quite comparable between the small and large-scale tests.

Values of hydraulic conductivity from the laboratory consolidation tests are shown versus void ratio in Figure 3c. This figure also includes another relationship based on data obtained from field tests and laboratory gradient ratio tests (ASTM D5101) performed in connection with a separate investigation of the filtration properties of geotextiles. The logarithm of k decreases linearly with decreasing e; however, the slope of the relationship is not one-half of the initial void ratio as has been reported for many clays (Mesri et al. 1994). Laboratory hydraulic conductivity values decrease from 7.8 x $10^{-6}$ m/s to 1.2 x $10^{-9}$ m/s as the void ratio decreases from 7.20 to 4.14. The following function was fitted to the hydraulic conductivity data:

$$\log k = 1.245e - 14.07 \qquad (2)$$

where k is vertical hydraulic conductivity (m/s). Equation 2 is similar in form to corresponding relationships observed for other high water content geomaterials; however, the magnitude of hydraulic conductivity and void ratio vary with material and composition (Wang and Tseng 1993). The slope of the linear relationship appears to be higher than that typically observed for clays.

*Small-Scale Oedometer Tests*

Results of the conventional (small-scale) oedometer tests are summarized in Figure 4. The slope of e-$\log\sigma'$ curve, i.e., compression index, $C_c$, progressively increases with increasing stress (Figure 4a). Values of $C_c$ for most natural clays are less than 1, and typically less than 0.5. The data in Figure 4 indicate that the MMSD sludge samples have $C_c$ = 1 to 2 and classify as highly compressible having $C_c/(1+e_o)$ greater than 0.2. The relationship between $a_v$ and $\sigma'$ is shown in Figure 3b.
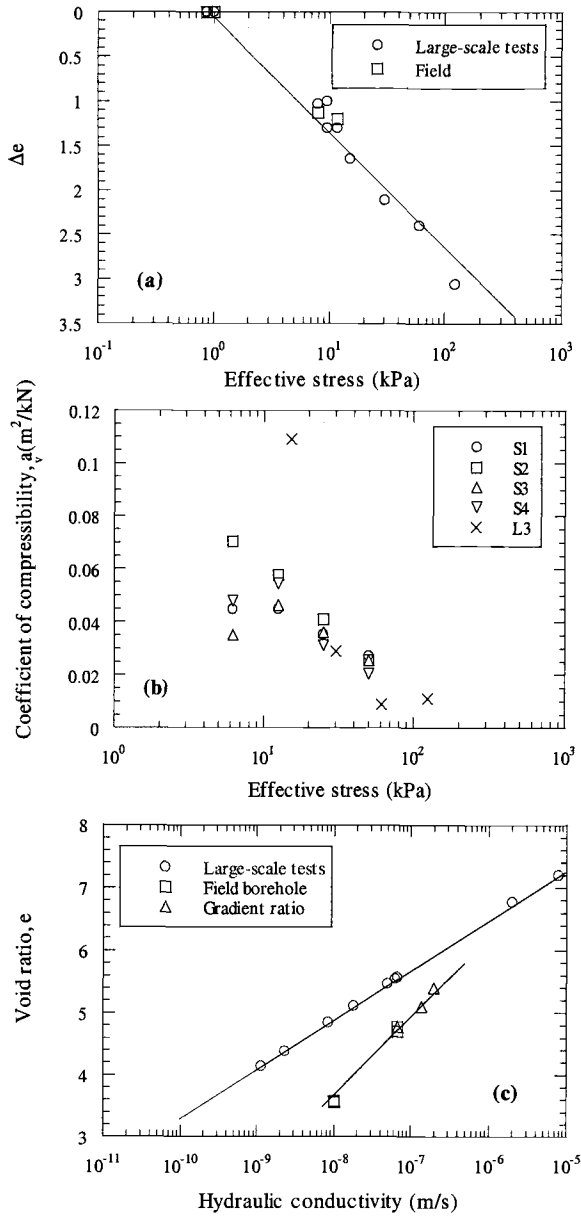
Figure 3 - *Results of large-scale consolidation tests*

Rate of compression was observed to decrease with time under any given load; however, the void ratio versus log-time relationship did not exhibit the classic "S" curve as observed for clays.    Nevertheless, coefficient of consolidation ($c_v$) values were calculated in accordance with the Taylor method and are given in Figure 4b. Due to the shape of the displacement versus time curves, the Casagrande method was not applicable. $c_v$ varies from $5.1 \times 10^{-8}$ to $1.7 \times 10^{-6}$ m$^2$/s for the sludge and, in general, decreases with increasing effective stress. The coefficient of consolidation typically varies from $3 \times 10^{-9}$ to $1 \times 10^{-7}$ m$^2$/s for most clays (Duncan 1993). The $c_v$ values obtained for MMSD sludge specimens are generally higher than those reported for clays, which indicates a higher rate of consolidation for this material.
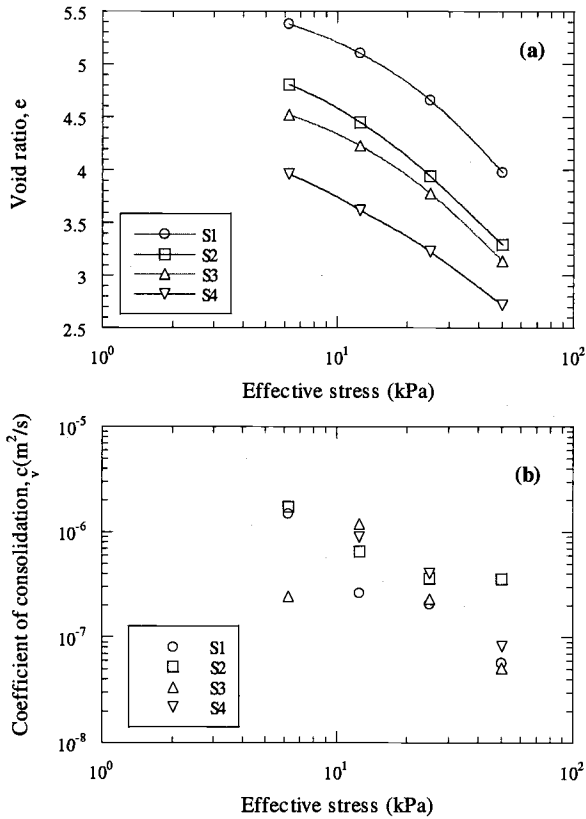


Figure 4 - *Results of small-scale (conventional) oedometer tests*

## Field Studies

To investigate the consolidation of MMSD sludge in the field, two test cells were capped using a light-weight fill (i.e., a wood chip/soil mixture).  The cells were constructed in two different seasons, summer and winter, to observe seasonal effects on constructability.  Total and differential settlement of the cap due to consolidation of the underlying sludge is an important design issue.  Geosynthetic reinforcement (a woven geotextile) was installed below the lightweight fill to provide stability.  It does not significantly affect the total settlement of the cap, however, the presence of a strong geotextile with good filtration characteristics helps to reduce differential settlement and retain sludge solids.

Test Cell 1 was constructed on a 24 m long by 19 m wide section of Lagoon 2A, on August 2, 1996 (Edil and Aydilek 1996).  The test cell was confined on three sides with dikes and open on the fourth side.  Before construction, the sludge had an average solids content of 25%, corresponding to a water content of 300%, and an average depth of 1.2 m.  The sludge was stored in the lagoon for more than 10 years; therefore, sedimentation and self-weight consolidation were assumed to be complete.  First, a woven slit-film polypropylene geotextile (mass per unit area = 203 $g/m^2$) was placed on the in-place sludge to facilitate placement of the cap.  The cap was composed of a wood chip/soil mixture with a wet unit weight ranging from 7.5 $kN/m^3$ to 10.4 $kN/m^3$ as determined from sand cone tests.  The west section of the cap was generally compacted more than the east section (Figure 5) due to a higher number of equipment passes during construction.  As a result, cap thickness and the applied stress was not uniform over the sludge.  The applied stress was approximately 11 kPa on the west section and 7.6 kPa on the east section (there are local areas where the applied stress was as low as 5.5 kPa) based on cap thickness and density measurements.

Settlement of the sludge was monitored using two settlement plates, one on the west section and the other on the east section, set on the geotextile (Figure 5).  Ten open tube piezometers placed at different locations and depths were used to observe groundwater
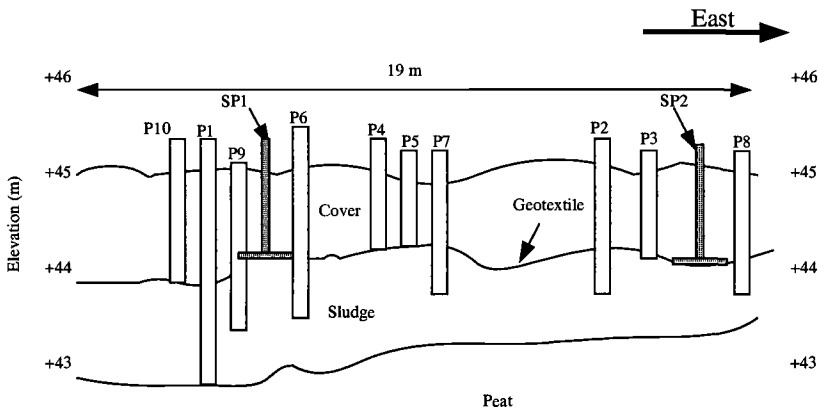


Figure 5 - *Instrumentation of field Test Cell 1*

levels and excess pore pressures during consolidation. Instrumentation of the cell also included nine surface survey blocks to monitor settlement of the cap.

The settlement plates indicated that a settlement of 0.16 m occurred on the west section of the cell (initial thickness, $H_o$ = 1.33 m) during construction and another 0.28 m of settlement was observed in the following 2 years; this corresponds to a total strain of 33%. Corresponding values for the east section ($H_o$ = 1.14 m) were 0.15 m, 0.21 m, and 31%, respectively. Post-construction surface movements, as indicated by the survey blocks, ranged from 0.05 to 0.14 m.

Excess pore pressures were computed from the difference in water levels for piezometers inserted in the sludge relative to those with their tips at the bottom of the cap. Figure 6 shows that excess pore pressures were close to zero on October 1, 1998 (nearly 800 days after construction) and consolidation was essentially complete. The maximum excess pore pressure was registered in piezometer P1 with its tip at the bottom of the sludge. This suggests that drainage into the peat at the bottom was limited.

To obtain the change in hydraulic conductivity due to settlement of the sludge, cased borehole slug tests were conducted before and after cap construction. A measured amount of water was added into the piezometers and the change in water level was determined over time. As this test is similar to the first stage of Boutwell borehole tests (Daniel 1989), the following equation was used to calculate the hydraulic conductivity:

$$k = \frac{D}{(t_2 - t_1)} \ln(\frac{H_1}{H_2}) \qquad (3)$$

where D is the inner diameter of the piezometer tube, and $H_1$ and $H_2$ are the initial and final heights of water in the piezometer, respectively, at times $t_1$ and $t_2$. Values of hydraulic conductivity measured by this method reflect mostly the effect of vertical flow; however, the effect of horizontal flow is also included to a certain extent.
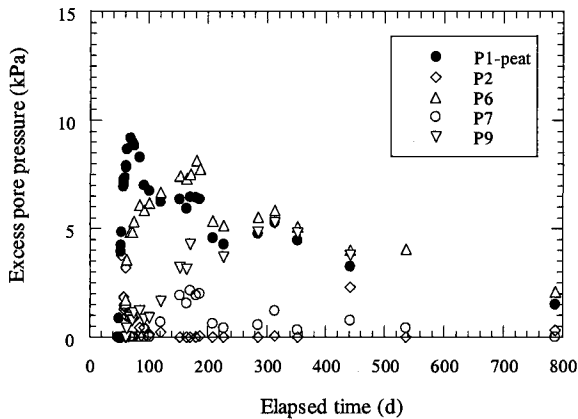


Figure 6 - *Excess pore pressures measured for Test Cell 1*

Figure 3c shows that field hydraulic conductivity values were higher than corresponding values obtained from the large-scale consolidation tests. This is most probably due to the heterogeneous structure of the sludge in the field and possible anisotropic effects. The decrease in field hydraulic conductivity with decreasing void ratio can be characterized by,

$$\log k = 0.78e - 10.86 \qquad\qquad (4)$$

where k is in m/s.

The construction of Test Cell 2 was performed during the winter (February 12, 1997) and was facilitated by a 60 mm thick layer of ice over a 0.3 m thick layer of frozen sludge. The frozen sludge was underlain by a 1 m thick layer of soft sludge. Test Cell 2 was constructed using the same reinforcement geotextile and wood/chip soil mixture. The wet unit weight of the cap material was 6.3 kN/m$^3$ on the northwest section and 10.5 kN/m$^3$ on the east section. The vertical stresses ranged from about 3 kPa to 9 kPa. These values were lower than those for Test Cell 1.

Before construction, the sludge had an average solids content of 18%, corresponding to a water content of 470%. To evaluate settlement behavior of the sludge, four settlement plates were placed on the sludge surface. The measurements indicated a settlement of 0.21 m at the east section of the cell through the spring thaw (2.5 months) and another 0.30 m of settlement in the following 17 months, giving a total strain of 36%. Values for the northwest section (where the applied stress was lower) were 0.075 m, 0.26 m, and 30%, respectively. Cap surface settlements determined from the survey blocks were comparable to those for the settlement plates, indicating that the post-construction cap compression was insignificant (Edil and Aydilek 1997). Because of thaw compression, consolidation of the sludge layer due to the cap load was not accurately known; therefore, the settlements of Test Cell 2 were not analyzed.

## Modeling of Consolidation

Conventional consolidation (Terzaghi) theory is an infinitesimal strain formulation. Specifically, the theory assumes that the hydraulic conductivity, compressibility, and thickness of the compressible layer remain constant during the consolidation process. However, high water content materials, such as the MMSD sludge, experience large strains during consolidation, thus invalidating these assumptions. To investigate these effects, settlement estimates obtained from conventional theory and a numerical finite strain model (CS2) were compared with measured values from the large-scale laboratory tests. CS2 estimates were also compared with measured field settlements for the two settlement plates of Test Cell 1.

CS2 is a piecewise-linear model for one-dimensional consolidation which accounts for vertical strain of the compressible layer (Fox and Berles 1997). The required input parameters for the program are the initial thickness of the soil layer, initial and final overburden effective stress conditions, initial void ratio at the top of the layer, specific gravity of solids, and void ratio-effective stress (e-$\sigma'$) and void ratio-hydraulic

conductivity (e-k) relationships.  The output file gives the settlement and excess pore pressure profile for specific values of time.  The model vertically divides the strata into $R_j$ elements. An $R_j$ value between 50 and 100 usually gives satisfactory results (Fox and Berles 1997).  Initial trials with different $R_j$ values verified these findings; therefore, $R_j$ = 50 was chosen for the simulations.  A $G_s$ value of 1.0 was specified to disable the effect of self-weight consolidation in the model.  Since the sludge had been stored in the lagoons for more than 10 years, self-weight consolidation was most likely completed. Therefore, CS2 was used to determine the consolidation due only to the applied surface load from the cap.

Figure 7 provides a comparison of estimates obtained from conventional theory and CS2 with the measurements for the incremental large-scale consolidation test (L3).  The $\Delta e$ values given by Equation (1) were subtracted from the initial void ratio ($e_o$) for each increment in order to obtain the necessary e-$\sigma'$ relationship for CS2.  The e-k relationship was given by Equation (2) based on the laboratory tests.  Estimates of average degree of consolidation, $U_{average}$, (i.e., settlement/initial height) versus time, as given by CS2, were generally in a good agreement with measured values from the laboratory test.  Estimates obtained using conventional theory based on initial values of $c_v$ underestimated the time for any given average degree of consolidation.  This is due to the limiting assumptions of conventional theory, especially the assumption of constant k.

Settlement estimates from CS2 were compared with measured values from Settlement Plates 1 (SP1) and 2 (SP2) in Test Cell 1 (Figure 8).  Equations (1) and (4) were used for the input values of e versus $\sigma'$ and e versus k in CS2.  CS2 estimates were in good agreement with observed values in terms of both magnitude and rate of settlement.  The use of Equation 2 based on laboratory hydraulic conductivity tests resulted in much slower rates of settlement than those observed in the field.

## Conclusions

The consolidation characteristics of a wastewater treatment sludge were investigated using laboratory and field tests.  The results were compared with estimates given by infinitesimal-strain and large-strain consolidation models.  The following conclusions are reached as a result of this study:

1) The consolidation characteristics of the sludge were different than those of natural clays.  Relative to most clays, the sludge exhibited higher compressibility, higher hydraulic conductivity, and a higher rate of consolidation due to high water content and the presence of organic matter.

2) Large-scale consolidation tests were more effective for the measurement of large compression of the sludge during the first load increment.  Both the void ratio and hydraulic conductivity varied with applied consolidation stress in a manner comparable to the behavior generally observed for high water content materials.

3) Field test cells indicated approximately 33% compression over a 2-year period for sludge with an initial thickness of 1.5 m and an initial water content of 300% under an applied stress of 8 to 11 kPa.  Winter frost in the sludge and formation of an ice layer over the sludge facilitates cap construction; however, significant compression occurs
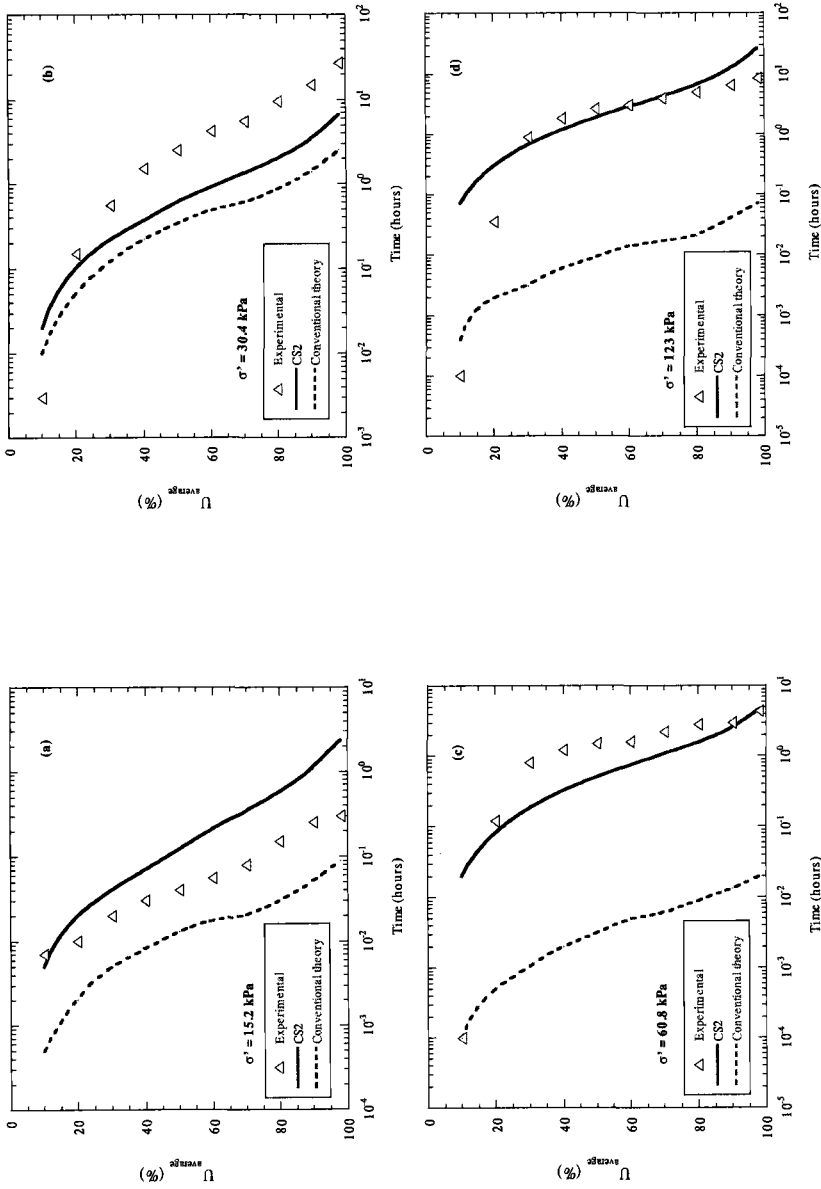
Figure 7. Comparisons of measured and estimated average degree of consolidation for large-scale laboratory test 3 (L3).
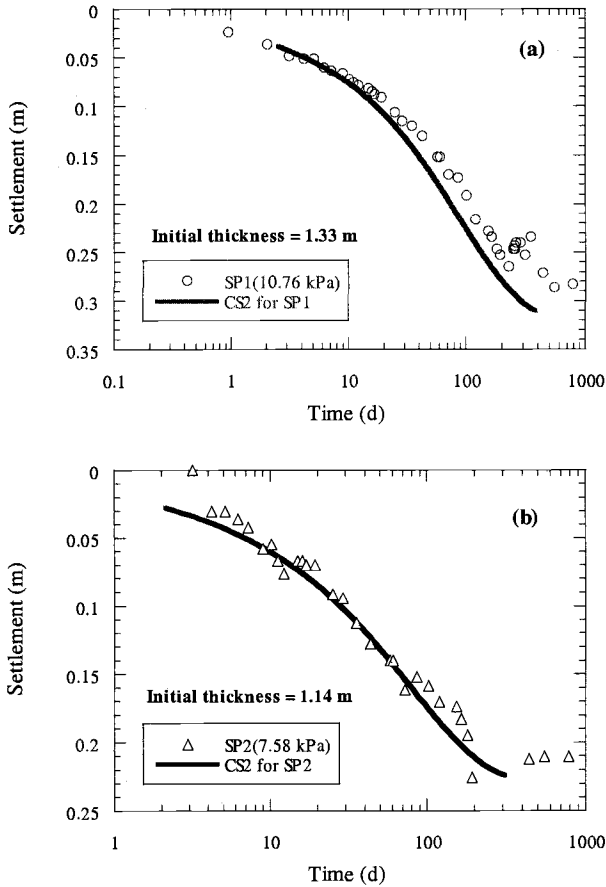
Figure 8 – *Observed and estimated settlements for Test Cell 1:*
*(a) SP1 location and (b) SP2 location*

during the subsequent spring thaw. Large-scale laboratory consolidation tests provided a satisfactory estimate of the magnitude of total settlement in the field.

4) CS2, a numerical code for large strain consolidation, successfully estimated the time required for a given settlement in the field. It also provided a reasonable representation of the large-scale laboratory consolidation tests. Conventional infinitesimal-strain (Terzaghi) theory underestimated the elapsed time for a given average degree of consolidation.

5) The time rate of consolidation is sensitive to the hydraulic conductivity-void ratio relationship. Use of the laboratory hydraulic conductivity-void ratio relationship resulted in an underestimate of the field rate of consolidation whereas the relationship

based on field hydraulic conductivity measurements resulted in good estimate of the field rate of consolidation.

## Acknowledgements

## References

Aydilek, A. H., 1996, "Solidification, Consolidation, and Filtration Characteristics of Madison Metropolitan Sewerage District Sludges," M.S. Thesis, University of Wisconsin-Madison, Madison, WI.

Daniel, D. E., 1989, "In Situ Hydraulic Conductivity Tests for Compacted Clay," *Journal of Geotechnical Engineering, ASCE*, Vol. 115, No. 9, pp. 1205-1226.

Duncan, J. M., 1993, "Limitations of Conventional Analysis of Consolidation Settlement," *Journal of Geotechnical Engineering, ASCE*, Vol. 119, No. 9, pp. 1333-1359.

Edil, T. B. and Aydilek, A. H., 1996, "Construction and Performance Analysis of Sludge Lagoon Test Cell Cap-Phase I," Progress Report submitted to the Madison Metropolitan Sewerage District.

Edil, T. B. and Aydilek, A. H., 1997, "Winter Construction and Performance Analysis of Sludge Lagoon Test Cell Cap-Phase II," Progress Report submitted to the Madison Metropolitan Sewerage District.

Edil, T. B. and Dhowian, A. W., 1979, "Analysis of Long-Term Compression of Peats" *Geotechnical Engineering,* Southeast Asian Society of Soil Engineering, Vol. 10, No. 2, pp. 159-178.

Fox, P. J. and Berles, J. D., 1997, "CS2: A Piecewise-Linear Model for Large Strain Consolidation," *International Journal for Numerical and Analytical Methods in Geomechanics,* Vol. 21, No. 7, pp. 453-475.

Fox, P. J., Roy-Chowdhury, N., and Edil, T. B., 1999, "Discussion of 'Secondary Compression of Peat with or without Surcharging,'" *Journal of Geotechnical and Geoenviromental Engineering, ASCE*, Vol. 125, No. 2, pp. 160-162.

Grefe, R. F., 1989, "Closure of Papermill Sludge Lagoons Using Geosynthetics and Subsequent Performance," *Proceedings of the 12<sup>th</sup> Annual Madison Waste Conference*, University of Wisconsin-Madison, Madison, WI, pp. 121-162.

Krizek, R. J. and Salem, A. M., 1974, "Behavior of Dredged Materials in Dyked Containment Areas" Technical Report No.5 by Northwestern University, Civil Engineering Department, submitted to the U. S. Environmental Protection Agency.

Mesri, G., Lo, D. O. K., and Feng, T. W., 1994, "Settlements of Embankments on Soft Clays," *Geotechnical Special Publication No.40, ASCE*, Vol. 1, pp. 8-56.

Sheeran, D. E. and Krizek, R. J., 1971, "Preparation of Homogeneous Soil Samples by Slurry Consolidometers," *Journal of Materials, ASTM*, No. 2, Vol. 6, pp. 356-373.

Wang, M. C. and Tseng, W., 1993, "Permeability Behavior of a Water Treatment Sludge," *Journal of Geotechnical Engineering, ASCE*, Vol. 119, No. 10, pp. 1672-1677.

Zeman, A. J., 1994, "Subaqueous Capping of Very Soft Contaminated Sediments," *Canadian Geotechnical Journal*, Vol. 31, No. 4, pp. 570-577.

M. Mehmet Berilgen, I. Kutay Özaydin,[1] and Tuncer B. Edil[2]

A Case History: Dredging and Disposal of Golden Horn Sediments

**Abstract:** Rehabilitation of the historic Golden Horn river outlet has been a major concern to people of Istanbul in the past two decades. Currently a major rehabilitation project is being implemented which involves the dredging of bottom sediments in the upstream one third of this waterway to provide for sufficient water depth needed for a clear marine environment and to make navigation possible for small vessels. The stability analyses have shown that the 6 (horizontal): 1(vertical) underwater slopes formed by dredging can be sustained. Among the several possible alternatives considered for the disposal of dredged bottom sediments, the most economical and environmentally safe alternative was storage of the sediments at an abandoned rock quarry pit at a distance of about 5 km. A 40-m- high, zoned earth dam constructed at the rock pit site enabled the storage of about 4 million cubic meters of dredged material, which is pumped via a pipeline. The pumped dredgings are undergoing large-strain self-weight consolidation. The paper presents this case history and the associated technical challenges. The geotechnical issues relating to the stability of the dredged channel as well as the result of the laboratory investigations on sedimentation and self-weight consolidation behavior of the dredged materials are presented together with the numerical prediction of field behavior at the disposal site.

**Keywords:** disposal of dredged material, self-weight consolidation, consolidation, settlement, large strain, numerical modeling

[1]Assistant Professor and Professor, Civil Engineering Faculty, Yildiz Technical University, Istanbul, Turkey, 80750
[2]Professor, Department of Civil and Environmental Engineering, University of Wisconsin, Madison, WI

## Introduction

The Golden Horn Bay is a long and narrow waterway dividing the European side of Istanbul and is the site of many historical monuments. In the past centuries, the region was used as a recreational area because of its picturesque surroundings. In addition to the silting caused by two small streams flowing into the Golden Horn and deposition of materials from the surrounding hills, disposal of untreated sewage and waste after the rapid growth of the city starting from early 1950's have largely filled this waterway and led to a highly polluted environment. Currently, a major effort is under implementation to rehabilitate the Golden Horn.

In this paper, first the geology and formation of Golden Horn is described and the geotechnical characteristics of the sea bottom sediments are presented. The results of the laboratory investigations carried out to study the sedimentation and self-weight consolidation characteristics of the dredged materials are utilized to predict field behavior. Two computer codes are used for numerical modeling of large-strain self-weight consolidation of dredged Golden Horn bottom sediments at the disposal site and the results are compared with observed behavior.

## The Golden Horn: Its Formation, Geology and Geotechnical Characteristics

It is generally accepted that the formation of Bosphorus and Golden Horn started approximately 8000 years ago with the flooding of ancient river valleys with the waters of the Mediterranean. Archeological findings indicate that these environmental changes have taken place concurrently with the start of human dwellings in the area. The thickness of deposits in the Golden Horn indicate a very high rate of deposition (approx. 7 m /1000 years), which is believed to be due to the elevation caused by young tectonic movements (Özaydin and Yildirim, 1997).

Golden Horn is located at a topography lowering towards the South. Alibey and Kagithane streams flowing southwards reach Golden Horn at its north end where it is about 450 m wide, then it extends first in southwest direction to Eyüp from that point on it continues in the southeast direction towards Bosphorus (Figure 1). On both shores of the Golden Horn, flat lands of about 150-m width with a few meters elevation from the sea level are encountered. The western shores of Golden Horn are gently sloping to heights of 40-60 m, whereas the eastern shores have higher slopes reaching to 80-140 m elevations.

Bottom elevations in Golden Horn are higher than those at Bosphorus and therefore Golden Horn can be considered a suspended valley. The rise due to tectonic movements caused the formation of three ridges in the sea bottom. It is postulated that the third ridge
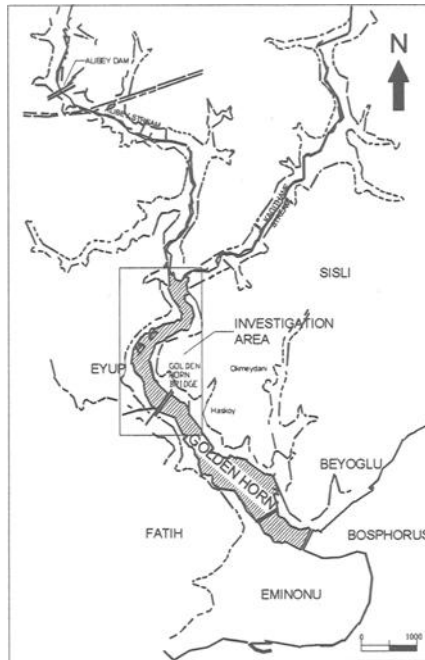
Figure 1 - *The Golden Horn*

sets a boundary for rapid deposition and filling, and the sections of Golden Horn beyond this point are under the influence of active marine and current environment.

The base formation around Golden Horn area consists of graywacke formation consisting of sandstone-siltstone-claystone rocks. Young Golden Horn deposits (Holocene) are directly seated on graywacke rocks thickness of which reach to 50-60 m, and they are comprised of mainly dark gray colored silty clays and clayey silts. Sands and sandy gravel pockets are also encountered within these alluvial deposits. The upper levels of young alluvial deposits are highly polluted and rich in organic content because of municipal and industrial wastes discharged into this low energy deposition environment. The shores of Golden Horn are covered with a thick artificial fill layer seated on these young deposits.

The rapid growth of population in the Golden Horn area due to industrialization starting from early 1950's and uncontrolled and untreated discharge of municipal and industrial waste until very recent years have led to an unacceptable situation. The upstream part of Golden Horn became almost completely filled. Water depth in this region was generally reduced to less than 1.0 m, and large areas were turned into swamps. Because of this situation, Alibey and Kagithane streams could no longer flow freely into the Golden Horn, the navigation became impossible even for small vessels, and due to lack of sufficient oxygen a very polluted environment with a dense odor was created.

A large number of soil borings have been drilled in the Golden Horn  area for different construction activities.  For rehabilitation project investigations, a total of 19 land (near shoreline) and marine soil borings were drilled, in-situ tests executed and soil samples (both bulk samples from the sea bottom and disturbed and undisturbed samples from various depths) were recovered for laboratory testing.  Findings of both the previous and new borings were utilized to prepare soil profiles for various sections of the Golden Horn.  In-situ tests (SPT, CPT and vane shear) were conducted in the boreholes and an extensive laboratory testing program has been carried out to determine the geotechnical characteristics of soil deposits at the project area.  In Figure 2 the variation of consistency limits and natural water content with depth are shown.
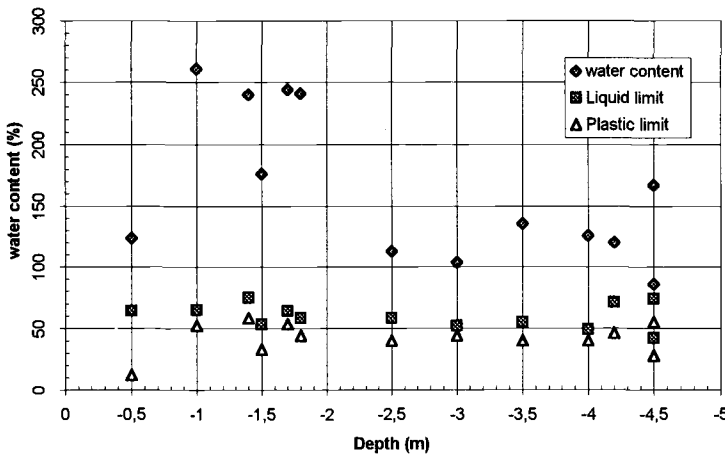


Figure 2 - *Variation of Consistency Limits and Natural Water Content with Depth*

The organic content of the sea bottom deposits are determined to vary between 3% to 6%, and samples are generally classified as sandy clayey silt (MH) according to Unified Soil Classification System.  From the combined evaluation of field and laboratory test results, the variation of in-situ undrained shear strength ($s_u$) with depth (z) to be used in the stability analyses is expressed with the following relationship

$$s_u \text{ (kPa)} = 6 \text{ (kPa)} + 0.7 \, z \text{ (m)} \tag{1}$$

From the results of consolidated undrained (CU) triaxial compression tests, the average drained shear strength parameters for cohesive Golden Horn sediments are determined to be c' = 0    and    $\phi'$ = 19°.

The compression characteristics of soil deposits were investigated with both large slurry consolidation tests performed on bulk samples collected from the sea bottom and standard oedometer tests performed on block samples prepared as a result of slurry consolidation.  The compression characteristics determined from these tests have shown

that the variation of compression index ($C_c$) with initial void ratio ($e_i$) can be defined quite well with a type of relationship proposed by Rendon-Herrero (1980)

$$C_c = 0.141G_s^{1.2}\left\{\frac{(1+e_i)}{G_s}\right\}^{2.38}$$  (2)

where $G_s$ is the specific gravity of solids (Yildirim and Özaydin, 1997).

## Rehabilitation Works

The Golden Horn Rehabilitation Project envisaged the dredging of sea bottom sediments at the upstream half to provide a minimum water depth of 5 m. Considering that large areas near the upstream end were completely filled, and to make the project more feasible and manageable, it was proposed that in these parts not the total area of the Golden Horn is dredged but only wide channels are formed by dredging for Alibey and Kagithane streams. Only beyond a certain point, the whole surface area was dredged to reach 5-m water depth. This would not only allow reducing the volume of material to be dredged, but also provide some storage area for dredged materials on the sides of the dredged channel.

Stability analysis was performed to determine the new geometry to be formed after dredging at Golden Horn. The results have shown that 6 (horizontal): 1 (vertical) side slopes formed by dredging could possess a sufficient degree of safety against sliding, allowing uniform surcharge loading of up 27.5 kPa for storage of dredged materials.

Most suitable alternatives for the disposal and storage of dredged sea bottom sediments were investigated taking into consideration the volume and characteristics of the dredge material and possible adverse environmental effects. After evaluation of all possible alternatives it was decided that the bulk of dredged material was to be transferred via a pipeline to an abandoned crushed rock quarry pit and stored there by means of two rock fill dams. Some of the dredged materials were planned to be stored behind berms formed along the newly opened channels and the low lands along the shoreline.

Experimental investigations have shown that sea bottom deposits dredged from the Golden Horn could attain the characteristics of natural soft-medium stiff cohesive soils upon consolidation. It is postulated that due to surface evaporation and consolidation, the storage areas for dredged material could be converted to fill areas suitable for recreational facilities and very much needed green areas in the center of the city.

Rehabilitation works for the Golden Horn were contracted to a Turkish-American joint venture in the beginning of 1997. After the preparation of the disposal site at the rock quarry, dredging operations started in April 1997 and continued for about 12 months. In-situ volume of the material to be dredged was estimated at 4 000 000 m$^3$ and it was realized during the time envisaged in the contract.

## Laboratory Investigation of Sedimentation and Self-Weight Consolidation

In order to study the sedimentation and self-weight consolidation behavior of dredged materials from the Golden Horn, a laboratory set up as described by Lee et al. (1993) was utilized (Figure 3). Laboratory behavior of dredged slurry at
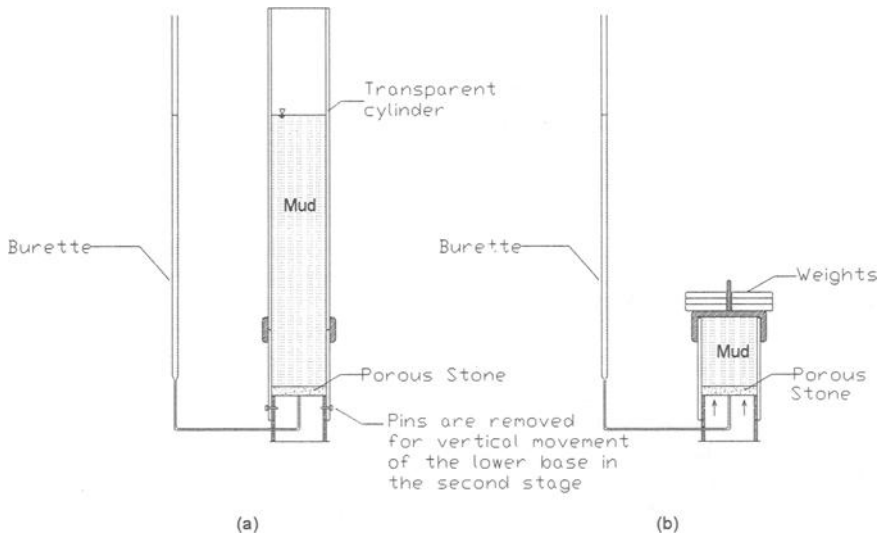


Figure 3 - *Self-Weight Consolidation Apparatus*

actual field (pumping) water contents was investigated by a three stage experimental study. In the first stage, the slurry was left for sedimentation and consolidation under its own weight during which the thickness and compression of the material deposited was monitored with time. In the second stage, the upper part of the equipment was removed and the time-dependent compression under incremental surcharge loading was measured on the lower part (slurry consolidation). In the third stage, a sample recovered from the block sample at the end of second stage was subjected to a conventional incremental loading oedometer test.

In the experimental investigation, samples of the dredgings collected from the discharge pipe were used. Samples were dark gray colored, generally silty clayey soils with some sand and contained organic material as well as some waste material. The samples were wet sieved through No. 40 sieve and brought to 1.17 g/cm$^3$ (pumping density) by addition of water with 0.8% salt in order to model the conditions at the disposal site. In Table 1, the properties of samples used in the experimental investigation and testing conditions are summarized.

Table 1- *Summary of Samples Properties and Test Conditions*

| Test No | Initial water content (%) | Initial slurry height (cm) | Bottom drainage condition | Water content (end of Sedimentation & Self weight consolidation) (%) | Water content (end of Slurry consolidation) (%)/Max.vert. stress (kPa) | Water content (end of oedometer test) (%)/ Final vert. Stress (kPa) |
|---|---|---|---|---|---|---|
| D1 | 445 | 40.0 | Drained | - | 93.2/20.5 | - |
| D2 | 480 | 69.0 | Drained | 156 | 74.7/51.1 | - |
| D3 | 300 | 39.5 | Drained | 149 | 75.7/51.1 | - |
| D4 | 300 | 73.3 | Undrained | 176 | 91.2/20.5 | - |
| D5 | 240 | 70.0 | Drained | 119 | 79.0/65.1 | 38.9/1200 |
| D6 | 230 | 38.0 | Drained | 135 | 83.0/40.9 | 38.0/1200 |
| D7 | 300 | 65.0 | Drained | 156 | 90.0/40.9 | 21.0/800 |
| D8 | 600 | 40.0 | Undrained | 316 | 90.0/40.9 | 20.0/800 |

## Sedimentation and Self-Weight Consolidation

The variation of effective vertical stress with height in slurry consolidating under its own weight is not known.  The experimental setup used in this stage of testing did not enable direct calculation of effective vertical stresses, therefore, experimentally determined void ratio and hydraulic conductivity values were used to estimate (calculate) the effective vertical stress.  For this purpose, a computer program (CS2) utilizing a piecewise-linear finite difference model for one-dimensional large strain consolidation of a soil column under its own weight was used (Fox and Berles, 1997).  CS2 requires relationships between effective vertical stress-void ratio ($\sigma'$-e) and hydraulic conductivity-void ratio (k-e). The constitutive relationships proposed by Somogyi (1979) were utilized in this study:

$$e = A(\sigma')^B \quad \text{and} \quad k = Ce^D \qquad (3)$$

where A, B,C and D are experimentally determined constants.

The rate of outflow during sedimentation and self-weight consolidation was monitored and used to estimate hydraulic conductivity assuming a constant-head flow condition.  The measured height of the sediment provided the void ratio and C and D were obtained from the k-e data by curve fitting.  Estimated values of A and B were used to compute the compression-time behavior using CS2 and, by comparison with the observed values of compression-time, the $\sigma'$-e relationship was calibrated.  In Table 2, the values of A, B, C and D as determined with the procedure described above are given.

Table 2 - *Soil Constants as Determined from Laboratory Tests*

| Test No | A[*] | B | C[*] | D |
|---------|-------|-------|------|-------|
| D2 | 5.710 | -0.24 | 9e-7 | 5.508 |
| D3 | 5.707 | -0.26 | 9e-7 | 5.507 |
| D5 | 5.708 | -0.23 | 9e-7 | 5.507 |
| D6 | 5.707 | -0.24 | 9e-7 | 5.512 |

[*]$\sigma'$ in kPa and k in m/day

## Consolidation Under Surcharge Loading

The dredged the Golden Horn sediments were stored the disposal site and left for self-weight consolidation. After the dredgings are consolidated to a certain degree and a desiccated crust formed, the disposal site is planned to be capped with a cover layer and turned into a recreational area. In order to analyze the compression behavior the dredging deposited at the disposal site under surcharge loading, soil samples prepared by self-weight consolidation were subjected to surcharge loading first in the sedimentation column (slurry consolidation) and than in a conventional oedometer apparatus. In Figure 4, a typical compression (e-log $\sigma'$) curve based on the three stages of consolidation are shown together.

## Prediction of Field Behavior

Field compression of the dredged material from the Golden Horn was studied using two numerical models. The pumping unit weight and water content, variable pumping rates through 12 months of pumping and the total volume of the slurry pumped into the disposal area were obtained from the contractor. The area of the storage site was about 200 000 m$^2$; the total volume of the slurry pumped (after diluting the dredgings for pumping) was 8 200 000 m$^3$, and the height of the dredged material at the end of pumping reached 40 meters. During pumping bottom drainage was provided using trench drains at the bottom (which are functioning effectively to this date) and the supernatant water at the surface was removed with special intakes. The water drained at the bottom and top were returned to the Golden Horn via a second pipeline while the height of deposited material was constantly monitored.

The field compression of deposited material was first studied with the computer code CS2 (Fox and Berles, 1997) which was discussed in the analysis of laboratory behavior. For this code, the total volume (height) of the self-weight consolidating material is assumed stored instantaneously and left to consolidate.
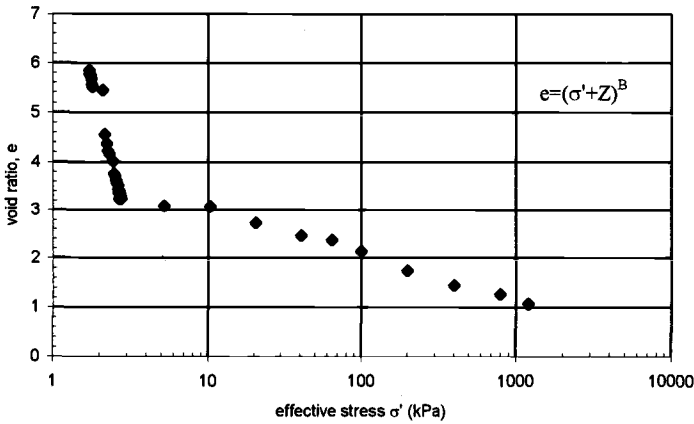
Figure 4 - *Laboratory  Compression Curve Obtained from Self-Weight Consolidation and Incremental Loading*

Using average values of constants in Table 2, the predicted field behavior is shown in Figure 5 with the actual field measurements.  A second computer code (CONDES0) modeling large-strain self-weight consolidation during filling as well as surface desiccation (Yao and Znidarcic, 1997) was also used to analyze the field behavior.  Because no surface desiccation has occurred to this date, the desiccation modeling option was not used for the simulation. CONDES0 uses  the relationship between effective stress-void ratio proposed by Liu and Znidarcic (1991)

$$e = A(\sigma'+Z)^{B} \qquad (4)$$

where A,B and Z are constants. In addition, hydraulic conductivity-void ratio variation is assumed the same as in relationship (3).  The values of constants A, B and Z were obtained by curve-fitting from the laboratory response (Figure 4) as

$$A = 5.7, \quad B = -0.24, \quad Z = 0.04$$

The CONDES0 computer code enables the modeling of actual field pumping rates.  In Figure 6, the field compression behavior of the dredged material stored is shown as predicted with  CONDES0 as well as the actual field measurements together with the loading curve (if there were no consolidation during pumping).  In the same figure the compression curve obtained from CS2 (instantaneous placement) is also shown for comparison.
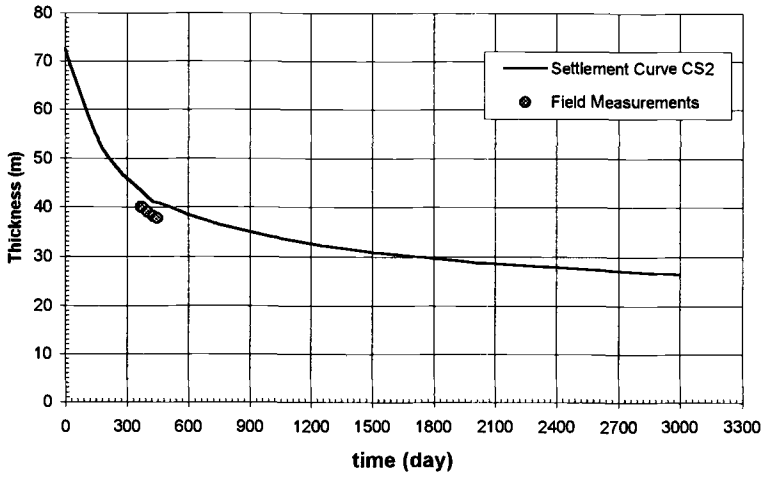
Figure 5 - *Predicted Consolidation Behavior of Dredged Material with CS2 Compared with Field Measurements*
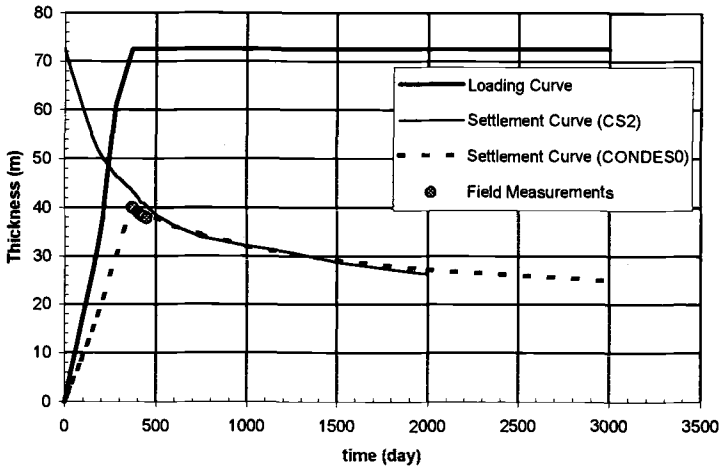


Figure 6 - *Predicted Consolidation Behavior of Dredged Material with CONDES0 and CS2 Compared with Field Measurements*

A parametric study was also completed to study the relationship between rate of the pumping and the self-weight consolidation rate, which is a key factor in storage capacity design. CONDES0 was used taking into consideration various constant pumping rates and curves showing the variation of stored height with time were obtained (Figure 7). In Figure 8, the variation of settlements expected during the pumping period are normalized with respect to the final consolidation settlement is shown as a function of pumping rate.

**Conclusions**

The Rehabilitation Project for the Golden Horn involved the dredging of 4 000 000 $m^3$ of soft bottom sediments, which are highly polluted. The bulk of the dredged material was transferred via a pipeline to a quarry pit for disposal and land reclamation. Laboratory investigations on sedimentation and self-weight consolidation of the dredged materials were performed to establish relationships between effective vertical stress-void ratio and permeability-void ratio, which were then used to predict the field behavior. Two different computer codes, CS2 (Fox and Berles, 1997) and CONDES0 (Yao and Znidarcic, 1997), were used for numerical modeling of large-strain self-weight consolidation. Material constants determined from the laboratory experiments provided satisfactory predictions of field compression behavior. It is shown that realistic estimates of self-weight consolidation behavior of dredged sea bottom sediments stored on land can be made, which is very important in storage capacity design and reclamation planning of such storage areas.

**Acknowledgments**
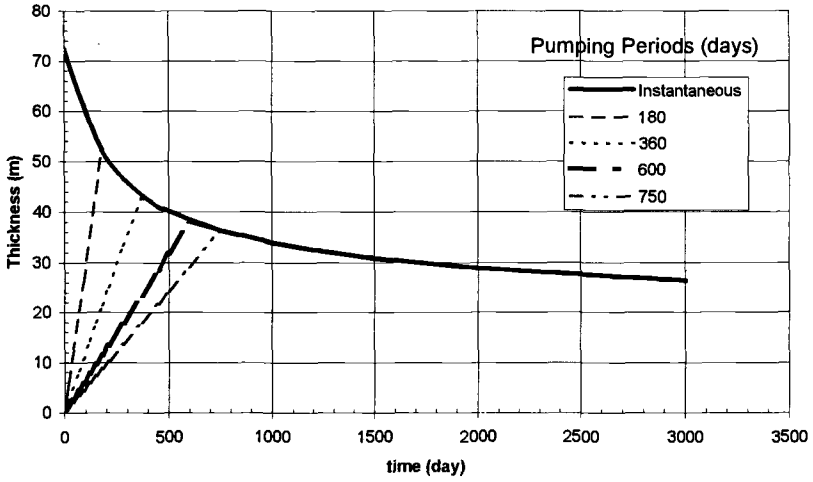
Figure 7 - *Effect of Pumping Rate on Settlement Behavior*
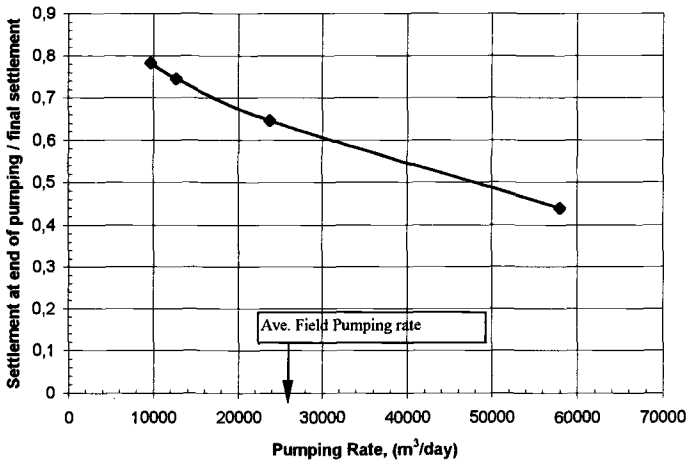


Figure 8 - *Variation of Normalized Settlement at the End of
Pumping with Pumping Rate*

## References

Fox, P. J. and Berles, J. D., 1997, "CS2: A Piecewise-Linear Model for Large Strain Consolidation," *Inter. J. For Numerical and Anal. Methods in Geomechanics*, Vol.21, pp.453-475.

Lee, K., Choa, V., Lee, S. H., and Quek, S. H., 1993, "Constant Rate of Strain Consolidation of Singapore Marine Clay", *Geotechnique*, Vol. 43, No. 3, pp. 471-488.

Liu, J. C. and Znidarcic, D., 1991, "Modeling One Dimensional Compression Characteristics of Soils," *Journal of Geotech. Engr., ASCE*, Vol. 117, No. 1, pp. 162-169.

Özaydin, I. K. and Yildirim, M., 1997, "The Golden Horn: Its Formation, Deterioration and Hopes for Rehabilitation," *Special Volume Honoring Prof. Vedat Yerlici*, Bogazici University, Istanbul, pp. 195-210.

Rendon-Herrero, O., 1980, "Universal Compression Index Equation", *Journal of Geotech. Engr., ASCE*, Vol. 106, No. 11, pp. 1179-1120.

Somogyi, F., 1979, "Analysis and Prediction of Phosphatic Clay Consolidation: Implementation Package," *Technical Report*, Florida Phosphatic Clay Research Project, Lakeland, Florida.

Yildirim, S. and Özaydin, I. K., 1997, " Geotechnical Investigation of The Golden Horn Deposits for Rehabilitation Works", *Green 2- 2nd International Symposium on Geotechnics and the Environment Theme: Contaminated and Derelict Land*, Bolton Institute, September 8-11, Krakow, Poland, pp. 97-102.

Yao, T. C. and Znidarcic, D., 1997, *"User's Manuel for Computer Program CONDES0,"* Numerical Solution Guide to One-dimensional Large Strain Consolidation and Desiccation by Finite Difference Implicit Method, Dep. of Civil, Environmental and Architectural Engineering, Univ. of Colorado, Boulder, CO, 80309, p. 98.

Alexander Abraham[1] and John E. Sankey[1]

**Design and Construction of Reinforced Earth Walls on Marginal Lands**

---

**Abstract:** Reinforced earth (RE) walls, a type of mechanically stabilized earth walls, are described in this paper as a composite system consisting of alternating layers of granular backfill and discrete steel reinforcements connected to precast concrete facing panels. This paper discusses the current procedures used for the design and construction of relatively flexible RE walls over marginally stable soils for roadway applications. Three case histories of RE walls constructed over very soft clays, organic deposits and/or compressible waste materials are provided, with particular emphasis on the technical and practical factors that influence the design of RE walls over marginal lands.

       Technical features that make RE walls a viable alternative to rigid cast-in-place structures for roadway applications are provided. The design of the facing panels, steel reinforcements, and backfill used in RE walls constructed over marginal soils is also discussed. Foundation improvement techniques that were used in the case histories to further reduce the risk of differential settlement due to the uncertainty in the predicted behavior of the material over time are also provided.

       It is demonstrated that RE walls may be designed to accommodate large total and differential settlements. Typically, simple construction techniques such as the use of vertical joints and staged construction may be used to increase flexibility and stability of RE walls. The paper concludes by providing a summary of the design and construction practices that will improve the aesthetics, cost, safety and durability of RE walls.

**Keywords:** Reinforced earth walls, steel reinforcements, precast concrete panels, total settlement, differential settlement, global stability, ground improvements.

**Introduction**

       Reinforced Earth (RE) walls consist of alternating layers of granular backfill and galvanized steel reinforcements connected to precast concrete facing panels (Figure 1). This paper discusses the design features of RE walls in relationship with their use over marginal lands. Case histories of RE walls constructed over very soft clays, organic

---

[1]Project Engineer and Vice-President, respectively, The Reinforced Earth Co., 8614 West Center Drive, Suite 1100 Vienna, VA 22182.

deposits and compressible waste materials are provided to illustrate how the design and construction procedures are modified to accommodate marginal soil conditions.

Select Granular Backfill

Precast Concrete
Facing Panels ———→

Reinforced
Volume

Random
Backfill

Temporary
Excavation

Unreinforced Concrete
Leveling Pad ——————

Reinforcing
Elements
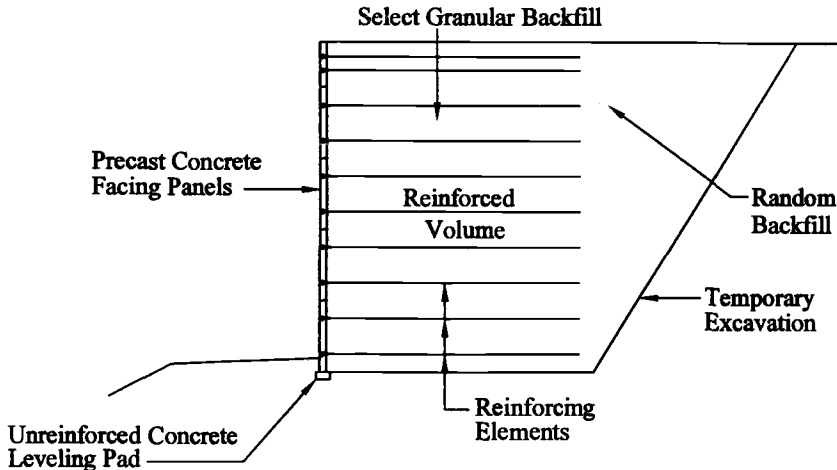
Figure 1- *Typical Section of a Reinforced Earth Wall*

**Design of RE Walls on Marginal Lands**

In a RE wall, the mechanical properties of a basic material - in this case granular backfill - are improved by reinforcing it parallel to the orientation of its greatest strains. The friction between the granular soil and the steel reinforcements allows the backfill, which can withstand only compressive and shear stresses, to transfer tensile stresses to the reinforcements. The combination of soil backfill, steel reinforcing elements and durable facing elements produces a composite material that is both strong and flexible. A description of the components with an emphasis on the modification to these components for construction on marginal lands are provided in the following sections.

*Facing Elements*

RE walls for permanent applications (defined as a design life of 50 to 100 years) predominantly use precast concrete facing panels with open joints in between the panels. The flexibility of a RE wall depends on the open joint between the precast modular facing elements. The open joints allow the panels to move relative to each other, thereby making it possible to undergo large amounts of deformation. The joints generally utilize 'bearing pads' made of elastomeric materials to provide a bearing surface between the top of one panel and the bottom of the panel. The bearing pads are typically 20 or 25 mm in thickness. For marginal soil applications, 25 mm thick pads may be used to

improve the flexibility along the facing.  These pad materials are highly resistant to ozone oxidation,  resistant to corrosive attack, retain resiliency and do not crack.  The weight of the overlying panels as well as the effect of long term creep usually results in a 10 to 15 percent compression of the bearing pads. The bearing pads provide the needed balance between compressibility under increased loads and ability to maintain an open joint during the design life.

By carefully monitoring a number of RE walls with precast facing panels which have undergone significant differential settlement, a maximum allowable value of  1 m of differential settlement per 100 m of wall length (1 percent) is recommended based on structural as well as aesthetic concerns.  However, several structures have undergone differential settlement in excess of the recommended limit without structural distress. Butler (1980) documents the case history of a ramp constructed at the Sprain Brook Parkway in New York which settled differentially 530 mm per 30.5 m of wall length (1.7 percent) without adverse structural effects.

For RE walls constructed on marginal lands, where the soil conditions are highly irregular (non-uniform), the potential exists for differential settlement in excess of 1 percent.  Differential settlements in excess of 1 percent will result in closing and opening of the joints between the panels. Spalling or cracking of the concrete panels may  in turn occur at some points along the closed joints depending on the magnitude of the settlement.  At locations where the predicted differential settlement is beyond the 1 percent limit,  the design and construction procedures should include provisions to accommodate the anticipated differential settlement.

*Backfill*

The current practice in the design and construction of RE walls is to use durable granular materials with no more than 15 percent particles finer than 0.075 mm (US Sieve No. 200) as backfill within the reinforced volume to enhance drainage, as well as constructability considerations at the work site [American Association of State Highway and Transportation Officials (AASHTO) 1996a].  In the range of loading normally associated with RE walls, the granular  materials behave elastically. Post-construction movements associated with internal yielding or readjustments of the backfill are not anticipated. The compacted granular backfill used in a RE wall deforms as an integral mass, with compression of the supporting subsurface materials below the embankment.

For certain applications, the global stability can be improved by using backfill materials with higher shear strength properties. In some cases, a reduction in settlement as well as an improvement in the global stability (rotational type) can be achieved by using lightweight backfills.  Lightweight backfills with unit weights as low as 10 kN/m$^3$ have been used in several projects.  When lightweight backfill materials are used, the stability against sliding and uplift is critical and should be checked if flooding is anticipated.

*Steel Reinforcements and Connection of Facing Elements to Reinforcements*

Discrete steel strips used in RE walls are classified as inextensible reinforcements, since the steel reinforcements deform much less readily than the backfill that envelops the reinforcements. Detailed procedures for the design of inextensible (steel) reinforcements are provided in the Standard Specifications prepared by AASHTO (1996b). For certain applications, the global stability can be improved by using longer reinforcements at the base and by varying the density (the quantity of reinforcement per unit volume of the embankment).

The connection between the facing elements and the reinforcements are selected based on a detailed evaluation of the anticipated stresses at the connection and the ease of connecting the reinforcing elements to the facing panels during construction. A well-designed connection will not allow separation to occur between the facing and the reinforcing elements. A positive connection also prevents movement between the facing and the backfill in the event of deformation due to external loads.

## Geotechnical Aspects of RE Walls on Marginal Lands

The provision of a comprehensive geotechnical evaluation of subsurface conditions plays an integral part in determining the future performance of a RE wall. Follow-up construction should include provisions for field monitoring and inspection to verify the evaluations made during design.

*Differential Settlement of Foundation Soils*

The effect of differential settlement can be evaluated based on the concept of regular and irregular differential settlement. Regular settlement occurs when the magnitude of settlement is essentially a function of the applied loads and the soil conditions are generally uniform along the entire length of the embankment. Regular settlement usually does not cause any damage to the elements of a RE wall since differential settlement resulting from regular settlement is usually within the maximum acceptable limit of 1 percent. Irregular settlement occurs when the settlement along the length of the embankment varies due to the rapid changes in the soil profile. Such rapid changes in soil profile are observed in areas underlain by landfill debris, fill materials placed in an uncontrolled manner, waste slime deposits or soil strata which contain isolated zones of highly organic materials. The differential settlements resulting from irregular settlements are very unpredictable and have the potential to exceed the 1 percent limit for RE walls. Several ground improvement techniques, such as partial replacement of the marginal soils, installation of wick drains, construction of preload embankments and dynamic compaction, are available to reduce differential settlements

to acceptable limits prior to the construction of the RE walls. For certain projects with large differential settlement potential, RE walls were constructed in stages using a flexible wire facing followed by attachment of precast concrete facing  elements with a flexible connection (Figure 2) after the settlement is essentially complete. The use of RE walls with flexible wire facing eliminates the costs associated with the construction and removal of a temporary preload embankment.
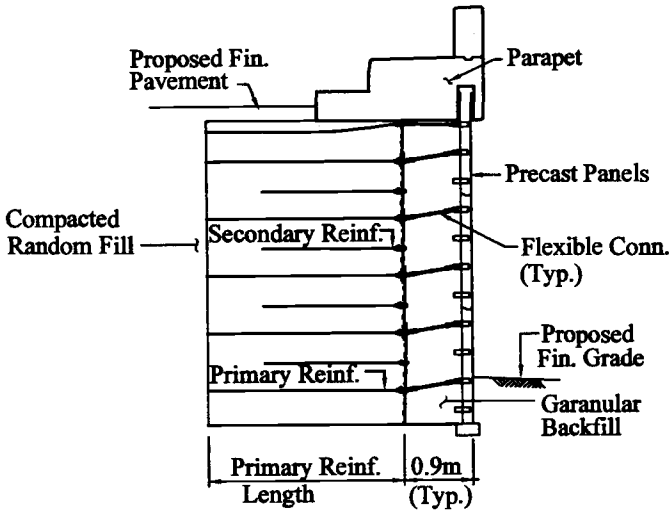


Figuere-2 *Typical Section of a Reinforced Earth Wall Constructed in Two Stages Using Flexible Wire Facing*

*Total Settlement*

For RE walls used in roadway applications,  there is no structural limit to the maximum total settlement as long as provisions are provided to account for the effect of settlement in road grades and on auxiliary systems such as drainage structures located within the RE volume.  Depending on the magnitude and rate of settlement, there are several methods to reduce the effect of settlement on the performance of RE walls. Settlements less than 100 mm are typically accommodated within the coping (Figure 3). If the expected total settlements are greater than $100\pm$ mm, the construction of the  RE walls are performed in several stages such that the upper row of panels and the drainage elements are installed after most of the foundation settlement is essentially complete (Figure 4).  For large settlements, the height of the upper row of panels will be adjusted based on the actual settlement. The techniques provided in figures 3 and 4 are feasible as long as the waiting periods can be accommodated within the schedule.   Slower settlements which can not be accommodated within the construction schedule must often be accelerated.  Methods for accelerating settlement include installation of the vertical

drains in the foundation soils within the zone of influence of the embankment and placement of temporary surcharge above the embankment.

Utilities and structures other than highway drainage are not recommended within RE walls built in marginal areas unless provisions are provided to reduce the impact of the expected total and differential settlements to levels acceptable to these structures. The effect of RE walls settlement on adjacent rigid structures (if present) should also be carefully evaluated during design.
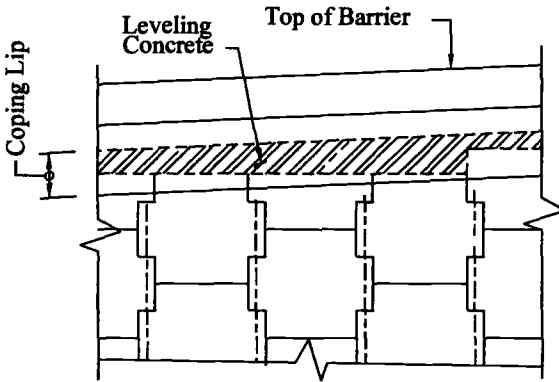


Figure 3- *Procedure for Accommodating Settlement within the Coping*
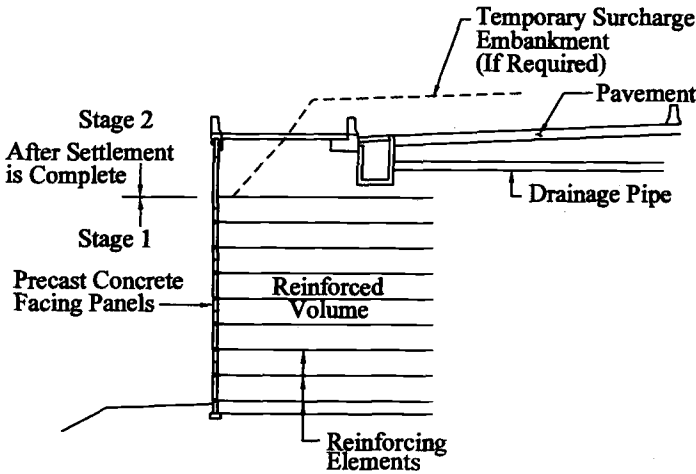


Figure-4 *Typical Section of a Reinforced Earth Wall Constructed in Two Vertical Stages*

*Bearing Capacity*

When analyzing foundation soils for bearing, the RE walls are modeled as continuous strip footings with a width and magnitude equivalent to that of the Meyerhof bearing pressure diagram (AASHTO 1996b). The resulting bearing pressure diagram is rectangular, with a width equal to the reinforcement length minus two times the eccentricity of the embankment.

When RE walls are constructed on marginal lands, the bearing capacity evaluations are performed for the short term as well as the long term conditions. For short term evaluations, analyses using the undrained (total stress) parameters  are generally used. The short term bearing capacity evaluations for high water content soils should also consider the potential strength gain of soils with time. Adequate factor of safety against  bearing can be maintained by constructing the embankment in two or three vertical stages, such that the load applied by the embankment do not exceed the allowable bearing capacity. If the design is based on the strength gain with time,  shear strength gains should be monitored during construction.  It is an acceptable practice to use drained (effective stress) parameters for long term bearing capacity evaluations. Such long term evaluations are based on an evaluation of the percentage of consolidation that is expected to occur over the life of the project.

In the case of RE walls, the use of a lower factor of safety against bearing failure is justified, since the uniform bearing pressure of the RE volume will not tend to increase if deformation of the embankment occurs (due to flexibility of the RE walls).  Factors of safety in the range of 2.0 to 3.0 are generally used based on an evaluation of the geotechnical information and the external loads applied on the RE wall.  The bearing capacity evaluations are generally based on the assumption that the critical mode of failure analysis is in general shear of the subsurface materials.  However, in the case of highly compressible soils, emphasis also should be placed on an evaluation of the punching shear as well.

*Global Stability*

On marginal foundation soils, it is possible to use the inherent flexibility of the RE walls without resorting to special foundation improvement procedures. The RE wall should be constructed in schedule-controlled lifts to minimize the build up of excess pore pressure and to allow the majority of settlement to occur during construction. During construction, the excess pore pressures developed within the subsurface materials and the settlement of the adjacent structures (if present) should be monitored to ensure that the observed behavior is in agreement with the predicted response. The gain in foundation soil shear strength with time may be monitored by retrieving samples of the foundation mass and performing triaxial shear tests over the course of the project.  The results of the field monitoring of the shear strength and pore pressure should be used to adjust the construction techniques as required.

For certain projects, the placement of a layer of granular material (may include tensile reinforcements) of sufficient thickness and width over marginal soils is a viable approach to improve the global stability. The placement of the granular layer also improves the constructability by providing a working platform for the construction of the RE wall. In marginal lands, RE walls can also be economically constructed after improving the soft soils with stone columns. Stone columns can be successfully installed to increase the rotational stability of RE walls.

*Sliding along the Base*

In the case of RE walls on marginal soils, one must determine that there is no risk of horizontal sliding along the base of the RE volume. The criteria for horizontal sliding is more critical when the RE wall is supporting a heavy surcharge; for example, when supporting a high, sloping embankment. When sliding along the base controls the design, because of the characteristics of the soils along the base, a lengthening of the reinforcements may be required to improve the sliding resistance. Undercutting the weak soils and replacing it with granular materials is another common technique used to improve the resistance to sliding along the base. Undercutting may be uneconomical when the required depth of undercut exceeds 2 to 3 m or the depth to ground water is relatively small.

**Construction Techniques**

This section provides a brief summary of several RE walls constructed on marginal soils. The case histories provide an overview of the various options available to designers and contractors to adapt the design and construction of RE walls to the subsurface conditions.

*A Two Hundred Meter Long RE Wall Constructed for Polk County Parkway, Lakeland, Florida*

This case history describes a 200 m long section of RE wall in Lakeland, Florida which incorporated significant short term settlements (Figure 5). Within the 200 m long section, the height of the RE wall varied from 6 to 9 m.

The soil conditions at the site consisted of uncontrolled fill approximately 0.6 to 3 m thick underlain by sand, clay and silt strata approximately 9 to 12 m thick. Isolated pockets of reddish brown fibrous peat and reddish brown sand with organics were encountered at several borings. Within the plan limits of the 200 m long section, the peat layer was 1.4 to 3 m thick and the peat layer existed at 5.5 m below the bottom of the RE

volume.  The standard penetration test resistance values (N values) as determined by ASTM Method for Penetration Test and Split-Barrel Sampling of Soils (D 1586) varied from Weight of Hammer (WOH) to 2 (PSI, Inc. 1994).
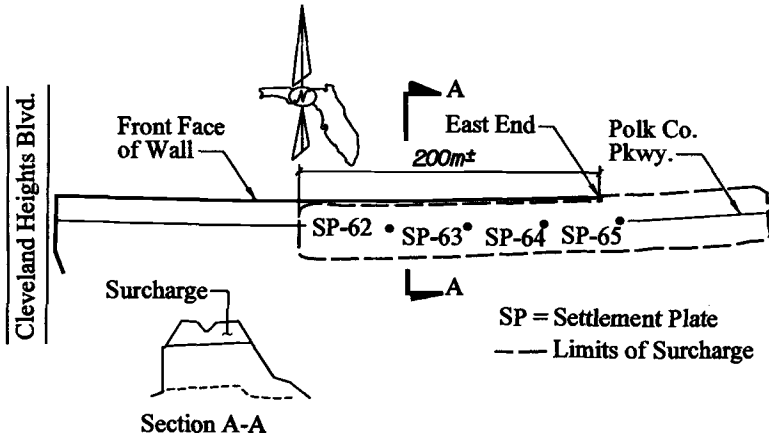


Figure-5  *Plan View of 200 m Long Section of Reinforced Earth Wall Constructed in Polk County, Florida*
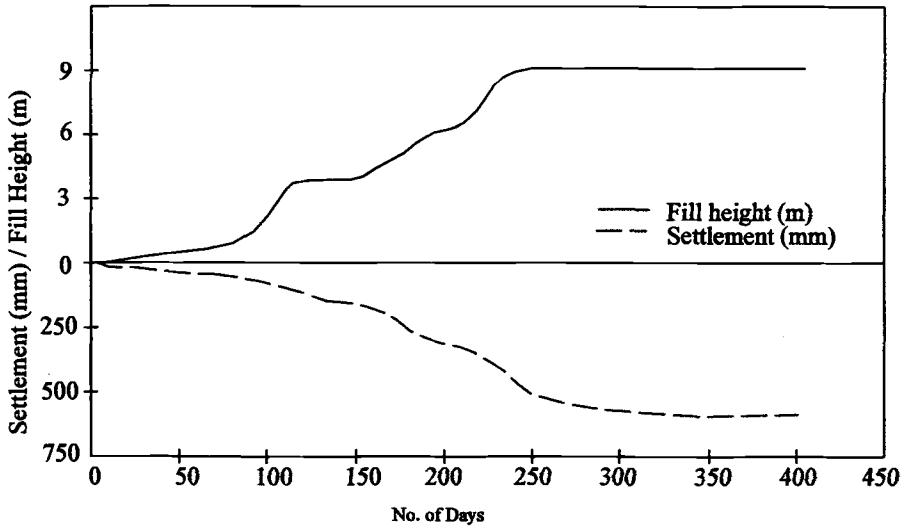


Figure-6  *Settlement and Fill Height vs. No. of Days after Construction  at Settlement Plate SP-63*

The facing panels used for the RE wall consist of cruciform shaped panels with a nominal area of 2.25 $m^2$. Additionally, vertical slip joints were provided at 15 m intervals along the entire length of the wall. Slip joints provide vertical breaks along the facing so that each 15 m section of the facing will act independently in the event of settlement of the isolated pockets of organic soils. Initially all the facing panels except the top row of panels were installed and a 4 m high surcharge embankment was constructed over the embankment. Inclinometer casings were provided at critical locations to monitor deformation. Most of the settlement occurred during the construction of the metallic stabilized embankment and the surcharge (Figure 6). The final set of settlement readings along the face of wall to determine the height of the top row of panels was taken at the end of 570 days after construction. The total settlement along the face of the wall at the end of 570 days varied from 0.18 m to 0.79 m (Figure 7). Based on the top of panel settlement measurements provided in figure 7, additional panels were cast and provided to the required height. The data obtained from the top of panel measurements follow the general trend observed in the settlement plates. The discrepancy between the settlement measurements along the facing and at the settlement plates is probably due to possible variation in the subsurface materials between the center line and face of the embankment, the duration of settlement measurements (570 vs. 400 days) and variations in the actual top of wall elevation prior to settlement compared to the design top of wall.

This case history demonstrates how the ability of a RE wall to accept deformation was successfully used to construct a retaining wall over marginal lands with high settlement potential without foundation improvement or deep foundations. This approach is suggested at locations where the waiting period can be accommodated within the construction schedule.



Distance along the Face (m)
Measured from the East End

Distance along the Face (m)
Measured from the East End

SP = Settlement Plate
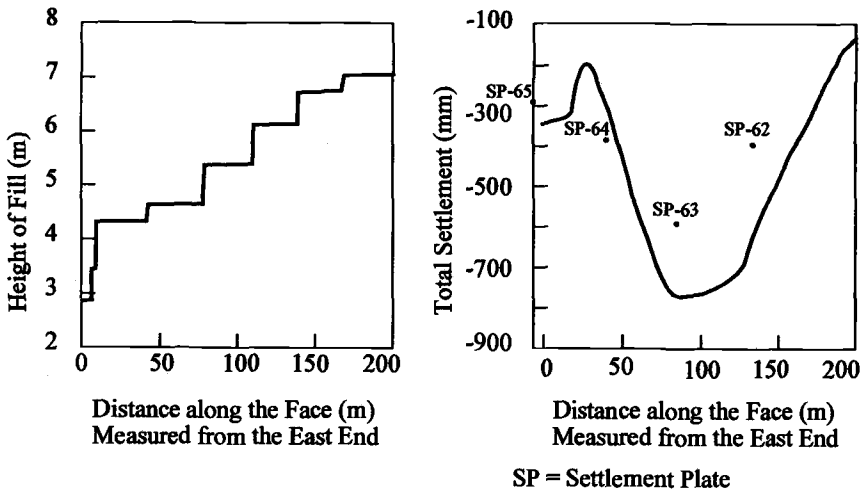
Figure-7 *Settlement along Reinforced Earth Wall*

*RE Walls (Walls 1 and 2) along Elizabeth Waterfront Boulevard in Elizabeth, New Jersey*

Four RE walls (walls 1 through 4) were constructed along the Elizabeth Waterfront Boulevard and Jersey Gardens Boulevard to provide access from the New Jersey Turnpike to a proposed Mall Development site in Elizabeth, New Jersey. Walls 1 and 2 incorporated ground modifications to improve global stability and to reduce settlement. Walls 1 and 2 included a total of 170-linear meter of RE walls with heights in the range of 3 m to 10 m. Geotechnical investigations indicated that the site surfaces along the alignment of walls 1 and 2 were found to be immediately underlain by 3 to 4 m thick layer of waste fill materials. The waste fill materials in this portion of the site consisted of loose to dense municipal solid waste intermixed in a matrix of silty sand soil. The waste consisted of durable materials such as tires, metal and glass, as well as materials more easily susceptible to decomposition such as cardboard and organic materials. Underlying the fill/waste materials, was a layer of soft to medium stiff peat and/or silty clay ranging from 0.3 to 1.5 m in thickness. The peat layer was found to be at its liquid limit and could not be assigned significant shear strength. Below the silty clay/ peat stratum, the borings encountered natural silty sands and sandy silts which increased in relative density with depth. Reddish brown shale bedrock was encountered below the soil layers. Groundwater measurements indicated perched water within the waste fill layer and a static groundwater table within the sand soils at depths ranging from 4.6 m to 7.6 m below the existing surface grades (PMK Group, Inc. 1995).
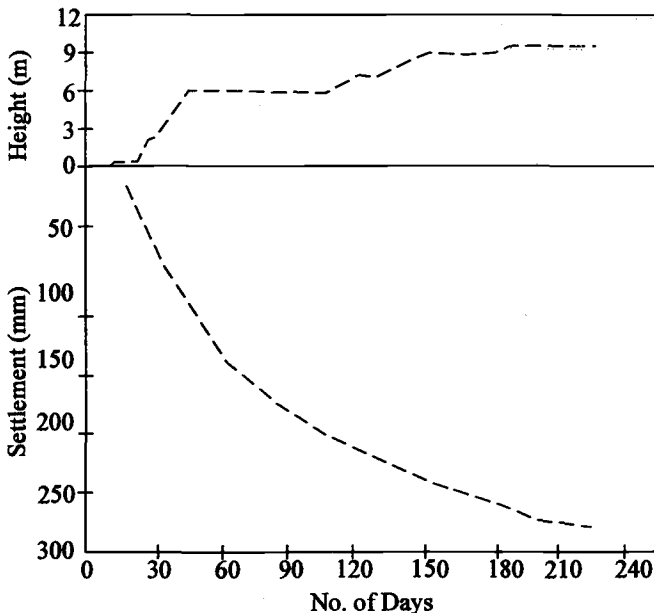


**Figure-8** *Settlement and Fill Height vs No. of Days after Construction*

Geotechnical analysis of the site conditions indicated that the design of the RE walls should consider the effect of the differential settlement of the waste fill layer and the stability against a slope failure through the thin organic clay layer. Settlement evaluations indicated that 0.9 m to 1.5 m settlement may occur within the waste fill layer due to the construction of a 9.5 m high embankment over the waste fill. Dynamic compaction was performed within the areas of influence of the embankment to limit potential differential settlements to less than 1 percent. Subsequent to the dynamic compaction, settlements on the order of 305 to 460 mm were expected. The design also provided a 0.9 m thick granular mat reinforced with high strength polyester geogrids below the embankment to prohibit a possible failure through the organic clay layer and to reduce the differential settlements.

The RE walls built for this project consisted of cruciform panels and steel reinforcements constructed above the 0.9 m thick granular mat. During construction of the RE walls, settlement readings were taken on a regular basis. Settlements up to 280 mm occurred at one location where the height of the RE wall was 9.5 m (Figure 8). Within the remaining portions of the wall, the total settlements were in the range of 15 to 170 mm. The calculated differential settlements were less than 1%.

The cost evaluations performed by the contractor for walls 1 and 2 indicated that the use of a RE wall in conjunction with ground improvement was significantly more cost effective than a cast-in-place wall supported on deep foundations. The objective of the ground improvement procedure was not only to reduce the potential differential settlement to less than 1 percent but also to improve the global (rotational) stability.

*RE walls (Walls 3 and 4) along Elizabeth Waterfront Boulevard in Elizabeth, New Jersey*

As discussed in the previous section, four RE walls (walls 1 through 4) were constructed along the Elizabeth Waterfront Boulevard and Jersey Gardens Boulevard to provide access from the New Jersey Turnpike to a proposed Mall Development site in Elizabeth, New Jersey. Walls 3 and 4 were planned adjacent to Spartina Marsh, an existing wetlands area and significant differential settlements were anticipated at this location. Wall 3 reached a maximum height of 10.7 m adjacent to the bridge crossing. Geotechnical explorations performed by PMK Group, Inc. (1997) at the wall location indicated the presence of 2 to 3 m layer of loose to dense silty sand fill materials overlying the marsh areas. Below the fill materials, the borings encountered silty clay and organic peat layers. The standard penetration test resistance values (N values) as determined by ASTM Method for Penetration Test and Split-Barrel Sampling of Soils (D 1586) within the peat layer varied from 3 to 5 blows per 0.3 m, which corresponds to soft to medium stiff consistency. The peat and clay layers were found to be uniformly underlain by medium dense to dense silty sand soils. Bedrock was encountered below these granular layers at about 15 m below ground surface.

Significant differential settlements were anticipated due to embankment construction over loose fill and compressible peat and clay. Evaluations indicated that

the settlements should take place within 2 to 5 months after embankment construction. The site conditions as well as the schedule dictated that the embankment should be constructed on the existing ground without any ground improvements. Therefore, the RE walls were constructed using a wire facing to ensure that all the potential differential settlements would occur prior to the placement of the concrete facing panels. Settlement plates were installed within the backfill to determine the settlement rates and magnitudes during construction. Once the settlement was essentially complete, based on the measurements from the settlement plates, concrete facing panels were attached to the embankment using a flexible connection (Figure 2).

At locations where ground improvement techniques to reduce differential settlements to less than 1 percent are not viable due to technical or economic considerations, the use of a RE wall constructed in stages using a flexible facing followed by a permanent facing should be considered. The use of precast concrete facing elements is generally more economical than a cast-in-place facing, and precast concrete facing elements with appropriate jointing are capable of handling additional foundation settlement which may occur during the design life of the project.

**Conclusion**

RE walls using modular facing panels, steel reinforcements and granular backfill are well-suited for the construction of retaining walls on marginal lands. The design of RE walls should include a comprehensive geotechnical evaluation of the subsurface materials. During construction, monitoring and inspection should be used to verify the evaluations made during design and to modify the construction procedures based on the field data.

The flexibility of a RE wall depends on the open joint between the precast modular facing elements. The open joints allow the panels to move relative to each other, thereby making it possible to undergo large amounts of deformation. By carefully monitoring a number of RE walls which have undergone significant differential settlement, a maximum allowable value of 1 m of differential settlement per 100 m of wall length (1 percent) is recommended.

The effect of total settlement on the top of the wall grades are usually adjusted within the coping and the top row of facing panels. Slower settlements which can not be accommodated within the construction schedule must often be accelerated. Methods for accelerating the settlement include installing wick drains, preloading the site and placing surcharge over the RE wall. At locations with large differential settlement potential, RE walls were also constructed in stages using a flexible wire facing followed by attachment of precast concrete facing elements with a flexible connection

For certain RE walls on marginal lands, the global stability can be improved by using longer reinforcements at the base of the embankment. Adequate factor of safety against bearing and global stability can be maintained by constructing the embankment in scheduled controlled lifts such that the load applied by the embankment do not exceed the allowable limits. If the design is based on the strength gain with time, shear strength

gains shall be monitored during construction.   Undercutting and replacement with competent soils (may include tensile reinforcements), stone columns, and dynamic compaction are some of the other techniques generally used to improve the foundation soils for RE walls.

Every RE wall built on marginal soils constitutes a new and unique project.  In each project, the optimum solution is obtained by taking into account the geotechnical information, the scheduling requirements and deadlines, the nature and magnitude of external loads and the flexible nature of the RE wall.

## Acknowledgments

## Limitations

Publication of this paper does not constitute an endorsement of the technology described in this paper by the owners, consultants and/or contractors mentioned herein.

## References

AASHTO (American Association of State Highway and Transportation Officials), 1996a, *Standard Specifications for Highway Bridges,* Division II - Construction, Section 7 - Earth Retaining Systems,  Sixteenth Edition, Washington, DC.

AASHTO (American Association of State Highway and Transportation Officials), 1996b, *Standard Specifications for Highway Bridges,* Division I - Design, Section 5 - Retaining Walls, Sixteenth Edition, Washington, DC.

Butler, B. E., 1980, "Use of Reinforced Earth for Construction of the SM Ramp on the Sprain Brook Parkway," *Earth Support Systems,* Seminar Sponsored by the New York City Metropolitan Section of the American Society of Civil Engineers.

PSI, Inc., August 1994, *Roadway Soil Survey, Polk County Parkway, Section 3, Polk County, Florida,* Tampa, Florida.

PMK Group, Inc., September 1995, *Geotechnical and Environmental Investigation, Kapkowski Road Extension, Section 1C, Elizabeth, New Jersey,* Kenilworth, New Jersey.

PMK Group, Inc., October 1997, *Geotechnical and Environmental Investigation, Kapkowski Road Extension, Section 2C, Elizabeth, New Jersey,* Kenilworth, New Jersey.

D. S. Ramer[1] and M. C. Wang[2]

**Performance of Roadway Embankment on Lime Waste**

**Abstract:** This paper presents the consolidation settlement and the excess pore pressure dissipation behavior of a four-lane highway embankment constructed over an abandoned quarry filled with a lime waste. The embankment was about 1000 ft (305 m) long and 45 to 50 ft (13.5 to 15 m) high with side slopes of 2(h):1(v). The supporting quarry, approximately 60 ft (18 m) deep, consisted primarily of a lime waste with very small amounts of asphalt coal tar, flyash, brick cinders, crushed limestone, and others. The lime waste was a residue derived from extraction of magnesium out of dolomitic rock and had calcium carbonate as the main chemical component. It had a natural water content as high as 124%, a specific gravity of 2.59, a liquid limit of 72%, and a plasticity index of 19.

   The field data showed that the embankment slopes were stable without visible lateral displacement, and that more than 10 ft (3 m) of consolidation settlement occurred at the deepest part of the quarry. The measured settlement and excess pore water pressure data were compared with the results of analysis. Possible causes for the observed discrepancy were discussed in detail.

**Keywords:** Lime waste, highway embankments, consolidation settlement, excess pore pressure, performance, field monitoring, field testing, laboratory testing, analysis

[1]Project Engineer, GTS Technologies, Inc., 851 South 19th Street, Harrisburg, PA 17104.
[2]Professor of Civil Engineering, 212 Sackett Building, Pennsylvania State University, University Park, PA 16802.

## Introduction

A four-lane highway embankment was constructed over an abandoned quarry filled with a lime waste. The embankment was installed with various instruments to monitor its performance. This paper presents the embankment performance data, which include the consolidation settlement and the excess pore pressure distribution behavior. The embankment performance was also analyzed using available theories. The monitored data were compared with the results of analysis. Possible causes for the observed discrepancy between the two sets of data are discussed. Meanwhile, potential applications of the research findings to embankment design and construction over highly compressible deposits such as lime waste are presented.

## Project Site Conditions

The roadway was a part of highway LR1010 located in Plymouth Township, Montgomery County, Pennsylvania. The embankment was about 1000 ft (305 m) long and 45 to 50 ft (13.5 to 15 m) high. The supporting quarry deposit consisted primarily of a lime waste with very small amounts of asphalt coal tar, flyash, brick cinders, crushed limestone, and others. The lime waste was a residue generated by a nearby Aluminum Plant which processed the Ledger Dolomite Bedrock for extraction of magnesium. The Aluminum Plant owned by Kaiser Industry, Inc. was located off Chemical Road near Plymouth Meeting, PA. Therefore, the primary chemical component of the lime waste was calcium carbonate.

The project site was located in the Piedmont physiographic province; the bedrock consisted of Cambrian dolomites and dolomitic limestones of the Ledger Formation. The overburden soil varied in thickness ranging approximately from 1 ft (0.3 m) to 10 ft (3 m), and contained varying proportions of sand, silt, and clay mixture. The quarry was capped with 4 ft (1.2 m) to 10 ft (3 m) of sandy soil and random fill material. The depth of the quarry generally ranged between 55 ft (18 m) and 65 ft (21 m), although at one location it was slightly deeper.

## Testing and Data Analysis

Both laboratory and in situ field testing were conducted to determine the properties of the lime waste. The laboratory testing performed on shelby tube samples included one-dimensional consolidation, consolidated-undrained triaxial compression, and constant head permeability tests, which were conducted following ASTM standard test procedures of D 2435, D 4767, and D 2434, respectively . In addition, particle size analyses (ASTM D 420), Atterberg limits tests (D 4318), and compaction tests (D 698) were performed on bag samples; the bag samples were disturbed soil samples which were contained in burlap bags.

The field testing conducted included the standard penetration test (SPT) (ASTM D 1586), cone penetration test (CPT)(ASTM D 3441), and dilatometer test (DMT); the dilatometer test followed the procedure of Schmertmann (1986). The standard penetration test together with boring and sampling was performed by Baddick and

Laskowski, Inc. Both cone penetration and dilatometer tests data were obtained by Pennsylvania Department of Transportation (PennDOT), and the results were analyzed by Schmertmann and Crapps, Inc. at Gainesville, Florida. The cone penetration tests were conducted at eleven sites; and the dilatometer tests were performed at two sites.

## Lime Waste Properties

Laboratory tests results showed that the lime waste had a natural water content as high as 124%, a specific gravity of 2.59, a void ratio of 3.2 and a saturated unit weight of 86.0 $lb_f/ft^3$ (13.5 $kN/m^3$). It contained approximately 97% fines (less than 0.075 mm) with about 54% clay size (less than 0.002 mm) and 43% silt size particles. The median grain size ($D_{50}$) was smaller than 0.001 mm. Its liquid limit, plastic limit, and plasticity index were about 72%, 53%, and 19, respectively. Also, the value of soil activity was about 0.2. The classifications according to AASHTO and Unified systems were A-5 and MH, respectively. Although the lime waste was classified as a silty soil, it had an abnormally high capacity of water adsorption when compared to typical silty soils.

Under the standard compaction effort, the maximum dry unit weight and optimum water content are 58.0 $lb_f/ft^3$ (9.1 $kN/m^3$) and 64.0%, respectively. Other laboratory test results indicate that the coefficient of permeability (k) is approximately 8.5 x $10^{-4}$ mm/s. The undrained cohesion (c) and internal friction angle ($\varphi$) equal 500 $lb_f/ft^2$ (24 $kN/m^2$) and 4°, respectively; and the drained cohesion (c′) and internal friction angle ($\varphi$′) are, respectively, near zero and 26°. The compression index ($C_c$) and swelling (or decompression) index ($C_s$) are approximately 1.30 and 0.03, respectively. Meanwhile, the coefficient of consolidation ($c_v$) ranges from 0.7 to 1.3 $ft^2$/day (45.0 to 84.0 $mm^2$/hr) within a consolidation pressure range of 500 to 32,000 $lb_f/ft^2$ (24 to 1,532 $kN/m^2$).

The standard penetration test results show that the blow count (N) value varies considerably from as low as 2 to more than 10, possibly due to the variation in water content and density as well as the intrusion of soil into the lime waste. From the eleven cone penetration tests, the ranges of cone resistance ($q_c$) and skin friction ($q_f$) are 4,000 to 40,000 $lb_f/ft^2$ (192 to 1915 $kN/m^2$), and 0 to 4,000 $lb_f/ft^2$ (0 to 192 $kN/m^2$), respectively. The dilatometer test data include a dilatometer modulus ($E_d$) of 6,000 to 26,000 $lb_f/ft^2$ (287 to 1245 $kN/m^2$), a material index ($I_D$) of 0.03 to 0.15, and a lateral stress index ($K_D$) of 1.05 to 2.01. These data were determined using the analysis method developed by Marchetti (1980). From these test data, the estimated lime waste properties are constrained modulus (M) of 6,000 to 20,000 $lb_f/ft^2$ (287 to 958 $kN/m^2$), lateral earth pressure coefficient ($K_o$) of 0.20 to 0.55, preconsolidation pressure ($p_c$) of 1,500 to 3,500 $lb_f/ft^2$ (72 to 168 $kN/m^2$), and over-consolidation ratio (OCR) of 0.30 to 0.91, which indicates that the lime waste was under-consolidated at the time of in situ testing. Meanwhile, the undrained shear strength ($c_u$) is estimated at 400 to 800 $lb_f/ft^2$ (19 to 38 $kN/m^2$). For comparison, the value of $c_u$ is also computed from the laboratory test results of c = 500 $lb_f/ft^2$ (20 $kN/m^2$) with $\varphi$ = 4° using $c_u$ = c tan (45° + $\varphi$/2). The computed value is $c_u$ = 540 $lb_f/ft^2$ (26 $kN/m^2$) which falls within the range of 400 to 800 $lb_f/ft^2$ (19 to 38 $kN/m^2$). This indicates that both laboratory and field tests provide a consistent shear strength property of the lime waste.

Based on the preceding test results, the lime waste is highly compressible with a very low shear strength. It is an under-consolidated soil with an abnormally high natural water content, high liquid limit, and relatively low plasticity index. The lime waste also has an unusual compaction behavior with a very low maximum dry unit weight and a high optimum water content.

**Embankment Construction and Instrumentation**

The roadway embankment under study was approximately 1000 ft (305 m) long and 45 to 50 ft (13.5 to 15 m) high with side slopes of 2 horizontally vs 1 vertically, i.e. 2(h): 1(v). The embankment construction was completed in just under 600 days. To compensate for the settlement due to the consolidation of the underlying lime waste deposit, an additional 8 ft (2.5 m) of embankment was used to reach the design grade. Meanwhile, berms were placed along the sides of embankment to increase embankment slope stability. Also, after embankment construction was complete, a 10 ft (3 m) high surcharge fill was placed for approximately 200 days to accelerate the primary consolidation settlement.

The embankment was instrumented to monitor its performance. The instrumentation layout presented in Figure 1 shows a total of 14 settlement platforms, 1 horizontal settlement indicator, 4 inclinometers, and 18 piezometers which were grouped into 6 setups each containing 3 piezometers. The piezometers used were vibrating wire piezometers. The 3-piezometer setup was used to obtain pore pressure readings at three different depths; the depths varied among the setups. As seen from Figure 1, of these 6 piezometers setups, four were arranged across the quarry and perpendicular to the roadway centerline; the other two were parallel to the centerline in the deepest part of the quarry.

The horizontal settlement indicator was approximately 705 ft (215 m) long and was installed perpendicularly to the roadway centerline with an access housing at each end. The indicator stopped functioning in the later stage of the project. At that time, 14 settlement platforms were installed on top of the embankment to continue settlement measurement. Of the 4 inclinometers, three were arranged equally spaced near the crest of west side and the fourth one was located near the bottom of the east side opposite to the middle one as shown in the layout. The inclinometers were installed to monitor possible slope movement.

**Results of Field Measurements**

The inclinometer data showed little lateral slope displacement indicating that the embankment slopes were stable. The measured embankment settlement during the stage of construction including fill placement and removal of surcharge fill is presented in Figure 2. It is seen, as would be expected, that the settlement increases as the construction progresses. After completion of construction, the embankment settlement continues to increase with time as shown in Figure 3. The spike formation exhibited in the settlement curves in both figures is possibly due to human and/or instrumental errors in the indicator readings. From Figure 2, the maximum embankment settlement at the end of fill

APPROXIMATE QUARRY LIMITS

PRECAST MONITORING VAULT

EMBANKMENT LIMIT

O

F ●

E ●

P4

CONRAIL RAILROAD

I2

I4

P3

N

G ●

J ●

I1

A ●

C

P5

P6

RAMP K CONSTR.  ℄

40

P2

42

1190

L.R. 1010 CONSTR.  ℄

H ●  K ●

B ●

D ●

I3

M

P1

L ●

I ●

RAMP B CONSTR.  ℄

EMBANKMENT LIMIT

APPROXIMATE QUARRY LIMITS

CHEMICAL ROAD

APPROX. NORTH

0          100

SCALE 1"=100'

LEGEND

[Horizon Settlement Indicator symbol]  Horizon Settlement Indicator

P1 -◯-  Piezometer

I1 ⊘  Inclinometer

A ●  Settlement Platform

Figure 1 - *Instrumentation Layout*
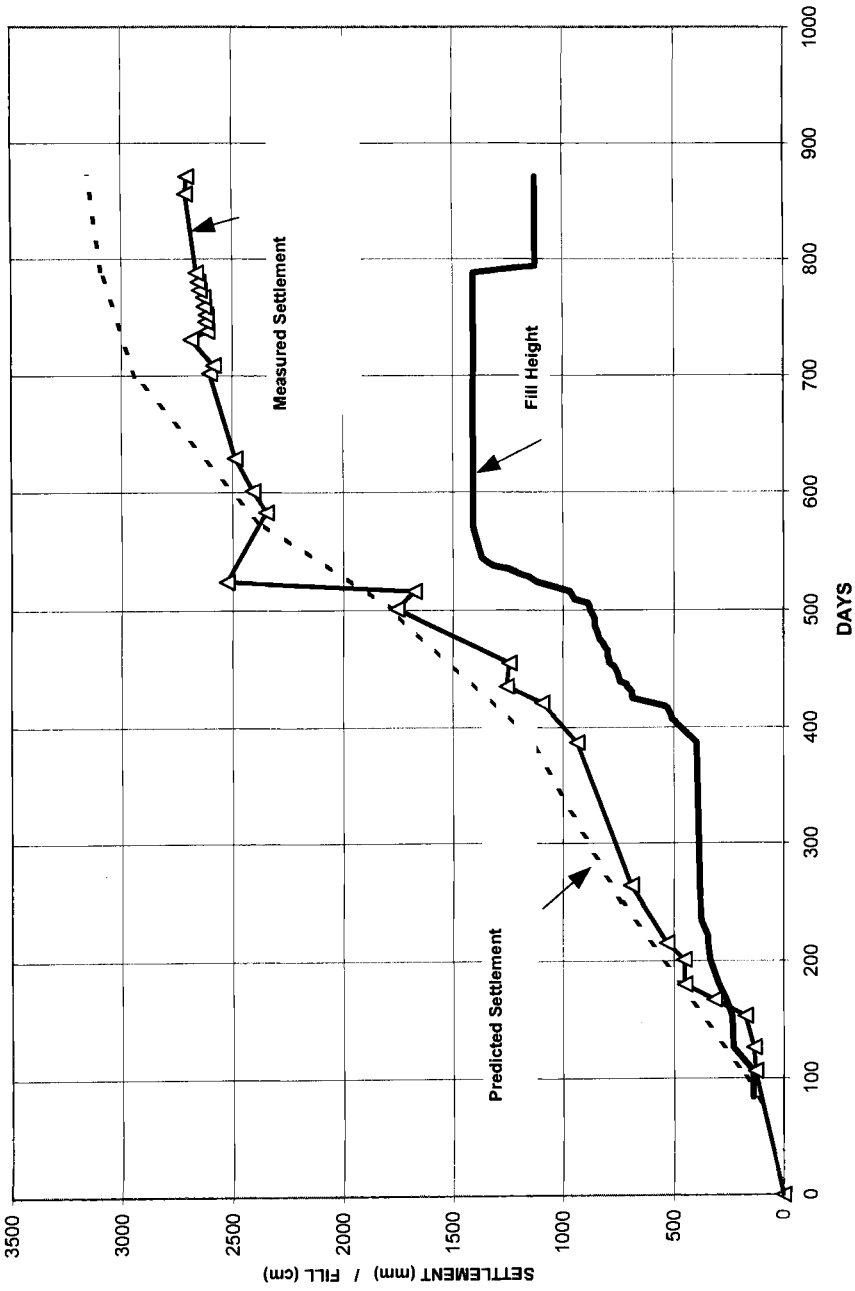
*Figure 2 - Embankment Settlement during Construction*
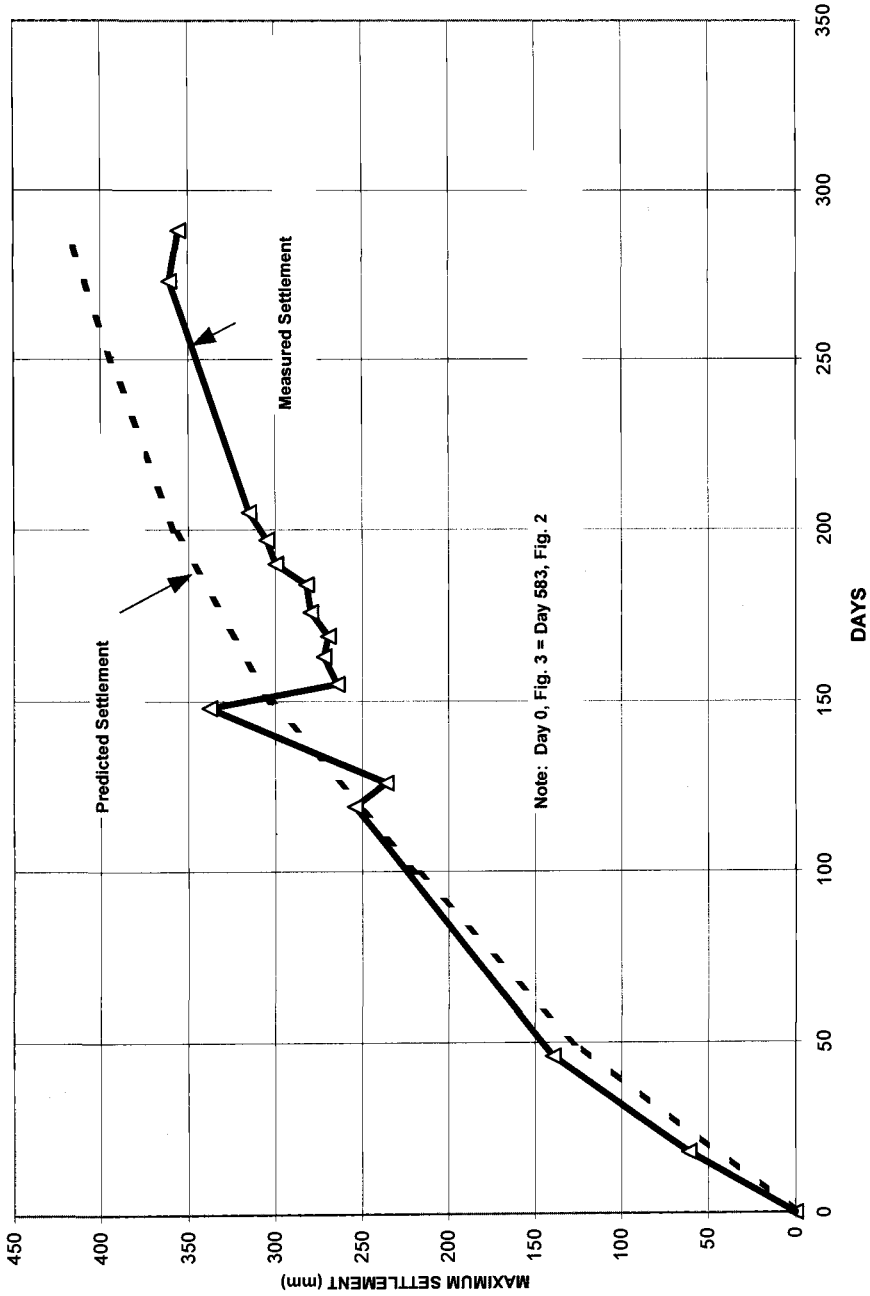
Figure 3 - *Embankment Settlement after Fill Operations*

placement is approximately 7.8 ft (2400 mm), and at 200 days after construction is about 8.8 ft (2700 mm). Thus, a total of about 1.0 ft (300 mm) settlement took place over 200 days after the embankment is constructed.

To this point in time, all of the settlement data were obtained from the horizontal settlement indicator. Three months later that was approximately 673 days from the start of construction, probably due to excessive bending of the horizontal settlement indicator's casing, it became impossible to run the instrument the whole way through the embankment to continue settlement monitoring. The subsequent settlement values obtained from the 14 settlement platforms indicate an additional maximum settlement of approximately 1.2 ft (370 mm) until the end of the observation period of three years. This gives a total cumulative maximum embankment settlement of approximately 10.0 ft (3000 mm) which occurred at the deepest part of the quarry.

The piezometer readings were fairly erratic. Only 9 of the 18 piezometers provided readings which showed a reasonable trend of excess pore pressure variation with load and time. Of the 9 sets of reasonable readings, three sets obtained from setup No. 3 are presented in Figure 4. This setup of piezometers was located in the deepest part of the quarry. The three piezometers in this setup were placed at different depths -- 60.6 ft (18.5 m) for piezometer 3-1, 40.8 ft (12.4 m) for piezometer 3-2, and 21.5 ft (6.6 m) for piezometer 3-3. Also presented in the figure is the fill placement curve. For this curve, the fill height was measured at the location of the piezometers. Therefore, this curve is not necessarily the same as that in Figure 2.

It is seen from Figure 4 that the excess pore pressure increased with increasing fill height to a peak. After the peak, it dissipated with time as would be expected. At any time, the magnitude of excess pore pressure varied with the fill height and the depth to the piezometer. Possibly due to human and/or instrumental errors involved in the monitoring, the readings of piezometer P3-2 were smaller than those of P3-1 only in the early stage of construction. Also, the readings of P3-3 showed a little change with time up to about 340 days suggesting that this piezometer exhibited less than desired sensitivity to load variation during this stage of monitoring. Thus, these excess pore pressure data appeared to be less dependable than the settlement data.

## Analyses and Discussions

Analyses were performed for consolidation settlement of the roadway embankment and excess pore water pressure in the lime waste at the deepest part of the quarry. In the analysis, the embankment loading was divided into a number of ramp loading, and the settlement and excess pore pressure due to each ramp loading was computed and superimposed. The soil properties needed in the analysis included saturated unit weight (86.0 lb/ft$^3$ or 13.5 kN/m$^3$), void ratio (3.2), compression index (1.30), swelling index (0.03), and the coefficient of consolidation (1.0 ft$^2$/day or 64.5 mm$^2$/hr). Also, a preconsolidation pressure of 2,500 lb/ft$^2$ (120 kN/m$^2$) was used. Since the bedrock underneath the quarry was weathered, double drainage condition was assumed. The analysis was made only for primary consolidation settlement. The effect of large settlement on the time rate of settlement was corrected based on the method proposed by
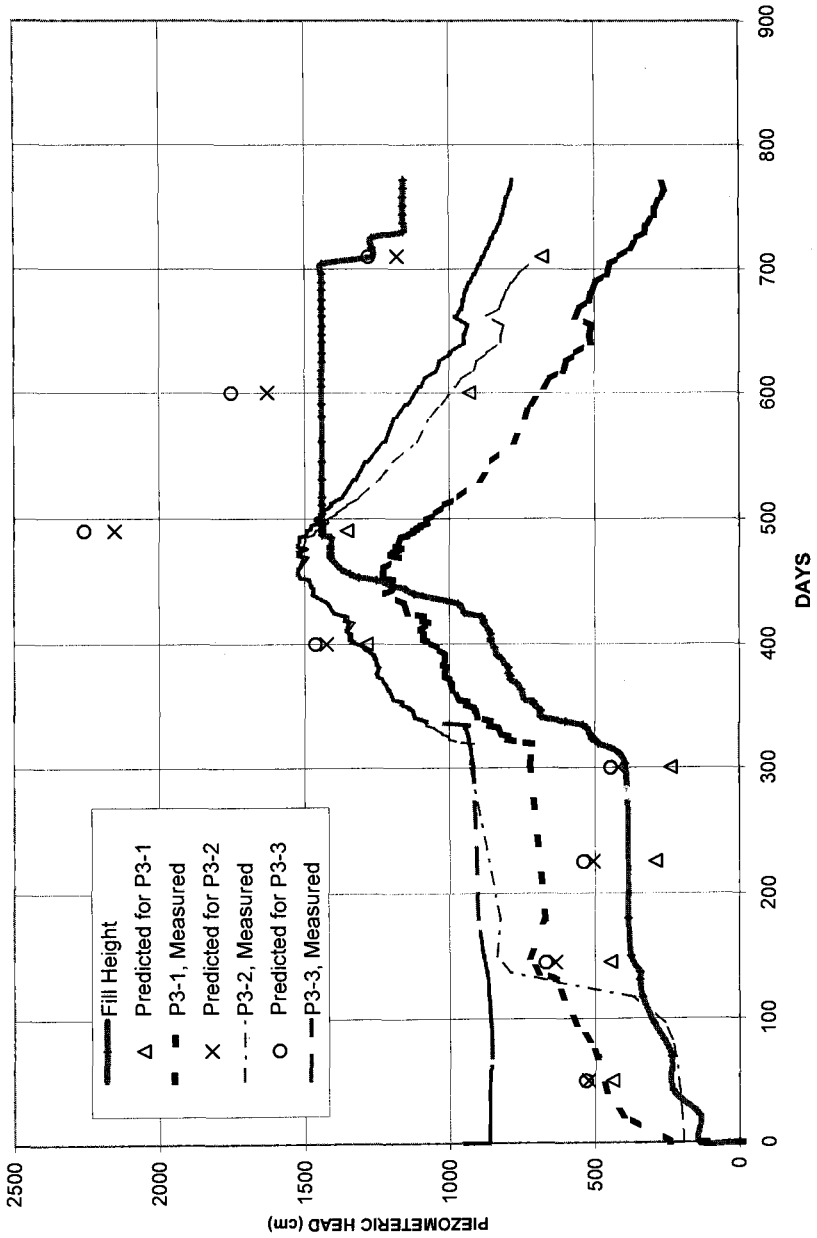
Figure 4 – Variation of Piezometer Readings with Time for Piezometer Setup 3

Olson and Ladd (1979). According to the method, the compressible layer thickness was reduced as follows:

$$H = H_o - \frac{S_{ult}}{2N} \qquad\qquad (1)$$

in which     $H$ = corrected layer thickness
$H_o$ = initial layer thickness
$S_{ult}$ = ultimate consolidation settlement
$N$ = number of drainage boundary

The average degree of consolidation due to a single ramp loading was determined using the method of Olson (1977).

The predicted settlement values are plotted along the measured data in Figure 2 for settlement during construction and in Figure 3 for settlement after construction. These two figures show that the predicted values agree fairly well with the measured data except in the later stage of measurement. Possible causes for the poor agreement between the two sets of data may include the following:

1. In the later stage of measurement, the horizontal settlement indicator has experienced excessive bending which may have resulted in less accurate readings.
2. The weathered bedrock at bottom boundary may have become less permeable due to the intrusion of lime waste into the fractures/cracks, thus reduced the validity of free draining assumption. As a result, the actual degree of consolidation at a time became smaller than the predicted value.

The excess pore pressure induced by a ramp loading was determined as follows: the average degree of consolidation due to the ramp loading was obtained first using the chart developed by Olson (1977). The degree of consolidation thus obtained was then used to find the time factor for an equivalent constant loading. Using this value of time factor, the consolidation ratio at any depth was obtained from an available chart for constant loading. From this consolidation ratio, the excess pore pressure was computed. The computed excess pore pressures for piezometer setup No. 3 are plotted along with the measured data in Figure 4.

The computed excess pore pressures presented in Figure 4 increase with increasing load and decrease with time as the load becomes constant. Such a pattern of variation of excess pore pressure with time and load is what would be expected according to the theory. The measured data follow the expected trend of variation from about 320 days. However, the magnitude of the data is considerably smaller than the computed values. During the first 320 days, the measured data show either little change with load (for P3-3) or erratic change with load (for P3-2). It appears that the piezometers were not functioning properly especially in the early stage of measurement. Thus, the poor agreement between the measured and computed excess pore pressure data can be attributed primarily to the instrumental factors. Although possible instrumentation factors have decreased the accuracy of the measured excess pore pressures, resulting in a poor agreement with the computed data, the agreement in settlement is encouraging.

There are many factors which may affect the result of settlement prediction; more important factors include nonhomogeneous lime waste properties as reflected by the SPT

N-values, non-uniform compressible layer thickness, irregular bottom profile of the quarry, drainage boundary, and non-uniform fill placement rate. Considering the possible effects of these many factors on settlement prediction, the agreement between the measured and computed settlement values is fairly good. Based on this comparison, it appears that the analysis using the conventional consolidation theory can provide sufficiently accurate consolidation settlement for embankment construction over highly compressible deposits such as lime waste.

## Summary and Conclusions

The performance of a four-lane highway embankment constructed over an abandoned quarry was presented. The roadway was a part of highway LR 1010 located in Plymouth Township, Montgomery County, PA. The embankment was about 1000 ft (305 m) long and 45 to 50 ft (13.5 to 15 m) high. The supporting quarry was approximately 60 ft (18 m) deep and contained a lime waste with very small amounts of asphalt coal tar, flyash, brick cinders, crushed limestone, and others. The lime waste had a natural water content as high as 124% with a liquid limit of approximately 72% and a plasticity index of 19. It was classified as A-5 and MH according to AASHTO and Unified classification systems, respectively.

The embankment was instrumented with settlement platforms, horizontal settlement indicators, inclinometers, and piezometers to monitor embankment settlement, slope movement, and pore water pressure. The embankment settlement and excess pore pressures were also analyzed. A comparison between the measured and analyzed data showed a fairly good agreement in settlement except in the later stage of measurement. In the later stage, the measured settlement was significantly smaller than the computed values due possibly to instrumental factors and drainage conditions. The piezometers data were fairly erratic, resulting in a poor agreement between the measured and analyzed excess pore pressures.

Based on the results of this study, it may be concluded that the lime waste, although classified as a silty soil, behaves differently from typical silty soils. It is highly compressible and can cause very large roadway settlements. The magnitude and time rate of settlement can be analyzed with satisfactory accuracy using the conventional consolidation theory.

## Acknowledgment

## References

Marchetti, S., March 1980, "In-Situ Tests by Flat Dilatometer", *Journal of the Geotechnical Engineering Division*, ASCE, Vol. 106, No. GT3, pp. 299-321.

Olson, R. E., January 1977, "Consolidation under Time Dependent Loading," *Journal of the Geotechnical Engineering Division*, ASCE, Vol. 103, No. GT1, pp. 55-60.

Olson, R. E. and Ladd, C. C., January 1979, "One-Dimensional Consolidation Problems," *Journal of the Geotechnical Engineering Division*, ASCE, Vol. 105, No. GT1, pp. 11-30.

Schmertmann, J. H., June 1986, "Suggested Method for Performing the Flat Dilatometer Test", *Geotechnical Testing Journal*, ASTM, Vol.9, No.2, pp.93-101.

Yong Shao[1] and Emir Jose Macari[2]

**Ground Water Control Associated with Deep Excavations**

---

**Abstract**: This paper discusses the principles and arrangement of pumping wells designed as part of a dewatering system to ensure the stability of deep soil excavations and the safety of adjacent structures. The paper presents a case study of a large-scale dewatering system in a deep excavation for an underground Power Transformer Station in Shanghai, People's Republic of China. Various construction methods are discussed to prevent excessive total and differential settlements that may result from dewatering. Theoretical predictions of settlement, based on the calculation of pore water pressure, are also presented, including the calculation of ground water table in the aquifers. The ground water table, pore water pressure and surface settlements were measured during the excavation process. This allows for comparisons between the measured values and the theoretical predictions. The paper concludes that the prediction of settlements, by the methods presented, is in good agreement with field measurements. These theoretical models can become powerful tools for the geotechnical engineer during the design stage of a dewatering system for an excavation project. Optimized designs will likely result from the use of theoretical models and allow the geotechnical engineer to present a variety of "what if" scenarios that will result in a well engineered dewatering system.

**Keywords:** dewatering system, diaphragm wall, deep excavation, surface settlement, seepage, ground water control, pore water pressure

## Introduction

The underground power transformer station discussed in this paper is located in the center of Shanghai City, China. The excavation was supported by means of a circular diaphragm wall retaining structure. The diaphragm wall, 1.2 m in thickness, extended to 38.2 m below the ground surface and the total excavation depth was 23.2 m. Figure 1 shows a section with detailed geometry.

Since the ground water table is high at the construction site (about 0.8 m below the ground surface), large water pressure gradients are generated during the excavation,

---

[1]Ph.D. Graduate Student, Georgia Institute of Technology, Atlanta, GA 30332-0355.
[2]Chairman/Bingham C. Stewart Professor, Louisiana State University, Baton Rouge, LA 70803. Formerly Associate Professor, Georgia Institute of Technology, Atlanta, GA 30332-0355.

especially when the excavation approaches the final depth. To alleviate such pressure gradients, a dewatering system was used, composed of several deep wells for pumping water from the ground and additional deep wells for pumping water back into the ground for the reasons discussed later. All the deep wells penetrated into the primary aquifer, a fine sand layer in this case.
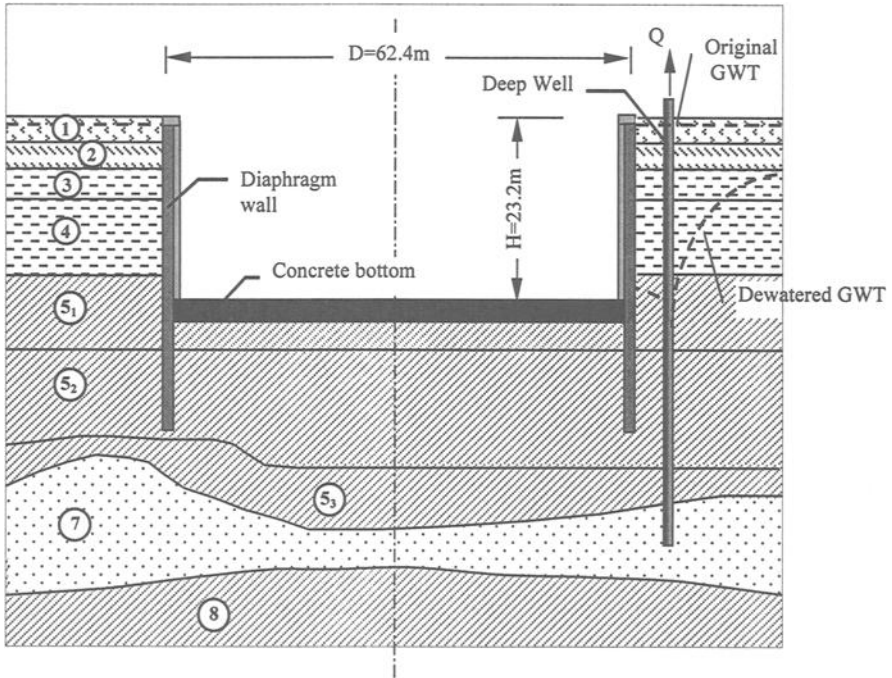


Figure 1 -- *Soil Profile along the Center Line of Excavation*

A dewatering system provides several benefits to the deep excavation design. First of all, it prevents water from seeping upward into the excavation pit, hence minimizing the possibility of piping. Second, de-watered ground gains shear strength, which may ensure the stability of the excavation and prevent shear failure and/or excess bottom heaving. Third, the lateral earth pressures on the diaphragm wall is reduced.

On the other hand, dewatering operations generally increase the effective stresses in the vicinity of the excavation pit, resulting from the reduction in pore water pressure. This stress increment often results in ground settlement that may cause damage to adjacent underground facilities. This issue was one of the major considerations in this project-- to safeguard a water supply pipeline (0.7 m diameter) that is located about 35 m away from the diaphragm wall.

It can therefore be stated that it is just as important to design an appropriate dewatering system as it is to design good supporting systems for a deep excavation. This paper discusses relevant issues of dewatering procedures by introducing the case history of an underground transformer station in Shanghai, People's Republic of China.

## Geological and Hydrological Conditions

The physical and mechanical engineering properties of the soil deposits in the study area are presented in Table 1. These data are the result of a geotechnical in-situ site investigation and a detailed laboratory test program.

Table 1 -- *Physical and Mechanical Engineering Properties of Soil*

| Layer no. | Soil description | Thickness $T$(m) | Elevation (m) | Water content $w$(%) | Void ratio $e$ | Permeability ($\times 10^{-9}$m/sec) $k_x$ | $k_y$ | CU test $c$(kPa) | $\phi$(°) |
|---|---|---|---|---|---|---|---|---|---|
| 1 | Fill | 0.7 ~ 3.4 | | | | | | | |
| 2 | Clay | 0.2 ~ 1.8 | 1.0 ~ 0.3 | | 1.26 | | | | |
| 3 | Silty clay | 3.6 ~ 5.0 | -3.1 ~ -4.2 | 43.0 | 1.21 | 3940 | 4.40 | 9.0 | 11 |
| 4 | Silty clay | 9.4 ~ 11.1 | -10.4 ~ -14.5 | 49.6 | 1.41 | 3940 | 4.40 | 9.5 | 7 |
| $5_1$ | Sandy clay | 12.2 ~ 13.8 | -26.3 ~ -27.3 | 36.4 | 1.06 | 5134 | 1.91 | 10.5 | 11 |
| $5_2$ | Sandy clay | 11.0 ~ 17.0 | -37.7 ~ -44.0 | 33.0 | 0.99 | 5134 | 1.91 | 13.0 | 14 |
| $5_3$ | Sandy clay | 1.5 ~ 10.4 | -39.2 ~ -53.4 | 28.2 | 0.85 | 5134 | 1.91 | 21.0 | 16 |
| 7 | Fine sand | 3.2 ~ 14.5 | -52.1 ~ -54.9 | 24.6 | 0.76 | 39600 | 12.54 | | 23 |
| 8 | Sandy clay | 17.8 ~ 23.5 | -72.5 ~ -76.6 | 30.9 | 0.91 | | | | 16 |

Note: $k_x$ -- Horizontal coefficient of permeability, $k_y$ -- Vertical coefficient of permeability

The geotechnical in-situ characterization program indicated that the soil deposits at the site were in hydrostatic equilibrium prior to excavation. This equilibrium condition would be destroyed as a result of the excavation or the groundwater pumping, because the rate of water flow (infiltration) for each layer is significantly different due to large differences in hydraulic conductivity. The pumping of the groundwater led to a rearrangement of the effective stresses in the soil deposits and to seepage of the groundwater into the primary layer of the aquifer. The primary layer of aquifer is the $7^{th}$ layer composed by fine sand.

## Layout of Dewatering System

Although the primary aquifer was located below the lowest point of the proposed excavation, the groundwater could still seep upward through the overlain sandy clay. The water head varies seasonally and it reaches the maximum of about 1 m below the ground surface. In addition, the 8 boreholes of the geotechnical investigation penetrated into the confined aquifer and it was expected that they could become conduits through which piping would occur. The main purpose of installing the dewatering system was to reduce the water pressure, hence, reducing the likelihood of the groundwater seeping into the excavation pit. Therefore, it was necessary to lower the water head to certain depth to prevent water from seeping into excavation pit.

After comparison of alternative pumping methods, deep well pumping was used for the dewatering system. The location, the number, and pumping rate of the extraction wells were determined according to the following criteria. (1) the water table would be maintained at a level that would ensure the stability of excavation and (2) the quantity of water pumped out of would be minimized in order to reduce ground settlement.

The cost of a dewatering system largely depends on the number of wells. Figure 2 shows the methodology used for the determination of the number of wells and of their locations.
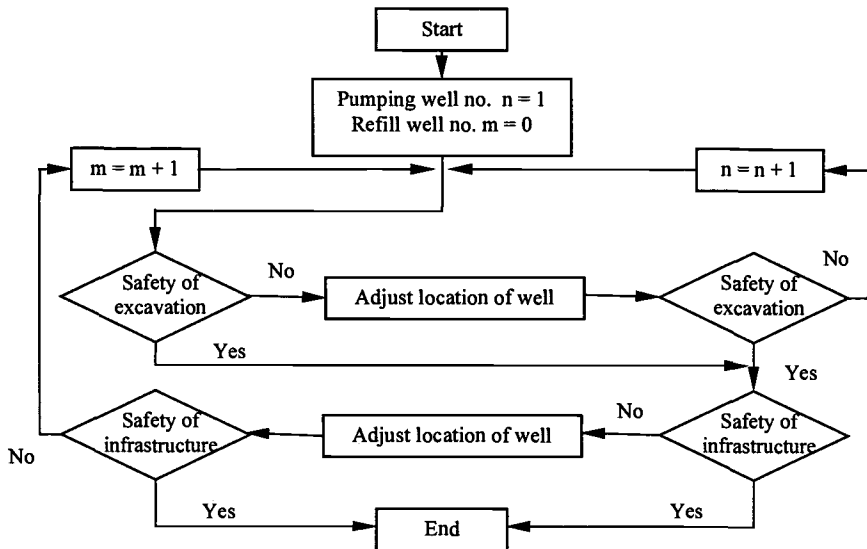


Figure 2-- *Methods for Arranging the Deep Well System*

The operational procedure was as follows:

1. Start with one pumping well and no recharge well.
2. Check the stability of the excavation under the full operation of the pump
   - If not stable, check if changing the location of the well would result in satisfactory stability.
   - If still not, increase the number of wells by one and repeat stability check; adding new wells and repeat the check until satisfactory stability is attained.
3. Check the safety of surrounding infrastructure
   - If not, check if the stability improves by adjusting the location of wells
   - If still not, increase the number of recharge wells by one and repeat the safety check of the infrastructures until required number of recharge wells is found.

The methodology discussed above led to the final layout for the dewatering system, that included 5 pumping wells outside of the circular diaphragm wall and 3 recharge wells near the protected underground water supply pipeline, as shown in Figure 3. The deep wells penetrated into the primary aquifer (7$^{th}$ layer of fine sand) having an approximate length of 60m. The groundwater discharge $Q$ for a single well pumping from confined aquifer may be determined according to equation (1), proposed by Su et al. (1995):

$$Q = \frac{2\pi k d l}{\ln \dfrac{1.32l}{r}}$$

$\qquad\qquad\qquad\qquad\qquad\qquad\qquad\qquad\qquad\qquad\qquad\qquad\qquad\qquad\qquad\;$ (1)

where,

| | | |
|---|---|---|
| $Q$ | = | volume rate of discharge, $m^3/day$ |
| $k$ | = | coefficient of permeability, $m/day$ |
| $d$ | = | drop of the GWT (ground water table) due to dewatering, $m$ |
| $l$ | = | length of screens of perforated section of well, $m$ |
| $r$ | = | radius of screens of perforated section of well, $m$ |
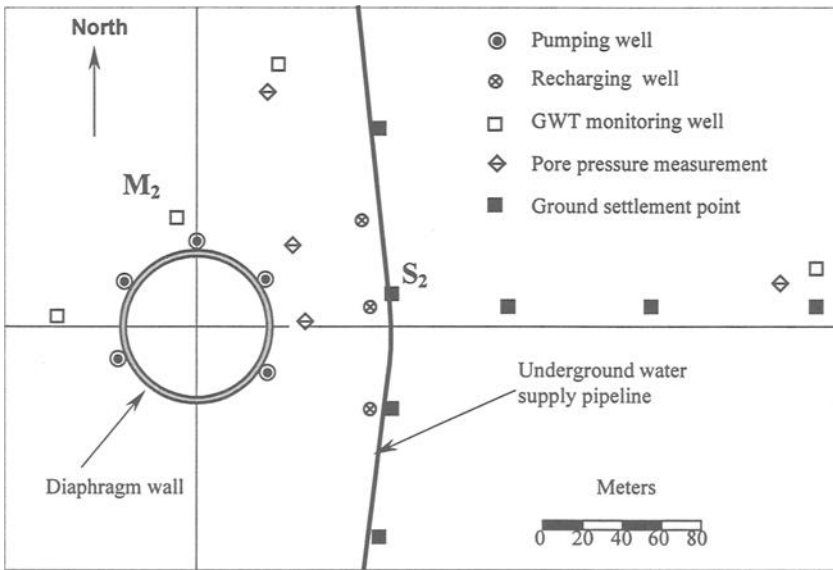


Figure 3 -- *Arrangement of Deep Well and Field Monitoring System*

The GWT was lowered to the excavated depth at each stage. The lowest GWT was about 17 meters below the ground surface as the designed maximum excavation depth was reached. After the first pouring of concrete for the bottom mat, the de-watered GWT was raised to 12 meters because the weight of the concrete counteracted the pressures from the ground water. The de-watered GWT was again raised to 8 meters after the second pouring of concrete and finally, the dewatering process was stopped when the concrete mat cured and reached its designed strength. According to field records, the total dewatering period was 197 days, and the total amount of water pumped out of the ground was about 285000 $m^3$, of which 35000 $m^3$ was re-pumped through recharge wells. The measured settlement at the surface directly above the 0.7 m diameter water supply pipeline was 8.7 mm; less than the allowable deformation of 1 cm.

## Ground Surface Settlement due to Dewatering and Its Control

As previously mentioned, when pumping begins, the groundwater flows towards the pumping wells and gradually forms the dewatering funnel. This procedure often generates non-uniform stresses between soil particles that may result in differential settlement in the ground. The non-uniform stress distribution in the soil mass often results in damage to adjacent structures and subsurface infrastructures. In this case one of the primary concerns was to protect a main underground water supply pipeline (700 mm in diameter) running by at a distance of 35 m away from the diaphragm wall. The allowable vertical displacement was restricted to 1 cm.

Besides minimizing the pumping out of water, other auxiliary measures might be helpful. Some of them were used in this project and proved to be effective. Details of these measures are presented below.

*Seal all potential gaps between the well and the surrounding ground.* Since the overlain silty clay and sandy clay have much lower vertical permeability than that of the primary aquifer fine sand, the pore water pressure in the overlain clay dissipates very slowly in the vertical direction when water is pumped out from the primary aquifers. However, if there were gaps left between the well and the surrounding ground after the installation of the well, the pore water in the overlain clay would be connected with primary aquifers. This would greatly accelerate dissipation of pore water pressure in the overlain clay in horizontal direction, which in turn may cause larger ground surface settlement.

*Incrementally deepen the de-watered GWT based on the excavated depth.* Since the excavation progresses in several stages, to minimize the settlement, the GWT within the excavation pit should only be lowered to the certain level (safety water level, *h*), which can be estimated according to the stability of the bottom against water pressure.

$$h = c - \frac{\gamma_{soil}(c - D)}{\gamma_{water} \cdot K} \tag{2}$$

where,

| | | |
|---|---|---|
| *h* | = | safety GWT within the excavation pit, *m* |
| *c* | = | elevation of top piezometric surface below the excavation pit, *m* |
| *D* | = | elevation of current excavation bottom, *m* |
| $\gamma_{soil}$ | = | average total unit weight of soil between the bottom of pit and the top surface of primary aquifer, $kg/m^3$ |
| $\gamma_{water}$ | = | unit weight of water, $kg/m^3$ |
| *K* | = | factor of safety (1.2 was used for this project) |

*Install recharge wells near the protected pipelines.* To reduce the variation of the GWT in the vicinity of the pipelines, it is helpful to install some deep recharge wells to pump water back into the primary aquifer. Three deep recharge wells were installed on the west side of the water supply pipeline as shown in Figure 3.

*Ensure that the deep wells are kept in working condition throughout the construction process.* Both laboratory test and field test have shown that the total settlement increased when pumping was suspended and restarted.

### Analytical Prediction of Ground Surface Settlement

*Determination of De-watered GWT*

In order to estimate the distribution of ground surface settlement at any given time, one must define the water drawdown $d$ of the GWT ($d = H - h$, $H$ is the original GWT and $h$ is the GWT during pumping) as a function of time $t$ during pumping. In other words, one must determine the equations for calculating the drop in GWT for transient-flow. By assuming that the well is pumped at a constant rate and the aquifer is homogeneous, isotropic, and of infinite horizontal extent, Lohman (1972) derived the basic equation for transient flow to a well as

$$\frac{1}{r} \cdot \frac{\partial h}{\partial r} + \frac{\partial^2 h}{\partial r^2} = \frac{S}{T} \cdot \frac{\partial h}{\partial t}$$

$$d(r,0) = 0 \qquad r \geq 0$$

$$d(\infty, t) = 0 \qquad t \geq 0$$

$$\lim_{r \to 0} r \frac{\partial d(r,t)}{\partial r} = -\frac{Q}{2\pi T} \tag{3}$$

where,

| | | |
|---|---|---|
| $S$ | = | storage coefficient or specific yield of the aquifer |
| $T$ | = | transmissivity of aquifer, $m^2/day$ |
| $r$ | = | radial distance from well center, $m$ |
| $t$ | = | time from constant pumping starts, $day$ |

The solution for equation (3) may be obtained (see Bouwer 1978) for a well of infinitesimally small diameter in a confined aquifer; the drawdown $d$ of the GWT is expressed as:

$$d = \frac{Q}{4\pi T} \int_u^\infty \left( \frac{e^{-u}}{u} \right) du \tag{4}$$

where, $Q$ is the volume of flow rate of well discharge, $m^3/day$, and

$$u = \frac{r^2 S}{4Tt} \tag{5}$$

Equation (4) is also written as

$$d = \frac{QW(u)}{4\pi T} \tag{6}$$

where, $W(u)$ is dimensionless, given by Ferris et al. (1962).

Being the overlain sandy clay not completely impermeable, one may treat the sandy clay as an absorbent or semi-confined aquifer. That is, the pumping action from a well connected to the primary aquifer causes a downward flow from the overburden to the aquifer. For this reason, Hantush and Jacob (1955) modified equation (6) to obtain the drawdown $d$ for a "leaky" aquifer by introducing a *leakage factor, L* as:

$$d = \frac{Q}{4\pi T} W(u, r/L) \tag{7}$$

When several deep wells operate simultaneously, the principle of superposition has been used (a good approximation for the case of a leaky aquifer). Thus if water is pumped from several wells in one aquifer, the drawdown $d$ at any given point is calculated as the sum of the drawdown at that point caused by each individual well. Mathematically, the drawdown at point $j$, $d_j$ may be written as:

$$d_j = \sum_{i=1}^{n} d_{ij} - \sum_{i=1}^{m} d_{ij} \tag{8}$$

where, $d_{ij}$ is the drawdown at point $j$ due to the pumping of well $i$, and $n$, $m$ are the number of pumping and recharge wells, respectively.

A pumping test was performed in the field and was simulated by using the model described by equation (3). From equation (3), the transmissivity, $T$, was determined to be 93 $m^2/day$, the storage coefficient, $S$, 0.000113, and the leakage factor, $L$, 2100 $m$. With these predetermined values, the de-watered GWT, due to the operation of pumping and recharging, may be predicted by using equation (8). The predicted GWT plotted with the measured values from the observations of well $M_2$ is shown in Figure 4.
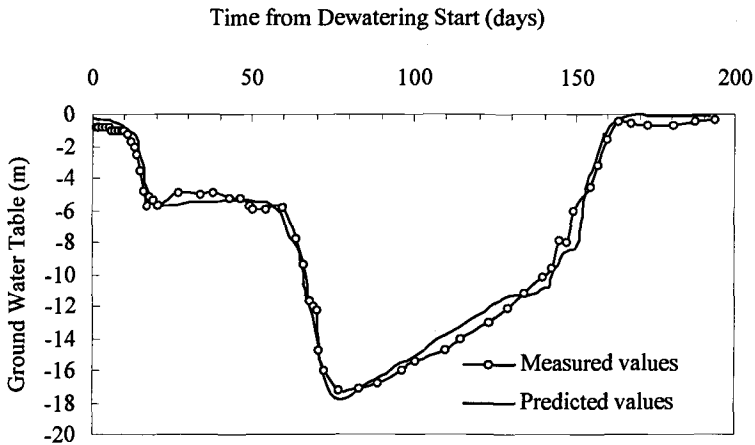


Figure 4 -- *Predicted and Measured Ground Water Table*

*Calculation of Change of Pore Water Pressure*

If one assumes that the pore water pressure in the overlain clay dissipates vertically, Terzaghi's one-dimensional consolidation theory may be considered to be applicable. The governing equation is then written as:

$$\frac{\partial u}{\partial t} = c_v \frac{\partial^2 u}{\partial z^2}$$

$$u \mid_{t=0} = u_i(z)$$

$$u \mid_{\Gamma_1} = u_1(t)$$

$$\frac{\partial u}{\partial z} \mid_{\Gamma_2} = q_2(t) \tag{9}$$

where,

| | | |
|---|---|---|
| $u$ | = | excess pore water pressure in the overlain clay, *kPa* |
| $c_v$ | = | coefficient of consolidation for the overlain clay, $m^2/day$ |
| $T$ | = | time, *day* |
| $z$ | = | depth, *m* |
| $u_i$ | = | initial pore water pressure in the overlain clay, *kPa* |
| $\Gamma_1$ | = | boundary surface formed by de-watered GWT *h(t)* |
| $\Gamma_2$ | = | bottom boundary of overlain clay, or the top surface of primary aquifer |
| $u_1(t)$ | = | pore water pressure at boundary $\Gamma_1$, $u_1(t) = \gamma_{water}h(t)$ |
| $q_2(t)$ | = | flow rate intensity at boundary $\Gamma_2$, $m^3/day.m^2$ |

From Table 1, one may notice that the permeability of soil changes with each layer, and hence the coefficient of consolidation, $c_v$, varies with depth. One may also notice that the pore water pressure at the boundary $\Gamma_1$, $u_1$ is a function of time. Therefore, equation (9) should be solved using appropriate numerical methods. The finite difference method was used to solve the governing equation (9), hence the pore water pressure distribution in the overlain clay for specific points and times was calculated. Detail procedures of the finite difference formulation is not presented, however, the readers may refer to Harr (1966) for detailed derivation and validation of this analysis.

*Evaluation of Ground Surface Settlement*

After estimating the change in pore water pressure in the overlain clay, it is much easier to calculate the corresponding ground surface settlements resulting from the dissipation of pore water pressure. By dividing the overlain clay into several thin layers, the total ground surface settlement is obtained as the sum of the deformation of individual layers as:

$$s = \sum_{i=1}^{n} \frac{a_{vi}\Delta u_i}{1+e_i} H_i \tag{10}$$

where,

| | | |
|---|---|---|
| $s$ | = | ground surface settlement, *m* |

$a_{vi}$    =    coefficient of compressibility for I layer, $(kPa)^{-1}$
$\Delta u_i$    =    average change of pore water pressure for I layer, $kPa$
$e_i$    =    average void ratio for I layer
$H_i$    =    thickness of I layer, $m$

Figure 5 shows the calculated ground surface settlements and are compared with measured values at point $S_2$.

Time from Dewatering Start (days)
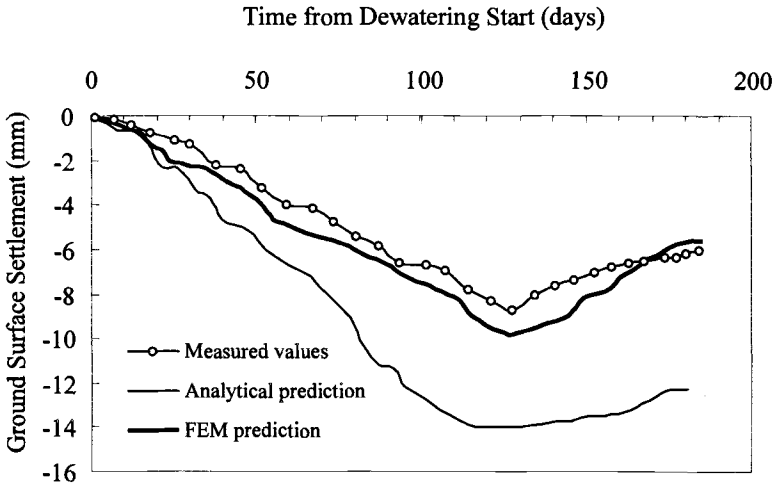


Figure 5 -- *Predicted and Measured Ground Surface Settlement at point $S_2$*

From Figure 5, one may notice that the predicted ground surface settlements follow the same trend as the measured values. However, the predicted values are larger than the measured values, having a maximum difference of about 70%. There are several reasons why these differences are obtained between the calculated and actual measured settlement values:

1.  The pore water pressure in the overlain clay dissipates in the vertical direction as well as in the horizontal direction. This means that the Terzaghi's one-dimensional consolidation theory should only be considered as an approximation.
2.  When one calculates the pore water pressure, the vertical coefficient of permeability $k_y$ used is the one determined from laboratory consolidation tests. The laboratory value is generally lower than field value for semi-permeable layer.
3.  Equation (10) only provides the ultimate values of ground settlement for the known values of pore water pressure changes. However, the measured values were not necessarily recorded after full dissipation of the pore water pressure.
4.  Pore water pressure dissipation is not the only cause of ground surface settlement. The excavation process, itself, may also be the cause of deformations of the ground surface. However, it is very difficult to separate dewatering induced settlements from total settlements.

In order to have a more accurate prediction, a finite element method that includes three-dimensional consolidation, should be used. This issue is further discussed in the next section.

*Predicting the Ground Surface Settlement using FEM*

One of the disadvantages of previously described methods for all accurate prediction of ground deformations is that the change of pore water pressures and the induced settlements are calculated separately following independent set of assumptions and theories, otherwise a solution would be too difficult to obtain analytically. On the other hand, the finite element method provides an opportunity to calculate settlements (or displacement) directly, by using a mixed element having, both, displacement nodes and pore water pressure nodes. The detailed description of the finite element formulation and procedures used in the study are beyond the scope of this paper. However, a brief discussion of the finite element model is presented in order to facilitate a better understanding of the results.

A simplification of the finite element analysis for the current problem was made by assuming that the de-watered GWT, evaluated by equation (7), represents the actual situation for each stage of the excavation. That is, instead of simulating the deep wells in the finite element model, the predetermined GWT for each stage was assumed. The FEM analysis calculates the displacement as a function of time, resulting from the change of GWT and excavation process itself.

The coupled pore fluid diffusion and stress analysis procedure (transient analysis) provided by the ABAQUS computer program was used for the analysis. This procedure treats the soil as a porous medium and adopts an effective stress principle to describe its behavior. The porous medium was modeled by attaching the finite element mesh to the solid phase (fluid can flow through this mesh.) The model also uses the continuity equation for the mass of water in a unit volume of the medium, and is written having the pore pressure (the average pressure in the water at a point in the porous medium) as the basic variable.

The axisymmetric case is the only scenario considered to approximate the actual three-dimensional problem of an excavation. In this nonlinear, isotropic elasticity analysis, where the stress varies as an exponential function of the volumetric strain, the soil is represented using mixed isoparametric finite elements (each with eight-displacement and four-corner pore-pressure nodes), while the diaphragm wall is modeled as a linear, elastic material with eight-noded solid elements.

The FEM results are also presented in Figure 5, which demonstrate an obvious improvement of prediction for the ground surface settlement as compared to the measured data.

**Conclusions**

1. When a deep excavation is performed in a soft clay formation overlain a confined aquifer, the installation of a dewatering system is recommended as a good construction practice. By dewatering the ground water table, the shear strength of soil below the excavation bottom will be increased and hence help to counteract the

potential of failure from seepage and/or shearing. An additional benefit of the dewatering process is that it will also decrease the lateral earth pressure exerted on the diaphragm wall.

2. Since dewatering often induces significant amount of ground surface settlement, caution must be exercised during the design stage for the dewatering system. The design principle that should be followed is the minimization of water pump-out as long as the excavation and environmental requirements are satisfied. With this in mind, the suggested methodology (Figure 2) for determining the number of deep wells and their locations is of great help for this design purpose.

3. The predicted values for the de-watered GWT are shown to be in good agreement with measured values. From the description of the proposed method, one may notice that the de-watered GWT is calculated based on couple of hydraulic properties of the ground and these need to be adequately determined. Therefore, a good field pump test is required for the accurate prediction of ground settlements.

4. The predicted ground surface settlement using the suggested analytical approach follows the general trend of the measured values. Although there is a relatively large difference between predicted and measured values (maximum overestimation up to about 70%), this method may still be used if one seeks simplicity and lower computational costs. In addition, this approach is often better accepted by practicing engineers. The overestimated ground surface settlement may be treated as a safety factor.

5. The finite element method used for these predictions is complicated and requires major computational effort. However, it provides much better estimation of the ground surface settlement. The largest difference between the FEM results and the measured values of ground settlement were in the order of 13%.

**References**

Bouwer, H., 1978, *Groundwater Hydrology*, McGraw-Hill Book Company, New York.

Ferris, J. G., et al., 1962, *Theory of Aquifer Tests*, U.S. Geological Survey Water Supply Paper 1536-E, pp. 69 - 174.

Hantush, M. S., and Jacob, C. E., 1955, "Non-steady Radial Flow in an Infinite leaky Aquifer," *Journal of Geophysics*, Vol. 36, pp. 95 - 100.

Harr, M. E., 1966, *Foundations of Theoretical Soil Mechanics*, McGraw-Hill Book Company, New York, 381 pp.

Lohman, S. W., 1972, *Groundwater Hydraulics*, U.S. Geological Survey Prof. Paper 708, 70 p.

Su, H., et al., 1995, *Foundation Engineering Construction Handbook*, Chinese Plan Press, 686 p. (In Chinese)

Giovanni Varosio[1]

## Peat Subsidence due to Ground Water Movements

**Abstract:** A wide seasonal variation of ground water level was observed near the town of
Angri, Italy. In the period 1989 to 1995, the water table dropped by 6 meters during the
summer and returned to normal levels in the fall. The water level variation led to
settlements which caused damage to an industrial building. The rational developed to
explain the soil behavior at the site, which includes layers of peat, illustrates the
important role of seepage pressures during rapid transients. During rapid lowering of the
phreatic surface, the initial soil compression is controlled by total stresses including the
weight of water. The soil investigation and monitoring to evaluate damages highlight this
unusual aspect of soil behavior, not yet completely documented, to the author's
knowledge, in the geotechnical literature.

**Keywords:** ground water flow, peat, seepage forces, soil settlement, building damages

## Nomenclature

| | |
|---|---|
| $G$, $\gamma_d$ | Specific gravity and dry unit weight (kN/m$^3$) |
| $n$ | Porosity (%) |
| $M$ | Oedometric modulus (MN/m$^2$) |
| $c'$, $\varphi'$ | Drained cohesion (MN/m$^2$) and drained friction angle, degrees |
| $c_v$ | Consolidation coefficient (cm$^2$/s) |
| $C_c$ | Primary consolidation index |
| $C_a$ | Secondary consolidation index |

---

[1] D'Appolonia S.p.A., Via San Nazaro 19, 16145 Genoa, Italy.

## Introduction

The lowering of phreatic ground water level in alluvial soils produces an effective stress increase, due to the reduction of buoyancy that in turn causes settlement of the ground surface. The opposite usually occurs when water levels raise. Soil behavior may be different in the case of confined aquifers. A good example was observed at the site of a decommissioned nuclear power plant, in Italy (D'Appolonia, unpublished data).

The reactor area is inside a diaphragm wall. The water table has been maintained in this area at about ten meters below the normal level. During a temporary shut down of the dewatering system, an apparently incongruous soil movement was observed. As the ground water rose, there was significant downward movement for some subsoil layers.

The diaphragm penetrates a silty clay aquitard, which separates two aquifers. Raising the water level inside the diaphragm area caused an increase of the total weight of the enclosed soil. This, in turn, increased the total stress on the underlying soils. Typically, the total stress increment is more than offset by the increased hydrostatic pressure and effective stress is reduced. The presence of the clay aquitard, however, interrupted hydraulic communication between the upper and lower layers, the lower soils experienced a total stress increase without compensating buoyancy, and tended to compress.

The compression of the confined aquifer was of the order of centimeters, although compensated from the heave of centimeters produced by the hydrostatic buoyancy of foundations inside the diaphragm area. The reactor moved down, even if for only a few millimeters, as a difference between the centimetric up and down movements above and below the aquitard. The experience described above was taken for reference to evaluate the soil movements during variations of ground water table levels, bearing in mind the effect of water weight in the initial behavior of soils.

The presence of compressible peat in the Angri soil profile produced more significant settlements than in the previous case. The movements damaged an industrial building. The building foundations are a combination of driven cast in situ Franki piles and slabs on grade supported on compacted fill. The tips of the driven cast in situ piles bear on a hard, pervious layer of tuff below compressible silt and peat.

The slabs underwent settlements of about 30 to 40 centimeters after construction. The settlement time exceeded the theoretical rate of consolidation induced by the fill. The interior walls of the building were damaged, and the equipment on the slab was inoperable. During this period the ground water table in an agricultural pit close to the plant was observed to lower about six meters from June to November, returning later to the initial level.

The plant damage after the end of construction was found to be mainly a consequence of subsidence produced by the water movements, with soil surface movements apparently in contrast with predictions.

## Site Geology and Hydrogeology

The town of Angri (Figure 1) is located close to Naples, in the area of the Sarno river.    The site is less than 10 kilometers west of Pompei, the famous town destroyed by the eruption of Vesuvius in 79 A. C. The site is at the south of the Campania carbonatic plane, which has been filled by thousands of meters of pyroclastic, alluvial and marine sediments (Celico et al. 1977). The area is bordered by the Somma Vesuvius Volcano to the north, by the Sarno Mountains to the east, and by the Lattari mountains to the south. It was covered by quaternary marshes, probably until recently, as indicated by the fibrous structure of the peat found at the site (Cascini et al. 1994).

The site aquifers are fed by abundant underground resources. They present variable permeability in vertical and horizontal directions. Groundwater flows according to a "two overlying water tables" model, with the exception of the coastal area, which has a single unconfined acquifer. The natural groundwater flow is presented in Figure 2.

The two separated aquifers are usually related to the presence of a layer of low permeability tuff, from a few to tenths of meters thick, interbedded with the marine, alluvial and pyroclastic sediments. Although at some locations the permeability of this layer is reported as low, and the tuff behaves as an aquitard, at the Angri site the tuff is a water bearing layer, as confirmed by local soil investigations. The tuff is overlain and underlain in this area by less permeable pozzolanic materials and sediments.  The peat layers close to the surface have intermediate permeability.
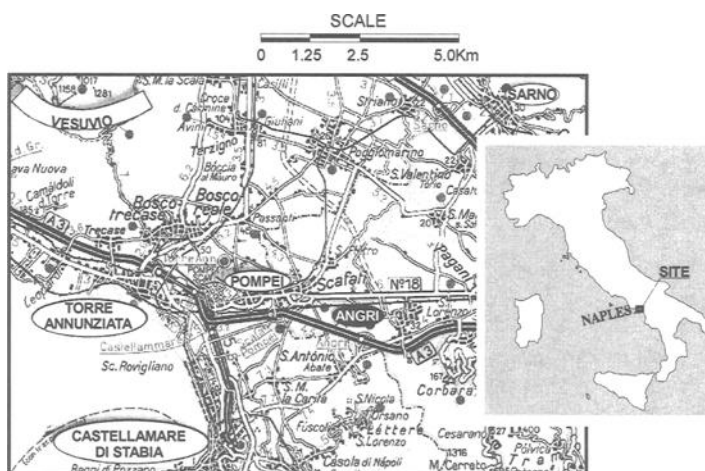


Figure 1- *Site Map*

## Foundations and Building Damages

A plan view of the area and of the damaged building are presented in Figure 3. The precast reinforced concrete structure was constructed on Franki piles with 540 millimeter diameter, bearing on a 5-meter thick layer of porous tuff. Lightly loaded areas and interior floors were on slabs placed on fill. Differential settlements occurred between piled foundations and the paved areas of the plant.
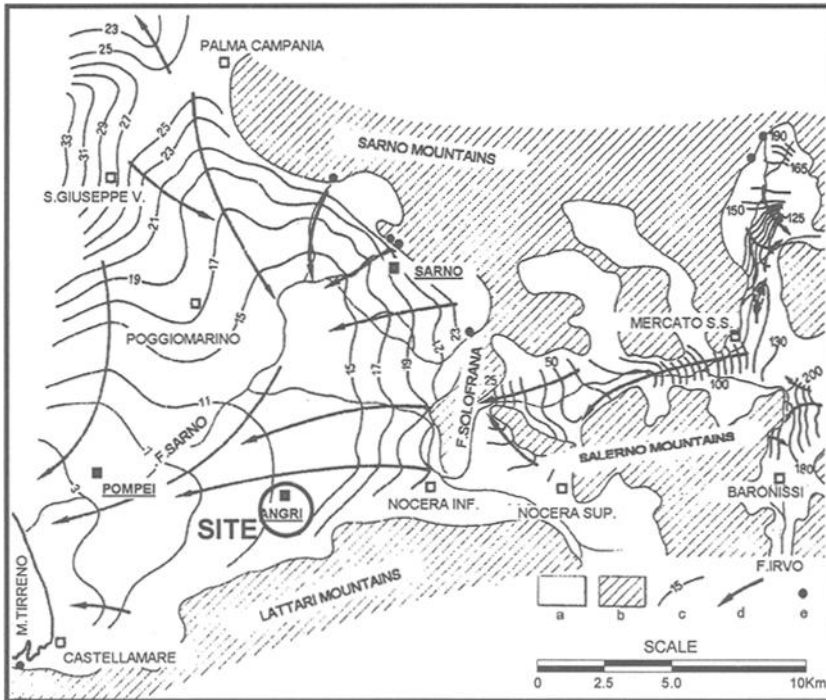


Legend: a) marine alluvial pyroclastic complex; b) calcareous and dolomitic complexes; c) isopiezometric contour lines; d) direction of ground water flow; e) main springs of aquifers.

Figure 2 - *Undisturbed Ground Water Flow*

The fill had a plate load test modulus of 30 MPa. Thus fill compression did not contribute significantly to the site settlements. The consolidation settlements produced by the weight of the fill were evaluated, and were also deemed to have no significant contribution after the end of construction. After the beginning of plant operations, however, cracks opened on interior walls founded on pavements. After these cracks were repaired, new cracks opened and widened in the following years.

## Ground Water

During the original soil investigation the water table was found at 4.5 meters below initial grade. In 1989, the owner started to measure the water levels in the irrigation well shown in Figure 3. The well, dug several decades ago, has an open underground chamber connected to the tuff.

Two open pipe piezometers were placed in 1994 during a soil investigation to study the building damage (Figure 3).

The first strong variation of water levels was reported the summer after construction. Similar variation was measured every summer thereafter (Figure 4). The water table variations appeared to be related to water withdrawal during the summer season.

LEGEND

S2,P:1994 BOREHOLES AND PIEZOMETERS

S3:1994 BOREHOLE

S2,P

S3

DAMAGED BUILDING

S1,P

AGRICULTURAL WELL

LEGEND

30 • MONUMENTS ON PILES
22 ■ MONUMENTS ON PAVEMENT

READINGS FOR THESE MONUMENTS ARE PRESENTED IN FIGURE 6
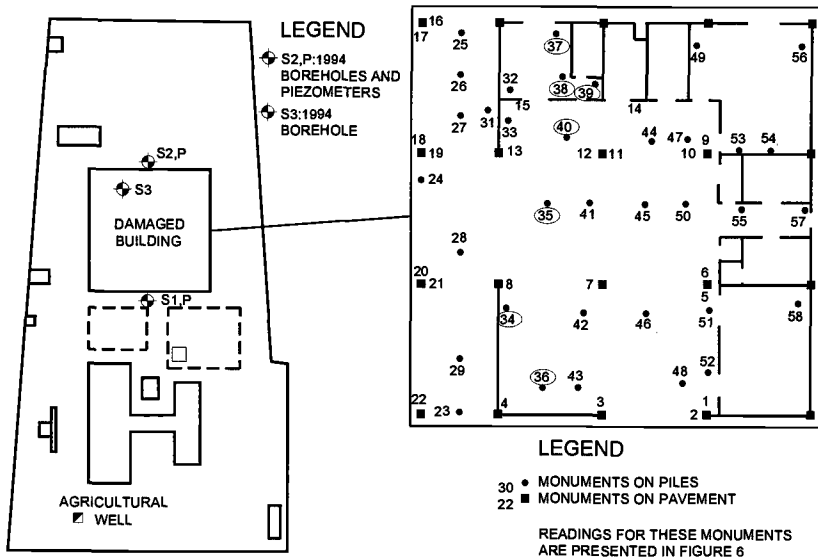
Figure 3 - *Plant Area and Building Monuments*

The 1994 piezometers are not hydraulically connected to the tuff of the irrigation well.    These piezometers measure pore pressures in the less pervious layers above the tuff. The readings of the 1994 piezometers, however, show the same variations as in the well with time delays of one to two months.

## Soil Profile and Peat Properties

Six soil investigations were carried out at the site; between 1983 and 1987 for the design, and from 1992 to 1995 during the studies to evaluate the building damage. A simplified soil profile is reported in Table 1.  A stratigraphic section across the area (Figure 5) shows the variability of peat thickness. The soil properties in Table 1 are based on in situ static and dynamic penetration tests and laboratory results.

Due to difficulties of sampling the very friable peat at the site, data from other geotechnical studies close to the Angri area was also considered. The Angri peat is fibrous, with an open primary structure (macropores), and a secondary structure of finer fibrous elements (micropores). The majority of the saturation water is not adsorbed. The primary consolidation can be related to the flow from the macropores, while secondary consolidation is more related to the water migration from micropores to macropores.

The confined moduli of the peat (M) range from 0.5 to 5.6 MPa, the consolidation index $(C_c)$ ranges from 0.34 to 1.60 and the vertical coefficient of consolidation $(c_v)$ varies from 1.6 to 8.2 x $10^{-3}$ cm$^2$/s. The coefficients of secondary consolidation $(C_a)$ of the peat, measured in the Angri area on samples with a relatively low organic content (15 per cent), range from 0.14 to 0.88 per cent, as a function of the load interval.

$C_a$ values on samples representative of the most organic portion of peat recovered in nearby areas range from 2.0 to 4.0 percent (Cascini et al. 1994; Mandolini et al. 1995).
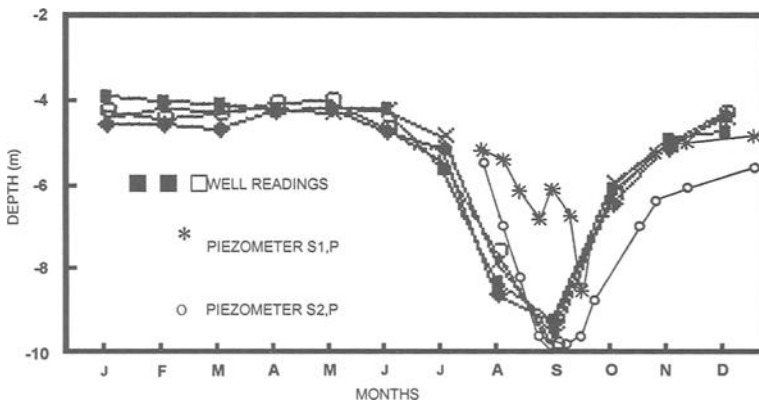


Figure 4 - *Average Water Levels 1989-1995*

Table 1 - *Simplified Soil Profile*

| Description | G | n % | $\gamma_d$ (kN/m$^3$) | M (MPa) | c' (MPa) | φ' |
|---|---|---|---|---|---|---|
| Fill and Sand | 2.7 | 0.4 | 16.2 | 30.0 | - | 35 |
| Peat and Pumices | 2.0 | 0.7 | 6.0 | 4.0 | - | 27 |
| Silt | 2.7 | 0.5 | 13.5 | 10.0 | - | 27 |
| Tuff | 2.4 | 0.5 | 12.0 | 300.0 | 1.0 | 38 |
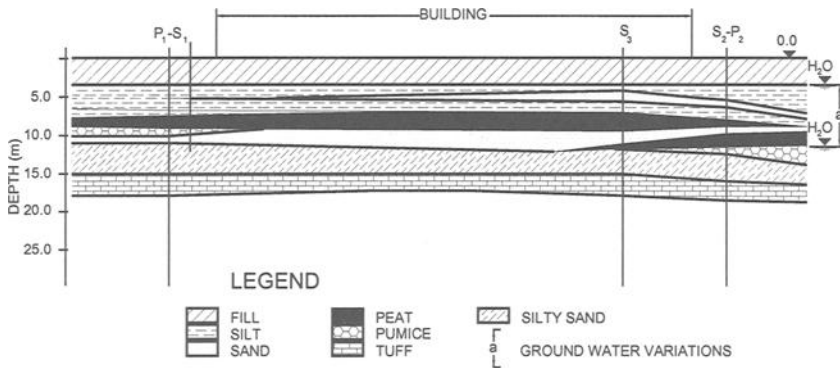


Figure 5 - *Soil Profile*

In the fibrous layers of the peat the permeability is reported to be $10^{-2}$ cm/s. The transmissivity of the top aquifer is from $10^{-2}$ m$^2$/s to 3 x $10^{-2}$ m$^2$/s (Piscopo et al. 1997); hence a permeability higher than $10^{-1}$ cm/s can be estimated for the tuff assuming an aquifer thickness of 15 meters and a tuff thickness of 5 meters.

The permeability of the pozzolanic soils above the tuff, measured in consolidation tests, is at least four orders of magnitude less. Because undisturbed sampling and consolidation tests are frequently made on the finest portion of soils, a permeability coefficient between $10^{-4}$ and $10^{-5}$ cm/s may apply to the mass permeability of the pozzolanic silts.

## Soil Movements

The field monitoring started in 1989, after wall damage was observed inside the building. Readings of monuments on the pile  foundations were found to be very small by the owner. Reference monuments were then placed on pile foundations for the readings for damage evaluation.

Monuments were monitored from July 1994 to May 1995. A summary of maximum and minimum values is presented in Table 2.  Partial graphs for this period are presented in Figure 6.  Only the readings of the 1994-1995 period were considered, as they provide the most continuous and complete record.

At least two cyclic vertical movements can be seen in Figure 6. The total displacement  is about two to three centimeters. Movements also occurred after the final readings shown in the figure.

Table 2 - *Measured Settlements, Extreme Values*

| Time | Maximum values, cm | Minimum values, cm |
|---|---|---|
| August 12, 1994 | + 3.0[1] | + 1.3 |
| September 5, 1994 | + 1.3 | - 1.0 |
| September 19, 1994 | + 2.7 | + 0.9 |
| November 9, 1994 | + 1.3 | - 0.5 |
| January 10,1995[2] | + 2.9 | + 0.7 |

[1] Plus for heave and minus for settlement.
[2] From January 10 to May 11, 1995, no meaningful movements were observed.
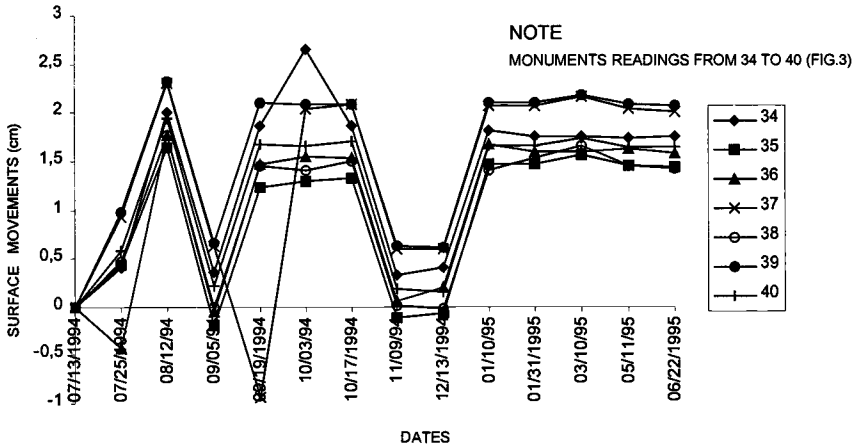


Figure 6 - *Soil Surface Movements*

## Evaluation of Soil Movements

In the attempt to understand the observed settlements, a series of simplified analyses were performed with the computer program FLAC (Itasca. 1995).

The stratigraphy given in Table 1 was modeled as a series of horizontal elastic layers. The layers were taken to be 5 m thick. The base of the model was assumed to coincide  with the comparatively rigid tuff. This was appropriate, as the ground surface settlements were measured with respects to the piles founded in the tuff.

The purpose of these analyses was to determine if the soil movements were consistent with the soil properties, based on lab testing, and with the forces induced by the ground water movements.
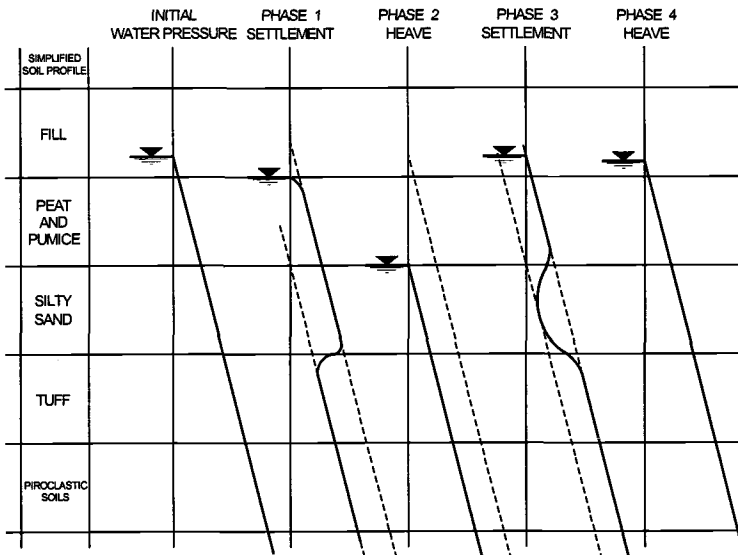


Figure 7 - *Idealize Hydrogeological Modeling*

As described in the following with reference to the transitory water levels, the computed settlement values approach the measured data.

Pore pressure variations and effective soil stresses can be represented as shown in Figure 7. The transitory phases in the surface aquifer can be described qualitatively as follows:

*Phase 1*

During the summer irrigation season, water is pumped from the porous tuff aquifer, causing a reduction in pore pressure. Water starts to flow downward from the shallow formations to the tuff. The silt between tuff and peat acts as an aquitard. This retards the pore pressure response in the upper soils. The time delay observed between the irrigation well in the tuff (Figure 3) and the piezometers in the silt above the tuff (Figure 4) is due to the retarding effect of the silt.

*Phase 2*

The downward flow during Phase 1 partially desiccates the peat. In the period from mid August to the end of September water levels are below the base of the layer and the peat quickly dries as water flows through the macropores. During this phase foundation heave was observed.

*Phase 3*

After the summer pumping, autumn rains saturate again the tuff and peat. The tuff is saturated first, due to the high permeability of this formation, by percolation from the nearby outcrops. The peat itself, once covering marsh areas, represents an easily flooded underground water collector.

*Phase 4*

The pozzolanic silt between peat and tuff saturates later, as water flows from above and below. Time lags observed between the abandoned irrigation well and the recently installed piezometers, confirm a delay in the restoration of pore pressures in the silt.

The effective stresses produced in Phase 1 can be expressed as:

$$F = i\, \gamma_w\, A \qquad\qquad (1)$$

Where:

$F$ = seepage force per unit area
$i$ = hydraulic gradient
$\gamma_w$ = water unit weight, and
$A$ = flow area.

For a vertical gradient close to one, and a unit area, the seepage force is equal to the unit weight of water. The settlement during Phase 1 can be computed considering the flow pressures in the peat and silt overlying the tuff. The computed settlement is about three centimeters. Measured settlements (Figure 6) do not include this settlement phase.

After the end of the downward flow, the effective stresses in the surface layers are reduced (Phase 2). To compute the new effective stresses, a water content of about ten percent was considered in the numerical model for the peat.

The reduction of vertical effective stress was computed to produce a surface heave of approximately 2.5 centimeters, consistent with the average heave (2.15 cm) measured on August 12 (Table 2) with reference to the initial zero reading. Differences between movements during Phase 1 and 2 were computed  to be five millimeters. The temporary elevation of the ground surface in Phase 2 was thus computed to be slightly below the undisturbed level.

Settlement is again produced by flooding of the peat in fall: it was computed to be close to two centimeters (Phase 3), equal to the average settlement observed on September 5 respect to August 12, 1994 (Table 2). Finally, after the saturation of the silt layers (Phase 4) the soil surface raised again to the undisturbed level, due to the reduction of effective stresses.

The first readings of 1994 were probably taken after the end of the downward flow. A soil heave was recorded in the first month thereafter, which corresponds to Phase 2. The peat plays an important role in these movements. Due to its high porosity the water flow is relatively fast. Peat compressibility amplifies the effects, making soil movements more observable.


**Concluding Remarks**


The movements observed were measured by means of a simple instrumentation system, designed according to the current practice. Further investigations on similar problems should include piezometer cells sealed in each formation.

The secondary consolidation properties of peat were evaluated according to standard procedures. They could  be also assessed  using simulation of the cyclic loading-unloading behavior. The correlation of secondary consolidation indexes with load histories could be useful in evaluating the soil movements in function of time.

Despite these limitations, the soil behavior was sufficiently documented. This was possible due to the relatively high water level variations, and the presence of soft porous peat which enhanced movements.

The observed soil behavior agrees in general with the rule that a reduction of the water level makes soils settle. The transitory phases have shown an unusual soil behavior, that is the result of temporary stress variations due to the ground water movements and to seepage pressures.

In the transitory phases, the effective pressures approach the total stresses. This was put in evidence by discontinuities of permeability and stiffness in the soil profile, and by the compressibility of peat.

## References

Cascini, L. and Di Maio, C., 1994, "Emungimento delle acque sotterranee e cedimenti nell'abitato di Sarno: Analisi Preliminare", *Rivista Geotecnica Italiana,*No.3, pp.217-231.

Celico, P., Civita, M., Macchi, A., and Nicotera, P., 1977, "Il sistema idrogeologico dei monti calcareo dolomitici di Salerno: idrodinamica, risorse globali e loro degradazione a seguito dello scavo della galleria ferroviaria S. Lucia", *Memorie e Note Istituto di Geologia Applicata*, No. 13, pp. 1-44.

Piscopo, V., Fusco, C., and Lamberti, A., 1997, "Idrogeologia dei Monti Lattari (Campania)", IV Convegno dei Giovani Ricercatori in Geologia Applicata, Italy.

Mandolini, A., Picarelli, L.,  and Viggiani, C., 1995, "Un rilevato Sperimentale su terreni limo argillosi organici di origine palustre", *Rivista Geotecnica Italiana*, No.2, pp 101-115.

Itasca Consulting Group, Inc.,1995, "FLAC3.30 User Manual", Minneapolis, Minnesota.

# Author Index

387

# Subject Index

## A

Accreting soil layers, 29
Adriatic Coast, peaty soils, 226
Adsorption wastewater sludges, 74
Australia, Melbourne sand washing slimes, 293

## B

Barrier layers, 91
Batch leaching tests, 123
Bentonite slurries, 137
Bulk density, 165, 243

## C

Calcium carbonate, 351
California Bearing Ratio, 152
Cam-clay model, 48
Capping, 74, 91, 255, 309
C-CORE Shear Wave Profiling System, 243
Cement-stabilized waste sludge, 123, 152
Cement treated soils, 196
Cement, water, ratio, 196
Centrifugal force, 279
Centrifuge, geotechnical, 165
China, transformer station/ dewatering system, 363
Chromium, 123
Clays, 91, 279
    kaolin, 165
    organic, 48
    paper, 108
    soft, 337
Compressibility, 3, 29, 74, 309
    secondary, 48
Compression
    secondary, 226
    soil, 375
    unconfined, 152
Compressional wave velocity, 165
Concrete panels, precast, 337

## Cone penetration, 152
Consolidation, 48, 209, 267, 375
    dewatering, 64
    effect evaluation, 255
    large strain model, 29
    peaty soil, 226
    self-weight, 165, 324
    settlement, 309, 351
    waste, 181
    wastewater sludges, 74
Creep, 48
CS4 piecewise-linear model, 29

## D

Densitometer, 243
Dewatering, 3, 279
    structures, 64
    system, 363
Diaphragm wall, 363
Diked impoundment area, 3
Dredge spoils, 64, 243
Dredging plan, New York and New Jersey, 152
Drying rate, 196
Dual probe method, 137

## E

Earth pressure at rest, 209
Earth, reinforced, wall stability, 337
Effective strength, 209
Embankments
    construction, 267
    highway, 351
Eulerian coordinate system, 29
Excavation, deep, dewatering system for, 363

## F

Field vane tests, 255
Finite element codes, 48
Flocs, 74